# Isolation of metalated ylides and their application in the synthesis of strong donor ligands for homogeneous catalysis and the stabilization of reactive main group compounds

Ruhr-Universität Bochum

Doctoral thesis
submitted in partial fulfilment
of the requirements
of the degree of Dr. rer. nat.

submitted by
Heidar Darmandeh

Bochum, 2021

# Isolation of metalated ylides and their application in the synthesis of strong donor ligands for homogeneous catalysis and the stabilization of reactive main group compounds

Ruhr-Universität Bochum

Doctoral thesis
submitted in partial fulfilment
of the requirements
of the degree of Dr. rer. nat.

submitted by
Heidar Darmandeh

Bochum, 2021

Submission on 03.05.2021
At the faculty of chemistry and biochemistry of the Ruhr-University Bochum, Germany.

Examiners of the dissertation:

1st Examiner: Prof. Dr. Viktoria H. Däschlein-Gessner
2nd Examiner: Prof. Dr. Stefan M. Huber
3rd Examiner: PD Dr. Rajeendra Ghadwal

Examiners of the oral doctoral examination:

1st Examiner: Prof. Dr. Viktoria H. Däschlein-Gessner
2nd Examiner: Prof. Dr. Stefan M. Huber
3rd Examiner: PD Dr. Rajeendra Ghadwal

Date of the doctoral examination: xxx, 2021

Date of the delivery of the doctoral certificate:

This doctoral thesis is based on the experimental work conducted within the period of time between October 2018 and April 2021 at the chair of Inorganic Chemistry II of the Ruhr-University Bochum under the supervision of Prof. Dr. Viktoria H. Däschlein-Gessner

# Danksagung

An erster Stelle möchte ich mich bei meiner Doktormutter Prof. Dr. Viktoria H. Däschlein-Gessner bedanken. Viktoria, danke für die freundliche Aufnahme in deine Arbeitsgruppe, für das Vertrauen, das du mir geschenkt hast und die Freiheiten, die du mir gewährt hast. Des Weiteren danke ich dir für deine hervorragende Betreuung. Deine Tür stand immer offen und wir konnten stets über Probleme und weitere Entwicklungen meiner Projekte sprechen – vielen Dank !

Prof. Dr. Stefan Huber danke ich für die Übernahme des Zweitgutachtens. Vielen Dank für die unkomplizierte Kommunikation und für den Input bei unserem First Year Supervision Meeting !

Ein großes Dankeschön geht an PD Dr. Rajeendra Ghadwal für die Übernahme des Drittgutachtens.

Ich danke allen aktuellen und ehemaligen Mitgliedern des AK Gessner: Dr. Kai-Stephan Feichtner, Dr. Thorsten Scherpf, Dr. Christopher Schwarz, Dr. Lennart Scharf, Dr. Alexander Kroll, Dr. Katharina Dilchert, Dr. Chandrajeet Mohapatra, Dr. Swamy Varre, Dr. Abir Sarbajna, Dr. Sebastien Lapointe, Dr. Richard Gauld, Dr. Tobias Stalder, Henning Steinert, Jens Tappen, Ilja Rodstein, Jana-Alina Zur, Michelle Schmidt, Jens Handelmann, Julian Löffler, Felix Krischer, Mike Jörges, Angela Großjohann – es war mir eine Freude mit euch gemeinsam im Labor zu arbeiten.

Ein besonderer Dank geht an Henning Steinert und Julian Löffler für umfangreiche DFT Rechnungen.

Dr. Bert Mallick danke ich für die Einführung in die Einkristall-Röntgenstrukturanalyse und für Hilfestellungen, wenn ich beim Lösen einer Struktur mal Probleme hatte.

Manuela Winter und Dr. Harish Parala danke ich für das Messen von Elementaranalysen. Außerdem möchte ich mich bei Dagmar Müller und Maurice Paaßen für reibungslose Abläufe im Laboralltag bedanken. Martin Gartmann danke ich für die ständige Erreichbarkeit / Problemlösung bei Fragen rund um unser NMR Gerät. Sabine Pankau danke ich für Ihre Unterstützung im Kampf gegen die Bürokratie.

Dr. Frank Richter bin ich zu tiefem Dank verpflichtet. Frank, danke für deinen ehrenamtlichen Einsatz. Unsere Mentoring-Kooperation hat mir viel Spaß gemacht. Vielen Dank für all die wertvollen Einblicke, Informationen und Diskussionen.

Der größte Dank gebührt meiner Familie. Ihr habt mich seit Tag 1 ermutigt, unterstützt und motiviert. Vom tiefsten Herzen danke ich meinen Eltern Abrahim und Houda, meinen Geschwistern Amina, Mohamed Ali und Rim und meiner Frau Lara für die bedingungslose Unterstützung während meines gesamten Studiums. Nur mit eurer Rückendeckung konnte ich das erreichen.

## List of abbreviations

| | |
|---|---|
| %$V_{\mathrm{bur}}$ | Percent buried volume |
| °C | Degree Celsius |
| Å | Angström |
| acac | Acetylacetonate |
| Ad | Adamantyl |
| aNHC | Abnormal N-Heterocyclic Carbene |
| approx. | approximately |
| APT | Attached Proton Test |
| Ar | Aryl substituent |
| $\mathrm{Ar}^{\mathrm{Mes}}$ | $C_6H_3$-2,6-$\mathrm{Mes}_2$ |
| $\mathrm{Ar}^{\mathrm{Tripp}}$ | $C_6H_3$-2,6-$\mathrm{Tripp}_2$ |
| AYC | Alkyl ylide carbene |
| B | Base |
| BHA | Buchwald-Hartwig Amination |
| Bn | Benzyl |
| CAAC | Cyclic alkyl amino carbene |
| cal | Calories |
| calc. | Calculated |
| CAYC | Cyclic alkyl ylide carbene |
| CGMT model | *Carter, Goddard, Malrieu* and *Trinquier* model |
| COD | 1,5-Cyclooctadiene |
| Cy | Cyclohexyl |
| dba | Dibenzylidenacetone |
| DCM | Dichloromethane |
| DEPT | Distortionless Enhancement by Polarization Transfer |
| DFT | Density functional theory |
| Dipp | Diisopropylphenyl |
| DMAP | 4-(Dimethylamino)-pyridine |
| DMF | Dimethylformamide |
| EDA | Energy decomposition analysis |
| eq. | Equivalent |
| Et | Ethyl |
| $Et_2O$ | Diethylether |
| exp | Experimental |
| FLP | Frustrated Lewis Pair |
| g | Gram |
| h | Hour |
| Hal | Halogen atom |
| HBcat | Catecholborane |
| HBpin | Pinacolborane |
| HMBC | Heteronuclear Multiple Bond Correlation |
| HMPA | Hexamethylphosphoramide |
| HOMO | Highest occupied molecular orbital |
| HSQC | Heteronuclear Single Quantum Coherence |
| Hz | Hertz |
| HMBC | Heteronuclear Multiple Bond Correlation |
| IAd | 1,3-Bis-(1-adamantyl)imidazol-2-ylidene |
| IAP | Imidazoline amino phosphines |
| IMe | 1,3-dimehtylimidazol-2-ylidene |
| IPr | 1,3-Bis-(2,6-diisopropylphenyl)-imidazol-2-yliden |
| *i*Pr | *Iso*-propyl |
| IR | Infrared |
| J | Joule |
| K | Kelvin |
| k | Kilo |
| KHMDS | Potassium bis(trimethylsilyl)amide |
| LDA | Lithium diisopropylamide |
| $L_n$ | Any Ligand |
| LUMO | Lowest unoccupied molecular Orbital |
| *m* | *Meta* |
| *M* | mol·L$^{-1}$ |
| M | Metal |
| Me | Methyl |
| Mes | 2,4,6-Trimethylphenyl |
| MHz | Megahertz |
| MIC | Mesoionic carbene |
| min | Minute |
| mmol | Millimolar |
| NaHMDS | Sodium bis(trimethylsilyl)amide |
| NBO | Natural Bond Orbital |
| *n*Bu | *n*Butyl |
| NFSI | N-Fluorbenzolsulfonimid |
| NHC | N-Heterocyclic-Carbene |
| NHI | N-Heterocyclic-Iminato |
| NHO | N-Heterocyclic-Olefin |
| NMP | *N*-Methyl-2-pyrrolidon |
| NMR | Nuclear Magnetic Resonance |
| *o* | *Ortho* |
| OA | Oxidative Addition |
| *p* | Para |
| p/a | per annum |
| PAP | Phosphazenyl phosphines |
| Ph | Phenyl |
| pm | Picometer |
| ppm | Parts per million |
| R | Any rest |
| r.t. | Room temperature |

| | |
|---|---|
| sIMes | 1,3-Bis(2,4,6-trimethylphenyl)-4,5-dihydroimidazol-2-ylidene |
| $t_{1/2}$ | Half-life |
| *t*Bu | *Tert*-Butyl |
| TEP | *Tolman electronic parameter* |
| *tert* | Tertiary |
| THF | Tetrahydrofuran |
| tht | Tetrahydrothiophene |
| TM | Transition-metal |
| TMS | Trimethylsilyl |
| TOF | Turnover frequency |
| Tol | p-Tolyl (4-Methylphenyl) |
| Tripp | 2,4,6-triisopropylphenyl |
| Ts | Tosyl |
| VT-NMR | Variable temperature NMR |
| WBI | Wiberg Bond indices |
| XRD | X-Ray structure determination |
| YPhos | Ylide-functionalized phosphine |
| $\Delta$ | Delta, difference |
| $\delta$ | Chemical shift |
| $\Delta E_{H\text{-}L}$ | HOMO-LUMO energy gap |
| $\Delta EN$ | Electronegativity difference |
| $\Delta E_{ST}$ | Singlet-triplet energy gap |
| $\Delta E_{\sigma+\pi}$ | Difference of the $\sigma$– and $\pi$– bond dissociation energy |
| $\eta$ | Hapticity |
| $\nu$ | Wave number |

# Index

1. Introduction ........ 1

1.1 Strong donor ligands in transition-metal catalysis ........ 1

1.2 Electronic and steric properties of tertiary phosphines ........ 4

1.3 N-Heterocyclic carbenes ........ 8

1.4 Low-valent main group species ........ 11

1.5 Ylides - a unique carbon-based ligand class ........ 22

1.5.1 Development of metalated ylides ........ 22
1.5.2 Structure and bonding motifs in metalated ylides ........ 26
1.5.3 Reactivity of metalated ylides in synthesis ........ 31
1.5.4 Ylides as stabilizing ligands for low-valent main group species ........ 35
2. Aims of this thesis ........ 47

3. Results and Discussion ........ 50

3.1 Synthesis, Isolation and Crystal Structures of the Metalated Ylides [$Cy_3P-C-SO_2Tol$]M (M = Li, Na, K) ........ 51

3.2 Synthesis of Low-Valent Dinuclear Group 14 Compounds with Element-Element Bonds by Transylidation ........ 60

3.3 Reactivity of ylide-stabilized acyclic germylenes and stannylenes ........ 66

3.4 Towards the synthesis of an ylide-stabilized acyclic silylene ........ 72

3.5 Au···H-C Hydrogen Bonds as Design Principle in Gold(I) Catalysis ........ 82

3.6 $^{Cy}$YPhos ligands in Pd catalysis ........ 94

4. Summary and Outlook ........ 99

5. Experimental Section ........ 113

5.1 Experimental Details for Section 3.1 ........ 115

5.2 Experimental Details for Section 3.2 ........ 118

5.3 Experimental Details for Section 3.3 ........ 121

5.4 Experimental Details for Section 3.4 ........ 123

5.5 Experimental Details for Section 3.5 ........ 127

5.6 Experimental Details for Section 3.6 ........ 133

5.7 Crystallographic details ........ 134

6. References ........ 141

7. Appendix ........ 155

# 1. Introduction

The central theme of this thesis was the synthesis of novel metalated ylides and their subsequent use for preparation of ylide-functionalized phosphines *and* ylide-stabilized low-valent main group element species. In the initial part of this introduction, the importance of ligand classes for transition-metal based homogeneous catalysis is explained briefly. Following this, the ability of low-valent main group compounds to mimic transition-metal like behavior is discussed and the importance of different ligand properties is explained. Finally, a historical survey of metalated ylides, followed by their electronic properties and reactivity is discussed.

## 1.1 Strong donor ligands in transition-metal catalysis

The development and design of strong donor ligands have led to fundamental advances in organometallic chemistry. Initially, molecular well defined, organometallic complexes were applied as homogeneous catalysts in academic laboratories as well as in industrial processes. Mild reaction conditions, increased selectivity and reactivity, as well as easily tunable steric and electronic properties of the applied complexes were some of the major advantages compared to heterogeneous catalysis. In the latter, the catalytically active species are most often not recognized and therefore the explanation of activity cannot be attributed to clear molecular interactions, which is why heterogeneous catalysis is often depicted as an alchemist's "black art"[1]. The ability of understanding reaction mechanisms at the molecular level by conducting stoichiometric experiments and subsequently adapting the molecular structure of the catalyst to solve distinct problems, is absolutely one of the key factors, why homogeneous catalysis has become so popular in use. In general, the catalytic cycle of a homogeneously catalyzed reaction is of course highly dependent on the reaction type. However, a few key features seem to be crucial for nearly every transition-metal catalyzed reaction. The abilities of transition-metals to switch between different oxidation states and binding modes and accessing different electronic structures are highly important. The catalytically active metal involved should be in an electronically unsatisfied state, hence providing access for further coordination by the substrate. This is often achieved by electron-rich, bulky supporting ligands, shielding the space around the metal center (kinetic stabilization) while simultaneously providing sufficient electron-donation to the metal atom (thermodynamic stabilization).[1] One of the first examples of applied organometallic catalysis in an industrial process is the famous hydroformylation reaction ('oxo' synthesis) developed by *Otto Roelen* at former Ruhrchemie AG (now OQ Chemicals) in 1938.[2] The reaction between olefins and a mixture of $H_2$/CO (so called *Syngas*) leading primary to important branched or linear aldehydes, is today conducted at a multimillion-ton p/a scale (Figure 1).[3] While the first catalysts used in this transformations were based on simple cobalt or rhodium hydride complexes (**1**), incorporating specified ligands (**2**) into the metal framework lead to an increase in selectivity (branched/linear product), stability and reactivity.[3,4] Further developments in ligand design (**3**) enabled even highly stereoselective variants of the hydroformylation process, thus impressively showing that the choice of the supporting ligand is highly important for catalyst reactivity and selectivity.[5]

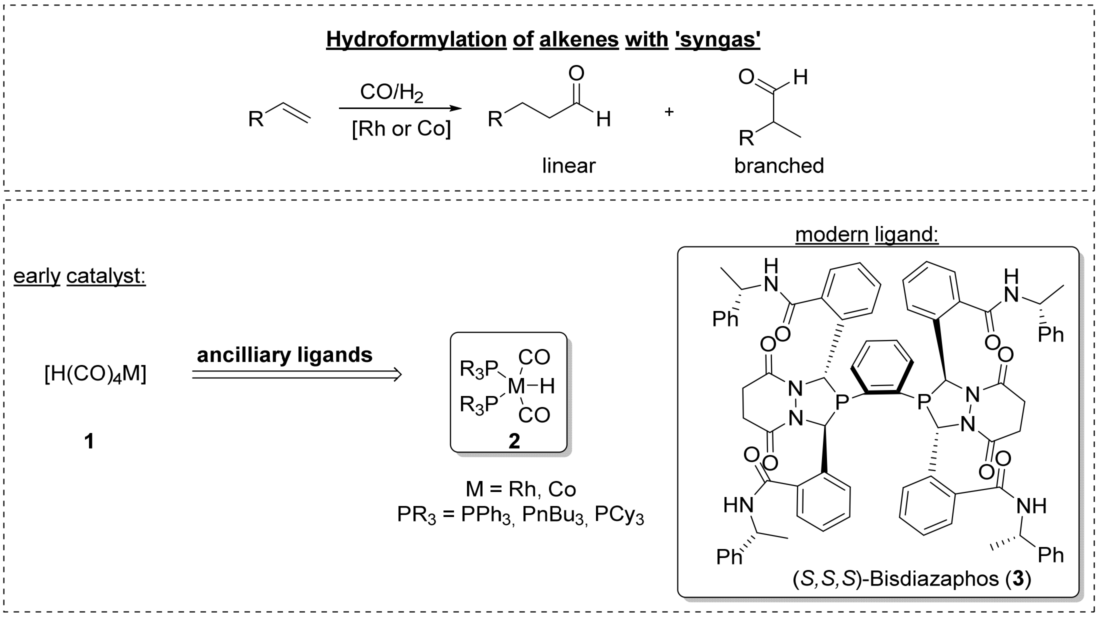
Hydroformylation of alkenes with 'syngas'
R
CO/H2
[Rh or Co]
O
R
H
linear
+
O
H
R
branched
early catalyst:
[H(CO)4M]
1
ancilliary ligands
R3P
R3P
CO
M–H
CO
2
M = Rh, Co
PR3 = PPh3, PnBu3, PCy3
modern ligand:
H
N
Ph
O
O
N
N
P
P
N
N
O
O
HN
Ph
H
N
Ph
NH
Ph
(S,S,S)-Bisdiazaphos (3)

**Figure 1.** Rhodium or Cobalt catalyzed 'oxo'-synthesis of linear and branched aldehydes from alkenes and syngas.

The invention of several industrial processes and scientific breakthroughs (Figure 2) like the selective catalytic hydrogenation of olefins (*Wilkinson's Hydrogenation*)[6], olefin metathesis (*Schrock*[7]/*Grubbs*[8,9,10], 'Shell's higher olefin process'[11]), stereoselective polymerizations (*Ziegler*[12], *Natta*[13] and *Kaminsky*[14]) or Pd- catalyzed cross-coupling reactions (*Kumada*[15,16], *Heck*[17], *Sonogashira*[18], *Negishi*[19], *Stille*[20] and *Suzuki*[21]), rely on the development of specialized ligand systems to enable these transformations and are thus mainly correlated to the progress achieved by the field of organometallic chemistry in general.

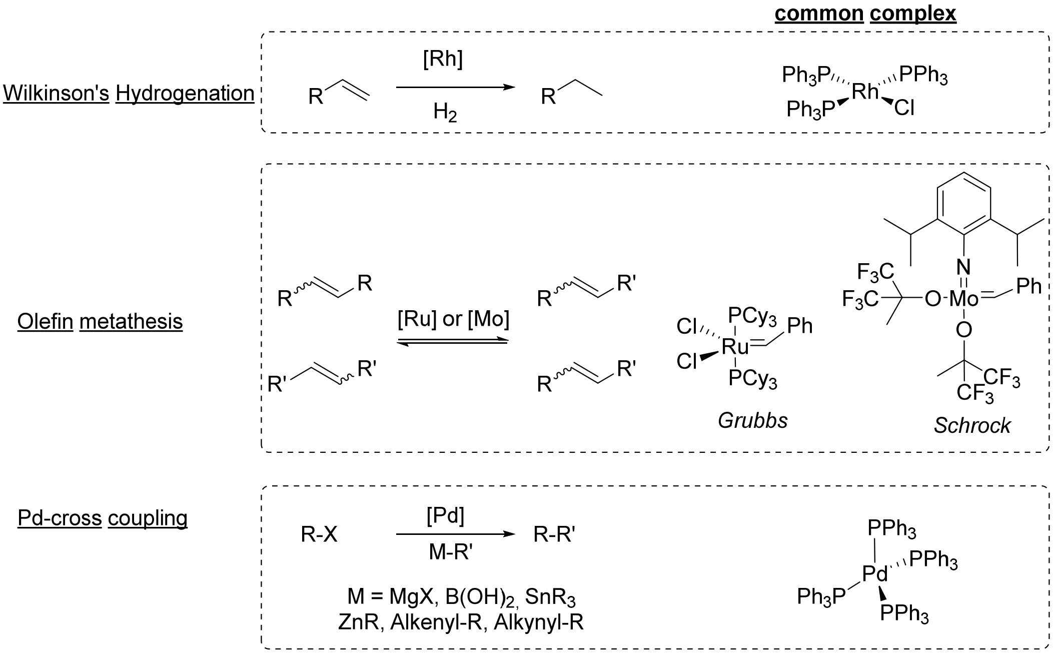
common complex
Wilkinson's Hydrogenation
R
[Rh]
H2
R
Ph3P
PPh3
Rh
Ph3P
Cl
Olefin metathesis
R
R
R'
R'
[Ru] or [Mo]
R
R'
R
R'
Cl
Cl
PCy3
Ru
PCy3
Ph
Grubbs
F3C
F3C
O
N
Mo
Ph
O
CF3
CF3
Schrock
Pd-cross coupling
R-X
[Pd]
M-R'
R-R'
M = MgX, B(OH)2, SnR3
ZnR, Alkenyl-R, Alkynyl-R
PPh3
Pd
PPh3
Ph3P
PPh3

**Figure 2.** Some important transition-metal based homogeneous catalyzed reactions and common complexes used as catalysts.

The above-mentioned reactions and processes show that ancillary ligands play a crucial role for efficient and selective homogeneous catalysis. Therefore, in the following chapters common ligand classes, as well as their electronic- and steric properties will be discussed briefly.

## 1.2 Electronic and steric properties of tertiary phosphines

When exploring the literature reporting about ligands for homogeneous catalysis, it is noticeable that the majority of examples rely on tertiary phosphines ($PR_3$, R = organic rest) and amines ($NR_3$). This is not surprising since they represent textbook examples of strong Lewis bases, enabling sufficient $\sigma$–donation to the metal center in organometallic complexes, hence being able to stabilize the most often highly oxidized catalytically active species. In particular, the synthesis of tertiary phosphines can be easily realized from cheap and commercially available starting materials, which makes them attractive for the use on industrial scale.[1,4] Furthermore, the electronic- and steric properties of phosphines can be easily tuned, explaining their versatility as ligands in metal complexes.[22] The phosphorus-metal bond can be mainly described by two major contributions (Figure 3): the phosphorus atom bears a free pair of electrons which can overlap with an unoccupied d-orbital of the metal center to give a $\sigma$–bond ($\sigma$-donor), while simultaneously an occupied metal orbital overlaps with an $\sigma$(P–R)*-orbital, resulting in $\pi$-backbonding ($\pi$-acceptor). The $\sigma$-donor / $\pi$-acceptor character of a phosphine can be modulated by the substituents directly bound to the phosphorus atom. Electron-withdrawing substituents stabilize the HOMO at the phosphorus atom, resulting in a decrease of the P–M $\sigma$-bond strength and in an increase of the M–P $\pi$-bond strength. On the other hand, electron-donating substituents destabilize the HOMO at the phosphorus atom, hence resulting in stronger $\sigma$-donation and weaker $\pi$-backbonding.[23]

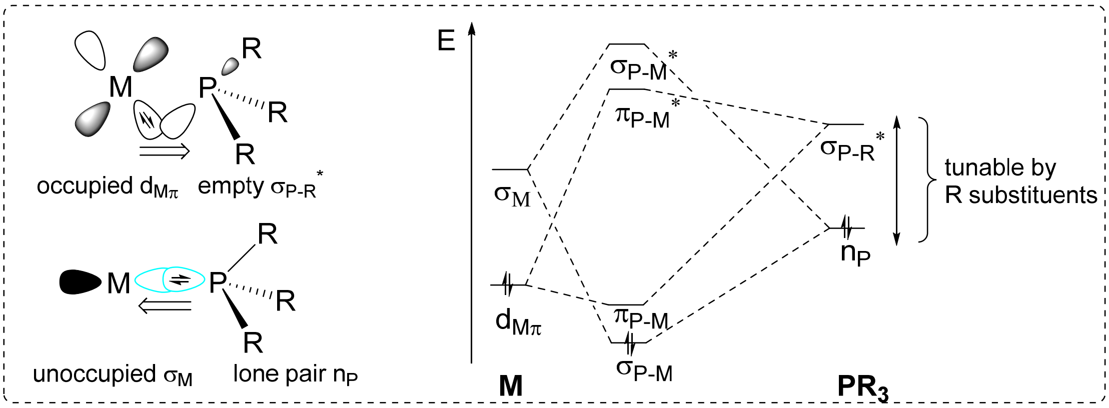

**Figure 3.** Bonding situation in metal-phosphine complexes.

To quantitatively describe the electronic properties of phosphines, *Tolman* et al. developed a method known as the *Tolman Electronic Parameter* (TEP).[24] Herein, a monodentate phosphine is reacted with $[Ni(CO)_4]$, resulting in ligand substitution giving the respective $[PR_3\text{-}Ni(CO)_3]$ complex. Its A1 stretching frequency $\nu_{CO}$ ($cm^{-1}$) can be measured by IR spectroscopy, giving direct information about the electronic situation at the metal center. A highly electron-rich phosphine can donate electron density to the metal which is then able to perform extensive $\pi$-backbonding to the attached CO ligands. While the metal-carbon bond is strengthened, the carbon-oxygen bond is weakened resulting in a decrease of the wavenumber for $\nu_{CO}$. Similar, if $PR_3$ is a good $\pi$–acceptor, it competes with the CO ligands for $\pi$-backbonding, resulting in an increase of $\nu_{CO}$. Today, substitutes for the highly toxic $[Ni(CO_4)]$ have been introduced and the TEP value can also be calculated by correlation of the stretching frequencies of other metal-phosphine carbonyl complexes such as $[PR_3\text{-}Rh(acac)CO]$[25] or $[PR_3\text{-}IrCl(CO)_2]$[26]. Besides the electronic properties of a ligand, geometrical factors also play a significant role in stabilizing highly reactive species. To further rationalize the steric bulk of phosphines, *Tolman* developed a semi-quantitative method based on a molecular model, the so-called *cone angle*.[24] The angle between the metal at the vertex and the peripheral edge of the van der Waals radii of the ligand atoms was used to determine the steric bulk of a large number of phosphines (Figure 4).

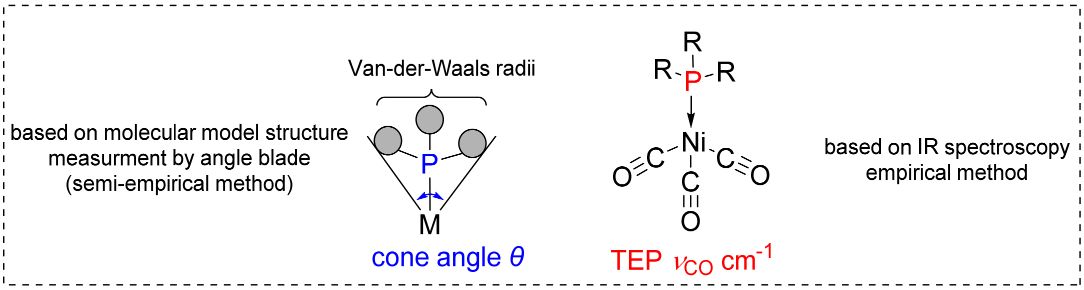

**Figure 4.** Models to quantify the steric demand (cone angle, left) and electronic properties of phosphines (TEP, right) developed by *Tolman*.

Some TEP values and cone angles of common phosphines are given in Table 1.

**Table 1.** TEP values and conge angles of simple alkyl- and arylphosphines.[24]

| Ligand | **$\text{TEP}_{\text{calc.}}$ [$\text{cm}^{-1}$]** | **cone angle [°]** |
|---|---|---|
| $PF_3$ | 2110.8 | 106 |
| $PCl_3$ | 2097.0 | 124 |
| $PPh_3$ | 2068.9 | 145 |
| P(*o*Tol)$_3$ | 2066.6 | 194 |
| $PMe_3$ | 2064.1 | 118 |
| P*i*Pr$_3$ | 2059.2 | 160 |
| $PCy_3$ | 2056.4 | 170 |
| P*t*Bu$_3$ | 2056.1 | 182 |

It can be easily seen that phosphorus ligands bearing electron-withdrawing substituents such as halogen atoms (e.g. $PF_3$, $PCl_3$, TEP = 2110.8 and 2097.0 $cm^{-1}$) have significantly higher TEP values than phosphines bearing aryl groups (e.g. $PPh_3$, TEP = 2068.9 $cm^{-1}$), clearly reflecting their high $\pi$-acceptor properties and thus their low donating ability. Furthermore, alkyl phosphines such as P*t*Bu$_3$ (TEP = 2056.1 $cm^{-1}$) are more electron-donating than their aryl counterparts, which can be explained by positive inductive effects of the alkyl chains. In addition, increasing the steric bulk of the substituents bound to the phosphorus atom, directly leads to an increase in the measured cone angle. This can be seen for example in the series of alkyl phosphines. While $PMe_3$ has a relatively low cone angle of 118°, attaching Cy- or *t*Bu-substituents instead, widens the angle to 170° and 182°, respectively. The limit by means of electron-releasing ability of a simple trialkylphosphine was for a long time P*t*Bu$_3$, which was only recently exceeded with the synthesis of tris-adamantylphosphine ($PAd_3$), reported by *Carrow*.[25] $PAd_3$ features a TEP value of 2052.1 $cm^{-1}$, significantly greater than the donor ability of P*t*Bu$_3$. However, the boundaries for phosphine donor strength in general, were pushed by recent reports about ylide-substituted phosphines (YPhos, TEP of up to 2044.6 $cm^{-1}$) by *Gessner*[27–33], imidazolin-2-ylidenamino phosphines (IAPs, TEP up to 2029.7 cm$^{-1}$) by *Dielmann*[34,35] and phosphazenyl phosphines (PAPs, TEP up to 2014.5 cm$^{-1}$) reported by *Sundermayer* (Figure 5).[36]

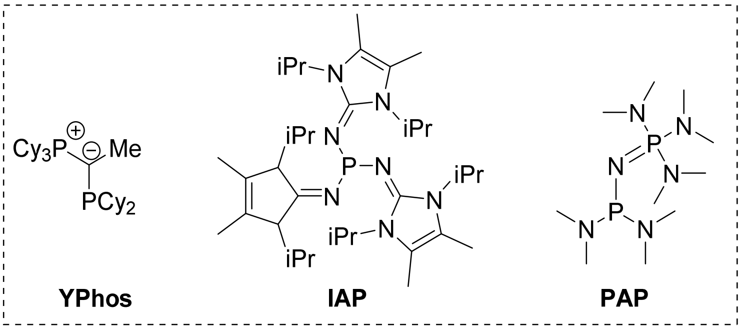

**Figure 5.** Examples of novel, highly electron-rich phosphines that exceed the common donor power of tertiary phosphines.

The beneficial effect of providing a ligand with high steric bulk and increased donor power in homogeneous catalysis can be seen for ruthenium catalyzed ring-closing metathesis reported by *Grubbs* (Scheme 1). [10]

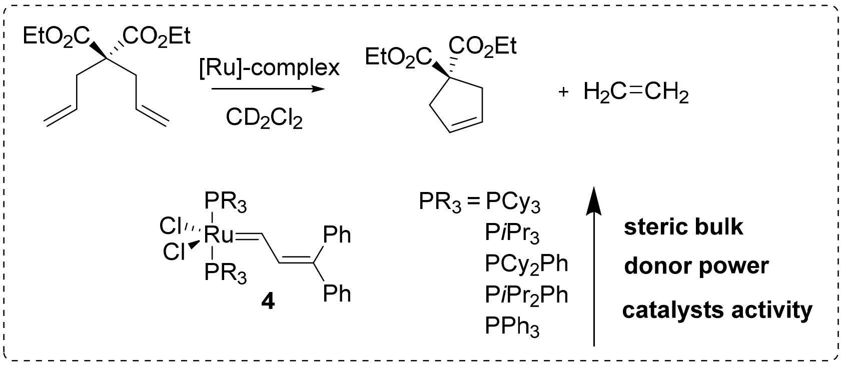

**Scheme 1.** Ring-closing metathesis catalyzed by Ru-complexes **4** bearing different phosphines.

Replacing the phenyl substituents of $PPh_3$ in complex **4** with more electron-releasing and bulkier *i*Pr or Cy groups, resulted in a dramatical increase of catalysts activity, with $PCy_3$ as the bulkiest and electron-richest phosphine giving the highest activity. The ability of bulky, electron-rich phosphines to stabilize a low-valent ruthenium 14 valence electron complex, which is regarded to be the catalytically active species[10], were responsible for these high catalytic activities. In addition to in ruthenium catalyzed metathesis reactions, bulky, electron-rich phosphines have found numerous applications as ancillary ligands for gold[37], palladium[38,39,40,41] and nickel catalysis[15,16,19,42]. Especially in palladium catalyzed cross-coupling reactions, trialkyl-phosphines[41,43] and dialkylbiaryl-phosphines (also known as *Buchwald* phosphines)[38,40,44] are extensively used as ligands. Recent reports on the beforementioned YPhos ligand class showed furthermore excellent catalytic activities in gold(I) catalyzed hydroamination[27,30,32] as well as Pd-catalyzed C–C[31,45,46] and C–N[28,29,33] bond forming reactions, even at room temperature. Because of their superior donor strength, it was reported that these phosphines are able to facilitate oxidative addition of aryl halides to the Pd(0) species, which is often the rate-determining step in the catalytic cycle.[47] Furthermore, their steric bulk eases reductive elimination by releasing steric pressure off the metal center, closing the catalytic cycle. However, donor strength and steric bulk are not the only factors that enable stabilization of low-valent metal centers. *Buchwald* phosphines for example, exhibit secondary metal-ligand interactions between the biaryl-motif and the metal center (Figure 6).[48] These interactions were e.g. observed in cationic coinage metal (Au(I), Ag(I), Cu(I))[48] (**5**) and Pd(0)[49] complexes of Buchwald phosphines and are believed to be beneficial for the stabilization of the catalytically active species in respective organic transformations, for instance in Au(I) or Cu (I)- hydroaminations and Pd-catalyzed Suzuki couplings.[40] Similarly, gold-arene interactions were found also in IAP-Au(I) complexes (**6**).[35] Moreover, agostic interactions between hydrogen atoms of bulky phosphine alkyl groups (e.g. **7** and **8**) and metal centers are believed to enhance rigidity of transition states and thus enhance the catalytic performance of the respective complexes, as for example can be seen in Pd-catalyzed cross-coupling reactions.[41,43]

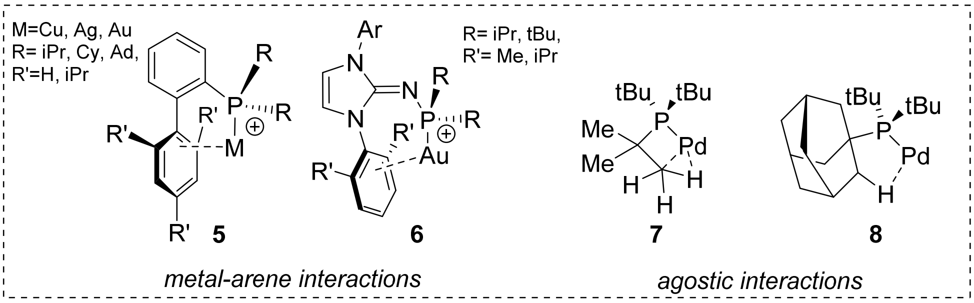
M=Cu, Ag, Au
R= iPr, Cy, Ad,
R'=H, iPr
R
R'
P
R
M
R'
R'
Ar
N
N
N
R
P
R'
R
Au
R'
R= iPr, tBu,
R'= Me, iPr
tBu
tBu
Me
P
Me
Pd
H
H
H
tBu
tBu
P
Pd
H
5
6
7
8
metal-arene interactions
agostic interactions

**Figure 6.** Examples for secondary metal-ligand interactions in phosphine-TM complexes.

Contrary to its neighbors, carbon centered Lewis bases such as carbenes or carbanions seem to be less important as ligand classes. Because of their high sensitivity, difficult isolation and further reactivity were for a long time regarded as impossible. However, progress in the stabilization of such species proved the way to new ligand classes, above all the so-called N-Heterocyclic-Carbenes (NHCs).

## 1.3 N-Heterocyclic carbenes

The first 'bottable' NHC, namely 1,3-bisadamantylimidazol-2-ylidene (**IAd**), was reported by *Arduengo* et al. in 1991[50], albeit seminal work performed by *Öfele*[51] and *Wanzlick*[52] in the 1960s clearly lead to important structural insights into stability and reactivity of NHCs. NHCs are singlet cyclic diamino carbenes, which are thermodynamically and/or kinetically stabilized and can be stored indefinitely under inert conditions. Free NHCs are usually synthesized by deprotonation of suitable imidazolium-salt precursors (Scheme 2). Their stability mainly arises from the incorporation of the carbon atom into a N,N-scaffold. The nitrogen atoms effectively decrease the electron density at the carbenic center ($\sigma$-withdrawing effect), while simultaneously donating into the vacant p-orbital ($\pi$-electron-donation). Furthermore, kinetic stabilization is provided by bulky substituents attached to the heteroatoms, suppressing dimerization. [53,54]

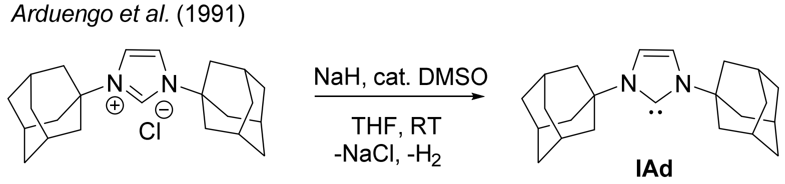
*Arduengo et al.* (1991)

**Scheme 2.** Synthesis of the first reported NHC by *Arduengo* et al.[50]

However, imidazol(in)e-based NHCs are more stabilized by electronic effects than by kinetics, making them thermodynamically stable. This can be seen for example by the isolation of **IMe**, with methyl groups attached to the nitrogen atoms.[55] Since their first isolation, NHCs evolved from laboratory curiosities into a highly valuable ligand class, being used for TM-catalysis[56], organocatalysis[54], material science[57], medicinal chemistry[58] or as strong donor substituents for stabilizing highly reactive low-valent main-group species[59]. Today, a plethora of NHCs with different heterocycles have been synthesized, for instance imidazol(in)- ('normal' NHCs), tetrahydropyrimidine[60]-, oxazole[61]-, thiazole[62]-, triazole[63]- or pyrrolidine (cyclic alkyl amino carbenes, **CAACs**[64], e.g. **9** and **10**) based carbenes are known.[54] Additionally, when the C2 position of the imidazoline scaffold is blocked, deprotonation in C3 position can occur (**11**, **12**), giving 'abnormal' NHCs (**aNHCs**) or sometimes called mesoionic carbenes (**MICs**).[65] Some common examples of NHCs are shown in Figure 7.

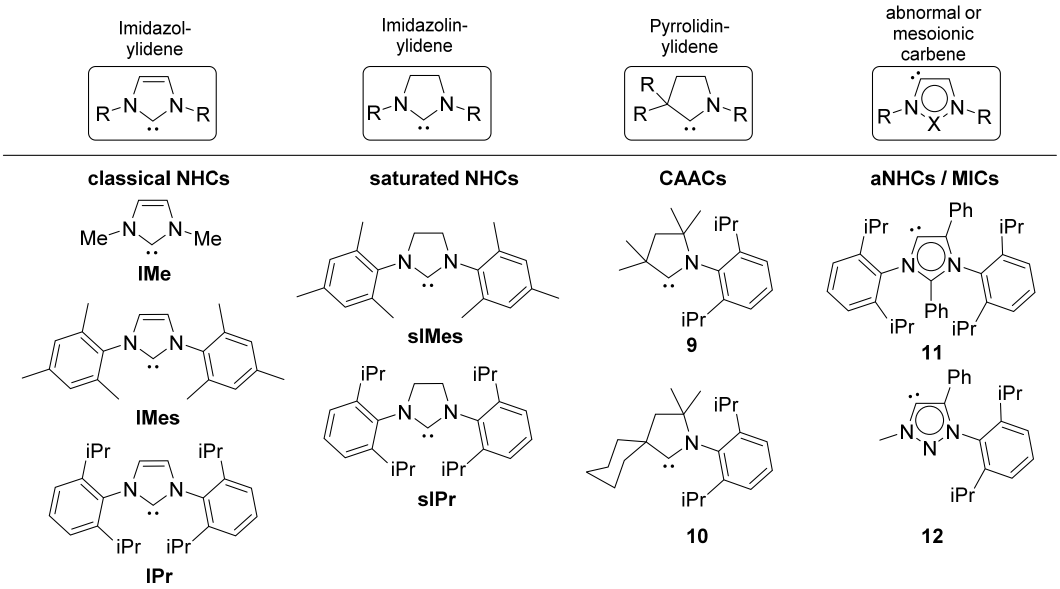
Imidazol-
ylidene
Imidazolin-
ylidene
Pyrrolidin-
ylidene
abnormal or
mesoionic
carbene
classical NHCs
saturated NHCs
CAACs
aNHCs / MICs
IMe
IMes
IPr
sIMes
sIPr
9
10
11
12

**Figure 7.** Important classes and examples of NHCs.

Classical NHCs are regarded as good $\sigma$-donors and weak $\pi$-acceptors. Their electronic properties can be evaluated by the same method as already applied for phosphines. TEP values of NHCs are significantly lower than for simple aryl- and alkylphosphines and usually lie in the range between 2049–2052 cm$^{-1}$, which makes them to very electron-rich ligands.[66] Steric properties of NHCs however, can not be evaluated by the same method as for phosphines. In contrast to phosphines, NHCs do not posses a symmetrical, cone-shaped steric profile, but a rather 'umbrella-like' asymmetric profile, which makes them unsuitable for measuring a cone angle (Figure 8).[67]

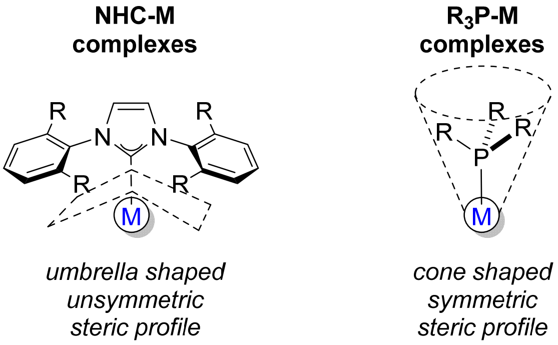
NHC-M
complexes
R$_3$P-M
complexes
umbrella shaped
unsymmetric
steric profile
cone shaped
symmetric
steric profile

**Figure 8.** Steric profiles of NHC-M complexes (left) and phosphine-metal complexes (right).[67]

In order to quantify the steric pressure brought by different ligand systems, *Nolan* and *Cavallo* developed a method based on 'the percent of a total volume of a sphere occupied by a ligand', the so-called *percent buried volume* %$V_{\text{bur}}$.[68] With a defined sphere radius and metal-ligand bond length, the metal being the center of the sphere, steric properties of different ligand systems can be easily calculated from suitable crystal structures and compared among themselves. Usually, L-AuCl-complexes are used for determination because the linear coordination environment minimizes the steric influences of other spectator ligands. That said, *Nolan* measured the %$V_{\text{bur}}$ of different NHCs clearly showing that the groups attached to the nitrogen atoms have the greatest impact, while backbone modification only has minor contribution to the steric profile.[69] Thus, the steric properties of NHCs can be easily adjusted to the need of the reaction. Moreover, metal-carbon bonds are stronger than metal-phosphorus bonds, resulting in more rigid and stable complexes. These properties render NHCs as potential ligands for homogeneous catalysis. Indeed, *Hermann* was the first one who reported on the use of NHCs as ancillary ligands for Pd-catalyzed Heck coupling reactions[70], followed by reports on NHC-Ru-complexes for olefin metathesis[71] and Pd-catalyzed cross-couplings.[72] Remarkably, substitution of the $PCy_3$ ligand in Grubbs' first generation metathesis catalysts (**Grubbs I**) with the saturated NHC **sIMes**, lead to an increase in reactivity and stability of the catalysts (Figure 9), which greatly shows the advantages of NHCs over phosphines in this transformation.[9]

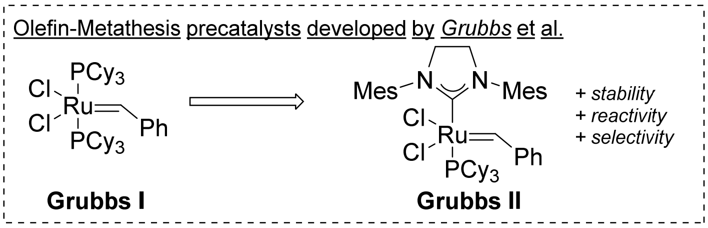

**Figure 9.** Substitution of one $PCy_3$ ligand in Grubbs I by the NHC sIMes giving the Grubbs II olefin-metathesis complex.

Nowadays, NHC based TM-catalysts are used for numerous organic transformations, including industrially important ones[73], challenging the status quo for phosphine ligands which are mainly used in TM-based homogeneous catalysis. Albeit the development of novel ligands that enable efficient TM-based homogeneous catalysis at low catalyst loadings and mild reaction conditions is highly important and remains a very active field of research, the use of often toxic, non-abundant and expensive transition-metals[74] and their difficult recovery is of concern in terms of sustainability, health issues and the concepts of green chemistry.[75] Since the last quarter of the 20th century, a growing interest in replacing transition-metals with non-toxic, abundant 'greener' alternatives has emerged. In this term, systems based on main-group (p-block) elements have shown promising transition-metal like reactivities and therefore are discussed briefly in the following section.

## 1.4 Low-valent main group species

Transition-metals usually possess partially occupied valence d-orbitals which lie close in energy. This characteristic has a pivotal role on their reactivity, hence enabling them to switch easily between different oxidation states, binding modes and coordination numbers.[76] These abilities are the main reason, why transition-metal complexes show catalytic activity, since oxidative addition, ligand dissociation/association, insertion reactions and reductive elimination are often crucial steps in catalytic cycles. However, main group compounds either do not have d-orbitals or they lie too high in energy to participate in bonding. Furthermore, the fundamentally lower number of valence electrons intrinsically limits the quantity of accessible oxidation states. Despite that, s- and p-orbitals in main-group molecules are either fully occupied or empty (*octet rule*) and often far apart in energy. From that point of view, two major requirements for accessing transition-metal like behavior with main-group compounds occur:[76]

- the presence of occupied and unoccupied molecular frontier orbitals with accessible energy levels and small energy gaps
- the resulting unsaturated, low-valent species should be stable to enable further chemistry

However, main-group compounds in unusual oxidation states are intrinsically highly reactive and tend to oligomerize/polymerize or to disproportionate into more stable species. To suppress typical decomposition pathways, stabilization is necessary. This stabilization can be achieved either by the use of extremely bulky substituents, suppressing oligomerization reactions and shielding the metal center from nucleophilic attack (kinetic stabilization), and/or by attaching substituents next to the metal center which can reduce the electron-density ($\sigma$-acceptor) at the HOMO and subsequently donate electron density ($\pi$-donor) to stabilize the LUMO (thermodynamic stabilization) (Figure 10).

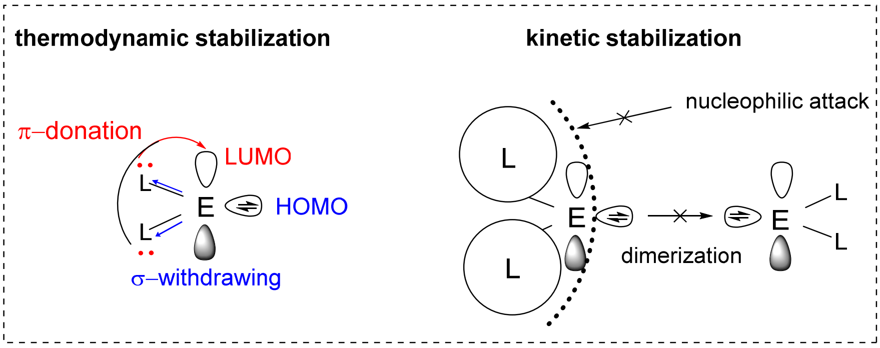

**Figure 10**. Illustration of thermodynamic stabilization (left) and kinetic stabilization (right) applied to isolate low-valent main group species.

### Landmark examples of low-valent main group compounds

It was long believed that stable heavier analogues of alkenes do not exist, due to the low tendency of the >2nd row elements to form homonuclear multiple bonds (double-bond rule).[77] However, with the development of suitable substituents, this rule was proven wrong. In the 1970s, *Lappert* et al. reported about the synthesis of heavier group 14 carbene analogues R-E-R (E= Ge, Sn, Pb), so-called tetrylenes, based on bulky silyl-substituted alkyl- or amido ligands (Scheme 3).[78–81] Both

[E(CH(SiMe$_3$)$_2$] **13a-c** and [E(N(SiMe$_3$)$_2$]**15a-c** were found to be monomeric species in solution, however the former dimerizing in the solid state to give heavier group 14 analogues of alkenes **14a-c**.

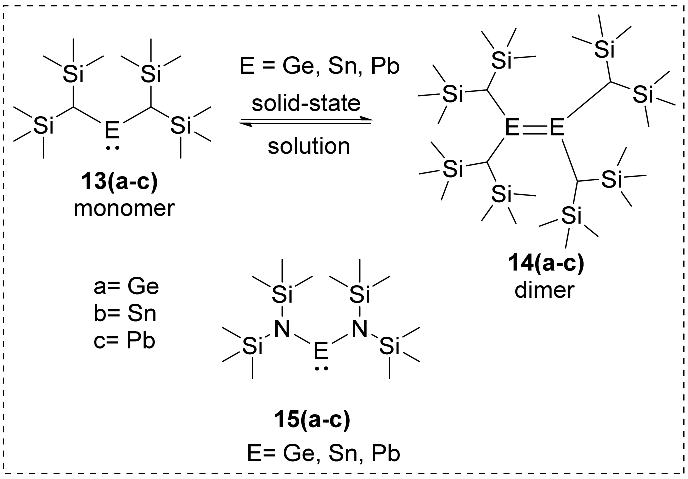

**Scheme 3.** First examples of isolated heavier tetrylenes and alkenes as reported by *Lappert*.[78–81]

XRD analyses of these species, showed that in contrast to classical alkenes which exhibit a strong and planar double bond, heavier tetrels form double-bonds with trans-bent geometries. This observation can be explained based on a valence bonding (VB) model developed by *Carter, Goddard, Malrieu* and *Trinquier* (CGMT model)[82]. In a computational experiment, a double bond is theoretically cleaved homolytically, giving two carbene fragments residing in a triplet state. Independently, the ground state of these fragment can be either a triplet state or a singlet state. The classical double bond energy consists of two main parts: 1) the bond-dissociation energies of the $\sigma$ and $\pi$ bond ($\Delta E_{\sigma+\pi}$) and 2) the singlet-triplet energy gap ($\Delta E_{ST}$). Now if the $\Delta E_{\sigma+\pi}$ is higher than the corresponding $\Delta E_{ST}$, a classical, planar double bond is formed. However, in contrast to methylene (H$_2$C:), basic group 14 carbene analogues :EH$_2$ (E = Si, Ge, Sn, Pb) all favor a singlet ground state over the triplet one, in which both electrons are located in the lower lying orbital with high s-character, while the higher lying p-orbital remains vacant.[83] This can be explained by the increasing effective nuclear charge going down the group, while simultaneously the size of the orbital increases, thus resulting in a decrease of electron-electron repulsion. This smaller electron repulsion and the reduced overlap between the corresponding s- and p orbitals, directly effects the tendency of hybridization. As a consequence, heavier carbene analogues favor the singlet ground state over the triplet state. That being said, the formation of a classical double bond between singlet heavier tetrylenes would result in repulsion of the lone pairs of electrons between both fragments. Instead, both fragments donate electron density from the filled s-type orbitals into the vacant p-orbitals, which results in a double donor-acceptor-type bond and as a consequence, trans-bent geometries are observed (Figure 11). According to the CGMT model, the degree of trans-bending can be correlated to the respective $\Delta E_{ST}$ values, smaller $\Delta E_{ST}$ give more planar double bonds, while large $\Delta E_{ST}$ values result in more trans-bent bonds. It should be noted that this model can be applied to heavier alkyne analogues in a same manner, giving rise to two doublet fragments which can form two similar donor-acceptor bonds and an additional $\sigma$-bond. However, the actual bond order of heavier alkynes, as well as heavier alkenes, highly depends on the element itself and furthermore on the additional substituent(s)[84], emphasizing that the model described here only relies on the valence-bonding theory, which of course simplifies the real situation. For instance, analyzing sub-van der Waals distances in molecular structures of **14a-c**, lead to the conclusion that also dispersion forces have a significant effect on the multiple bond stabilities.[85]

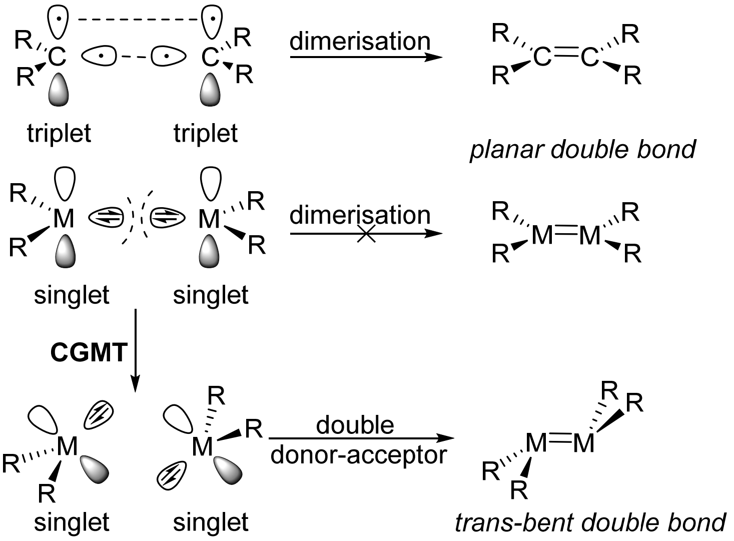

**Figure 11.** Formation of double bonds for alkenes and for heavier group 14 tetrylenes based on the CGMT model.

The seminal work by *Lappert*, kicked off the development of sterically extremely crowded substituents with tunable electronic properties which enabled the isolation of highly interesting low-valent main group compounds all over the p-block. Such ligand classes are for instance bulky amido-, silyl, alkyl or aryl groups. *West* and coworkers for instance, reported in 1981 on the first stable silicon (II) compound, namely disilene **18.**[86] Disilene **18** was synthesized via photolysis of its trisilane precursor **16**, giving the transient silylene intermediate **17** which dimerizes to give **18** (Scheme 4). The isolation of this compound was solely attributed to the highly steric nature of the used mesityl substituents, providing kinetic stabilization, as other less bulkier substituents only lead to polymerized or decomposed products. In the same year, also the first synthesis of molecules with a P=P double bond[87] and a Si=C double bond[88] were reported using a similar approach of kinetic stabilization.

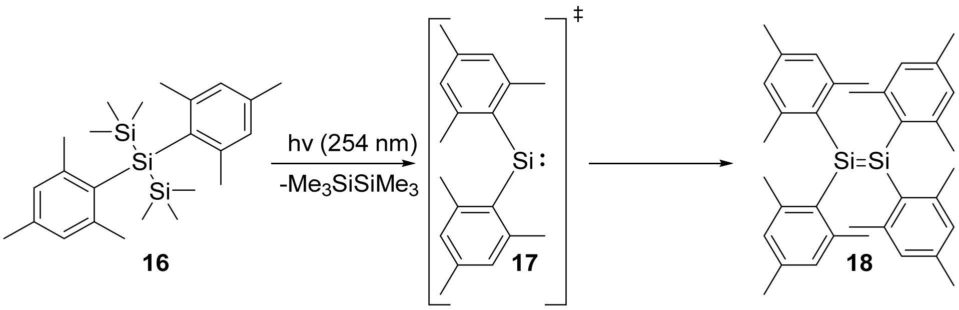

**Scheme 4.** The synthesis of the first isolable disilene **18** from precursor **16** via photolysis as reported by *West*.

As already mentioned, low-valent main group compounds can also be stabilized by a mix of thermodynamic and kinetic stabilization, for instance like in Lappert's stannylene **15a**. While its carbon-substituted congener does dimerize to give the respective distannene, the amido-substituted stannylene **15a** retains its structure also in the solid state, the same applies for the respective Ge and Pb compounds. With the concept of mixed thermodynamic and kinetic stabilization, a plethora of low-valent main group species could be isolated to date. This holds true not only for heavier group 14 compounds like carbenes, alkenes and alkynes, also different low-valent group 13 and group 15 compounds were isolated. Some landmark examples are given in Figure 12.

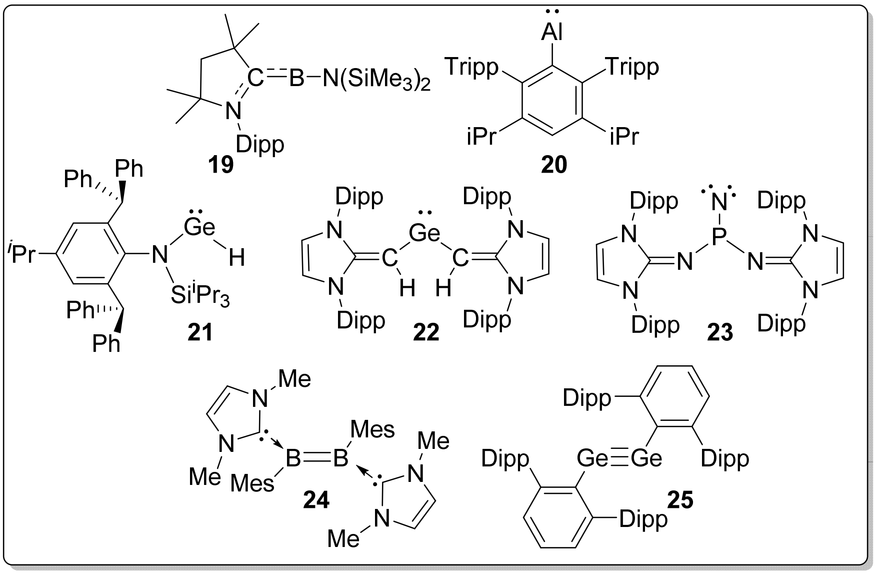

**Figure 12.** Landmark examples of low-valent main group species.

Hence, the use of extremely hindered substituents paved the way for the isolation of a variety of low valent main-group element species. Carbene analogues of group 13 such as the CAAC-stabilized borylene **19** (*Bertrand et al.*)[89] or the NHC stabilized diborene **24** reported by *Braunschweig*[90], as well as the only recently published monocoordinated Al(I)-species **20** by *Power*[91], are excellent examples of how even highly electron-deficient species can be stabilized by choosing the 'right' substituent. The latter exploits the extreme bulkiness of *ortho*-terphenyl groups, which are substituted by sterically demanding alkyl-groups in the *meta*-position, a common substituent class introduced by *Power*. The use of terphenyl-substituents enabled the isolation of several heavier p-block multiple bonded species both, homo-and heterobimetallic[92], with germyne **25** being the first example of a heavier group 14 alkyne.[93] Further, *Bertrand* reported on the isolation of the first stable nitrene **23**[94] by exploiting strongly $\pi$-donating N-Heterocyclic-Iminato (NHI) substituents. Similarly, N-Heterocyclic-Olefins (NHOs) are suitable for the isolation of tetrylenes such as germylene **22**, as shown by *Rivard.*[95] *Jones* also showed that by increasing the steric bulk of amido substituents, the observation of a monomeric germylene-hydride (**21**) in solution is possible.[96] These landmark examples demonstrate the importance of ligand design for the isolation of stable low-valent main group species. In the next section, the ability of selected examples with focus on group 14 tetrylenes to mimic transition-metal like behavior will be discussed briefly.

### Tetrylenes as transition-metal mimics

In 2005, the group of *Power* reported on the synthesis of digermyne **25** and its ability to activate dihydrogen at room-temperature and low pressures (1 bar) without any catalysts, affording a mixture of mono-, di- and tri-hydrogenated products.[93] This transformation is remarkable, since it was long believed that only transition-metals are capable of activating important small molecules like $H_2$. This seminal report kicked off the field of small molecule activation by simple main-group compounds. Several other main-group systems which possess donor/acceptor type frontier orbitals with modest energy gaps were reported to activate $H_2$ such as alkyl amino carbenes **26/27**[97] or FLPs **28**[98] (Scheme 5). Additionally, $NH_3$ is nucleophilically activated by **26/27**, which is remarkable because even TM are normally unable to perform the activation of ammonia, caused by the formation of Werner-type donor-complexes. Small molecule activation is furthermore not limited to main group systems with closed shell configuration. Only recently, *Ghadwal* and coworkers reported on singlet Ge(I) and Sn(I) diradicals that activate $H_2$ under ambient conditions.[99]

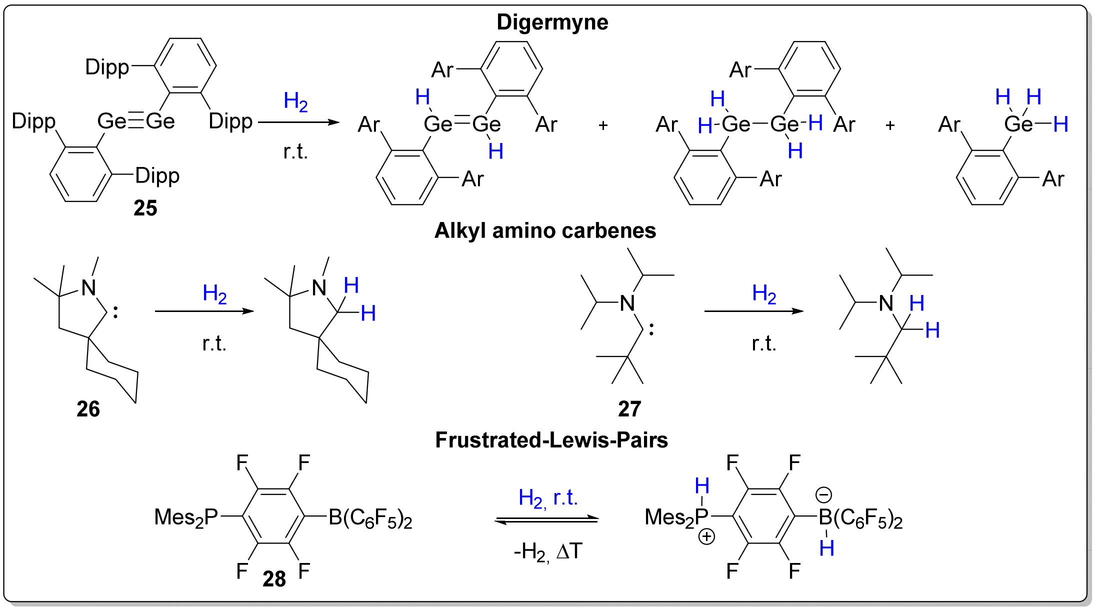

**Scheme 5.** Ability of different main-group compounds to activate dihydrogen at mild conditions.

Heavier carbene analogues have shown remarkable reactivities in the activation of catalytically relevant small molecules, especially acyclic tetrylenes. In 2012 *Power* et al. reported on the isolation of the first acyclic silylene, stabilized by two bulky thiolato-substituents.[100] **30** was synthesized via reduction of its dibrominated Si(IV) precursor **29** with *Jones* Mg(I) reagent (Scheme 6).[101] However, **30** turned out to not activate dihydrogen, which was attributed to the relatively wide HOMO-LUMO and $\Delta E_{ST}$ gaps. This might be caused by the electronegative nature of the thiolato-ligands which increases the energy separation of the silicon lone pair and the vacant p-orbital, hence making a synergic interaction between the frontier orbitals of $H_2$ and **30** unlikely to occur. However, **30** turned out to reversibly bind ethylene at room-temperature, giving siliranes **31**.[102] This observation is remarkable since the ability of alkyne complexation was almost entirely the property of transition-metals and which is often an important step in catalytical processes.

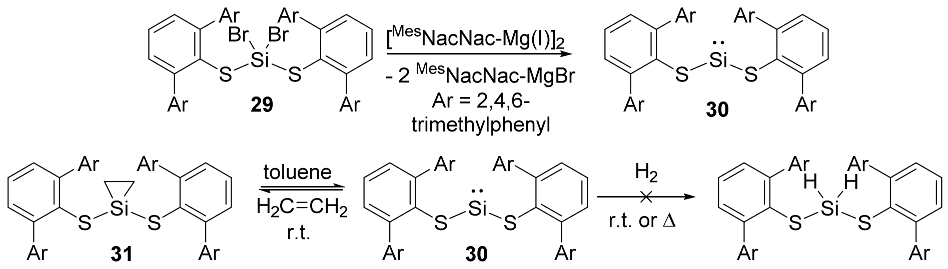

**Scheme 6.** Synthesis of the first acyclic silylene **30** via reduction of its dibrominated precursor **29** and the reactivity of **30** towards ethylene and $H_2$.

In the same year, *Aldridge* et al. reported on the isolation of an unsymmetric substituted acyclic silylene **35**, bearing a bulky $\pi$–donating amido and a strongly electropositive boryl-substituent (Scheme 7).[103] **35** was synthesized in a one-step procedure from tribromosilane precursor **32** and two equivalents of boryllithium **36**. In this reaction boryllithium **36** acts not only as a nucleophile but also as a reducing agent. The reaction is believed to procced first via a bromine/lithium exchange, affording a transient bromosilylenoid species **33** and the boryl bromide as a side product. Subsequently, nucleophilic attack of the second boryllithium equivalent on the Si(II) center gives another silylenoid species **34** which upon elimination of LiBr, yields silylene **35**.

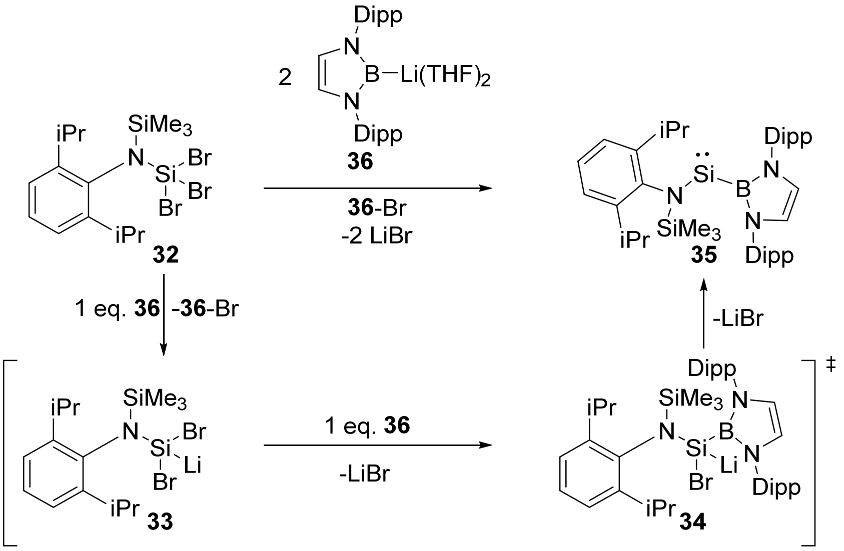

**Scheme 7.** Synthesis of acyclic boryl-silylene **35** from tribromosilane **32**.

This special ligand combination proved to successfully decrease the ΔEST, resulting in narrow frontier-orbital separation which could allow a fine interplay between the Si(II) and Si(IV) oxidation state, thus enabling selective activation of strong enthalpic bonds. Indeed, **35** was able to activate $H_2$ even at 0 °C giving dihydrosilane **37**. In contrast to alkyl amino carbenes which activate dihydrogen via a more nucleophilic pathway[97], DFT calculations revealed that silylene **35** approaches $H_2$ in a side-on manner, which is reminiscent to transition-metals. This was mainly attributed to the true electrophilic nature of silylene **35**. In addition to the activation of dihydrogen, **35** showed to react with $CO_2$ under abstraction of one oxygen atom leading to the liberation of CO and the oxidized species **38**. Additionally, when a solution of **35** is exposed to an excess of CO gas, the selective formation of **39** is observed, which is expected to proceed via reductive coupling of CO to give a ethynediolate anion that subsequently inserts into the Si–B bond (Scheme 8).[104] The reductive coupling of CO is known for transition-metal systems[105], however this was the first example of a p-block element performing this reaction.

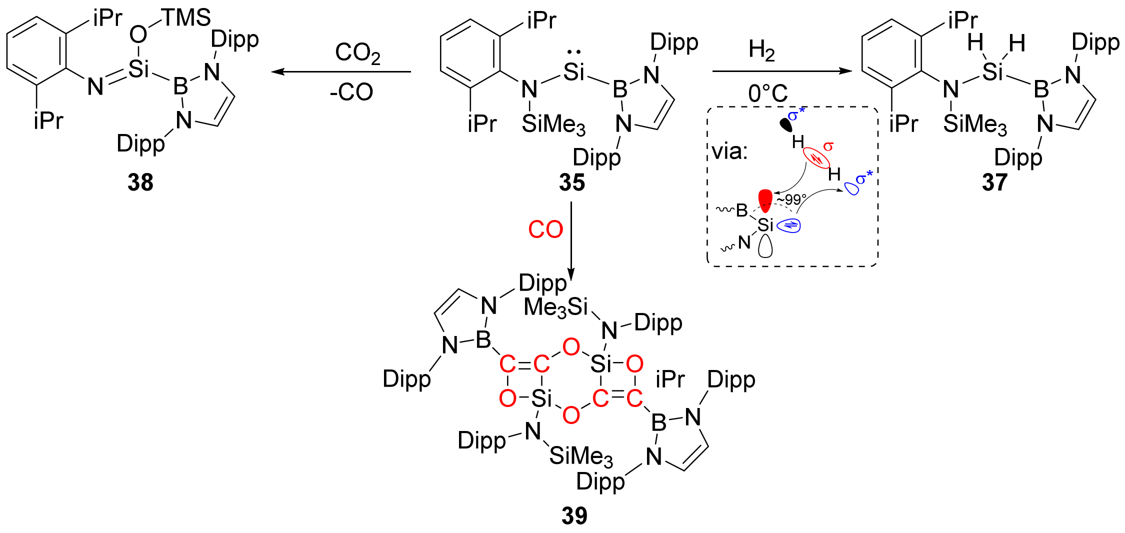

**Scheme 8.** Reactivity of **35** towards small molecules.

The synthetic approach, which enabled to access **35**, was shortly later used to give silylsilylene **40** with potassium hypersilanide KSi(SiMe$_3$)$_3$ as a nucleophile and the reducing agent.[106] Silylsilylene **40** showed a similar reactivity towards H$_2$ as its boryl substituted congener, strongly underlying that the combination of a $\pi$–donating substituent and an intrinsically electropositive substituent gives access to highly reactive silylenes. **40** was later reported by *Inoue* and *Rieger* to enable not only the activation of ethylene to afford siliranes (**42**), but also to perform the first reported migratory insertion (**43**) of an olefin into the Si–Si bond (**44**) accessed via a low valent silicon species (Scheme 9).[107] This clearly emphasizes the potential of acyclic silylenes to mimic typical reactions which are usually observed only with transition-metals.

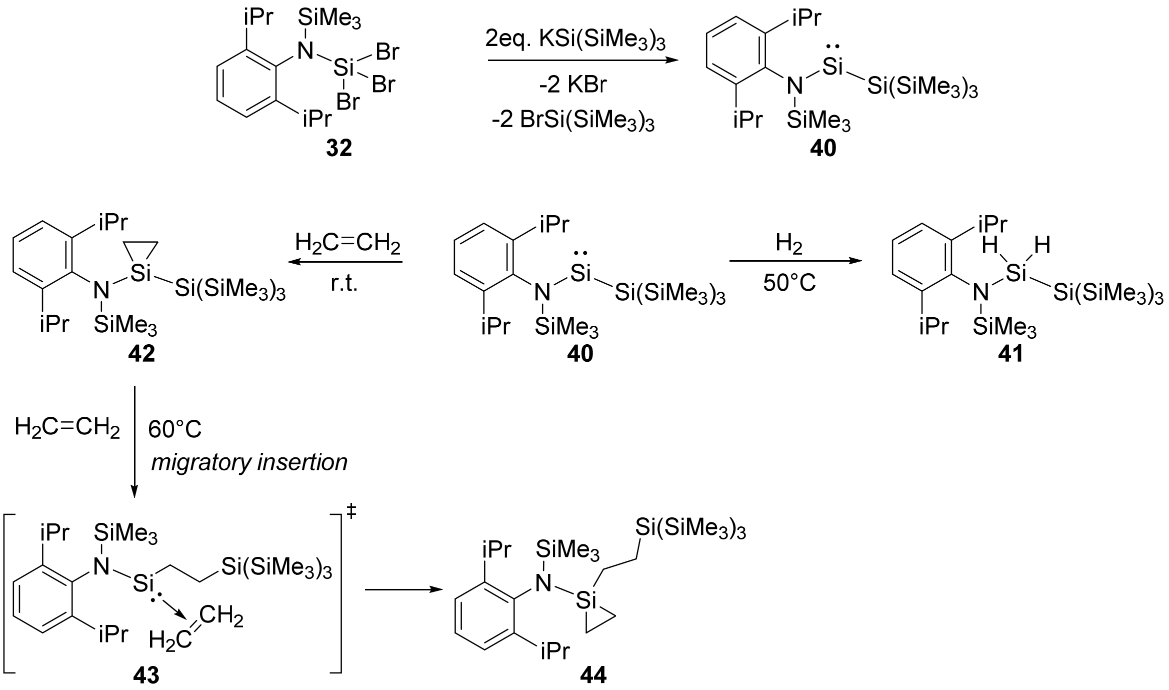

**Scheme 9.** Synthesis and reactivity of silylsilylene **40**.

Following the same synthetic approach, the groups of *Inoue* and *Jones* reported on the isolation of Iminosilylsilylene **46**[108] and Vinyl(silyl)silylene **47**[109], respectively (Scheme 10).

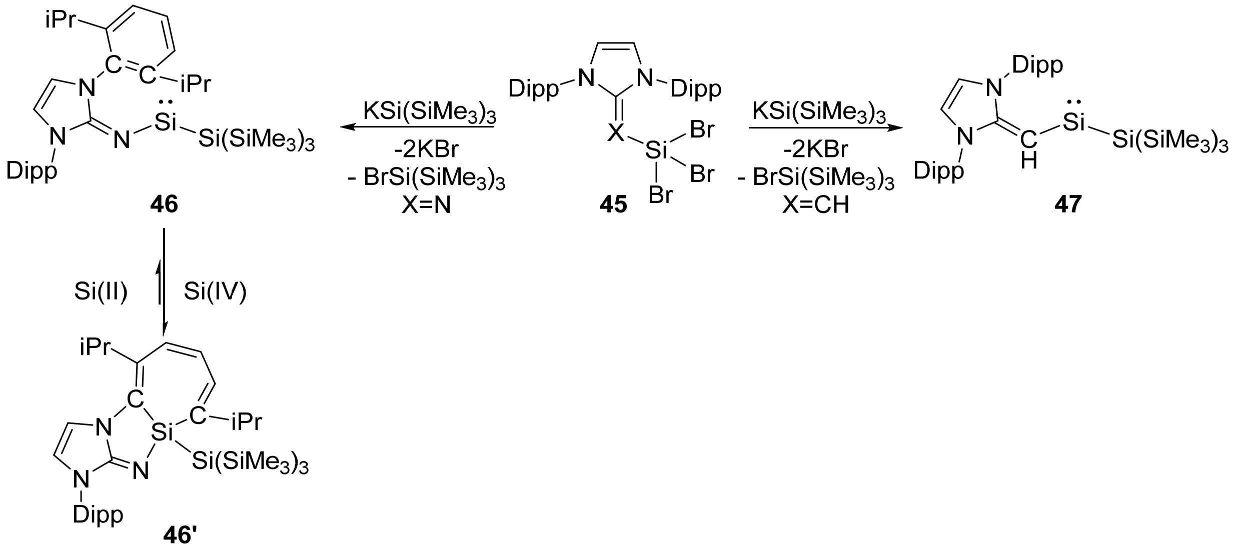

**Scheme 10.** Synthesis of Silylsilylenes **46/46'** and **47** from NHI and NHO-derived precursor **45**, respectively.

Iminosilylsilylene **46** was reported to reversibly insert into the C–C bond of its ligand framework, giving silepin **46'**, which is is a rare example of a reversible redox-process, involving a low-valent main-group species going from Si(II) to Si(IV) and back (Scheme 11). This oxidative addition / reductive elimination process is reminiscent to transition-metal-catalyzed reaction steps and thus shows that when put into the right environment, main group compounds can mimic their behavior. Although the equilibrium heavily lies on the silepin site at room temperature, further transformation revealed its reactivity as silylene equivalent **46**. As such, **46'** reacts readily with $H_2$ to give the respective dihalosilane **48** and furthermore also activates $CO_2$ to give silicon carbonate **49**. Similar to **30**, it also reacts with ethylene at room temperature to give silirane **50**, however not in a reversible process. Also, the reaction of **46'** with $N_2O$ delivered one of the first examples of a crystalline silanone **51**.[110]

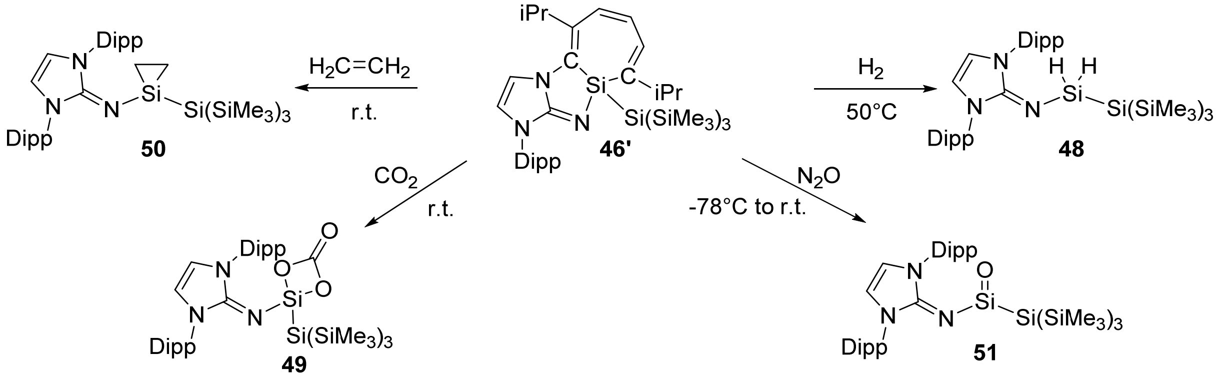

**Scheme 11.** Reactivity of silylene equivalent **46'** towards small molecules.

Vinyl(silyl)silylene **47** showed to be able to activate other strong enthalpic bonds like the B-H bond of pinacolborane giving **52**, the Si–H bond of trichlorosilane (**53**) and even the P–P bond in white phosphorus (**54**) (Scheme 12).

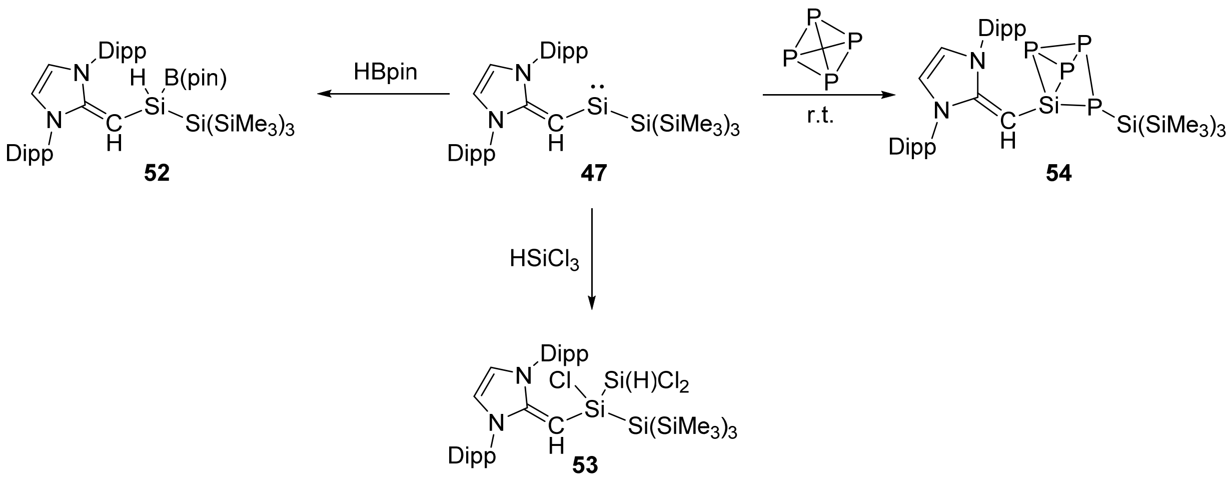

**Scheme 12.** Reactivity of Silylsilylene **47** towards B–H, Si–Cl and P–P bonds.

Similarly, germylenes and stannylenes based on bulky terphenyl, boryl, amido or imino-substituents were also highly efficient towards the activation of small molecules. For instance, *Power* et al. reported the synthesis of simple diaryl-germylenes (**55a-b**)[111], based on bulky terphenyl substituents (Scheme 13). These germylenes are capable of activating dihydrogen at elevated temperatures (70°C), depending on the steric bulk, giving either monoaryl-substituted (R = Dipp, **56a**) or diaryl-substituted germanes (R = Mes, **56b**).

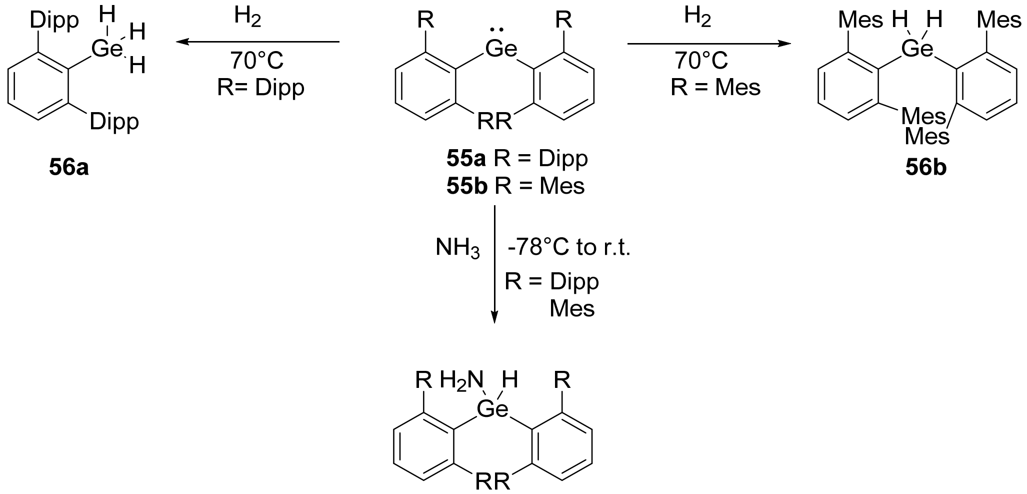

**Scheme 13.** Reactivity of germylenes **55a-b** towards $NH_3$ and $H_2$.

In addition, both germylenes were also able to oxidatively add ammonia to the germanium center, giving diaryl-amino-germanes **57a-b**, under very mild conditions. In the case of the corresponding stannylenes (**58a-b**)[112] however, the reaction with $H_2$ and $NH_3$ did not give the expected oxidative addition products (Scheme 14). While the stannylene (**58b**) with mesityl-groups attached to the terphenylring does not react with dihydrogen, its bulkier analogue with diisopropylphenyl-groups (**58a**) does activate $H_2$, furnishing a symmetric -Sn(II)(μ-H)$_2$Sn(II)- dimer (**59**) and one equivalent of the protonated parent-arene as the products. DFT studies indicate that this reaction proceeds via the expected Sn(IV) oxidative addition product with subsequent reductive elimination, promoted by the extreme steric bulk. The reactivity of **58a** towards $H_2$ was attributed to its extremely wide C–Sn–C angle of 117.6°, which results in a more triplet state reactivity. That also explains why its slightly less bulky analogue **58b** did not react with $H_2$. However, both stannylenes were able to cleave the N–H bond of ammonia giving similar bridged dimers **60a-b**.

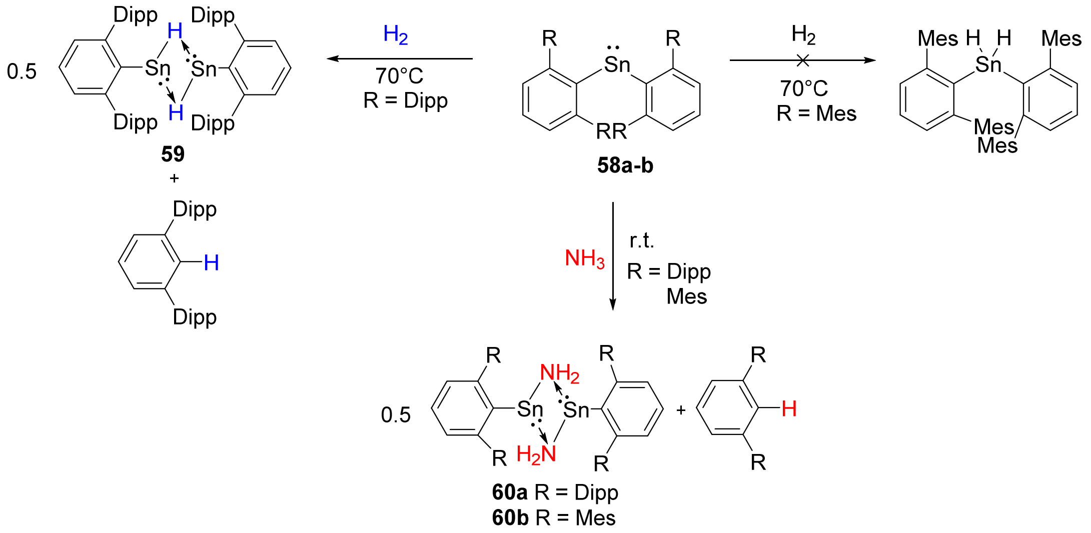
0.5
Dipp
Dipp
H
Sn
Sn
H
59
+
H
H2
70°C
R = Dipp
R
R
Sn
RR
58a-b
H2
70°C
R = Mes
Mes H H Mes
Sn
Mes
Mes
NH3
r.t.
R = Dipp
Mes
NH2
H2N
60a R = Dipp
60b R = Mes

**Scheme 14.** Reactivity of stannylenes **58a-b** towards $H_2$ and $NH_3$.

*Aldridge* et al. recently published an extensive study on how the substitution pattern of acyclic germylenes influences their reactivity towards small molecules.[113] Similar as already observed for acyclic silylenes, with incorporation of strongly $\sigma$-donating substituents like hypersilyl (**61**) or boryl (**62**), a dramatic increase in reactivity is observed (Scheme 15). As such, germylene **61** reacts with dihydrogen and ammonia under mild conditions giving the oxidative additions products (**63a-b**), while **62** undergoes a rare intramolecular C–H– bond reaction with its ligand framework (**64**) at room temperature. This reactivity is consistent with its extremely narrow HOMO-LUMO energy gap (119 kJ/mol).[113]

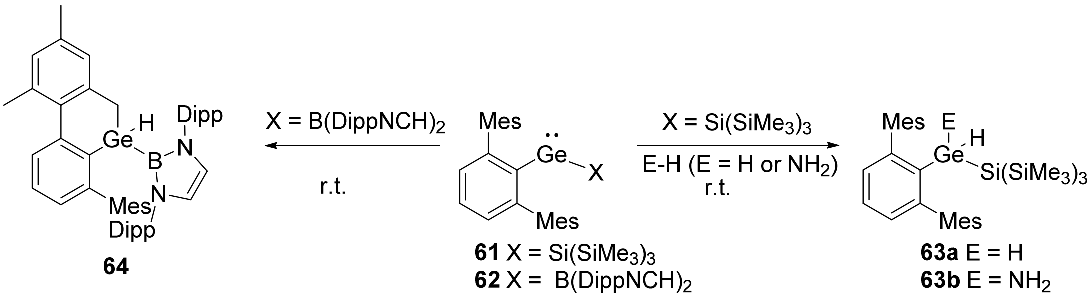
Ge
H
Dipp
B
N
N
Mes
Dipp
64
X = B(DippNCH)2
r.t.
Mes
Ge
X
Mes
61 X = Si(SiMe3)3
62 X = B(DippNCH)2
X = Si(SiMe3)3
E-H (E = H or NH2)
r.t.
Mes E
Ge
H
Si(SiMe3)3
Mes
63a E = H
63b E = NH2

**Scheme 15.** Reactivity of aryl-germylenes **61/62**.

The examples discussed above impressively show the ability of heavier tetrylenes to mimic transition-metal like behavior such as oxidative additions of E-H bonds (E = H, N, B etc.), reversible binding of alkenes such as ethylene, migratory insertion reactions or the activation of simple small molecules like CO and $CO_2$. Low-valent main-group species are capable of performing crucial reaction steps that are normally only found in transition-metal based homogeneous catalysis cycles and thus should be able to act as molecular catalysts. Indeed, first reports on the use of low-valent heavier group 14 compounds as molecular catalysis exist. For instance, *Jones* et al reported on catalytic hydroboration of ketones and aldehydes[96], as well as the reduction of $CO_2$[114], with Ge(II) (**65a**) and Sn(II)-hydrides (**65b**) (Figure 13). With TOFs of up to 13300 $h^{-1}$ and 1188 $h^{-1}$, respectively, these main-group metal catalyzed systems can definitely compete with their transition-metal rivals. From a mechanistic point of view, the catalytic hydroboration is believed to proceed via two $\sigma$-bond metathesis steps. In the first one, the hydridic hydrogen atom of **65** is transferred to the substrate, giving an oxy-tetrylene intermediate (**66**). This intermediate is prone to another $\sigma$-bond metathesis where the hydrogen atom from HBpin is transferred to the low-valent metal center, while at the same time a boron-oxygen bond is formed, ultimately leading to the product and giving back the hydrido-tetrylene.

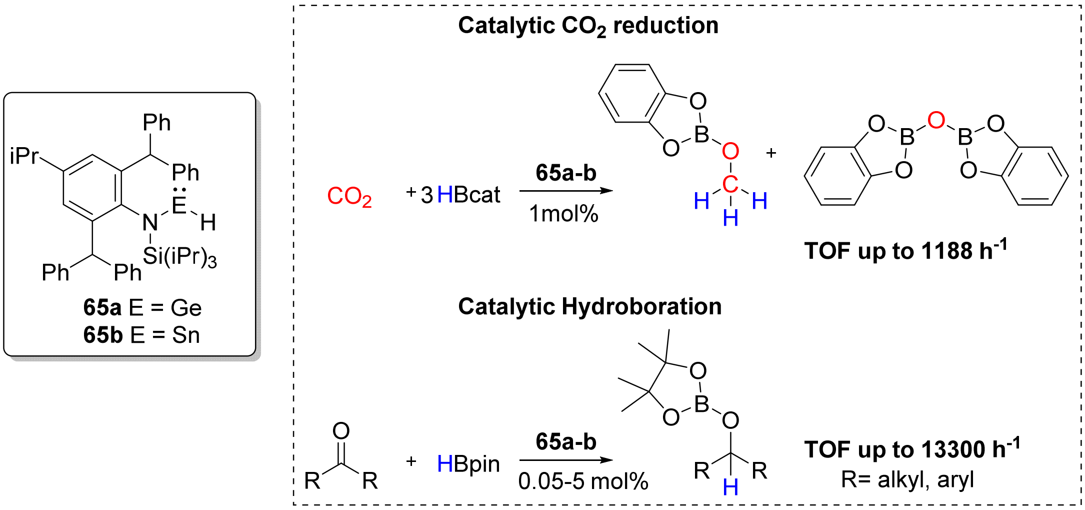
iPr
Ph
Ph
N
E
H
Si(iPr)3
Ph
Ph
65a E = Ge
65b E = Sn
Catalytic CO2 reduction
CO2
+ 3 HBcat
65a-b
1mol%
+
TOF up to 1188 h-1
Catalytic Hydroboration
+ HBpin
65a-b
0.05-5 mol%
TOF up to 13300 h-1
R= alkyl, aryl

Catalytic cycle for the hydroboration proposed by DFT

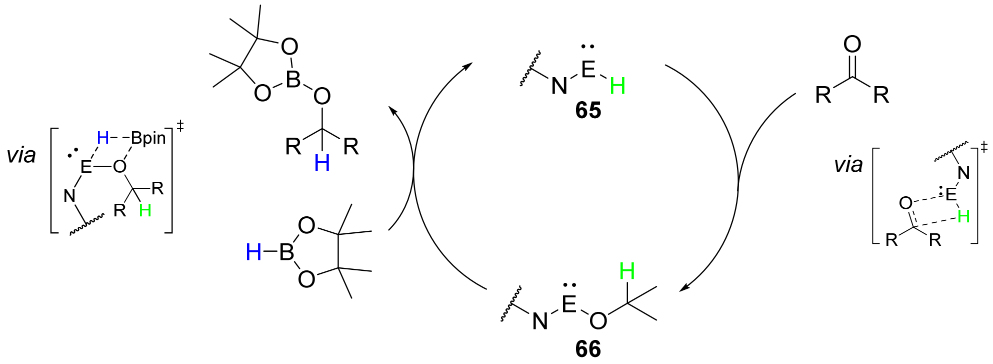
65
66
via
H- -Bpin
E—O
N
R
R
H
‡
H–B
via
N
E
O
H
R
R
‡

**Figure 13.** Catalytic $CO_2$ reduction and hydroboration with low-valent tetrylene hydrides **65a-b** (top) and the proposed catalytic cycle for the **65**-catalyzed hydroboration (bottom).

Although still in its infancy, these results clearly raise the hope for homogeneous catalysis based on fairly abundant, non-toxic and cheap main-group compounds. However, further investigations especially by means of alternative ligand classes are necessary to find novel reactivity patterns and bonding modes. In this regard, metalated ylides as carbon-based $\pi$- and $\sigma$-donor ligands have recently gained considerable attention for the stabilization of low-valent species and will be discussed in detail in the next sections.

## 1.5 Ylides - a unique carbon-based ligand class

### 1.5.1 Development of metalated ylides

Since their first synthesis more than a century ago[115], ylides have evolved from laboratory curiosities to versatile reagents in synthetic transformations.[116] An ylide is described as an inner salt (Figure 14), where a negatively charged (normally carbon) atom is attached to a positively charged heteroatom, with both atoms remaining their octet and thus giving a 1,2 dipolar structural motif (**A**). Usually, when speaking about ylides, phosphonium based phosphorus ylides are meant. However, a broad range of ylides with e.g. sulfonium[117]-, ammonium[118]-, iminosulfonium[119]-, arsenium[120]- or imidazolium[121] groups are also known. Because of the negative charge located at the carbon atom, ylides are in general highly nucleophilic species and hence have a diverse chemistry. Above all, the reaction of phosphorus ylides with carbonyl compounds yielding olefins with a new C=C bond, had an outstanding impact on organic chemistry. The so-called *Wittig* reaction, named after its explorer *Georg Wittig*, is used in numerous synthesis protocols as a standard method for incorporating a new C=C bond and has also found various applications in industrial processes.[122] With this outstanding scientific contribution, *Georg Wittig* was awarded the Nobel prize in chemistry. Phosphorus ylides can formally also be described by a non-polar 'ylene' structure (**B**), with a P=C double bond. It was believed that the phosphorus atom with its empty d-orbitals interacts with the lone pair of electrons at the carbanionic center hence enabling $\pi$ bonding and thus forming a double bond. However, this hypothesis could be falsified by theoretical calculations, revealing that the empty d-orbitals of the phosphorus atom lie too high in energy to participate in any significant bonding interactions.[123] Instead, a highly polarized bond with strong coulomb interactions between the phosphonium moiety and the carbanionic center is postulated, which fits very well to theoretical calculations.

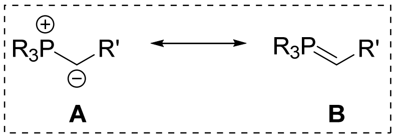

**Figure 14.** Possible resonance structures of phosphonium ylides with the ylidic form **A** and the ylene form **B**.

Phosphorus ylides are usually synthesized by deprotonation of their corresponding phosphonium salts (Scheme 16), the latter being accessible via nucleophilic substitution of e.g. organic halides with phosphines.[124]

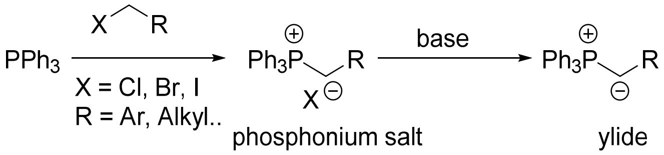

**Scheme 16.** Common synthesis strategy for phosphorus ylides via formation of a phosphonium salt from the nucleophilic attack of a tertiary phosphine (here $PPh_3$) at an appropriate electrophile (e.g. alkyl halide) and subsequent deprotonation yielding an ylide.

Due to the stabilizing effect of the phosphonium group, phosphonium salts are in general most acidic in alpha position to the phosphorus atom. Depending on the substituents attached to the carbon atom, mild to strong bases are necessary for deprotonation and thus ylides are classified as either non-stabilized (EDG, e.g. alkyl group like in **67**), semi-stabilized (aryl or alkenyl, **68**) or stabilized (EWG, e.g.

carboxyl groups, **69**) (Figure 15), with $pK_a$ values of the parent phosphonium salts ranging from 4 to 26 (DMSO scale).[125]

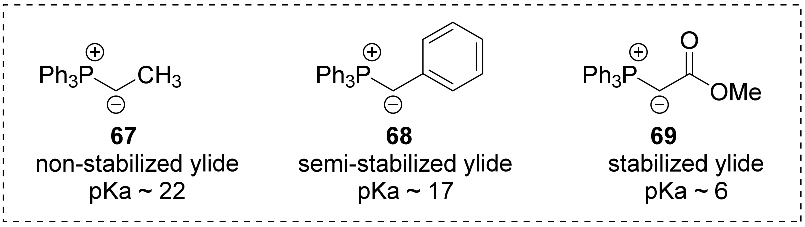

**Figure 15.** Examples for different stabilization degrees and associated p*Ka* values (DMSO scale) found for ylides.

The nucleophilicity and thus reactivity of an ylide is directly correlated with its degree of stabilization. Usually, highly reactive non-stabilized ylides are not isolated but used *in-situ* for further transformation caused by the lability of these species. For instance, compound **67** is not stable under ambient conditions, instantaneously getting hydrolyzed by traces of water. Ylide **69** on the other hand, can be isolated as a moisture- and air-stable solid. In general, one can think about a further deprotonation of the ylidic carbon atom, giving rise to an even more reactive species, the so called metalated ylides or yldiides (Scheme 17). Metalated ylides can be regarded as mono-anionic species in which the central carbon atom bears two lone pairs of electrons, one of $\pi$- and one of $\sigma$-symmetry. In theory, yldiides should hence be able to act as both, $\sigma$– and $\pi$– donors, making them to promising reagents for stabilizing highly reactive, electron-deficient species

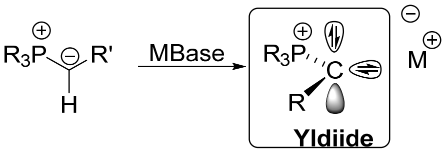

**Scheme 17.** Deprotonation of an ylide with a strong metal base to yield a monoanionic yldiide, bearing two lone pairs of electrons.

The first report of a metalated ylide was given in 1966 by *Schlosser* et al. who investigated ligand exchange reactions at pentaphenyl phosphorane **70** (Scheme 18).[126] Treatment of **70** at -78°C with excess of *n*BuLi and subsequent quenching with DBr yielded the geminal di-deuterated phosphonium salt **70-D₂** in a yield of 14%.

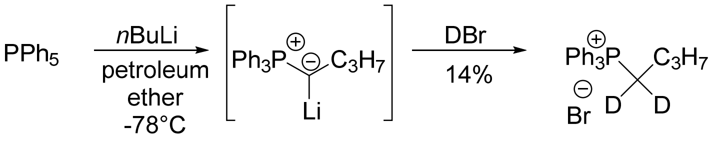

**70** **70-Li** **70-D₂**

**Scheme 18.** Preparation of **70-Li** via reaction of *n*BuLi with $PPh_5$ at -78°C and subsequent quenching with DBr yielding phosphonium salt **70**-$D_2$ as reported by *Schlosser* et al.**[126]**

The authors concluded that a metalated intermediate, namely the yldiide **70-Li** must have been formed. In 1972 *Strating* et al. reported on the reaction of the sulfonyl-substituted ylide **71** with *n*BuLi to form the metalated ylide **71-Li**, which was used *in-situ* in the reaction with ethyl chloroformate to form ylide **72** (Scheme 19).[127] Notably, the parent ylide **71** did not react with ethyl chloroformate, giving further evidence for the existence of **71-Li**.

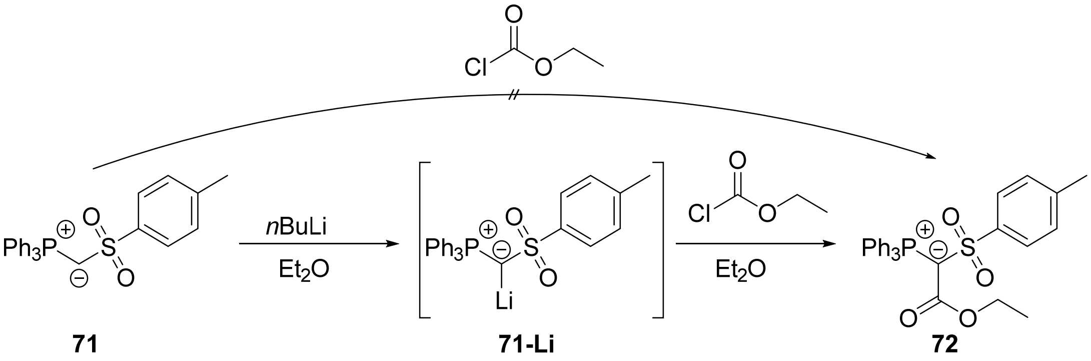

**Scheme 19.** Reported metalation of **71** with *n*BuLi forming **71-Li** and subsequent quenching with ethylchloro formate yielding **72**. No activity was observed when **71** was treated with the chloro formate without *n*BuLi.

*Corey* and *Kang* reported in 1982 about the synthesis of α-lithiomethylene triphenylphosphorane (**73-Li**) by deprotonation of methylen triphenylphosphorane (**73**) with *t*BuLi at -40°C (Scheme 20).[128] Again, the existence of this species was postulated only due to the enhanced reactivity in *Wittig* type reactions e.g. with sterically hindered ketones which did not react with the protonated precursor **73**. Contrary to this report, *Schlosser* et al. claimed that the species reported by *Corey* was not **73-Li** but more probably the *ortho*-metalated ylide **73-*o*Li,** which could also explain the observed enhanced activity in *Wittig* reactions.[129] This hypothesis could be further proved by reactivity studies.[130] When the intermediate species is treated with methyl iodide, ethyl-dipheynl-*o*-tolyl phosphonium iodide **74** is formed in good yield, giving direct evidence for the existence of **73-*o*Li**. However, **73-Li** could be conveniently prepared by the reaction of the brominated phosphonium salt **73-HBr** with phenyllithium forming ylide **73-Br**, followed by metal/halogen exchange with *t*BuLi. Moreover, the formation of **73-Li** could be also be proved by detail assignment of $^1$H-NMR shifts and a distinct high field shift of the $^{31}$P-NMR signal, compared with the starting material **73** and **73-*o*Li**, indicating a different electronic environment around the phosphorus atom. The deprotonation of **73** with *t*-BuLi was further repeated by *Sundermayer* et al. who could prove the observations made by *Schlosser* and even give evidence, that during the formation of **73*o*-Li**, no *α*-metalated ylide is present at all.[131]

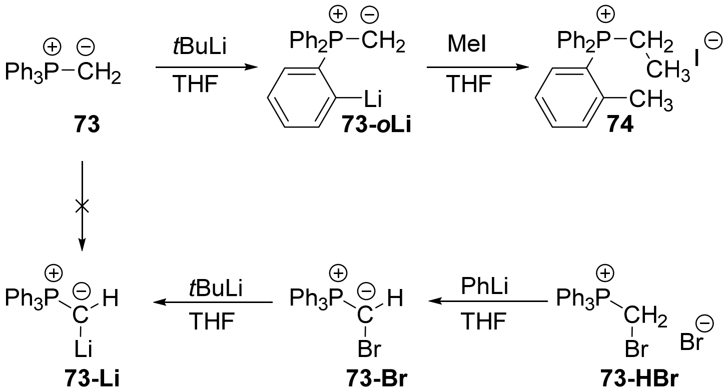

**Scheme 20.** Synthesis of **6-*o*Li** via ortho-metalation of **73** with *t*BuLi and subsequent methylation with MeI to **74** as reported by *Schlosser* (top). *In-situ* preparation of **73-Li** via ylide formation (**73-Br**) from **73-HBr** and metal/halogen exchange with *t*BuLi (bottom).

Again, the metalated ylide **73-Li** was not stable and decomposed upon warming to room temperature. The fact that no yldiide could be isolated via deprotonation of non- or semi-stabilized ylides, shows that the metalated congeners require extra stabilization to enable an isolation at room temperature. Indeed, *Bestmann* and *Schmidt* recognized this issue and reported in 1987 about the first isolation of a metalated ylide (Scheme 21). With the strong electron-withdrawing cyano group in the backbone, metalation of ylide **75** was feasible with $NaN(SiMe_3)_2$ as the base, giving **75-Na** as a room temperature stable, highly moisture- and air-sensitive yellow solid.[132] The electron-withdrawing cyano-substituent sufficiently stabilizes the high negative charge on the carbon atom, resulting in an increased stability compared to simple aryl- or alkyl groups, hence making the yldiide isolable at room temperature.

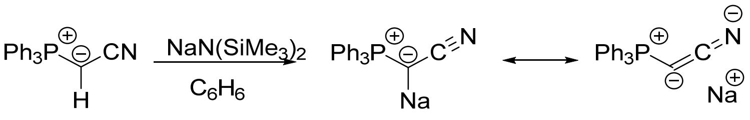

**75** **75-Na** **75-Na'**

**Scheme 21.** Synthesis of the first isolable metalated ylide **75-Na** by deprotonation of **75** with NaHMDS in benzene.

However, yldiide **75-Na** can also be described with a ketenimine-like resonance structure **75-Na'**, indicating a further stabilization effect by reducing the bond order of the C-N bond and thus shifting electron-density from the ylidic carbon atom towards the nitrogen atom of the cyano-group. The existence of such a mesomeric resonance structure could be further underlined by IR-spectroscopic analysis of its $\nu_{CN}$ stretching frequency. The IR band of the nitrile group in **75-Na** ($\nu_{CN}$= 2000 $cm^{-1}$) is strongly shifted towards smaller wavenumbers compared to its protonated analogue **75** ($\nu_{CN}$= 2130 $cm^{-1}$).[132] Deprotonation of ylides bearing highly stabilizing groups was already reported in the 1970s. *Bestmann* and coworkers showed that triphenylphosphonium ylides with (thio)carboxy-substituents (**76 a-b**) can be deprotonated by strong metal bases, however, not leading to isolable metalated ylides. Instead, a rearrangement and subsequent elimination of the metal alkoxide as a good leaving group along with triphenylphosphoraneylidene ketene (**77a**) or the corresponding thio-analogue (**77b**) is observed.[133] With ketones as stabilizing groups (**78**), selective deprotonation of the ylidic carbon atom seems to be possible, giving metalated ylides (**78-Li**) as reported by *Broquet* and coworkers (Scheme 22).[134] However, this type of compounds could also be described as ylidic enolates (**78-Li'**), but since no spectroscopic data nor reactivity data was provided, no structural assignment could be made.

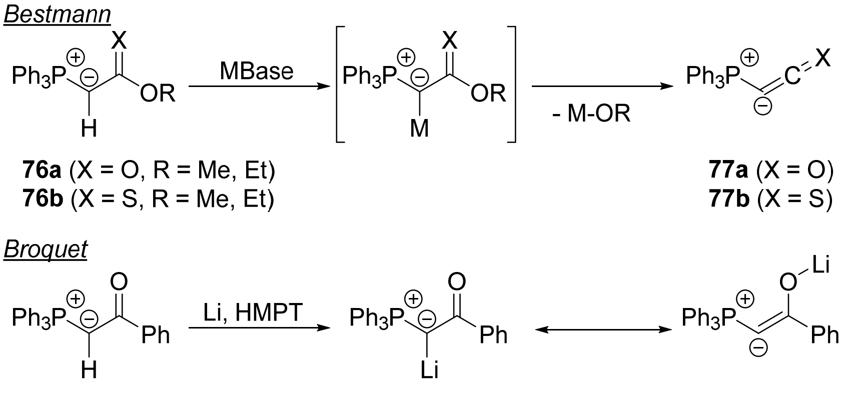

**76a** (X = O, R = Me, Et)
**76b** (X = S, R = Me, Et)

**77a** (X = O)
**77b** (X = S)

**78** **78-Li** **78-Li'**

**Scheme 22.** Preparation of triphenyphosphoraneylidene ketenes (**77a** and **77b**) from the deprotonation of carboxy-substituted ylides **(76a**,**76b**) via a transient metalated yide (top). Synthesis of metalated ylides or ylidic enolates (**78-Li/78-Li'**) from the protonated precursor **78** and Li in HMPT (bottom).

### 1.5.2 Structure and bonding motifs in metalated ylides

The first structural evidence for the synthesis of a metalated ylide was reported in 1997 by *Niecke* et al. with the isolation of lithium phosphorane ylides **79(a-b)-Li** by deprotonation of the corresponding protonated precursors **79(a-b)** with *n*-butyllithium (Scheme 23).[135] XRD analyses revealed monomeric structures with direct lithium-carbon contacts and short C–P bonds of 1.632(5) Å for **79a** and 1.624(5) Å for **79b**, respectively, confirming the deprotonation in α-position to the phosphorus atom and furthermore, corroborating with a partial-double bond or increased Coulomb interactions due to the presence of an additional negative charge on the ylidic carbon atom. However, since these compounds do not exhibit a four-coordinate phosphorus atom, they can also be regarded as metalated phosphalkenes (**79(a-b)-Li'**). It was *Bertrand* who reported on the first fully characterized α-metalated phosphonium ylide.[136] **80-Li** is the only yldiide which was synthesized via a unique 1,2-addition of *n*-butyllithium to phosphinocarbene **80**. **80-Li** features also a direct C–Li contact and a short C–P bond length of 1.636 Å, which is comparable to that observed for **78**. Additionally, a short distance of 1.755(10) Å is observed for the C–Si bond, which could be explained by strong negative hyperconjugation effects.

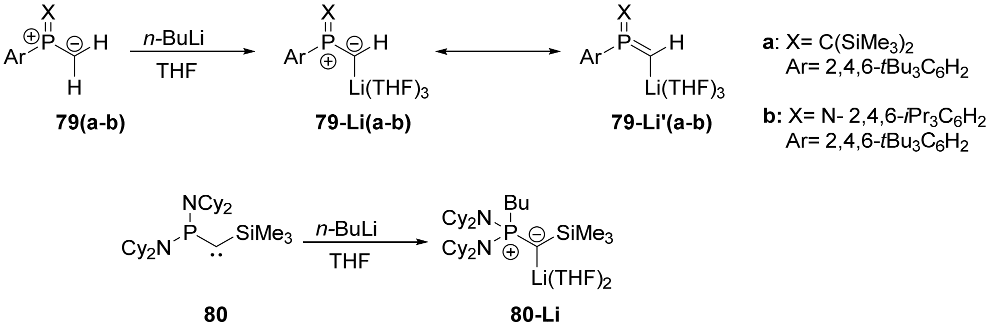

**Scheme 23.** Preparation of metalated ylides / phosphaalkenes (**79-Li/79-Li'**) by deprotonation of **79** with *n*BuLi as reported by *Niecke* (top) and 1,2-addition of *n*BuLi to **80** giving the first phosphonium yldiide **80-Li** reported by *Bertrand* (bottom).

*Gessner* et al. only recently confirmed the before mentioned existence for the metalated ylides **71-M** (M=Li, Na, K)[137] and **75-M** (M=Li, Na, K)[138] by XRD and furthermore, optimized their reaction conditions, leading to the first isolation of metalated ylides in gram scale, which opened up new ways for applications (*vide infra*). In 2007, *Baceiredo* et al. reported on the isolation of a sulfinyl substituted lithium-yldiide (**81-Li**)[139], with a diamino functionalized phosphonium group, completing the number of structurally characterized metalated ylides known till the writing of this thesis, which are summed up in Figure 16.

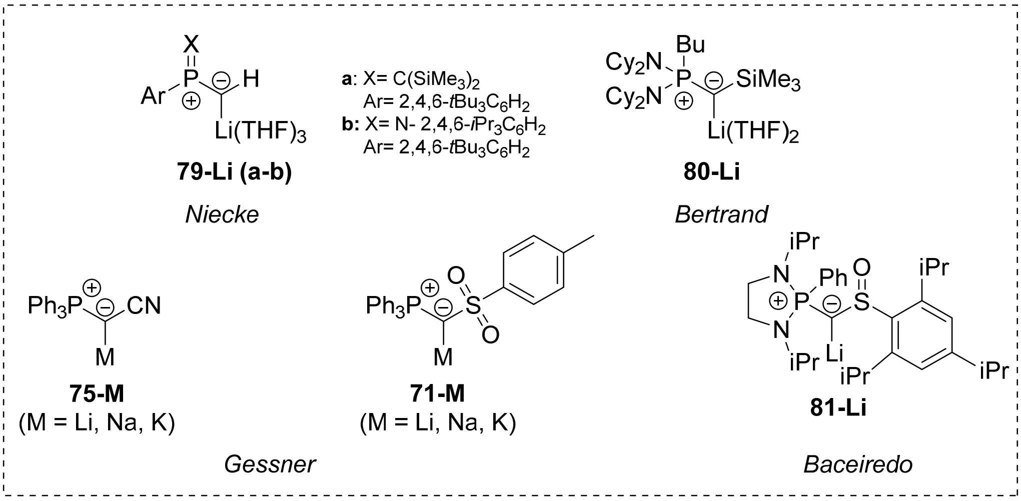
X
Ar
P
H
Li(THF)3
a: X= C(SiMe3)2
Ar= 2,4,6-tBu3C6H2
b: X= N- 2,4,6-iPr3C6H2
Ar= 2,4,6-tBu3C6H2
79-Li (a-b)
Niecke
Bu
Cy2N
Cy2N
P
SiMe3
Li(THF)2
80-Li
Bertrand
Ph3P
CN
M
75-M
(M = Li, Na, K)
Ph3P
S
O
O
M
71-M
(M = Li, Na, K)
Gessner
iPr
N
Ph
O
P
S
N
iPr
Li
iPr
iPr
iPr
81-Li
Baceiredo

**Figure 16.** All literature known examples for fully characterized, stable yldiides.

Contrary to yldiides **79-Li** and **80-Li**, which are monomeric in the solid state and where lithium cations only coordinate to the ylidic carbon atom and additional solvent molecules, **71-M**, **75-M** and **81-Li** showed a different behavior (Figure 17). For instance, **71-Na** crystallized as a dimer, consisting of three yldiides in the asymmetric unit, with $(NaO)_4$ cubes as a face-connected, central structural motif, resulting from coordination of the sodium cation with the ylidic carbon atom and oxygen atoms of the sulfonyl group. **71-K** is monomeric with the addition of an equivalent of 18-crown-6, which complexed the potassium atom and leaves back an almost 'naked' yldiide. The solid-state structure of **75-M** is highly dependent on the alkali metal cation. While the alkali metal in **75-K** prefers the coordination of both carbon atoms at the same time in the nitrile function ($\eta^2$-coordination), the harder alkali metals (**75-Li, 75-Na**) prefer coordination via the nitrogen atom. **81-Li** shows a similar behavior as already observed for **71-M**, the lithium cation is complexed by the ylidic carbon atom, as well as by the sulfinyl oxygen atom, resulting in a dimeric structure.

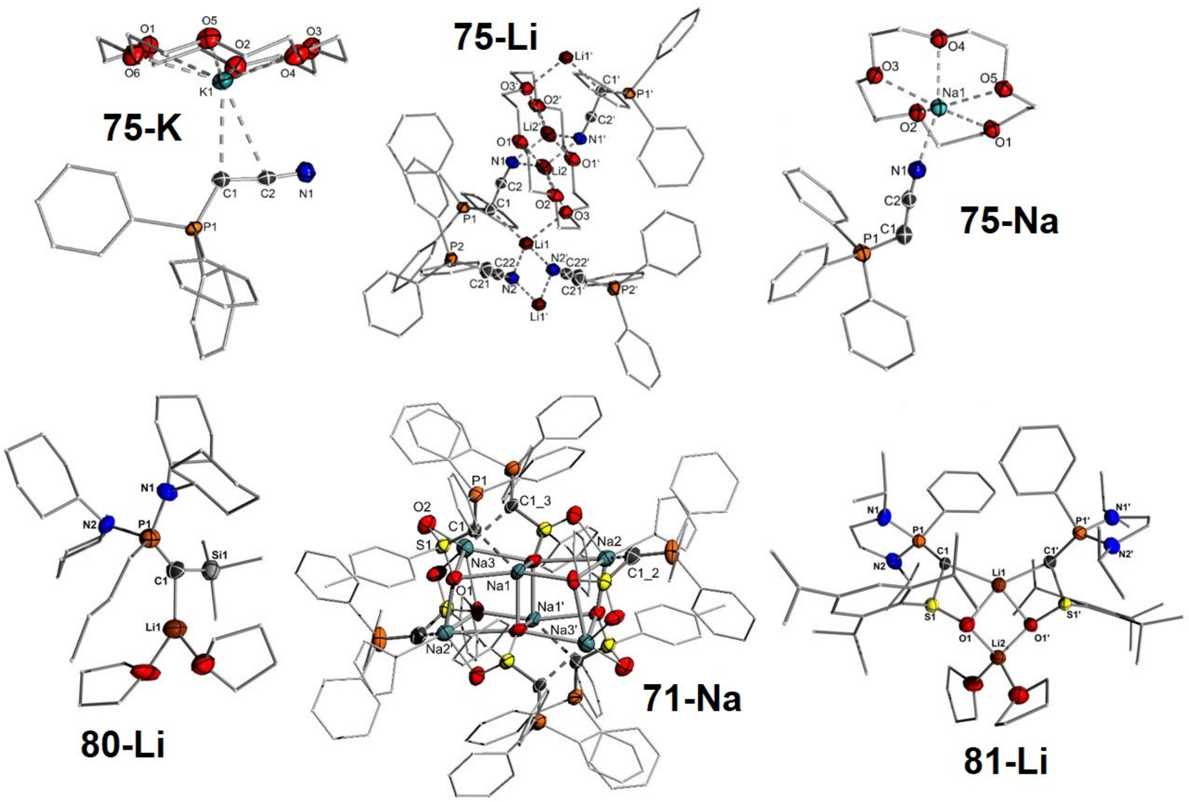
75-K
O1
O5
O3
O6
O2
O4
K1
C1
C2
N1
P1
75-Li
Li1'
C1'
P1'
O3'
O2'
Li2'
C2'
N1'
O1
N1
O1'
C2
Li2
C1
O2
O3
P1
P2
Li1
N2'
C22'
C22
C21
N2
C21'
P2'
Li1'
O4
O3
Na1
O5
O2
O1
N1
C2
C1
P1
75-Na
N1
N2
P1
C1
Si1
Li1
80-Li
P1
C1_3
O2
C1
S1
Na3
Na2
Na1
C1_2
O1
Na1'
Na3'
Na2'
71-Na
N1
P1
N2
C1
S1
O1
Li1
C1'
P1'
N1'
N2'
S1'
O1'
Li2
81-Li

**Figure 17.** Solid-state structures of known metalated phosphonium ylides in literature.[136–139] Reproduced/Adapted from the given sources with permission from John Wiley & Sons

Some interesting NMR-spectroscopic and XRD-structural features can be observed when a metalated ylide is compared with its parent ylide (Table 2), which will be discussed for example based on **71-M**.

**Table 2.** Important bond lengths and angles as well as NMR spectroscopic values for **71-Na** and **71-H**.

| | **71-Na** | **71-H** |
|---|---|---|
| P−C [Å] | 1.646(2) | 1.700(3) |
| S−C [Å] | 1.626(2) | 1.683(3) |
| P−$C_{Ph}$ [Å] | 1.806(2)<br>1.837(3)<br>1.861(3) | 1.793(2)<br>1.805(3)<br>1.814(3) |
| S−$C_{Tol}$ [Å] | 1.801(2) | 1.776(3) |
| S−O [Å] | 1.477(1)<br>1.479(1) | 1.442(2)<br>1.450(2) |
| $^{31}P\{^1H\}$-NMR [ppm] | −11.1 | 14.2 |
| $^{13}C\{^1H\}$-NMR [ppm] | 41.2<br>($^1J_{CP}$ = 38.0 Hz) | 34.5<br>($^1J_{CP}$ = 123.3 Hz) |

Upon deprotonation, the bond length of the the ylidic C–P bond shortens dramatically from 1.700(3) Å to 1.646(2) Å, reflecting the increased electrostatic interaction due to the higher negative charge located at the ylidic carbon atom. The same effect causes contraction of the P–C–S linkage, reflected by longer S–O and S-$C_{Tol}$ bonds. Because of the decreased positive charge, electrostatic interactions between these atoms becomes weaker. At the same time, the P–C bond from the phosphorus atom to the phenyl groups increases, reflecting strong negative hyperconjugation from the free lone pairs at the ylidic carbon atom into the $\sigma(\mathrm{P{-}C_{Ph}})^*$ orbitals (Figure 18).

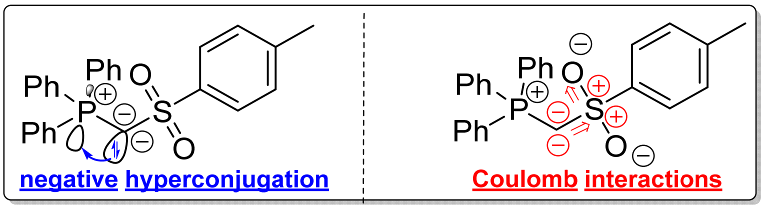

**Figure 18.** Stabilizing, electronic effects in metalated ylides

Furthermore, the coupling constant $^{1}J_{CP}$ decreases from 123.3 Hz for **71-H** to 38.0 Hz for **71-Na**. This is a good indication for successful yldiide formation, since this trend was also observed in other yldiides like in **81-Li**. This decrease is attributed to an elevation of $\sigma$-electron density at the ylidic carbon atom and a higher p-character in the P–C linkage. Another characteristic for successful yldiide formation is the $^{31}$P-NMR shift. Upon metalation, the signal is shifted towards higher field, compared with its protonated precursor. Additionally, the shift-difference is strongly dependent on the alkali-metal cation, since lithium yldiides give a relatively small shift difference, while potassium-yldiides give the most high-field shifted signals. This was observed for **71-M**, the potassium yldiide **71-K** resonated at $\delta_P$ = -16.6 ppm, compared to **71-Na** at $\delta_P$ = -11.1 ppm and the parent ylide **71-H** at $\delta_P$ = 14.2 ppm. The same trend was also observed for **75-M**. The observations revealed by XRD and NMR spectroscopy could also be underlined via computational studies. For instance, DFT calculations on **75-M** revealed the presence of two lone-pairs of electrons at the ylidic carbon atom, with one of $\pi$– and one of $\sigma$-symmetry, which was further confirmed via natural bond orbital analysis. Additionally, it was found that upon metalation an increase of the negative charge at the ylidic carbon atom occurs (from -1.05 for **75-H** to -1.33 for **75-M**), which is in line with the presence of a high electron-density already indicated by the two lone pairs of electrons. This is also reflected by the calculated gas phase proton affinities (PA) of **75-M**. Indeed, the 1st PA of 351.7 indicates a very high basicity. The calculated WBI of 1.43 for the $\mathrm{P{-}C_{ylide}}$ bond in **75-M** indicates a strong electrostatic interaction resulting in bond shortening compared to **75-H**, which could be confirmed via XRD (*vide supra*). The same trends have also been observed by *Baceiredo* et al. who performed calculations on **81-Li**.[139] Since a controversial discussion on the bonding in related compounds such as bisylides emerged[140], *Gessner* et al. recently studied the bonding situation of metalated ylides in detail.[141,142]

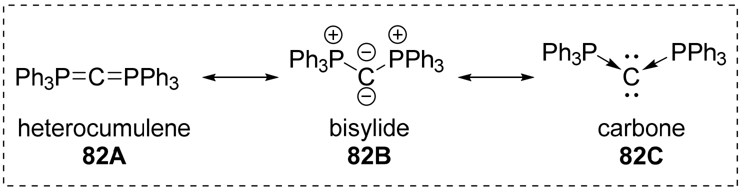

**Figure 19.** Possible resonance structures for a bisylide.

Neutral bisylides such as carbodiphosphorane **82** (Figure 19) could be described with a heterocumulene structure **82A**, with P–C single bonds and two negative charges on the central carbon atom as well as one positive charge on each phosphorus atom like in **82B**, or with dative bonds from two tertiary phosphines to a carbon-atom in an oxidation state of zero **82C** ('carbone'). However, describing **82** with a heterocumulene structure can not be considered as genuine. Molecular structures found for **82** revealed also bent bonding angles[143] and more importantly, double bonds between phosphorus and carbon require d-orbitals at the phosphorus atom, which however lie to high in energy to participate in bonding. It was long believed that resonance form **82B** describes the bonding in bisylides best. *Frenking* et al. suggested by NBO- and energy decomposition analysis (EDA) that resonance form **82C** with donor-acceptor interactions describes the bonding and reactivity of bisylides and related compounds like carbodicarbenes better.[144] Since metalated ylides are somewhat the mono-anionic congeners of bisylides, the bonding situation was also elucidated with these methods. However, *Gessner* et al. revealed that in metalated ylides no clear-cut picture could be given.[141] Initiated by the asymmetric structure of ylides, several fragmentation patterns were similar in energy, thus different electronic structure seem to be equally valid. For instance, the phenyl derivative (**83**) of **71-M** was investigated (Figure 20).

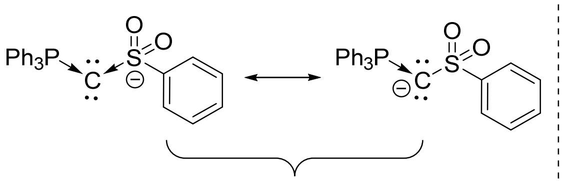

**83**

**Figure 20.** Canonical structures that describe the bonding in metalated ylide **83** best, according to EDA and NBO analysis performed by *Gessner* and coworkers.

Here, a combination of both, ylidic bonds and dative interactions, seem to be most suitable for the description of the bonding in **83**. However, ylidic bonds describe the reactivity of these species way better, as can be seen from the following chapter.

### 1.5.3 Reactivity of metalated ylides in synthesis

Early reactivity studies were reported on the use of metalated ylides as 'activated' Wittig reagents. For instance, *Corey* et al. reported that **73-Li** easily undergoes Wittig olefination with the sterically hindered fenchone **84**, while its non metalated congener **73** does not show any conversion to the exo-methylene derivative **85**.[128] In this transformation **73-Li** initially reacts in the first step as a typical organolithium reagent with a 1,2-addition to the carbonyl group, while subsequently performing a classical Wittig reaction in the second step (Scheme 24). The enhanced reactivity was attributed to the higher nucleophilicity of **73-Li** compared with **73**. Furthermore, **73-Li** showed an interesting behavior when reacting with epoxides like **86**. First, a nucleophilic ring opening furnished oxido-ylide (**87**), which could be further reacted with benzaldehyde to give homo-allyl alcohol **88** in a one-pot reaction. Similar, reaction of **73-Li** with aldehydes like **89a-b** initially gave *β*-oxido ylides (**90a-b**), which reacted with another equivalent of aldehyde giving *trans*-allyl alcohols **91a-b**.

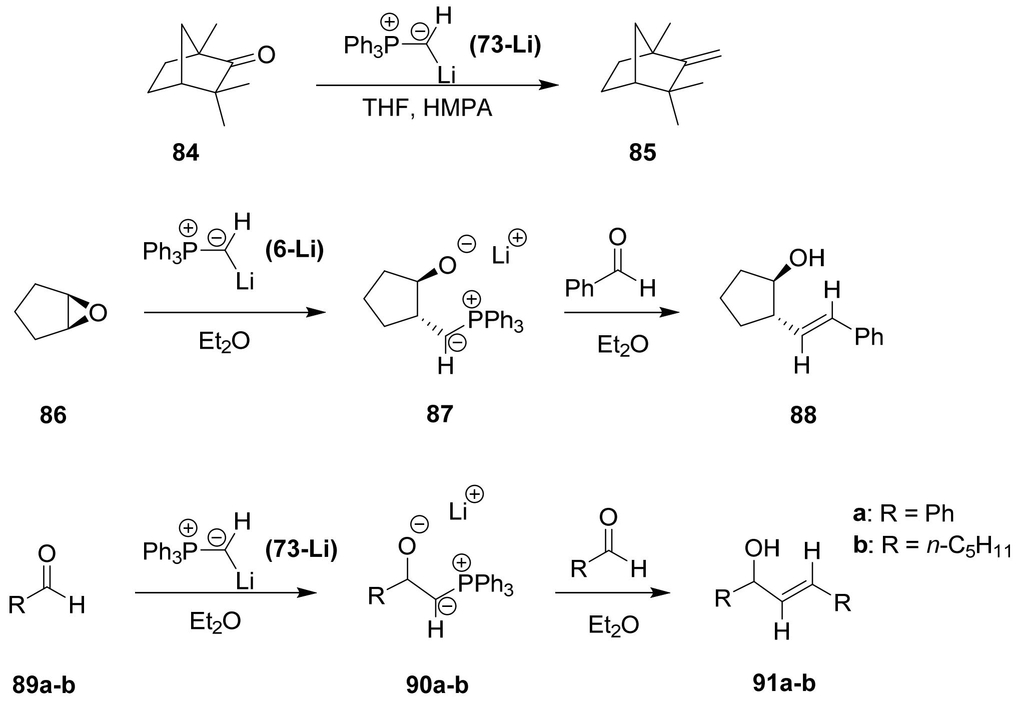

**Scheme 24.** Reactivity of **73-Li** towards carbonyl compounds and expoxides.

The yldiide **75-Na** reacted with epoxides in a similar manner, providing also oxido-ylides **92a-c**, which showed a very versatile chemistry (Scheme 25). Due to the attached nitrile function, different transformations depending on the reaction partners occurred, giving access to interesting cascade-like reactions. Acidic hydrolysis with HCl gave *γ*-nitrile functionalized alcohols **93a-c**, whereas hot hydrolysis initially furnished carboxylic acids functionalized with an alcohol functional group in *γ*-position **94a-c**, which further condensated to give lactones **95a-c**.[145]

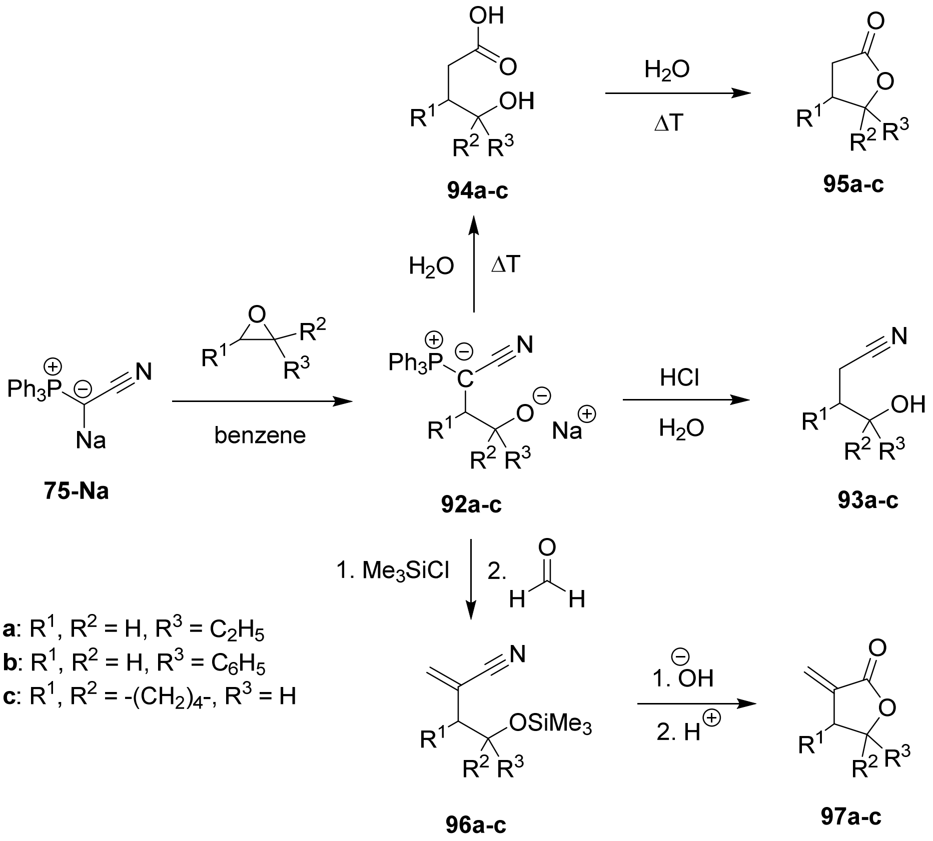
75-Na
benzene
92a-c
HCl
H2O
93a-c
ΔT
94a-c
95a-c
1. Me3SiCl
2.
96a-c
1. OH
2. H
97a-c
a: R1, R2 = H, R3 = C2H5
b: R1, R2 = H, R3 = C6H5
c: R1, R2 = -(CH2)4-, R3 = H

**Scheme 25.** Cascade-type reactions initiated by the metalated ylide **75-Na**,giving access to different functionalized organic molecules.

Protecting the alcohol function of **92a-c** and subsequently performing a Wittig reaction with formaldehyde, furnished acryl-nitriles **96a-c**. These could be further hydrolyzed under basic conditions to yield $\alpha$-methylene lactones **97a-c.** On the other hand, when the aldehyde function is protected in the first step, facile access to cyclized $\alpha,\beta$-unsaturated nitriles is possible (**98**/**99**) (Scheme 26).[132]

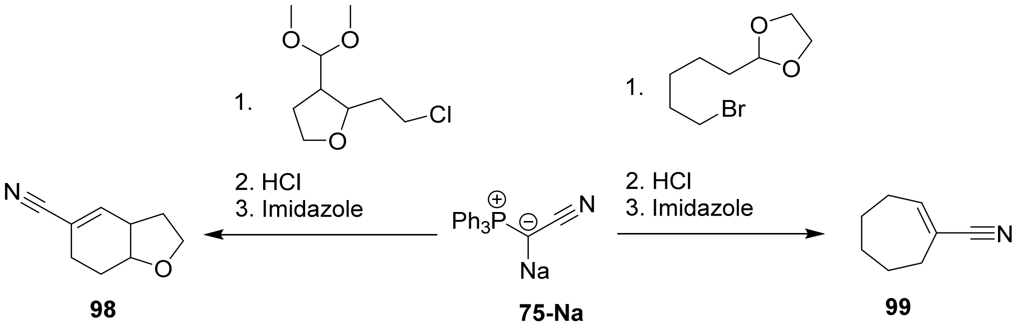
1.
2. HCl
3. Imidazole
1.
2. HCl
3. Imidazole
98
75-Na
99

**Scheme 26.** Access to $\alpha,\beta$-unsaturated nitriles.

Contrary to the observations made with **73-Li**, *Gessner* et al. recently showed that reaction of the metalated ylide **71-Na** with aldehydes does not result in typical Wittig reactivity. Instead, novel ylide-functionalized carbonyl compounds (**100**/**101**) are formed when **71-Na** reacted with benzaldehyde or pentafluoro phenyl aldehyde, respectively (Scheme 27).[137] Due to the highly stabilizing effect of the sulfonyl-moiety, only little classical elimination of $PPh_3=O$ occurs, while formal elimination of either sodium hydride in the case of benzaldehyde or formal elimination of pentafluorophenyl sodium occurs.

This observation shows that the reactivity of metalated ylides highly dependents on the attached substituents, which influence their steric- and electronic properties.

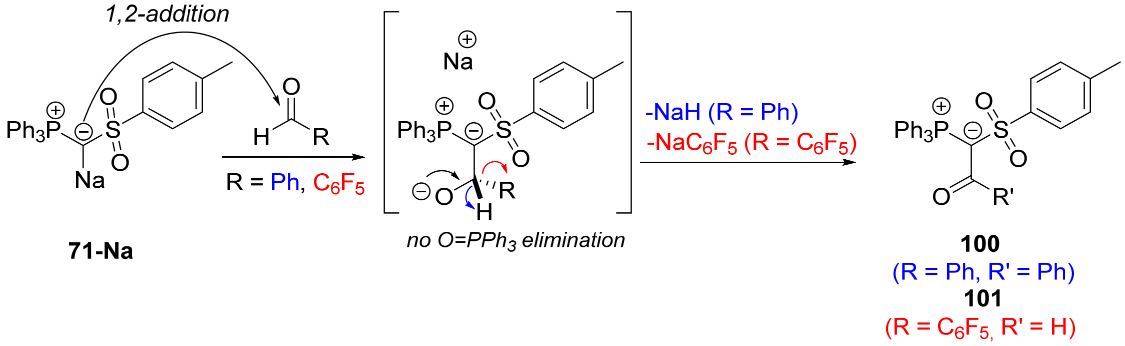
1,2-addition
R = Ph, C6F5
no O=PPh3 elimination
-NaH (R = Ph)
-NaC6F5 (R = C6F5)
71-Na
100
(R = Ph, R' = Ph)
101
(R = C6F5, R' = H)

**Scheme 27.** Reactivity of **71-Na** towards aldehydes.

Despite the already mentioned reactivities, the fundamental advantage of yldiides is their ability to perform highly selective salt metathesis reactions with organic and inorganic halides. As such, simple one-step procedures for ylide-functionalization via metalated ylides exist. First reports on salt metathesis reactivity was provided by *Bestmann* et al. who showed that **75-Na** easily reacts under sodium halide elimination with methyl iodide, benzyl chloride, silyl halides or elemental bromine to give the respective ylide functionalized compounds **102a-e** (Scheme 28).[132]

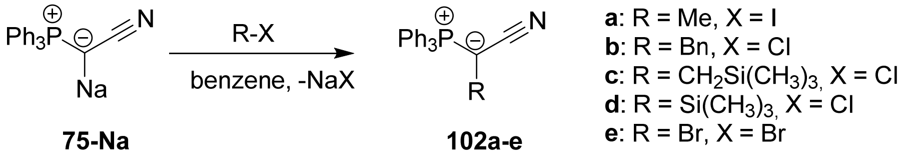
R-X
benzene, -NaX
75-Na
102a-e
a: R = Me, X = I
b: R = Bn, X = Cl
c: R = CH2Si(CH3)3, X = Cl
d: R = Si(CH3)3, X = Cl
e: R = Br, X = Br

**Scheme 28.** Salt metathesis reactions of **75-Na** with different organic halides.

Similarly, *Bertrand* reported on the reaction of **80-Li** with different electrophiles R-X , including diphenyl chlorophosphine, giving an ylide-functionalized phosphine (**103c**)[136], while *Niecke* et al. showed that also organometallic complexes such as the mono- and di-ylide mercury complexes (**104** and **105**, respectively) can be accessed by salt metathesis with $HgCl_2$ (Scheme 29).[135]

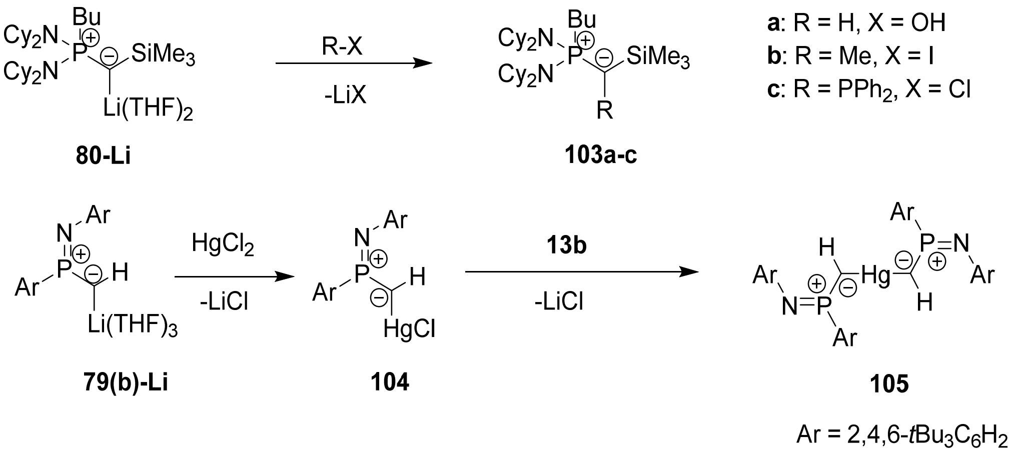
R-X
-LiX
80-Li
103a-c
a: R = H, X = OH
b: R = Me, X = I
c: R = PPh2, X = Cl
HgCl2
-LiCl
13b
-LiCl
79(b)-Li
104
105
Ar = 2,4,6-tBu3C6H2

**Scheme 29.** Reactivity of the metalated ylides **79(b)-Li** and **80-Li** towards different electrophiles.

This reaction is the only reported example to date, where an isolated yldiide is used for the formation of an $C_{ylide}$-transition metal bond via direct salt metathesis. Such species, also known as alkylidene-complexes, are usually prepared by deprotonation of suitable protonated ylide-transition metal precursors or by the reaction of phosphines with suitable carbine complexes.[146] Gessner et al. recently reported on the synthesis of ylide-functionalized silanes (**106a-b**) by reacting **71-Na** or **75-K** with phenyldichlorosilane (Scheme 30).[147] Furthermore, the authors showed also that the reaction of the corresponding yldiides with NFSI delivered the first structurally characterized *α*-fluorinated phosphorus ylides **107a** and **107b**.[147]

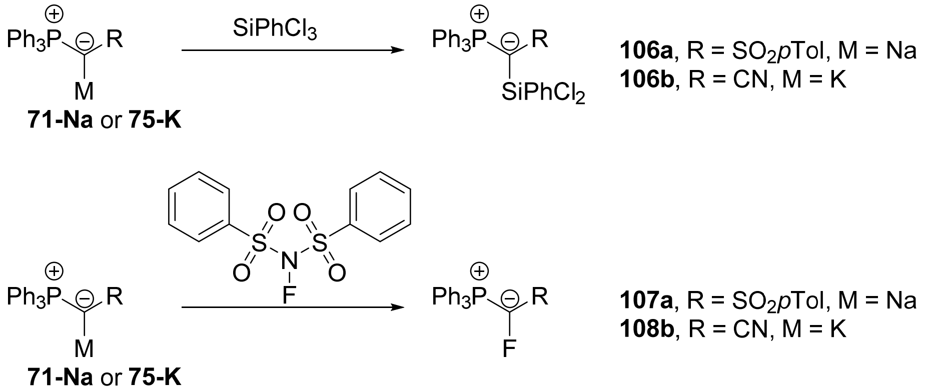

**Scheme 30.** Synthesis of ylide-functionalized silanes via salt-metathesis of **71-Na** and **75-K** with trichlorosilane (top) and preparation of the first fluoro-phosphonium ylides by reaction of NFSI with **71-Na** or **75-K**.

Both fluorinated ylides were also characterized by XRD and showed a huge deviation from the classical planar geometry (sum of angles around the carbon atom ~ 360°), which is usually observed in these compounds. Fluorination results in distinct pyramidalization of the ylidic carbon atom which can be explained by a change in hybridization from $sp^2$ to $sp^3$, caused by an increased p-character introduced by the fluorine atom. Moreover, compound **108b** exhibits a longer carbon-phosphorus bond and a 'normal' carbon-fluorine bond length, indicating that this species could also be described as a phosphine stabilized carbene species **108b**', since the phosphonium moiety might be the 'best leaving group' in this species (Figure 21). Reports on the use of fluorinated sulfonium ylides as fluoromethylene transfer agents, also suggest the formation of intermediate fluoro-carbene species.[148] This could also explain the extreme liability of **108** since its isolation was always concomitant with several decomposition products.

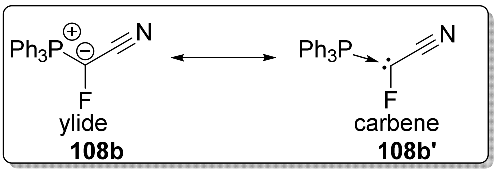

**Figure 21.** Possible ylidic and carbenic resonance structures of **108b**.

### 1.5.4 Ylides as stabilizing ligands for low-valent main group species

Despite being excellent reagents in organic transformations, ylides have been also studied as strong donor ligands for the stabilization of low-valent main-group compounds. Since only few metalated ylides are known, the majority of ylide-substituted main-group compounds was synthesized by direct coordination of suitable phosphonium precursors, followed by deprotonation. In this section, the preparation and reactivity of low-valent main group compounds stabilized by ylide substituents will be discussed concisely.

#### Ylide-stabilized group 13 compounds

Reports on the synthesis of ylide-functionalized group 13 compounds are extremely rare and thus the chemistry of group 13-ylide species is underexplored. However, *Bestmann* et al. reported on the preparation of ylide-functionalized boranes via reaction of phosphonium ylides with alkyldichloroboranes (Scheme 31).[149] This reaction proceeds via transylidation from **109**, giving the desired chloroboranes (e.g. **110**) and one equivalent of the parent phosphonium salt as the products. Attempts to prepare ylides which feature a P–C=B-R moiety such as **111** via base induced HCl elimination failed. Instead, a second transylidation reaction lead to boron-containing bis-ylides (**112**).

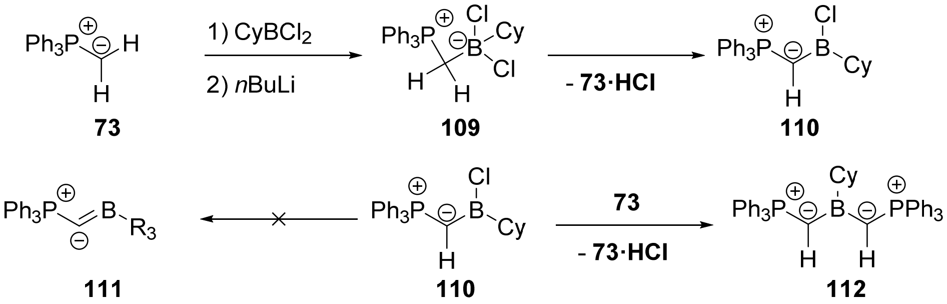

**Scheme 31.** Synthesis of ylide-functionalized boranes.

Furthermore, the synthesis of an ylide-functionalized lithium borate (**113-Li**) via the reaction of **75-H** with $BH_3 \cdot SMe_2$ and subsequent deprotonation with *n*BuLi was demonstrated (Scheme 32).[150] However, further reactivity studies were not provided.

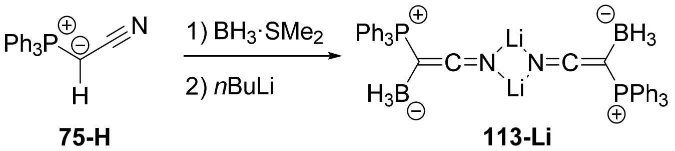

**Scheme 32.** Preparation of ylide-functionalized lithium-borate **113-Li**.

Recently, *Breher* et al. showed that $\alpha$-borylated ylides like **114** can activate small molecules such as CO, $CO_2$ and $NH_3$ by a FLP-type reactivity (Scheme 33).[151] While **114** reacts with CO and $CO_2$ to furnish cyclic insertion products like **115** and **116**, the reaction with ammonia results in a cleavage of the $C_{ylide}$–B bond, giving the parent ylide and the respective amino-borane. The reactivity towards these small molecules was attributed to a highly polarized carbon-boron bond, in which both atoms compete for the lone pair of electrons, hence resembling a frustrated electronic situation in which neither the carbon- , nor the boron atom is fully satisfied.

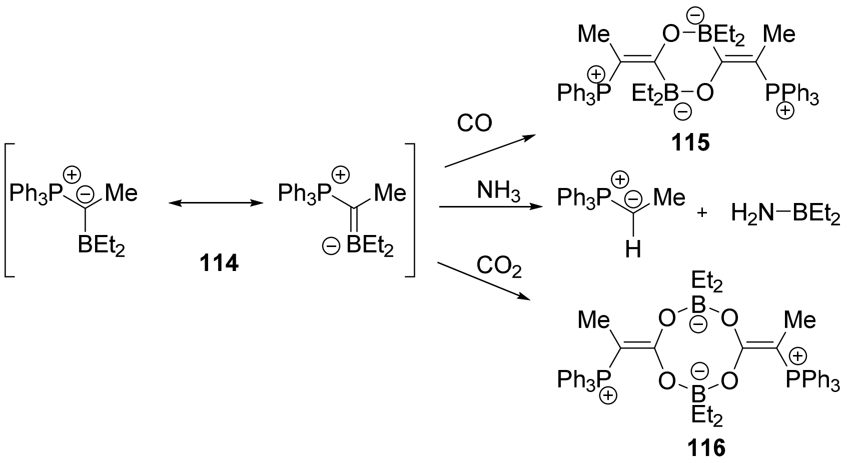

**Scheme 33.** Reactivity of borylated ylide **114** towards small molecules.

The first and only example of a low-valent group 13 compound stabilized by ylide substituents was recently reported by *Gessner*.[152] Reaction of the metalated ylide **71-Na** with $BH_3$·THF resulted in the formation of the di-ylide functionalized borane **117**(Scheme 34). Subsequent halide abstraction with trityl salts gave rise to the first di-ylide stabilized boron-cations **118a-d**. XRD studies on **118-d** revealed an additional coordination by one oxygen atom of the sulfonyl group, hence rendering this compounds as borenium cations rather than di-coordinated borinium species.

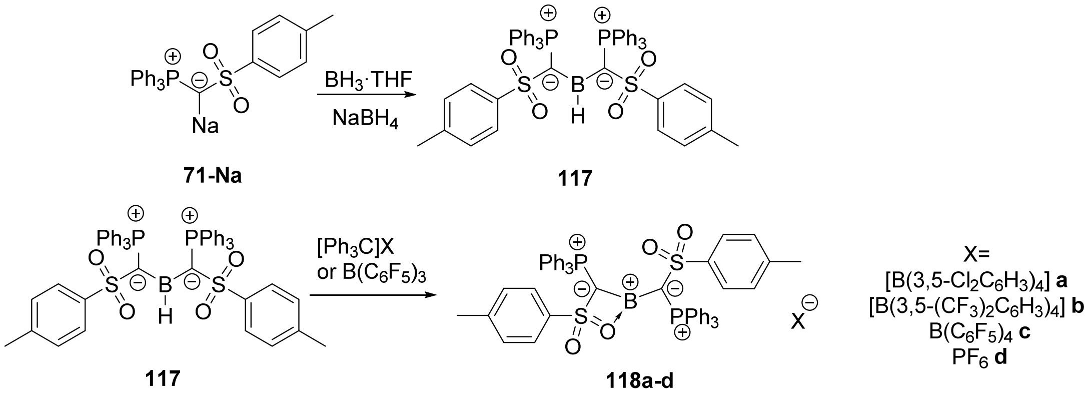

**Scheme 34.** Preparation of di-ylide functionalized borane **117** via reaction of **71-Na** with $BH_3$·THF and subsequent synthesis of the first example of a low-valent ylide-substituted boron compound, namely borenium cation **118**.

The solid-state data indicate strong *π*-donation from the ylidic carbon atoms to the boron center, resulting in short C–B distances of 1.481(7) Å and 1.510(9) Å, for the exo-cyclic and endo-cyclic-bond, respectively. This *π*-bond interaction could be furthermore proved by NBO analysis, which showed that the HOMO-1 reflects *π*-delocalization over the whole C-B-C linkage. However, the LUMO is predominantly localized at the boron center. Hence, independently from the strong *π*-donation of the ylidic carbon atoms, the boron atom remains the most electrophilic center of the molecule. The electrophilicity of borenium cation **118** could be demonstrated by its prompt fluorination with KF giving **119** and subsequent elimination of $KPF_6$. Additionally, **118** demonstrated its Lewis acidity by forming simple Lewis acid base pairs with DMAP, DMF or NMP (**120a-c**). When **118** is treated with a primary or secondary amine, the N–H bond is activated across the C–B–C linkage, resulting in a cleavage of the ylide fragments with subsequent formation of tris(amino)boranes (**121a-c**), the parent phosphonium salt **71-H**$_2$ and ylide **71-H** (Scheme 35). The reactivity of **118** towards primary and secondary amines is surprising but reflects the strongly polarized nature of the C–B bonds.

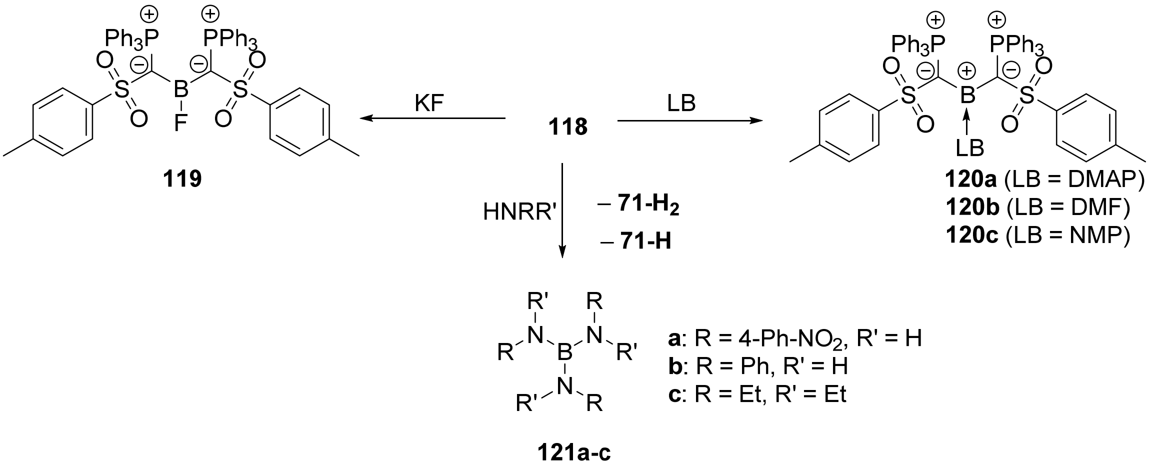

**Scheme 35.** Reactivity of borenium cation **118**.

Despite **118**, no further ylide-stabilized low-valent group 13 compound was reported. However, the preparation of **118** showed that metalated ylides can act as both, strong $\sigma$- and $\pi$-donor ligands, being able to stabilize even highly electrophilic species like boron cations. This observation indicates the high potential of ylides as stabilizing ligands for inherent electron-deficient group 13 elements, which was recently also recognized by *Phukan* and coworkers.[153] Theoretical calculations revealed that ylide functionalization could indeed enable the isolation of so-far elusive, stable borylenes.

### Ylide-stabilized group 14 compounds

The chemistry of stable singlet carbenes and their heavier analogues has already been discussed in a previous chapter of this thesis. The isolation of several of these species was only possible by the 'right' choice of steric- and electronic properties delivered by the ligand framework, which is mainly achieved by bulky $\alpha$-nitrogen substituents like in NHCs, CAACs or diaminocarbenes (*vide supra*). Stabilization of these low-valent species is often accomplished via $\pi$-interaction of the heteroatoms' lone-pair of electrons and the empty $p_\pi$-orbital at the tetrel center. Such stabilization could also be achieved by replacing, e.g. one of the nitrogen-groups in NHCs by an ylidic motif, yielding so-called cyclic amino(ylide) carbenes or **CAYCs**. Because of the lower electronegativity of carbon compared to nitrogen, CAYCs are expected to exhibit similar donor power as CAACs, while retaining the $\pi$-acceptor properties of NHCs and are thus interesting species, for instance as highly electron-rich ligands in main-group chemistry and homogeneous catalysis. This interested *Facchin* and *Michelin*, who prepared the first CAYC platinum-complexes (**123**) by a based induced cyclization of a phosphonium-isonitrile scaffold (**122**) in the late 1980's.[154] A similar approach, reported by *Alcarazo*, synthesized the first acyclic Au(I)-AYCs complexes (**124**) (Scheme 36).[155]

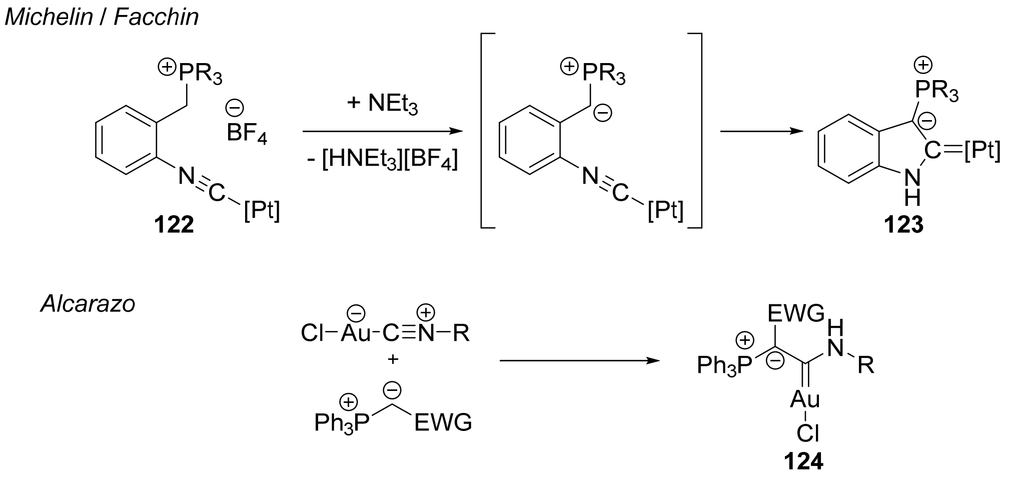
Michelin / Facchin
⊕PR3
⊖ BF4
N≡C–[Pt]
122
+ NEt3
- [HNEt3][BF4]
⊕PR3
⊖
N≡C–[Pt]
⊕ PR3
⊖
C=[Pt]
N H
123
Alcarazo
Cl–Au–C≡N–R
+
Ph3P EWG
EWG
H
N R
Ph3P
Au
Cl
124

**Scheme 36.** Examples for the preparation of CAYC complexes.

In 2008, the research groups of *Kawashima*[156], *Fürstner*[157] and *Bertrand*[158] reported independently on synthesis attempts of free CAYCs by deprotonation of suitable phosphonium salt precursors with strong metal bases. For instance, deprotonation of phosphonium salt **125** with mesityl-lithium was studied by *Kawashima* et al., however not leading to a stable carbene (**126**). Instead, transfer of a phenyl group to the carbene carbon atom occurred, giving **127** (Scheme 37). However, a trapping reaction with elemental sulfur revealed the existence of CAYC **126** at low-temperatures, since the corresponding thio-derivative could be isolated from the product mixture (**128**). Furthermore, the formation of the corresponding [**CAYC-**Rh(CO)$_2$Cl] complex **129** proved the superior donor properties compared to diamino or alkyl(amino)carbenes.

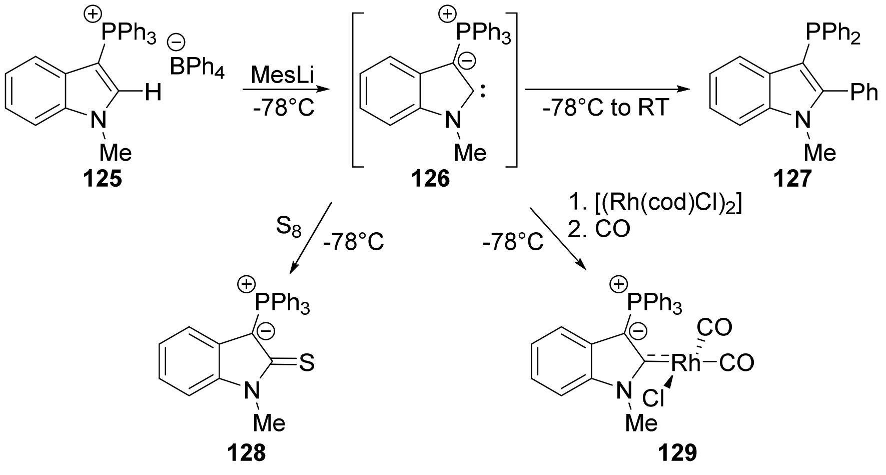
⊕PPh3 ⊖
BPh4
H
N
Me
125
MesLi
-78°C
⊕PPh3
⊖
N
Me
126
-78°C to RT
PPh2
Ph
N
Me
127
S8
-78°C
-78°C
1. [(Rh(cod)Cl)2]
2. CO
⊕PPh3
⊖
S
N
Me
128
⊕PPh3
⊖
CO
Rh–CO
N Cl
Me
129

**Scheme 37.** Attempted synthesis of CAYC **126** and performed trapping reactions as reported by *Kawashima*.

Similar observations were made by *Fürstner* and coworkers, who succeeded in the preparation of complexes **130**/**131** and thio-compound **132**, while *Bertrand* et al. observed the deprotonation of phosphonium salt **133** with MeLi, giving the lithium adduct **134**, formed by cleavage of a labile P–C(sp$^2$) bond (Scheme 38).

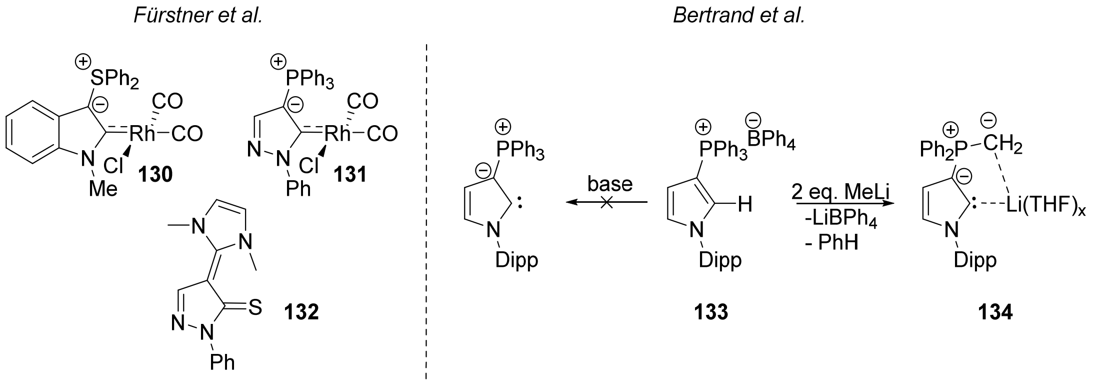
Fürstner et al.
Bertrand et al.
SPh2
CO
Rh–CO
Cl
N
Me
130
PPh3
CO
Rh–CO
N–N
Cl
Ph
131
N
N
S
N–N
Ph
132
PPh3
N
Dipp
base
PPh3
BPh4
H
N
Dipp
133
2 eq. MeLi
-LiBPh4
- PhH
Ph2P–CH2
Li(THF)x
N
Dipp
134

**Scheme 38.** Prepared CAYC Rh-complexes and thio-derivative by *Fürstner* (left). Synthesis attempts towards a CAYC by *Bertrand* and coworkers (right).

Recently, *Gessner* et al. reported on synthesis attempts of CAYCs bearing trialkyl-onium groups[159], which should be less prone to bond-cleaving reactions because of the intrinsically higher bond strength of C($sp^3$)-X bonds (Scheme 39). However, the deprotonation of tricyclohexyl phosphonium precursor **135** did not take place at the 'carbenic' carbon atom, instead a deprotonation in $\alpha$-position to the phosphorus atom was observed, forming ylide **136**. Similarly, deprotonation of sulfonium salt **137** gave presumably ylide **138** which eliminates ethene in a Corey–Chaykovsky type reaction sequence to afford thioether **139**.

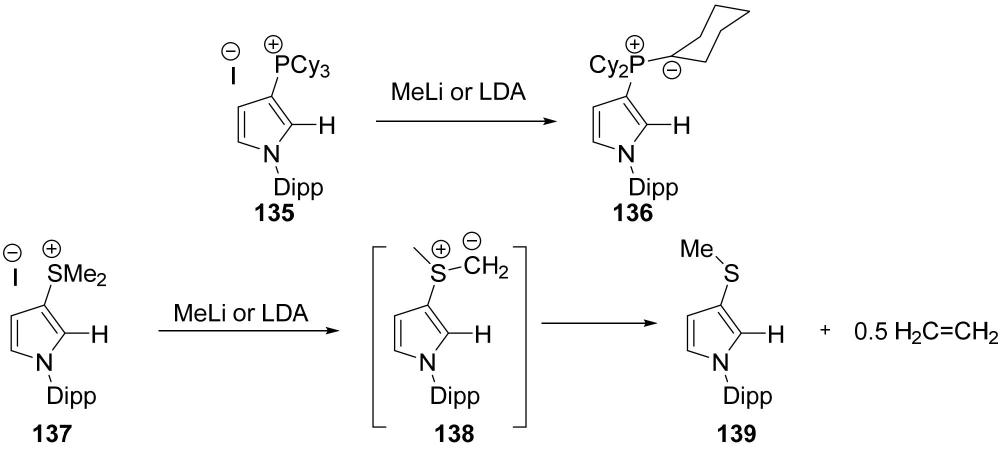
I
PCy3
H
N
Dipp
135
MeLi or LDA
Cy2P
H
N
Dipp
136
I
SMe2
H
N
Dipp
137
MeLi or LDA
S–CH2
H
N
Dipp
138
Me
S
H
N
Dipp
139
+ 0.5 H2C=CH2

**Scheme 39.** Synthesis attempts of CAYCs bearing trialkylphosphonium-and sulfoxonium groups as reported by *Gessner*.

The authors concluded from DFT studies that deprotonation in $\alpha$-position to the heteroatom is thermodynamically always favored over carbene formation and furthermore, even if AYCs might be accessible at low temperatures, proton shifts from the trialkyl-onium group to the carbene center are more likely to occur, even from $\beta$-positions such as from *t*Bu groups. Solely the use of adamantyl groups might provide access to stable CAYCs (**140**), because here the deprotonation in $\beta$-position would give a double bond at a bridgehead carbon atom (**141**), violating *Bredt's* rule (Scheme 40). Thus, the isolation of a room-temperature stable CAYC (e.g. **142**) might be possible with incorporation of triadamantyl-phosphonium group but remains elusive until today.

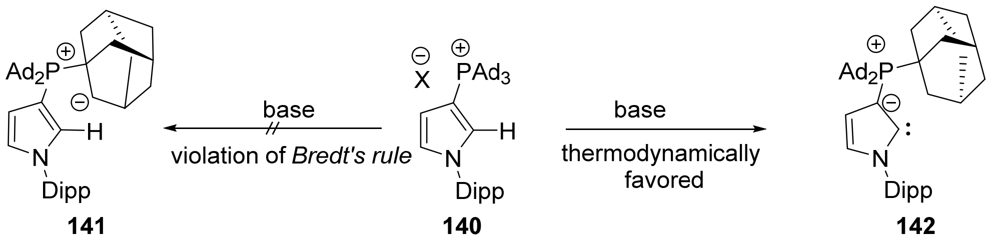
Ad$_2$P
H
N
Dipp
141
base
violation of *Bredt's rule*
X
PAd$_3$
H
N
Dipp
140
base
thermodynamically favored
Ad$_2$P
N
Dipp
142

**Scheme 40.** Possible synthesis of a stable CAYC based on a triadamantyl-phosphonium group.

In contrast, a few examples of isolable heavier ylide stabilized tetrylenes have been reported. In 1998, *Schmidtpeter* et al. succeeded in isolating the first di-ylide stabilized stannylene **144** by reaction of di-ylide **143–H** with [Sn(N(SiMe$_3$)$_2$] (Scheme 41).[160] **144** could not be structurally characterized by XRD, however NMR data suggest a symmetric di-valent tin center stabilized by flanked ylide-substituents. Since **144** is incorporated into an aromatic cycle, several resonance structure can be formulated, indicating an electron-rich tin center.

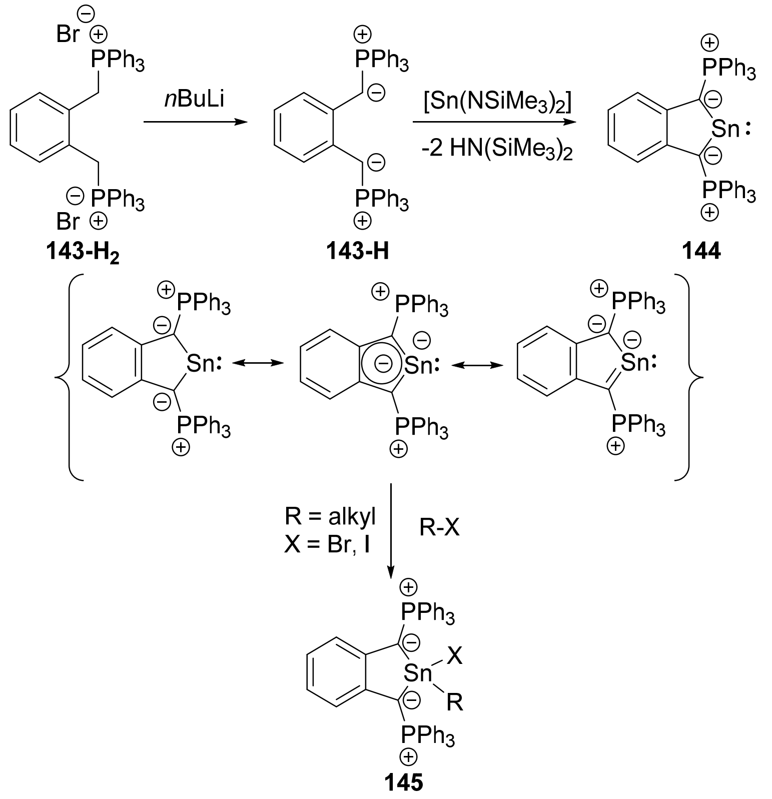
Br
PPh$_3$
PPh$_3$
Br
143-H$_2$
*n*BuLi
PPh$_3$
PPh$_3$
143-H
[Sn(NSiMe$_3$)$_2$]
-2 HN(SiMe$_3$)$_2$
PPh$_3$
Sn
PPh$_3$
144
R = alkyl
X = Br, I
R-X
PPh$_3$
Sn
X
R
PPh$_3$
145

**Scheme 41.** Synthesis and reactivity of diylide-stabilized stannylene **144**.

The electron-rich nature of **144** was also indicated by the $^{13}C\{^1H\}$-NMR shift of the ylidic carbon atom, appearing at $\delta_C$ = 122.4 ppm, revealing strong $\pi$-donation from the lone pairs of electrons into the vacant $p_\pi$-orbital. Additionally, simple oxidative addition of alkyl bromides or iodides to the low-valent tin center (**145**) clearly demonstrates the ability of di-ylide stannylene **144** to act as an electron-rich species. *Driess* and coworkers reported in 2001 on the isolation of silylene **147**, the silicon analogue of **144** (Scheme 42).[161] The synthesis proceeds with the bis-phosphonium salt **143–H$_2$**, which is reacted with excess KHMDS and SiBr$_4$, giving di-ylide dibromosilanes **146a-b**. Reduction of **146** with either KC$_8$ or *Jones* Mg(I) dimers gave rise to the first diylide functionalized silylenes **146a-b**.

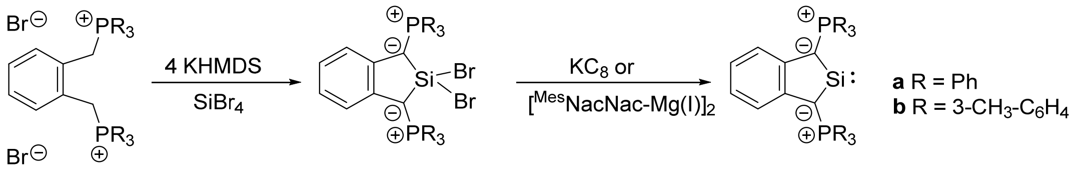

**143(a-b)-H$_2$** **146a-b** **147a-b**

**Scheme 42.** Synthesis of the first diylide-stabilized cyclic silylenes **147a-b**.

Albeit no structure characterization of **147a-b** via XRD was performed, the existence of these species was confirmed via NMR spectroscopy and trapping reactions. The $^{29}$Si-NMR signal of **146b** appears as a triplet at low-field $\delta_{Si}$ = 213.3 ppm, with a coupling constant of $^2J_{SiP}$ = 38.5 Hz. This low-field shift is typical for silicon(II) species and indicates the successful formation of a silylene. Similar to **144**, the $^{13}$C{$^1$H}-NMR shift of the ylidic carbon atom appears significantly low-field (~ $\delta_C$ = 90 ppm) compared to the precursor (*cf.* $\delta_C$ = 37.5 ppm ), indicating $\pi$-delocalization, as already expected by the resonance structures for **144**, which could further be proven by DFT calculations. As expected for silylenes, **147a-b** undergoes selective [4+2] cycloaddition with 3,5-di-tert-butyl-o-benzoquinone to give spirocyclic silanes **148ab** (Scheme 43).

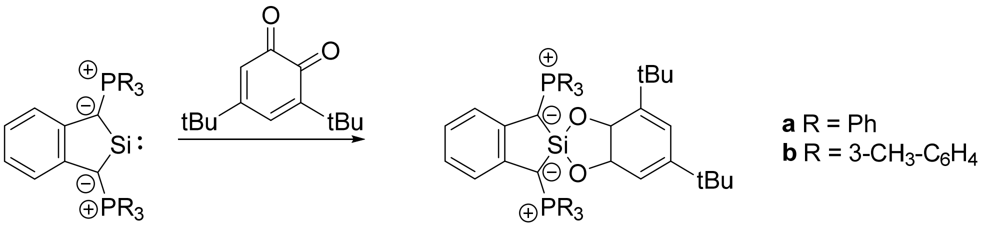

**147a-b** **148a-b**

**Scheme 43.** Reactivity of silylenes **147a-b** towards 3,5-di-tert-butyl-o-benzoquinone, giving spirocyclic silanes **148a-b**, as reported by *Driess* and coworkers.

*Kato* et al. described in 2016 the synthesis of an asymmetric amido-/ylide-substituted silylene **151** from deprotonation of dichloro-silane precursor **149** with LDA and subsequent reduction of the corresponding ylide **150** with two equivalents of elemental potassium (Scheme 44).[162]

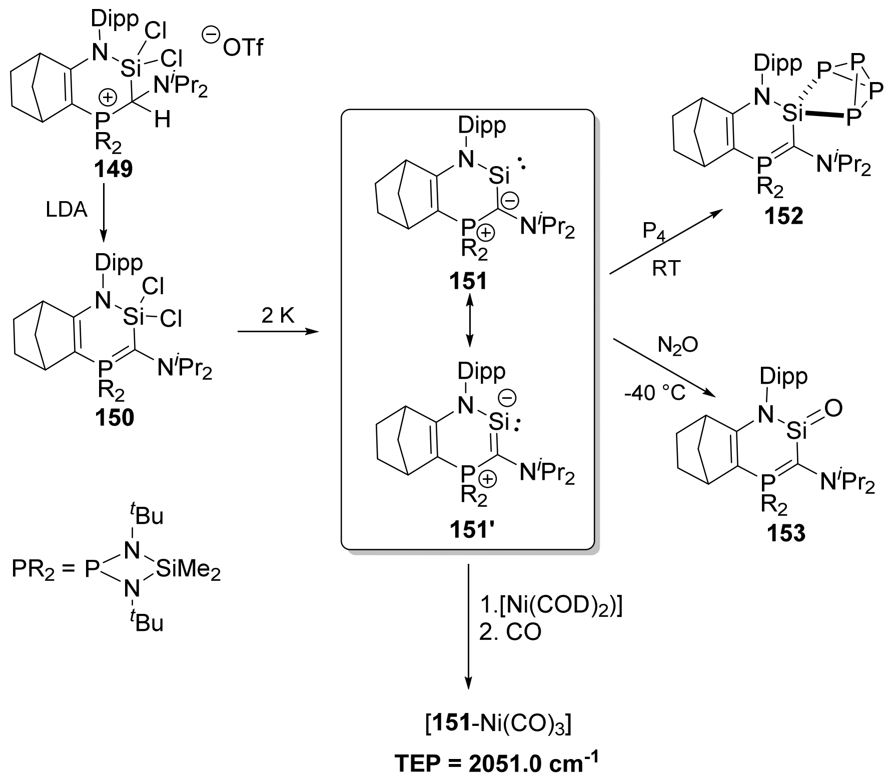

**Scheme 44.** Synthesis and reactivity of a cyclic amido-/ylide substituted silylene **151**.

Silylene **151** is characterized by significant downfield shifts for the silicon atom (202.2 ppm, *d*, $^2J_{\mathrm{SiP}}$ = 9.2 Hz) and the ylidic carbon atom (137.7 ppm, *d*, $^1J_{\mathrm{CP}}$ = 61.2 Hz) in the $^{29}$Si-and $^{13}$C-NMR spectra, respectively. The downfield shift for the signal of the silicon atom is similar to that observed for **147**, while the $^{13}$C-NMR signal for the ylidic carbon atom is way more downfield shifted. This indicates very strong $\pi$-bonding character of the Si–C bond. Indeed, this strong $\pi$-bonding interaction could be proved by the first XRD analysis of an ylide-substituted tetrylene. The Si–C bond length of 1.798(2) Å lies between classical single and double bonds and is shorter than the calculated Si–C bonds (1.871 Á) for **147**, thus silylene **151** is best described by resonance structure **151'**, with a strongly polarized Si–C double bond. Silylene **151** reacts with small molecules such as $P_4$ and $N_2O$ (Scheme 44). While **151** inserts into a P–P bond of white phosphorus giving **152**, reaction with $N_2O$ provided the first structurally characterized base-free silanone **153**. Albeit **153** possesses only limited stability ($t_{1/2}$ = 5 h) and dimerizes at RT, it reflects the unique stabilizing character of the ylide-motif. Furthermore, the donor ability of **151** could be measured by means of its TEP value, obtained from the CO-stretching frequency of the corresponding [**151**–Ni(CO)$_3$] complex. With a TEP value of 2051.0 cm$^{-1}$ silylene **151** turned out to be strongly electron-donating, surpassing the donor power of cyclic silylenes like NHSis (2076.0 cm$^{-1}$) as well as common tertiary phosphines and thus its donor strength is comparable to NHCs (~2050-2054.0 cm$^{-1}$). This donor power could be even exceeded by replacing the phosphonium ylide moiety in **151** by a bora-ylide-substituent like in **154**, reported by *Kato* in 2017 (Scheme 45).[163] With an even smaller difference in electronegativity ($\Delta_{\mathrm{EN}}$ (B-Si) = 0.1), the electron-density at the divalent silicon center is further increased and thus the corresponding [**154-**Ni(CO)$_3$] complex gave rise to a stretching frequency as low as 2046.0 cm$^{-1}$. With its higher donor capacity, the corresponding silanone **155** was with $t_{1/2}$ = 4 d even more stable than its carbon-based ylide analogue **153**.[164]

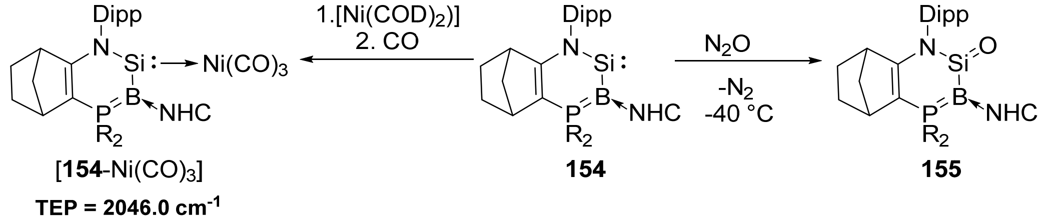

**Scheme 45.** Reactivity of amido-/bora-ylide substituted silylene **154** towards $N_2O$ giving silanone **155** and preparation of complex [**154**-$Ni(CO)_3$] from [$Ni(COD)_2$] and CO.

Despite ylide-stabilized silylenes, *Kato* and coworkers reported on germylenes similar to **151** that could be accessed by a rare isomerization reaction of germynes **156a-b** above -30°C, yielding to germylenes **157a-b** (Scheme 46).[165] However, no further reactivity of these species was reported, which may be caused by the rather difficult access to these ligand classes.

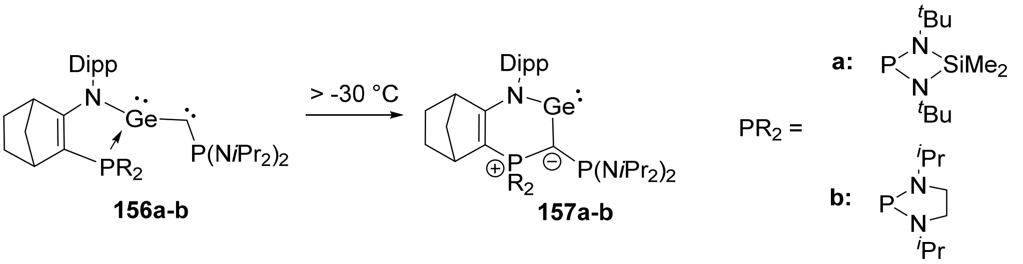

**Scheme 46.** Isomerization reaction of germynes **156a-b** to the corresponding germylenes **157a-b**.

In 2018, *Gessner* et al. reported on the facile synthesis of the first acyclic di-ylide substituted germylene **158** and stannylene **159** (Scheme 47).[166] These compounds were obtained by simple salt-metathesis of the metalated ylide **71-Na** with half an equivalent of the respective halide salt ($ECl_2$ with E = Ge, Sn), being the first and only reported example of utilizing an alkali metal yldiide as a one-step entry into low-valent ylide-functionalized main-group species.

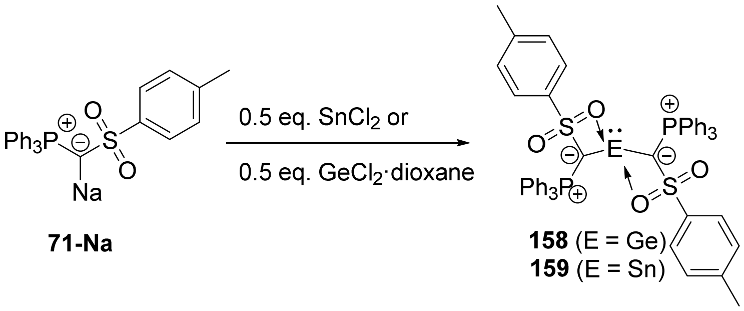

**Scheme 47.** One-step synthesis of the first acyclic di-ylide stabilized germylene **158** and stannylene **159** from via salt metathesis from **71-Na** and half an equivalent of the respective element chlorides.

In contrast to all other reported ylide-stabilized tetrylenes, **158** and **159** exhibit unusually high field shifted signals for the ylidic carbon atoms in the $^{13}C\{^1H\}$-NMR spectra at approximately $\delta_C = 52$ ppm. This indicates that the ylide-substituents do not act as $\pi$-donors. Indeed, XRD analysis of **158** and **159** revealed a unique electronic situation, in which both ylide groups (P–C–S plane) are perpendicular arranged to the C–E–C linkage, thus suggesting that no $\pi$-donation into the vacant p-orbital of the tetrel center is possible. This results in a unique bonding situation, where three lone pairs of electrons are located next to each other (Figure 22) conformer 1. As a consequence, the metal-carbon bond lengths are in the range of single bonds. This unusual arrangement can be explained by the strong ability of the sulfonyl group to stabilize the negative charge at the ylidic carbon atom and its coordination to the metal, hence pointing out that the substitution pattern on the ylidic backbone has a tremendous effect on structure, electronic properties and reactivity of ylidic compounds. Furthermore, this unusual electronic structure has an impact on the energies of the frontier orbitals of di-ylide tetrylenes **158** and **159**, boosting the HOMO and LUMO orbitals to higher energies compared to the hypothetical conformer where the ylidic carbon atoms donates electron density towards the central tetrel atom (Figure 22, conformer 2). Compared to all other reported acyclic germylenes for instance diaryl-, diamido- or amido/boryl-germylenes shown in Figure 22, **158** possesses the highest donor strength and its calculated TEP value of 2032.3 cm$^{-1}$ shows that its donor power lies within the range of strongly donating CAACs.

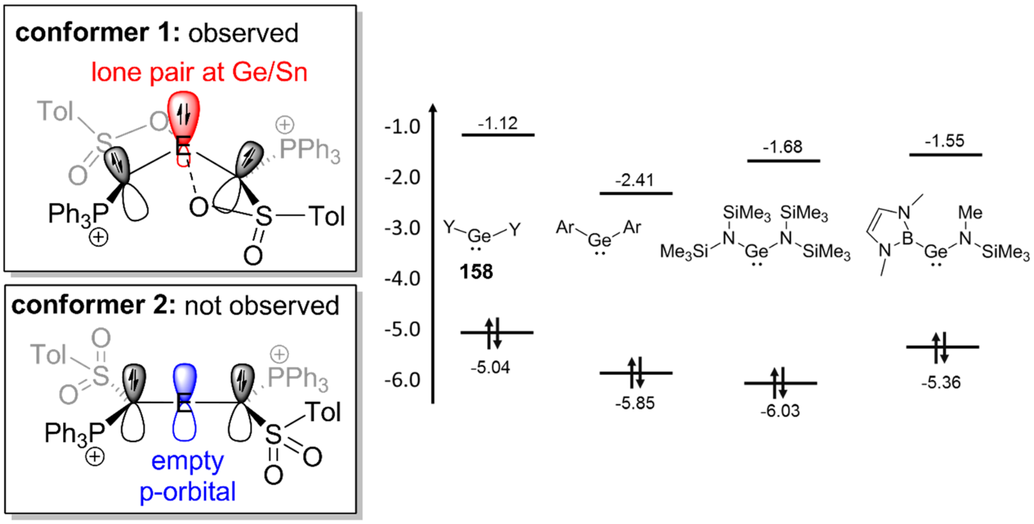
conformer 1: observed
lone pair at Ge/Sn
Tol
S
O
O
E
PPh3
Ph3P
O
S
Tol
O
conformer 2: not observed
Tol
O
S
O
PPh3
Ph3P
Tol
S
O
O
empty
p-orbital
-1.0
-2.0
-3.0
-4.0
-5.0
-6.0
-1.12
-2.41
-1.68
-1.55
Y
Ge
Y
158
Ar
Ge
Ar
SiMe3
SiMe3
Me3Si
N
Ge
N
SiMe3
N
B
N
Ge
Me
N
SiMe3
-5.04
-5.85
-6.03
-5.36

**Figure 22.** Conformers of the tetrylenes **158/159** and energy levels of the frontier orbitals (in eV) of **158** in comparison with other germylenes.[166] Reproduced/Adapted from the given sources with permission from John Wiley & Sons

This remarkably high donor power was further proved by the reactivity of **158** (Scheme 48). While **159** shows an indefinite stability in THF solution, **158** undergoes an intramolecular C–H activation reaction of one of the $PPh_3$ phenyl groups even at room temperature to give tetragermane **160** along with free ylide **71–H**. DFT calculations on the mechanism of this reaction showed that the activation presumably proceeds across the Ge–C$_{ylide}$ linkage, indicating that based on ylide-functionalization, metal-ligand cooperation is possible. Similar to other tetrylenes, **158** and **159** reacted with 3,5-di-tert-butyl-o-benzoquinone in a [4+2] cycloaddition reaction, giving spirocyclic germanes (**161a**) and stannanes (**161b**), respectively. Additionally, **159** reacts with elemental sulfur, yielding a di-ylide substituted compound **162** with an unusual $Sn_2S_3$ five-membered ring.

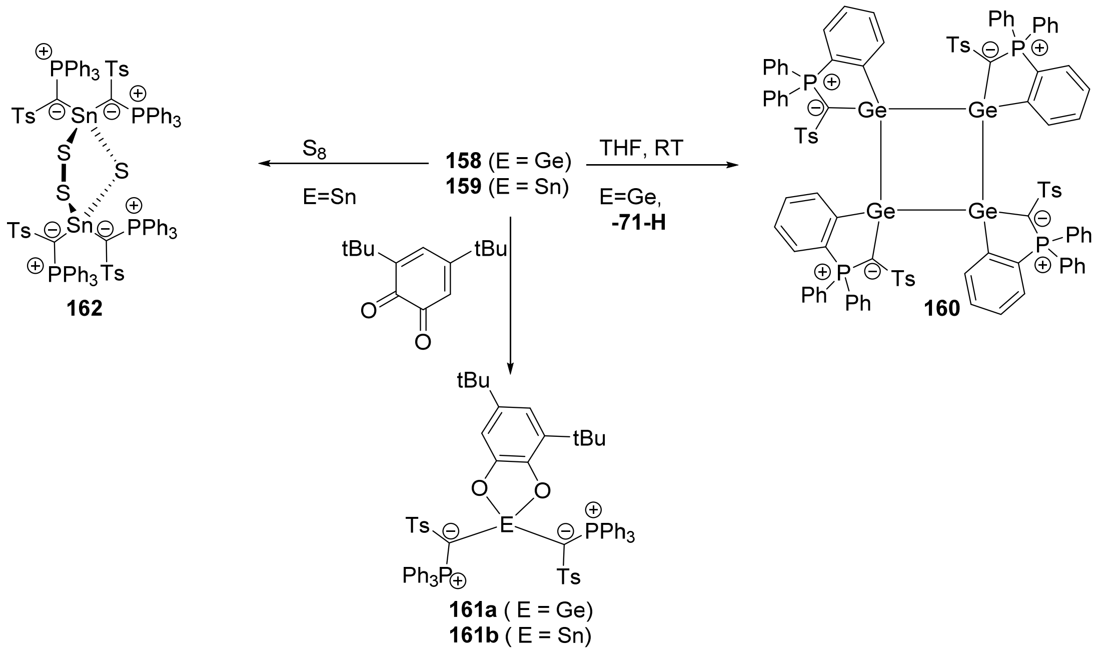

**Scheme 48.** Reactivity of diylide-tetrylenes **158/159**.

These first examples of low-valent ylide functionalized group 14 compounds impressively show the ability of ylidic substituents to function as supporting ligands, enabling the isolation of highly reactive species with unusual structural motifs and bonding situations.

### Ylide-stabilized group 15 compounds

Phosphorus compounds bearing ylide-substituents gained considerable attention in the 1990s. The groups of *Schmidtpeter* and *Nöth* in particular, were extensively engaged with the chemistry of ylide-functionalized halophosphines (**163a-e**)[167], studying the impact of electron-rich ylide fragments on the phosphorus-halogen bond (Figure 23). Compared to non-$\pi$ donating substituents, ylides cause a remarkable polarization of the P–X bond, which results in bond elongation via negative hyperconjugation from the lone pair of electrons at the ylidic carbon atom into the $\sigma^*$(P–X) orbital (**164a-e**).[168]

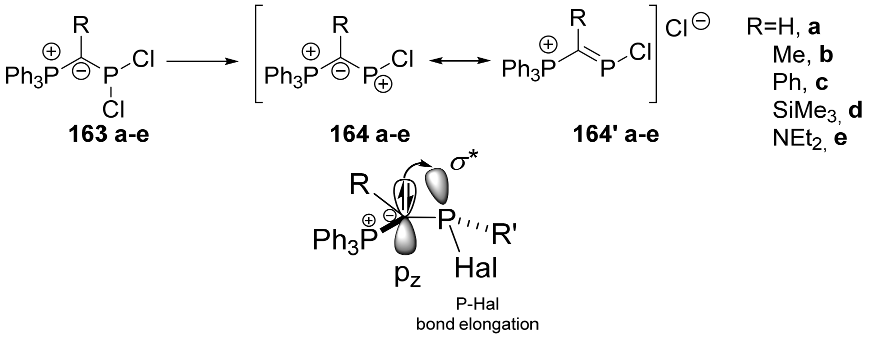

**Figure 23.** Dissociation of chloride-substituents from ylide-functionalized chloro-phosphines initiated by negative hyperconjugation.

Depending on the strength of this negative hyperconjugation, even spontaneous dissociation of the halogen atom can occur, as observed with halophosphines bearing two strong $\pi$-donating substituents like in bisylidyl-phosphenium **166** or amino/ylidyl phosphenium **167**, which are accessible via TMSCl elimination from ylide **165** upon reaction with $PCl_3$ (Scheme 49).[167,169]

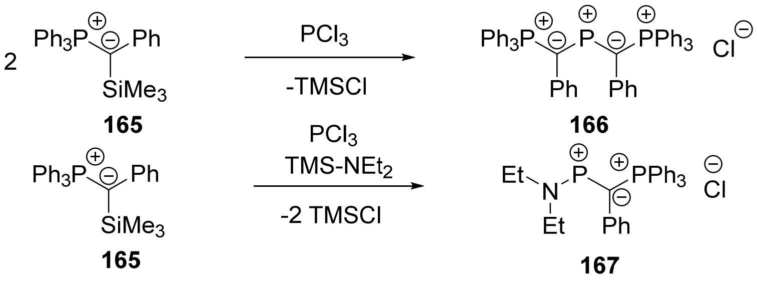
2
Ph3P Ph
SiMe3
165
PCl3
-TMSCl
Ph3P P PPh3 Cl
Ph Ph
166
Ph3P Ph
SiMe3
165
PCl3
TMS-NEt2
-2 TMSCl
Et N P PPh3 Cl
Et Ph
167

**Scheme 49.** Synthesis of phosphenium cations **166/167** via TMSCl elimination upon reaction of **165** with $PCl_3$.

The resulting cationic, divalent phosphorus compounds, so-called phosphenium cations, are isoelectronic to carbenes and thus highly interesting species. Similar to carbenes, phosphenium ions can acts as $\sigma$-donors and $\pi$-acceptors.[170] However, the donating ability is strongly reduced, caused by the overall positive charge (Figure 24). Depending on the substitution pattern, the positive charge is either mainly localized on the phosphorus atom, e.g. in 2-phosphaallyl-cations[171], its substituents, like diamino-phosphenium cations[172], or distributed over the whole ligand framework, as for instance observed in cyclic diylide-phosphenium cations.[173]

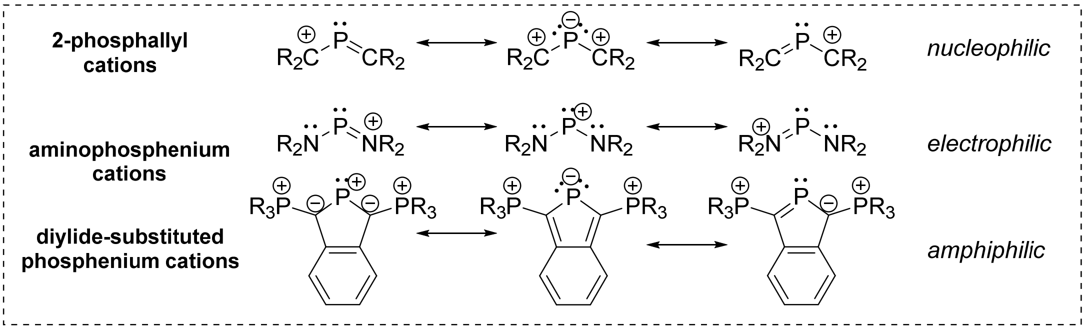
2-phosphallyl cations
R2C P CR2
nucleophilic
aminophosphenium cations
R2N P NR2
electrophilic
diylide-substituted phosphenium cations
R3P P PR3
amphiphilic

**Figure 24.** Overview of differently substituted phosphenium cations and their electronic behavior.[174]

Therefore, according to the ligand design, phosphenium ions can be either classified as rather nucleophilic, electrophilic or as amphiphilic species. As such, this special class of carbene analogues exhibits a diverse chemistry. However, while reactions with simple Lewis bases and the coordination chemistry of especially diamino-substituted phosphenium ions is well explored[174,175], the ability of phosphenium cations to perform bond activation reactions is still in its infancy.[176] In this regard, the chemistry of ylide-substituted phosphenium cations is lacking reports and thus remains highly underexplored, providing space for future research. It is noteworthy to mention that also heavier analogues of phosphenium cations are known, e.g. arsenium cations such as **168** were reported.[177]

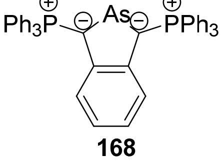

**168**

**Figure 25.** Reported example of a di-ylide substituted arsenium ion.

However, further reports on the reactivity of arsenium ions like **168** were not provided.

# 2. Aims of this thesis

Ylides are a unique class of carbon bases and their potential as $\sigma$- and $\pi$-donating ligands for the stabilization of low-valent main group species was only recently recognized. Despite the fact that several ylide functionalized low-valent main group compounds could be isolated successfully, their synthesis is often complex and requires multi-step procedures to reach the target species. *Gessner* et al. where the first to overcome this issue by applying $\alpha$-metalated ylides (like **71-Na**) in salt-metathesis procedures (e.g. with $GeCl_2$·dioxane), leading directly to low-valent main group compounds (for instance **158**). However, due to the incorporation of labile P–C($sp^2$) and C–H($sp^2$) bonds in the ligand design, activation reactions were observed during further studies in main-group chemistry and homogeneous catalysis, which limits the use of these compounds.

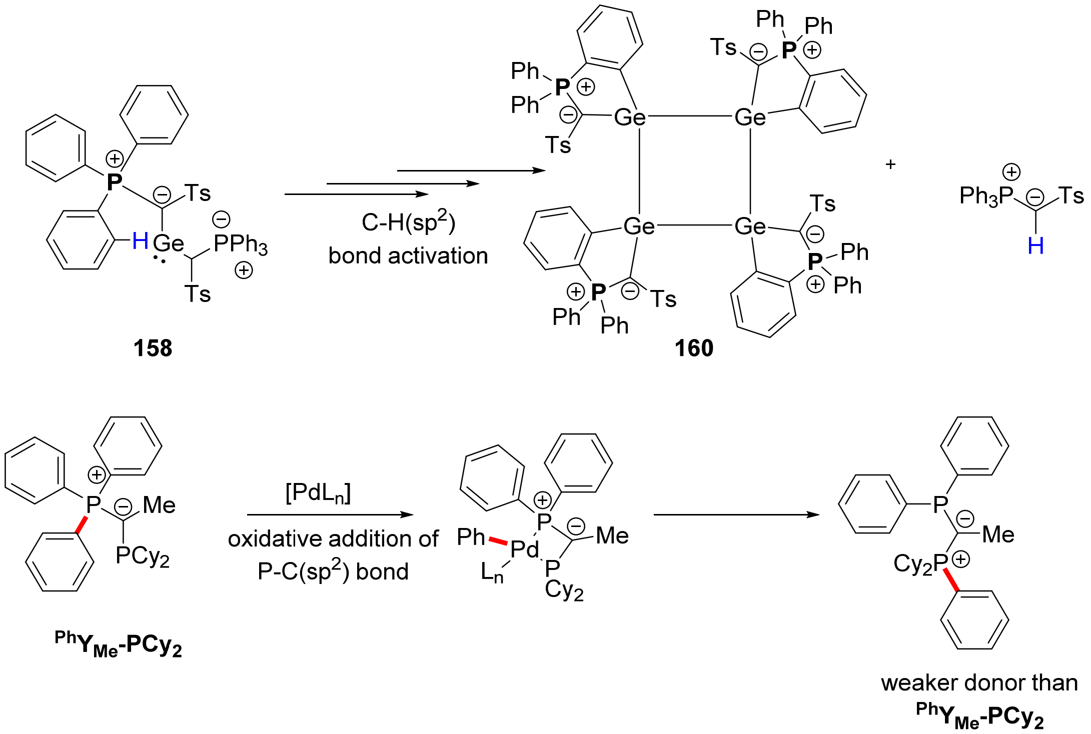

**Scheme 50.** Observed bond activation reactions of triphenylphosphonium-based ylidic compounds that permit the further use of ylide-functionalized species in low-valent main group chemistry[166] (top) and homogeneous catalysis[28] (bottom).

To overcome this issue and to further exploit the potential of yldiides as stabilizing ligands for low-valent main group species, the synthesis of a more stable metalated ylide should be explored. For instance, replacing the triphenylphosphonium group in **71-Na**, with a tricyclohexylphosphonium moiety, should lead to a stability increase, caused by stronger C–P($sp^3$) and C–H($sp^3$) bonds. That said, the first aim of this thesis is the synthesis, isolation and characterization of **$^{Cy}$Y-M** (M = Li, Na, K), the tricyclohexyl-phosphonium analogue of **71-M**.

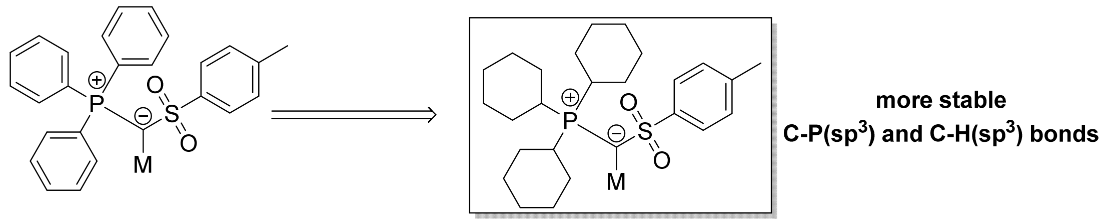

more stable
C-P(sp$^3$) and C-H(sp$^3$) bonds

**71-M**

**$^{Cy}$Y-M**
M = Li, Na, K

**Figure 26.** Substitution of the triphenylphosphonium group in **71-M** with a tricyclohexyl-moiety (**$^{Cy}$Y-M**) should result in a stability increase.

After successful synthesis, **$^{Cy}$Y-M** should be applied as a stabilizing ligand for low-valent main group species, with focus on group 14. For instance, the di-ylide stabilized tetrylenes **$^{Cy}$Y$_2$E** (E = Si, Ge, Sn) should be synthesized via salt-metathesis from suitable E(II) dihalide precursors.

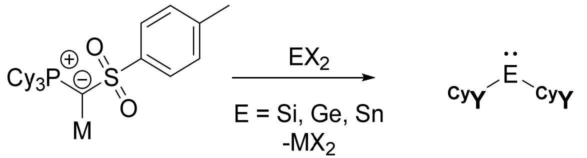

**$^{Cy}$Y-M**
M = Li, Na, K

**Scheme 51.** Preparation of di-ylide functionalized tetrylenes via salt-metathesis reactions of **$^{Cy}$Y-M** with respective element(II) halides.

In addition, the novel tetrylenes should be fully characterized, and their electronic properties should be elucidated via DFT methods. Since these tetrylenes are expected to be strongly electron-donating, their ability to form homo-and heterometallic group 14 donor-acceptor complexes as well as respective cationic species should be explored. Next, their reactivity towards different small molecules (CO, CO$_2$, H$_2$) should be probed.

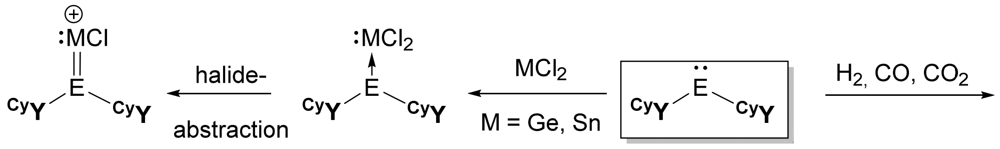

**$^{Cy}$Y$_2$E**
E = Si, Ge, Sn

**Scheme 52.** Planned reactivity studies of the di-ylide tetrylenes **$^{Cy}$Y$_2$E** with MCl$_2$ (M = Ge, Sn) to get access to heavier vinyl-analogues via halide abstraction from tetrylene stabilized dichloro-metal complexes (left) and bond-activation chemistry (right).

As already described earlier, transition metal complexes bearing YPhos ligands exhibit remarkable activities in different organic transformations. Thus, to further explore structure-reactivity relations in YPhos TM-based homogeneous catalysis, **$^{Cy}$Y-M** should be used for the synthesis of novel highly electron-rich phosphines. The isolated **$^{Cy}$YPhos** ligands should be fully characterized and their electronic- and steric properties should be determined via state-of-the art methods. Subsequently, **$^{Cy}$YPhos** should be applied in the preparation of well-defined transition-metal complexes and their potential as catalysts should be probed. Gold and palladium complexes are of special interest, since related YPhos systems showed high reactivities in Au(I)- and Pd(0) catalyzed organic transformations.

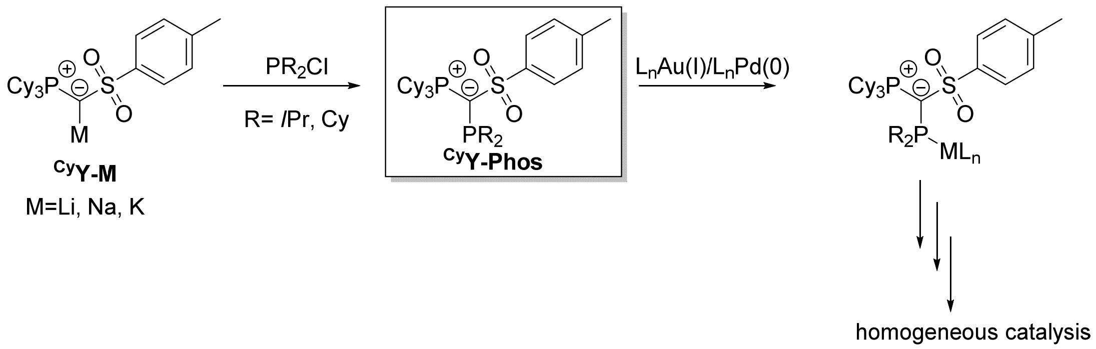
Cy3P
M
CyY-M
M=Li, Na, K
PR2Cl
R= iPr, Cy
PR2
CyY-Phos
LnAu(I)/LnPd(0)
R2P
MLn
homogeneous catalysis

**Scheme 53.** Planned synthesis of ylide-functionalized phosphines and their use as ligands for homogeneous catalysis.

Furthermore, their catalytic ability should be compared to related YPhos systems, enabling direct structure-reactivity correlations and hence the optimization of future YPhos ligand design.

# 3. Results and Discussion

The results of this thesis are presented in a semi-cumulative approach. Original, peer-reviewed publications or manuscript drafts will be presented here and the contribution of the respective authors towards the presented work is given in detail. Additional, unpublished results on the same/or a related topic will be given in an extra chapter right after the publications. Tags, labels and numbering of compounds are decoupled from the introductory section and only consistent within a specific research chapter.

## 3.1 Synthesis, Isolation and Crystal Structures of the Metalated Ylides [$Cy_3$P-C-$SO_2$Tol]M (M = Li, Na, K)

| | |
|---|---|
| Title: | "Synthesis, Isolation and Crystal Structures of the Metalated Ylides [$Cy_3$P-C-$SO_2$Tol]M (M = Li, Na, K)" |
| Publishing Status: | published online, Full Article |
| Publisher: | Wiley VCH |
| Journal: | Zeitschrift für Anorganische und Allgemeine Chemie |
| DOI: | 10.1002/zaac.201900333 |
| Authors: | Heidar Darmandeh, Thorsten Scherpf, Kai-Stephan Feichtner, Christopher Schwarz and Viktoria H. Gessner* |

Contribution: H. Darmandeh planned and executed all experimental work and wrote the manuscript. T. Scherpf, K.-S. Feichtner and C. Schwarz did the XRD measurements. V.H. Gessner finalized the manuscript and supervised all the performed work.

Journal of Inorganic and General Chemistry
ZAAC
Zeitschrift für anorganische und allgemeine Chemie
DOI: 10.1002/zaac.201900333
ARTICLE

# Synthesis, Isolation, and Crystal Structures of the Metalated Ylides $[Cy_3P\text{-}C\text{-}SO_2Tol]M$ (M = Li, Na, K)

Heidar Darmandeh,[a] Thorsten Scherpf,[a] Kai-Stephan Feichtner,[a] Christopher Schwarz,[a] and
Viktoria H. Gessner*[a]

*Dedicated to Manfred Scheer on Occasion of his 65th Birthday*

**Abstract**. The preparation and isolation of the metalated ylides $[Cy_3PCSO_2Tol]M$ ($^{Cy}$**1-M**) (with M = Li, Na, K) are reported. In contrast to its triphenylphosphonium analogue the synthesis of $^{Cy}$**1-M** revealed to be less straight forward. Synthetic routes to the phosphonium salt precursor $^{Cy}$**1-H$_2$** via different methods revealed to be unsuccessful or low-yielding. However, nucleophilic attack of the ylide $Cy_3P = CH_2$ at toluenesulfonyl fluoride under basic conditions proved to be a high-yielding method directly leading to the ylide $^{Cy}$**1-H**. Metalation to the yldiides was finally achieved with strong bases such as *n*BuLi, $NaNH_2$, or BnK. In the solid state, the lithium compound forms a tetrameric structure consisting of a $(C–S–O–Li)_4$ macrocycle, which incorporates an additional molecule of lithium iodide. The potassium compound forms a $C_4$-symmetric structure with a $(K_4O_4)_2$ octahedral prism as central structural motif. Upon deprotonation the P–C–S linkage undergoes a remarkable contraction typical for metalated ylides.

## Introduction

Since the first synthesis of an ylide more than one century ago and the pioneering work by *Wittig*, *Staudinger* and others,[1] ylides have become an important class of reagents. They are nowadays routinely used in organic synthesis in a variety of transformations, as well as in catalysis, e.g. as group transfer reagents, or as ligands in coordination chemistry.[2] Besides simple ylides, also their metalated congeners, the so-called yldiides, have early been discussed and applied in synthesis.,[3,4] For example, *Corey* reported on an enhanced reactivity of yldiides in Wittig reactions with hindered ketones,[5] while *Bestmann* demonstrated their potential in a number of cascade reactions, such as for the syntheses of alkynes and carbacycles.[6] Despite these early reports in the 1980s, their isolation was for a long time limited to very few examples.[6a] This is mostly due to the high reactivity of metalated ylides, which is strongly connected with the high charge concentration at the ylidic carbon atom.

Until today, only five metalated ylides have been isolated and also structurally characterized (Figure 1),[7] whereat only **1-M**[8] and **2-M**[9] (with M = Li, Na, K) have been prepared in gram-scale and applied in synthesis. For example, our group demonstrated that **1-M** and **2-M** are excellent reagents for ylide-functionalizations,[10] which represents a powerful tool for the electronic manipulation of main group compounds.,[11,12] As such, electron-deficient species like borenium ions and tetrylenes were successfully isolated starting from **1-Na**.[13] Likewise, a series of ylide-substituted phosphines were prepared which turned out to be excellent ligands for homogeneous catalysis.[14]

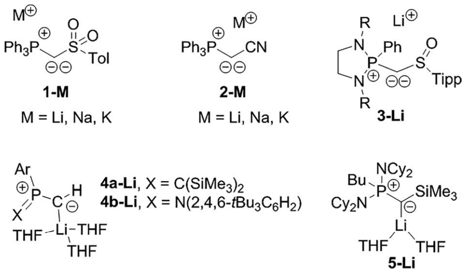

**Figure 1**. Isolated and structurally characterized metalated ylides.

During our studies on the use of **1-M** in main group chemistry we observed the C–H activation at one of the phenyl groups of the phosphonium moiety as side-reaction leading to the protonation and subsequently to the cleavage of an ylide ligand from the main group metal.[13a] In order to further exploit the use of metalated ylides for the stabilization of reactive compounds we thus became interested in replacing the $PPh_3$ moiety by a tricyclohexyl phosphonium moiety which should less tend to undergo any CH activation processes and hence lead

---

* Prof. Dr. V. H. Gessner
E-Mail: viktoria.gessner@rub.de
[a] Chair of Inorganic Chemistry II
Faculty of Chemistry and Biochemistry
Ruhr University Bochum
Universitätsstrasse 150
44780 Bochum, Germany

Supporting information for this article is available on the WWW under **http://dx.doi.org/10.1002/zaac.201900333** or from the author.

© 2020 The Authors. Published by Wiley-VCH Verlag GmbH & Co. KGaA. • This is an open access article under the terms of the Creative Commons Attribution-NonCommercial License, which permits use, distribution and reproduction in any medium, provided the original work is properly cited and is not used for commercial purposes.

to more stable products. Here, we report on the preparation of $^{\mathrm{Cy}}$**1-M**, the cyclohexyl derivative of **1-M**. Despite this rather small change in the molecular structure the synthesis of $^{\mathrm{Cy}}$**1-M** turned out to be surprisingly more difficult than expected.

## Results and Discussion

For the preparation of $^{\mathrm{Cy}}$**1-M**, we at first addressed a synthetic route analogous to that reported for the $PPh_3$ system.[8] Thus, tricyclohexylphosphine and (iodomethyl)tolylsulfone were reacted at different temperatures to access the phosphonium salt $^{\mathrm{Cy}}$**1-H$_2$** in the first reaction step (Route A, Scheme 1). However, in contrast to the phenyl compound no selective formation of $^{\mathrm{Cy}}$**1-H$_2$** was observed due to several competing side-reactions such as reduction of the sulfonyl group, oxidation of $PCy_3$ and deprotonation by the more basic $PCy_3$. This reaction was observed under different reaction conditions (in $C_6D_6$ or without solvent; at 60 °C or room temperature). Likewise, reaction of the halo phosphonium salts $[Cy_3PX]X$ (with X = Br, I) with lithiated methyl(*p*-tolyl)sulfone proved to be unsuccessful (Route C). No product formation was observed by NMR spectroscopy. In contrast, treatment of the (iodomethyl)phosphonium salt with sodium sulfinate (Route B) delivered the desired phosphonium salt $^{\mathrm{Cy}}$**1-H$_2$**, albeit only in small quantities together with a series of by-products. Due to the low nucleophilicity of the sulfinate harsh reaction conditions in refluxing DMF or DMSO were necessary to observe detectable amounts of $^{\mathrm{Cy}}$**1-H$_2$**. Albeit $^{\mathrm{Cy}}$**1-H$_2$** could be isolated in pure form by this method and spectroscopically as well as structurally characterized (see below), it was impossible to further improve the reaction to reliably yield sufficient amounts of $^{\mathrm{Cy}}$**1-H$_2$** for further synthesis.

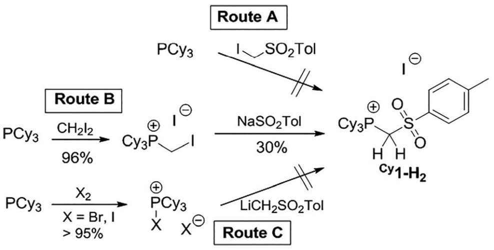

**Scheme 1.** Examined pathways for the synthesis of the tricyclohexylphosphonium salt $^{\mathrm{Cy}}$**1-H$_2$**.

In order to obtain high quantities of the ylide precursor for its metalation we turned our attention towards a further synthetic pathway, the nucleophilic attack of the methylenephosphorane, $Cy_3PCH_2$, on a suitable sulfonyl electrophile (Scheme 2). To this end, tricyclohexylphosphonium methylide, $Cy_3PCH_2$, was in situ formed from $[Cy_3PMe]I$ and sodium hexamethyldisilazide (NaHMDS) and subsequently treated with tosyl fluoride. Sulfonyl fluorides have proven to be excellent electrophiles for the formation of C–S bonds.[15,17] NMR spectroscopic studies of the reaction mixture revealed the direct formation of ylide $^{\mathrm{Cy}}$**1-H** under the reaction conditions since ylide $Cy_3P{=}CH_2$ simultaneously acts as reagent as well as base and deprotonates the initially formed phosphonium salt $^{\mathrm{Cy}}$**1-H$_2$** thus yielding $^{\mathrm{Cy}}$**1-H** and $[Cy_3PMe]F$. Therefore, under optimized conditions $Cy_3PCH_2$ was treated with one equiv. of tosyl fluoride in the presence of a further equiv. NaHMDS to prevent the reformation of $[Cy_3PMe]F$. Thus, $^{\mathrm{Cy}}$**1-H** could be obtained in only one reaction step as colorless solid in excellent yields of 90 %. $^{\mathrm{Cy}}$**1-H** was characterized by NMR and IR spectroscopy as well as XRD and elemental analysis. The ylide exhibits a singlet at $\delta_P = 26.8$ ppm in the $^{31}P\{^1H\}$ NMR spectrum and a doublet at $\delta_H = 1.86$ ppm with a coupling constant of $^2J_{PC} = 8.4$ Hz in the $^1H$ NMR spectrum. The $^{13}C\{^1H\}$ NMR signal of the ylidic carbon appears at $\delta = 26.1$ ppm with a large $^1J_{PC}$ coupling constant of 105 Hz (cf. 44.5 ppm; $^1J_{CP} = 31.3$ Hz in $^{\mathrm{Cy}}$**1–H$_2$**), which is in line with the increased s-character in the P–C bond of $^{\mathrm{Cy}}$**1-H** compared to the phosphonium salt precursor $^{\mathrm{Cy}}$**1–H$_2$**. This is also reflected in the larger P–C–S angle in the molecular structure (Figure 2, Table 1) of $^{\mathrm{Cy}}$**1-H** (127.63(19)°] compared to that observed in $^{\mathrm{Cy}}$**1-H$_2$** [117.85(9)°].

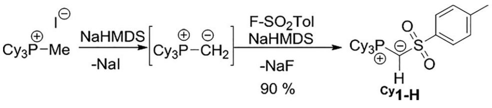

**Scheme 2.** Preparation of ylide $^{\mathrm{Cy}}$**1-H**.

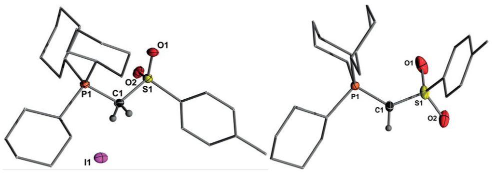

**Figure 2.** Molecular structures of phosphonium salt $^{\mathrm{Cy}}$**1-H$_2$** and ylide $^{\mathrm{Cy}}$**1-H**. Thermal ellipsoids at the 50 % probability level. Selected bond lengths and angles are given in Table 1. Crystallographic details are given in the Supporting Information.

With ylide $^{\mathrm{Cy}}$**1-H** in hand, we next attempted its metalation to $^{\mathrm{Cy}}$**1-M**. At first, alkali metal HMDS bases were tested which were successfully applied to access the $PPh_3$ analogue **1-M**. However, no reaction was observed with $^{\mathrm{Cy}}$**1-H** even after a prolonged reaction time. This suggests, that the more electron-rich $PCy_3$ unit significantly lowers the CH acidity of the ylide. Accordingly, stronger metal bases were tested. Indeed, monitoring of the metalation reaction by $^{31}P\{^1H\}$ NMR spectroscopy revealed the successful formation of the different alkali metal yldiides $^{\mathrm{Cy}}$**1-M**, when using *n*-butyllithium, benzyl potassium (BnK), and sodium amide, respectively (Scheme 3). The formation of the alkali metal yldiides is evidenced by a distinct high-field shift of the signal in the $^{31}P\{^1H\}$ NMR spectrum compared to the ylide precursor $^{\mathrm{Cy}}$**1-H** (Table 1). For example, addition of BnK or $NaNH_2$ gave rise to a broad singlet at 3.2 ppm and 6.1 ppm, respectively (cf. 26.7 ppm for $^{\mathrm{Cy}}$**1-H**). Albeit all reactions were highly selective as judged by NMR

© 2020 The Authors. Published by WILEY-VCH Verlag GmbH & Co. KGaA, Weinheim

**Table 1**. Important NMR spectroscopic and crystallographic properties of **$^{Cy}$1-H$_2$**, **$^{Cy}$1-H**, and its metalated congeners **$^{Cy}$1-Li** and **$^{Cy}$1-K**.

| | **$^{Cy}$1-H$_2$** | **$^{Cy}$1-H** | **[$^{Cy}$1-Li]$_4$·LiI** | **[$^{Cy}$1-K]$_8$** |
|---|---|---|---|---|
| P–C1 /Å | 1.8279(17) | 1.718(3) | 1.676(2) | 1.669(6) |
| S–C1 /Å | 1.7846(17) | 1.662(3) | 1.602(2) | 1.591(6) |
| S–O1 /Å | 1.4423(13) | 1.450(3) | 1.4800(18) | 1.494(4) |
| S–O2 /Å | 1.4381(13) | 1.451(3) | 1.4953(16) | 1.471(4) |
| P–$C_{Cy}$ $^{a)}$ /Å | 1.8237(12) | 1.836(8) | 1.855(16) | 1.850(6) |
| M-C1 /Å | – | – | 2.159(5) | 2.906(6) |
| P–C1–S /° | 117.85(9) | 127.63(19) | 127.48(15) | 127.20(4) |
| $\delta$ = $^{31}$P /ppm | 35.4 | 26.8 | 10.1 | 3.1 |

a) Average values.

studies, isolation turned out to be most facile for the lithium and the potassium compound. Reaction of a suspension of **$^{Cy}$1-H** in *n*-pentane with one equiv. *n*BuLi yielded the highly soluble **$^{Cy}$1-Li**, which can easily be purified by filtration from the insoluble starting materials and thus could be isolated as yellow solid in 90 % yield. **$^{Cy}$1-Li** was characterized by multinuclear NMR spectroscopy, elemental and XRD analysis. The $^{7}$Li NMR signal appears as broad singlet at 0.6 ppm, the $^{31}$P NMR signal at $\delta$ = 10.1 ppm and is thus the most downfield shifted signal in the whole series of the alkali metal yldiides **$^{Cy}$1-M**. The potassium compound **$^{Cy}$1-K** could also be isolated as pure solid in excellent yields of up to 98 %.

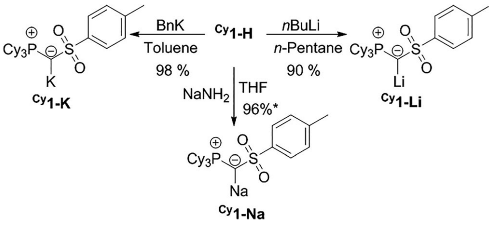

**Scheme 3.** Metalation of **$^{Cy}$1-H** with alkali metal bases to **$^{Cy}$1-M** (M = Li, Na, K) (* = NMR yield).

Single crystals of **$^{Cy}$1-Li** were grown by slow vapor diffusion of *n*-pentane into a saturated THF solution of the yldiide at –30 °C and analyzed by XRD techniques. The yldiide crystallizes in the tetragonal space group $P4_2/n$ (Figure 3) as a $S_4$ symmetric tetramer with an additional molecule of lithium iodide (present from the synthesis of **$^{Cy}$1-H** via route B).[16] The monomeric subunit (asymmetric unit) consists of one yldiide, in which the lithium ion is coordinated by the ylidic carbon atom, one oxygen of the sulfonyl group and a THF molecule. Aggregation of the monomers to the tetramer is realized through the coordination of the second oxygen atom of the sulfonyl moiety, which bridges the lithium ions of monomeric subunits. Thus, a highly symmetric (C–S–O–Li)$_4$ macrocycle is formed (Figure 4), whose outer sphere is fully covered by the coordinating THF molecules and phosphonium groups. This structure is most probably responsible for the high solubility of the compound also in hydrocarbon solvents, since the polar moieties of the complex are well covered in the inner core of the structure. In this context it is interesting to note that the macrocycle itself adopts not a planar but a bowl-like geometry. The additional lithium ion Li2 is complexed in the center of the resulting pocket and lies on the $S_4$ axis of the molecule.

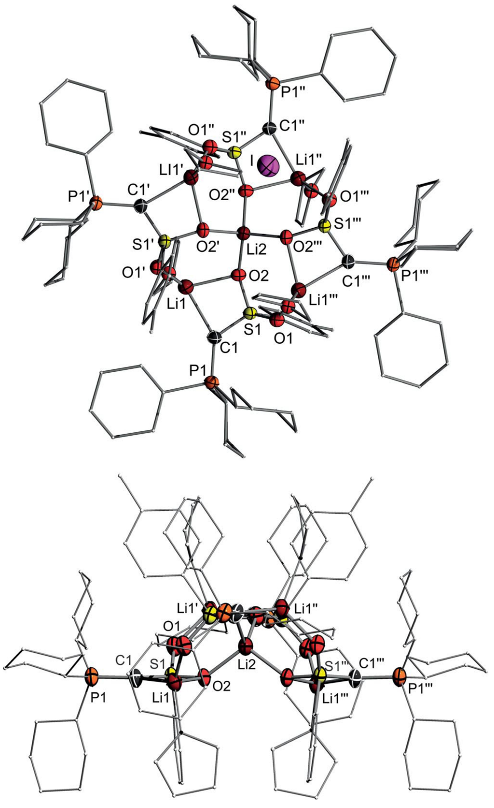

**Figure 3.** Molecular structure of (**$^{Cy}$1-Li**)$_4$·LiI·4THF. (Top) Top view, (bottom) side view; the counter-anion is not shown. Ellipsoids at the 50 % probability level. Selected bond lengths /Å and angles /°: Li1–C1 2.159(5) Å; Li1–O2 2.022(5), Li1–O1' 1.875(5), Li2–O2 1.9354(15). S1–C1–P1 127.48(15), S1–C1–Li1 86.07(15), P1–C1-Li 146.41(18). Further structure parameters are provided in Table 1, crystallographic details are given in the Supporting Information.

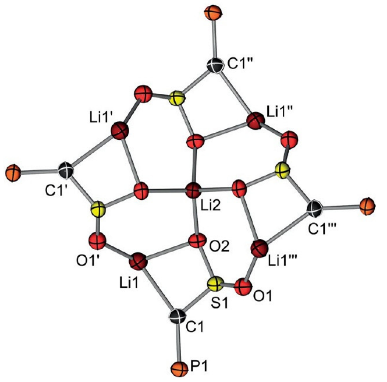

**Figure 4.** Drawing of the inner core of the structure of $^{\mathrm{Cy}}$**1-Li**.

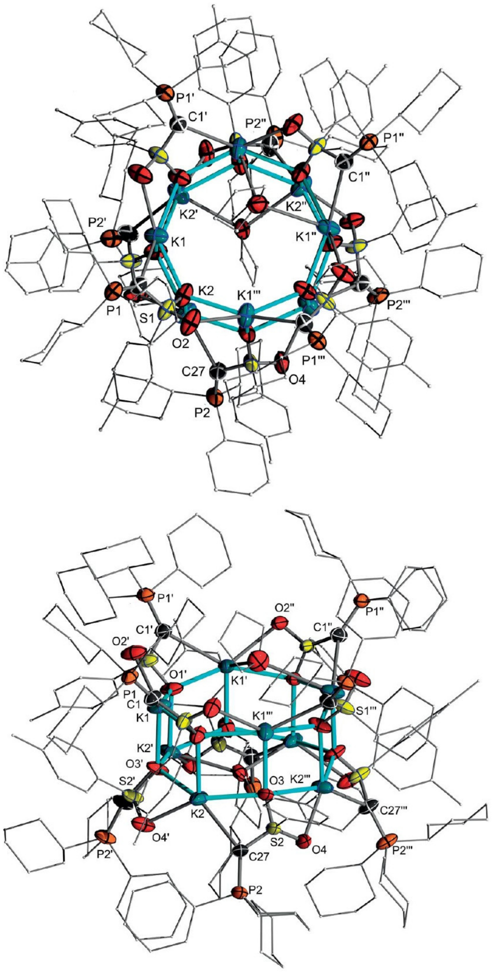

**Figure 5.** Molecular structure of [($^{\mathrm{Cy}}$**1-K**)$_8$·2THF]. (Top) side view, (bottom) top view. Ellipsoids at the 50 % probability level. Non-coordinating THF solvent molecules as well as disordered moieties are omitted for clarity. Selected bond lengths /Å and angles /°: K1–C1 2.906(6), K2–C27 2.906(6), K1–O3 2.672(4), K1–O1 2.709(4), K1–O1' 2.764(4), K1–O2' 2.767(5). Further structure parameters are provided in Table 1, crystallographic details are given in the Supporting Information.

In the molecular structure of $^{\mathrm{Cy}}$**1-Li**, the ylidic carbon atom C1 adopts a planar arrangement with an ideal sum of angles of 360.0(2)°. The C1–Li1 distance amounts to 2.159(5) Å and is thus in the typical range for organolithium aggregates.[17] A comparison of the important bond lengths and angles in $^{\mathrm{Cy}}$**1-Li** in comparison to its protonated precursors is given in Table 1. As already observed for yldiide **1-K**, the central P–C–S linkage undergoes a remarkably contraction upon each deprotonation step due to increased electrostatic attractions with increasing charge at the central carbon atom. The S–C and P–C bonds thus shorten from 1.785(2) and 1.828(1) Å in $^{\mathrm{Cy}}$**1–H$_2$** to 1.602(2) and 1.676(2) Å in $^{\mathrm{Cy}}$**1-Li**. Likewise, the S–O and P–C$_{\mathrm{Cy}}$ bonds lengthen slightly because of negative hyperconjugation effects. Furthermore, the P-C-S angle widens from 117.9(1)° in the phosphonium salt to 127.6(2)° in the yldiide indicating an increase of s-character upon deprotonation, which is retained after the second deprotonation.

Overall, the changes in the bond lengths and angles in $^{\mathrm{Cy}}$**1-Li** relative to its protonated precursors is similar to the trends observed for the PPh$_3$-substituted compounds.[8] However, it is interesting to note that in comparison to the PPh$_3$-substituted compounds, the S–C bonds in the PCy$_3$-substituted compounds are shorter by approx. 20–30 pm. This can be explained by the lower ability of the PCy$_3$ compared to the PPh$_3$ group to stabilize the negative charge at the ylidic carbon atom by electrostatic and negative hyperconjugation effects. Therefore, the electrostatic attraction in the C-S linkage increases and hence the bond shortens.

Besides the structure of the lithium yldiide we also attempted the elucidation of structure of the potassium and sodium compound. While no crystals of sufficient quality could be obtained for $^{\mathrm{Cy}}$**1-Na**, single-crystals of $^{\mathrm{Cy}}$**1-K** could be obtained by storage of a saturated THF solution at –30 °C. $^{\mathrm{Cy}}$**1-K** crystallizes as *C*4-symmetric octamer in the tetragonal space group *P*4/n with two additional THF molecules on the *C*4 axis (only one orientation shown in Figure 5).[18] Unfortunately, the quality of the crystals was rather low due to highly disordered solvent molecules (see ESI). However, the trends in the bond lengths are similar to those observed for the lithium compound discussed above (Table 1).

The central structural motif of $^{\mathrm{Cy}}$**1-K** consists of an octagonal prism formed by the potassium and oxygen atoms of the sulfonyl group with K–O distances between 2.672(4) and 2.767(5) Å (Figure 6). The O–K–O angles amount to approx. 83.4(1)° within each $K_2O_2$ face and to approx. 133° between the faces. Each potassium atom is coordinated by the ylidic carbon atom, four oxygens of the sulfonyl groups as well as by the two loosely bound THF molecules on top and below the octahedral prism and weak C-H interactions with the cyclohexyl moieties (not shown in Figure 4). The P–C and S–C bonds are shortened compared to the ylide and the phosphonium salt and in the range of those found in the lithium compound $^{Cy}$**1-Li**.

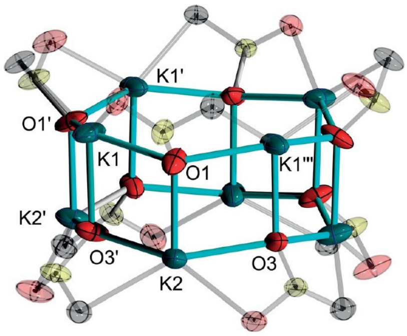

Figure 6. Drawing of the inner core of the structure of $^{Cy}$**1-K**.

## Conclusions

In conclusion, we have successfully developed a synthetic protocol for the high-yielding isolation of the tricyclohexylphosphonium-substituted metalated ylides $[Cy_3PCSO_2Tol]M$ ($^{Cy}$**1-M**) (with M = Li, Na, K). The synthesis was accomplished by reaction of tricyclohexylphosphonium methylide with tosyl fluoride under basic conditions thus directly forming the ylide precursor $^{Cy}$**1-H**, which was subsequently deprotonated with strong metal bases. This deprotonation was found to be considerably less facile than in case of the $PPh_3$ analogue thus demonstrating the pronounced acidifying properties of a $PPh_3$ moiety compared to the $PCy_3$ unit. The molecular structures of the lithium and potassium yldiide could be elucidated by XRD analysis. In the solid state, $^{Cy}$**1-Li** forms a $S_4$-symmetric tetrameric structure with one additional lithium iodide molecule, while $^{Cy}$**1-K** exhibits a $C_4$ symmetric structure with an octahedral prism as central structural motif. In the structures, the central P–C and S–C bonds are shortened compared to the ylide precursor due to electrostatic interactions. Current studies are focusing on the application of the yldiide in main group chemistry.

## Experimental Section

**Experimental Details:** Details regarding the synthesis of $^{Cy}$**1-H$_2$** via route A, B and C are given in the Supporting Information.

**General Methods:** All experiments were carried out in a dry, oxygen-free argon atmosphere using standard Schlenk techniques. Involved solvents were dried using an MBraun SPS-800 (THF, Toluene, $Et_2O$, DCM, *n*-Pentane, *n*-Hexane) or dried in accordance with standard procedures. $^1H$, $^{13}C\{^1H\}$, $^{31}P\{^1H\}$, $^7Li$ NMR spectra were recorded on Avance-500 or Avance-400 spectrometers at 25 °C if not stated otherwise. All values of the chemical shift are in ppm regarding the $\delta$-scale. All spin-spin coupling constants (*J*) are printed in Hertz (Hz). To display multiplicities and signal forms correctly the following abbreviations were used: s = singlet, d = doublet, m = multiplet, br = broad signal. Signal assignment was supported by DEPT, APT, HSQC and HMBC experiments. Elemental analyses were performed on an Elementar vario MICRO-cube elemental analyzer.

**Synthesis of [Cy$_3$P-Me]I:** Tricyclohexylphosphine (16.00 g, 57.05 mmol, 1.00 equiv.) was dissolved in toluene (200 mL). Methyl iodide (3.8 mL, 61.05 mmol, 1.07 equiv.) was added dropwise to the solution at room temp. During the addition, a white solid precipitated out of the solution. The reaction mixture was stirred at room temperature until full precipitation was achieved (2 h). Next, the suspension was filtered and washed with $Et_2O$ (3 × 10 mL). The solid was dried in vacuo ($1 \times 10^{-3}$ mbar) for 4 h, giving $[Cy_3P\text{-}Me]I$ as a white, amorphous powder (98 %, 23.50 g). **$^1$H NMR** ($CD_2Cl_2$, 400 MHz): $\delta$ = 2.5 (m, 3 H, PCy-CH), 2.0–1.9 (m, 11 H, PCy-$CH_2$), 1.9 (d, *J* = 12.1 Hz, 3 H, $CH_3$), 1.8–1.8 (m, 3 H, PCy-$CH_2$), 1.6–1.2 (m, 16 H, PCy-$CH_2$) ppm. **$^{31}$P{$^1$H} NMR** ($CD_2Cl_2$, 161.9 MHz): $\delta$ = 33.7 (s) ppm. The obtained signals are in accordance with literature values.[19]

**Synthesis of $^{Cy}$1-H:** $[Cy_3P\text{-}Me]I$ (10.00 g, 23.68 mmol, 1.00 equiv.) and NaHMDS (8.77 g, 47.82 mmol, 2.02 equiv.) were placed in a 500 mL Schlenk flask. THF (150 mL) was added, giving a white suspension which was stirred for 30 min at room temp. In a second Schlenk flask, *p*-toluenesulfonyl fluoride (4.12 g, 23.68 mmol, 1.00 equiv.) was dissolved in THF (25 mL) and this solution was slowly added to the suspension via cannula, upon which a color change from white to a deep brown occurred. The reaction mixture was stirred overnight, and the solvent was removed in vacuo. The residue was taken up in a dichloromethane/toluene mixture (50 mL/250 mL) and the resulting suspension was subsequently filtered over celite to obtain a clear yellow solution. Removal of the solvent under reduced pressure yielded an off-white solid, which was washed with *n*-hexane (5 × 25 mL). After drying in vacuo ($1 \times 10^{-3}$ mbar) for 4 h at 70 °C, the pure product was obtained as a white solid (90 %, 9.80 g). **$^1$H NMR** ($CD_2Cl_2$,400 MHz): $\delta$ = 7.69 (d, $^2J_{HH}$ = 8.2 Hz, 2 H, *o*-CH), 7.18 (d, $^2J_{HH}$ = 7.9 Hz, 2 H, *m*-CH), 2.36 (s, 3 H), 2.27–2.09 (m, 3 H, $PCy_3$-CH), 1.86 (d, $^2J_{PH}$ = 8.4 Hz, 1 H, PCHS), 1.85–1.75 (m, 11 H, $PCy_3$–$CH_2$), 1.73–1.65 (m, 3 H, $PCy_3$–$CH_2$), 1.47–1.32 (m, 6 H, $PCy_3$–$CH_2$), 1.31–1.06 (m, 10 H, $PCy_3$–$CH_2$). **$^{13}$C{$^1$H} NMR** ($CD_2Cl_2$, 100.6 MHz): $\delta$ = 149.7 (*ipso*-C), 140.2 (*p*-C), 129.5 (*m*-CH), 125.5 (*o*-CH), 33.1 (d, $^2J_{CP}$ = 50.8 Hz, $PCy_3$-CH), 27.8 (d, $^3J_{CP}$ = 3.1 Hz, $PCy_3$–$CH_2$), 27.6 (d, $^2J_{CP}$ = 12.3 Hz, $PCy_3$–$CH_2$), 26.5 (d, $^4J_{CP}$ = 1.6 Hz, $PCy_3$–$CH_2$), 26.1 (d, $^2J_{PH}$ = 105 Hz, PCS), 21.6 (*p*-Tol-$CH_3$). **$^{31}$P{$^1$H} NMR** ($CD_2Cl_2$, 161.9 MHz): $\delta$ = 26.8 (s) ppm. EA: calcd: C: 69.61, H: 9.21, S: 7.15 %, found C 69.26, H: 9.04, S: 7.38 %.

**Synthesis of $^{Cy}$1-Li: $^{Cy}$1-H** (3.63 g, 8.09 mmol, 1.0 equiv.) was suspended in *n*-pentane (100 mL). *n*BuLi (1.53 M in hexanes, 5.29 mL, 1.0 equiv.) was added dropwise to the suspension at 0 °C. The reaction mixture was warmed to room temp. and stirred for 1 h. The suspension was filtered via cannula furnishing a yellow solution. Removal of the solvent under reduced pressure and drying in vacuo ($1 \times 10^{-3}$ mbar) for 4 h at 40 °C afforded $^{Cy}$**1-Li** as a yellow powder (90 %, 3.33 g). **$^1$H NMR** ([$D_8$]THF, 400 MHz): $\delta$ = 7.85 (d, $^2J_{HH}$ = 7.7 Hz, 2 H, *m*-CH), 6.96 (d, $^2J_{HH}$ = 7.7 Hz, 2 H, *o*-CH), 2.28 (s, 3 H, *p*-Tol-$CH_3$), 1.95–1.84 (m, 10 H, PCy-CH+CH$_2$), 1.70–1.65 (m, 6 H,, PCy-CH$_2$), 1.61–1.57 (m, 3 H,, PCy-CH$_2$), 1.43–1.38 (m, 4 H,, PCy-CH$_2$), 1.20–1.10 (m, 10 H,, PCy-CH$_2$). **$^{13}$C{$^1$H} NMR** ([D$_8$]THF, 100.6 MHz): $\delta$ = 155.5 (*ipso*-C), 137.1 (*p*-C) 128.4 (*m*-CH), 126.9 (*o*-CH), 36.9 (d, *J* = 52.8; PCy$_3$-CH), 28.7 (PCy$_3$–CH$_2$), 28.6 (d, *J* = 8.4, PCy$_3$–CH$_2$), 27.5 (PCy$_3$–CH$_2$), 21.4 (*p*-Tol-CH$_3$). The signal for the PCS bridge could not be observed. **$^{31}$P{$^1$H} NMR** ([D$_8$]THF,162 MHz): $\delta$ = 10.1 (s) ppm. **$^7$Li NMR** ([D$_8$]THF, 155.6 MHz): $\delta$ = 0.6 (s) ppm. EA: calcd.: C: 68.70, H: 8.87, S: 7.05 %; found: C: 68.73, H: 8.84, S: 7.03 %

**Synthesis of $^{Cy}$1-K:** Benzyl potassium (0.32 g, 2.45 mmol, 1.1 equiv.) and **$^{Cy}$1-H** (1.00 g, 2.22 mmol, 1.0 equiv.) were placed into a Schlenk tube and toluene (25 mL) was added. The red reaction mixture was stirred for 5 min at room temp. and was subsequently filtered via a filter cannula. A dark yellow solution was obtained. The solvent was removed under reduced pressure and the residue was dried in vacuo ($1 \times 10^{-3}$ mbar) for 3 h at 40 °C to yield $^{Cy}$Y$_S$-K as a dark yellow powder (98 %, 532 mg). Single crystals of **$^{Cy}$1-K** were grown by storage of a saturated THF solution at –30 °C. **$^1$H NMR** ([D$_8$]THF,400 MHz): $\delta$ = 7.79 (br., 2 H, *m*-CH), 6.91 (br., 2 H, *o*-CH), 2.28 (s, 3 H, *p*-Tol-CH$_3$), 1.87–1.75 (m, 8 H, PCy-CH+CH$_2$), 1.71–1.66 (m, 6 H, PCy-CH$_2$), 1.61–1.57 (m, 3 H, PCy-CH$_2$), 1.42–1.31 (m, 6 H, PCy-CH$_2$), 1.17–1.02 (m, 10 H, PCy-CH$_2$). **$^{13}$C{$^1$H} NMR** ([D$_8$]THF, 100.6 MHz): $\delta$ = 157.3 (*ipso*-C), 136.2 (*p*-C) 128.6 (*m*-CH), 126.3 (*o*-CH), 37.4 (d, *J* = 52.5 Hz; PCy$_3$-CH), 28.9 (PCy$_3$–CH$_2$), 28.8 (PCy$_3$–CH$_2$), 27.7 (PCy$_3$–CH$_2$), 21.5 (*p*-Tol-CH$_3$). The signal for PCS bridge could not be observed. **$^{31}$P{$^1$H} NMR** ([D$_8$]THF,162 MHz): $\delta$ = 3.2 (s, br) ppm. EA: calcd.: C: 64.16, H: 8.28, S: 6.59 %; found: C: 64.50, H: 8.30, S: 6.88 %.

**Synthesis of $^{Cy}$1-Na:** Sodium amide (5 mg, 128 µmol, 1.01 equiv.) and **$^{Cy}$1-H** (57 mg, 127 µmol, 1.0 equiv.) were placed into a J. Young NMR tube and [D$_8$]THF (0.5 mL) was added. The tube was shaken on an IKA® ROCKER 3D digital at room temp. overnight. $^{31}$P-NMR spectroscopy revealed full conversion of **$^{Cy}$1-H** and the formation of **$^{Cy}$1-Na** (ca. 96 %). Attempts to purify **$^{Cy}$1-Na** resulted in the instant protonation of the ylidic carbon atom. **$^1$H NMR** ([D$_8$]THF,400 MHz): $\delta$ = 7.80 (br., 2 H, *m*-CH), 6.90 (br., 2 H, *o*-CH), 2.27 (s, 3 H, *p*-Tol-CH$_3$), 1.86–1.78 (m, 8 H, PCy-CH+CH$_2$), 1.71–1.64 (m, 6 H, PCy-CH$_2$), 1.61–1.56 (m, 3 H, PCy-CH$_2$), 1.43–1.34 (m, 6 H, PCy-CH$_2$), 1.18–1.04 (m, 10 H, PCy-CH$_2$) ppm. **$^{31}$P{$^1$H} NMR** ([D$_8$]THF,162 MHz): $\delta$ = 6.1 (s, br) ppm.

**Single-crystal X-ray Diffraction Analyses:** Data collection of all compounds was conducted with Rigaku XtaLAB Synergy (**$^{Cy}$1-H, $^{Cy}$1-H, $^{Cy}$1-Li·LiI, $^{Cy}$1-K**). The structures were solved by direct methods, refined with the Shelx software package and expanded using Fourier techniques. The crystals of all compounds were mounted in inert oil (perfluoropolyalkylether). Crystal structure determinations were affected at 100 K. The structures were solved by direct methods, refined using full-matrix least-squares techniques on $F^2$ with the Shelx software package[20] and expanded using Fourier techniques. Data collection parameters are given in Tables S1 and S2 (Supporting Information).

Crystallographic data (excluding structure factors) for the structures in this paper have been deposited with the Cambridge Crystallographic Data Centre, CCDC, 12 Union Road, Cambridge CB21EZ, UK. Copies of the data can be obtained free of charge on quoting the depository numbers CCDC-1971569, CCDC-1971570, CCDC-1971571, and CCDC-1971572. (Fax: +44-1223-336-033; E-Mail: deposit@ccdc.cam.ac.uk, http://www.ccdc.cam.ac.uk)

**Supporting Information** (see footnote on the first page of this article): ■■ ((<=Author: please give a short description of the supporting information.)) ■■

## Acknowledgements

This project has received funding from the European Research Council under the European Union's Horizon 2020 research and innovation program(no 677749).

**Keywords:** Alkali metals; Ylides; Carbanions; Structure elucidation; Phosphorus ligands

## References

[1] a) A. Michaelis, H. Gimborn Hv, *Ber. Dtsch. Chem. Ges.* **1894**, *27*, 272; b) H. Staudinger, J. Meyer, *Helv. Chim. Acta* **1919**, *2*, 635; c) G. Wittig, C. Geissler, *Liebig Ann. Chem.* **1953**, *44*, 580; d) G. Wittig, *Science* **1980**, *210*, 600.
[2] For reviews, see: a) O. I. Kolodiazhnyi, *Phosphorus Ylides: Chemistry and Application* in *Organic Synthesis*, Wiley-VCH, **1999**; b) M. Alcarazo, *Struct. Bonding (Berlin)* **2018**, *177*, 25; c) R. Oost, J. D. Neuhaus, J. Merad, N. Maulide, *Struct. Bonding (Berlin)* **2018**, *177*, 73; d) S. Liu, W.-C. Chen, T.-G. Ong, *Struct. Bonding (Berlin)* **2018**, *177*, 51; e) A. C. B. Burtoloso, R. M. P. Dias, I. A. Leonarczyk, *Eur. J. Org. Chem.* **2013**, 5005; f) D. Kaiser, I. Klose, R. Oost, J. Neuhaus, N. Mulide, *Chem. Rev.* **2019**, *119*, 8701.
[3] H.-J. Cristau, *Chem. Rev.* **1994**, *94*, 1299.
[4] a) M. Schlosser, T. Kadibelban, G. Stanihoff, *Justus Liebigs Ann. Chem.* **1971**, *743*, 25; b) B. Schaub, T. Jenny, M. Schlosser, *Tetrahedron Lett.* **1984**, *25*, 4097; c) B. Schaub, M. Schlosser, *Tetrahedron Lett.* **1985**, *26*, 1623; d) R. S. Mc Dowell, A. Streitwieser, *J. Am. Chem. Soc.* **1984**, *106*, 4047.
[5] a) E. J. Corey, J. Kang, *J. Am. Chem. Soc.* **1982**, *104*, 4724; b) E. J. Corey, J. Kang, K. Kyler, *Tetrahedron Lett.* **1985**, *26*, 555; c) M. Schlosser, H. BaTuong, J. Raspondek, B. Schaub, *Chimia* **1983**, *37*, 10.
[6] a) H. J. Bestmann, M. Schmidt, *Angew. Chem. Int. Ed. Engl.* **1987**, *26*, 79; b) H. J. Bestmann, M. Schmidt, *Tetrahedron Lett.* **1987**, *28*, 2111.
[7] a) S. Goumri-Magnet, H. Gornitzka, A. Baceiredo, G. Bertrand, *Angew. Chem. Int. Ed.* **1999**, *38*, 678; b) T. Baumgartner, B. Schinkels, D. Gudat, M. Nieger, E. Niecke, *J. Am. Chem. Soc.* **1997**, *119*, 12410; c) A. Garduno-Alva, R. Lenk, Y. Escudié, M. L. González, L. Bousquet, N. Saffon-Merceron, C. A. Toledano, X. Bagan, V. Branchadell, E. Maerten, A. Baceiredo, *Eur. J. Inorg. Chem.* **2017**, 3494.
[8] T. Scherpf, R. Wirth, S. Molitor, K.-S. Feichtner, V. H. Gessner, *Angew. Chem. Int. Ed.* **2015**, *54*, 8542; *Angew. Chem.* **2015**, *127*, 8662.
[9] C. Schwarz, L. T. Scharf, T. Scherpf, J. Weismann, V. H. Gessner, *Chem. Eur. J.* **2019**, *25,11*, 2793.
[10] a) C. Schwarz, T. Scherpf, I. Rodstein, J. Weismann, K.-S. Feichtner, V. H. Gessner, *ChemistryOpen* **2019**, *8*, 621; b) L. T. Scharf, D. M. Andrada, G. Frenking, V. H. Gessner, *Chem. Eur. J.* **2017**, *23*, 4422.
[11] For reviews: a) L. T. Scharf, V. H. Gessner, *Inorg. Chem.* **2017**, *56*, 8599; b) V. H. Gessner, , *Struct. Bonding (Berlin)* **2018**, *177*, 117.
[12] For examples: a) A. Fürstner, M. Alcarazo, K. Radkowski, C. W. Lehmann, *Angew. Chem. Int. Ed.* **2008**, *47*, 8302; b) S. Nakafuji, J. Kobayashi, T. Kawashima, *Angew. Chem. Int. Ed.* **2008**, *47*, 1141; c) M. Asay, S. Inoue, M. Driess, *Angew. Chem. Int. Ed.* **2011**, *50*, 9589; d) I. Alvardo-Beltran, A. Baceiredo, N. Saffon-Merceron, V. Branchadell, T. Kato, *Angew. Chem. Int. Ed.* **2016**, *55*, 16141; e) J. Berthe, J. M. Garcia, E. Ocando, T. Kato, N. Saffon-Merceron, A. De Cózar, F. P. Cossío, A. Baceiredo, *J. Am. Chem. Soc.* **2011**, *133*, 15930; f) N. Del Rio, A. Baceiredo, N. Saffon-Merceron, D. Hashizume, D. Lutters, T. Müller, T. Kato,

© 2020 The Authors. Published by WILEY-VCH Verlag GmbH & Co. KGaA, Weinheim

Journal of Inorganic and General Chemistry
ZAAC
Zeitschrift für anorganische und allgemeine Chemie
ARTICLE

*Angew. Chem. Int. Ed.* **2016**, *55*, 4753; g) N. Del Rio, M. Lopez-Reyes, A. Baceiredo, N. Saffon-Merceron, D. Hashizume, D. Lutters, T. Müller, T. Kato, *Angew. Chem. Int. Ed.* **2017**, *56*, 1365.

[13] a) T. Scherpf, K.-S. Feichtner, V. H. Gessner, *Angew. Chem. Int. Ed.* **2017**, *56*, 3275; b) C. Mohapatra, L. Scharf, T. Scherpf, B. Mallick, K.-S. Feichtner, C. Schwarz, V. H. Gessner, *Angew. Chem. Int. Ed.* **2019**, *58*, 7459.

[14] a) T. Scherpf, C. Schwarz, L. T. Scharf, J.-A. Zur, A. Helbig, V. H. Gessner, *Angew. Chem. Int. Ed.* **2018**, *57*, 12859; b) P. Weber, T. Scherpf, I. Rodstein, D. Lichte, L. T. Scharf, L. J. Gooßen, V. H. Gessner, *Angew. Chem. Int. Ed.* **2019**, *58*, 3203; c) X.-Q. Xu, D. Lichte, I. Rodstein, A.-K. Seitz, T. Scherpf, V. H. Gessner, L. J. Gooßen, *Org. Lett.* **2019**, *21*, 7558; d) C. Schwarz, J. Handelmann, D. M. Baier, A. Ouissa, V. H. Gessner, *Catal. Sci. Technol.* **2019**, *9*, 6808; e) I. Rodstein, J. Tappen, K. McGuire, A. Großjohann, J. Löffler T. Scherpf, V. H. Gessner, *Chem. Eur. J.* **2020**, doi.org/10.1002/chem.201905535.

[15] a) A. M. van Leusen, B. A. Reith, A. J. W. Iedema, J. Strating, *Recl. Trav. Chim. Pays-Bas* **1972**, *91*, 37; b) J. Dong, L. Krasnova, M. G. Finn, K. B. Sharpless, *Angew. Chem. Int. Ed.* **2014**, *53*, 9430.

[16] Single crystals could only be obtained with LiI being present in the solution of $^{\mathrm{Cy}}$**1-Li** in THF. Despite many affords, we so far failed to grow crystals of pure $^{\mathrm{Cy}}$**1-Li**.

[17] a) V. H. Gessner, C. Däschlein, C. Stohmann, *Chem. Eur. J.* **2009**, *15*, 3320; b) F. Mongin, A. Harrison-Marchand, *Chem. Rev.* **2013**, *113*, 7563.

[18] In the crystal, the THF molecules on the rotational axis symmetrically occupy the space on top and below the octahedral prism and thus coordinate to all potassium atoms. These THF molecules are present with 95 % occupancy. 5 % of the space is filled by KI. Repeated crystallization gave the same structure, yet always with poor quality due to heavily disordered cyclohexyl and solvent molecules.

[19] E. M. Leitao, S. R. Dubberley, W. E. Piers, Q. Wu, R. McDonald, *Chem. Eur. J.* **2008**,*14*, 11565.

[20] a) G. Sheldrick, A short history of SHELX, *Acta Crystallogr., Sect. A: Found. Crystallogr.* **2008**, *64*, 112; b) G. Sheldrick, Crystal structure refinement with SHELXL, *Acta Crystallogr., Sect. C: Struct. Chem.* **2015**, *71*, 3.

Received: December 12, 2019

© 2020 The Authors. Published by WILEY-VCH Verlag GmbH & Co. KGaA, Weinheim

Journal of Inorganic and General Chemistry
ZAAC
Zeitschrift für anorganische und allgemeine Chemie

**ARTICLE**

*H. Darmandeh, T. Scherpf, K.-S. Feichtner, C. Schwarz, V. H. Gessner** ................................................................. **1–8**

Synthesis, Isolation, and Crystal Structures of the Metalated Ylides [$Cy_3P$-C-$SO_2$Tol]M (M = Li, Na, K)

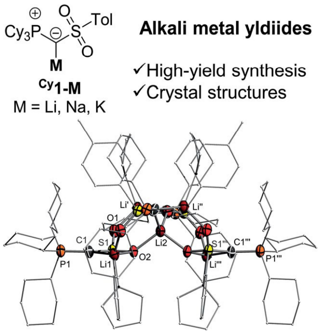
⊕
O
Cy3P
⊖
S
Tol
O
M
Cy1-M
M = Li, Na, K
Alkali metal yldiides
✓High-yield synthesis
✓Crystal structures
Li'
Li''
O1
C1
S1
P1
Li1
O2
Li2
S1'''
C1'''
P1'''
Li'''

© 2020 The Authors. Published by WILEY-VCH Verlag GmbH & Co. KGaA, Weinheim

## 3.2 Synthesis of Low-Valent Dinuclear Group 14 Compounds with Element-Element Bonds by Transylidation

| | |
|---|---|
| Title: | Synthesis of Low-Valent Dinuclear Group 14 Compounds with Element-Element Bonds by Transylidation |
| Publishing Status: | published online, Communication |
| Publisher: | Wiley VCH |
| Journal: | Chemistry – A European Journal |
| DOI: | 10.1002/chem.202004242 |
| Authors: | Chandrajeet Mohapatra‡, Heidar Darmandeh‡, Henning Steinert, Bert Mallick, Kai-Stephan Feichtner, Viktoria H. Gessner* |

‡ These authors contributed equally

Contribution: C. Mohapatra and H. Darmandeh planned and executed all experimental work and wrote the manuscript. C. Mohapatra synthesized and characterized all $^{Ph}$Y-substituted compounds. H. Darmandeh synthesized and characterized all $^{Cy}$Y-substituted compounds. H. Steinert performed the theoretical calculations. H. Darmandeh, Bert Mallick and K.-S. Feichtner performed the XRD measurements. V.H. Gessner finalized the manuscript and supervised all the performed work.

Chemistry–A European Journal
Communication
doi.org/10.1002/chem.202004242
Chemistry Europe
European Chemical Societies Publishing

## Main Group Chemistry

# Synthesis of Low-Valent Dinuclear Group 14 Compounds with Element–Element Bonds by Transylidation

Chandrajeet Mohapatra+, Heidar Darmandeh+, Henning Steinert, Bert Mallick, Kai-Stephan Feichtner, and Viktoria H. Gessner*[a]

*Dedicated to Professor Manfred Scheer on the occasion of his 65th birthday*

**Abstract:** Dinuclear low-valent compounds of the heavy main group elements are rare species owing to their intrinsic reactivity. However, they represent desirable target molecules due to their unusual bonding situations as well as applications in bond activations and materials synthesis. The isolation of such compounds usually requires the use of substituents that provide sufficient stability and synthetic access. Herein, we report on the use of strongly donating ylide-substituents to access low-valent dinuclear group 14 compounds. The ylides not only impart steric and electronic stabilization, but also allow facile synthesis via transfer of an ylide from tetrylene precursors of type $^{R}Y_2E$ to $ECl_2$ (E = Ge, Sn; $^{R}Y = TolSO_2(PR_3)C$ with R = Ph, Cy). This method allowed the isolation of dinuclear complexes amongst a germanium analogue of a vinyl cation, $[(^{Ph}Y)_2GeGe(^{Ph}Y)]^-$ with an electronic structure best described as a germylene-stabilized $Ge^{II}$ cation and a ylide(chloro)digermene $[^{Cy}Y(Cl)GeGe(Cl)^{Cy}Y]$ with an unusually unsymmetrical structure.

The ability of elements to form homonuclear bonds is most pronounced for carbon. This propensity is the basis of organic chemistry and the chemistry of life. However, compared to carbon, the heavier elements form weaker homonuclear bonds due to the weaker overlap of the orbitals and the increased Pauli repulsion.[1] Low-valent compounds with an additional element–element bond are thus extremely rare species, but of special interest, since they typically exhibit unique reactivities such as towards small molecules and offer prospects to study unusual bonding situations and structural properties.[2] Heavier alkene and alkyne analogues were the first examples which demonstrated the unique reactivity of such compounds and thus paved way to the exploration of the transition-metal-like behavior of the main group elements.[3] Cationic and low-valent species with E–E multiple bonds are only little investigated, particularly with Ge and Sn due to the decreasing E–E bond strength.[4] Landmark examples in case of germanium are the stable germanium vinylidene **A** by Aldridge[5] and Scheschkewitz's silagermenylidene **B** (Figure 1).[6] However, often no multiple bonds but only single or dative bonds are formed[7] such as in Driess' three coordinate $[Ge:]^{2+}$ complex **D**[8] as well as in allene-like structures $R_2E{=}E{=}ER_2$,[9] such as germylone **C**[10] or the di(germylene)-substituted germene **E**.[11]

The most common strategy to access such low-valent compounds is the reduction of halo precursors which upon treatment with strong reducing agents form a new element–element bond (e.g. to **A**, **B**, **E**). Alternatively, bonds between the heavier elements can also be formed by donor-acceptor interactions using heavier carbenes as Lewis base. For example, Rivard and co-workers used the NHC-coordinated $GeCl_2$ adduct

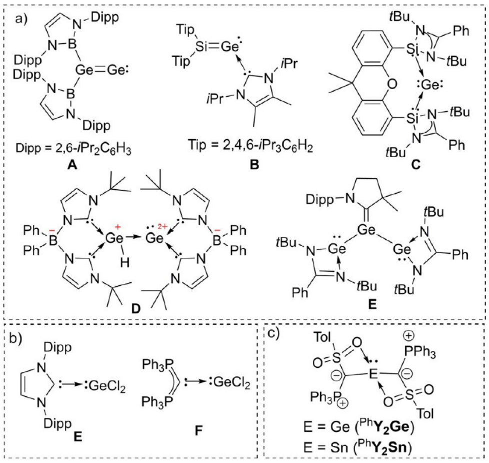

**Figure 1.** (a) Examples of low-valent germanium compounds with a Ge–Ge/Si bond, (b) donor-stabilized $GeCl_2$ and (c) diylidetetrylenes $^{Ph}$**Y$_2$Ge** and $^{Ph}$**Y$_2$Sn**.

---

[a] Dr. C. Mohapatra,+ H. Darmandeh,+ H. Steinert, Dr. B. Mallick, Dr. K.-S. Feichtner, Prof. V. H. Gessner
Chair of Inorganic Chemistry II, Faculty of Chemistry and Biochemistry
Ruhr-University Bochum, Universitätsstraße 150, 44801 Bochum (Germany)
E-mail: viktoria.gessner@rub.de

[+] These authors contributed equally to this work.

Supporting information and the ORCID identification numbers for the authors of this article can be found under: https://doi.org/10.1002/chem.202004242.

© 2020 The Authors. Published by Wiley-VCH GmbH. This is an open access article under the terms of Creative Commons Attribution NonCommercial-NoDerivs License, which permits use and distribution in any medium, provided the original work is properly cited, the use is non-commercial and no modifications or adaptations are made.

**E**, which reacts with $GeCl_2$ to branched and linear germanes.[12] The same strategy was applied by Alcarazo using the carbodiphosphorane adduct **F**[13] as well as by So using an amidinato germylene[14] and by Driess in the synthesis of germylone **C** and **D**.[10]

Recently, we reported on the isolation of the diylidegermylene $^{Ph}$**Y$_2$Ge** and stannylene $^{Ph}$**Y$_2$Sn** which exhibited high donor strengths due to the alignment of the three lone pairs in the C–E–C linkage.[15] We hypothesized that this donor strength should be ideal for generating donor-acceptor complexes and hence for the formation of unique homo- and heterodimetallic compounds. Furthermore, the donor ability of the ylide-substituents[16] should also be suited to access unusual cationic compounds which are difficult to isolate with other classes of substituents.

To test this hypothesis, germylene $^{Ph}$**Y$_2$Ge** was treated with tin and germanium dichloride, respectively, with the intention to isolate germylene-coordinated $ECl_2$ complexes, which upon halide abstraction would give rise to heavier vinyl cations of type $Y_2Ge{=}E(Cl)^+$. Reaction of $^{Ph}$**Y$_2$Ge** with 1 equiv $GeCl_2$·dioxane unfortunately gave a mixture of inseparable products. However, applying the same procedure with $SnCl_2$ yielded two products in an approx. 1:1 ratio along with free ylide. The two products could be separated by sequential precipitation and identified by XRD analysis as the germylene-coordinated $SnCl_2$ **1** and the digermanium cation **2**$^+$ (Scheme 1). Both compounds could be isolated in 89 and 26% yield, respectively. Most interestingly, the same products are formed from the reaction of $^{Ph}$**Y$_2$Sn** with $GeCl_2$·dioxane. This suggests that the diylidetetrylenes readily transfer ylide substituents to other metals. Such transylidation processes are known for transition-metal complexes[17] and hypervalent halonium compounds,[18] but not to and from low-valent main group species.[19]

Complex **1** is a rare example of a donor-stabilized monomeric $SnCl_2$, which for example was reported by Rivard using an *N*-heterocyclic carbene,[20,21] and by So using an amidinato silylene or germylene.[14] **1** features two doublets at 22.4 and 27.1 ppm in the $^{31}P\{^1H\}$ NMR and a singlet at 58.0 ppm in the $^{119}Sn$ NMR spectrum, which is significantly downfield-shifted compared to Rivard's IPr·$SnCl_2$ (−68.7 ppm).[20] XRD analysis revealed that one ylide ligand in the germylene underwent an intramolecular cyclometallation, which results in unsymmetrical NMR patterns in the $^1H$ and $^{13}C\{^1H\}$ NMR spectra. Such a cyclometallation reaction has previously been observed for $^{Ph}$**YGe** and was found to proceed via C–H activation across the Ge–$C_{ylide}$ linkage.[15]

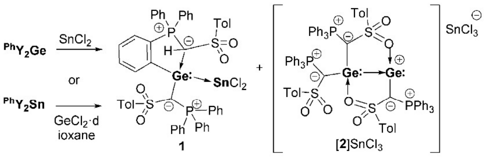

**Scheme 1.** Preparation of **1** and **2**[$SnCl_3$] (Tol = *p*-$CH_3C_6H_4$).

In the crystal (Figure 2a), **1** features a Ge–Sn distance of 2.7493(5) Å, which is considerably shorter than the $Sn^{II}$–$Ge^{II}$ bond length reported by So (2.8520(3) Å).[14] Nonetheless, the Sn–Ge bond in **1** is longer than the Ge=Sn double bond reported by Weidenbruch (2.5065(5) Å),[22] but similar to distances observed by Power and Driess for a $Ge^{IV}$–$Sn^{II}$[23] and a $Ge^{I}$–$Sn^{I}$ bond.[24] The Ge–C bonds to the ylide ligands in **1** are distinctly different, thus reflecting the different bonding situations (Ge–C1: 2.1245(3) and Ge–C2: 1.940(4) Å).

The digermanium(II) cation **2**$^+$ crystallizes with $SnCl_3^-$ as counter anion and was characterized by NMR spectroscopy as well as elemental and XRD analysis. The cation features two sets of signals in a 2:1 ratio in the $^1H$ and $^{13}C\{^1H\}$ NMR spectrum, thus being in line with the different ylide substituents at the two Ge centers. The $^{31}P\{^1H\}$ NMR spectrum showed two broad signals at 9.9 and 13.1 ppm which suggest fluctional behavior in solution. The crystal structure confirms that the two Ge centers are coordinated by three ylide substituents and two sulfonyl groups. The unsymmetrical coordination of the two ylide ligands at Ge1 is probably the origin of the broadening of the signals in the $^{31}P\{^1H\}$ NMR spectrum. **2**$^+$ features a $Ge^{II}$–$Ge^{II}$ bond distance of 2.489(1) Å. This bond is clearly longer than the Ge=Ge double bond in digermavinylidene **A** (2.312(1) Å)[5] and other digermenes,[25] but shorter than the Ge–Ge bond in Rivard's $GeCl_2$ adduct with **E** (2.630 Å),[12] in Driess' cation **D** (2.556 Å) and in Jones's digermyne with a Ge–

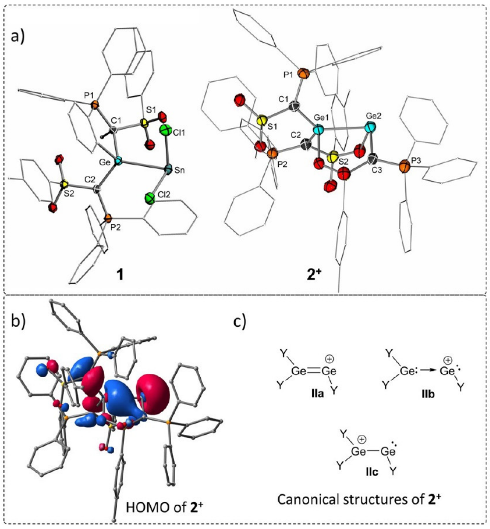

**Figure 2.** (a) Molecular structures of **1** and **2**$^+$. Hydrogens, solvent molecules and $SnCl_3^-$ omitted for clarity; ellipsoids at 50% probability. Selected bond lengths [Å] and angles [°]: (**1**): Sn1–Cl1 2.4883(10), Sn–Cl2 2.5263(10), Sn–Ge 2.7493(5), Ge–C1 2.125(3), Ge–C2 1.940(4), Ge–C3 1.970(4); Cl1-Sn-Ge 90.64(3), Cl1-Sn-Cl2 92.64(3), Cl2-Sn-Ge 88.76(3). (**2**$^+$): P1–C1 1.730(7), C1–C1 1.670(7), C1–Ge1 1.996(7), Ge1–Ge2 2.489(1), P1-C1-S1 116.148(3), C1-Ge1-Ge2 88.243(2), C27-Ge2-Ge1 104.530(2). (b) HOMO (isosurface value 0.4) and (c) possible canonical structures of **2**$^+$.

© 2020 The Authors. Published by Wiley-VCH GmbH

Chemistry–A European Journal | Communication doi.org/10.1002/chem.202004242 | Chemistry Europe European Chemical Societies Publishing

Ge single bond (2.709 Å).[26] The Ge–C bond distances vary between 1.918(6) and 1.996(6) Å and are thus shorter than in the free germylene **$^{Ph}Y_2Ge$** (approx. 2.042 Å). This can be explained by a decreased repulsion between the lone pairs at the carbon atoms and germanium or an increased s-character in the Ge–C bond due to the involvement of the lone pair at Ge1 in the bonding to Ge2.

Several canonical structures can be formulated for **$2^+$** depending on the bonding situations between the two germanium centers (Figure 2c): a digermavinyl cation (**IIa**), a germylene-stabilized germanium(II) cation (**IIb**) and a germylene-substituted germylium ion (**IIc**).[27] The rather long Ge–Ge distance found in the crystal structure suggests that **$2^+$** cannot be regarded as a true digermavinyl cation with a Ge=Ge double bond. This is also confirmed by computational studies (PW6B95D3/def2tzvp; see Supporting Information). The HOMO of **$2^+$** indicates the presence of a lone pair at Ge2 (in line with structures **IIb** and **IIc**), as well as a σ bond between the two germanium atoms polarized towards Ge1. The latter is indicative for a dative bond, which is also confirmed by natural bond orbital (NBO) analysis which describes the Ge–Ge bond as a single bond with a predominant contribution of Ge1 (62%). The Wiberg bond index of 0.861 is smaller than the one found for Ge=Ge double bonds (WBI = 1.528 for $Ph_2Ge{=}GePh_2$; WBI = 1.668 for **A**), but almost identical to the value calculated for the single bond in $Ph_3Ge–GePh_3$ (WBI = 0.863). Thus, **$2^+$** is best described by resonance structures **IIb** and **IIc**. The shorter Ge-Ge distance in **$2^+$** compared to **D** with dicarbene ligands indicates that **IIc** is more important for **$2^+$**.[28]

The unexpected formation of **1** and **$2^+$** from **$^{Ph}Y_2Ge$** with $SnCl_2$ and from **$^{Ph}Y_2Sn$** with $GeCl_2$ suggests that ylide transfer from the tetrylenes proceeds rapidly. However, the formation of **1** indicates that C–H activation of the phenyl group might be an additional driving force in this reaction. To better understand the transylidation process and to probe its generality we turned our attention towards $PCy_3$-substituted analogues which should be less prone to C–H activation. **$^{Cy}Y_2Ge$** and **$^{Cy}Y_2Sn$** were obtained via salt metathesis from the metallated ylide **$^{Cy}Y$-M**[29] and half an equiv $GeCl_2$·dioxane or $SnCl_2$ (Figure 3) as pale-yellow solids in good yields (71 and 75%). The important structural features (e.g. alignment of the lone-pairs in the C–E–C) are almost identical to **$^{Ph}Y_2Ge$** and **$^{Ph}Y_2Sn$**,

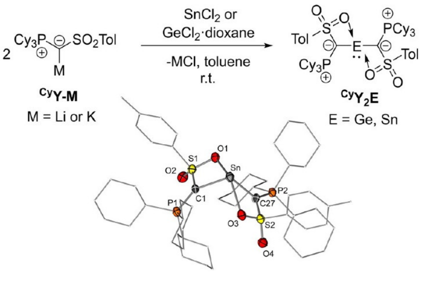

**Figure 3.** Synthesis of **$^{Cy}Y_2Sn$** and **$^{Cy}Y_2Ge$** and molecular structure of **$^{Cy}Y_2Sn$**.

indicating no significant changes in the electronic properties upon replacement of $PPh_3$ by $PCy_3$.

Next, the reactivity of the tetrylenes was tested. The reaction of **$^{Cy}Y_2Ge$** with $SnCl_2$ in $C_6D_6$ revealed to be slow but could be accelerated by sonication. After 1 h, full consumption of **$^{Cy}Y_2Ge$** and selective formation of a single new species in solution along with a colorless precipitate was observed. The precipitate was identified as chloro(ylide)stannylene **3** (Scheme 2). **3** forms a chloro-bridged dimer in the crystal but was found to be in equilibrium with stannylene **$^{Cy}Y_2Sn$** and presumably $SnCl_2$ in THF solution (see below). In $^{31}P\{^1H\}$ and in the $^{119}Sn$ NMR spectrum, **3** exhibits broad singlets at $\delta_P = 24.0$ ppm and at $\delta_{Sn} = -184.6$ ppm, respectively. The second product was isolated from the reaction solution as colorless crystals in 54% yield and identified as 1,2-dichlorodigermene **4**. XRD analysis (Figure 4) showed an unsymmetrical coordination of the two Ge centers by the two ylide-substituents, which thus results in two sets of signals in the $^1H$ and $^{13}C\{^1H\}$ NMR spectrum. Like-

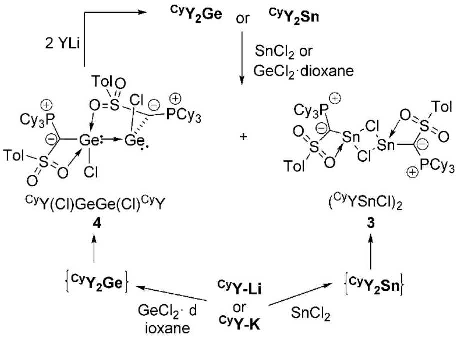

**Scheme 2.** Formation of germylene $(^{Cy}YSnCl)_2$ (**3**) and $^{Cy}Y(Cl)Ge\text{-}Ge(Cl)^{Cy}Y$ **4** from **$^{Cy}Y_2Ge$** and stannylene **$^{Cy}Y_2Sn$**.

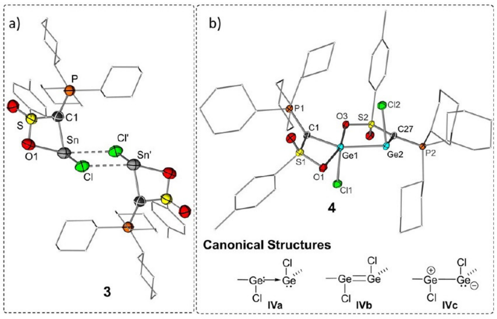

**Figure 4.** (a) Molecular structure of **3** and (b) molecular and canonical structures of **4**. Selected bond lengths [Å] and angles [°]: (**3**): P1–C1 1.735(5), S1–C1 1.659(5), Sn–C1 2.191(5), Sn–Cl 2.5681(12), Sn–Cl" 3.0695(11), C-Sn1-Cl 100.9(1); (**4**): P1–C1 1.743(2), P2–C27 1.742(2), S1–C1 1.685(2), S2–C27 1.660(2), Ge1–C1 1.923(2), Ge2–C27 2.030(2), Ge1–Ge2 2.4908(4), Ge1–O1 2.451(2), Ge1–O3 1.976(2), C1-Ge1-C27 143.5(1), C27-Ge2-Ge1 85.5(1), Cl1-Ge1-Ge2 103.8(2), Ge1-Ge2-Cl2 93.2(2).

© 2020 The Authors. Published by Wiley-VCH GmbH

wise, two signals at $\delta = 33.1$ and 24.1 ppm are observed in the $^{31}$P{$^1$H} NMR spectrum, thus suggesting a dimeric structure also in solution. In the solid state, the two Ge$^{II}$ centers exhibit remarkably different coordination environments. Ge1 is five-coordinate due to the interaction with two sulfonyl groups and adopts a square-pyramidal geometry, whereas Ge2 is only three-coordinate. Thus, in contrast to conventional 1,2-halogermenes[25] no *trans*-bent structure is found in **4**. Instead, C1 is almost in plane with the Cl-Ge-Ge-Cl unit with an acute Cl1-Ge1-C1 angle of 109.6(1)°. This suggests that the lone pair at Ge1 is involved in the bonding to Ge2, which itself retains its lone pair. Hence, **4** is better described as a germylene-stabilized germylene (structure **IVa**, Figure 4), rather than a digermene with a Ge=Ge double bond (**IVb**). This is also in line with the Ge–Ge distance of 2.4908(4) Å, which is comparable to the one found in **2**$^+$ and in the range of a single bond.[30] In principal, also a dipolar structure (**IVc**) with a single rather than a dative bond between the two germanium centers is reasonable, but presumably less dominant. This is suggested by the facile cleavage of the Ge–Ge bond upon reaction of **4** with two equiv of the metallated ylide **$^{Cy}$YLi** thus resulting in the formation of the germylene **$^{Cy}$Y$_2$Ge**. Nonetheless, **4** exhibits a remarkable stability and contrary to many other reported digermenes[31] retains its dimeric structure even in coordinating solvents such as acetonitrile or THF.

It is noteworthy that tin prefers the formation of the symmetric dimeric chloro(ylide)stannylene **3**, while germanium forms the unsymmetrical digermylene **4**. This is due to the weaker metal–metal interaction of Sn compared to Ge, as was already noted by Power.[25a] DFT calculations show that for Ge structure **4** is preferred over any other isomer (see Table S19 and S20) and 68.7 kJ mol$^{-1}$ more stable than a structure similar to **3**. For tin, however, both structures as well as the complex $^{Cy}$Y$_2$Sn$\rightarrow$SnCl$_2$ lie within only 6 kJ mol$^{-1}$ of energy. This small energy difference corroborates with the fact that no pure NMR spectra of **3** could be obtained. Even when dissolving crystals of **3**, mixtures of **3**, stannylene $^{Cy}$Y$_2$Sn and presumably SnCl$_2$ are obtained indicating the existence of an equilibrium between all species in solution.

To test whether the chloro(ylide)tetrylenes **3** and **4** can directly be accessed from the metallated ylide, **$^{Cy}$Y-M** was treated with one equiv SnCl$_2$ and GeCl$_2$·dioxane, respectively. In both cases, the diylidetetrylenes formed initially but reacted further to **3** and **4**. While **4** was obtained in good yields of 75%, **3** could only be isolated in 50% yield since purification was complicated by the equilibrium between **3**, **$^{Cy}$Y$_2$Sn** and SnCl$_2$ (Scheme 2). Overall, these observations clearly confirm the facile transfer of ylide substituents from Ge$^{II}$ and Sn$^{II}$ compounds. Even the reaction of **$^{Cy}$Y$_2$Ge** with one equiv SnCl$_2$ was found to proceed via intermediate formation of the stannylene. This demonstrates that transylidation is a viable process in low-valent group 14 compounds which does not require an additional driving force through C–H activation and thus may be used as a general tool in this chemistry.

In conclusion, we reported on the formation of homo- and heterodinuclear low-valent germanium and tin compounds stabilized by ylide-substituents. These compounds are uniquely formed by transfer of an ylide substituent from tetrylene precursors. Together with the propensity of ylide substituents to act as strong donor substituents, this migratory ability discloses new possibilities for the preparation and isolation of reactive main group compounds. This was demonstrated by the isolation of a germylene-stabilized Ge$^{II}$ cation, a formal germanium-analogue of a vinyl cation, as well as a chloro(ylide)digermene with an unusual, unsymmetrical structure. These results clearly prove the aptitude of ylide substituents to access reactive main group compounds. Transylidation constitutes a mild synthetic method suggesting that more unusual species with unique reactivities should be isolable with these substituents.

## *Acknowledgements*

This project has received funding from the European Research Council (ERC) under the European Union's Horizon 2020 research and innovation programme (Starting Grant: 677749) and was funded by the Deutsche Forschungsgemeinschaft (DFG, German Research Foundation) under Germany's Excellence Strategy—EXC 2033–390677874—RESOLV. Open access funding enabled and organized by Projekt DEAL.

## Conflict of interest

The authors declare no conflict of interest.

**Keywords:** cations · germanium · structure elucidation · tetrylenes · ylides

[1] E. Rivard, *Chem. Soc. Rev.* **2016**, *45*, 989.

[2] H. Jacobsen, T. Ziegler, *J. Am. Chem. Soc.* **1994**, *116*, 3667–3679.

[3] a) P. P. Power, *Nature* **2010**, *463*, 171; b) C. Weetman, S. Inoue, *ChemCatChem* **2018**, *10*, 4213; c) R. L. Melen, *Science* **2019**, *363*, 479.

[4] a) P. Ghana, M. I. Arz, U. Das, G. Schnakenburg, A. C. Filippou, *Angew. Chem. Int. Ed.* **2015**, *54*, 9980; *Angew. Chem.* **2015**, *127*, 10118; b) A. F. Richards, A. D. Phillips, M. M. Olmstead, P. P. Power, *J. Am. Chem. Soc.* **2003**, *125*, 3204; c) W.-P. Leung, Z.-X. Wang, H.-W. Li, T. C. W. Mak, *Angew. Chem. Int. Ed.* **2001**, *40*, 2501; *Angew. Chem.* **2001**, *113*, 2569.

[5] A. Rit, J. Campos, H. Niu, S. Aldridge, *Nat. Chem.* **2016**, *8*, 1022.

[6] A. Jana, V. Huch, D. Scheschkewitz, *Angew. Chem. Int. Ed.* **2013**, *52*, 9980; *Angew. Chem.* **2013**, *125*, 10164.

[7] Examples, of Ge cations with no Ge–Ge bond: a) I. Krummenacher, I. Fernández, H. Rügger, F. Weigand, F. Breher, *Dalton Trans.* **2009**, 5335; b) T. Ochiai, T. Szilvási, D. Franz, E. Irran, S. Inoue, *Angew. Chem. Int. Ed.* **2016**, *55*, 11619; *Angew. Chem.* **2016**, *128*, 11791.

[8] Y. Xiong, T. Szilvási, S. Yao, G. Tan, M. Driess, *J. Am. Chem. Soc.* **2014**, *136*, 11300.

[9] a) N. Wiberg, H.-W. Lerner, S.-K. Vasisht, S. Wagner, K. Karaghiosoff, H. Nöth, W. Ponikwar, *Eur. J. Inorg. Chem.* **1999**, 1211; b) S. Ishida, T. Iwamoto, C. Kabuto, M. Kira, *Nature* **2003**, *421*, 725; c) M. Kira, T. Iwamoto, S. Ishida, H. Masuda, T. Abe, C. Kabuto, *J. Am. Chem. Soc.* **2009**, *131*, 17135.

[10] Y. Wang, M. Karni, S. Yao, Y. Apeloig, M. Driess, *J. Am. Chem. Soc.* **2019**, *141*, 1655.

[11] Y. Li, K. C. Mondal, J. Lübben, H. Zhu, B. Dittrich, I. Purushothaman, P. Parameswaran, H. W. Roesky, *Chem. Commun.* **2014**, *50*, 2986.

[12] S. M. I. Al-Rafia, M. R. Momeni, R. McDonald, M. J. Ferguson, A. Brown, E. Rivard, *Angew. Chem. Int. Ed.* **2013**, *52*, 6390; *Angew. Chem.* **2013**, *125*, 6518.

[13] S. Khan, G. Gopakumar, W. Thiel, M. Alcarazo, *Angew. Chem. Int. Ed.* **2013**, *52*, 5644; *Angew. Chem.* **2013**, *125*, 5755.

Chemistry–A European Journal | Communication
doi.org/10.1002/chem.202004242
Chemistry Europe
European Chemical Societies Publishing

[14] a) Y.-L. Shan, B.-X. Leong, H.-W. Xi, R. Ganguly, Y. Li, K. H. Lim, C.-W. So, *Dalton Trans.* **2017**, *46*, 3642; b) M. L. Bin Ismail, C.-W. So, *Chem. Commun.* **2019**, *55*, 2075.

[15] a) C. Mohapatra, L. T. Scharf, T. Scherpf, B. Mallick, K.-S. Feichtner, C. Schwarz, V. H. Gessner, *Angew. Chem. Int. Ed.* **2019**, *58*, 7459; *Angew. Chem.* **2019**, *131*, 7537; b) T. Scherpf, R. Wirth, S. Molitor, K.-S. Feichtner, V. H. Gessner, *Angew. Chem. Int. Ed.* **2015**, *54*, 8542; *Angew. Chem.* **2015**, *127*, 8662.

[16] a) T. Scherpf, K.-S. Feichtner, V. H. Gessner, *Angew. Chem. Int. Ed.* **2017**, *56*, 3275; *Angew. Chem.* **2017**, *129*, 3323; b) L. T. Scharf, V. H. Gessner, *Inorg. Chem.* **2017**, *56*, 8599; c) A. Sarbajna, V. S. V. S. N. Swamy, V. H. Gessner, *Chem. Sci.* **2020**, https://doi.org/10.1039/D0SC03278F.

[17] a) X. Li, M. Schopf, J. Stephan, K. Harms, J. Sundermeyer, *Organometallics* **2002**, *21*, 2356; b) W. C. Kaska, D. K. Mitchell, R. F. Reichelderfer, W. D. Korte, *J. Am. Chem. Soc.* **1974**, *96*, 2847.

[18] a) M. Ochiai, N. Tada, T. Okada, A. Sota, K. Miyamoto, *J. Am. Chem. Soc.* **2008**, *130*, 2118; b) M. Ochiai, T. Okada, N. Tada, A. Yoshimura, *Org. Lett.* **2008**, *10*, 1425.

[19] For ylide-transfer by TMSCl elimination: a) A. Schmidpeter, H. Nöth, G. Jochem, H.-P. Schrödel, K. Karaghiosoff, *Chem. Ber.* **1995**, *128*, 379; b) A. Schmidpeter, G. Jochem, *Tetrahedron Lett.* **1992**, *33*, 471.

[20] a) K. C. Thimer, S. M. I. Al-Rafia, M. J. Ferguson, R. McDonald, E. Rivard, *Chem. Commun.* **2009**, 7119.

[21] a) A. K. Swarnakar, M. J. Ferguson, R. McDonald, E. Rivard, *Dalton Trans.* **2016**, *45*, 6071; b) S. M. I. Al-Rafia, A. C. Malcolm, S. K. Liew, M. J. Ferguson, E. Rivard, *J. Am. Chem. Soc.* **2011**, *133*, 777; c) S. M. I. Al-Rafia, O. Shynkaruk, S. M. McDonald, S. K. Liew, M. J. Ferguson, R. McDonald, R. H. Herber, E. Rivard, *Inorg. Chem.* **2013**, *52*, 5581.

[22] A. Schäfer, W. Saak, M. Weidenbruch, *Organometallics* **2003**, *22*, 215.

[23] W. Setaka, K. Sakamoto, M. Kira, P. P. Power, *Organometallics* **2001**, *20*, 4460.

[24] W. Wang, S. Inoue, S. Yoa, M. Driess, *Chem. Commun.* **2009**, 2661.

[25] a) L. Pu, A. D. Phillips, A. F. Richards, M. Stender, R. S. Simons, M. M. Olmstead, P. P. Power, *J. Am. Chem. Soc.* **2003**, *125*, 11626; b) M. Stender, L. Pu, P. P. Power, *Organometallics* **2001**, *20*, 1820; c) K. Suzuki, Y. Numata, N. Fujita, N. Hayakawa, T. Tanikawa, D. Hashizume, K. Tamao, H. Fueno, K. Tanaka, T. Matsuo, *Chem. Commun.* **2018**, *54*, 2200; d) N. Hayakawa, T. Sugahara, Y. Numata, H. Kawaai, K. Yamatani, S. Nishimura, S. Goda, Y. Suzuki, T. Tanikawa, H. Nakai, D. Hashizume, T. Sesamori, N. Tokitoh, T. A. Matsuo, *Dalton Trans.* **2018**, *47*, 814; e) K. W. Klinkhammer, T. F. Fässler, H. Grützmacher, *Angew. Chem. Int. Ed.* **1998**, *37*, 124; *Angew. Chem.* **1998**, *110*, 114; f) M. Stürmann, M. Weidenbruch, K. W. Klinkhammer, F. Lissner, H. Marsmann, *Organometallics* **1998**, *17*, 4425; g) Y. Suzuki, T. Sasamori, J.-D. Guo, N. Tokitoh, *Chem. Eur. J.* **2018**, *24*, 364.

[26] J. Li, C. Schenk, C. Goedecke, G. Frenking, C. Jones, *J. Am. Chem. Soc.* **2011**, *133*, 18622.

[27] Note that further canonical structures including the dative bonds between the sulfonyl groups and the Ge atoms can be formulated. These interactions are not considered for simplicity reason.

[28] For a silicon analogue: T. Yamaguchi, M. Asay, A. Sekiguchi, *J. Am. Chem. Soc.* **2012**, *134*, 886.

[29] H. Darmandeh, T. Scherpf, K.-S. Feichtner, C. Schwarz, V. H. Gessner, *Z. Anorg. Allg. Chem.* **2020**, *646*, 835.

[30] P. Pyykkö, M. Atsumi, *Chem. Eur. J.* **2009**, *15*, 186.

[31] a) P. Jutzi, C. Leue, *Organometallics* **1994**, *13*, 2898; b) T. Ohtaki, W. Ando, *Organometallics* **1996**, *15*, 3103.

---

Manuscript received: September 18, 2020
Accepted manuscript online: September 21, 2020
Version of record online: October 19, 2020

© 2020 The Authors. Published by Wiley-VCH GmbH

## 3.3 Reactivity of ylide-stabilized acyclic germylenes and stannylenes

Following the reactivity of **$^{Cy}Y_2E$** towards Group 14 element (II) chlorides, which was reported in the previous section, their ability to activate small molecules was explored next. First, it was tested if **$^{Cy}Y_2Ge$** is more stable than its phenyl analogue, which undergoes an intramolecular C–H activation reaction at one of the phenyl groups across the C–E–C linkage (vide supra). To this end, a solution of **$^{Cy}Y_2Ge$** in $C_6D_6$ was heated to reflux over night (Scheme 54). As expected, no sign of decomposition was observed by $^{31}P\{^1H\}$-NMR spectroscopy, confirming the superior stability of **$^{Cy}Y_2Ge$** over its phenyl analogue, the latter decomposing already slowly at room temperature.[166]

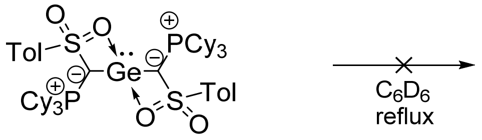

**$^{Cy}Y_2Ge$**

**Scheme 54.** Thermal stability of **$^{Cy}Y_2Ge$**.

Next, the reactivity of the di-ylide tetrylenes towards small molecules like CO, $CO_2$ and $H_2$ was probed (Scheme 55). Pressurizing benzene solutions of the tetrylenes with the respective gaseous small molecules did not afford any sign of conversion even at elevated temperatures.

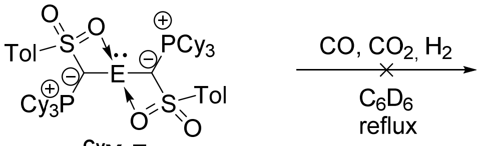

**$^{Cy}Y_2E$**
E= Ge, Sn

**Scheme 55.** Attempted reactions of the novel tetrylenes with small molecules.

This lack of reactivity prompted us to investigate the electronic structures of the tetrylenes via DFT methods. *Henning Steinert* from the Gessner group performed calculations on the PW6B95D3/def2tzvp level of theory. Analysis of the frontier orbitals of **$^{Cy}Y_2E$** showed that the HOMOs mainly consist of a lone pair which is centered on the tetrel center, while the LUMO(+4) is constituted primarily of the vacant p-orbital. It can be easily seen from Figure 27 that both, the HOMOs and the LUMOs lie high energy, resulting in relatively large energy gaps ($\Delta E_{H-L}$), which can explain the lack of reactivity towards strong enthalpic bonds.

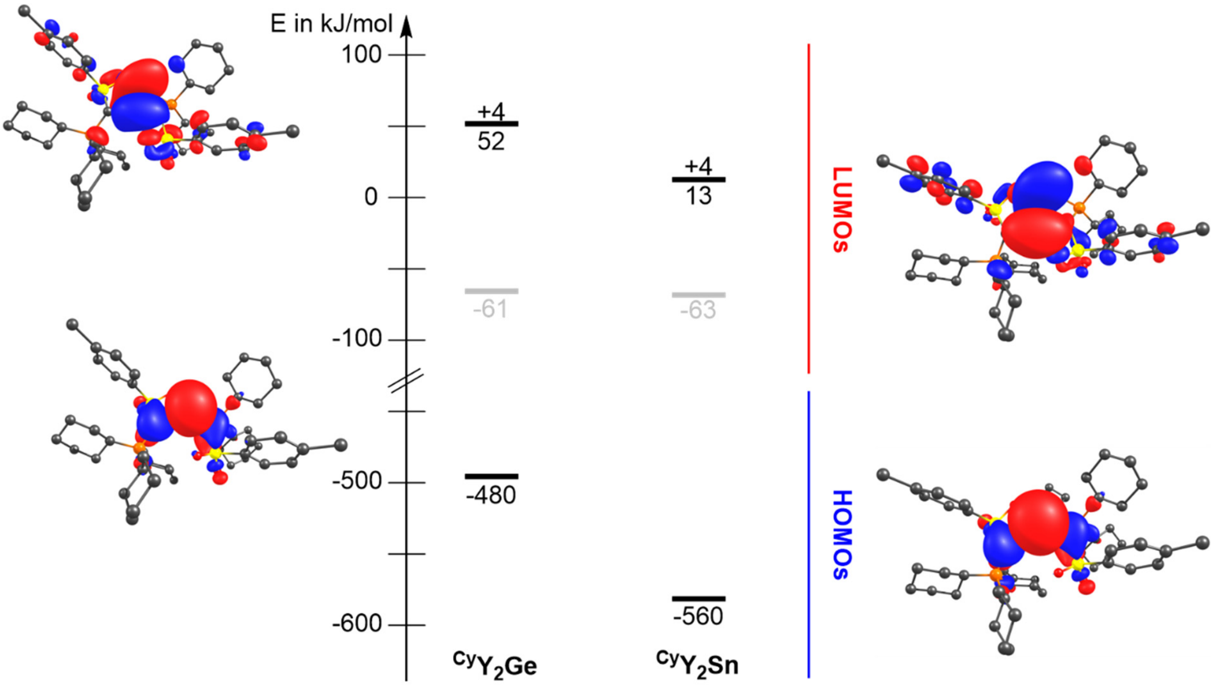

**Figure 27.** DFT calculated energy values (kJ/mol) and appearance of frontier orbitals of the di-ylide substituted germylene **$^{Cy}Y_2Ge$** (left, HOMO bottom, LUMO+4 top) and stannylene **$^{Cy}Y_2Sn$** (right, HOMO bottom, LUMO+4 top). Calculations were performed on PW6B95D3/def2tzvp level of theory.

While the former corroborates with a high donor ability, the latter describes the low Lewis acidity of these systems. The high lying LUMO energies are the main reason for the wide HOMO-LUMO energy gaps and are caused by additional coordination of the sulfonyl groups oxygen atoms to the metal center. This extra electron-donation into the vacant p-orbital results in an increased stability and subsequently lowers the reactivity of the tetrylenes. For instance, **$^{Cy}Y_2Ge$** exhibits a wide HOMO-LUMO energy gap of 532 kJ/mol, while highly reactive germylenes like *Aldridges* boryl-amido system or *Powers* diaryl-germylenes (*vide supra*) posses narrower frontier orbital energies, due to lower lying LUMOs. From this point of view, replacing one of the sulfonyl-ylides from **$^{Cy}Y_2E$** with a substituent which does not posses an additional donor site, should decrease the LUMO stability, while retaining the high donor capacity. This electronic situation should result in an enhanced reactivity towards small molecules.

In order to access such monoylide-tetrylenes with a further substituent, the ylide chlorotetrylenes species $^{Cy}$Y(Cl)Ge-Ge(Cl)Y$^{Cy}$ (**169**) and ($^{Cy}$YSnCl)$_2$ (**170**) were selected as starting materials. A suitable substituent that already has proven its ability to narrow the HOMO-LUMO energy gap of tetrylenes is for example the strongly $\sigma$-donating hypersilyl group –Si(SiMe$_3$)$_3$. To access ylide-/silyl substituted tetrylenes of type $^{Cy}$Y-E-Si(SiMe$_3$)$_3$, the chloro(ylide)stannylene dimer **170** and 1,2-dichlorogermene **169** were treated with two equivalents of K-Si(SiMe$_3$)$_3$, respectively (Scheme 56).

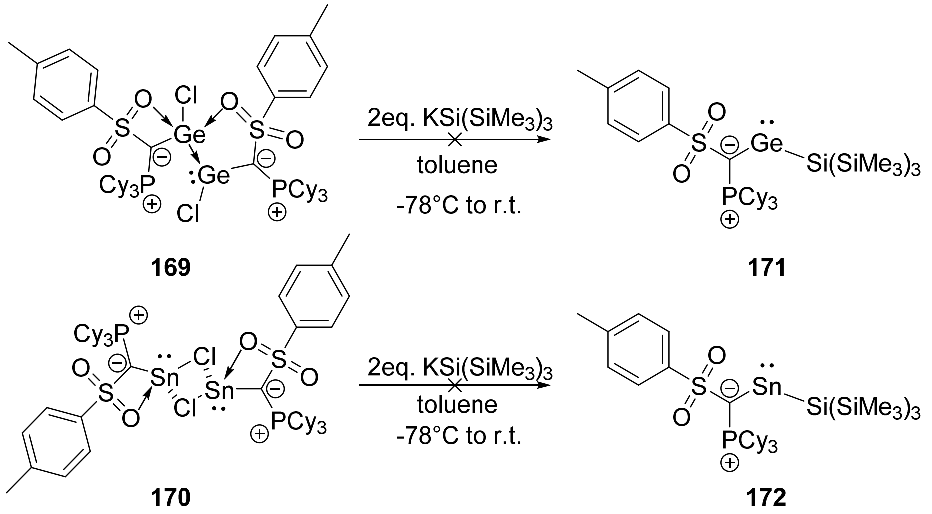

**Scheme 56.** Synthesis attempts towards ylide-/silyl substituted tetrylenes **171** and **172**.

Analysis of the crude reaction mixtures via NMR spectroscopy indicated the formation of diylide-tetrylenes **$^{Cy}$Y$_2$Ge** and **$^{Cy}$Y$_2$Sn**, respectively, along with minor amounts of the protonated ylide **$^{Cy}$Y-H**. No other phosphorus containing products could be detected, indicating that the desired products were not formed at all. Further attempts to access the target species via variation of the reaction's parameters such as stoichiometry, temperature or solvent, also repeatedly failed. More reactive ylide-substituted tetrylenes may be also achieved by replacing one of the ylide ligands by bulky terphenyl substituents. Tetrylenes containing extremely sterically demanding terphenyl substituents, were shown to exhibit wide bonding angles between the main group element and the substituents, leading to narrower HOMO-LUMO energy gaps and thus to high reactivities.[111] To probe if this also applies to $^{Cy}$Y-functionalized tetrylenes, **169** was reacted with two equivalents of (2,6-Tripp$_2$-C$_6$H$_3$)-Li·Et$_2$O (**Ar$^{Tripp}$-Li**) in toluene (Scheme 57).

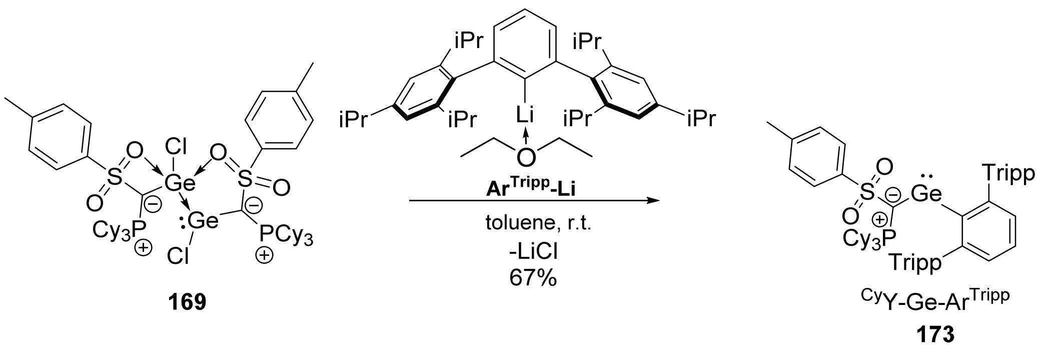

**Scheme 57.** Synthesis of $^{Cy}$Y-Ge-Ar$^{Tripp}$ (**173**) from (chloro)digermylene **169** and Ar$^{Tripp}$-Li.

The reaction revealed to be highly selective, as estimated by $^{31}$P{$^{1}$H}-NMR spectroscopy, affording a single new product that resonates at $\delta_P$ = 27.3 ppm, which is significantly high field shifted compared to **$^{Cy}$Y$_2$Ge** (*cf.* $\delta_P$ = 19.7 ppm). This already indicates a different electronic environment around the phosphorus atom. Storage of a saturated *n*-pentane solution of the reaction mixture at -30°C gave yellow crystals of **173** in 67% yield. These crystals were suitable for XRD analysis. Indeed, the formation of the target compound **173** could be unambiguously confirmed, albeit only crystals of minor quality were obtained, thus a detailed discussion on bonding parameters can not be given. However, as can be seen from Figure 28, the structure of **173** differs extremely from its di-ylide congener **$^{Cy}Y_2Ge$** (see section 3.2 Synthesis of Low-Valent Dinuclear Group 14 Compounds with Element-Element Bonds by Transylidation).

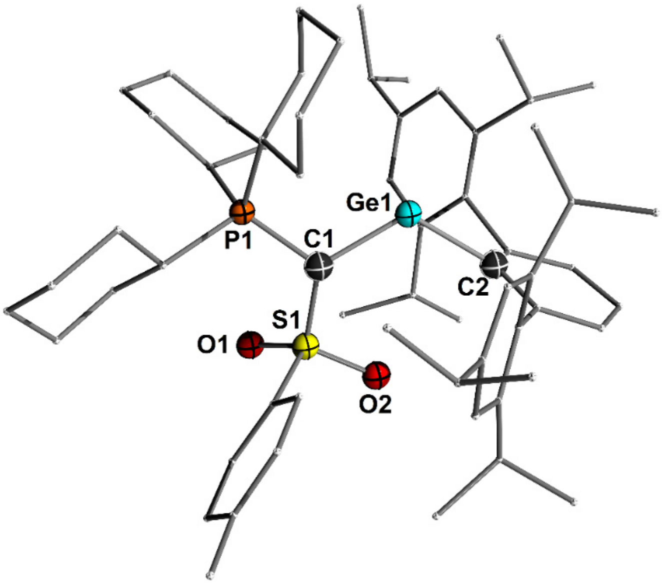

**Figure 28.** Molecular structure of $^{Cy}$Y-Ge-Ar$^{Tripp}$ (**173**), due to low data quality only the constitution of the molecule is given here.

Contrary to **$^{Cy}Y_2Ge$**, the P–C–S plane is not perpendicular arranged to the C–E–C linkage, which should enable a pronounced degree of $\pi$-donation from the ylidic carbon atom into the vacant p-orbital of the germanium center. Furthermore, no additional coordination from the sulfonyl's oxygen atoms is observed. Interestingly, the resonance for the ylidic carbon atom in the $^{13}C\{^1H\}$-NMR spectrum appears at $\delta_C$ = 101.4 ppm (d, $^1J_{CP}$ = 32.8 Hz), which is significantly high field shifted compared to **$^{Cy}Y_2Ge$** (*cf* $\delta_C$ = 45.7 ppm), further suggesting $\pi$-delocalization. To gain further insights into the bonding situation and the electronic properties of **173**, DFT calculations on PW6B95D3/def2tzvp level of theory were performed by *Julian Löffler* from the *Gessner* group. The Wiberg bond index of 0.97 for the Ge–C$_{ylide}$ bond confirms a certain degree of $\pi$-delocalization and is in the range of values found for related $\pi$-donor stabilized germylenes, while the WBI of 0.73 for the Ge–C$_{Aryl}$ bond fits perfectly to values obtained for other aryl-germylenes.[166] Additionally, NBO analysis of **173** suggests a partial double bond character, thus **173** could also be described by a resonance structure with a Ge–C double bond (Figure 29). Furthermore, the lone-pair of electrons resides in an orbital which has a high s-character.

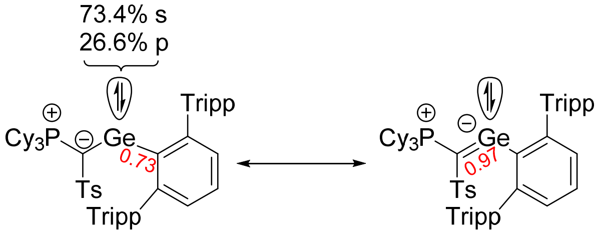

**173**

**Figure 29.** Possible canonical structures for **173** and calculated WBIs.

Compared to **$^{Cy}Y_2Ge$**, the frontier orbital energies calculated for **173** are indeed closer in energy. As anticipated, the LUMO is considerably more destabilized due to the lack of additional electron donation from the sulfonyl oxygen atoms, causing a shift in energy of approximately -60 kJ/mol. However, due to $\pi$-donation from the lone pair of electrons residing at the ylidic carbon atom, the relative energy of the LUMO is still higher than values calculated for related terphenyl-germylenes without an $\pi$–donor substituent. At the same time, the energy level of the HOMO is decreased by about 38 kJ/mol compared to the HOMO energy of **$^{Cy}Y_2Ge$**, resulting from the higher ability of the arene-carbon atom to withdraw electron-density from the metal center (-I effect), compared with the anionic ylidic carbon atom. Considering both effects, due to the exchange of one ylide substituent in **$^{Cy}Y_2Ge$** with **Ar$^{Tripp}$**, the HOMO-LUMO energy gap is efficiently decreased by about 118 kJ/mol, giving a $\Delta E_{H\text{-}L}$ of 414 kJ/mol for **173**. To allow a comparison between ylide-stabilized germylenes and related literature known aryl-germylene systems, the frontier orbital energies of the latter were calculated with the same method as described above. Figure 30 displays the HOMO and LUMO energies of the ylide-germylenes **$^{Cy}Y_2Ge$, 173** and of amido/aryl germylene DippHN-Ge-Ar$^{Mes}$ (**174**) as well as of boryl/aryl germylene (HCDippN)$_2$B-Ge-Ar$^{Mes}$ (**175**).

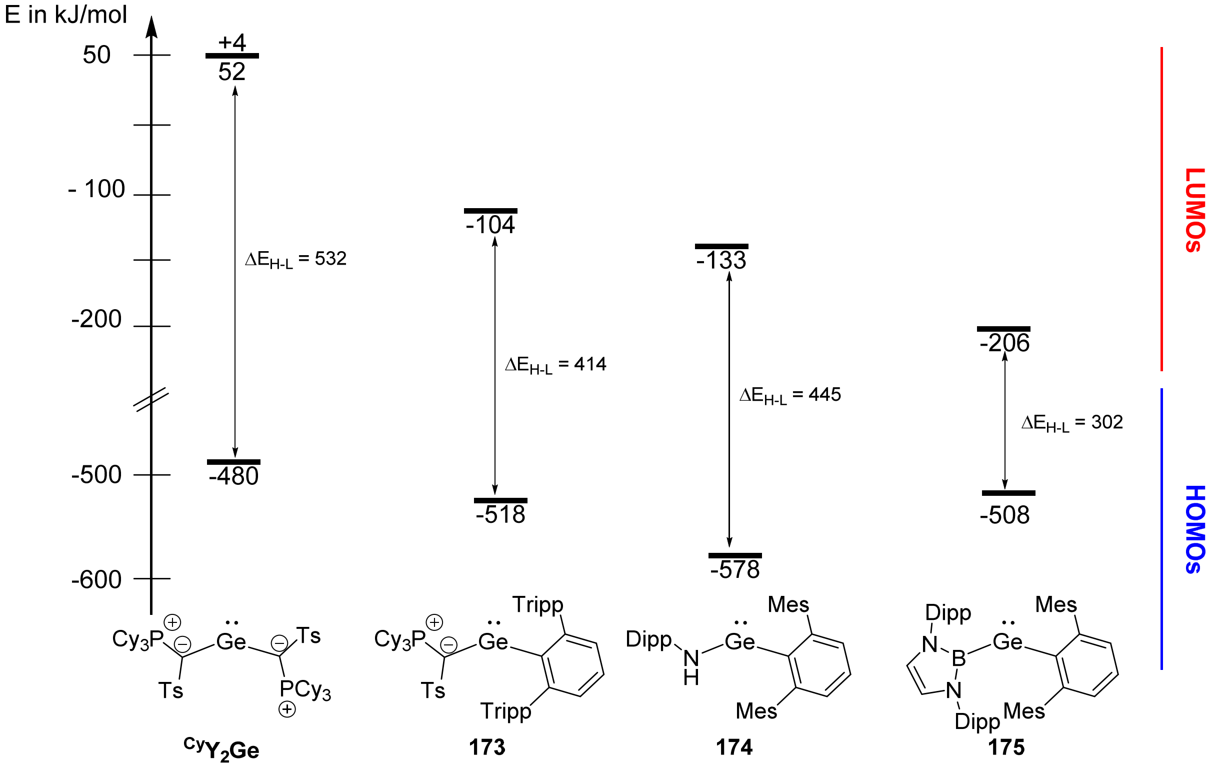

**Figure 30.** Comparison of DFT calculated frontier orbital energies and HOMO-LUMO energy gaps ($\Delta E_{H\text{-}L}$) of different terphenyl-germylenes in kJ/mol. Calculations were performed on the PW6B95D3/def2tzvp level of theory.

As already described, di-ylide germylene **$^{Cy}Y_2Ge$** exhibits the highest HOMO energy, but at the same time has the widest $\Delta E_{H\text{-}L}$ observed for these systems, due to its high lying LUMO(+4). Interestingly, the amido/aryl germylene **174** is a better acceptor than **173**, indicating that in the former less $\pi$-donation from the lone pair into the LUMO is observed, leading to a difference in the LUMO energies of about 31 kJ/mol. Simultaneously, the HOMO (-578 kJ/mol) of **174** lies lower in energy than its ylidic congener (-518 kJ/mol), resulting from the stronger ability of nitrogen to withdraw electron-density from the lone-pair due to its higher electronegativity compared to carbon. As expected, boryl/aryl germylene **175** is calculated to have the narrowest $\Delta E_{H\text{-}L}$ with 302 kJ/mol. This is also consistent with its reported reactivity towards strong enthalpic bonds.[113] Due to the lack of additional $\pi$–donation, the LUMO of **175** is destabilized to –206 kJ/mol, while at the same time the electropositive nature of the B–Ge bond results in effective $\sigma$-donation to the metal center, boosting the HOMO energy of **175** to -508 kJ/mol.

The obtained results clearly demonstrate that the donor/acceptor properties of germylenes can be easily tuned by choosing the right substitution pattern. More interestingly, ylidic substituents like **$^{Cy}$Y** can act as both $\sigma$– and $\pi$– donors, depending on the exact environment. Since the $\Delta E_{H\text{-}L}$ of **173** lies between those calculated for **$^{Cy}Y_2Ge$** and **175** it should be examined if the calculated energy gap of 414 kJ/mol is narrow enough to promote activation of strong enthalpic bonds. Therefore, **173** was dissolved in $C_6D_6$ and subsequently pressurized with 1 bar of hydrogen gas.

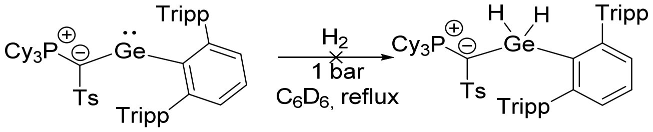

**Scheme 58.** Attempted activation of $H_2$ with **173**.

However, $^{31}P\{^1H\}$-NMR spectroscopy revealed no sign of conversion at room temperature. Consequently, the reaction mixture was heated to reflux over night. Unfortunately, subsequent NMR analysis did not afford any sign of conversion. This result clearly emphasizes that for efficient $H_2$ activation based on ylide-stabilized germylenes an even narrower $\Delta E_{H\text{-}L}$ is necessary. This may be achieved by combining for instance the boryl substituent used in **175** with the ylide group **$^{Cy}$Y**, which should result in a small $\Delta E_{H\text{-}L}$. Additionally, **173** may be suitable for the activation of other strong enthalpic bonds like the more polar N–H bonds in ammonia. Unfortunately, due to time constraints no further studies could be performed yet but should be further explored in the near future.

## 3.4 Towards the synthesis of an ylide-stabilized acyclic silylene

As already described in the introductory section, due to in general smaller HOMO-LUMO energy gaps, acyclic silylenes exhibit a remarkable reactivity towards small molecules and are thus reminiscent to TM. Only few ylide substituted silylenes were reported in literature, which already indicate that their superior donor strength results in special reactivities (vide supra). In order to further explore the properties and reactivity of silylenes bearing ylide-substituents, the novel metalated ylide **$^{Cy}$Y-M** should serve as a potential building block to access the first acyclic ylide-stabilized silylenes. Silylenes are generally synthesized by reduction of suitable Si(IV) precursors, however with the isolation of a stable Si(II) source by *Roesky* and coworkers, namely **IPr·SiCl$_2$**[178], direct access to silylenes via salt metathesis is also possible.[179] Since direct metathesis of **$^{Cy}$Y-Li** with GeCl$_2$·dioxane and SnCl$_2$ delivered stable and isolable di-ylide tetrylenes **$^{Cy}$Y$_2$E** (E=Ge, Sn), preparation of the respective silylene was also probed. To this end, **$^{Cy}$Y-Li** was reacted with half an equivalent of **IPr·SiCl$_2$** in C$_6$D$_6$ at room temperature (Scheme 59).

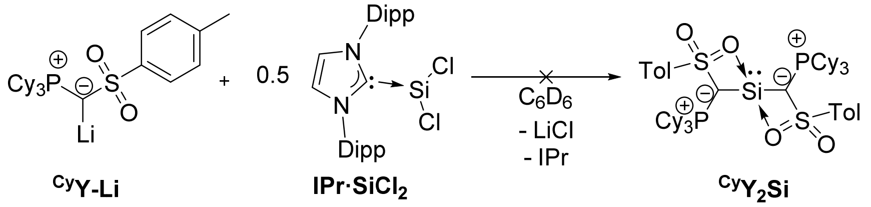

**Scheme 59.** Reaction of the metalated ylide **$^{Cy}$Y-Li** with half an equivalent of NHC-stabilized dichlorosilylene **IPr·SiCl$_2$** to yield the desired acyclic silylene **$^{Cy}$Y$_2$Si**.

Analysis of the crude reaction mixture via $^{31}$P{$^1$H}-NMR spectroscopy revealed the clean formation of the parent protonated ylide **$^{Cy}$Y$_S$-H**. Furthermore, the $^1$H-NMR spectrum indicated the presence of free IPr in solution, whereas no resonances were found in the $^{29}$Si{$^1$H}-NMR spectrum. This observations clearly suggest simple protonation of the metalated ylide, however, the proton source remains unknown at this point. Due to the high basicity of **$^{Cy}$Y-Li**, deprotonation of the imidazoline-backbone could explain the observed formation of the free ylide $^{Cy}$Y-H. Since under these reaction conditions deprotonation seems to be favored over nucleophilic attack, the reaction was repeated at low temperatures (-78°C). Interestingly, the yellow reaction mixture changed its colour from yellow to red upon warming to approx. -40°C. However, stirring the mixture further while warming to room temperature, resulted in a brownish suspension again with $^{Cy}$Y-H as the only phosphorus containing product. This could indicate the formation of di-ylide silylene **$^{Cy}$Y$_2$Si** at low temperatures, which may decomposed upon warming. However, the formation of a silylene could not be proved via low-temperature NMR studies, neither by trapping reactions, indicating that the formed reddish solution did not result from a silylene species and may be caused by other side reactions. Because the synthesis of **$^{Cy}$Y$_2$Si** seems not to be viable via this route, an alternative synthesis strategy was probed (Scheme 60). To this end, **$^{Cy}$Y-Li** should be reacted with half an equivalent of trichlorosilane to yield di-ylide functionalized silane **$^{Cy}$Y$_2$SiHCl**. This species should then be prone to a base-induced HCl elimination, eventually yielding the silylene target compound.

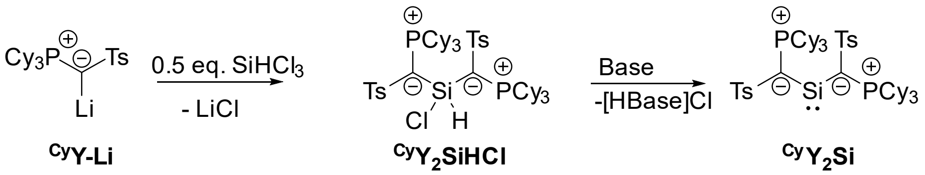

**Scheme 60.** Planned synthesis towards **$^{Cy}Y_2Si$** via reaction of trichlorosilane with yldiide **$^{Cy}$Y-Li** and subsequent base induced HCl elimination.

To probe the feasibility of this approach, a solution of the metalated ylide in toluene was cooled to -78°C and a highly diluted solution of half an equivalent $SiHCl_3$ was slowly added. Upon warming, the yellowish reaction mixture turned colourless and further stirring gave a colourless precipitate. The precipitate was analyzed via NMR spectroscopy. $^{31}P\{^1H\}$-NMR spectroscopy showed a singlet peak at $\delta_P$ = 28.9 ppm. $^1H$-NMR analysis indicated the formation of the mono-ylide-substituted dichlorosilane **$^{Cy}Y$-$SiHCl_2$**, due to the 2:1 integration of the characteristic signals of the tosyl group with the Si–H proton signal found for the unknown species at $\delta_H$ = 5.77 ppm (d, $^3J_{PH}$ = 4.8 Hz). In addition, XRD analysis on colourless crystals, obtained by storing a saturated dichloromethane solution of **$^{Cy}YSiHCl_2$** at -30°C, unambiguously confirmed the suggested connectivity. Unfortunately, the obtained structure is of very poor quality, as such no detailed discussion on bond lengths and angles can be given here. To test whether a sequential substitution to the desired diylidlylsilane is possible, the crude solid was treated with another equivalent of metalated ylide (Scheme 61). $^{31}P\{^1H\}$-NMR spectra of the reaction mixture showed only the presence of protonated ylide $^{Cy}$Y-H and small amounts of unreacted **$^{Cy}YSiHCl_2$**. Presumably, instead of acting as a nucleophile, the metalated ylide just deprotonates **$^{Cy}YSiHCl_2$**, to give ylide $^{Cy}$Y-H and an unstable chloro-silicon species which decomposes.

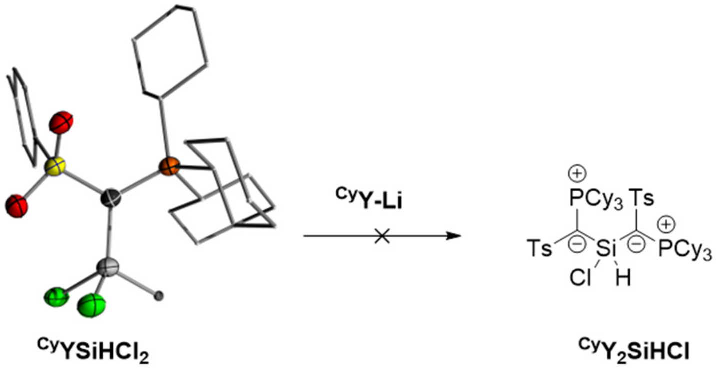

**Scheme 61.** Failed reaction of mono-ylide substituted dichlorosilane **$^{Cy}YSiHCl_2$** with another equivalent of metalated ylide to give di-ylide functionalized silane **$^{Cy}Y_2SiHCl$**.

Because this synthesis route did not yield the desired target compound, another approach was probed (Scheme 62). Therefore, the metalated ylides **$^{Cy}$Y-M** (M=Li and K) were reacted with half an equivalent of $SiX_4$ (X=Cl, Br, I) to yield the respective bis-ylide substituted dihalosilanes **$^{Cy}Y_2SiX_2$** (X=Cl, Br, I). These species should then serve as suitable Si(IV) precursors that would yield the aimed silylene upon reduction.

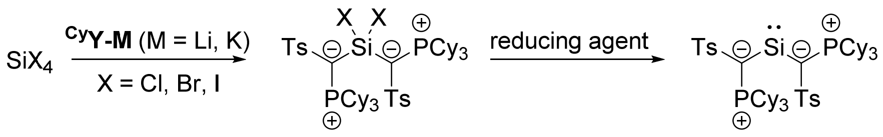

**$^{Cy}Y_2SiX_2$** **$^{Cy}Y_2Si$**

**Scheme 62.** Planned synthesis route of **$^{Cy}Y_2Si$** starting from silicon(IV)-tetrahalides.

Unfortunately, all attempts to identify or isolate a defined ylidic species from the reaction mixtures failed. Even more, in case of X= **I** no resonances were found in the $^{29}Si\{^1H\}$-NMR spectrum, indicating that the metalated ylides prefer nucleophilic attack on the halide, instead of the expected reaction at the silicon center. The last approach probed to access a di-ylide substituted silylene of type **$^{Cy}Y_2Si$**, was to use the concept of transylidation (see 3.2 Synthesis of Low-Valent Dinuclear Group 14 Compounds with Element-Element Bonds by Transylidation). Therefore, the isolated di-ylide germylene **$^{Cy}Y_2Ge$** and stannylene **$^{Cy}Y_2Sn$** were treated with $SiI_4$ in different stoichiometric ratios (Scheme 63). Again, no silicon-containing product was found in solution, as indicated by $^{29}Si\{^1H\}$-NMR studies. Similarly, reaction of the tetrylenes with $IPr{\cdot}SiCl_2$ did not afford a new silicon containing species. No further attempts to access the di-ylide stabilized silylene **$^{Cy}Y_2Si$** were probed.

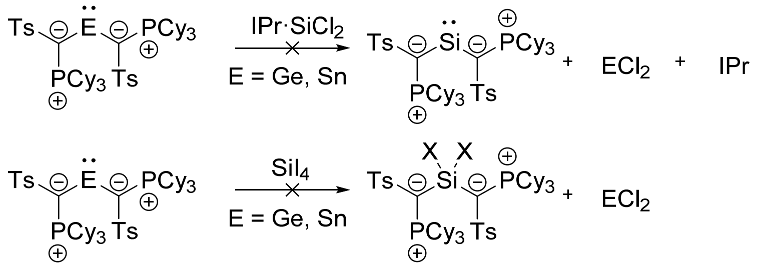

**Scheme 63.** Synthesis attempts towards **$^{Cy}Y_2Si$** via transylidation from $Y_2E$ (E=Ge,Sn).

Overall, the **$^{Cy}Y$**-substituent seems not to be suitable for the isolation of a silylene. Thus, we turned our attention towards other ylide-substituents, which do not bear a sulfonyl moiety. Since these ylides can not be easily deprotonated to yield the respective metalated ylides and to undergo subsequent salt-metathesis reactions, an alternative synthesis route towards ylide-functionalized Si(IV) precursor has to be used. Therefore, a process called Trans-Silylation, originally developed by *Schmidbaur*[180], seems to be a viable alternative to access such species. Here, trimethylsilyl (TMS)-functionalized ylides react with halosilanes via TMS-X (X= Cl, Br) elimination to yield the respective ylide-functionalized silanes. The advantage of this method is, that TMS-ylides can be used as mild "yldiide" equivalents and furthermore, are easily accessible. That said, two different TMS-ylides were prepared. **$^{Cy}Y_{Me}$-TMS** and **$^{Cy}Y_{Ph}$-TMS** were chosen as the target molecules, to vary the steric and electronic properties. **$^{Cy}Y_{Me}$-TMS**, is accessible via a one pot-procedure from its parent phosphonium salt **$^{Cy}Y_{Me}$-H$_2$**. The latter is deprotonated with *n*BuLi to form ylide **$^{Cy}Y_{Me}$-H** which is then reacted with TMS-Cl, presumably forming an intermediate silyl-phosphonium salt, which is instantaneously deprotonated by **$^{Cy}Y_{Me}$-H**, giving half an equivalent of **$^{Cy}Y_{Me}$-TMS** and **$^{Cy}Y_{Me}$-H$_2$** as the products (Scheme 64). **$^{Cy}Y_{Me}$-TMS** was isolated as a colourless solid in 50% yield. Its $^{31}P\{^1H\}$-NMR spectrum shows a singlet resonance at $\delta_P = 30.3$ ppm.

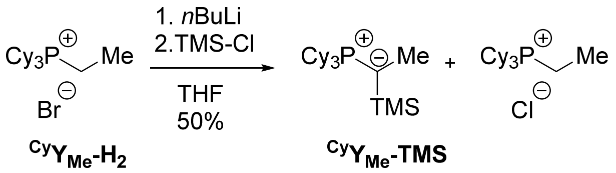

**Scheme 64.** Preparation of **$^{Cy}Y_{Me}$-TMS**.

The phenyl analogue **$^{Cy}Y_{Ph}$-H** is a weaker base and weaker nucleophile, therefore the reaction has to be performed with TMS-I, yielding a stable $\alpha$-silyl-phosphonium salt, which can be deprotonated by addition of KO*t*Bu giving the TMS-ylide **$^{Cy}Y_{Ph}$-TMS** (Scheme 65). **$^{Cy}Y_{Ph}$-TMS** is characterized by a singlet signal at $\delta_P$ = 21.9 ppm in the $^{31}P\{^1H\}$-NMR spectrum and was isolated as a colourless powder in 70% overall yield.

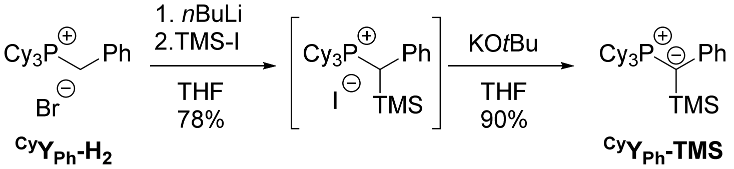

**Scheme 65.** Synthesis of **$^{Cy}Y_{Ph}$-TMS**.

With the TMS-ylides in hand, they were reacted with half an equivalent of $SiCl_4$, respectively, to access the di-ylide substituted dichlorosilanes **($^{Cy}Y_Z$)$_2$-SiCl$_2$** (Scheme 66). The reaction mixtures were stirred at room temperature for 12h and subsequently analyzed via NMR spectroscopy. In both cases, $^{31}P\{^1H\}$-NMR spectroscopy showed the selective formation of a new product, along with approximately one equivalent of the respective starting material. This observation indicates that only a mono-substitution took place. The phosphorus atoms of **$^{Cy}Y_{Me}$-SiCl$_3$** and **$^{Cy}Y_{Ph}$-SiCl$_3$** resonate at $\delta_P$ = 33.7 ppm and $\delta_P$ = 26.5 ppm, respectively. Furthermore, mono-substitution is confirmed by $^{29}Si\{^1H\}$-NMR spectroscopy, which showed doublets as expected for the coupling with only a single phosphorus nucleus. **$^{Cy}Y_{Me}$-SiCl$_3$** gives a signal at $\delta_{Si}$ = -11.7 ppm ($^2J_{SiP}$ = 41.2 Hz), while the silicon atom of **$^{Cy}Y_{Ph}$-SiCl$_3$** resonates at $\delta_{Si}$ = -15.0 ppm with a similar coupling constant of $^2J_{SiP}$ = 40.3 Hz.

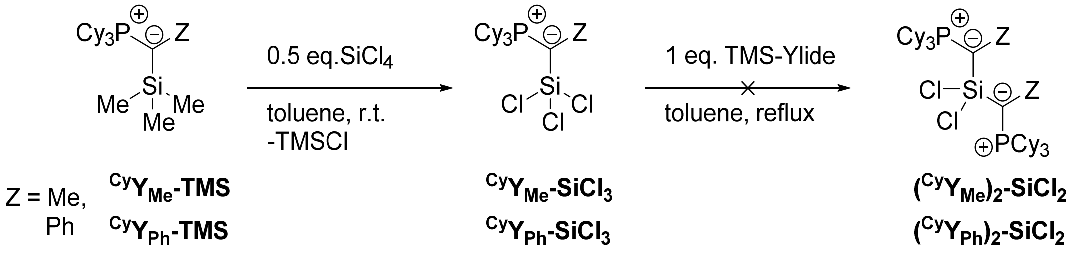

**Scheme 66.** Attempted synthesis of di-ylide substituted dichlorosilanes via TMS-Cl elimination.

Attempts to force a second substitution by refluxing toluene solutions of **$^{Cy}Y_{Me}$-SiCl$_3$** and **$^{Cy}Y_{Ph}$-SiCl$_3$** with another equivalent of the respective TMS-ylides failed. The question, whether the lack of a second substitution is caused by steric or electronic effects or a combination of both, arises. Therefore, colourless crystals of **$^{Cy}Y_{Ph}$-SiCl$_3$** and its precursor **$^{Cy}Y_{Ph}$-TMS** were grown by slow evaporation of respective benzene solutions and subsequently analyzed by XRD. The obtained molecular structures are shown in Figure 31.

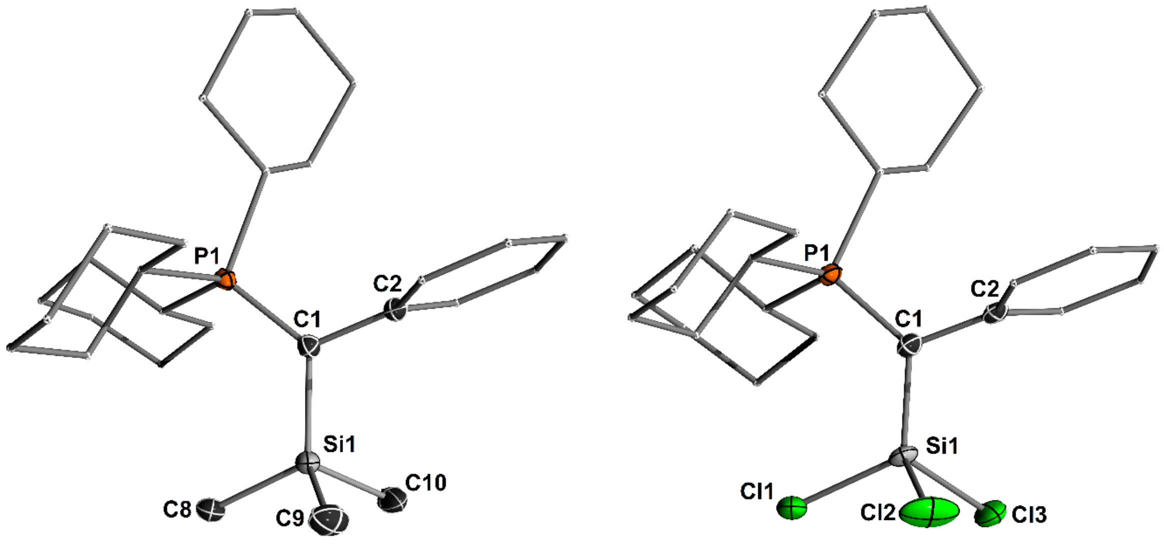

**Figure 31.** Molecular structures of **$^{Cy}$Y$_{Ph}$-TMS** (left) and **$^{Cy}$Y$_{Ph}$-SiCl$_3$** (right). Thermal ellipsoids drawn at 50% probability. Hydrogen atoms omitted for clarity.

The obtained solid-state structures unambiguously confirm the suggested connectivity. On the first look, no obvious changes in the structures arise. However, by taking a closer look into the bonding parameters (Table 3), significant differences can be observed.

**Table 3.** Important bond lengths and angles for **$^{Cy}$Y$_{Ph}$-TMS** and **$^{Cy}$Y$_{Ph}$-SiCl$_3$**.

| | **$^{Cy}$Y$_{Ph}$-TMS** | **$^{Cy}$Y$_{Ph}$-SiCl$_3$** |
|---|---|---|
| P1–C1 [Å] | 1.7029(12) | 1.7257(15) |
| C1–C2 [Å] | 1.5027(16) | 1.514(2) |
| Si1–C1 [Å] | 1.8311(12) | 1.7635(16) |
| Si1–Cl$_{average}$ [Å] | - | 2.0597(3) |
| Si1–CH3$_{average}$ [Å] | 1.882(2) | - |
| P1–C1–Si1 [°] | 127.27(7) | 127.30(9) |
| Si1–C1–C2[°] | 113.75(8) | 113.50(10) |

The P1–C1–C2 and Si1–C1–C2 bond angles are very similar and suggest no difference in the steric-profile upon substitution of the methyl groups with chlorine atoms. Furthermore, in both molecules the silicon atom adopts an essentially tetrahedral geometry. On the other hand, the Si1–C1 bond dramatically shortens upon substitution. Due to the large difference in electronegativity, the Si–Cl bond is highly polarized, thus enabling strong electrostatic interactions between the positively charged silicon atom and the negatively charged ylidic carbon atom. At the same time, the electrostatic pressure is released off from the P–C–C linkage, as indicated by longer P1–C1 and C1–C2 bond lengths. Of course, one could argue that negative hyperconjugation from the lone-pair of the ylidic carbon atom into the $\sigma$*(Si–Cl) orbitals would result in a similar C1–Si1 bond shortening. However, the corresponding Si1–Cl bonds should be simultaneously weaker and thus a bond lengthening should be observed. This is not the case for the Si1–Cl bonds in **$^{Cy}$Y$_{Ph}$-SiCl$_3$**, with an average bond length of approx. 2.06 Å, which is a typical value found for covalent Si–Cl single bonds.[181] Additionally, weaker Si–Cl bonds lengths would also result in an increased reactivity towards nucleophiles, which is obviously not the case, since a second substitution on **$^{Cy}$Y$_{Ph}$-SiCl$_3$** was not possible. That said, the obtained data suggest that the silicon atom in **$^{Cy}$Y$_{Ph}$-SiCl$_3$** is highly stabilized and electronically satisfied, due to electrostatic effects induced by the ylide substituent, thus making it unreactive towards nucleophiles. Since a further substitution neither with an additional ylide substituent, nor with other donor-ligands (e.g. amides like $KN(SiMe_3)_2$) was possible, further attempts to isolate an acyclic di-ylide stabilized silylene were abandoned. Instead, the synthesis of a silylene with only one ylide-substituent and an additional $\sigma$-donating ligand was pursued. To this end, we followed a synthetic approach previously reported by *Rivard* and *Inoue* for the synthesis of NHI/NHO substituted silylsilylenes.[108,109] We hypothesized that a similar approach as outlined in (Scheme 67) would lead to an isolable ylide-functionalized silyl-silylene.

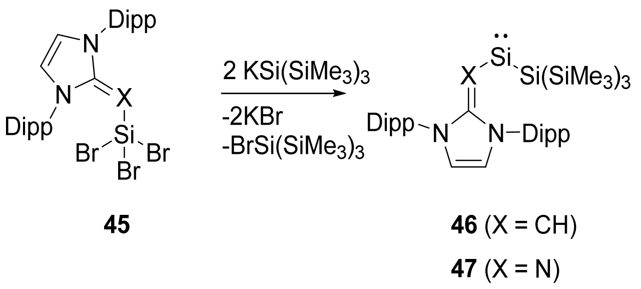

**Scheme 67.** Reported synthesis of NHI/NHO stabilized silyl-silylenes by Inoue and Rivard, respectively.[108,109]

Since the synthesis routes developed by *Inoue* and *Rivard* made use of the respective tribromosilanes, probably due to the more facile reduction of Si–Br bonds compared to their Cl analogues, the synthesis of a highly electron-donating, yet more sterically demanding tribromosilyl-ylide was probed. Therefore, the mesityl-substituted tricyclohexylphosphonium salt (**$^{Cy}$Y$_{Mes}$-H$_2$**) was deprotonated *in-situ* and the formed ylide was reacted with one equivalent of $SiBr_4$ in toluene (Scheme 68). Surprisingly, the formation of a white precipitate was observed, which turned out to consists of the respective phosphonium salt **[$^{Cy}$Y$_{Mes}$-SiBr$_3$]Br**. This salt could be isolated as a colourless solid in 82% yield.

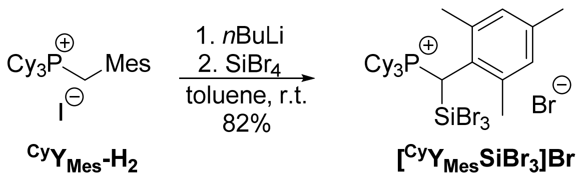

**Scheme 68.** Reaction of **$^{Cy}$Y$_{Mes}$-H** with one equivalent of $SiBr_4$ in toluene.

Unfortunately, no crystals suitable for XRD analysis of this species to confirm its structure could be obtained, but its salt-like character suggest the formation of a $\alpha$-silyl-phosphonium salt, instead of a simple Lewis adduct. This is also indicated by its $^{31}P\{^1H\}$-NMR shift of $\delta_P$ = 43.9 ppm, a typical value for $PCy_3$-substituted onium salts and its $^{29}Si\{^1H\}$-NMR shift of $\delta_{Si}$ = -35.5 ppm (d, $^2J_{SiP}$ = 3.0 Hz), which is considerably downfield shifted compared to $SiBr_4$ (*cf.* -90.8 ppm).[182] An additional coordination of the silicon atom would result in a more high field shifted signal.[183] However, the product formation might also depend on the solvent used. For example the reaction of IPr with $SiBr_4$ in toluene yields the respective adduct IPr·$SiBr_4$[184], while the salt [IPr·$SiBr_3$]Br is obtained in *n*-hexane.[185]

Next, the deprotonation of the *α*-tribromosilyl substituted phosphonium salt was probed using an equimolar amount of $KN(SiMe_3)_2$ to yield the respective tribromosilyl-ylide **$^{Cy}Y_{Mes}$-SiBr$_3$** (Scheme 69). However, $^{31}P\{^1H\}$-NMR spectroscopic data of the reaction mixture revealed only partial conversion into a new species, characterized by a singlet peak at $\delta_P = 13.4$ ppm along with minor amounts of some side products, and approx. 50% of unreacted starting material. Addition of another equivalent base lead to nearly full conversion. The novel species could be isolated as a colourless solid in 52% yield and crystals suitable for XRD analysis were obtained by slow diffusion of n-hexane into a saturated DCM solution. Surprisingly, the isolated compound turned not out to be the expected tribromosilane **$^{Cy}Y_{Mes}$-SiBr$_3$**. Instead, an ylide-substituted dibromo-silane **176** with a four-membered ring formed by silylation of one of the cyclohexyl groups is obtained. While the mechanism of this transformation is not clear at this point, it could be possible that in the first step of this reaction deprotonation to **$^{Cy}Y_{Mes}$-SiBr$_3$** occurs, which is then prone to a second deprotonation at the cyclohexyl-group, with subsequent elimination of KBr. The proposed mechanism is depicted in Scheme 69.

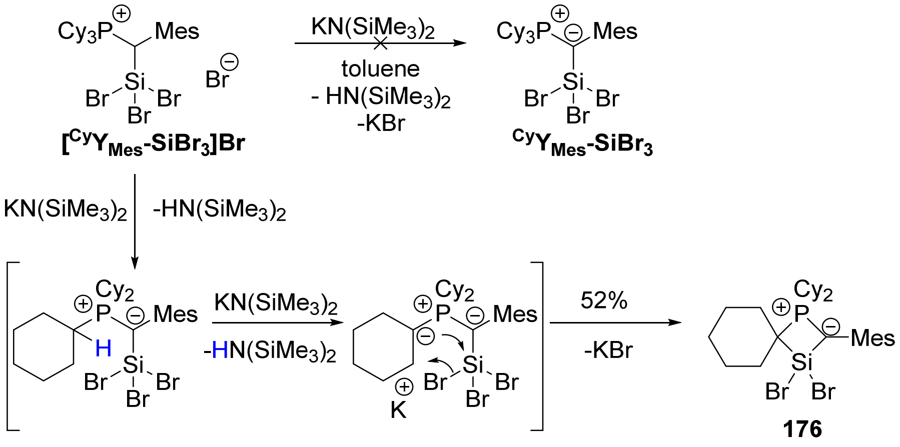

**Scheme 69.** Attempted synthesis of **$^{Cy}Y_{Mes}$-SiBr$_3$** (top) and formation of cyclo di-bromo silane **176** via double-deprotonation with $KN(SiMe_3)_2$ (bottom).

**176** is characterized by a doublet in the $^{29}Si\{^1H\}$-NMR spectrum at $\delta_{Si} = -46.2$ ppm with a coupling constant of $^2J_{SiP} = 24.2$ Hz. Additionally, $^1H$-NMR analysis confirms the deprotonation of one of the cyclohexyl-groups of the phosphonium moiety, while the quaternary ylidic carbon atom resonates at $\delta_C = 45.1$ ppm (d, $^2J_{CP} = 34.6$ Hz) in the $^{13}C\{^1H\}$-NMR spectrum. **176** crystallizes as a monomer in the monoclinic P 2(1)/m space group without any additional solvent molecules. As expected, the ylidic carbon atom adopts a trigonal-planar geometry, while the geometry around the silicon atom is highly distorted due to the strained, planar four-membered ring. This can be seen for instance from the sum of bonding angles of 425°, which is a significant deviation from the expected value of 438° for a perfect tetrahedron. As expected, the smallest angle at silicon is found within the four-membered ring and amounts to only 91.1(2)°. As already observed for **$^{Cy}Y_{Ph}$-SiCl$_3$**, the C1–Si1 bond in **176** is with 1.755(3) Å significantly shorter than a common C–Si single bond[186], probably also caused by electrostatic interactions. On the other hand, the Si1–C2 bond accounts to 1.908(3) Å and lies within the expected range for a single bond, the same holds true for both Si–Br bonds (2.26 Å).[187]

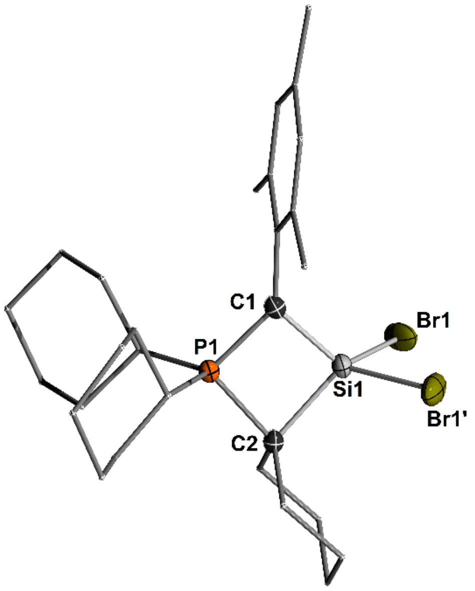

**Figure 32.** Molecular structure of **176**. Thermal ellipsoids at 50% probability level, hydrogen atoms omitted for clarity. Selected important bond lengths [Å] and -angles [°]: Si1–Br1/1' 2.2586(6), Si1–C1 1.755(3), Si1–C2 1.908(3), P1–C1 1.723(3), P1–C2 1.883(3), C1–Si1–C2 91.13(15), Br1–Si1–Br1' 101.83(4), C2–Si1–Br1' 114.90(6), C1–Si1–Br1 117.45(6), C1–Si1–C2–P1 -0.000(106).

Although the target precursor for the synthesis of an ylide/silyl-silylene was not obtained via this route, the reduction of dibromosilane **176** could also lead to either an ylide silylene (**177**) or to its dimer, an ylide-substituted disilene (**178**) (Scheme 70).

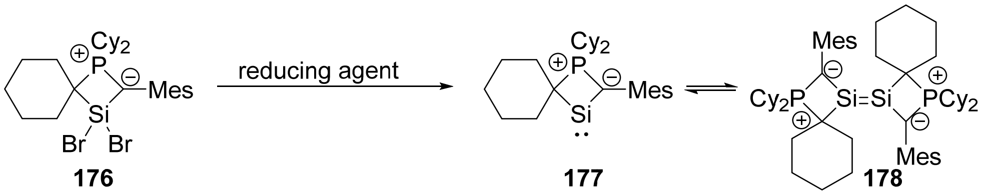

**Scheme 70.** Possible synthesis of ylide-functionalized silylene **177** or its dimer (**178**) upon reduction of **176**.

For the formation and isolation of such species, a suitable reducing agent is necessary. Therefore, *Jones* Mg(I) dimer [$^{Mes}$NacNacMg(I)–Mg(I)NacNac$^{Mes}$][101] was chosen. It is a mild and soluble reducing agent, which can be used in stoichiometric amounts, thus minimizing the risk of overreduction which is often observed with more forcing reducing agents such as $KC_8$ or Li-Naphtalenide.[188] To this end, **176** was treated with one equivalent of the $^{Mes}$NacNac-Mg(I) dimer in $C_6D_6$ at room temperature. The $^{31}P\{^1H\}$-NMR spectrum of the reaction mixture confirmed full consumption of the starting material and the formation of a new species which resonates at $\delta_P$ = 26.6 ppm. In the $^{29}Si\{^1H\}$-NMR spectrum a new signal at around $\delta_{Si}$ = -18.9 ppm is observed. Interestingly, this signal appears as a doublets of doublets with coupling constants of $^2J_{SiP}$ = 30.5 Hz and $^3J_{SiP}$ = 7.1 Hz, proving the existence of a dimeric species. Simultaneously, $^1$H-NMR analysis of the reaction mixture indicated the presence of unreacted Mg(I) species. To get further insights into the molecular composition of this product, XRD analysis on colourless crystals obtained from the reaction mixture was performed. The novel compound turned out to be indeed a dimeric species, however not bearing a low valent Si center. As can be seen from Figure 33, an ylide substituted bromo-disilane **179** is obtained. The one-electron reduction product, resulting from abstraction of one bromine atom from **176** was probably formed, which upon dimerization gave **179** (Scheme 71).

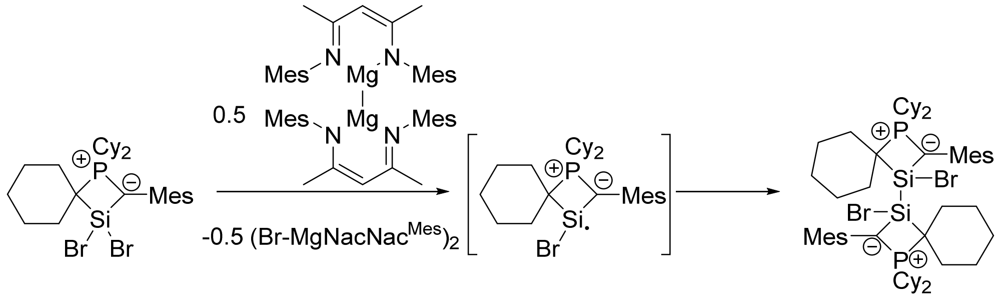

**176** **179**

**Scheme 71.** Possible formation of **179**.

The $C_i$ symmetric molecular structure of **179** differs significantly from its dibrominated precursor.

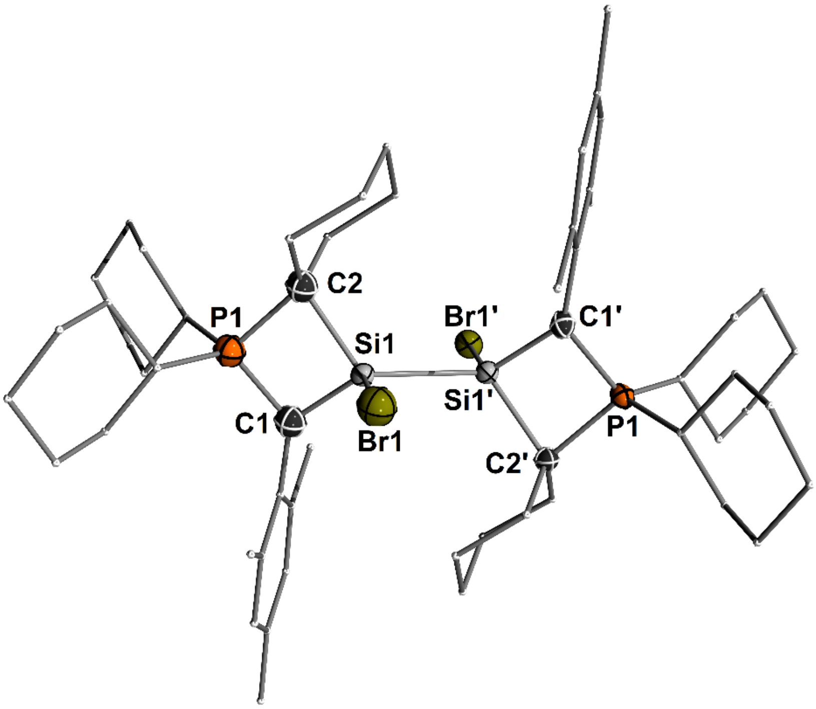

**Figure 33.** Molecular structure of **179**. Thermal ellipsoids at 50% probability level, hydrogen atoms omitted for clarity. Selected important bond lengths [Å] and -angles [°]: Si1–Si1' 2.3959(14), Si1–Br1/1' 2.3208(9), Si1–C1 1.801(3), Si1–C2 1.944(3), P1–C1 1.728(3), P1–C2 1.855(3), C1–Si1–C2 88.09(13) , Br1–Si1–Si1' 100.83(4), C2–Si1–Si1' 121.20(10), C1–Si1–Br1 114.94(10), C1–Si1–C2–P1 11.147(121), C1–Si1–Si1'–C1' -180.00(16) , C2–Si1–Si1'–C1' -180.000(141), Br1–Si1–Si1'–Br1' 180.000(29).

For instance, the four-membered cycle is not planar, twisted out of the plane as indicated by the Si1–C1–P1–C2 torsion angle of approx. 12° , probably induced by coordination of Si1 to Si1'. The Si1–Si1' bond length accounts to 2.3959(14) Å, being in the expected range for Si(IV)-Si(IV) single bonds.[189] Furthermore, the C1–Si1 bond length is elongated to 1.801(3) Å, indicating weaker electrostatic interactions between the ylidic carbon atom and the silicon center. Due to the inversion symmetry, all substituents adopt a perfect antiperiplanar conformation around the Si–Si bond with ideal torsion angles of 180°. The formation of the disilane **179** from its precursor **176** is surprising, since one-electron reductions with *Jones* Mg(**I**) complex are not very common.[188] One explanation for this unusual reactivity could be the steric bulk of the used reducing agent [$^{\text{Mes}}$NacNacMg(**I**)–Mg(**I**)NacNac$^{\text{Mes}}$], which only enables a single-electron-transfer due to steric congestion with the substrate. However, longer reaction times or applying mild heating did not result in a further reduction of **179**. Furthermore, the brominated-disilane could not be isolated as a pure solid, caused by contamination with the BrMgNacNac$^{\text{Mes}}$ by-product. **176** may be instead directly reduced under harsher conditions, generating the target disilene species via in-situ formation and subsequent reduction of **179**. However, due to time constraints no further attempts to obtain ylide-stabilized low-valent silicon species were performed, but with the results shown in this section, an isolation of such species may seem possible by further optimizing the steric and electronic structure of the ylide.

## 3.5 Au···H-C Hydrogen Bonds as Design Principle in Gold(I) Catalysis

Title: Au···H-C Hydrogen Bonds as Design Principle in Gold(I) Catalysis

Publishing Status: draft , Communication

Publisher: -

Journal: draft

DOI:

Authors: Heidar Darmandeh, Julian Löffler, Nikolaos V. Tzouras, Thorsten Scherpf, Kai-Stephan Feichtner, Sofie Vanden Broeck, Marina Saab, Kristof Van Hecke, Catherine S. J. Cazin, Steven P. Nolan* and Viktoria H. Gessner*

Contribution: H. Darmandeh planned and executed the synthesis, isolation and full characterization of novel ylide-substituted phosphine ligands and their respective gold(I) complexes. Additionally, H. Darmandeh synthesized and fully characterized the novel gold(I) complex of Cy-$^{Cy}$JohnPhos. H. Darmandeh performed the presented Au(I)-catalyzed hydroamination reactions and their analysis and wrote the manuscript. Julian Löffler performed all DFT studies. Nikolaos V. Tzouras synthesized novel YPhos-Au(I)-aryl complexes as well as cationic YPhos digold complexes and applied them as catalysts in hydrophenoxylation and hydrocarboxylation reactions. H. Darmandeh, T. Scherpf and K.-S. Feichtner performed the XRD analysis of all novel compounds, except YPhos-Au-aryl- and cationic digold complexes. The latter were measured and solved by members of the XRD department of Ghent University. Calorimetry studies were performed by members of the Nolan group. V.H. Gessner and S.P. Nolan supervised the work performed by their group members and finalized the manuscript.

# Au···H-C Hydrogen Bonds as Design Principle in Gold(I) Catalysis

Heidar Darmandeh[a], Julian Löffler[a], Nikolaos V. Tzouras[b], Thorsten Scherpf[a], Kai-Stephan Feichtner[a], Sofie Vanden Broeck[b], Kristof Van Hecke[b], Marina Saab[b], Catherine S. J. Cazin[b], Steven. P. Nolan[b]* and Viktoria H. Gessner[a]*

To the memory of Professor Paul C. J. Kamer

---

[a] M.Sc. H. Darmandeh, M. Sc. J. Löffler, Dr. T. Scherpf, Dr. K.-S. Feichtner, Prof. V. H. Gessner
Chair of Inorganic Chemistry II, Faculty of Chemistry and Biochemistry
Ruhr-University Bochum
Universitätsstraße 150, 44801 Bochum, Germany
E-mail: viktoria.gessner@rub.de
[b] N. V. Tzouras, S. Vanden Broek, M. Saab, Prof. Dr. K. Van Hecke, Prof. Dr. C. S. J. Cazin, Prof. Dr. S. P. Nolan
Department of Chemistry and Centre for Sustainable Chemistry
Ghent University
Krijgslaan 281, S-3, 9000 Ghent, Belgium
E-mail: steven.nolan@ugent.be

**Abstract:** Secondary ligand metal interactions are decisive in many catalytic transformations. While arene-gold interactions have repeatedly been reported as critical structural feature in many high-performance gold catalysts, we herein report that these interactions can also be replaced by Au···H-C hydrogen bonds without suffering any reduction in catalytic performance. Systematic experimental and computational studies on a series of ylide-substituted phosphines featuring either a $PPh_3$ ($^{Ph}$YPhos) or $PCy_3$ ($^{Cy}$YPhos) moiety showed that the arene-gold interaction in the aryl-substituted compounds is efficiently compensated by the formation of Au···H-C hydrogen bonds. The strongest interaction is found with the C-H moiety next to the onium center, which due to the polarization results in remarkably strong interactions with the shortest Au···H-C hydrogen bonds reported to date. Calorimetric studies on the formation of the gold complexes further confirmed that the $^{Ph}$YPhos and $^{Cy}$YPhos ligands form similarly stable complexes. Consequently, both ligands showed the same catalytic performance in the hydroamination, hydrophenoxylation and hydrocarboxylation of alkynes, thus demonstrating that Au···H-C hydrogen bonds are equally suited for the generation of highly effective gold catalysts than gold-arene interactions. The generality of this observation was confirmed by a comparative study between a biaryl phosphine ligand and its cyclohexyl-substituted derivative, which again showed identical catalytic performance. These observations clearly support Au···H-C hydrogen bonds as fundamental secondary interactions in gold catalysts, thus further increasing the number of design elements that can be used for future catalyst construction.

## Introduction

Gold catalysis has undergone a rapid development in the past two decades.[1] As is the case for numerous other metal-catalysed transformations, this success story is oftentimes associated with the development of ligands and the tailoring of their properties to meet the specific requirements of the metal and targeted reaction. In gold(I) catalysis, a cationic $LAu^+$ complex is usually the catalytically active species.[2] In order to stabilize these species and to generate highly active and efficient catalysts, secondary ligand metal interactions have been reported as being important in ligand design and have fuelled numerous advances in the field of homogenous catalysis. Particularly gold-arene interactions have repeatedly been described to being beneficial in gold(I) catalysis.[3] This was, for example, illustrated in the Buchwald biarylphosphine ligands (Figure 1), in which the lateral arene ring is involved in bonding to the metal center.[4] This design principle was adopted in several other phosphines and *N*-heterocyclic carbenes,[5] such as in the imidazo[1,5-a]pyridin-3-ylidene platform first described by Lassaletta and Glorius[6] or in Alcarazo's *N*-arylpiperidino-phosphines.[7]

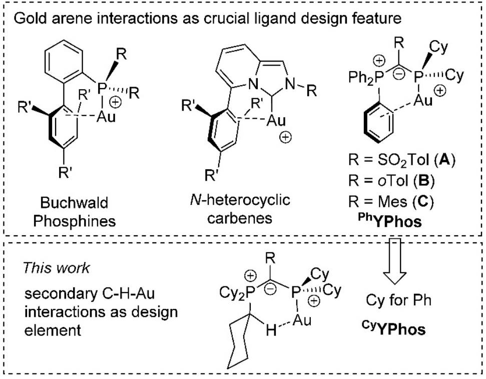

**Figure 1.** Recent examples of phosphine and carbene gold(I) complexes with postulated gold-arene interactions (top) and $^{Ph}$YPhos ligands with gold-arene interaction vs. Au···H-$C_{sp3}$ interaction and their novel $^{Cy}$YPhos analogues described in this work. (R= alkyl or aryl).

Recently, we reported on transition metal catalysts based on ylide-functionalized phosphines (YPhos), which showed very high activities in Pd- and Au-catalysed reactions.[8] Especially in gold(I)-catalyzed transformations, both with moderately (**A**)[8a] as well as highly electron-rich (**B** and **C**),[9] YPhos systems exhibit exceptionally high turnover numbers (Figure 1). Recent studies have indicated that the stabilization of the carbanionic center in the ylide backbone of the YPhos ligand is critical for high catalytic activity, since equally electron-rich, but smaller YPhos ligands, were not nearly as efficient due to competing decomposition of the catalytically active species initiated by the intrinsic reactivity of the highly basic ylidic carbon atom. All of these catalyst systems so far have relied on triphenyl phosphonium groups which were shown to foster arene-gold interactions, thus further contributing to the stability and high catalytic performance of the corresponding LAu(I)$^+$ -species.

The understanding of such secondary ligand metal interactions is important for future ligand design and for the development of high-performance catalysts. Thus, we wondered if these interactions were indeed necessary or if equally high activities can also be achieved without such stabilizing arene-gold interactions. Therefore, we turned our attention towards tricyclohexyl phosphonium substituted YPhos analogues ($^{Cy}$YPhos). Herein, we describe the synthesis of a series of novel $^{Cy}$YPhos ligands, their AuCl-complexes and analysis of their catalytic activity in the hydroamination of phenylacetylene. Surprisingly, these studies reveal that the arene-gold interactions are not necessary and that stabilizing hydrogen bonds are equally suited in generating highly active catalysts.

## Results and Discussion

### Ligand Synthesis

To probe the importance of supporting interactions between gold and the phosphonium moiety, we present a detailed study of the performance of the three PCy$_3$-substituted ligands $^{Cy}Y_{S}PCy_2$ (**L1**), $^{Cy}Y_{oTol}PCy_2$ (**L2**) and $^{Cy}Y_{Mes}PCy_2$ (**L3**) as congeners to **A**, **B** and **C**. Ligands **L2** and **L3** have previously been designed for the selective Pd-catalysed monoarylation of small primary amines.[10] Additionally, the *iso*-propyl-derivative of **L1**, $^{Cy}Y_{S}P\textit{i}Pr_2$ (**L4**) was synthesized to evaluate the influence of the lower steric bulk of the smaller alkyl group on the catalytic ability. **L1** and **L4** were prepared on gram scale as white solids by reaction of the metalated ylide $^{Cy}Y_{S}$-Li with Cy$_2$PCl and *i*Pr$_2$PCl in good yields of 75% and 70%, respectively.[11]

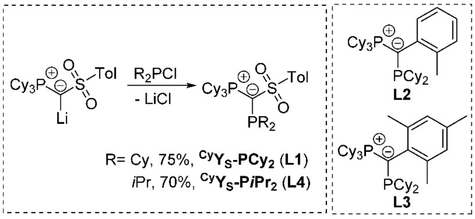

**Scheme 1**. Synthesis of $^{Cy}Y_{S}$-PR$_2$ by reaction of the metalated ylide $^{Cy}Y_{S}$-Li with dialkyl chlorophosphines (PR$_2$Cl with R=*i*Pr or Cy).

Both phosphines were fully characterized by means of multi-nuclear NMR spectroscopy, elemental analysis and diffraction studies on single crystals. **L1** features two sets of doublets in the $^{31}$P{$^1$H}-NMR spectrum at 31.7 and -7.3 ppm, with a coupling constant of $^2J_{PP}$ = 106.8 Hz, while **L4** displays resonances at 31.5 and 1.5 ppm with a slightly smaller coupling constant of $^2J_{PP}$ = 105.7 Hz. In addition to the obtained new ligands, **L1** and **L4**, we targeted a completely arene-free $^{Cy}$YPhos derivative, to eliminate any possible metal-arene interaction. Therefore, we tackled the synthesis of $^{Cy}Y_{SF}PCy_2$ (**L5**), an analogue of **1** in which the *p*-tolyl motif is replaced by a perfluorobutyl chain. To access this ligand, the metalated ylide $^{Cy}Y_{SF}$-Li first had to be synthesized. By analogy to the procedure reported for $^{Cy}Y_{S}$-Li,[11] the protonated precursor $^{Cy}Y_{SF}$-H was prepared in a one-pot reaction from the easily accessible phosphonium salt [Cy$_3$P-CH$_3$]I and the commercially available perfluorobutanesulfonyl fluoride in the presence of two equiv. of KHMDS in a very good yield of 83% (Scheme 2). $^{Cy}Y_{SF}$-H was isolated as a pale-yellow powder and fully characterized (see SI for details).

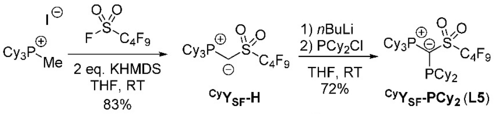

**Scheme 2**. Synthesis of the ylide precursor $^{Cy}Y_{SF}$-H from perfluorobutyl sulfonyl fluoride, KHMDS and the phosphonium salt [Cy$_3$P-Me]I and subsequent reaction with *n*BuLi and PCy$_2$Cl to yield $^{Cy}Y_{SF}$-PCy$_2$ (**L5**).

Deprotonation of $^{Cy}Y_{SF}$-H with *n*-butyllithium afforded the metalated ylide $^{Cy}Y_{SF}$-Li which was used in-situ and directly reacted with PCy$_2$Cl to yield $^{Cy}Y_{SF}$-PCy$_2$ (**L5**) as a colorless solid in 72% yield. **L5** was fully characterized by elemental analysis, single-crystal X-ray diffraction (XRD) analysis and multi-nuclear NMR spectroscopy. With $\delta_P$ = 32.3 and -0.7 ppm, its $^{31}$P{$^1$H} NMR signals are in the same range as observed for **L1** and **L4**, while with $^2J_{PP}$ = 95.0 Hz, the coupling constant is significantly smaller. Important NMR spectroscopic and crystal structure parameters are given in Table 1. XRD analyses confirm the expected connectivity and show the typical arrangement of PCy$_3$ substituted YPhos ligands, were the alkyl groups attached to the phosphorus atom point away from the phosphonium group to minimize the steric pressure.

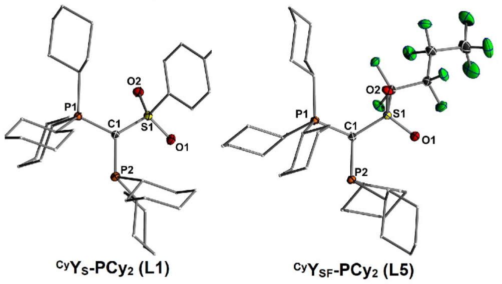

**Figure 2**. Molecular structures of $^{Cy}Y_{S}$-PCy$_2$ (**L1**) (left) and $^{Cy}Y_{SF}$-PCy$_2$ (**L5**) (bottom). Thermal displacement ellipsoids of selected atoms drawn at 50% probability level; hydrogen atoms are omitted for clarity.

**Table 1.** $^{31}$P{$^1$H} NMR spectroscopic data and selected crystal structure details for **L1**, **L4** and **L5**.

| | $^{Cy}$**Y$_S$-PCy$_2$ (L1)** | $^{Cy}$**Y$_S$-PiPr$_2$ (L4)** | $^{Cy}$**Y$_{SF}$-PCy$_2$ (L5)** |
|---|---|---|---|
| $\delta_P$ (PCy$_3$) [ppm] | 31.7 | 31.5 | 32.3 |
| $\delta_P$ (PR$_2$) [ppm] | -7.3 | 1.5 | -0.7 |
| $^2J_{PP}$ [Hz] | 106.8 | 105.7 | 95.0 |
| P1-C1 [Å] | 1.7570(15) | 1.7614(14) | 1.7688(11) |
| P1-C1-P2 [°] | 114.66(8) | 115.83(7) | 113.97(6) |

To evaluate the ligand electronic properties, we calculated the Tolman electronic parameter (TEP) by analyzing the carbonyl stretching frequencies of the corresponding [Rh($^{Cy}$YPhos)(acac)(CO)] complexes (Table 2). As expected, $^{Cy}$Y$_S$-PCy$_2$ (**L1**), with a TEP$_{calc}$ of 2057.0 cm$^{-1}$, is more electron-releasing than its isopropyl-substituted congener **L4** (TEP$_{calc}$ 2058.7 cm$^{-1}$). Furthermore, the stabilizing effect of the sulfonyl moiety becomes evident, by comparison with aryl substituted YPhos ligands **L2** and **L3**, which are significantly more electron-donating than **L1** and **L4**. Interestingly, $^{Cy}$Y$_{SF}$-PCy$_2$ (**L5**) with a TEP$_{calc}$ value of 2059.8 cm$^{-1}$ is even less electron-releasing than the simple alkyl phosphine PCy$_3$ (TEP$_{calc}$ 2058.1 cm$^{-1}$). This result clearly demonstrates the further increased electron-withdrawing nature of the perfluorobutylsulfonyl moiety and thus shows how easily the electronics of YPhos ligands can be tuned via backbone modification.

Table 2. Comparison of the TEP values for different alkylphosphines and YPhos ligands.

| Ligand | $\nu_{CO}$ **Rh [cm$^{-1}$]** | **TEP$_{calc.}$ [cm$^{-1}$]$^{[a]}$** |
|---|---|---|
| PPh$_3$$^{[a]}$ | 1978.0 | 2069.1 |
| PCy$_3$$^{[a]}$ | 1958.7 | 2058.1 |
| $^{Ph}$Y$_S$PCy$_2$ (**A**)$^{[b]}$ | 1953.5 | 2055.1 |
| $^{Ph}$Y$_{oTol}$PCy$_2$ (**B**)$^{[c]}$ | 1947.5 | 2051.7 |
| $^{Cy}$Y$_{oTol}$PCy$_2$ (**L2**)$^{[d]}$ | 1941.1 | 2048.0 |
| $^{Cy}$Y$_{Mes}$PCy$_2$ (**L3**)$^{[d]}$ | 1941.8 | 2048.4 |
| $^{Cy}$Y$_S$PCy$_2$ (**L1**) | 1956.8 | 2057.0 |
| $^{Cy}$Y$_S$P*i*Pr$_2$ (**L4**) | 1959.7 | 2058.7 |
| $^{Cy}$Y$_{SF}$PCy$_2$ (**L5**) | 1961.7 | 2059.8 |

[a] TEPs were determined by $\nu_{CO}$ in the [Rh(acac)(CO)(L)] complexes using the linear relationship between $\nu_{CO}$ for [Ni(CO)$_3$(L)] and [Rh(acac)(CO)(L)] reported in ref. 12. [b] Values taken from reference 8a. [c] Values taken from reference 9a. [d] Values taken form reference 10.

### Synthesis and Structures of the Gold complexes

With the novel ligands in hand, we next prepared [Au($^{Cy}$YPhos)Cl] complexes from the free ligands and [Au(tht)Cl] (**Scheme 3**). [Au($^{Cy}$Y$_S$PCy$_2$)Cl] (**P1**), [Au($^{Cy}$Y$_S$P*i*Pr$_2$)Cl] (**P4**) and [Au($^{Cy}$Y$_{SF}$-PCy$_2$)Cl] (**P5**) were isolated as colorless solids in good to quantitative yield. All complexes were characterized by NMR spectroscopy, XRD and elemental analysis. As expected, the $^{31}$P{$^1$H} NMR resonances are shifted significantly downfield upon complexation together with a decrease of the coupling constant, e.g. from 31.7 and -7.3 ppm ($^2J_{PP}$ = 106.8 Hz) in **L1** to 40.7 and 29.9 ppm ($^2J_{PP}$ = 35.6 Hz) for **P1**. Interestingly, in contrast to the phosphine precursors, the protons of the tertiary carbon atoms in the phosphonium group appeared as a slightly broadened signal in the $^1$H-NMR spectrum of complexes **P1** and **P4**. The corresponding carbon atom shows a similar behavior in the $^{13}$C{$^1$H} NMR spectrum and appears as a broad doublet at around 36.9 ppm. This broadening is even more pronounced for complex **P5** and could be caused by an attractive Au···H–C(sp$^3$) interaction. Indeed, VT-NMR studies of a solution of **P5** in DCM-d$^2$ showed a splitting of the signal at around 263 K with one proton signal being downfield shifted from 3.5 ppm to 4.4 ppm (see Figure S27 and S28). Such a downfield shift has also recently been reported for other Au···H–C interactions, but has controversially been discussed.[13] In the case of complex **P1**, no splitting of the PC*H* signal was observed thus suggesting a weaker gold hydrogen bond.

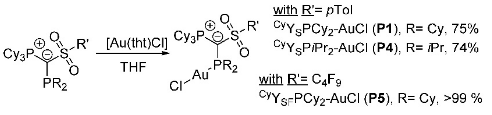
Cy3P
R'
[Au(tht)Cl]
THF
PR2
Au
Cl
with R'= pTol
CyYSPCy2-AuCl (P1), R= Cy, 75%
CyYSPiPr2-AuCl (P4), R= iPr, 74%
with R'= C4F9
CyYSFPCy2-AuCl (P5), R= Cy, >99 %

**Scheme 3**. Preparation of [Au)($^{Cy}$Y$_S$PR$_2$)Cl] complexes (with R= *i*Pr and Cy) from the reaction of L1, **L4** and L5 with [Au(tht)Cl] in THF.

The existence of Au···H-X hydrogen bonds has controversially been discussed in the literature,[14] but were experimentally and computationally proven in recent studies.[15] For example, the groups of Bourissou,[16] Berger and Monkowius[17] as well as Rulíšek[18] demonstrated that N$^+$-H ammonium or pyridinium groups are suitable donors for the formation of N-H···Au hydrogen bonds. Other strong donors such as O-H, F-H, NH$_3$ and HCN were also found to form close-contact interactions with gold.[19] Au···H-C interactions have very recently been reported, but have never been discussed as structural motif for ligand design in catalysis.[20] Despite numerous early discussions, it is now well established that the Au atom in these Au···H-X interactions acts as an electron donor and the C-H moiety as an acceptor, which is in contrast to "classical" agostic interactions which rely on the donation of electron density into an empty orbital at the metal center.[21] Accordingly, these interactions were named anagostic interactions or "contra-electrostatic" hydrogen bonds.[22] The later term emphasises the relation to classical H-bonds, which however differ in the charge of the C and H atom upon approximation of the donor (gold versus the H-bond acceptor).

Further proof of the Au···H-C interactions in the YPhos-gold complexes is manifested in their molecular structures (Figure 3). Indeed, with 2.39(4) Å and 2.38(5) Å in **P1** and **P5** respectively, the Au···H-C distances are remarkably short and significantly shorter than their sum of Van-der Waals radii (2.86 Å)[23] as well as hydrogen bonds previously reported.[20] For example, Koshini and coworkers reported on Au-H distances between 2.60 and 2.65 Å in gold clusters supported by a phenylene-bridged diphosphine ligand.[16a] To the best of our knowledge the Au-H9 distance of 2.38(5) Å in **P5** is the shortest distance reported to date for a Au···H-C hydrogen bond. Presumably, this interaction is stronger than those found with other C-H moieties due to the stronger polarization of this entity next the positively charged phosphorus centre.

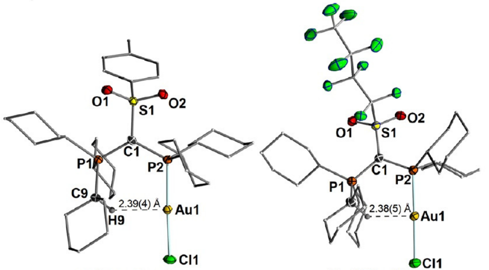

[Au($^{Cy}$Y$_S$-PCy$_2$)Cl]
**P1**

[Au($^{Cy}$Y$_{SF}$-PCy$_2$)Cl]
**P5**

**Figure 3**. Molecular structures of [Au($^{Cy}$Y$_S$-PCy$_2$)Cl] (**P1**) (left) and [Au($^{Cy}$Y$_{SF}$-PCy$_2$)Cl] (**P5**) (right). Thermal displacement ellipsoids of selected atoms drawn at 50% probability level; hydrogen atoms omitted for clarity.

Of course, one could argue that the interaction might also be caused by steric pressure within the molecule. However, the latter should be less critical in the structure of the complex with *i*Pr-substituted phosphine **L4**. Here, the smaller alkyl groups should give rise to a more flexible ylide structure and allow a widening of the P-C-P angle, which was found to be decisive for the approach of the phosphonium group to the metal center and hence for secondary metal ligand interactions.[24] Unfortunately, no crystals of **P4** of sufficient quality could be obtained to allow for the direct location of the hydrogen atom in the electron density map. However, the observed Au-C distance clearly indicates that also short interactions between gold and the PCy$_3$ unit are present in **P4** (Table 3). It is interesting to note, that **P2** and **P3** with aryl groups in the ylide-backbone showed considerably longer C-H···Au distances. Nonetheless, they are shorter than the sum of Van-der Waals radii, thus suggesting that weak secondary ligand metal interactions are still present in these complexes. These differences in the C-H···Au distances can be explained by the different bulk of the sulfonyl and the aryl groups. Whereas the flexible sulfonyl group allows the complexes **P1**, **P4** and **P5** to adopt the preferred geometry with a planar Au-P-C-P unit,[25] the rigid tolyl and mesityl substituents enforce a deformation, which results in the rotation of the PCy$_2$ moiety and hence the coordination of AuCl "outside" the center of the pocket formed by the PCy$_3$ and PCy$_2$ units (see Figure S36). This also results in a slightly reduced steric pressure of the aryl-substituted ligands directed towards the metal center as measured by the percent buried volume ($V_{bur}$%) (**Table 3**).[26] While all ligands are highly sterically demanding, covering more than half of the sphere defined in the model, it is slightly lower for the YPhos ligands **L2** and **L3** with an aryl group in the ylidic backbone. With 54.8 $V_{bur}$% **L1** is slightly bulkier than **L4** (53.2 $V_{bur}$%) and **L5** (52.5 $V_{bur}$%), but similar demanding than the PPh$_3$ substituted analogue **A**.

**Table 3.** $^{31}$P{$^1$H} NMR data, $V_{bur}$% and important crystal structure bond lengths and angles for the novel $^{Cy}$YPhos complexes.

| | P1 | P2[a] | P3[a] | P4[b] | P5 |
|---|---|---|---|---|---|
| $V_{bur}$% | 54.8 | 49.4 | 50.7 | 53.2 | 52.5 |
| $C_{PCy3}$-H-Au [Å] | 2.39(4) | 2.70(3) | 2.73(3) | n.d. | 2.38(5) |
| $C_{PCy3}$-Au [Å] | 3.264(3) | 3.49(3) | 3.407(2) | 3.312(15) | 3.301(4) |
| $C_{PCy3}$-H-Au [°] | 141.1(1) | 136.4(1) | 128.9(1) | n.d. | 138.6(1) |
| P1-C1-P2 | 122.7(2) | 121.2(1) | 123.7(1) | 124.8(7) | 119.6(2) |
| P2-Au-Cl [°] | 177.2(1) | 177.9(1) | 179.5(1) | 178.4(1) | 178.6(1) |

[a] Values taken from reference 10. [b] crystallographic values taken from one molecule of the asymmetric unit; data was not of sufficient quality for reliable determination of CH-Au interaction. [c] Calculated with the SambVca 2.1 program for the [Au(L)Cl] complexes; M-P distance = 2.28 Å, including H atoms.

### Calorimetric Studies

In order to gain further insights into the relative stability of cyclohexyl- vs phenyl-substituted YPhos ligands bound to gold, we initiated a solution calorimetry study focusing on ligand substitution of the labile dimetylsulfide (DMS) ligand in the common gold synthon, [Au(DMS)Cl]. Results are presented in Scheme 5.

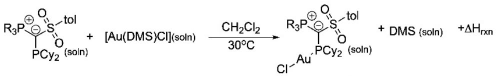

| R | −ΔH$_{rxn}$ (kcal/mol) |
|---|---|
| Ph (**A**) | 19.6 ± 0.4 |
| Cy (**L1**) | 18.3 ± 0.4 |

**Scheme 5**. Enthalpy of ligand substitution (kcal/mol) associated with the formation of [Au($^R$Y$_S$PCy$_2$)Cl] (R =Ph (**A**) and Cy (**L1**)) complexes.

The batch solution calorimetry results clearly show the very similar enthalpy of reaction values (-19.6 ± 0.4 (for **A**) and -18.3 ± 0.4 (for **L1**) kcal/mol) obtained for this simple ligand substitution. These data clearly indicate, that within 1 kcal/mol, both ligands possess similar binding energies to the metal center. The enthalpy values, we will emphasize, reflect all interactions with the metal ($\sigma$,$\pi$ and secondary interactions). The TEP value for **A**, 2055.1 cm$^{-1}$, (vs 2057.0 cm$^{-1}$ for **L1**) indicates that **A** is a better donor ligand just on an electronic basis. The infrared data suggest that more negative enthalpies of ligand substitution should be expected for the reaction in Scheme 5 involving **A**, and experimental results validate this expectation.

### Catalytic Activity

Next, we turned our attention to the catalytic activity of the [Au($^{Cy}$YPhos)Cl] complexes. We selected the hydroamination of phenylacetylene with aniline as first test reaction since this would permit a comparison with the previously reported PPh$_3$-substituted YPhos ligands. Furthermore, the effectiveness of gold catalysts in this reaction is severely influenced by the stability of the cationic gold species, which in turn is affected by secondary metal-ligand interactions, thus making it an ideal test reaction.[27] To this end, the [Au(YPhos)Cl] complexes of **A**, **B** and **C** as well as their direct PCy$_3$ analogues [Au($^{Cy}$Y$_S$PCy$_2$)Cl]

(**P1**), [Au($^{Cy}Y_{oTol}PCy_2$)Cl] (**P2**) and [Au($^{Cy}Y_{Mes}PCy_2$)Cl] (**P3**) were compared under identical reaction conditions (0.1 mol% of respective ligand and NaBAr$^F$, neat, 50°C). Additionally, we also tested **P4** to investigate the effect of the size of the alkyl groups attached to the phosphorus (III) atom on the catalytic activity. Furthermore, we also examined complex [Au($^{Cy}Y_{SF}PCy_2$)Cl] (**P5**) with the perfluorinated "aryl-free" ligand **L5**, which excludes the presence of any arene-gold interactions and hence gives direct information about the importance of these secondary interaction in the YPhos ligands.

Figure 4 shows the conversion time plots of the comparison between the $^{Ph}$YPhos and $^{Cy}$YPhos ligands. Note that without the addition of NaBAr$^F$ no conversion was observed. To our delight, the cyclohexyl-substituted complexes also proved to be highly active catalysts (Figure 4, left). They were equally efficient as their $PPh_3$-substituted analogues, (e.g. **A** and **P1**) or only slightly less active (**B** / **C** vs. **P2** / **P3**). Overall **P1** and **P3** performed superbly, leading to almost full conversion to the imine after approx. 5h of reaction time. Only the tolyl-substituted catalyst is slightly less effective. Changing the phosphine alkyl groups from cyclohexyl in **P1** to isopropyl in **P4**, led only to a moderate drop in activity (Figure 4, right). Most interestingly, the completely arene-free $^{Cy}$YPhos complex **P5** also gave nearly full conversion after 24h, thus demonstrating that the absence of arene-metal interaction also leads to highly active gold catalysts. The slightly lower activity of **P5** compared to its tosylate analogue **P1** can be attributed to more electron-withdrawing nature of the $C_4F_9$-substituents. Most importantly, the $PCy_3$-substituted YPhos ligands also preserved their high activity at lower catalyst loadings of only 0.05 mol% (Figure 4, right, dashed lines). Again, **P1** performed equally well compared to **A**. This is an important finding, since ligand design has so far focussed on the introduction of aryl substituents to incorporate arene gold interaction for stabilizing the catalytically active Au(I)$^+$ species. Our results clearly demonstrate that the active species with $^{Ph}$YPhos and $^{Cy}$YPhos are equally active thus suggesting that Au ···H-C interactions are equally suited for the generation of highly active gold catalysts, which even operate at very low catalyst loadings. This observation points to new possibilities for ligand design in gold catalysis.

To further prove the comparable performance of $^{Ph}$YPhos and $^{Cy}$YPhos we synthesized well-defined, cationic digold complexes bearing these ligands and examined their activity in the hydrophenoxylation and in the hydrocarboxylation of diphenylacetylene. In order to gain access to digold hydroxides, we chose to follow a new route which utilizes Au-Aryl complexes as precursors to cationic complexes (Scheme 6).[28] Therefore, after synthesizing the corresponding Au-Aryl complexes **1a** and **1b**, addition of acid to their acetonitrile suspensions, followed by evaporation of the solvent and extractions with DCM/$H_2O$ led to the desired digold hydroxide complexes **2a** and **2b** bearing the two YPhos ligands.[29,30] The complexes **1a**, **1b** and **2b** were also characterized by XRD analysis. Most interestingly, **1b** also exhibited short Au-H interactions (< 2.5 Å),[31] thus demonstrating that hydrogen bonds are not limited to the AuCl complexes.

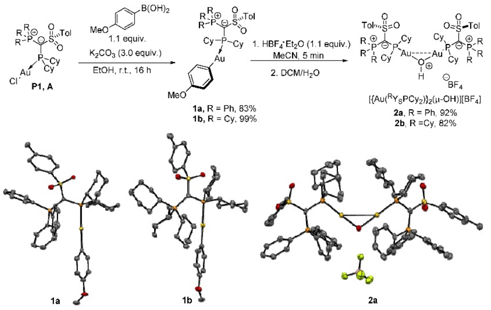

**Scheme 6.** Preparation of well-defined, cationic [{Au($^{R}Y_SPCy_2$)}$_2$($\mu$-OH)][$BF_4$] complexes (with R= Ph and Cy). Molecular structures of complexes **1a**, **1b** and **2a** are presented, showing thermal displacement ellipsoids at the 50% probability level and hydrogen atoms omitted for clarity.

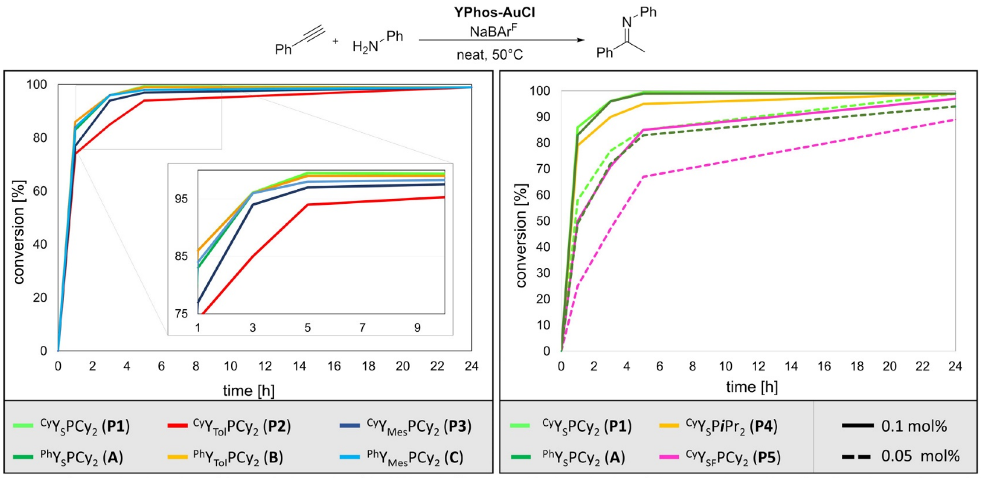

**Figure 4.** Conversion-time plots of the catalysis results of the YPhos-AuCl catalyzed hydroamination of phenyacetylene with aniline. Reaction conditions: 0.1 mol% YPhos ligand and 0.1 mol% NaBAr$^F$, neat, 50°C.

The complexes were evaluated in terms of their catalytic activity in the hydrophenoxylation and hydrocarboxylation of diphenylacetylene (Scheme 7).[32,33] In the hydrophenoxylation to **3**, both complexes displayed lower activity than the state of the art digold complex bearing the IPr ligand (IPr = *N,N'*-bis[2,6-(di-isopropyl)phenyl]imidazol-2-ylidene).[29] However, their overall performance was essentially the same, irrespective of the structure of the $^{R}$Y$_S$Phos (R = Ph or Cy) ligand. In hydrocarboxylation to **4**, their activity was higher when compared to that in hydrophenoxylation.[29] Again, the same trend is observed with both complexes displaying comparable catalytic activities. It seems that the bulky, electron-donating YPhos ligands can participate in dual gold catalysis as well, albeit leading to decreased activity in comparison with IPr. This is still significant, considering that both the ligand and the counterion (and their specific combination) are targets for optimization as they markedly affect the outcomes of these reactions. Of note, activation of the corresponding AuCl complexes with NaBAr$^F$ did not lead to product formation in either reaction shown in scheme 7, under various conditions (inert atmosphere, under air, premixing of the gold complex and the chloride abstractor). Synthesis and evaluation of other well-defined, cationic complexes of this kind will be pursued further.

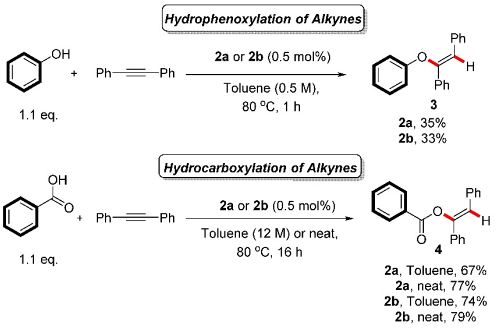

**Scheme 7.** Evaluation of well-defined, cationic [{Au($^{R}$Y$_S$PCy$_2$)}$_2$($\mu$-OH)][BF$_4$] complexes (**2a** with R = Ph and **2b** with R = Cy) in the hydrophenoxylation and hydrocarboxylation of diphenylacetylene. Yields were determined by $^1$H-NMR using 1,3,5-trimethoxybenzene as the internal standard and were reproduced once.

## Computational Studies

To further evaluate the stability and the nature of the secondary interactions between gold and the different $^{Cy}$YPhos ligands we performed computational studies on the PW6B95D3/def2tzvp (MWB60 for Au) level of theory. We were particularly interested in answering the following questions: i) Are C-H··Au interactions the most favored interactions or can the aryl or the sulfonyl groups in the ylide backbone of the $^{Cy}$Y$_S$-substituted YPhos ligands also bind and thus stabilize the metal center? ii) Are the short contacts between the CH protons of the PCy$_3$ moiety and the gold atom in **P1** and **P5** observed by XRD analysis present in the gas phase and solution structures and iii) what is the nature of these C(sp$^3$)–H···Au interactions?

To confirm that the conformer of **P1** observed in the crystal structure (**C1**) is also the preferred conformation in the cationic gold complexes a series of structures were optimised (Table 4). Local energy minima were found for the conformers **C2**, in which the ylidic substituent is rotated by ~160° about the P2-C1 bond and the gold atom is coordinated by the sulfonyl group, and **C3**, in which the ylidic substituent is rotated by ~180° and an arene – gold interaction can be observed. Energy optimization showed that conformer **C1** with the experimentally observed C(sp$^3$)-H··Au interaction is thermodynamically preferred over the structures exhibiting an S=O··Au (ΔΔG = 72 kJ·mol$^{-1}$) or arene-Au interaction (47.6 kJ·mol$^{-1}$). This preference is even more pronounced in **P5** with the perfluorobutyl group. It is noteworthy that also for **P3** with the mesityl substituent in the ylide backbone the conformer with the PCy$_3$ moiety oriented towards gold is preferred over a **C3** analogue with a mesityl-Au interaction (ΔΔG = 65 kJ/mol, see SI). Hence, the calculations clearly confirm the favourable C-H···Au interaction.

**Table 4.** Energies [kJ·mol$^{-1}$] of the different possible conformers of **P1** and **P5** and their cations with and without additional coordination of phenylacetylene (**pa**) relative to the energy of conformer **C1**.

| Complex | ΔΔG [kJ·mol$^{-1}$] 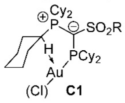 **C1** | ΔΔG [kJ·mol$^{-1}$] 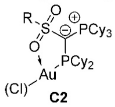 **C2** | ΔΔG [kJ·mol$^{-1}$] 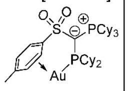 **C3** |
|---|---|---|---|
| **P1**<br>(R = *p*Tol) | ±0.0 | +72.3 | +47.6 |
| **L1·Au$^+$**<br>(R = *p*Tol) | ±0.0 | +39.6 | +3.5 |
| **L1·Au(pa)$^+$**<br>(R = *p*Tol) | ±0.0[a] | +29.4[a,b] | +19.0[a,c] |
| **P5**<br>(R = $C_4F_9$) | ±0.0 | +116[b] | +84.1[c] |
| **L5-Au$^+$**<br>(R = $C_4F_9$) | ±0.0 | +61.5[b] | +82.9[c] |
| **L5-Au(pa)$^+$**<br>(R = $C_4F_9$) | ±0.0[a] | +68.8[a,b] | +105.8[a,c] |

[a] including solvent effects using a polarizable continuum model with aniline as solvent. b] 90° rotation around P2-C1, S=O··Au interaction. [c] 90° rotation around P2-C1. No additional secondary ligand gold interaction. [

Interestingly, the preference of the hydrogen bonded conformer **C1** is also observed for the cationic gold complexes, which are more important in the catalysis. This also holds true for a gold complex with additional coordination of phenylacetylene (pa) including aniline as solvent (PCM model), which reflects the reaction conditions during catalysis. As shown in Table 4 the preference of the hydrogen bonded conformer is still significant for these complexes [LAu(pa)]$^+$, albeit being slightly less pronounced than in the neutral LAuCl complexes due to the decreased electron density at gold and the resulting weaker electron donation from Au to the C-H bond (*vide infra*). To obtain an estimate for the strength of the C-H··Au interactions we calculated a conformer of **C1** in which the cyclohexyl group is rotated about the P-C bond to prevent any C-H··Au interaction. This conformer revealed to be energetically disfavored over **C1** by 65 kJ·mol$^{-1}$.[34]

Having established that the C(sp$^3$)-H··Au interactions give rise to the thermodynamically most favoured structures, we next turned our attention towards studying the nature of this bonding interaction. To this end, natural bond orbital (NBO), quantum theory of atoms-in-molecules (QTAIM) and noncovalent interaction (NCI) analyses on the gold complexes **P1** and **A** were performed (including solvent effects: PCM for aniline). Overall, the computational studies in unison confirm the presence of attractive C-H gold interactions. The QTAIM studies show several bond critical points (BCP) in each of the gold complexes between the Au and the hydrogen atoms of CH and $CH_2$ in the $PCy_3$ and $PCy_2$ moieties. The BCP's with the highest electron density ρ(r) and Laplacian $\nabla^2\rho(r)$ are always found between the Au atom and the CH group in the $PCy_3$ moiety and range between ρ(r) = 0.015–0.024 e·bohr$^{-3}$ and $\nabla^2\rho(r)$ = 0.0432-0.0646 e·bohr$^{-5}$ (Table 5). These values are smaller than those reported for an Au···H-N hydrogen bond (ρ(r) = 0.033 e·bohr$^{-3}$ and $\nabla^2\rho(r)$ = 0.08 e·bohr$^{-5}$)[18], but higher than those of the Au···H-C hydrogen bond in a gold cluster with a phenylene-bridged diphosphine ligand (ρ(r) = 0.016 e·bohr$^{-3}$ and $\nabla^2\rho(r)$ = 0.037 e·bohr$^{-5}$).[20] The NCI plots show a blue isosurface around these BCP's, indicating a strong attractive interaction (Figure 5). Furthermore, the calculated C-H bonds involved in the hydrogen bond are slightly elongated compared to the non-interacting C-H bonds of the $PCy_3$ moiety (e.g. from 1.0949 to 1.1004 Å in **P1**. NBO analysis also shows a higher occupancy of the σ*(C-H) orbital of 0.030e to 0.040e while the occupancy of the binding σ orbital is not significantly decreased. Overall, the data clearly argue for weak hydrogen bonds with the Au atom acting as electron donor and the C-H moiety as an acceptor.[22] Most interestingly, the calculations indicate that the strongest Au···H-C is present in complex **P5** thus being in line with the data obtained from XRD and VT NMR studies (see above). This also corroborates with the calculated positive charges at the phosphorus atom in phosphonium group, which is slightly higher in **P5** ($q_P$ = +1.63) than in **P1** ($q_P$ = +1.62).

Besides the C-H···Au interactions with the CH moiety of the $PCy_3$ group further BCP's were found between Au and H atoms from $CH_2$ moieties in the $PCy_3$ and $PCy_2$ groups, however with lower values of the electron density and Laplacian ranging from ρ(r) = 0.0055–0.0164 e·bohr$^{-3}$ and $\nabla^2\rho(r)$ = 0.0169-0.0405 e·bohr$^{-5}$. The NCI plot shows a green coloured isosurface in the respective areas, indicating a weaker interaction. The observed occupancy of the C-H σ* orbitals is also consistent with lower values of <0.0210 e.

To compare the observed C(sp$^3$)-H···Au interaction with aryl···Au interactions, QTAIM and NCI analysis were also performed for the YPhos-AuCl complex **A** with the $PPh_3$ substituted ligand. The calculations revealed an arene···Au and a C(sp$^3$)H···Au interaction between the $PPh_3$ phenyl and the $PCy_2$ group, respectively, and the gold center. At the corresponding BCP's an electron density of ρ(r) = 0.0141 and 0.0121 e·bohr$^{-3}$ is found, which – in contrast to our initial expectation – is considerably lower than the electron density observed at the BCP for the C(sp$^3$)H···Au interaction in **P1**. Furthermore, the NCI scatterplot of **P1** clearly shows the additional spike at sign($\lambda_2$)ρ ~0.022, representing the strongly attractive C(sp$^3$)H···Au interaction, while the attractive interactions in **A** only extend to sign($\lambda_2$)ρ ~0.018 further confirming the weaker nature of the arene···Au and C(sp$^2$)H···Au interactions.

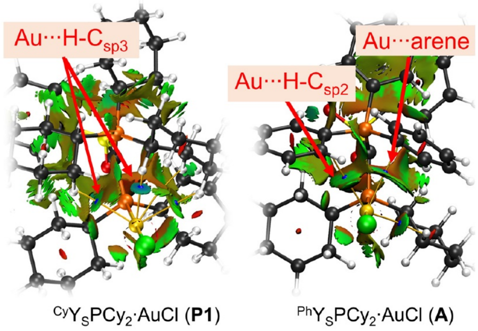

$^{Cy}Y_SPCy_2\cdot AuCl$ (**P1**)  $^{Ph}Y_SPCy_2\cdot AuCl$ (**A**)

**Figure 5**. NCI plots for **P1** and **A**. Coloured in a blue-green-red scheme over the range of (−0.035 < sign($\lambda_2$)ρ < 0.02) and isosurface of RDG = 0.5. Blue indicates strong attraction, green indicates weak interaction, and red indicates repulsion.

We further analysed the corresponding cationic gold complexes with phenylacetylene as additional ligand, which are considered to be the catalytically active species. Most importantly, it was found that the C(sp$^3$)H···Au interactions still persist, albeit with slightly lower values for ρ(r), $\nabla^2\rho(r)$ and a lower occupancy of the C-H σ* orbitals. This is well in line with the weaker donor capacity of the cationic gold centre which ultimately leads to a weaker hydrogen bond. This was already indicated by the relative energies of the different conformers (Table 4).

**Table 5**. Results of the computational studies on the secondary ligand gold interactions in the **P1**, **A**, **P3** and **P5**. For further details, see the Supporting Information. Calculations were performed on the PW6B95D3/def2tzvp (MWB60 for Au) level of theory including a PCM model with aniline as solvent.

| Complex | **LAuCl complex** | | | | | **LAu(dpa)$^+$ complex** | | | |
|---|---|---|---|---|---|---|---|---|---|
| | **d(CH-Au) [Å] exp.** | **d(CH-Au) [Å] calc.** | **ρ(r) [e.bohr$^{-3}$]** | **$\nabla^2$ρ(r) [e.bohr$^{-5}$]** | **occ($\sigma^*_{C-H}$)** | **d(CH-Au) [Å] calc.** | **ρ(r) [e.bohr$^{-3}$]** | **$\nabla^2$ρ(r) [e.bohr$^{-5}$]** | **occ($\sigma^*_{C-H}$)** |
| $^{Cy}Y_S$-$PCy_2$ (**P1**) | 2.39(4) | 2.438 | 0.0219 | 0.0603 | 0.0380 | 2.475 | 0.0204 | 0.0563 | 0.0357 |
| $^{Ph}Y_S$-$PCy_2$ (**A**) | 3.238(2) | 3.207 (Au-C) | 0.0141 | 0.0417 | - | 3.252 (Au-C) | 0.0133 | 0.0389 | - |
| | 2.84(3) | 2.844 (to $PCy_2$) | 0.0121 | 0.0386 | 0.0149 | 2.832 | 0.0118 | 0.0359 | 0.0210 |
| $^{Cy}Y_{Mes}$-$PCy_2$ (**P3**) | 2.73(3) | 2.642 | 0.0153 | 0.0432 | 0.0299 | 2.680 | 0.0142 | 0.0407 | 0.0287 |
| $^{Cy}Y_{SF}$-$PCy_2$ (**P5**) | 2.38(5) | 2.394 | 0.0238 | 0.0646 | 0.0397 | 2.387 | 0.0126 | 0.0329 | 0.0372 |

### Proof of concept

Having established that gold-hydrogen interactions are equally well suited for highly efficient YPhos based gold(I) catalysis, we next wanted to explore the generality of the concept. Au-complexes supported by *Buchwald*-type *biaryl*phosphines have shown remarkable performance in gold(I) catalysis. We wondered if substitution of the biaryl moiety with a phenyl-2-cyclohexyl group would enable gold-hydrogen interactions and thus eventually lead to similar high catalytic performance. To this end, we choose $^{Cy}$JohnPhos as the parent *Buchwald*-type phosphine and synthesized its phenyl-2-cyclohexyl analogue Cy-$^{Cy}$JohnPhos (**L6**) according to a previously reported procedure.[35] The corresponding gold complex (**P6**) was prepared from the free phosphine and [Au(tht)Cl] and could be isolated as colourless solid in quantitative yield. Strikingly, elucidation of the molecular structure of **P6** revealed – similar to the YPhos ligands – a relatively short Au···H-C distance of 2.77(4) Å, thus indicating the presence of a gold-hydrogen interaction in the solid-state structure. Broad signals between 48–25 ppm in the $^{31}P\{^1H\}$ NMR spectrum and at $\delta_H$ = 3.91 ppm in the $^1H$ NMR spectrum for the C*H*-proton of the phenyl-bound cyclohexyl group also indicate the existence of this interaction in solution. Furthermore, the lower buried volume of **L6** (%$V_{bur}$ = 38.1) compared to the YPhos ligands suggests that this interaction is not only enforced by steric bulk and hindered confirmational changes. The presence of the CH···Au hydrogen bond is also confirmed by DFT studies. QT/AIM as well as NBO analyses show similar values than those obtained for the YPhos ligands, for instance an electron density of $\rho(r)$ = 0.0204 e·bohr$^{-3}$ and a Laplacian of $\nabla^2\rho(r)$ = 0.0545 e·bohr$^{-5}$ at the bond critical point in **P6**.

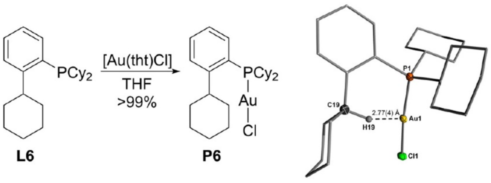

**Figure 6.** Synthesis of **P6** from [Au(tht)Cl] and free phosphine **L6** (left) and molecular structure of **P6** (right). Hydrogen atoms (except H19) omitted for clarity, ellipsoids drawn at the 50% probability level.

Having established the presence of the CH···Au hydrogen bond in **P6**, we next compared the performance of **$^{Cy}$JohnPhos·AuCl** and **P6** in the hydroamination of phenylacetylene with aniline under exact same conditions (0.1 mol%, 50°C) as applied above. Based on the results obtained with the YPhos ligands (see above), we expected similar catalytic performance of both complexes. Indeed, both ligands performed equally well (Table 6), giving full conversion to the imine after approx. 5h reaction time. This observation impressively confirms that arene-gold interactions are no prerequisite for the design of efficient gold catalysts, but that Au···H-C bonds are equally suited as design principle in ligands other than ylide-substituted phosphines.

**Table 6**. Results of the hydroamination of phenyacetylene with aniline catalyzed by the gold complexes with **L6** and CyJohnPhos. Reaction conditions: 0.1 mol% YPhos ligand and 0.1 mol% NaBAr$^F$, neat, 50°C.

| Reaction time [h] | Conversion with **CyJohnPhos** [%] | Conversion with **P6** [%] |
|---|---|---|
| 1 | 81 | 86 |
| 3 | 96 | 96 |
| 5 | 98 | 98 |
| 24 | >99 | >99 |

## Conclusion

In conclusion, we have performed a systematic study on $PPh_3$ and PCy.substituted YPhos ligands to elucidate the importance of different secondary ligand metal interactions for catalysis. Whereas earlier investigations have demonstrated that the $PPh_3$ group is involved in gold-arene interactions, NMR spectroscopic studies as well as XRD analyses of the cyclohexyl-substituted ligands, $^{Cy}$YPhos, revealed the presence of remarkably strong Au···H-C hydrogen bonds, amongst the shortest Au-H interaction reported to date. Computational studies further confirmed the bonding interaction between the gold center and the $PCy_3$ moiety and clearly showed that the metal acts as hydrogen bond donor. A direct comparison of the stability of the gold complexes of a $Ph_3P$-substituted ligand and its $PCy_3$ analogue by calorimetric studies showed that both ligands bind similarly strong to the metal. Strikingly, the $PCy_3$-substituted ligands delivered highly potent gold catalysts, which showed equal performance to their phenyl-substituted analogues. The generality of the ability of hydrogen bonds to support stable gold catalysts was demonstrated by means of a cyclohexyl substituted derivative of the widely used biaryl phosphines. Also for this class of phosphine ligands an identical catalytic performance was observed for the biaryl and the cyclohexyl-substituted system.

Overall, these observations clearly demonstrate that gold-arene interactions are no prerequisite for the design of highly effective gold catalysts, which has often been assumed in the literature, but can be replaced by hydrogen bonds. Thus, not only flanking arene substituents but also hydrogen bond acceptors may be introduced as stabilizing moieties in the ligand structures thus further expanding the tools available for future ligand design in gold catalysis.

## Acknowledgements

This work was supported by RESOLV, funded by the Deutsche Forschungsgemeinschaft (DFG, German Research Foundation) under Germany's Excellence Strategy – EXC-2033 - Projektnummer 390677874 and by the European Research Council (Starting Grant: YlideLigands 677749). We also gratefully acknowledge VLAIO (SBO project CO2PERATE), for support. The Special Research Fund (BOF) of Ghent University is also acknowledged (starting and advanced grants to SPN). The Research Foundation – Flanders (FWO) is thanked for PhD fellowships to N.V.T (11I6921N) and S.V.B (1S99819N). KVH and MS thank the Research Foundation – Flanders (FWO) (project AUGE/11/029) and the Special Research Fund (BOF) –

UGent (project 01N03217) for funding. Umicore AG is acknowledged for generous gifts of materials.

**Keywords:** Phosphines · secondary interactions · gold · catalysis · steric and electronic properties

---

[1] For selected reviews, see: a) S. Budagumpi, R. S. Keri, G. Achar, K. N. Brinda, *Adv. Synth. Catal.* **2020**, *362*, 970-997; b) A. S. K. Hashmi, *Chem. Rev.* **2007**, *107*, 3180-3211; c) W. Zi, F. D. Toste, *Chem. Soc. Rev.* **2016**, *45*, 4567-4589; d) S. A. Shahzad, M. A. Sajid, Z. A. Khan, D. Conseco-Gonzalez, *Synth. Commun.* **2017**, *47*, 735-755; e) D. B. Huple, S. Ghorpade, R.-S. Liu, *Adv. Synth. Catal.* **2016**, *358*, 1348-1367; f) D. P. Day, P. W. H. Chan, *Adv. Synth. Catal.* **2016**, *358*, 1368-1384; M. Jia, M. Bandini, *ACS Catal.* **2015**, *5*, 1638–1652; g) A. S. K. Hashmi, *Chem. Rev.* **2013**, *107*, 3180–3211; h) D. Garayalde, C. Nevado, *ACS Catal.* **2012**, *2*, 1462–1479; i) N. Krause, C. Winter, *Chem. Rev.* **2011**, *111*, 1994–2009; j) A. Corma, A. Leyva-P¦rez, M. J. Sabater, *Chem. Rev.* **2011**, *111*, 1657–1712; k) S. M. Abu Sohel, R.-S. Liu, *Chem. Soc. Rev.* **2009**, *38*, 2269–2281; l) A. Fürstner, *Chem. Soc. Rev.* **2009**, 38, 3208–3221; m) E. Jiménez-Núñez, A. M. Echavarren, *Chem. Rev.* **2008**, *108*, 3326–3350; n) N. T. Patil, Y. Yamamoto, *Chem. Rev.* **2008**, *108*, 3395–3442; o) D. J. Gorin, F. D. Toste, *Nature* **2007**, *446*, 395–403.

[2] Examples for isolated cationic Au(I) complexes: a) P. de Frémont, E. D. Stevens, M. R. Fructos, M. M. Díaz-Requejo, P. J. Pérez, S. P. Nolan *Chem. Comm.* **2006**, 2045-2047; b) M. P. Mingos, J. Yau, *J. Organomet. Chem.* **1994**, *479*, C16.

[3] For example: a) J. Iglesias-Sigüenza, C. Izquierdo, E. Diez, R. Fernandez and J. M. Lassaletta, *Dalton Trans.* **2016**, *45*, 10113–10117; b) C. Burstein, C.W. Lehmann and F. Glorius, *Tetrahedron* **2005**, *61*, 6207–6217; c) H. Tinnermann, L. D. M. Nicholls, T. Johannsen, C. Wille, C. Golz, R. Goddard and M. Alcarazo, *ACS Catal.* **2018**, *8*, 10457–10463; d) L. Shengrong, P. Alessio, C. Xinpeng, M. Xu, Z. Giuseppe, L. Zhang, *Angew. Chem. Int. Ed.* **2018**, *57*, 8250–8254; e) T. Witteler, H. Darmandeh, P. Mehlmann, F. Dielmann, *Organometallics*, **2018**, *37*, 3064-3072.

[4] P. Pérez-Galán, N. Delpont, E. Herrero-Gómez, F. Maseras and A. M. Echavarren, *Chem. Eur. J.* **2010**, *16*, 5324–5332.

[5] a) S. Handa, L. M. Slaughter, *Angew. Chem. Int. Ed.* **2012**, *51*, 2912-2915; b) L. Noël-Duchesneau, N. Lugan, G. Lavigne, A. Labande, V. César, *Organometallics*, **2014**, *33*, 5085-5088; c) L. Shengrong, P. Alessio, C. Xinpeng, M. Xu, Z. Giuseppe, L. Zhang, *Angew. Chem. Int. Ed.* **2018**, *57*, 8250–8254.

[6] (a) J. Iglesias-Sigüenza, C. Izquierdo, E. Diez, R. Fernandez and J. M. Lassaletta, *Dalton Trans.* **2016**, *45*, 10113–10117. (b) C. Burstein, C.W. Lehmann and F. Glorius, *Tetrahedron* **2005**, *61*, 6207–6217; c) J. Francos, F. Grande-Carmona, H. Faustino, J. Iglesias-Sigüenza, E. Díez, I. Alonso, R. Fernández, J. M. Lassaletta, F. López, J. L. Mascarenas, *J. Am. Chem. Soc.* **2012**, 134, 14322–14325; d) F. Grande-Carmona, J. Iglesias-Sigüenza, E. Álvarez, E. Díez, R. Fernández, J. M. Lassaletta, *Organometallics* **2015**, *34*, 5073–5080.

[7] H. Tinnermann, L. D. M. Nicholls, T. Johannsen, C. Wille, C. Golz, R. Goddard and M. Alcarazo, *ACS Catal.* **2018**, *8*, 10457–10463.

[8] a) T. Scherpf, C. Schwarz, L. T. Scharf, J.-A. Zur, A. Helbig and V. H. Gessner, *Angew. Chem. Int. Ed.* **2018**, *57*, 12859-12864; b) C. Schwarz, J. Handelmann, D. M. Baier, A. Ouissa, V. H. Gessner, *Catal. Sci. Tech.* **2019**, *9*, 6808-6815. c) P. Weber, T. Scherpf, I. Rodstein, D. Lichte, L. T. Scharf, L. J. Gooßen and V. H. Gessner, *Angew. Chem. Int. Ed.* **2019**, *58*, 3203-3207; d) X.-Q. Hu, D. Lichte, I. Rodstein, P. Weber, A.-K. Seitz, T. Scherpf, V. H. Gessner and L. J. Gooßen, *Org. Lett.* **2019**, *21*, 7558-7562; e) Z. Hu, X.-J. Wei, J. Handelmann, A.-K. Seitz, I. Rodstein, V. H. Gessner, L. J. Gooßen, *Angew. Chem. Int. Ed.* **2021**, *60*, 6778–6783; f) T. Scherpf, H. Steinert, A. Großjohann, K. Dilchert, J. Tappen, R. Rodstein, V. H. Gessner, *Angew. Chem. Int. Ed.* **2020**, *59*, 20596-20603; g) I. Rodstein, J. Tappen, K. McGuire, A. Großjohann, J. Löffler T. Scherpf, V. H. Gessner, *Chem. Eur. J.* **2020**, *26*, 4281-4288

[9] J. Handelmann, C. Naga Babu, H. Steinert, C. Schwarz, T. Scherpf, A. Kroll, V. H. Gessner, *Chem. Sci.* **2021**, *DOI: 10.1039/D1SC00105A*.

[10] I. Rodstein, D.S. Prendes, L. Wickert, M. Paaßen, V.H. Gessner, *J. Org. Chem.* **2020**, 85, 14674-14683.

[11] H. Darmandeh, T. Scherpf, K.-S. Feichtner, C. Schwarz, V. H. Gessner, *Z. Anorg. Allg. Chem.* **2020**, *646*, 835-841.

[12] L. Chen, P. Ren, and B. P. Carrow, *J. Am. Chem. Soc.* **2016**, *138*, 6392-6395.

[13] J. Vícha, C. Foroutan-Nejad, M. Straka, *Nat. Commun.* **2019**, *10*, 1643.

[14] a) A. Ilie, C. I. Rat, S. Scheutzow, C. Kiske, K. Lux, T. M. Klapçtke, C. Silvestru, K. Karaghiosoff, *Inorg. Chem.* **2011**, *50*, 2675–2684; b) F. Kraus, H. Schmidbaur, S. S. Al-juaid, *Inorg. Chem.* **2013**, *52*, 9669–9674; c) H. Schmidbaur, H. G. Raubenheimer, L. Dobrzanska, *Chem. Soc. Rev.* **2014**, *43*, 345–380; d) H. Schmidbaur, H. G. Raubenheimer, L. Dobrzanska, *Chem. Soc. Rev.* **2014**, *43*, 345-380.

[15] H. Schmidbaur, *Angew. Chem. Int. Ed.* **2019**, *58*, 5806-5809.

[16] M. Rigoulet, S. Massou, E. D. Sosa Carrizo, S. Mallet-Ladeira, A. Amgoune, K. Miqueu, D. Bourissou, *Proc. Natl. Acad. Sci. USA* **2019**, *116*, 46-51.

[17] R. J. F. Berger, J. Schoiber, U. Monowius, *Inorg. Chem.* **2017**, *56*, 956.

[18] M. Straka, E. Andris, J. Vícha, A. Růžička, J. Roithová, L. Rulížek, *Angew. Chem. Int. Ed.* **2019**, *58*, 2011-2016; *Angew. Chem.* **2019**, *131*, 2033-2038.

[19] a) F. Groenewald, J. Dillen, H. G. Raubenheimer, C. Esterhuysen, *Angew. Chem. Int. Ed.* **2016**, *55*, 1694-1698; *Angew. Chem.* **2016**, *128*, 1726-1730; b) M. Kumar, J. S. Francisco, *J. Am. Chem. Soc.* **2020**, *142*, 6001-6006; c) F. Groenewald, H. G. Raubenheimer, J. Dillen, C. Esterhuysen, *Dalton Trans.* **2017**, *46*, 4960-4967; d) L. Estévez, *Dalton Trans.* **2020**, *49*, 4797-4804. For an Si-H-Au interaction, see: e) F. Rekhroukh, L. Estévez, C. Bijani, K. Miqueu, A. Amgoune, D. Bourissou, *Angew. Chem. Int. Ed.* **2016**, *55*, 3414-3418.

[20] a) M. A. Bakar, M. Sugiuchi, M. Iwasaki, Y. Shichibu, K. Konishi, *Nat. Commun.* **2017**, *8*, 576; b) M. Vaddamanu, A. Sathyanarayana, Y. Masaya, S. Sugiyama, O. Kazuhisa, K. Velappan, K. Subramaniyam, K. Hisano, O. Tsutsumi, G. Prabusankar, *Organometallics* **2020**, *39*, 2202−2206; c) M. K. Pandey, H. S. Kunchur, D. Mondal, L. Radhakrishna, B. S. Kote, M.S. Balakrishna, *Inorg. Chem.* **2020**, *59*, 3642−3658; d) M. Guitet, P. Zhang, F. Marcelo, C. Tugny, J. Jimenez-Barbero, O. Buriez, C. Amatore, V. Mouries-Mansuy, J.-P. Goddard, L. Fensterbank, Y. Zhang, S. Roland, M. Menand, M. Sollogoub, *Angew. Chem. Int. Ed.* **2013,** *52*, 7213; e) S. K. Verma, S. N. Ansari, P. Kumari, S. M. Mobin, *Organometallics* **2019**, *38*, 2591-2596.

[21] a) M. Brookhart, M. L. H. Green, G. Parkin, *Proc. Natl. Acad. Sci. USA* **2007**, *104*, 6908-6914; b) W. Scherer, A. C. Dunbar, J. E. Barquera-Lozada, D. Schmitz, G. Eickerling, D. Kratzert, D. Stalke, A. Lanza, P. Macchi, N. P. M. Casati, J. Ebad-Allah, C: Kuntscher, *Angew. Chem., Int. Ed. Engl.* **2015**, *54*, 2505-2509.

[22] a) G. P. Gomes, G. Xu, X. Zhu, L.-M. Chamoreau, O. Bistri-Aslanoff, S. Roland, I. V. Alabugin, M. Sollogoub, *ChemRxiV*, **2020**, doi: 10.26434/chemrxiv.12167916. (b) D. Braga, F. Grepioni, E. Tedesco, K. Biradha, G. R. Desiraju, *Organometallics* **1997**, *16*, 1846-1856.

[23] CRC Handbook of Chemistry and Physics; Haynes, W. M., Ed.; CRC Press: Boca Raton, FL, **2010**.

[24] L. T. Scharf, I. Rodstein, M. Schmidt, T. Scherpf, V. H. Gessner, *ACS Catal.* **2020**, *10*, 999-1009.

[25] This geometry is preferred since it results in a perpendicular arrangement of the lone pairs at C1 and P2 and hence in a minimization of electronic repulsion. For details, see reference 7a.

[26] L. Falivene, Z. Cao, A. Petta, L. Serra, A. Poater, R. Oliva, V. Scaraon, L. Cavallo, *Nat. Chem.* **2019**, *11*, 872-879.

[27] W. Wang, G. B. Hammond, B. Xu, *J. Am. Chem. Soc.* **2013**, *134*, 5697-5705.

[28] N. V. Tzouras, M. Saab, W. Janssens, T. Cauwenbergh, K. Van Hecke, F. Nahra, S. P. Nolan, *Chem. Eur. J.* **2020**, *26*, 5541-5551.

[29] A. Gómez-Suárez, Y. Oonishi, S. Meiries, S. P. Nolan, *Organometallics* **2013**, *32*, 1106-1111.

[30] F. Nahra, N. V. Tzouras, A. Collado, S. P. Nolan, *Nat. Protoc.* **2021**, DOI 10.1038/s41596-020-00461-6.

---

[31] **1b** features two molecules in the asymmetric unit, which show short Au-H bond lengths of 2.32(7) and 2.49(7) Å. The Au-C distances amount to 3.279(8) and 3.281(8) Å, respectively.

[32] Y. Oonishi, A. Gómez-Suárez, A. R. Martin, S. P. Nolan, *Angew. Chem. Int. Ed.* **2013**, *52*, 9767-9770.

[33] S. Dupuy, D. Gasperini, S. Nolan, *ACS Catal.* **2015**, *5*, 6918-6921.

[34] Note, that this value does not reflect the CH-Au bond strength but is the sum of energy changes caused by the rotation about the P-C bond. Second order perturbation calculations within the NBO analysis give to contributions of the CH-Au interaction with a total energy of 14.6 kJ·mol$^{-1}$, which is in the range of typical hydrogen bonds.

[35] H. Riihimäki, T. Kangas, P. Suomalainen, H. K. Reinius, S. Jääskeläinen, M. Haukka, A. O. I. Krause, T. A. Pakkanen, J. T. Pursiainen, *J. Mol. Cat. A. Chem.* **2003**, *200*, 81-94.

## Entry for the Table of Contents

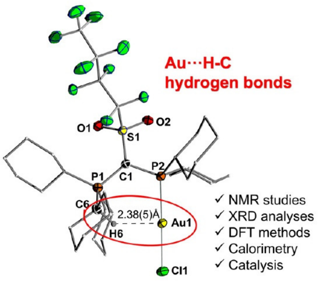
Au···H-C
hydrogen bonds
O1
O2
S1
P1
C1
P2
C6
2.38(5)Å
H6
Au1
Cl1
✓ NMR studies
✓ XRD analyses
✓ DFT methods
✓ Calorimetry
✓ Catalysis

**Hydrogen bond.** Systematic experimental and computational studies on $PPh_3$ and $PCy_3$-substituted ylide-functionalized phosphines as well as on a biaryl and a cyclohexyl-aryl phosphine demonstrate that Au···H-C hydrogen bonds can serve as secondary metal ligand interactions similar gold-arene interactions often used in ligand design for the stabilization of catalytically active species. Remarkably short Au-H bonds are observed which give way similar catalytic activities compared to the phenyl-substituted analogues.

Institute and/or researcher Twitter usernames: @ViktoriaGessner

## 3.6 $^{Cy}$YPhos ligands in Pd catalysis

Motivated by the outstanding results achieved with the novel $^{Cy}$YPhos ligands in Au(I) catalysis, we next became interested if the same ligands would enable Pd-catalyzed organic transformations. Recently, our group reported on palladium-complexes bearing electron-rich tricyclohexyl-phosphonium based YPhos ligands with aryl (**joYPhos**, **pinkYPhos**, **mesYPhos**) or alkyl groups (**keYPhos**, **trYPhos**) in the backbone, which were highly potent catalysts for C–C and C–N cross coupling reactions.[29,31,33,45,46]

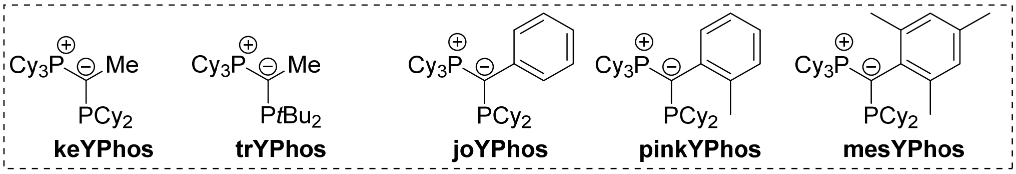

**Figure 34.** Important examples of YPhos ligands, suitable for high-performance Pd-catalysis.

Especially in *Buchwald-Hartwig* aminations (BHA), the use of these ligands unraveled one of the most potent catalysts systems known to date for this transformation, enabling even highly electron-deficient aryl-chlorides to be coupled at low catalyst loadings (0.5 mol%) and at ambient conditions (Scheme 72), thus outperforming most of the known phosphine and NHC-based palladium complexes normally used as catalysts for this type of reactions.

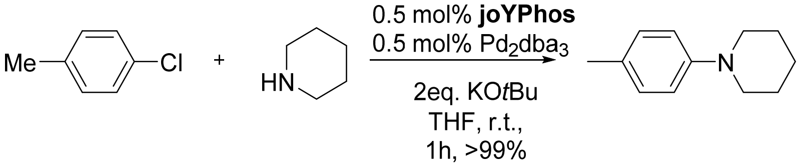

**Scheme 72.** Example of an Pd-catalyzed amination of *p*-chlorotoluene with piperidine at room temperature enabled by the **joYPhos** ligand system.

However, their high activity comes also with some drawbacks. Caused by their strong electron-donating properties, some of these ligand systems are highly sensitivity towards elevated reaction temperatures[31], which are sometimes needed for difficult or sterically demanding substrates, ultimately leading to catalyst decomposition and thus to reduced long-term activities. For the same reason, also incompatibilities with sensitive functional groups were observed.[31] The novel $^{Cy}$YPhos systems developed in this work differ from the already described ligands in two key points: First, due to the electron-withdrawing nature of the sulfonyl-group, they are only moderately electron-rich and thus should be less sensitive towards side reactions compared to their alkyl and aryl counterparts, which should result in a higher functional group tolerance. Second, the incorporation of the sulfonyl-moiety should enable an additional O-coordination to the Pd-center and thus a higher stability at elevated temperatures should be achieved. Moreover, the additional donation from the sulfonyl's oxygen atom may act as an anchoring side arm, which easily opens up, rendering an in-situ formed open coordination side when necessary for substrate coordination (Scheme 73).

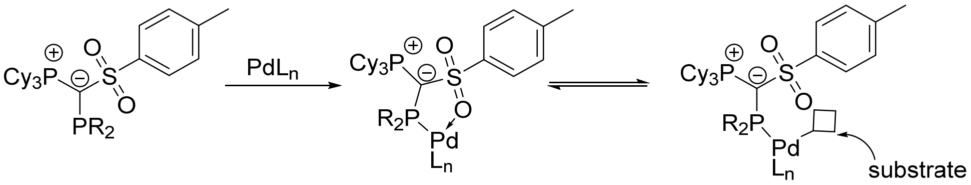

**Scheme 73.** Attempted, reversible coordination of one of the sulfonyl's oxygen atoms to the palladium center.

To test if the sulfonyl substituted $^{Cy}$YPhos ligands are able to form palladium complexes, **$^{Cy}$Y$_S$-PCy$_2$** was mixed with an equimolar amount of Pd$_2$dba$_3$ and THF-d$_8$ was added.

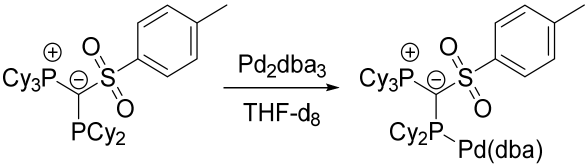

**$^{Cy}$Y$_S$-PCy$_2$** **$^{Cy}$Y$_S$-PCy$_2$-Pd(dba)**

**Scheme 74.** Preparation of **$^{Cy}$Y$_S$-PCy$_2$-Pd(dba)** via reaction of **$^{Cy}$Y$_S$-PCy$_2$** with Pd$_2$dba$_3$ in THF.

The reaction was analyzed by $^{31}$P{$^1$H}-NMR spectroscopy and revealed to be highly selective. The formed product gives rise to a signal that appears high field shifted compared to the free ligand (*cf.* $\delta_P$ = 31.7, -7.3 ppm), resonating at $\delta_P$ = 32.5 (d, $^2J_{PP}$ = 34.4 Hz) and 22.1 ppm (brd, $^2J_{PP}$ = 35.1 Hz), respectively. However, after 1h still around 10% of starting material was present and full conversion could not be achieved also after a prolonged reaction time. From the reaction mixture, a block shaped, black crystal suitable for XRD analysis was obtained. The molecular structure is depicted in Figure 35.

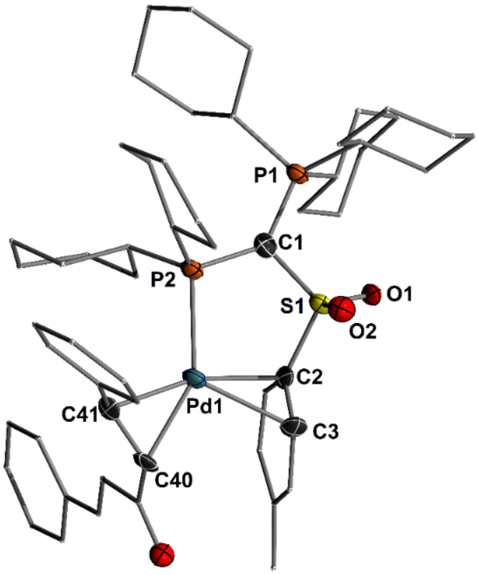

**Figure 35.** Molecular structure of **$^{Cy}$Y$_S$-PCy$_2$-Pd(dba)**. Due to low data quality, only the constitution of the molecule is given here.

Unfortunately, the obtained crystal was only of low quality, thus a detailed discussion on bond lengths and angles can not be made. However, the obtained structure clearly confirms the formation of the **$^{Cy}$Y$_S$-PCy$_2$-Pd(dba)** complex, albeit the coordination mode is not as anticipated. The palladium atom favors coordination of the arene moiety over the sulfonyl's oxygen atom. Additionally, one dba ligand is also coordinated. However, such a $\eta^2$ coordination is often observed in Pd(0) complexes and is in general reversible.[190] Since the **$^{Cy}$Y$_S$-PCy$_2$-Pd(dba)** complex is formed relatively fast in THF, studies on the catalytic ability were performed *in-situ*. The rate determining-step in palladium-catalyzed transformations is often the oxidative addition of the aryl-halide. Since this is also the case for BHA and the beforementioned YPhos ligands are able to perform this step at room temperature even with non-activated aryl chlorides, the ability to perform similar oxidative additions on **$^{Cy}$Y$_S$-PCy$_2$-Pd(dba)** was probed. Therefore, an excess amount of *p*-chlorotoluene was added to a freshly prepared solution of **$^{Cy}$Y$_S$-PCy$_2$-Pd(dba)** at room temperature and the reaction was monitored via $^{31}$P{$^1$H}-NMR spectroscopy.

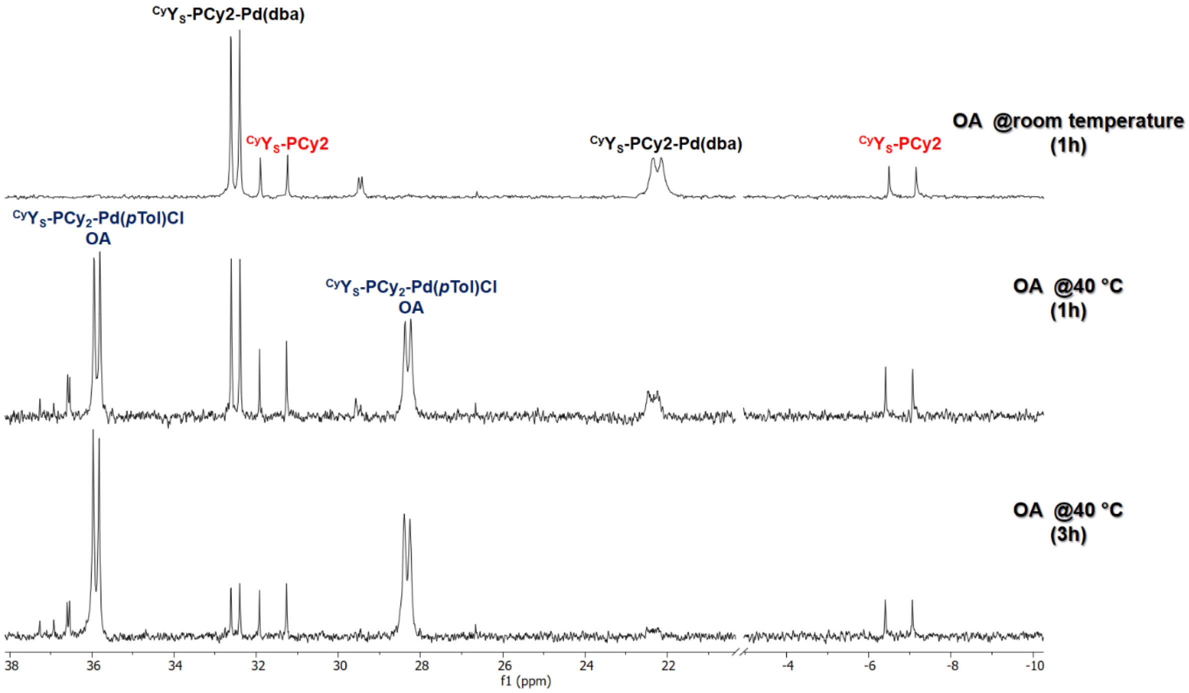

**Figure 36.** Oxidative addition of *p*-chlorotoluene on **$^{Cy}$Y$_S$-PCy$_2$-Pd(dba)** at different reactions temperatures and -times: room temperature, 1h (top); 40°C, 1h (middle); 40°C, 3h (bottom).

As can bee seen from Figure 36, oxidative addition did not proceed under ambient conditions (top). This was expected, because with an only moderate electron-richness, **$^{Cy}$Y$_S$-PCy$_2$** does not posses enough donor power to enable oxidative addition of the strong enthalpic C–Cl bond of *p*-chlorotoluene at room temperature. However, moderate heating to 40°C for 1h, results in the formation of the (presumably) oxidative addition product **$^{Cy}$Y$_S$-PCy$_2$-Pd(*p*Tol)Cl** (middle). Prolonged heating (3h) at 40°C resulted in almost complete conversion of the **$^{Cy}$Y$_S$-PCy$_2$-Pd(dba)** complex (bottom). **$^{Cy}$Y$_S$-PCy$_2$-Pd(*p*Tol)Cl** is characterized by more low field shifted signals in the $^{31}$P{$^1$H}-NMR spectrum, resonating at $\delta_P$ = 35.9 (brd, $^2J_{PP}$ = 23.0 Hz) and 28.3 ppm (brd, $^2J_{PP}$ = 35.1 Hz). Furthermore, one can observe that the resolution of the spectra gets worse upon heating. This can be attributed to the precipitation of the assumed product from the reaction mixture. From this mixture, a colourless crystal was isolated which was suitable for XRD analysis.

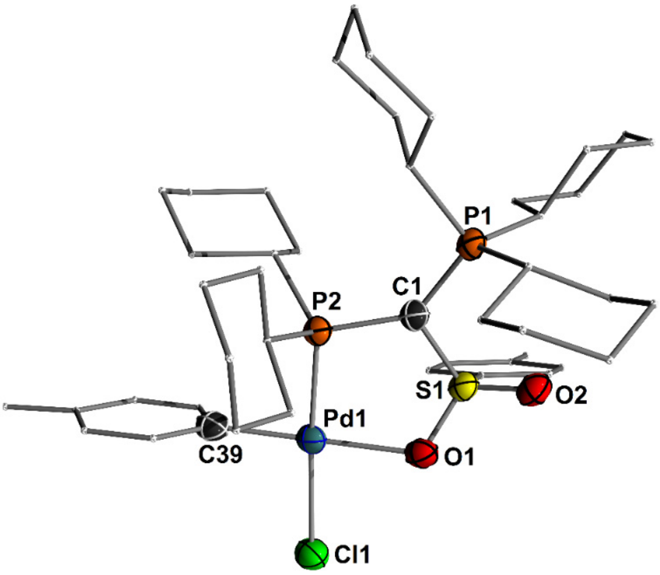

**Figure 37.** Molecular structure of **$^{Cy}Y_S$-PCy$_2$-Pd(*p*Tol)Cl**. Due to low data quality, only the constitution of the molecule is given here.

Again, the obtained data was not of sufficient quality to discuss specific bond lengths and angles. However, as can be seen from Figure 37, the XRD analysis clearly confirmed the successful oxidative addition. The Pd(II) atom adopts a square planar geometry, being coordinated by the **$^{Cy}Y_s$-PCy$_2$** ligand via the phosphine phosphorus atom and as anticipated also via one of the oxygen atoms of the sulfonyl group. As a consequence, the *p*-tolyl group and the chlorine atom are placed on the same side, thus adopting a *cis*-geometry. It must be noted that the sulfonyl coordination leads to the formation of a monomeric complex. This contrasts other YPhos ligands which formed dimeric oxidative addition products.[191]

With the established reaction parameters for the oxidative addition of *p*-chlorotoluene in hand, the catalytic amination with this ligand system was tested. That said, a freshly prepared THF solution of **$^{Cy}Y_S$-PCy$_2$-Pd(dba)** (0.5 mol%) was added to a THF solution containing piperidine, *p*-chlorotoluene, KO*t*Bu and 1,3,5-trimethoxybenzene (internal standard) and stirred at 40°C. The reaction mixture was monitored via $^1$H-NMR spectroscopy. However, even after stirring over night, no conversion was detected. This is surprising, since oxidative addition is feasible at this reaction temperature and thus this usually rate-determining-step should not hamper the catalytic activity. Albeit oxidative addition was already achieved at 40°C, the reaction was repeated with refluxing THF to speed up this reaction step. To our surprise, also under these reaction conditions no conversion at all was observed. Similarly, varying the amine scope or using the bromo-toluene derivative, which should be easier to couple, did not result in any detectable conversion to the desired products. To investigate why no conversion was obtained with **$^{Cy}Y_S$-PCy$_2$-Pd(dba)**, further single steps of the catalytic cycle were explored. After confirming that oxidative addition is feasible, the next step would be the coordination of the amine. Therefore, a freshly prepared solution of **$^{Cy}Y_S$-PCy$_2$-Pd(*p*Tol)Cl** was treated with an excess of piperidine and the mixture was monitored via $^{31}$P{$^1$H}- NMR spectroscopy (Figure 38).

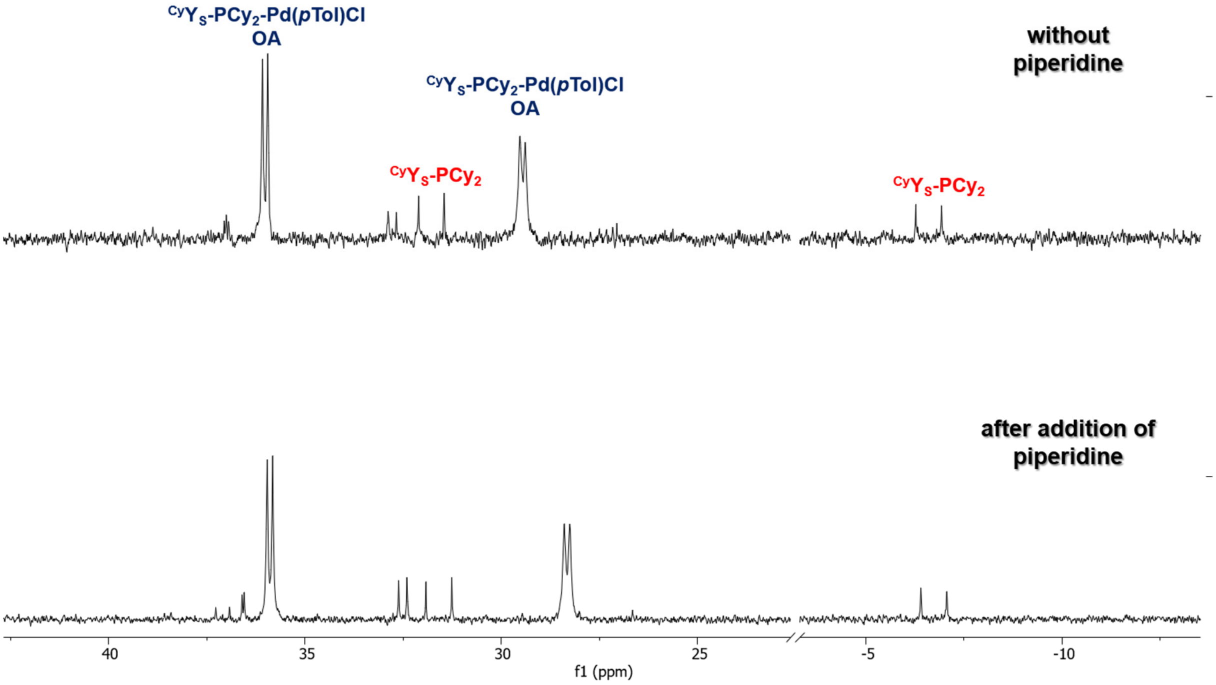

**Figure 38.** $^{31}P\{^1H\}$-NMR spectrum from the reaction mixture of **$^{Cy}$Y$_S$-PCy$_2$-Pd(*p*Tol)Cl** before (top) and after the addition of piperidine (bottom).

As can be seen from the obtained spectra, upon addition of piperidine only a slight shift towards lower field is observed, while no additional signals appear. This is a strong indication for the absence of any formation of the respective amine-complex. One explanation for this observation could be the inability of the oxidative addition complex **$^{Cy}$Y$_S$-PCy$_2$-Pd(*p*Tol)Cl** to perform a dissociation of the O–Pd bond. As a consequence, no additional coordination at the Pd(II) center is possible, explaining the lack of reactivity in catalysis.

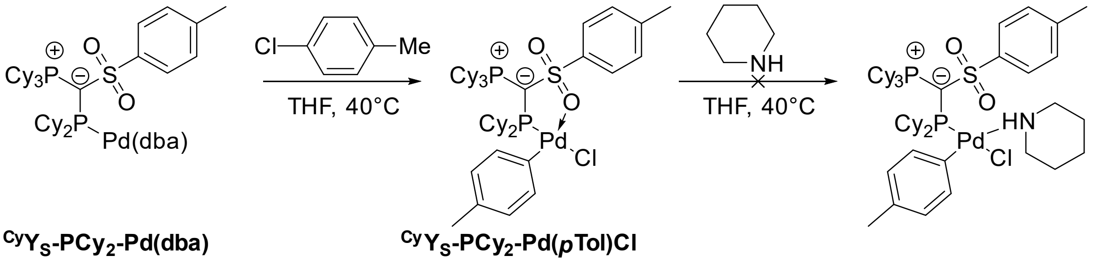

**Scheme 75.** Synthesis of the oxidative addition complex **$^{Cy}$Y$_S$-PCy$_2$-Pd(*p*Tol)Cl** and subsequent failed attempt to prepare its amine-coordinated species with piperidine.

To prove this hypothesis, DFT calculations were performed on the PBE0/def2svp//PBE0/def2tzvp level of theory by *Henning Steinert* from the Gessner group. Indeed, it was found that **$^{Cy}$Y$_S$-PCy$_2$-Pd(*p*Tol)Cl** with a palladacycle is 23.4 kJ/mol more stable in energy than its de-coordinated analogue. In the latter, the Pd atom is only stabilized by weak Pd–H agostic interactions, thus explaining why in **$^{Cy}$Y$_S$-PCy$_2$-Pd(*p*Tol)Cl** the additional coordination via a stronger Pd–O bond is preferred. Furthermore, the kinetic barrier to break this bond seems also to be high in energy, since also in refluxing THF no conversion was observed. Due to this reasons, no further attempts to use the novel sulfonyl-substituted YPhos ligands in Pd catalyzed C–N cross coupling reactions were performed.

# 4. Summary and Outlook

The aim of this thesis was the synthesis, isolation and characterization of a tricyclohexyl-phosphonium yldiide (**$^{Cy}$Y-M**) and its subsequent application in group 14 and 15 chemistry. The first part focused on the use of the yldiide as a stabilizing ligand for low-valent group 14 compounds, above all, heavier carbene analogues. The electronic properties as well as the reactivity of the novel ylide-tetrylenes were investigated via DFT calculations and experimental methods. In the second section of this thesis, the preparation of **$^{Cy}$Y**-functionalized phosphines, the elucidation of their electronic-and steric properties as well as their ability to function as strong donor ligands for TM catalysis were explored.

### Synthesis, Isolation and Crystal Structures of the Metalated Ylides
### [$Cy_3P$-C-$SO_2$Tol]M (M = Li, Na, K)

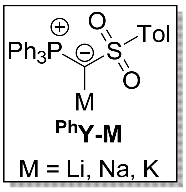

**$^{Ph}$Y-M**
M = Li, Na, K

Our group recently reported on the synthesis of a triphenylphosphonium based metalated ylide (**$^{Ph}$Y-M**) and its application as a strongly donating ligand for the isolation of low-valent main-group compounds. However, during our studies on **$^{Ph}$Y** stabilized main-group compounds C–H(sp$^2$) activation reactions were observed, leading to the cleavage of the ylide substituent from the main-group element. Thus, to further exploit the use of metalated ylides as stabilizing ligands in main-group chemistry, the synthesis of the tricyclohexylphosphonium substituted metalated ylide (**$^{Cy}$Y-M**) was addressed in the first part of this thesis. This yldiide was expected to be less prone to bond activation reactions due to stronger C–H(sp$^3$) bonds. The metalated ylide **$^{Cy}$Y-M** was synthesized from the corresponding ylide **$^{Cy}$Y-H** which could be obtained by reaction of *in-situ* formed tricyclohexyl phosphonium methylide ($Cy_3P=CH_2$) with tosyl fluoride. In this reaction, $Cy_3P=CH_2$ acts not only as a nucleophile, but also as a base, thus delivering directly **$^{Cy}$Y-H** and one equivalent of [$Cy_3P$–Me]F. To prevent the formation of [$Cy_3P$–Me]F, under optimized reaction conditions $Cy_3P=CH_2$ was treated with one equivalent of tosyl fluoride in the presence of another equivalent of base, thus delivering **$^{Cy}$Y-H** in a single reactions step as a colourless solid in excellent yields of up to 90% (Figure 39). **$^{Cy}$Y-H** was fully characterized and furthermore, its preparation could be performed on large scale (>10 g).

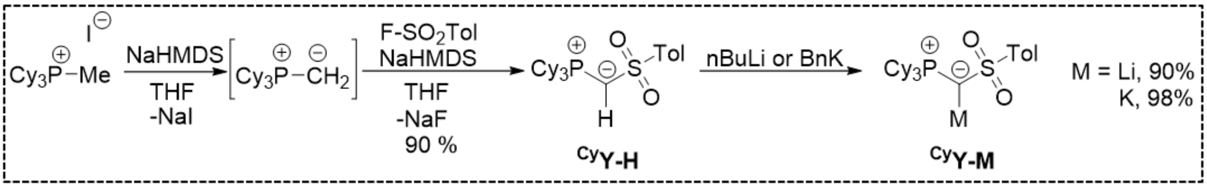

**Figure 39.** One-pot synthesis of **$^{Cy}$Y-H** via reaction of $Cy_3P=CH_2$ with tosyl fluoride in the presence of NaHMDS and subsequent metalation of **$^{Cy}$Y-H** with strong metal bases to yield the yldiides **$^{Cy}$Y-M** (M = Li, K).

With the ylide in hand, its metalation was subsequently probed with HMDS bases, which were successfully applied to access its $PPh_3$ analogue. However, no reaction was observed, which is in line with the decreased CH-acidity of **$^{Cy}$Y-H**, due to the more electron-rich $PCy_3$ unit. Thus, successful metalation of **$^{Cy}$Y-H** was achieved with benzyl potassium, *n*-BuLi and $NaNH_2$ delivering the respective metalated ylides **$^{Cy}$Y-M** (M = Li, Na, K).

All metalations turned out to be highly selective, however gram-scale isolation was most facile for **$^{Cy}$Y-Li** and **$^{Cy}$Y-K**, delivering the metalated ylides as yellow, highly air-and moisture sensitive solids in excellent yields. Both yldiides were fully characterized by NMR spectroscopy, elemental analysis and XRD studies. Their molecular structures are depicted in Figure 40 and show some interesting features.

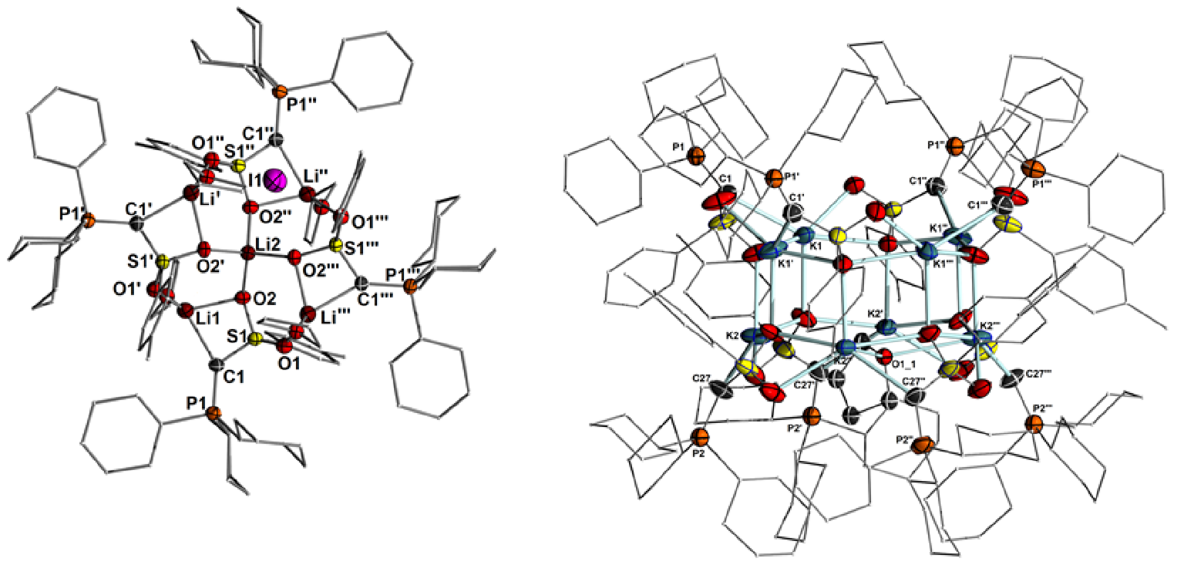

**Figure 40.** Molecular structures of ($^{Cy}$**Y-Li**)$_4$·LiI·4THF (left) and ($^{Cy}$**Y-K**)$_8$·2THF (right). Ellipsoids drawn at the 50% probability level, non coordinating THF solvents as well as disordered moieties and hydrogen atoms are omitted for clarity.

$^{Cy}$**Y-Li** crystallizes as $S_4$ symmetric tetramer and incorporates an additional molecule of LiI, while $^{Cy}$**Y-K** forms a $C_4$ symmetric structure with an octahedral prism consisting of $(K_4O_4)_2$ units. Compared to the protonated precursor $^{Cy}$**Y-H**, a remarkable contraction of the P–C–S linkage is observed upon deprotonation.

### Synthesis of Low-Valent Dinuclear Group 14 Compounds with Element-Element Bonds by Transylidation

With the novel metalated ylides in hand, their ability to stabilize low-valent main group species was next addressed. Therefor, the synthesis of a di-ylide stabilized germylene ($^{Cy}$**Y$_2$Ge**) and stannylene ($^{Cy}$**Y$_2$Sn**) via salt metathesis with $^{Cy}$**Y-M** and half an equiv. of $ECl_2$ (E=Ge, Sn) was attempted in a similar way as previously described for the $PPh_3$-substituted analogue.[166]

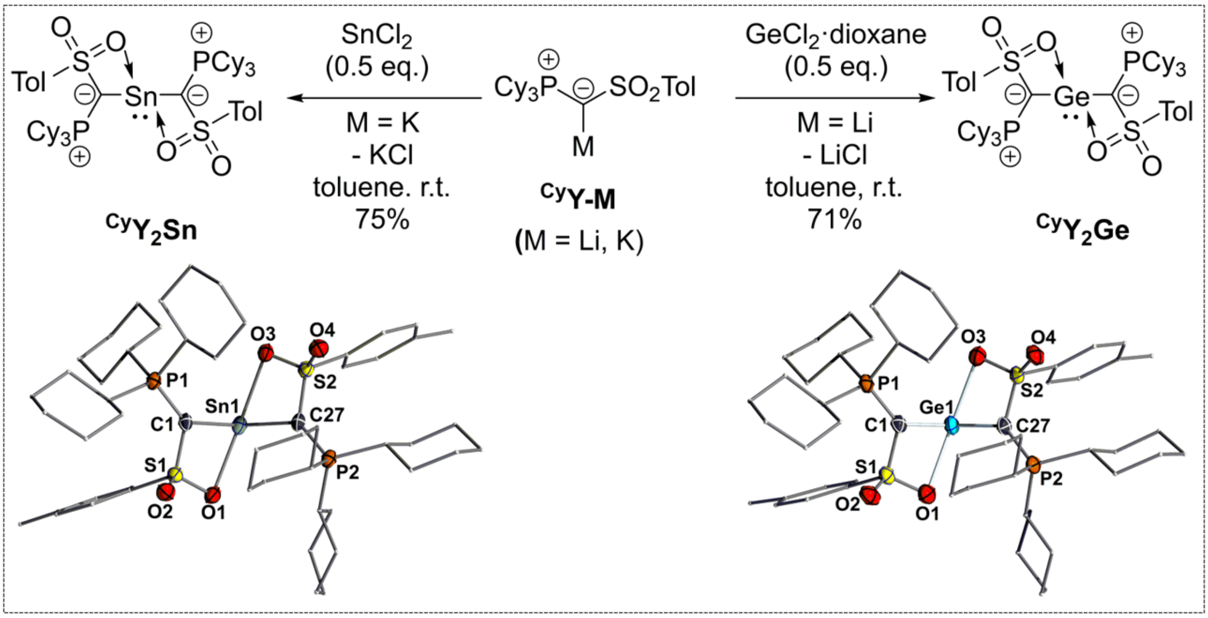

**Figure 41.** Syntheses of di-ylide tetrylenes $^{Cy}$**Y$_2$E** (E = Ge, Sn) from salt metathesis reactions between metalated ylides $^{Cy}$Y-M (M = Li, K) and E(II)Cl$_2$ precursors (top); molecular structures of $^{Cy}$**Y$_2$Sn** (bottom, left) and $^{Cy}$**Y$_2$Ge** (bottom, right). Ellipsoids drawn at the 50% probability level, disordered moieties and hydrogen atoms omitted for clarity.

Indeed, by following this synthesis route, $^{Cy}$**Y$_2$Ge** and $^{Cy}$**Y$_2$Sn** could be obtained as pure, pale yellow solids in good yields (Figure 41) and fully characterized. Their molecular structures show essentially the same properties as their PPh$_3$-substituted analogues. For instance, the unusual alignment of the three lone pairs of electrons in the C–E–C linkage is retained, thus confirming the high donating ability of the tetrylenes. Next, it was tested if replacement of the PPh$_3$ group with a PCy$_3$ moiety really leads to an increase in stability. Indeed, refluxing a benzene solution of $^{Cy}$**Y$_2$Ge** did not show any sign of decomposition as judged by NMR analysis. With both tetrylenes in hand, their reactivity towards Lewis acids such as GeCl$_2$·dioxane and SnCl$_2$ was probed, with the intention to exploit their exceptional donor strength for the formation of donor-acceptor complexes, which upon halide abstraction would give access to ylide-stabilized heavier vinyl cations of type $^{Cy}$Y$_2$E=E(Cl)$^+$ (E = Ge or Sn). However, the reaction of $^{Cy}$**Y$_2$Ge** and $^{Cy}$**Y$_2$Sn** with the group 14 metal chlorides turned out to not delivered the respective donor-acceptor complexes. Instead, a unique ylide-transfer from one metal to another is observed. As such, the reaction of $^{Cy}$**Y$_2$Ge** with SnCl$_2$ or $^{Cy}$**Y$_2$Sn** with GeCl$_2$·dioxane in equimolar amounts, delivered the chloro(ylide)stannylene dimer ($^{Cy}$YSnCl)$_2$ (**170**) and 1,2-dichloro(ylide)digermene $^{Cy}$Y(Cl)Ge-Ge(Cl)$^{Cy}$Y (**169**). These (formally) dimers of the chloro(ylide)tetrylenes, could also be prepared from the metalated ylide $^{Cy}$**Y-M** and one equivalent of GeCl$_2$·dioxane and SnCl$_2$ , respectively. Interestingly, the di-ylide tetrylenes $^{Cy}$**Y$_2$E** were formed as intermediates in these reactions, which subsequently reacted further to **170** and **169**, respectively (Figure 42).

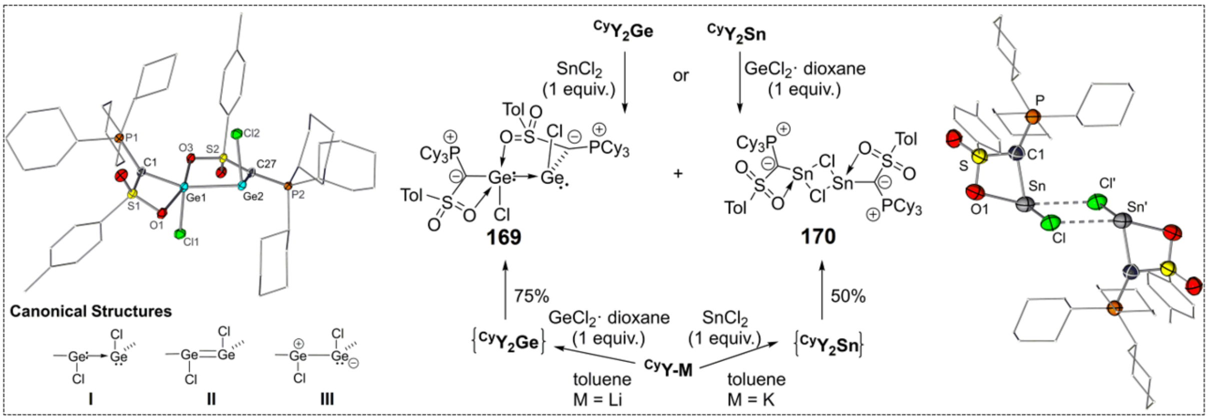

**Figure 42.** Synthesis of chloro(ylide)tetrylenes **169** and **170** via trans-ylidation (middle); molecular structure of **170** (right) and molecular- as well as canonical structures of **169** (left).

**169** and **170** could be isolated as pure solids and were fully characterized by means of NMR spectroscopy, elemental- and XRD analysis. **169** exhibits an unusual, unsymmetrical structure, while **170** forms a symmetric chloro-bridged dimer in the solid-state. Due to a relatively long Ge(II)–Ge(II) bond of 2.4908(4) Å, **169** can not be considered as a true digermene with a Ge=Ge bond (**II**) but should be rather described as a germylene stabilized germylene (**I**) or with a polar Ge–Ge single bond (**III**). However, the facile cleavage of this bond (*vide infra*) indicates that canonical structure (**III**) is presumably less pronounced. The observed ylide-transfer reactivity is remarkable and might offer new ways for the synthesis of other ylide-stabilized low-valent main-group compounds under mild conditions and thus should be studied in the near future.

### Reactivity of ylide-stabilized acyclic germylenes and stannylenes

Next, the ability of the novel di-ylide tetrylenes to activate small molecules like $CO_2$, CO and $H_2$ was tested. However, pressurizing benzene solutions of **$^{Cy}Y_2Ge$** and **$^{Cy}Y_2Sn$** with the respective small molecules did not result in any reaction, even under harsh conditions. Due to this lack of reactivity, the electronic properties of the di-ylide tetrylenes were elucidated via DFT methods. The calculated frontier orbital energies of **$^{Cy}Y_2E$** (E = Ge, Sn) show that both tetrylenes are strong donors, reflected by their high lying HOMOs. However, due to additional coordination of the sulfonyl oxygen atoms to the metal center, the respective LUMOs are well stabilized, resulting in large HOMO-LUMO energy gaps. Since narrow frontier orbital energies are essential for the activation of strong enthalpic bonds, the synthesis of more reactive ylide-substituted tetrylene systems was attempted. Therefor, the replacement of one ylide-substituent by a more electropositive ligand without an additional coordination site was attempted, with the aim to lower the respective LUMO energy. Unfortunately, introduction of the hypersilyl group by reaction of the chloro(ylide)tetrylenes **169** and **170** with two equivalents of $KSi(SiMe_3)_3$, repeatedly failed. However, preparation of a terphenyl-substituted system proved to be more successful. Terphenyl-substituted tetrylenes have shown to exhibit wide angles between the main group element and the sterically demanding substituents, ultimately leading to narrower frontier orbital energies and thus to high reactivities.[111,112] Reaction of **169** with two equivalents of (2,6-$Tripp_2$-$C_6H_3$)-Li·$Et_2O$ (**Ar$^{\text{Tripp}}$-**

**Li**) lead to ylide-/terphenyl-stabilized tetrylene **173**, which could be successfully isolated as a yellow solid in good yield.

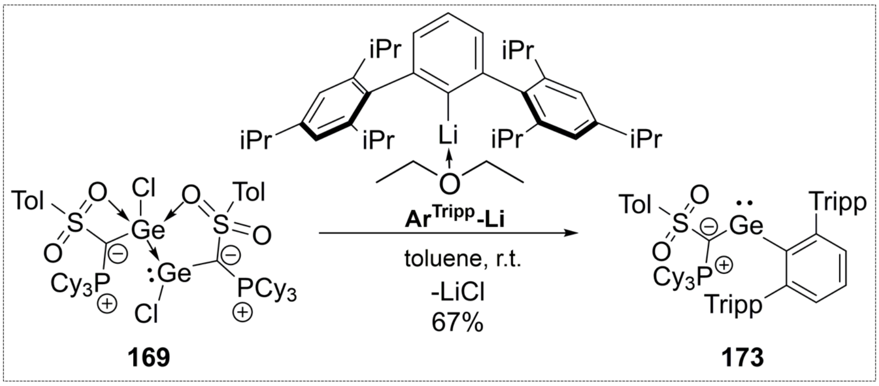

**Figure 43.** Synthesis of the ylide-/terphenyl-stabilized tetrylene **173**.

Contrary to $^{\mathbf{Cy}}\mathbf{Y_2Ge}$, in the molecular structure of **173** the C–E–C linkage is not perpendicular arranged to the P–C–S plane of the ylide substituent, thus enabling *π*-donation from the ylidic carbon atom to the metal center. This was also confirmed by the calculated WBI and NBO analyses. Substitution of one ylide substituent in $^{\mathbf{Cy}}\mathbf{Y_2Ge}$ with $\mathbf{Ar^{Tripp}}$ indeed results in a narrower HOMO-LUMO energy gap (Figure 44). As anticipated, the LUMO is destabilized compared to its di-ylide congener, due to the missing electron-donation from the sulfonyl's oxygen atoms into the empty p-orbital at Ge. However, the LUMO of **173** lies still higher in energy than those of related terphenyl-germylenes without an additional *π*-donor substituent like the boryl-stabilized germylene **175**. Since the $\Delta E_{H\text{-}L}$ of **173** lies between those calculated for $^{\mathbf{Cy}}\mathbf{Y_2Ge}$ and **175**, it should be examined if the calculated energy gap of 414 kJ/mol is narrow enough to promote activation of strong enthalpic bonds. Therefor, a solution of **173** was pressurized with 1 bar of hydrogen gas. However, no sign of conversion was observed.

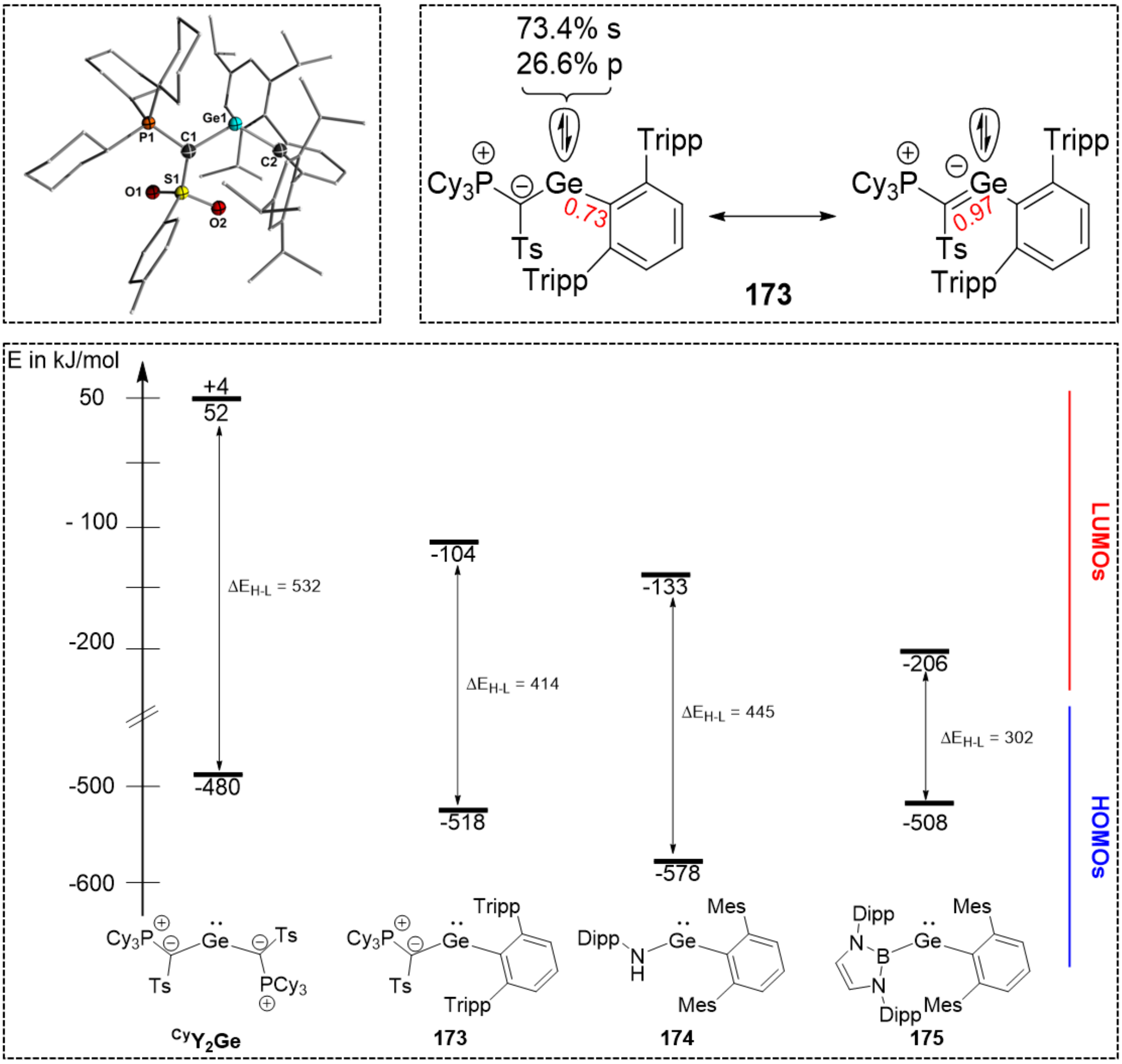
P1
C1
Ge1
C2
S1
O1
O2
73.4% s
26.6% p
Cy3P
Ge
0.73
Ts
Tripp
Tripp
173
Cy3P
Ge
0.97
Ts
Tripp
Tripp
E in kJ/mol
50
- 100
-200
-500
-600
+4
52
ΔEH-L = 532
-480
-104
ΔEH-L = 414
-518
-133
ΔEH-L = 445
-578
-206
ΔEH-L = 302
-508
LUMOs
HOMOs
Cy3P
Ge
Ts
Ts
PCy3
CyY2Ge
Cy3P
Ge
Ts
Tripp
Tripp
173
Dipp
N
H
Ge
Mes
Mes
174
Dipp
N
B
N
Dipp
Ge
Mes
Mes
175

**Figure 44.** Resonance structures of **173** including WBIs and properties of the HOMO (right, top); molecular structure of **173** (left, top); calculated HOMO-LUMO energy values and $\Delta E_{H\text{-}L}$ for different terphenyl-stabilized germylenes (bottom).

These results clearly emphasize that for efficient $H_2$ activation based on ylide-stabilized germylenes an even narrower $\Delta E_{H\text{-}L}$ is necessary. This may be achieved by combining for instance the boryl substituent used in **175** with the ylide group $^{\mathbf{Cy}}\mathbf{Y}$, which should result in a germylene with an extremely narrow $\Delta E_{H\text{-}L}$. Additionally, **173** may be suitable for the activation of other strong enthalpic bonds like the more polar N–H bonds in ammonia. However, from the obtained results it is clear that the chemistry of strongly donating acyclic ylide-substituted germylenes and stannylenes is still in its infancy and that more exciting results such as with respect to their coordination chemistry or to reactivity changes by variations in the ylidic backbone can be expected in the future.

### Towards the synthesis of an ylide-stabilized acyclic silylene

After the successful isolation of **$^{Cy}$Y**-stabilized acyclic germylenes and stannylenes, the quest for a possible preparation of **$^{Cy}$Y$_2$Si** emerged. Since the former could be easily accessed via salt-metathesis from their E(II) chlorides, a similar strategy to access **$^{Cy}$Y$_2$Si** was used. To this end, the metalated ylide **$^{Cy}$Y-Li** was reacted with half an equivalent of NHC stabilized silicon dichloride (**IPr·SiCl$_2$**). However, several attempts to access the silylene via this route failed and only the protonation of the ylide as well as free IPr were observed. Similarly, attempts to prepare di-ylide chloro silane precursor from $SiHCl_3$ or $SiX_4$ (X = Cl, Br, I) which upon base induced HCl elimination or reduction would give the desired silylene, failed. Instead, either only mono-substitution took place (**$^{Cy}$Y-SiHCl$_2$**) or the reactions were highly unselective and only gave inseparable product mixtures ($SiX_4$). Since the classical methods for preparation of a silylene were unsuccessful, it was probed if transylidation would be a viable method to access this species. Therefor, the already isolated di-ylide tetrylenes **$^{Cy}$Y$_2$E** (E = Ge, Sn) were used as the low-valent precursors, which upon reaction with **IPr·SiCl$_2$** or $SiX_4$ (X = Cl, Br, I) would transfer their ylide substituents to silicon, yielding either directly a silylene or a suitable Si(IV) precursor. Unfortunately, both attempts were unsuccessful and in no case the formation of a silylene species was observed. Thus, acyclic silylenes based on the **$^{Cy}$Y**-substituent seem not to be easily accessible.

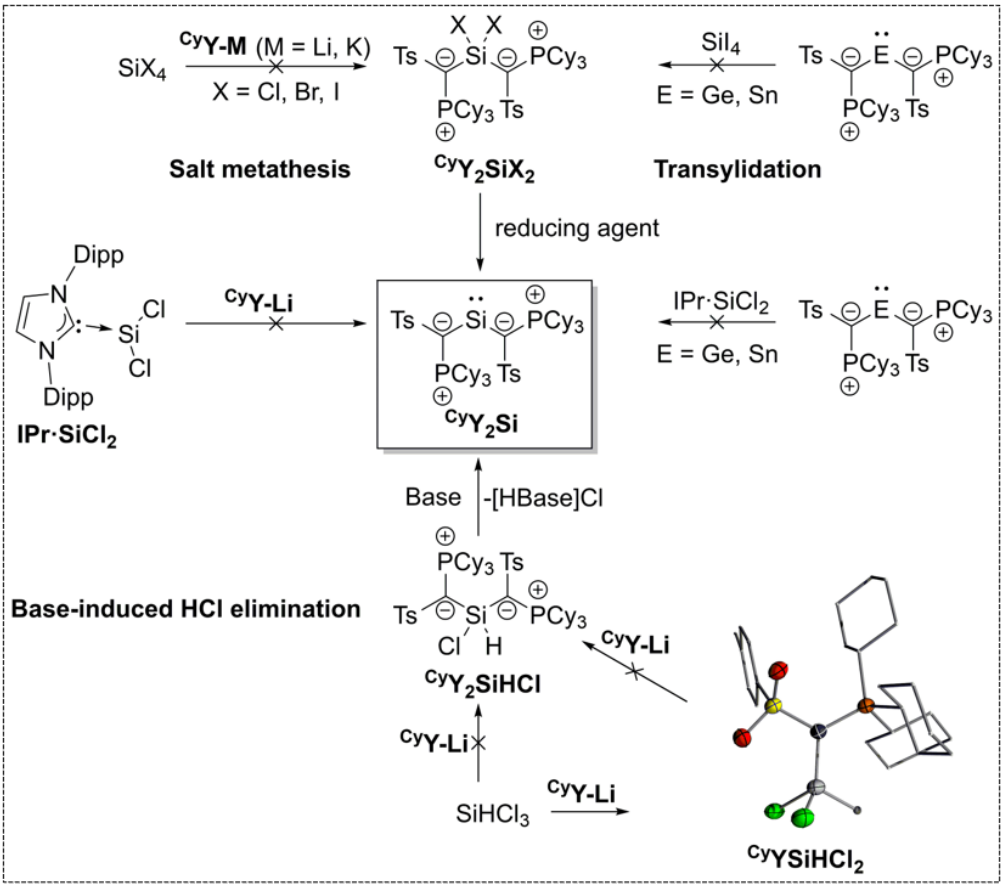

**Figure 45.** Different synthesis attempts towards **$^{Cy}$Y$_2$S**i.

Thus, the synthesis of a silylene with methyl- and phenyl-substituted ylide moieties was addressed. Since the synthesis of the corresponding metalated ylides is not possible, we aimed at the preparation of the di-ylide chlorosilanes via TMS-Cl elimination from TMS-ylides. The TMS-ylides were prepared from their respective parent phosphonium salts via deprotonation and subsequent reaction with TMS-

Cl or TMS-I. With the novel TMS-ylides in hand, they were reacted with half an equivalent of SiCl$_4$ to gain access to the respective dichloro-silane species. Unfortunately, only mono-substituted products (**$^{Cy}$Y$_{Me}$-SiCl$_3$** and **$^{Cy}$Y$_{Ph}$-SiCl$_3$**) were obtained and attempts to prepare the di-ylide substituted silanes under more forcing conditions repeatedly failed. XRD analysis on single crystals of **$^{Cy}$Y$_{Ph}$-SiCl$_3$** revealed a very short C$_{ylide}$–Si bond, indicating that the silicon atom is highly stabilized by electrostatic effects and thus inert to nucleophilic attacks. No further attempts to isolate an di-ylide stabilized acyclic silylene were undertaken.

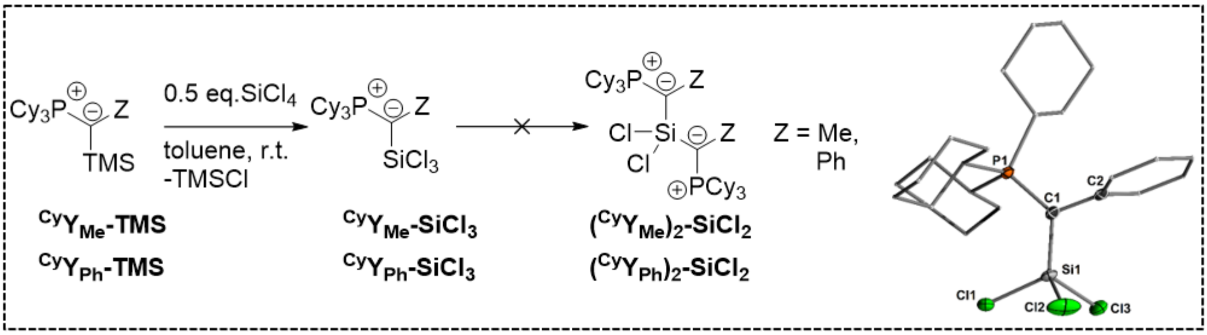

**Figure 46.** Preparation of TMS-ylides and subsequent attempts to obtain di-ylide substituted dichlorosilanes upon TMS-Cl elimination; Molecular structures of $^{Cy}$Y$_{Ph}$-TMS (top) and $^{Cy}$Y$_{Ph}$-SiCl$_3$ (bottom).

As an alternative to di-ylidyl silylenes, the synthesis of a monoylide substituted silylene was next explored. It was recently demonstrated that silylenes bearing strongly donating substituents together with a hypersilyl group are highly reactive species and competent in bond activation reactions,[108,109] thus the quest arose if ylide-/silyl-silylenes would show the same reactivity. To this end, the synthesis of a silyl-silylene with a highly-sterically demanding and electron-rich **$^{Cy}$Y$_{Mes}$**-substituent was attempted. The parent phosphonium salt **$^{Cy}$Y$_{Mes}$-H$_2$** was at first deprotonated and treated with SiBr$_4$ thus giving the respective *a*-silyl-phosphonium salt **[$^{Cy}$Y$_{Mes}$-SiBr$_3$]Br**. Surprisingly, deprotonation delivered ylide-substituted dibromo-silane **176** with a four-membered ring by deprotonation of one of the cyclohexyl groups, instead of the anticipated **$^{Cy}$Y$_{Mes}$-SiBr$_3$** species (Figure 47). **176** could be isolated in moderate yield and fully characterized.

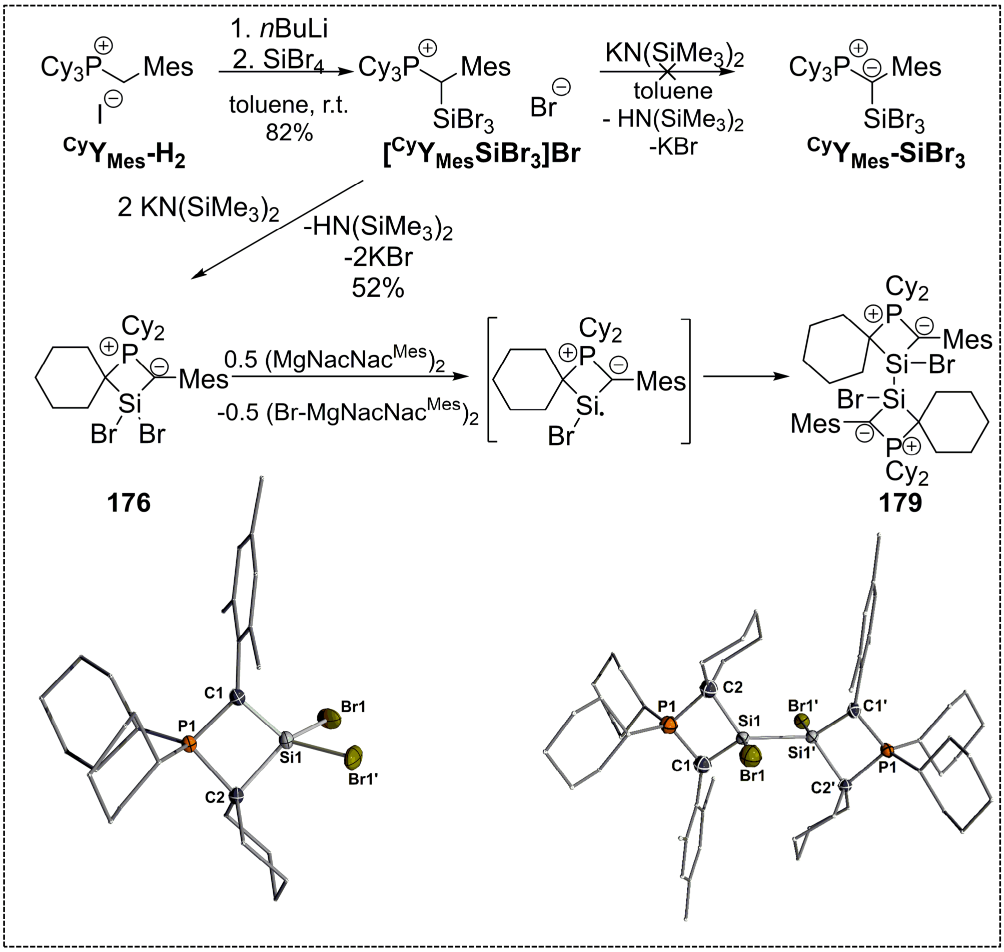
1. nBuLi
2. SiBr4
toluene, r.t.
82%
CyYMes-H2
[CyYMesSiBr3]Br
KN(SiMe3)2
toluene
- HN(SiMe3)2
-KBr
CyYMes-SiBr3
2 KN(SiMe3)2
-HN(SiMe3)2
-2KBr
52%
0.5 (MgNacNacMes)2
-0.5 (Br-MgNacNacMes)2
176
179
C1
Br1
P1
Si1
Br1'
C2
Br1'
C1'
Si1'
Br1
C1
C2'

**Figure 47.** Preparation of **[$^{Cy}$Y$_{Mes}$-SiBr$_3$]Br** and its subsequent deprotonation to yield **176**, as well as reduction of **176** with *Jones* Mg(I) reagent to yield the dimerized one-electron reduction product **179** (top); Molecular structures of **176** (bottom, left) and **179** (bottom, right).

Although the target precursor for the synthesis of an ylide/silyl-silylene was not obtained via this route, the reduction of dibromosilane **176** could also lead to interesting low-valent silicon species. Thus, **176** was reacted with *Jones* Mg(I) dimer.[101] However, instead of a Si(II) species, an ylide substituted bromo-disilane **179** was obtained. **179** is probably formed by dimerization of the respective one-electron reduction product, which is either too reactive to undergo a second reduction, or steric congestion with the used reducing agent did not enable a further electron-transfer. However, **176** may be reduced with more reactive reducing agents in the future to yield low-valent silicon compounds. Additionally, halide abstraction from either **176** or **179** may provide access to highly reactive silicon cations, which could be used for instance in Lewis acid catalysis.

In the second section of this thesis, the preparation of tricyclohexylphosphonium based ylide-functionalized phosphines ($^{Cy}$YPhos) and their subsequent application as strong donor ligands for TM-metal catalysis was explored.

## Au···H-C Hydrogen Bonds as Design Principle in Gold(I) Catalysis

Gold(I) complexes bearing triphenylphosphonium based YPhos ligands ($^{Ph}$YPhos) have shown a remarkable catalytic activity in several organic transformations. In particular, Au(I)–$^{Ph}$YPhos complexes with sulfonyl (**A**) or aryl (**B**, **C**) groups in the backbone gave extraordinarily good catalysts.[27,30] The outstanding catalytic activity of these systems in Au(I) catalysis is believed to rely mainly on their ability to stabilize the catalytically active Au(I)$^+$-species. Among other factors like ligand donor strength or sterical demand, the existence of additional Au-arene interactions is believed to be crucial for stabilization of the cationic species and hence for the observed high catalytic activities. The design element of incorporating arene groups in close proximity to the metal center to foster secondary metal ligand interactions has been described before. Highly sophisticated NHCs[192] or *Buchwald* phosphines[48] rely on the same principle (Figure 48). Thus, the fundamental question arises if these Au-arene interactions are really necessary for efficient Au(I) catalysis or if these could also be replaced by other design elements.

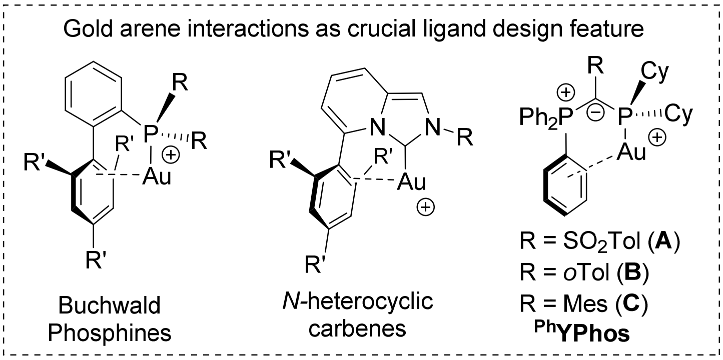

**Figure 48.** Highly sophisticated ligands in which gold-arene interactions where postulated.

To answer this question, tricyclohexylphosphonium congeners to **A**, **B** and **C** should be prepared. These ligands should not exhibit these interactions in their respective gold complexes and thus would allow for a direct comparison in catalysis. While the preparation of the **$^{Cy}$YPhos** congeners to **B** and **C** were already described in literature, namely **$^{Cy}$Y$_{oTol}$-PCy$_2$ (L2)** and **$^{Cy}$Y$_{Mes}$-PCy$_2$** (**L3**), the preparation of the former had to be developed. That said, the metalated ylide **$^{Cy}$Y-Li** was reacted with chloroalkyl phosphines (PR$_2$Cl, R = *i*Pr, Cy) to deliver **$^{Cy}$Y$_S$-PCy$_2$ (L1)** and **$^{Cy}$Y$_S$-P*i*Pr$_2$ (L4)**, respectively. The latter was prepared to investigate the influence of the smaller alkyl group on catalytic activity. Furthermore, to exclude any possible Au-arene interaction, the tolyl group was substituted by a perfluorobutyl chain, delivering a completely arene-free derivative of **L1**. **$^{Cy}$Y$_{SF}$-PCy$_2$ (L5)** was prepared by *in-situ* deprotonation of its ylide precursor **$^{Cy}$Y$_{SF}$-H** leading to the respective metalated ylide which is then reacted with PCy$_2$Cl. All phosphines could be isolated as colourless solids in good yields and were fully characterized by NMR spectroscopy, elemental- and XRD analysis. Next, their respective $^{Cy}$YPhosAu(I)-Cl (**P1**, **P4** and **P5**) were synthesized

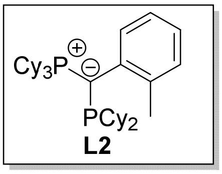

**L2**

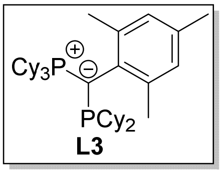

**L3**

via reaction of the free phosphines with (tht)AuCl. The complexes were obtained as colourless solids and were fully characterized including XRD analysis. In the latter, remarkably short $Au\cdots H–C_{sp3}$ distances were observed, thus strongly indicating the presence of gold-hydrogen bonds. Specifically, the obtained $Au\cdots H–C_{sp3}$ distances for **P1** 2.39(4) Å and **P5** 2.38(5) Å represent the shortest Au–C–H bonds reported to date. The presence of attractive bonding interactions between the gold atom and the cyclohexyl's hydrogen atoms could be observed furthermore by NMR spectroscopy and was also proved via different DFT methods. The latter revealed that the $Au\cdots H–C$ bonds are of anagostic nature, thus the Au atom acts as an electron-donor, while the C–H moiety acts as an acceptor. Furthermore, it was confirmed that these interactions are also present in the gas-phase and most important, are preferred over any other possible interaction e.g., coordination via the sulfonyl group or arene-interaction with the tolyl motif.

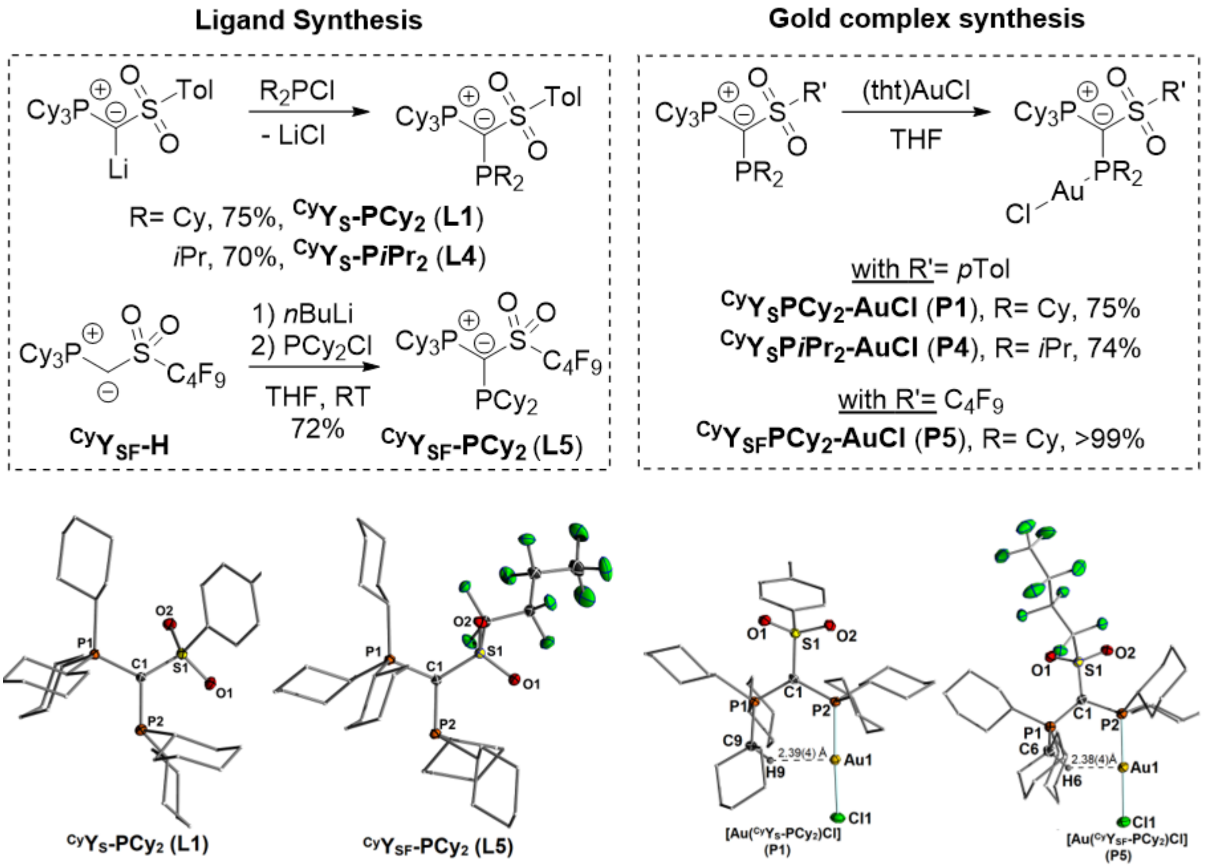
Ligand Synthesis
Gold complex synthesis
R₂PCl
- LiCl
R= Cy, 75%, CyYS-PCy2 (L1)
iPr, 70%, CyYS-PiPr2 (L4)
1) nBuLi
2) PCy2Cl
THF, RT
72%
CyYSF-H
CyYSF-PCy2 (L5)
(tht)AuCl
THF
with R'= pTol
CyYSPCy2-AuCl (P1), R= Cy, 75%
CyYSPiPr2-AuCl (P4), R= iPr, 74%
with R'= C4F9
CyYSFPCy2-AuCl (P5), R= Cy, >99%
CyYS-PCy2 (L1)
CyYSF-PCy2 (L5)
[Au(CyYS-PCy2)Cl] (P1)
[Au(CyYSF-PCy2)Cl] (P5)
2.39(4) Å
2.38(4) Å

**Figure 49.** Synthesis of novel $^{Cy}$YPhos ligands **L1** and **L5** (left, top) and preparation of the corresponding complexes (**P1** and **P5**) (right, top); molecular structures of the novel phosphines (bottom, left) and Au-complexes (bottom, right).

To examine the electronic properties of the novel phosphines, their TEP value was determined by analyzing the carbonyl stretching frequencies of the corresponding [Rh($^{Cy}$YPhos)(acac)(CO)] complexes. As expected, **L1** turned out to be more electron donating than **L4**, while the highly electron-withdrawing effect of the perfluorobutyl group becomes evident in **L5**, making it even less electron-releasing than its parent tricyclohexylphosphine. This result clearly shows how easily the electronics of YPhos ligands can be tuned via backbone modification. Furthermore, the novel $^{Cy}$YPhos ligands turned out to be highly sterically demanding, covering more than half of the metal's sphere according to their calculated $V_{bur}$%. The obtained values are essentially similar to the respective $PPh_3$ analogues, thus confirming that the overall electronic and steric properties do not change upon substitution with $PCy_3$. This was also confirmed by batch solution calorimetry studies performed in the *Nolan* group, which exhibit same reaction enthalpy's for the formation of gold-complexes from [Au(DMS)Cl] and **A** or **L1**.

**Table 4.** Steric and electronic-properties of $^{Cy}$YPhos ligands.

| | **L1** | **L2** | **L3** | **L4** | **L5** |
|---|---|---|---|---|---|
| $V_{bur}$% [%][a] | 54.8 | 49.4 | 50.7 | 53.2 | 52.5 |
| TEP [$cm^{-1}$][b] | 2057.0 | 2048.0 | 2048.4 | 2058.7 | 2059.8 |

[a] Calculated with the SambVca 2.1 program for the Au(L)Cl complexes; M-P distance = 2.28 Å, including H atoms.[193]; [b] TEPs were determined by $\nu_{CO}$ in the [Rh(acac)(CO)(L)] complexes using the linear relationship between $\nu_{CO}$ for [Ni(CO)$_3$(L)] and [Rh(acac)(CO)(L)].[25]

Next, the ability of the $^{Cy}$YPhos-Au-(I) complexes to catalyze the hydroamination of phenylacetylene with aniline was tested under the exact same conditions already applied for **A**, **B** and **C**. The $^{Cy}$YPhos-Au(I) complexes **P1**–**P3** turned out to be highly active catalysts and were furthermore similarly effective as their $PPh_3$-substituted congeners. Moreover, substitution of the cyclohexyl-groups on the P(III) phosphorus atom in **P1** with isopropyl-groups (**P4**) leads only to a moderate drop in reactivity. Most interestingly, the completely arene-free derivative **P5** gave also nearly full conversion after 24 h of reaction time, thus confirming that Au···C$_{arene}$ interactions are not necessary to yield efficient catalysis. In addition, **P1** and **P5** retained their catalytic activity also at lower catalyst loading, with **P1** being similarly efficient as **A** under these conditions, thus impressively demonstrating that stabilization of the catalytically active cationic Au(I) species is equally well performed by Au···H–C interactions. Additionally, the generality of this concept could be proved by substitution of the biaryl-motif of *Buchwald* ligand $^{Cy}$JohnPhos with a (phenyl-2-cyclohexyl)-group, ultimately leading to the gold complex **P6**. Similar to the $^{Cy}$YPhos ligands, **P6** exhibits Au···H-C interactions as proved by XRD analysis and DFT calculations. Most importantly, **P6** is as active as its parent biaryl congener $^{Cy}$JohnPhos·AuCl in the hydroamination of phenylacetylene with aniline.

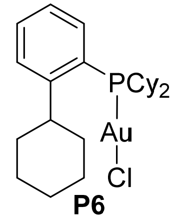

**P6**

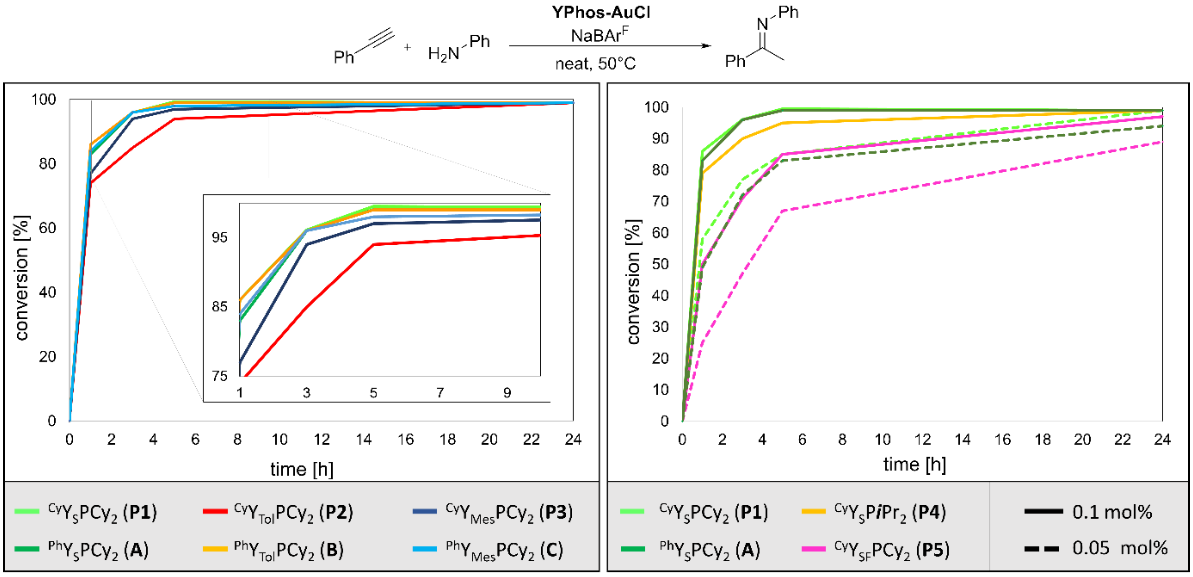

**Figure 50.** Comparison of the catalytic activity of the novel $^{Cy}$YPhos-Au(I) complexes in the hydroamination of phenylacetylene with aniline with their $PPh_3$ congeners.

Reports in literature have often assumed that gold-arene interactions are prerequisites for the design of highly-active gold catalysts. However, the results presented in this work clearly underline, that gold-hydrogen bonds are equally well suite, enabling efficient gold(I) catalysis even at low-catalyst loadings. These novel secondary ligand interactions may open new possibilities for future catalyst design.

### $^{Cy}$YPhos ligands in Pd catalysis

Motivated by the results achieved with the novel $^{Cy}$YPhos ligands in gold(I) catalysis, their ability to perform Pd-catalyzed C–N cross couplings was next explored. First, it was tested if the sulfonyl-substituted YPhos ligands are suitable for the formation of Pd(0) complexes. Therefore, **$^{Cy}$Y$_S$-PCy$_2$** was reacted with an equimolar amount of Pd$_2$dba$_3$. However, albeit the respective **$^{Cy}$Y$_S$-PCy$_2$Pd·dba** could be successfully synthesized, and its structure unambiguously confirmed via XRD, it turned out that this complex was inactive in the C–N cross coupling reaction of *p*-chlorotoluene with piperidine at room temperature. Subsequently its ability to perform single steps of the catalytic cycle was explored. While **$^{Cy}$Y$_S$-PCy$_2$Pd·dba** does not perform the oxidative addition of *p*-chlorotoluene at room temperature, almost full conversion to the oxidative addition product (**$^{Cy}$Y$_S$-PCy$_2$-Pd(*p*Tol)Cl**) could be achieved after 3 h at 40°C. XRD analysis on single crystals obtained from the reaction mixture confirmed the formation of the anticipated oxidative addition complex , and furthermore the existence of a coordination of the Pd center by one of the sulfonyl's oxygen atoms. However, albeit the oxidative addition of p-chlorotoluene could be proven, no catalytic activity was observed even in refluxing THF. Thus, to check whether the next step of the catalytic cycle is working, piperidine was added to **$^{Cy}$Y$_S$-PCy$_2$-Pd(*p*Tol)Cl**. $^{31}$P{$^1$H} NMR analysis showed no conversion to a new product, thus strongly indicating that that no adduct formation is possible. The lack of reactivity might be explained by the inability of **$^{Cy}$Y$_S$-PCy$_2$-Pd(*p*Tol)Cl** to break its Pd(II)–O bond, thus the Pd-atom remains always fully saturated allowing no further coordination by the amine. DFT calculations support this hypothesis, since breaking the Pd(II)–O is thermodynamically unfavored in comparison with the respective palladacycle.

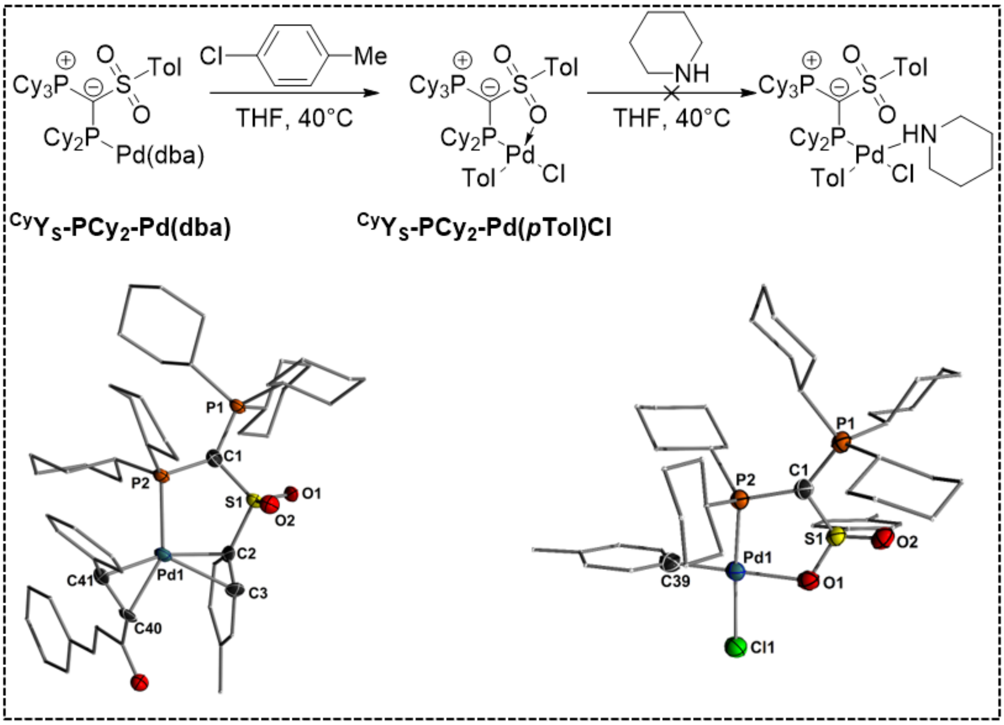

**Figure 51.** Oxidative addition of *p*-chlorotoluene to **$^{Cy}$Y$_S$-PCy$_2$Pd·dba**, yielding to the **$^{Cy}$Y$_S$-PCy$_2$-Pd(*p*Tol)Cl** complex, and subsequent attempt to prepare the amine-coordination complex with piperidine (top); molecular structures of **$^{Cy}$Y$_S$-PCy$_2$Pd·dba** (bottom, left) and **$^{Cy}$Y$_S$-PCy$_2$-Pd(*p*Tol)Cl** (bottom, right).

This results indicate that Pd-complexes based on sulfonyl-substituted YPhos ligands seem not to be suitable to catalyze BHA reactions. However, these ligand systems might be useful for catalytic transformations in which no substrate coordination is necessary, for instance catalytic cycles involving transmetallation reactions. Thus, the ability of the novel sulfonyl-substituted YPhos Pd-complexes to perform catalysis with other cross-coupling protocols should be tested in the future.

Overall, the results presented in this thesis provided a valuable contribution to the field of ylide-stabilized low-valent main group species as well as homogeneous catalysis based on $^{Cy}$YPhos-TM complexes. The full potential of this special donor class in main-group chemistry and TM-catalysis is by no means exhausted. Important findings obtained in this thesis will help to optimize future ylide ligand design, which might enable the isolation of more reactive ylide-stabilized main group compounds and more efficient TM-catalysts based on ylide-functionalized ligand systems.

# 5. Experimental Section

## General Remarks

Full syntheses procedures, computational details and crystallographic data of the compounds published in peer-review journals can be found in the respective supporting information file by following the given DOI number. However, to keep the consistency of this thesis, synthetic procedures for already published compounds will be presented here as well. Experimental details will be given sequentially, following the section in which they appeared first. Crystallographic data for unpublished molecules is given in a separate appendix.

All experiments were carried out under a dry, oxygen-free argon atmosphere using standard Schlenk techniques or inside a glovebox. Involved solvents ($Et_2O$, THF, acetonitrile, toluene, DCM, *n*-hexane and *n*-pentane) were dried via a solvent purification system (MBraun SPS 800) or according to standard procedures (cyclohexane, DMSO), degassed and stored over molecular sieves. Deuterated solvents were purchased from commercial suppliers (Euroisotop, Sigma-Aldrich or Deuterio), degassed and stored over molecular sieves. Glassware was oven-dried (130 °C) before use.

$^{1}H$, $^{13}C\{^{1}H\}$, $^{31}P\{^{1}H\}$, $^{19}F\{^{1}H\}$, $^{119}Sn\{^{1}H\}$, $^{29}Si\{^{1}H\}$, $^{7}Li$ NMR spectra were recorded on a Bruker Avance III HD 400 MHz spectrometer at 25 °C (if not otherwise stated). All values of the chemical shift are in ppm regarding the $\delta$–scale. All spin-spin coupling constants ($J$) are printed in Hertz (Hz). $^{1}H$ NMR and $^{13}C\{^{1}H\}$ NMR spectra were referenced to the respective residual solvent signals. NMR spectra of other nuclei were referenced to their respective external standards. To display multiplicities and signal forms correctly the following abbreviations were used: s = singlet, d = doublet, dd = doublets of doublets, t = triplet, m = multiplet, br = broad signal. Signal assignment was supported by DEPT, APT, HSQC and HMBC experiments.

Elemental analyses were performed on an Elementar vario MICRO-cube elemental analyzer. XRD analyses were performed with Oxford SuperNova (Cu-microsource, Atlas detector). Data collection, absorption correction and cell determination were conducted with CrysAlisPro (Agilent Technologies, version 1.171.36.24)., while structure refinement was performed with SHELXL14/SHELXL18/3[194].

DFT calculations were performed by *Henning Steinert* and *Julian Löffler*. All computational studies were carried out without symmetry restrictions. If it was not possible to obtain starting coordinates from crystal structures, GaussView 6.0[195] was used. Calculations were performed with the Gaussian16 Revision B.01[196] or the Gaussian16 Revision C.01[197] program packages using Density-Functional Theory (DFT).[198] Energy optimizations were carried out with the PW6B95D3 functional[199] and def2svp or def2tzvp basis set.[200] As implemented in Gaussian, MWB60 ECP[201] together with GRIMMES D3 dispersion correction with Becke-Johnson damping was used for Au, while MWB46 ECP was used for Sn.[202] To determine the nature of the structure harmonic vibrational frequency analyses were performed on the same level of theory. No imaginary frequencies were observed for the optimized structures. NBO Analysis was performed with NBO Version 7.0.[203] The optimized structures were used for the quantum theory of atoms in molecule (QTAIM)[204] and noncovalent interaction (NCI)[205] analyses using

Multiwfn.[206] The results were visualized using the VMD 1.9.4a51 software.[207] Chemcraft 3D[208] and Gimp[209] were used for graphical representation.

Benzyl potassium[210], *p*Tol–$SO_2CH_2I$[211], Li–$CH_2SO_2$-*p*Tol[212], K–Si($SiMe_3$)$_3$[213], $Ar^{Tripp}$–Li[214], IPr·$SiCl_2$[178], $^{Cy}Y_{Me}$-$H_2$[28,215], $^{Cy}Y_{Ph}$-$H_2$[33] , $^{Cy}Y_{Mes}$-$H_2$[29], $^{Mes}$NacNac–Mg(I) dimer[216], $NaBAr^F_4$ [217], $^{Cy}Y_{oTol}$-$PCy_2$ (**L2**)[29], [Au($^{Cy}Y_{oTol}$-$PCy_2$)Cl] (**P2**)[29], $^{Cy}Y_{Mes}$-$PCy_2$ (**L3**)[29], [Au($^{Cy}Y_{Mes}$-$PCy_2$)Cl] (**P3**)[29] , $[RhCl(CO)_2]_2$[218] and Cy-$^{Cy}$JohnPhos (**L6**)[219] were prepared according to literature procedures. All other reagents were purchased from commercial suppliers and used without further purification. Organolithium bases were titrated against diphenylacetic acid before use.

## 5.1 Experimental Details for Section 3.1

**Synthesis of [Cy$_3$PCH$_2$I]I:**

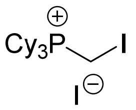

Tricyclohexylphosphine (10.00 g, 35.7 mmol, 1.00 eq.) was dissolved in toluene (200 mL). Diiodomethane (3 mL, 37.1 mmol, 1.04 eq.) was added dropwise to the solution at RT. During the addition, a white solid precipitated out of the solution. The reaction mixture was stirred at RT until full precipitation was achieved (36 h). Next, the suspension was filtered and washed with Et$_2$O (3 x 10 mL). The solid was dried *in vacuo* (1 x $10^{-3}$ mbar) for 4 h, giving the product as a white, amorphous powder (89%, 17.40 g).

**$^1$H NMR** (DMSO-*d$_6$*, 400 MHz): $\delta$ (ppm) = 3.49 (d, $^2J_{PH}$ = 7.3 Hz, 2H, CH$_2$I), 2.69 – 2.55 (m, 3H, PCy-CH), 2.00 – 1.92 (m, 6H, PCy-CH$_2$), 1.88 (m, 6H, PCy-CH$_2$), 1.76 – 1.71 (m, 2H, PCy-CH$_2$), 1.58 (m, 6H, PCy-CH$_2$), 1.44 – 1.18 (m, 10H, PCy-CH$_2$).

**$^{13}$C{$^1$H} NMR** (DMSO-*d$_6$*, 100.6 MHz): $\delta$ (ppm) = 30.1 (d, $^1J_{CP}$ = 40.9 Hz, PCy$_3$-CH), 26.0 (PCy$_3$-CH$_2$), 25.9 (PCy$_3$-CH$_2$), 25.9 (d, $^2J_{CP}$ = 12.6 Hz, CH$_2$), 24.9 (PCy$_3$-CH$_2$).

**$^{31}$P{$^1$H} NMR** (DMSO-*d$_6$*, 161.9 MHz): $\delta$ (ppm) = 30.9 (s).

**CHNS**: calculated: C: 41.62%, H: 6.43%, found: C: 41.68%, H: 6.06%.

**Synthesis of $^{Cy}$Y-H$_2$:**

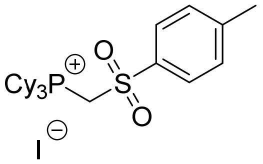

**[Cy$_3$PCH$_2$I]I** (5.40 g, 9.85 mmol, 1.00 eq.) and sodium *p*-tolylsulfinate (3.51 g, 19.7 mmol, 2.00 eq.) were dissolved in 30 mL DMSO. The suspension was heated at 100 °C for 36 h. After cooling the suspension down to RT, the solvent was removed under reduced pressure and the residue was redissolved in dichloromethane (30 mL). The dark suspension was filtrated over celite, giving a dark brown solution. The solution was reduced to 10 mL and toluene (40 mL) was added, which resulted in the precipitation of phosphonium salt **$^{Cy}$Y-H$_2$**. The solid was filtrated off, washed with 3 x 5 mL of toluene and dried *in vacuo* (1 x $10^{-3}$ mbar, 60 °C, 12 h) giving the title compound as a white, amorphous powder (1.7 g, 30%).

**$^1$H NMR** (CD$_2$Cl$_2$, 400 MHz): $\delta$ (ppm) = 8.03 (d, *J* = 8.0 Hz, 2H), 7.46 (d, *J* = 8.0 Hz, 2H), 5.00 (d, $^2J_{PH}$ = 11.4 Hz, 2H, PCH$_2$S), 3.07 – 2.90 (m, 3H, PCy-CH), 2.47 (s, 3H, CH$_3$-Tol), 2.13 – 2.04 (m, 6H, PCy-CH$_2$), 1.99 – 1.90 (m, 6H, PCy-CH$_2$), 1.85 – 1.69 (m, 9H, PCy-CH$_2$), 1.55 – 1.32 (m, 9H, PCy-CH$_2$).

**$^{13}$C{$^1$H} NMR** (CD$_2$Cl$_2$, 100.6 MHz): $\delta$ (ppm) = 147.1 (*p*-C), 137.5 (d, $^3J_{CP}$ = 3.4 Hz, *ipso*-C), 130.8 (*m*-C), 128.6 (*o*-C), 44.5 (d, $^1J_{CP}$ = 31.3 Hz, PCH$_2$S), 32.0 (d, $^1J_{CP}$ = 36.7 Hz, PCy-CH), 27.8 (d, $^3J_{CP}$ = 3.9 Hz, PCy-CH$_2$), 27.0 (d, $^2J_{CP}$ = 12.7 Hz, PCy-CH$_2$), 25.8 (d, $^4J_{CP}$ = 1.8 Hz, PCy-CH$_2$).

**$^{31}$P{$^1$H} NMR** (CD$_2$Cl$_2$, 161.9 MHz): $\delta$ (ppm) = 35.4 (s).

**CHNS**: calculated: C: 54.16%, H: 7.34%, S: 5.56%, found C: 54.55%, H: 7.55%, S: 5.21%

**Synthesis of [Cy$_3$P-Me]I:**

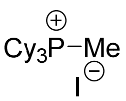

Tricyclohexylphosphine (16.00 g, 57.05 mmol, 1.00 eq.) was dissolved in toluene (200 mL). Methyl iodide (3.8 mL, 61.05 mmol, 1.07 eq) was added dropwise to the solution at RT. During the addition, a white solid precipitated out of the solution. The reaction mixture was stirred at r.t. until full precipitation was achieved (2 h). Next, the suspension was filtered and washed with $Et_2O$ (3 x 10 mL). The solid was dried *in vacuo* (1 x $10^{-3}$ mbar) for 4 h, giving **[$Cy_3$P-Me]I** as a white, amorphous powder (98%, 23.50 g).

**$^1$H NMR** ($CD_2Cl_2$, 400 MHz): $\delta$ (ppm) = 2.5 (m, 3H, PCy-CH), 2.0 – 1.9 (m, 11H; PCy-$CH_2$), 1.9 (d, *J* = 12.1 Hz, 3H; $CH_3$), 1.8 – 1.8 (m, 3H; PCy-$CH_2$), 1.6 – 1.2 (m, 16H; PCy-$CH_2$).

**$^{31}$P{$^1$H} NMR** ($CD_2Cl_2$, 161.9 MHz): $\delta$ (ppm) = 33.7 (s).

The obtained signals are in accordance with literature values.[x]

### Synthesis of $^{Cy}$Y-H:

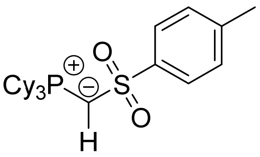

**[$Cy_3$P-Me]I** (10.00 g, 23.68 mmol, 1.00 eq.) and NaHMDS (8.77 g, 47.82 mmol, 2.02 eq.) were placed into a 250 mL schlenk flask. THF (150 mL) was added, giving a white suspension. The mixture was stirred for 30 min at room temperature. In a separate schlenk flask, *p*-Toluenesulfonyl fluoride (4.12 g, 23.68 mmol, 1.00 eq.) was dissolved in THF (25 mL) and this solution was slowly added to the suspension via cannula, upon which a color change from white to a deep brown occurred. The reaction mixture was stirred over night and the solvent was removed *in vacuo*. Dichloromethane (100 mL) was added to the residue, the resulting suspension was centrifugated (20 min, 2000 rpm) and subsequently filtrated over celite to obtain a clear yellowish solution. Removal of the solvent under reduced pressure yielded an off-white solid, which was washed with *n*-hexane (5 x 25 mL). After drying *in* vacuo (1 x $10^{-3}$ mbar) for 4 h at 70 °C, the pure product was obtained as a white solid (90%, 9.80 g).

**$^1$H NMR** ($CD_2Cl_2$ ,400 MHz): $\delta$ (ppm) = 7.61 (d, $^2J_{HH}$=8.2 Hz, 2H, *o*-CH), 7.10 (d, $^2J_{HH}$=7.9 Hz, 2H; *m*-CH), 2.28 (s, 3H), 2.25–2.13 (m, 3H, $PCy_3$-CH), 1.77 (d, $^2J_{PH}$=8.4 Hz, 1H; PCHS), 1.83 – 1.74 (m, 12H, $PCy_3$-$CH_2$), 1.74 – 1.64 (m, 3H, $PCy_3$-$CH_2$), 1.47–1.33 (m, 6H, $PCy_3$-$CH_2$), 1.32 – 1.05 (m, 9H, $PCy_3$-$CH_2$).

**$^{31}$P{$^1$H} NMR** ($CD_2Cl_2$, 161.9 MHz): $\delta$ (ppm) = 26.8 (s).

**$^{13}$C{$^1$H} NMR** ($CD_2Cl_2$, 100.6 MHz): $\delta$ (ppm) = 149.7 (ipso-C), 140.2 (*p*-C), 129.5 (*m*-CH), 125.5 (*o*-CH), 33.1 (d, $^2J_{CP}$= 50.8 Hz, $PCy_3$-CH), 27.8 (d, $^3J_{CP}$= 3.1 Hz, $PCy_3$-$CH_2$), 27.6 (d, $^2J_{CP}$ = 12.3 Hz, $PCy_3$-$CH_2$), 26.5 (d, $^4J_{CP}$= 1.6 Hz, $PCy_3$-$CH_2$), 26.1 (d, $^2J_{PH}$ = 105 Hz, PCS), 21.6 (*p*-Tol-$CH_3$).

**CHNS**: calculated: C: 69.61%, H: 9.21%, S: 7.15%, found C: 69.26%, H: 9.04%, S: 7.38%.

### Synthesis of $^{Cy}$Y-Li:

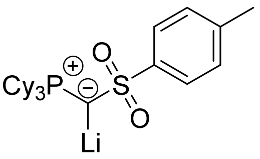

**$^{Cy}$Y-H** (3.63 g, 8.09 mmol, 1.0 Äq.) was suspended in *n*-Pentane (100 mL). *n*BuLi (1.53 M in hexanes, 5.29 mL, 1.0 Äq.) was added dropwise to the suspension at 0°C. The reaction mixture was warmed to r.t. and stirred for 1 h. The suspension was filtered via cannula and a yellow solution was obtained. Removal of the solvent under reduced pressure and drying *in* vacuo (1 x $10^{-3}$ mbar) for 4 h at 40 °C afforded **$^{Cy}$Y-Li** as a yellow powder (90%, 3.33 g)

**$^1$H NMR** (THF-$d_8$, 400 MHz): $\delta$ (ppm) = 7.85 (d, $^2J_{HH}$ = 7.7 Hz, 2H, *m*-CH), 6.96 (d, $^2J_{HH}$ =7.7 Hz, 2H, *o*-CH), 2.28 (s, 3H, *p*-Tol-$CH_3$), 1.95 – 1.84 (m, 10H, PCy-CH+$CH_2$), 1.70 – 1.65 (m, 6H; , PCy-$CH_2$), 1.61 – 1.57 (m, 3H; , PCy-$CH_2$), 1.43 – 1.38 (m, 4H; , PCy-$CH_2$), 1.20 – 1.10 (m, 10H; , PCy-$CH_2$).

**$^{31}$P{$^{1}$H} NMR** (THF-$d_8$,162 MHz): $\delta$ (ppm) = 10.1 (s)

**$^{13}$C{$^{1}$H} NMR** (THF-$d_8$, 100.6 MHz): $\delta$ (ppm) = 155.5 (*ipso*-C), 137.1 (*p*-C) 128.4 (*m*-CH), 126.9 (*o*-CH), 36.9 (d, *J*=52.8; PCy$_3$-CH), 28.7 (PCy$_3$-CH$_2$), 28.6 (d, *J*=8.4, PCy$_3$-CH$_2$), 27.5 (PCy$_3$-CH$_2$), 23.4 (PCy$_3$-CH$_2$), 21.4 (*p*-Tol-CH$_3$). The signal for PCS bridge could not be observed.

**$^{7}$Li NMR** (THF-$d_8$, 155.6 MHz): $\delta$ (ppm) = 0.6 (s).

**CHNS**: calculated: C: 68.70%, H: 8.87%, S: 7.05%, found C: 68.73%, H: 8.84%, S: 7.03%

**Synthesis of $^{Cy}$Y-K:**

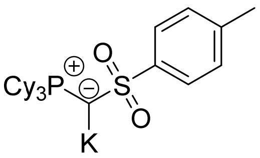

Benzyl potassium (0.32 g, 2.45 mmol, 1.1 eq.) and **$^{Cy}$Y-H** (1.00 g, 2.22 mmol, 1.0 eq.) were placed into a schlenk tube and toluene (25 mL) was added. The red reaction mixture was stirred for 5 min at room temp. and was subsequently filtered via cannula. A dark yellow solution was obtained. The solvent was removed under reduced pressure and the residue was dried *in vacuo* (1 x 10$^{-3}$ mbar) for 3 h at 40 °C to yield **$^{Cy}$Y-K** as a dark yellow powder (98%, 1.06 g).

**$^{1}$H NMR** (THF-$d_8$ ,400 MHz): $\delta$ (ppm) = 7.79 (br, 2H, *m*-CH), 6.91 (br, 2H, *o*-CH), 2.28 (s, 3H, *p*-Tol-CH$_3$), 1.87 – 1.75 (m, 8H, PCy-CH+CH$_2$), 1.71 – 1.66 (m, 6H, PCy-CH$_2$), 1.61 – 1.57 (m, 3H, PCy-CH$_2$), 1.42 – 1.31 (m, 6H, PCy-CH$_2$), 1.17 – 1.02 (m, 10H, PCy-CH$_2$).

**$^{31}$P{$^{1}$H} NMR** (THF-$d_8$,162 MHz): $\delta$ (ppm) = 3.2 (s, br)

**$^{13}$C{$^{1}$H} NMR** (THF-$d_8$, 100.6 MHz): $\delta$ (ppm) = 157.3 (*ipso*-C), 136.2 (*p*-C) 128.6 (*m*-CH), 126.3 (*o*-CH), 37.4 (d, *J*=52.5; PCy$_3$-CH), 28.9 (PCy$_3$-CH$_2$), 28.8 (PCy$_3$-CH$_2$), 27.7 (PCy$_3$-CH$_2$), 21.5 (*p*-Tol-CH$_3$). The signal for PCS bridge could not be observed.

**CHNS**: calculated: C: 64.16, H: 8.28, S: 6.59, found C: 64.50, H: 8.30, S: 6.88.

## 5.2 Experimental Details for Section 3.2

**Synthesis of $^{Cy}Y_2Ge$:**

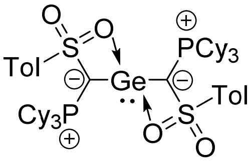

**$^{Cy}$Y-Li** (197 mg, 0.432 mmol, 2.0 eq.) and $GeCl_2$·dioxane (50 mg, 0.216 mmol, 1.0 eq.) were placed into a Schlenk tube and 20 mL of toluene was added. The reaction mixture was stirred at room temp. for 1h, during which LiCl precipitates out of the solution. The yellow suspension was filtered, and the obtained clear solution was evaporated in vacuo to full dryness (4h, 50 °C, 1 x $10^{-3}$ mbar). The residue was redissolved in a small amount of ice-cold toluene (5 mL) and filtered again. Removing the solvent in vacuo furnished the title compound as a pale-yellow solid (148 mg, 0.153 mmol, 71 %). X-Ray quality crystals were grown by slow evaporation of a saturated benzene solution.

**$^1$H NMR** ($C_6D_6$, 400 MHz): $\delta$ (ppm) = 1.13 – 1.43 (m, 20H, $PCy_3$-C$H_2$), 1.45 – 1.56 (m, 6H, $PCy_3$-C$H_2$), 1.58 – 1.64 (m, 6H, $PCy_3$-C$H_2$), 1.67 – 1.74 (m, 10H, $PCy_3$-C$H_2$), 1.74 – 1.85 (m, 12H, $PCy_3$-C$H_2$), 1.98 (s, 6H, C$H_3$), 2.20 – 2.34 (m, 6H, $PCy_3$-C$H_2$), 2.49 – 2.62 (m, 6H, $PCy_3$-C$H$), 6.92 (d, $^2J_{HH}$ =7.9, 4H, C$H_{\mathrm{STol,meta}}$), 8.36 (d, $^2J_{HH}$ =7.9, 4H; C$H_{\mathrm{STol,ortho}}$).

**$^{13}$C{$^1$H} NMR** ($C_6D_6$, 101 MHz): $\delta$ (ppm) = 21.1 (C$H_3$), 26.7 ($PCy_3$-C$H_2$), 27.0 – 27.8 (m, $PCy_3$-C$H_2$), 28.0 ($PCy_3$-C$H_2$), 28.5 ($PCy_3$-C$H_2$), 34.4 (d, $^1J_{PC}$ = 49.8 Hz, $PCy_3$-C$H$), 47.64 (d, $^1J_{PC}$ = 55.6 Hz, PCS), 127.0 (C$H_{\mathrm{STol,ortho}}$) , 129.0 (C$H_{\mathrm{STol,meta}}$), 139.2 (C$H_{\mathrm{STol,para}}$), 150.85 (C$H_{\mathrm{STol,ipso}}$).

**$^{31}$P{$^1$H} NMR** ($C_6D_6$, 162 MHz): $\delta$ (ppm) = 19.7.

**CHNS:** for $C_{52}H_{80}O_4P_2S_2Ge_1$: C, 64.53; H, 8.33; S, 6.62. found: C, 64.57; H, 8.39; S, 6.67

**Synthesis of $^{Cy}Y_2Sn$:**

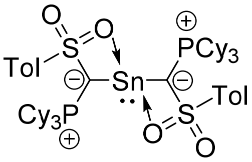

**$^{Cy}$Y-K** (257 mg, 0.527 mmol, 2.0 eq.) and finely ground $SnCl_2$ (50 mg, 0.264 mmol, 1.0 eq.) were placed into a Schlenk tube and 20 mL of toluene and a few drops of THF were added. The reaction mixture was stirred at room temp. overnight, during which KCl precipitates out of the solution. The volume of the yellow suspension was reduced to approximately 5 mL, cooled with an ice-bath and filtered, giving a clear slightly yellow solution. Removing the solvent in vacuo furnished the title compound as a pale-yellow solid (201 mg, 0.199 mmol, 75 %). Crystals suitable for XRD analysis were grown by slow evaporation of a saturated benzene solution.

**$^1$H NMR** ($C_6D_6$, 400 MHz): $\delta$ (ppm) = 1.17 – 1.33 (m, 20H, $PCy_3$-C$H_2$), 1.48 – 1.54 (m, 6H, $PCy_3$-C$H_2$), 1.58 – 1.62 (m, 6H, $PCy_3$-C$H_2$), 1.66 – 1.72 (m, 10H, $PCy_3$-C$H_2$), 1.75 – 1.85 (m, 12H, $PCy_3$-C$H_2$), 1.98 (s, 6H, C$H_3$), 2.18 – 2.26 (m, 6H, $PCy_3$-C$H_2$), 2.33 – 2.44 (m, 6H, $PCy_3$-C$H$), 6.89 (d, $^2J_{HH}$ =7.9 Hz, 4H, C$H_{\mathrm{STol,meta}}$), 8.24 (d, $^2J_{HH}$ = 7.9 Hz, 4H; C$H_{\mathrm{STol,ortho}}$).

**$^{13}$C{$^1$H} NMR** ($C_6D_6$, 101 MHz): $\delta$ (ppm) = 21.1 (C$H_3$), 26.7 ($PCy_3$-C$H_2$), 27.4 – 27.8 (m, $PCy_3$-C$H_2$), 28.0 ($PCy_3$-C$H_2$), 28.5 ($PCy_3$-C$H_2$), 34.8 (d, $^1J_{PC}$ = 50.2 Hz, $PCy_3$-C$H$), 50.4 (d, $^1J_{PC}$ =50.5 Hz, PCS), 127.0 (C$H_{\mathrm{STol,ortho}}$) , 129.0 (C$H_{\mathrm{STol,meta}}$), 139.2 (C$H_{\mathrm{STol,para}}$), 151.1 (C$H_{\mathrm{STol,ipso}}$).

**$^{31}$P{$^1$H} NMR** ($C_6D_6$, 162 MHz): $\delta$ (ppm) = 18.6.

**$^{119}$Sn{$^1$H} NMR** ($C_6D_6$, 149 MHz): $\delta$ (ppm) = –99.4 (t, $^2J_{SnP}$ = 43.6 Hz).

**CHNS:** for $C_{52}H_{80}O_4P_2S_2Sn_1$: C, 61.60; H, 7.95; S, 6.32. found: C, 61.49; H, 8.00; S, 6.23

### Synthesis of ($^{Cy}$YSnCl)$_2$ (170):

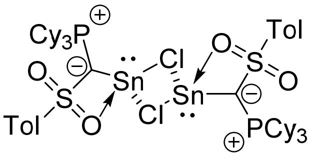

A freshly prepared solution of **$^{Cy}$Y$_2$Ge** (51 mg, 0.053 mmol, 1.0 eq. in in 0.5 mL $C_6D_6$) was filtered into a *J.-Young-style* NMR tube containing finely ground $SnCl_2$ (10 mg, 0.053 mmol, 1.0 eq.). The tube was placed into an ultra-sound bath and was sonicated for 1h, upon which a white precipitate formed. The reaction mixture was filtered into another NMR tube and the residue was washed with a small amount of $C_6D_6$ (0.1 mL), re-dissolved in THF (0.3 mL), filtered into a glass vial and stored at –30 °C for one week, giving colorless crystals of **170** (15 mg, 0.013 mmol, 47 %), suitable for X-ray analyses. The filtrate was identified as **169** (*vide infra*).

Independent synthesis of **170** starting from the metalated ylide **$^{Cy}$Y-K**:

**$^{Cy}$Y-K** (77 mg, 0.16 mmol, 1.0 eq.) and finely ground $SnCl_2$ (30 mg, 0.16 mmol, 1.0 eq.) were placed into a glass vial and were dissolved in 0.7 mL THF-*d$_8$*. The reaction mixture was shaken for 10 min at room temp., filtered into a *J.-Young-style* NMR tube and analyzed by NMR spectroscopy. The $^{31}$P{$^1$H}-NMR spectrum showed the selective formation of **170** and **$^{Cy}$Y$_2$Sn** in a ratio of approximately 1 to 0.5. The addition of another equivalent $SnCl_2$ yielded full conversion to **170**. Upon standing over night, **170** precipitates out of the solution. The solid was filtered off, washed with a small amount of toluene (0.1 mL) and dried in the glovebox atmosphere for 12 h, giving the title compound as a white solid (48 mg, 0.08 mmol, 50%). Re-dissolving this solid in THF-*d$_8$*, gave a mixture of **170** and **$^{Cy}$Y$_2$Sn** in the $^{31}$P{$^1$H]-NMR spectrum. When dissolving pure crystals of **170**, this product mixture could also be observed, strongly indicating an equilibrium between **170**, **$^{Cy}$Y$_2$Sn** and $SnCl_2$. NMR data for characterization were collected from a freshly prepared sample of **($^{Cy}$YSnCl)$_2$** with an excess of $SnCl_2$ in THF-*d$_8$*.

**$^1$H NMR** (THF-*d*$_8$, 400 MHz): *δ* (ppm) = 1.09 – 1.32 (m, 10H, PCy$_3$-C*H$_2$*), 1.39 – 1.53 (m, 6H, PCy$_3$-C*H$_2$*), 1.59 – 1.71 (m, 8H, PCy$_3$-C*H$_2$*), 1.73 – 1.81 (m, 6H, PCy$_3$-C*H$_2$*), 2.33 (s, 3H, C*H$_3$*), 2.43 – 2.55 (m, 3H, PCy$_3$-C*H*), 7.19 (d, $^2J_{HH}$ = 8.2 Hz, 2H, C*H*$_{\mathrm{STol,meta}}$), 7.90 (d, $^2J_{HH}$ = 8.2 Hz, 2H, C*H*$_{\mathrm{STol,ortho}}$).

**$^{13}$C{$^1$H} NMR** (THF-*d*$_8$, 101 MHz**):** *δ* (ppm) = 21.4 (C*H$_3$*), 27.1 (d, $^4J_{PC}$ = 1.6 Hz, PCy$_3$-C*H$_2$*), 28.1 (d, $^2J_{PC}$ =12.1 Hz), 28.6 (d, $^3J_{PC}$ =3.0 Hz), 34.6 (d, $^1J_{PC}$ = 49.2 Hz, PCy$_3$-C*H*), 127.4 (C*H*$_{\mathrm{STol,ortho}}$), 129.7(C*H*$_{\mathrm{STol,meta}}$), 140.8 (C*H*$_{\mathrm{STol,para}}$), 149.7(C*H*$_{\mathrm{STol,ipso}}$). No resonance for the ylidic carbon atom could be detected, probably due broadening and low solubility of the compound.

**$^{31}$P{$^1$H} NMR** (THF-*d*$_8$, 162 MHz): *δ* (ppm) = 24.0 (br).

**$^{119}$Sn{$^1$H} NMR** (THF-*d*$_8$, 149 MHz): *δ* (ppm) = −165.5 (s, br)

**CHNS:** for $C_{52}H_{80}Cl_2O_4P_2S_2Sn_2$: C, 51.89; H, 6.70; S, 5.33 found: C, 51.54; H, 6.61; S, 5.62.

### Synthesis of $^{Cy}$Y(Cl)Ge-Ge(Cl)$^{Cy}$Y (169):

The filtrate of the above-mentioned reaction mixture was dried *in vacuo* and subsequently re-dissolved in acetonitrile (0.3 mL). The solution was overlayed with 3 mL of cyclohexane and kept at room temperature for 2 weeks, yielding colourless crystals of **169** (16 mg, 0.014 mmol, 54 %), which were suitable for X-ray structure determination.

Independent synthesis of **169** starting from the metalated ylide **$^{Cy}$Y-Li** :

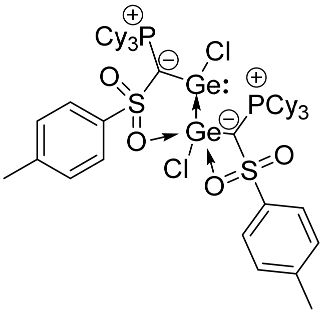

**$^{Cy}$Y-Li** (490 mg, 1.08 mmol, 1.0 eq.) and $GeCl_2$·dioxane (250 mg, 1.08 mmol, 1.0 eq.) were placed into a Schlenk tube and 10 mL of toluene was added. The reaction mixture was stirred at room temp. for 12h, during which LiCl precipitates out of the solution. The yellow suspension was filtered, and the obtained clear yellow solution was evaporated in vacuo to full dryness (4h, 50 °C, 1 x $10^{-3}$ mbar) furnishing **169** (450 mg, 0.81 mmol, 75 %) as a pale-yellow solid.

**$^1$H NMR** ($C_6D_6$, 400 MHz): $\delta$ (ppm) = 8.64 (d, $^2J_{HH}$ =7.9, 2H, $CH_{\mathrm{STol,ortho}}$), 8.57 (d, $^2J_{HH}$ =7.9, 2H, $CH_{\mathrm{STol,ortho}}$), 7.13 – 6.86 (m, 4H, $CH_{\mathrm{STol,meta}}$), 2.74 – 2.57 (m, 3H, $PCy_3$-C*H*), 2.55 – 2.38 (m, 3H, $PCy_3$-C*H*), 2.02 (s, 3H, $CH_3$), 1.95 (s, 3H, $CH_3$), 1.84 – 1.44 (m, 44H, $PCy_3$-$CH_2$), 1.30 – 1.09 (m, 16H, $PCy_3$-$CH_2$).

**$^{13}$C{$^1$H} NMR** ($C_6D_6$, 101 MHz): $\delta$ (ppm) =147.4 ($CH_{\mathrm{STol,ipso}}$), 147.1($CH_{\mathrm{STol,ipso}}$), 141.1 ($CH_{\mathrm{STol,para}}$), 140.7 ($CH_{\mathrm{STol,para}}$), 129.2 – 129.1 (br, $CH_{\mathrm{STol,meta}}$), 129.1 – 129.0 (br, $CH_{\mathrm{STol,ortho}}$), 47.2 (d, $^1J_{PC}$ = 65.8 Hz, PCS), 44.0 (d, $^1J_{PC}$ = 49.7 Hz, PCS), 34.6 (d, $^1J_{PC}$ = 48.3 Hz, $PCy_3$-C*H*), 33.2 (d, $^1J_{PC}$ = 48.1 Hz, $PCy_3$-C*H*), 28.2 – 28.0 (m, $PCy_3$-$CH_2$), 27.8 – 27.4 (m, $PCy_3$-$CH_2$), 27.4 – 27.1 (m, $PCy_3$-$CH_2$), 26.4 – 26.1 (m, $PCy_3$-$CH_2$), 21.4 – 20.9 (m, $CH_3$).

**$^{31}$P{$^1$H} NMR** ($C_6D_6$, 162 MHz): $\delta$ (ppm) = 33.1, 24.1.

**CHNS:** for $C_{52}H_{80}O_4P_2S_2Ge_2Cl_2$: C, 56.20; H, 7.26; S,5.77. found: C, 56.19; H, 7.30; S,5.67

## 5.3 Experimental Details for Section 3.3

### Attempted activation of small molecules with $^{Cy}Y_2E$ (E = Ge,Sn)

The respective di-ylide tetrylene (0.05 mmol) were filled into *J*. Young type NMR tubes and $C_6D_6$ was added (0.5 mL). The tubes were cycled onto a Schlenk line, degassed by the Freeze-pump-thaw method (three times) and subsequently 1 bar of $H_2$, $CO_2$ or CO was applied, respectively. No reaction was apparent from $^{31}P\{^1H\}$ NMR analysis, thus the respective tubes were heated to reflux for 12 h. Again, no reaction was observed.

### Attempted synthesis of $^{Cy}Y$-Ge-Si(SiMe$_3$)$_3$ (171):

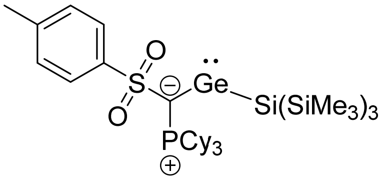

**169** (50 mg, 0.05 mmol, 1eq.) and KSi(SiMe$_3$)$_3$ (26 mg, 0.1 mmol, 2eq.) were placed into separate Schlenk tubes, dissolved in toluene under stirring (5 mL each) and cooled down to -78°C.The KSi(SiMe$_3$)$_3$ solution was then added slowly via cannula to the tube containing **169**. The reaction mixture was allowed to reach room temp. and stirred overnight. The reaction mixture was filtered via cannula and the obtained clear solution was evaporated to dryness. The yellowish residue was subsequently analyzed via $^{31}P\{^1H\}$ NMR spectroscopy and revealed to consists mostly of the protonated ylide $^{Cy}Y$-H ($\delta_P$ = 26.7 ppm). A reversed addition (digermylene to KSi(SiMe$_3$)$_3$) gave similar results.

### Attempted Synthesis of $^{Cy}Y$-Sn-Si(SiMe$_3$)$_3$ (172):

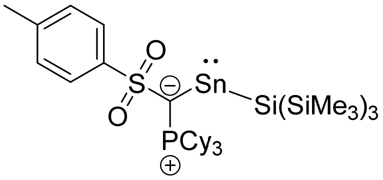

**170** (60 mg, 0.05 mmol, 1.0 eq.) and KSi(SiMe$_3$)$_3$ (29 mg , 0.1 mmol, 2.0 eq.) were placed into separate Schlenk tubes, dissolved in toluene under stirring (5 mL each) and cooled down to -78°C.The KSi(SiMe$_3$)$_3$ solution was then added slowly via cannula to the tube containing **170**. The reaction mixture was allowed to reach room temp. and stirred overnight. The reaction mixture was filtered via cannula and the obtained clear solution was evaporated to dryness. The yellowish residue was subsequently analyzed via $^{31}P\{^1H\}$ NMR spectroscopy and revealed to consists mostly of the protonated ylide $^{Cy}Y$-H ($\delta_P$ = 26.7 ppm). A reversed addition (chloro-stannylene to KSi(SiMe$_3$)$_3$) gave similar results.

**Synthesis of 173:**

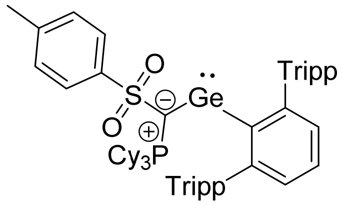

To a freshly prepared toluene (20 mL) solution of **169** (612 mg, 0.55 mmol, 1.0 eq.), (2,6-Tripp$_2$-C$_6$H$_3$)-Li·Et$_2$O (619 mg, 1.1 mmol, 2.0 eq.) dissolved in 10 mL Et$_2$O, was added dropwise at room temperature. The yellow reaction mixture was stirred over night and the solvent was subsequently removed in *vacuo*. To the obtained yellow residue, *n*-pentane (10 mL) was added and the suspension was filtered via cannula. The clear orange filtrate was concentrated to approx. 4 mL and stored at -30°C for 12 h, upon which the title compound crystallized as orange needles. The supernatant was removed via syringe and the residue was dried in *vacuo* giving the title compound as an orange powder (740 mg, 67%).

**$^1$H NMR** (C$_6$D$_6$, 400 MHz): $\delta$ (ppm) = 7.27 (d, $^2J_{HH}$ = 7.0 Hz, 2H, *m*-H/p-Tol), 7.26 – 7.18 (m, 7H, Terph), 6.84 (d, $^2J_{HH}$ =7.9 Hz, 2H, *o*-H/*p*-Tol), 3.77 – 3.70 (m, 3H, *i*PrCH), 2.98 (p, *J* =7.0 Hz, 7.0 Hz, 6.8 Hz, 6.8 Hz, 3H, *i*PrCH), 2.52 (q, *J*= 12.1 Hz, 12.1 Hz, 12.1 Hz, 3H, PCy$_3$-CH), 2.11 (s, 3H, *p*Tol-CH$_3$), 1.63 (s, 6H, PCy$_2$-CH$_2$), 1.53 – 1.45 (m, 16H, PCy$_2$-CH$_2$), 1.37 (d, $^2J_{HH}$ = 6.9 Hz, 18H), 1.21 (d, $^2J_{HH}$ = 6.8 Hz, 18H), 1.14 – 0.98 (m, 8H, PCy$_2$-CH$_2$).

**$^{13}$C{$^1$H}-NMR** (C$_6$D$_6$, 101 MHz): $\delta$ (ppm) = 165.04 (d, $^3J_{CP}$ = 10.9 Hz, *i*-Ph), 148.44 (*o*-Ph), 147.51 (*i*-Tripp), 146.96 (*p*-Tol), 146.88 (*p*-Tripp), 142.63 (*i*-Tol), 139.34 (*o*-Tripp), 130.51 (*p*-Ph), 128.84 (*o*-Tol), 128.18 (*m*-Tol), 125.23 (*m*-Ph), 120.78 (*m*-Tripp), 101.78 (d, $^1J_{CP}$ = 32.7 Hz, PC$_{\text{ylide}}$), 34.47 (*p*-*CH*(CH$_3$)$_2$), 33.65 (d, $^1J_{CP}$ = 45.7 Hz, PCy$_3$-CH), 30.88 (*m*-*CH*(CH$_3$)$_2$), 27.88 (d, $^3J_{CP}$ =3.4 Hz, PCy$_3$-CH$_2$), 27.56 (d, $^2J_{CP}$ = 12.0 Hz, PCy$_3$-CH$_2$), 26.20 (PCy$_3$-CH$_2$), 24.61 (*m*-CH(CH$_3$)$_2$), 24.49 ((*p*-CH(*C*H$_3$)$_2$), 24.46 ((*m*-CH(*C*H$_3$)$_2$), 21.17 (*C*H$_3$-Tol).

**$^{31}$P{$^1$H} NMR** (C$_6$D$_6$, 161.9 MHz): $\delta$ (ppm) = 27.2 (s).

## 5.4 Experimental Details for Section 3.4

**Attempted syntheses of $^{Cy}Y_2Si$:**

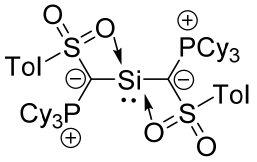

via salt-metathesis from IPr·SiCl$_2$:

**$^{Cy}$Y-Li** (150 mg, 0.330 mmol, 1.0 eq) and IPr·SiCl$_2$ (80 mg, 0.165 mmol, 0.5 eq.) were placed into a Schlenk tube and cooled down to -78°C. To this tube, precooled (-78°C) toluene (10 mL) was added and the mixture was stirred at -78°C for 1h. Subsequently, the mixture was allowed to warm up to room temperature. At this point the solvent was removed in *vacuo* and the crude was dissolved in $C_6D_6$ and analyzed via NMR spectroscopy. $^{31}P\{^1H\}$ NMR spectrum revealed the formation of $^{Cy}$Y-H, while $^1H$ NMR analysis proved the formation of free IPr. No indication for the formation of the target compound was observed. Additionally, varying the reaction conditions (e.g. separate addition of the compounds or different solvents/temperatures) gave similar results.

via formation of ylide chlorosilanes

**$^{Cy}$Y-Li** (227 mg, 0.5 mmol, 1.0 eq.) was dissolved in toluene (10 mL) and the mixture was cooled to -78°C. SiHCl$_3$ (0.025 mL, 0.25 mmol, 0.5 eq., dissolved in 5 mL toluene) was added slowly via cannula and the resulting orange reaction mixture was stirred rapidly till it reached room temperature and additionally over night. Further stirring over night, resulted in the precipitation of a white solid, which turned out to mainly consist of $^{Cy}$Y-SiHCl$_2$ (as proved by NMR and XRD analysis). Attempts to install a second ylide-substituent by isolating this solid and subsequently react it with another equivalent of $^{Cy}$Y-Li repeatedly failed. Instead, only protonation to the respective ylide was observed.

via formation of di-ylide halosilanes

**$^{Cy}$Y-M** (M=Li, K) (0.5 mmol, 1.0 eq.) was dissolved in toluene (10 mL) and the mixture was cooled to -78 °C. SiX$_4$ (X= Cl, Br, I) (1.0 mmol, 2.0 eq. in 20 mL toluene) was added slowly via cannula and the resulting orange reaction mixture was stirred rapidly till it reached room temperature. Subsequently the solvent was removed in *vacuo* and the residue was analyzed via NMR spectroscopy. $^{31}P\{^1H\}$ NMR analysis revealed mostly ylide formation along with unidentified products. Furthermore, no signals were found in the $^{29}Si\{^1H\}$ NMR spectrum. Additionally, varying the reaction conditions (e.g. reverse addition of the compounds or different solvents/temperatures) gave similar results.

via transylidation from di-ylide tetrylenes to IPr·SiCl$_2$

A precooled (-78 °C) toluene solution of **$^{Cy}Y_2E$** (E=Ge, Sn, 0.5 mmol in 3 mL) was added dropwise via cannula to a precooled (-78 °C) toluene solution of IPr·SiCl$_2$ (0.25 mmol in 1 mL). The reaction mixture was stirred rapidly till it reached room temperature and additionally over night. Subsequently the solvent was removed in *vacuo* and the residue was analyzed via NMR spectroscopy. $^{31}P\{^1H\}$ NMR analysis revealed mostly ylide formation along with unreacted **$^{Cy}Y_2E$**. Furthermore, no additional signals were found in the $^{29}Si\{^1H\}$ NMR spectrum. Additionally, varying the reaction conditions (e.g. reverse addition of the compounds or different solvents/temperatures) gave similar results.

via transylidation from di-ylide tetrylenes to SiI$_4$

A precooled (-78 °C) toluene solution of **$^{Cy}Y_2E$** (E=Ge, Sn, 0.5 mmol in 3 mL) was added dropwise via cannula to a precooled (-78 °C) toluene solution of SiI$_4$ (0.25 mmol in 1 mL). The reaction mixture was stirred rapidly till it reached room temperature and additionally over night. Subsequently the solvent was removed in *vacuo* and the residue was analyzed via NMR spectroscopy. $^{31}P\{^1H\}$ NMR analysis revealed mostly ylide formation along with unreacted **$^{Cy}Y_2E$**. Furthermore, no additional signals were found in the $^{29}$Si{$^1$H} NMR spectrum. Additionally, varying the reaction conditions (e.g. reverse addition of the compounds or different solvents/temperatures) gave similar results.

**Synthesis of $^{Cy}Y_{Me}$-TMS:**

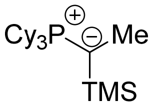

**$^{Cy}Y_{Me}$-H$_2$** (6.14 g, 15.77 mmol, 1 eq.) was suspended in 100 ml THF. To this suspension, 10.00 mL of *n*BuLi (1.57 M in hexanes, 15.77 mmol, 1 eq.) was added dropwise at room temp. until all solid was dissolved. The reaction mixture was stirred for 30 min, subsequently filtered and 1.00 mL (0.856 g, 7.88 mmol, 0.5 eq.) of trimethylsilyl chloride was added dropwise to the solution. The solution was stirred overnight and a white solid slowly precipitated. The solvent was removed *in vacuo* and 10 mL of toluene was added. The suspension was cooled down to 0 °C and the solution was filtered off. The remaining solid was dried in *vacuo*, giving the title compound as a white solid (1.51 g, 3.97 mmol, 50 %).

**$^1$H NMR** (THF-d$_8$, 400 MHz): $\delta$ (ppm) = 2.25 – 2.03 (m, 3H, PCy$_3$-CH), 1.89 – 1.77 (m, 12H, PCy$_3$-CH$_2$), 1.77 – 1.68 (m, 3H, PCy$_3$-CH$_2$), 1.58 (d, $J$ = 16.2 Hz, 3H, CH$_3$), 1.54 – 1.36 (m, 6H, PCy$_2$-CH$_2$), 1.32 – 1.18 (m, 9H, PCy$_3$-CH$_2$), 0.02 (s, 9H, TMS).

**$^{13}$C {$^1$H} NMR** (THF-d$_8$, 101 MHz): $\delta$ (ppm) = 34.7 (d, $J$ = 49.8 Hz, PCy$_3$-CH), 28.8 (d, $J$ = 2.2 Hz, PCy$_3$-CH$_2$), 28.6 (d, $J$ = 11.1 Hz), 27.6 (d, $J$ = 1.5 Hz, PCy$_3$-CH$_2$), 15.0 (PCy$_3$-CH$_2$), 3.1 (d, $J$ = 1.4 Hz, CH$_3$), -10.9 (d, $J$ = 93.4 Hz, PCy$_3$-C-TMS).

**$^{31}$P {$^1$H} NMR** (THF-d$_8$, 162 MHz): $\delta$ (ppm) = 31.3.

**Synthesis of $^{Cy}Y_{Ph}$-TMS:**

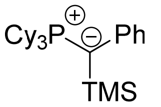

**$^{Cy}Y_{Ph}$-H$_2$** (1.00 g, 2.21 mmol, 1,0 eq.) was placed into a schlenk flask and toluene (50 mL) was added. The flask was cooled down to -78°C and nBuLi (1.6 M, 1.42 mL, 1.0 eq.) was added dropwise. The flask was allowed to warm to room temp. and the formed ylide was subsequently treated *in-situ* with TMS–I (0.32 mL, 2.32 mmol, 1.05 eq,) at 0°C. The reaction mixture was stirred over night, upon which a colourless solid precipitated. The solvent was removed in vacuo, KO*t*Bu (0.27 g, 2.43 mmol, 1.1 eq.) and THF (30 mL) were added to the flask. The reaction mixture was stirred for 2h at room temperature. THF was removed in *vacuo* and toluene (50 mL) was added, the suspension filtered, and the obtained clear solution was dried in *vacuo* to afford the title compound as a colorless solid (0.70 g, 70%). Colorless crystals suitable for XRD analysis were grown by overlaying a DCM solution of **$^{Cy}Y_{Ph}$-TMS** with *n*-hexane.

**$^1$H NMR** (C$_6$D$_6$, 400 MHz): $\delta$ = 7.54 – 7.47 (m, 2H, Ph), 7.25 (t, $J$=7.4 Hz, 7.4 Hz, 2H, Ph), 7.09 (ddt, $J$=7.3 Hz, 5.5 Hz, 1.6 Hz, 1.6 Hz, 1H, Ph), 2.02 – 1.82 (m, 9H PCy$_3$-CH+CH$_2$), 1.72 – 1.62 (m, 6H, PCy$_3$-CH$_2$), 1.60 – 1.51 (m, 3H, PCy$_3$-CH$_2$), 1.41 (qt, $J$=12.4 Hz, 12.4 Hz, 12.4 Hz, 3.2 Hz, 3.2 Hz, 6H, PCy$_3$-CH$_2$), 1.15 – 0.92 (m, 9H, PCy$_3$-CH$_2$), 0.38 (s, 9H, TMS).

**$^{13}$C NMR** (C$_6$D$_6$, 101 MHz): $\delta$ (ppm) = 139.8 (d, $J_{CP}$ = 4.1 Hz), 139.0 (d, $J_{CP}$ = 1.6 Hz), 128.5 (d, $J_{CP}$ = 2.5 Hz), 126.3 (d, $J_{CP}$ = 2.7 Hz), 34.8 (d, $^1J_{CP}$ = 49.9 Hz), 28.9 (d, $^3J_{CP}$ = 3.1 Hz, PCy$_3$ -CH$_2$), 28.3 (d, $^2J_{CP}$ = 11.8 Hz, PCy$_3$ -CH$_2$), 27.2 (d, $^4J_{CP}$ = 1.5 Hz, PCy$_3$ -CH$_2$), 1.5 (TMS).

**$^{31}P\{^1H\}$ NMR** ($C_6D_6$, 162 MHz): $\delta$ (ppm) = 21.9.

**CHNS:** calc. for $C_{28}H_{47}PSi$: C: 75.96; H: 10.70; found: C: 75.16; H: 10.52.

### Attempted syntheses of di-ylide substituted dichlorosilanes via TMS-Cl elimination:

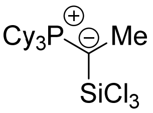

**$^{Cy}Y_{Me}$-TMS** (332 mg, 0.87 mmol, 1.0 eq.) was dissolved in 10 mL of toluene and $SiCl_4$ (0.05 mL, 0.44 mmol, 0.5 eq.) was added dropwise at room temperature. The reaction mixture was stirred overnight, upon which a colourless solid precipitated. The supernatant was removed via syringe and the solid was collected via filtration, washed with small amounts of toluene and dried in vacuo. The filtrate and the collected solid were analyzed by NMR spectroscopy. The latter turned out to be almost pure **$^{Cy}Y_{Me}$-$SiCl_3$**, while the former contained mainly the starting material. Attempts to install a second ylide substituent sequentially by adding another equivalent of TMS-ylide to the obtained **$^{Cy}Y_{Me}$-$SiCl_3$** in refluxing toluene failed.

**$^{31}P\{^1H\}$ NMR** ($C_6D_6$, 162 MHz): $\delta$ (ppm) = 33.7.

**$^{29}Si\{^1H\}$ NMR** ($C_6D_6$, 80 MHz): $\delta$ (ppm) = -11.7 (d, $^2J_{SiP}$ = 41.9 Hz).

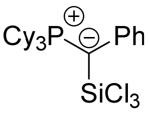

Similarly, using **$^{Cy}Y_{Ph}$-TMS** (386 mg, 0.87 mmol, 1.0 eq.) and $SiCl_4$ (0.05 mL, 0.44 mmol, 0.5 eq.) delivered mostly **$^{Cy}Y_{Ph}$-$SiCl_3$**, which was also not prone to a second substitution. Colourless crystals suitable for XRD analysis were obtained by slow evaporation of a saturated benzene solution of **$^{Cy}Y_{Ph}$-$SiCl_3$**.

**$^{31}P\{^1H\}$ NMR** ($C_6D_6$, 162 MHz): $\delta$ (ppm) = 26.5

**$^{29}Si\{^1H\}$ NMR** ($C_6D_6$, 80 MHz): $\delta$ (ppm) = -15.0 (d, $^2J_{SiP}$ = 40.3 Hz).

### Synthesis of [$^{Cy}Y_{Mes}$-$SiBr_3$]Br:

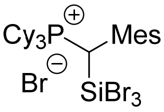

$^{Cy}Y_{Mes}$-$H_2$ (2.00 g, 3.70 mmol, 1.0 eq.) was suspended in toluene (50 mL) and *n*BuLi (2.31 mL, 1.60 M in hexanes, 3.70 mmol, 1.0 eq.) was added dropwise at room temperature. After stirring the mixture for 1 h at room temperature, the cloudy suspension was left to stand to let most of the formed LiI settle down. Subsequently, the solid was filtered off, and $SiBr_4$ (0.5 mL, 4.03 mmol, 1.09 eq.) was added to the clear filtrate. This mixture was stirred over night, upon which a colourless solid precipitated. The solid was collected via filtration and washed with *n*-pentane (3 x 10 mL), giving the title compound as a white powder (2.16 g, 77%).

**$^1H$ NMR** ($CD_2Cl_2$, 400 MHz): $\delta$ = 7.03 (d, $J$ = 11.4 Hz, 2H, CH-Mes), 4.59 (d, $^2J_{PH}$ = 22.2 Hz, 1H), 2.82 – 2.70 (m, 3H, $PCy_3$-CH), 2.61 (s, 3H, Mes-$CH_3$), 2.43 (s, 3H), 2.30 (s, 3H, Mes-$CH_3$), 2.07 – 1.88 (m, 10H, $PCy_3$-$CH_2$), 1.82 – 1.74 (m, 3H, $PCy_3$-$CH_2$), 1.67 – 1.56 (m, 3H, $PCy_3$-$CH_2$), 1.53 – 1.16 (m, 14H, $PCy_3$-$CH_2$).

**$^{13}C\{^1H\}$ NMR** ($CD_2Cl_2$, 101 MHz) δ = 141.0 (d, $J$ = 2.7 Hz, *p-C*), 139.5 (d, $J$ = 5.5 Hz, *ipso*-C), 138.6 (d, $J$ = 2.7 Hz, *o*-C), 132.3 (d, $J$ =2.1 Hz, *m*-CH), 132.2 (d, $J$ =2.7 Hz, *m*-CH), 35.6 (d, $J$ =33.3 Hz, PC*H*C), 32.3 (d, $J$ = 23.8 Hz, $PCy_3$-CH), 29.3 (d, $J$ =4.9 , $PCy_3$-$CH_2$), 28.8 (d, $J$ = 4.5 Hz, $PCy_3$-$CH_2$), 27.6 (d, $J$= 11.8 Hz, $PCy_3$-$CH_2$), 27.4 (d, $J$ = 11.7 Hz, $PCy_3$-$CH_2$), 25.6 (d, $J$ = 1.8 Hz, $PCy_3$-$CH_2$), 25.5 (*m*-$CH_3$), 23.8 (*m*-$CH_3$), 21.0 (*p*-$CH_3$).

**$^{31}P\{^1H\}$ NMR** ($CD_2Cl_2$, 162 MHz): $\delta$ = 42.8.

**$^{29}Si\{^1H\}$ NMR** ($C_6D_6$, 80 MHz): $\delta$ (ppm) = -35.5 (d, $^2J_{SiP}$ = 3.0 Hz).

**CHNS:** calc. for $C_{28}H_{45}Br_4PSi$: C: 46.23; H:5.97; found: C: 46.69; H: 6.07.

**Synthesis of 176:**

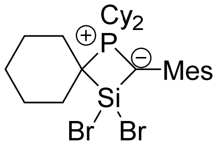

**[$^{Cy}Y_{Mes}$-SiBr$_3$]Br** (1.00 g, 1.32 mmol, 1.0 eq.) and KHMDS (0.54 g, 2.71 mmol, 2.05 eq.) were placed into a Schlenk tube and toluene (30 mL) was added. The reaction mixture was stirred over night, filtered subsequently and the solvent was removed in *vacuo*. Acetonitrile (20 mL) was added to the crude material and the resulting suspension was stirred rapidly for 3 h. The suspension was then filtered over a frit and the obtained pale-yellow solid was washed with acetonitrile (5 mL) and *n*-pentane (3 x 15 mL). The solid was dried in *vacuo* to yield pure **176** as a white powder (410 mg, 52%). Colourless crystals, suitable for XRD analysis were obtained by storage of a saturated toluene solution of **176** at -30°C for one week.

**$^1H$ NMR** ($C_6D_6$, 400 MHz): $\delta$ (ppm) = 6.85 (s, 2H, CH-Mes), 2.65 (s, 6H, $CH_3$-Mes), 2.57 (d, *J*=12.2, 2H, PCy-$CH_2$), 2.13 (s, 3H, $CH_3$-Mes), 2.09 – 1.90 (m, 6H, PCy-$CH_2$+PCy$_2$-CH), 1.90 – 1.80 (m, 2H, PCy-$CH_2$), 1.78 – 1.65 (m, 5H, PCy-$CH_2$), 1.59 – 1.44 (m, 6H, PCy-$CH_2$), 1.28 – 1.18 (m, 2H, PCy-$CH_2$), 1.14 – 0.98 (m, 9H, PCy-$CH_2$).

**$^{13}C$ $\{^1H\}$ NMR** ($C_6D_6$, 101 MHz): $\delta$ (ppm) = 140.9 (d, $^2J_{CP}$ = 5.1 Hz, Mes-*ipso*-C), 134.3 (d, $^5J_{CP}$ = 3.2 Hz, Mes-*para*-C), 132.9 (d, $^3J_{CP}$ = 3.9 Hz, Mes-*ortho*-C), 128.7 (d, $^4J_{CP}$ = 2.6 Hz, Mes-*meta*-C), 47.8 (d, $^1J_{CP}$ = 28.1 Hz, PCy$_2$-CH), 47.1 (PC$_{cyclic}$Si), 45.5 (d, $^1J_{CP}$ = 34.6 Hz, PC$_{ylide}$Si), 31.9 (d, $J_{CP}$ = 4.5 Hz, PCy-$CH_2$), 30.1 (d, $J_{CP}$ = 4.6 Hz, PCy-$CH_2$), 29.5 (d, $J_{CP}$ =3.1 Hz, PCy-$CH_2$), 28.2 (d, $J_{CP}$ =11.3 Hz, PCy-$CH_2$), 27.6 (d, $J_{CP}$ =11.1 Hz, PCy-$CH_2$), 26.7 (d, $J_{CP}$ =1.7 Hz, PCy-$CH_2$), 26.0 – 25.7 (m, PCy-$CH_2$), 22.7 (Mes-*o*-$CH_3$), 21.0 (Mes-*p*-$CH_3$).

**$^{31}P\{^1H\}$ NMR** ($C_6D_6$, 162 MHz): $\delta$ (ppm) = 13.4.

**$^{29}Si\{^1H\}$ NMR** ($C_6D_6$, 80 MHz): $\delta$ (ppm) = -46.2 (d, $^2J_{SiP}$ = 24.2 Hz).

**CHNS:** calc. for $C_{28}H_{43}Br_2PSi$: C: 56.19; H:7.24; found: C: 56.26; H: 7.47.

**Synthesis of 179:**

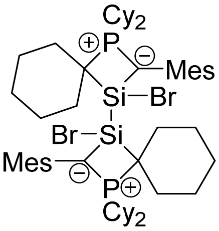

**179** (50 mg, 0.083 mmol, 1.0 eq.) and $^{Mes}$NacNac-Mg(I) dimer (34 mg, 0.042 mmol, 0.5 eq.) were placed into a *J.* Young type NMR tube and $C_6D_6$ (0.5 mL) was added. The tube was shaken for 30 min at room temperature. The reaction mixture was then subsequently analyzed via NMR spectroscopy, confirming full conversion to the title compound. Attempts to purify the disilane species failed, because the formed $^{Mes}$NacNac–Mg–Br could not be removed completely. X-Ray quality crystals were formed after filtration of the reaction mixture into a glass vial, which was left to stand over night.

**$^{31}P\{^1H\}$ NMR** ($C_6D_6$, 162 MHz): $\delta$ (ppm) = 26.6.

**$^{29}Si\{^1H\}$ NMR** ($C_6D_6$, 80 MHz): $\delta$ (ppm) = -18.9 (dd, $^2J_{SiP}$ = 30.5 Hz, $^3J_{SiP}$ = 7.1 Hz).

## 5.5 Experimental Details for Section 3.5

**Synthesis of $^{Cy}$Y$_S$-PCy$_2$ (L1):**

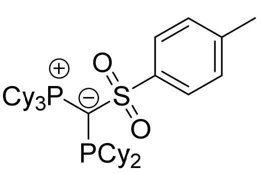

**$^{Cy}$Y$_S$-Li** (3.00 g, 6.60 mmol, 1.00 eq.) was dissolved in toluene (30 mL) and PCy$_2$Cl (1.50 mL, 6.73 mmol, 1.02 eq.) was added dropwise at room temperature. The orange reaction mixture was stirred for 1h at room temperature, giving the precipitation of LiCl. The suspension was filtered via a filter cannula and the solvent of the obtained clear solution was removed under reduced pressure. Acetonitrile (20 mL) was added and the waxy-like suspension was stirred over night, during which a white precipitate formed. The white solid was collected with a glass frit, washed with acetonitrile (2 mL) and *n*-hexane (3 x 10 mL) and dried in vacuo, giving **$^{Cy}$Y$_S$-PCy$_2$** as a white amorphous powder (75%, 3.20 g). Colorless crystals suitable for X-ray structure determination were grown via slow evaporation of a saturated benzene solution.

**$^1$H NMR** ($C_6D_6$, 400 MHz): $\delta$ (ppm) = 8.19 (d, $J_{HH}$ = 8.0 Hz, 2H, *m*-CH), 6.96 (d, $J_{HH}$ = 7.9 Hz, 2H, *o*-CH), 3.04 – 2.83 (m, 3H, PCy$_3$-CH), 2.66 – 2.50 (m, 2H, PCy$_2$-CH), 2.50 – 2.37 (m, 2H; PCy-CH$_2$), 2.31 – 2.19 (m, 2H, PCy-CH$_2$), 2.02 (s, 3H, *p*-Tol-CH$_3$), 1.99 – 1.95 (m, 4H, PCy-CH$_2$), 1.90 – 1.79 (m, 4H, PCy-CH$_2$), 1.76 – 1.62 (m, 14H, PCy-CH$_2$), 1.62 – 1.52 (m, 4H, PCy-CH$_2$), 1.51 – 1.40 (m, 4H, PCy-CH$_2$), 1.40 – 1.05 (m, 16H, PCy-CH$_2$).

**$^{13}$C{$^1$H} NMR** ($C_6D_6$, 101 MHz): $\delta$ (ppm) = 149.1 (*ipso*-CH), 140.2 (*p*-CH) 128.8 (*m*-CH), 127.6 (*o*-CH), 37.6 (dd, $J_{CP}$ = 4.2, 12.9 Hz, PCy$_2$-CH), 36.0 (dd, $^1J_{CP}$ = 61.8, $^1J_{CP}$= 87.1 Hz, PCP), 35.2 (dd, $^3J_{CP}$ = 11.3, $^1J_{CP}$ = 49.0 Hz, PCy$_3$-CH), 34.5 (d, $^2J_{CP}$ = 19.6, PCy-CH$_2$), 32.5 (d, $^2J_{CP}$ = 15.6 PCy-CH$_2$), 28.6 (d, $^2J_{CP}$ = 13.5, PCy-CH$_2$), 28.7 – 28.4 (m, PCy-CH$_2$), 28.2 (d, $^3J_{CP}$ = 10.4, PCy-CH$_2$), 27.7 (d, $^3J_{CP}$ = 11.9, PCy-CH$_2$), 27.4 (PCy-CH$_2$), 26.5 (PCy-CH$_2$), 21.1 (*p*-Tol-CH$_3$).

**$^{31}$P{$^1$H} NMR** ($C_6D_6$, 162 MHz): $\delta$ (ppm) = 31.7 (d, $^2J_{PP}$ = 106.8 Hz), -7.3 (d, $^2J_{PP}$ = 106.8 Hz).

**CHNS**: calc. for $C_{38}H_{62}O_2P_2S$: C: 70.77, H: 9.69, S: 4.97, found C: 70.86, H: 9.85, S: 4.72.

**Synthesis of $^{Cy}$Y$_S$-P*i*Pr$_2$ (L4):**

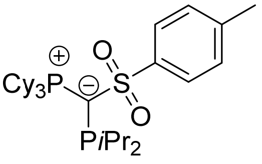

$^{Cy}$Y$_S$-Li (1.00 g, 2.20 mmol, 1.00 eq.) was dissolved in toluene (30 mL) and P*i*Pr$_2$Cl (0.36 mL, 2.27 mmol, 1.03 eq.) was added dropwise at room temperature. The orange reaction mixture was stirred for 1h at room temperature, giving the precipitation of LiCl. The suspension was filtered via a filter cannula and the solvent of the obtained clear solution was removed under reduced pressure. Acetonitrile (20 mL) was added and the waxy-like suspension was stirred over night, during which a white precipitate formed. The white solid was collected with a glass frit, washed with acetonitrile (2 mL) and *n*-hexane (3 x 10 mL) and dried in vacuo, giving **$^{Cy}$Y$_S$-P*i*Pr$_2$** as a white amorphous powder (70%, 870 mg). Colorless crystals suitable for X-ray structure determination were grown via slow evaporation of a saturated benzene solution.

**$^1$H NMR** (THF-*d*$_8$, 400 MHz): $\delta$ (ppm) = 7.80 (d, $J$ = 8.3 Hz, 2H, *m*-CH), 7.18 (d, $J$ = 8.0 Hz, 2H, *o*-CH), 2.93 –2.76 (m, PCy$_3$-CH), 2.45 – 2.21 (m, 5H, P*i*Pr$_2$-CH+*p*-Tol-CH$_3$), 2.00 – 1.87 (m, 6H, PCy$_3$-CH$_2$), 1.86 – 1.76 (m, 6H, PCy$_3$-CH$_2$), 1.72 – 1.59 (m, 8H, PCy$_3$-CH$_2$), 1.40 – 1.20 (m, 10H, PCy$_3$-CH$_2$), 1.10 (dd, $^1J_{HH}$ = 6.9, $^2J_{PH}$ = 13.8 Hz, 6H, P*i*Pr$_2$-CH$_3$), 0.98 (dd, $^1J_{HH}$ = 7.2, $^2J_{PH}$ = 16.3 Hz, 6H, P*i*Pr$_2$-CH$_3$).

**$^{13}$C{$^1$H} NMR** (THF-$d_8$, 101 MHz): δ (ppm) = 149.5 (*ipso*-CH), 141.1 (*p*-CH), 129.3 (*o*-CH), 128.1 (*m*-CH), 38.3 (dd, $^1J_{CP}$ = 61.8 Hz, $^1J_{CP}$ = 87.3 Hz, PCP), 35.9 (dd, $^3J_{CP}$ = 11.2, $^1J_{CP}$ = 49.0 Hz, PCy$_3$-CH), 29.08 (m, *J* = 2.9, 2.9 Hz, PCy$_3$-CH$_2$), 29.2 – 28.9 (m, PCy$_3$-CH$_2$), 28.5 (d, *J*=12.0, PCy$_3$-CH$_2$), 27.4 (dd, $^3J_{CP}$ = 4.7 Hz, $^1J_{CP}$ = 13.4 Hz, P*i*Pr$_2$-CH), 27.3 – 27.1 (m), 24.4 (d, $^2J_{CP}$ =21.7), 21.8 (d, $^2J_{CP}$ =18.4), 21.4 (*p*-Tol-CH$_3$).

**$^{31}$P{$^1$H} NMR** (THF-$d_8$, 162 MHz): δ (ppm) = 31.5 (d, $^2J_{PP}$ = 105.7 Hz), 1.5 (d, $^2J_{PP}$ = 105.7 Hz).

**CHNS**: calc. for $C_{32}H_{54}O_2P_2S$: C: 68.05, H: 9.64, S: 5.68, found C: 68.33, H: 9.72, S: 5.69.

### Synthesis of [Au($^{Cy}$Y$_S$-PCy$_2$)Cl] (P1):

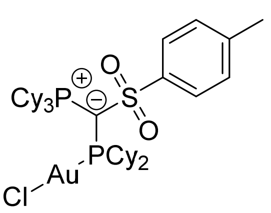

**$^{Cy}$Y$_S$-PCy$_2$** (70 mg, 0.11 mmol, 1.02 eq.) and thtAuCl (34 mg, 0.11 mmol, 1.00 eq.) were placed into a schlenk tube, dissolved in 5 mL of toluene and stirred for 30 min at room temperature. The reaction mixture was overlayed with 15 mL of *n*-pentane and left to stand over night, during which colorless crystals formed. The solution was removed via a filter cannula and the residual crystals were washed with a small amount of *n*-pentane (5 mL). The colorless crystals were dried in vacuo, furnishing **[Au($^{Cy}$Y$_S$-PCy$_2$)Cl]** as a white solid. (75%, 72 mg). Colorless crystals were suitable for X-ray structure determination.

**$^1$H NMR** (THF-$d_8$, 400 MHz): δ (ppm) = 7.75 (d, $J_{HH}$ = 8.0 Hz, 2H, *m*-CH), 7.30 (d, $J_{HH}$ = 8.0 Hz, 2H. *o*-CH), 3.45 – 3.29 (brm, 3H, PCy$_3$-CH), 2.85 – 2.78 (m, 2H, PCy$_2$-CH), 2.60 – 2.48 (br, 2H, PCy$_2$-CH$_2$), 2.38 (s, 3H, *p*-Tol-CH$_3$; 2.25 – 2.11 (br, 2H, PCy$_2$-CH$_2$), 1.97 – 1.86 (m, 8H; PCy$_3$-CH$_2$+PCy$_2$-CH$_2$), 1.86 – 1.78 (m, 2H; PCy$_3$-CH$_2$+PCy$_2$-CH$_2$), 1.77 – 1.64 (m, 10H, PCy$_3$-CH$_2$+PCy$_2$-CH$_2$), 1.63 – 1.49 (m, 10H, PCy$_3$-CH$_2$+PCy$_2$-CH$_2$), 1.48 – 1.14 (m, 14H, PCy$_3$-CH$_2$+PCy$_2$-CH$_2$).

**$^{13}$C{$^1$H} NMR** (THF-$d_8$, 101 MHz): δ (ppm) = 148.5 (*ipso*-C), 142.5 (*p*-C), 130.0 (*m*-C), 127.5 (*o*-C), 43.9 (d, $^1J_{CP}$ = 38.0 Hz, PCy$_2$-CH) , 38.0 (dd, $^1J_{CP}$ = 37.8 Hz, $^1J_{CP}$ = 73.3 Hz, PCP), 36.9 (brd, $^1J_{CP}$ = 49.4 Hz, PCy$_3$-CH), 29.9 – 28.9 (m, PCy$_3$-CH$_2$/PCy$_2$-CH$_2$), 28.5 (d, $J_{CP}$ = 14.4 Hz, PCy$_3$-CH$_2$/PCy$_2$-CH$_2$), 28.2 (d, $J_{CP}$ = 15.3 Hz, PCy$_3$-CH$_2$/PCy$_2$-CH$_2$), 28.1 (d, $J_{CP}$ = 12.3 Hz, PCy$_3$-CH$_2$/PCy$_2$-CH$_2$), 27.2 (d, $J_{CP}$ = 2.0 Hz, PCy$_3$-CH$_2$/PCy$_2$-CH$_2$), 27.0 (d, $J_{CP}$ = 1.6 Hz, PCy$_3$-CH$_2$/PCy$_2$-CH$_2$), 21.4 (*p*-Tol-CH$_3$).

**$^{31}$P{$^1$H}** NMR (THF-$d_8$; 162 MHz): δ (ppm) = 40.7 (d, $^2J_{PP}$ = 35.6 Hz), 29.9 (d, $^2J_{PP}$ = 35.6 Hz).

CHNS: calc. for $C_{38}H_{62}AuClO_2P_2S$ : C: 52.02, H: 7.12, S: 3.65, found C: 52.25, H: 7.01, S: 3.67.

### Synthesis of [Au($^{Cy}$Y$_S$-P*i*Pr$_2$)Cl] (P4):

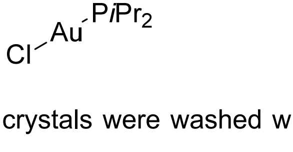

**$^{Cy}$Y$_S$-P*i*Pr$_2$** (100 mg, 0.18 mmol, 1.02 eq.) and thtAuCl (56 mg, 0.17 mmol, 1.00 eq.) were placed into a schlenk tube, dissolved in 5 mL of toluene and stirred for 30 min at room temperature. The reaction mixture was overlayed with 15 mL of *n*-pentane and left to stand over night, during which colorless crystals formed. The solution was removed via a filter cannula and the residual crystals were washed with a small amount of *n*-pentane (5 mL). The colorless crystals were dried in vacuo, furnishing **[Au($^{Cy}$Y$_S$-P*i*Pr$_2$)Cl]** as a white solid. (74%, 102 mg). Colorless crystals were suitable for X-ray structure determination.

**$^1$H NMR** (THF-*d*$_8$, 400 MHz): *δ* (ppm) = 7.74 (d, $J_{HH}$ = 8.1 Hz, 2H, *m*-CH), 7.26 (d, $J_{HH}$ = 8.0 Hz, 2H, *o*-CH), 3.42– 3.25 (m, 3H, PCy$_3$-CH), 3.12 – 2.95 (m, 2H, P*i*Pr$_2$-CH), 2.34 (s, 3H), 1.93 – 1.80 (m, 6H, PCy$_3$-CH$_2$), 1.71 – 1.62 (m, 10H, PCy$_3$-CH$_2$), 1.62 – 1.50 (m, 6H, PCy$_3$-CH$_2$), 1.47 (d, *J* = 7.1 Hz, 3H, P*i*Pr$_2$-CH$_3$), 1.43 (d, *J* = 7.1 Hz, 3H, P*i*Pr$_2$-CH$_3$), 1.37 (d, *J* = 6.9 Hz, 3H, P*i*Pr$_2$-CH$_3$), 1.32 – 1.02 (m, 12H, P*i*Pr$_2$-CH$_3$ + PCy$_3$-CH$_2$).

**$^{13}$C{$^1$H} NMR** (THF-*d*$_8$, 101 MHz): *δ* (ppm) = 148.2 (*ipso*-C), 142.6 (*p*-C), 130.1 (*m*-C), 127.7 (*o*-C), 39.6 (dd, $^1J$ = 38.6 Hz, 73.3 Hz, PCP), 36.9 (brd, $^1J$ = 45.8 Hz, PCy$_3$-CH), 33.9 (d, $^1J$ = 38.6 Hz, P*i*Pr$_2$-CH) , 29.32 (br, PCy$_3$-CH$_2$), 28.13 (d, $^3J$ = 12.2 Hz, PCy$_3$-CH$_2$), 27.0 (d, $^4J$ = 1.7 Hz, PCy$_3$-CH$_2$), 24.42 (P*i*Pr$_2$-CH$_3$), 23.54 (P*i*Pr$_2$-CH$_3$), 21.37 (*p*-Tol-CH$_3$)

**$^{31}$P{$^1$H} NMR** (THF-*d*$_8$, 162 MHz): *δ* (ppm) = 50.8 (d, $^2J_{PP}$ = 35.9 Hz), 29.7 (d, $^2J_{PP}$ = 35.9 Hz).

**CHNS**: calc. for $C_{32}H_{54}AuClO_2P_2S$: C: 48.21, H: 6.83, S: 4.02, found C: 48.58, H: 6.93, S: 4.28.

### Synthesis of $^{Cy}Y_{SF}$-H:

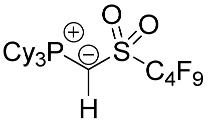

**[Cy$_3$P-Me]I** (3.00 g, 7.10 mmol, 1.00 eq.) and KHMDS (3.26 g, 16.34 mmol, 2.30 eq.) were placed into a 100 mL schlenk flask and suspended in 50 mL THF. Perfluorobutane sulfonyl fluoride (1.40 mL, 7.81 mmol, 1.1 eq.) was slowly added to the white suspension via a syringe, upon which a color change to a deep brown occurred. The reaction mixture was stirred for 30 min at room temperature. Subsequently, the solvent was removed under reduced pressure and dichloromethane (30 mL) was added. The suspension was filtered trough a glass frit equipped with a pad of dry celite, giving a clear dark solution. Removal of the solvent under reduced pressure furnished an orange powder, which was further washed with cold *n*-hexane (3 x 10 mL) and dried for 6h at 70°C in vacuo. The title compound was obtained as a pale-yellow powder (83%, 3.40 g). Block shaped, colorless crystals suitable for X-ray structure analyses were obtained by slow evaporation of a saturated benzene solution.

**$^1$H NMR** (THF-*d*$_8$, 400 MHz): *δ* (ppm) = 2.42 – 2.25 (m, 3H, PCy$_3$-CH), 2.05 – 1.92 (m, 6H, PCy$_3$-CH$_2$), 1.90 (d, $^2J_{PH}$ = 8.4, 1H, PCHS), 1.89 – 1.78 (m, 6H, PCy$_3$-CH$_2$), 1.72 – 1.68 (m, 4H, PCy$_3$-CH$_2$), 1.66 – 1.48 (m, 6H, PCy$_3$-CH$_2$), 1.42 – 1.19 (m, 8H, PCy$_3$-CH$_2$).

**$^{13}$C{$^1$H} NMR** (THF-*d*$_8$, 101 MHz): *δ* (ppm) = 33.7 (d, $^1J_{PC}$ = 49.9 Hz, PCy$_3$-CH), 28.0 (d, $^2J_{PC}$ = 9.8 Hz, PCy$_3$-CH$_2$), 28.0 –27.8 (m, PCy$_3$-CH$_2$), 27.0 (d, $^4J_{PC}$ = 1.8 Hz, PCy$_3$-CH$_2$), 23.8 (d, $^1J_{PC}$ = 105.0 Hz, PCHS). Resonances for fluorine substituted carbon atoms could not be detected.

**$^{19}$F{$^1$H} NMR** (THF-*d*$_8$, 377 MHz): *δ* (ppm) = -81.82 (t, *J* = 10.1, 10.1 Hz, 3F), -113.61 (t, *J* = 13.8, 13.8 Hz, 2F), -121.12 (dt, *J* = 7.6, 7.6, 15.7 Hz, 2F), -126.55 (td, *J* = 4.7, 13.3, 13.5 Hz, 2F).

**$^{31}$P{$^1$H} NMR** (THF-*d*$_8$, 162 MHz): *δ* (ppm) = 29.1 (s).

**CHNS**: calc. for $C_{23}H_{34}F_9O_2PS$: C: 47.92%, H: 5.94%, S: 5.56%, found C: 47.61%, H: 6.14%, S: 5.23%.

### Synthesis of $^{Cy}Y_{SF}$-PCy$_2$ (L5):

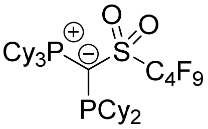

**$^{Cy}Y_{SF}$-H** (2.00 g, 3.47 mmol, 1.00 eq.) was dissolved in THF (30 mL) and *n*BuLi (1.59 M, 2.20 mL, 1.01 eq) was added dropwise at RT and stirred for 30 min. Then PCy$_2$Cl (0.80 mL, 3.63 mmol, 1.05 eq.) was added dropwise at room temperature.

The orange reaction mixture was stirred for 1h at room temperature. The solvent was removed in vacuo and the residue was redissolved in toluene (50 mL). The suspension was filtered via a filter cannula and the solvent of the obtained clear solution was removed under reduced pressure. Acetonitrile (10 mL) was added, and the waxy-like suspension was stirred overnight, during which a white precipitate formed. The white solid was collected with a glass frit, washed with acetonitrile (2 mL) and *n*-hexane (3 x 10 mL) and dried in vacuo (1 x $10^{-3}$ mbar, 8 h), giving **$^{Cy}$Y$_{SF}$-PCy$_2$** as a white amorphous powder (72%, 1.94 g). Block-shaped, colorless crystals suitable for X-ray structure analyses were obtained by slow evaporation of a saturated benzene solution.

**$^{1}$H NMR** (THF-*d*$_8$, 400 MHz): *δ* (ppm) = 3.11 – 3.00 (m, 1H, PCy$_2$-CH), 2.83 – 2.71 (m, 4H, PCy$_3$-CH+PCy-CH$_2$), 2.71 – 2.63 (m, 1H, PCy-CH$_2$), 2.24 – 2.13 (m, 1H, PCy-CH$_2$), 2.14 – 2.05 (m, 2H, PCy-CH+ PCy-CH$_2$), 1.97 – 1.84 (m, 6H, PCy-CH$_2$), 1.84 – 1.71 (m, 6H, PCy-CH$_2$), 1.70 – 1.58 (m, 8H, PCy-CH$_2$), 1.57 – 1.37 (m, 16H, PCy-CH$_2$), 1.21 – 0.99 (m, 10H, PCy-CH$_2$).

**$^{13}$C{$^{1}$H} NMR** (THF-*d*$_8$, 101 MHz): *δ* (ppm) = 42.7 (dd, $^{1}J_{CP}$= 14.3 Hz, $^{3}J_{CP}$ = 3.8 Hz, PCy$_2$-CH), 38.9 (dd, $^{1}J_{CP}$= 80.0, 73.0 Hz, PCP), 36.4 (PCy$_2$-CH$_2$), 36.1 (PCy$_2$-CH$_2$), 36.1 (dd, $^{1}J_{CP}$= 12.5 Hz, $^{3}J_{CP}$ = 3.0 Hz, PCy$_2$-CH), 34.3 (dd, $^{1}J_{CP}$= 47.2 Hz, $^{3}J_{CP}$ = 9.9 Hz, PCy$_3$-CH), 33.9 (d, $^{2}J_{CP}$ = 8.4 Hz, PCy$_3$-CH$_2$), 33.6 (PCy$_2$-CH$_2$), 33.3 (PCy$_2$-CH$_2$), 30.6 (PCy$_2$-CH$_2$), 29.3 (PCy$_2$-CH$_2$), 29.1 (PCy$_2$-CH$_2$), 28.4 – 28.2 (m, PCy-CH$_2$), 28.2 – 28.1 (m, PCy-CH$_2$), 28.1 – 28.0 (m, PCy-CH$_2$), 27.9 – 27.7 (m, PCy-CH$_2$), 27.7 – 27.5 (m, PCy-CH$_2$), 27.5 – 27.4 (m, PCy-CH$_2$), 27.4 – 27.2 (m, PCy-CH$_2$), 27.0 (PCy-CH$_2$), 26.3 (PCy-CH$_2$). Resonances for fluorine substituted carbon atoms could not be detected.

**$^{19}$F{$^{1}$H} NMR** (THF-*d*$_8$, 377 MHz): *δ* (ppm) = -80.8 – -80.9 (m, 3F), -108.8 – -112.2 (m, 2F), -119.1 – -121.8 (m, 2F), -123.9 – -126.8 (m, 2F).

**$^{31}$P{$^{1}$H} NMR** (THF-*d*$_8$, 162 MHz): *δ* (ppm) = 32.3 (d, $^{2}J_{PP}$ = 95.0 Hz), -0.7 (d, $^{2}J_{PP}$ = 95.0 Hz).

**CHNS**: calc. for $C_{35}H_{55}F_9O_2P_2S$: C: 54.40, H: 7.17, S: 4.15, found C: 54.29, H: 7.12, S: 4.28.

**Synthesis of [Au($^{Cy}$Y$_{SF}$-PCy$_2$)Cl] (P5):**

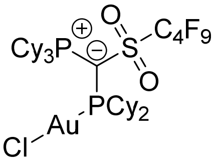

**$^{Cy}$Y$_{SF}$-PCy$_2$** (70 mg, 0.11 mmol, 1.00 eq.) and thtAuCl (29 mg, 0.11 mmol, 1.00 eq.) were placed into a schlenk tube, dissolved in 5 mL of toluene and stirred for 30 min at room temperature. The solvent was removed in vacuo (1 x $10^{-3}$ mbar, 3 h, 40 °C) furnishing [Au($^{Cy}$Y$_{SF}$-PCy$_2$)Cl] as a white solid (quantitative yield, 91 mg). Colorless crystals suitable for X-ray structure analyses were obtained storage of a saturated solution of P5 in *n*-pentane at -30°C.

**$^{1}$H NMR** ($CD_2Cl_2$, 400 MHz): *δ* (ppm) = 3.47 (br, 3H, PCy$_3$-CH), 2.82 – 2.75 (m, 1H, PCy-CH), 2.42 – 2.16 (m, 5H, PCy-CH+ PCy-CH$_2$), 2.09 – 2.00 (m, 6H, PCy-CH$_2$), 1.90 – 1.68 (m, 20H, PCy-CH$_2$), 1.49 – 1.23 (m, 20H, PCy-CH$_2$).

**$^{13}$C{$^{1}$H} NMR** ($CD_2Cl_2$, 101 MHz): *δ* (ppm) = 44.6 (dd, $^{1}J_{CP}$= 34.1, $^{3}J_{CP}$ = 2.1, PCy$_2$-CH), 41.8 (d, $^{1}J_{CP}$ =33.8 Hz, PCy$_2$-CH), 40.8 (dd, $^{1}J_{CP}$ = 67.5, 24.9 Hz, PCP), 38.2 – 37.9 (m, PCy-CH$_2$), 37.4 – 37.1 (m, PCy-CH$_2$), 36.8 (br, PCy$_3$-CH), 32.2 (d, *J*=1.8 Hz, PCy-CH$_2$), 31.6 (PCy-CH$_2$), 30.4 (PCy-CH$_2$), 29.2 (PCy-CH$_2$), 28.8 (PCy-CH$_2$), 28.3 (PCy-CH$_2$), 28.1 (PCy-CH$_2$), 27.9 – 27.5 (m, PCy-CH$_2$), 27.3 (PCy-CH$_2$), 27.2(PCy-CH$_2$), 26.8 – 26.6 (m, PCy-CH$_2$), 26.6 – 26.2 (m, PCy-CH$_2$), 26.1 (PCy-CH$_2$). Resonances for fluorine substituted carbon atoms could not be detected.

**$^{19}F\{^1H\}$ NMR** ($CD_2Cl_2$, 377 MHz): $\delta$ (ppm) = -80.7 – -81.5 (m, 3F), -106.4 – -109.7 (m, 2F), -120.0 – -122.5 (m, 2F), -124.8 – -126.9 (m, 2F).

**$^{31}P\{^1H\}$ NMR** ($CD_2Cl_2$, 162 MHz): $\delta$ (ppm) = 43.3 (d, $^2J_{PP}$ = 26.8 Hz), 34.8 (d, $^2J_{PP}$ = 26.8 Hz).

**CHNS**: calc. for $C_{35}H_{55}AuClF_9O_2P_2S$: C: 41.82, H: 5.52, S: 3.19, found C: 41.91, H: 5.75, S: 3.22.

**Synthesis of [Au(Cy-$^{Cy}$JohnPhos)Cl] (P6):**

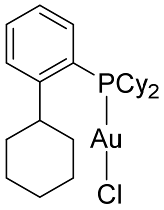

**Cy-$^{Cy}$JohnPhos (L6)** (100 mg, 0.280 mmol, 1.0 eq.) and [Au(tht)Cl] (90 mg, 0.280 mmol, 1.0 eq.) were placed into a schlenk tube and THF (5 mL) was added. The mixture was stirred for 10 min at room temperature. Subsequently, all volatiles were evaporated and the residue was dried for several hours in vacuo, giving the title compound as a pure colourless solid in quantitative yield (165 mg, 0.280 mmol). Colourless crystals suitable for X-ray structure determination were obtained by overlaying a saturated DCM solution of P6 with *n*-pentane.

**$^1H$-NMR** ($CD_2Cl_2$, 400 MHz) $\delta$ (ppm) = 7.57 – 7.42 (m, 3H, *CH*), 7.31 – 7.24 (m, 1H, *CH*), 4.02 – 3.81 (m, 1H, Cy-*CH*), 2.40 – 2.22 (m, 2H, $PCy_2$-*CH*), 2.22 – 2.08 (m, 2H, $CH_2$), 1.89 – 1.79 (m, 6H, $CH_2$), 1.80 – 1.72 (m, 2H, $CH_2$), 1.72 – 1.09 (m, 20H, $CH_2$).

**$^{13}C\{^1H\}$-NMR** ($CD_2Cl_2$, 101 MHz): $\delta$ (ppm) = 154.0 (d, $J$ = 9.2 Hz, $C_{ipso}$), 134.5 (*CH*), 132.1 (d, $J$ = 2.5 Hz, *CH*), 129.1 (d, $J$ = 8.2 Hz, *CH*), 126.3 (d, $J$ = 9.4 Hz, *CH* ), 122.6 (d, $J$ = 51.7 Hz, $C_{ortho}$), 43.3 (d, $J$=9.7 Hz, Cy-*CH*), 36.3 (d, $J$ = 34.1 Hz, $PCy_2$-*CH*), 35.4 ($CH_2$), 31.4 (d, $J$ = 3.6 Hz, $CH_2$), 29.8 ($CH_2$), 27.3 – 26.9 (m, $CH_2$), 26.6 ($CH_2$), 26.3 (d, $J$ = 1.8 Hz, $CH_2$).

**$^{31}P\{^1H\}$-NMR** ($CD_2Cl_2$, 162 MHz): $\delta$ (ppm) = 47.9 – 24.8 (vbr).

**CHN**: calc. for $C_{24}H_{37}AuClP$: C:48.95, H.6.33; found: C: 48.77, H: 6.25

**Procedure for the determination of TEP values :**

IR spectra were recorded on a Nicolet iS5 FT-IR in transmission mode with a Specac “Omni-cell” with KBr plates and a 0.1 mm spacer at 22 °C.

Procedure for $\tilde{\nu}_{(CO)}$Rh determination: 5.00 mg (19.4 µmol) $Rh(acac)(CO)_2$ were dissolved in 1 mL of DCM in a glovebox. 19.4 µmol of the phosphine were added to the solution and the solution was stirred for 15 min until gas evolution ceased. The solution was added into the IR cell using a syringe. The cell was closed, taken outside the glovebox and an IR spectrum was recorded. The TEP value was calculated *via* the linear correlation of TEP and $\tilde{\nu}_{(CO)}$Rh described by Carrow.[25]

**Table 5.** Determined $\tilde{\nu}_{(CO)}$ frequencies of the novel $^{Cy}$YPhos ligands and their corresponding $TEP_{calc.}$ values.

| **Compound** | **$\tilde{\nu}_{(CO)}$Rh** | **calcd. TEP** |
|---|---|---|
| $^{Cy}Y_S$-$PCy_2$ (L1) | 1956.8 | 2057.0 |
| $^{Cy}Y_S$-P*i*$Pr_2$ (L4) | 1959.7 | 2058.7 |
| $^{Cy}Y_{SF}$-$PCy_2$ (L5) | 1961.7 | 2059.8 |

**Procedure for Au(I) catalyzed hydroamination reactions:**

The reaction was conducted in a similar fashion as previously described by our group. A 2 mL glass vial with a rubber cap and a stir bar was charged in a glovebox with the indicated amount of LAuCl and NaBAr$^F$. The amine (5.25 mmol) and the alkyne (5.00 mmol) were added via syringe. The vial was heated on a hotplate to the indicated temperature while stirring. Small aliqouts were removed via a syringe and added directly to an NMR tube to monitor the reaction progress. Yields were calculated by integration of the peak for the alkyne starting material with respect to the peak for the imine product in the $^1$H-NMR spectrum.

**Table 6.** Results and reaction conditions for the Au(I) catalyzed hydroamination of phenylacetylene with aniline.

| Catalyst | P1 | P2 | P3 | P4 | P5 | P6 | P1 | P5 |
|---|---|---|---|---|---|---|---|---|
| Loading [mol%] | 0.1 | 0.1 | 0.1 | 0.1 | 0.1 | 0.1 | 0.05 | 0.05 |
| Temp. [°C] | 50 | 50 | 50 | 50 | 50 | 50 | 50 | 50 |
| 0 h | 0 | 0 | 0 | 0 | 0 | 0 | 0 | 0 |
| 1 h | 86 | 74 | 77 | 79 | 50 | 86 | 58 | 25 |
| 3 h | 96 | 84 | 94 | 90 | 71 | 96 | 77 | 47 |
| 5 h | 99 | 94 | 97 | 95 | 85 | 98 | 85 | 67 |
| 24 h | >99 | >99 | >99 | >99 | 95 | >99 | >99 | 89 |

## 5.6 Experimental Details for Section 3.6

**Synthesis of $^{Cy}$Y$_S$-PCy$_2$-Pd(dba):**

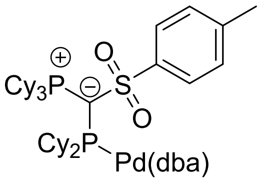

**$^{Cy}$Y$_S$-PCy$_2$** (32.3 mg, 0.05 mmol) and Pd$_2$dba$_3$ (5.3 mg, 0.05 mmol) were placed into a *J*. Young type NMR tube and THF-d$_8$ (0.6 mL) was added. The tube was shaken at room temperature for 30 min and subsequently a $^{31}$P{$^1$H} NMR spectrum was measured. NMR data revealed approx. 90% conversion to the title compound. A prolonged reaction time did not result in an increase of conversion and attempts to isolate the complex in pure form failed. Thus, for further studies the complex was prepared *in-situ* and used as it is.

**$^{31}$P{$^1$H} NMR** (THF-d$_8$, 162 MHz): $\delta$ (ppm) = 32.5 (d, $^2J_{PP}$ = 34.4 Hz), 22.1 ppm (brd, $^2J_{PP}$ = 35.1 Hz).

**Oxidative Addition of *p*-chlorotoluene to $^{Cy}$Y$_S$-PCy$_2$-Pd(dba):**

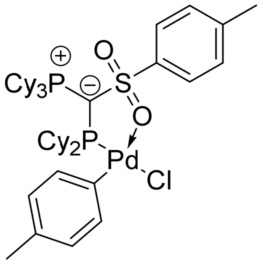

To a solution containing **$^{Cy}$Y$_S$-PCy$_2$-Pd(dba)** (prepared as explained above) was added 0.1 mL of *p*-chlorotoluene (0.85 mmol, 17 eq.) and the mixture was shaken for 1 h at room temperature. $^{31}$P{$^1$H} NMR analysis indicated no conversion, thus the reaction mixture was heated to 40°C and subsequently monitored via NMR spectroscopy. After 1 h, approx. 65% conversion was observed. Prolonged heating (3 h) at 40°C resulted in almost full conversion to the oxidative addition product **$^{Cy}$Y$_S$-PCy$_2$-Pd(*p*Tol)Cl**.

**$^{31}$P{$^1$H} NMR** (THF-d$_8$, 162 MHz): $\delta$ (ppm) = 35.9 (brd, $^2J_{PP}$ = 23.0 Hz) , 28.3 ppm (brd, $^2J_{PP}$ = 35.1 Hz).

**Buchwald-Hartwig amination catalysis attempts:**

For the C–N cross coupling attempts a similar procedure as described earlier by our group was used.[33]

To a 5 mL vial containing 1,3,5-trimethoxy benzene (143 mg, 0.85 mmol,1.0 eq.), KO*t*Bu (189 mg, 1.69 mmol, 2 eq.), *p*-chlorotoluene (0.1 mL, 0.85 mmol, 1.0 eq.) and piperidine (0.92 mmol, 1.1 eq.) dissolved in THF (4 mL), was added a THF solution (0.5 mL) of **$^{Cy}$Y$_S$-PCy$_2$-Pd(dba)** (0.1 mol%, preformed as described above). The mixture was heated to 40°C and stirred at this temperature.

For reaction monitoring, small aliquots of the reaction mixture were quenched with 0.2 ml of water and the organic phase was separated. The latter was filtered through a pipette, the solvent was allowed to evaporate, and the residue was dissolved in CDCl$_3$ for recording an $^1$H NMR spectrum. The conversion was determined by integration of the product peaks in comparison to 1,3,5- trimethoxybenzene as an internal standard.

No conversion was observed after 12 h of reaction time. Repeating this procedure except that the mixture was heated for reflux for 12 h, did not result in any conversion. Additionally, varying the amine or aryl halide scope did not result in any conversion

## 5.7 Crystallographic details

**Table 7.** Crystal data and structure refinement details of compounds **$^{Cy}$Y-H$_2$**, **$^{Cy}$Y-H** and **$^{Cy}$Y-Li·LiI**.

| **Compound** | **$^{Cy}$Y-H$_2$** | **$^{Cy}$Y-H** | **$^{Cy}$Y-Li·LiI** |
|---|---|---|---|
| CCDC No. | 1971570 | 1971569 | 1971572 |
| Empirical formula | $C_{26} H_{42} I O_2 P S$ | $C_{27} H_{43} Cl_2 O_2 P S$ | $[C_{120}H_{192}Li_5O_{12}P_4S_4]I$ |
| Formula weight | 576.52 | 533.54 | 560.11 |
| Temperature (K) | 100(2) | 100(2) | 100(2) |
| Wavelength | 1.54184 Å | 1.54184 Å | 1.54184 Å |
| Crystal system | Monoclinic | Orthorhombic | Tetragonal |
| Space group | $P2_1/n$ | $P2_12_12_1$ | $P_4 2/n$ |
| a (Å) | 9.31921(4) | 16.16138(9) | 18.9729(2) |
| b (Å) | 22.93106(10) | 17.05308(10) | 18.9729(2) |
| c (Å) | 25.75996(9) | 20.30115(13) | 17.3367(3) |
| α (°) | 90 | 90 | 90 |
| β (°) | 95.0980(4) | 90 | 90 |
| γ (°) | 90 | 90 | 90 |
| Volume (Å$^3$) | 5483.11(4) | 5595.02(6) | 6240.71(17) |
| Z | 8 | 8 | 2 |
| Density (calculated) | 1.397 Mg/m$^3$ | 1.267 Mg/m$^3$ | 1.192 Mg/m$^3$ |
| Absorption coefficient | 10.581 mm$^{-1}$ | 3.488 mm$^{-1}$ | 3.547 mm$^{-1}$ |
| F(000) | 2384 | 2288 | 2400 |
| Crystal dimensions (mm$^3$) | 0.143 x 0.084 x 0.074 | 0.164 x 0.123 x 0.078 | 0.113 x 0.069 x 0.013 |
| Theta range (°) | 2.584 to 74.497°. | 3.385 to 74.997°. | 3.294 to 67.076° |
| Index ranges | -11<=h<=11,<br>-27<=k<=28,<br>-22<=l<=32 | -20<=h<=13,<br>-21<=k<=21,<br>-25<=l<=23 | -21<=h<=22,<br>-22<=k<=22,<br>-20<=l<=20 |
| Reflections collected | 52241 | 43872 | 83544 |
| Independent reflections | 11182<br>[R(int) = 0.0269] | 11453<br>[R(int) = 0.0554] | 5579<br>[R(int) = 0.1182] |
| Data / restraints / parameters | 11182 / 0 / 811 | 11453 / 70 / 654 | 5579 / 102 / 438 |
| Goodness-of-fit on F$^2$ | 1.047 | 1.055 | 1.094 |
| Final R indices [I>2sigma(I)] | R1 = 0.0225,<br>wR2 = 0.0568 | R1 = 0.0442,<br>wR2 = 0.1206 | R1 = 0.0592,<br>wR2 = 0.1773 |
| R indices (all data) | R1 = 0.0231,<br>wR2 = 0.0572 | R1 = 0.0456,<br>wR2 = 0.1219 | R1 = 0.0647,<br>wR2 = 0.1823 |
| Largest diff. peak and hole | 0.444 and -0.857 e.Å$^{-3}$ | 0.496 and -0.667 e.Å$^{-3}$ | 1.004 and -0.574 e.Å$^{-3}$ |

**Table 8.** Crystal data and structure refinement details of compounds **$^{Cy}$Y-K**, **$^{Cy}$Y$_2$Ge** and **$^{Cy}$Y$_2$Sn**.

| **Compound** | **$^{Cy}$Y-K** | **$^{Cy}$Y$_2$Ge** | **$^{Cy}$Y$_2$Sn** |
|---|---|---|---|
| CCDC No. | 1971571 | 1977236 | 2012936 |
| Empirical formula | $[(C_{208}H K_8O_{16}P_8S_8)\cdot(KI)_{0.05}(2THF)_{0.95}]9\ THF$ | $C_{52}H_{80}O_4P_2S_2Ge$ | $C_{58}H_{86}O_4P_2S_2Sn$ |
| Formula weight | 1172.01 | 967.81 | 1092.01 |
| Temperature (K) | 100.0(4) K | 100.0(2) | 100.01(10) |
| Wavelength | 1.54184 Å | 1.54184 Å | 1.54184 Å |
| Crystal system | Tetragonal | Triclinic | Monoclinic |
| Space group | P4/n | *P*-1 | *P*2$_1$/n |
| a (Å) | 26.6751(5) | 10.3275(3) | 10.94240(10) |
| b (Å) | 26.6751(5) | 12.3453(3) | 26.7086(2) |
| c (Å) | 17.8721(5) | 24.6532(6) | 18.7537(2) |
| α (°) | 90 | 89.529(2) | 90 |
| β (°) | 90 | 86.210(2) | 95.0080(10) |
| γ (°) | 90 | 76.341(2) | 90 |
| Volume (Å$^3$) | 12717.1(6) | 3047.52(14) | 5459.96(9) |
| Z | 2 | 2 | 4 |
| Density (calculated) | 1.224 Mg/m$^3$ | 1.055 Mg/m$^3$ | 1.328 Mg/m$^3$ |
| Absorption coefficient | 2.847 mm$^{-1}$ | 2.089 mm$^{-1}$ | 5.332 mm$^{-1}$ |
| F(000) | 5071 | 1036.0 | 2312.0 |
| Crystal dimensions (mm$^3$) | 0.328 x 0.113 x 0.075 | 0.185 × 0.031 × 0.019 | 0.128 × 0.111 × 0.048 |
| Theta range (°) | 2.976 to 67.077° | 3.594 to 76.969 | 2.887 to 77.058 |
| Index ranges | -30<=h<=31,<br>-28<=k<=31,<br>-21<=l<=31 | $-12 \le h \le 13$ ,<br>$-15 \le k \le 15$ ,<br>$-27 \le l \le 31$ | $-11 \le h \le 13$,<br>$-31 \le k \le 33$,<br>$-22 \le l \le 23$ |
| Reflections collected | 77580 | 42241 | 45191 |
| Independent reflections | 11363<br>[R(int) = 0.1134] | 12406<br>[*R*(int) = 0.0649] | 11125<br>[*R*(int)= 0.0549] |
| Data / restraints / parameters | 11363 / 2040 / 1162 | 12406/184/733 | 11125/0/606 |
| Goodness-of-fit on F$^2$ | 1.106 | 1.036 | 1.065 |
| Final R indices [I>2sigma(I)] | R1 = 0.1100,<br>wR2 = 0.2440 | $R_1$ = 0.0744,<br>$wR_2$ = 0.2158 | $R_1$ = 0.0416,<br>$wR_2$ = 0.1064 |
| R indices (all data) | R1 = 0.1268,<br>wR2 = 0.2560 | $R_1$ = 0.0844,<br>$wR_2$ = 0.2264 | $R_1$ = 0.0464,<br>$wR_2$ = 0.1091 |
| Largest diff. peak and hole | 0.615 and -0.815 e.Å$^{-3}$ | 1.80 and -0.70 e.Å$^{-3}$ | 0.828 and -1.024 e.Å$^{-3}$ |

**Table 9**. Crystal data and structure refinement details of compounds **169**, **170** and **$^{Cy}$Y$_{Ph}$-TMS**.

| **Compound** | **169** | **170** | **$^{Cy}$Y$_{Ph}$-TMS** |
|---|---|---|---|
| CCDC No. | 2012937 | 2012933 | |
| Empirical formula | $C_{60}H_{95}Cl_2Ge_2NO_4P_2S_2$ | $C_{30}H_{48}ClO_3PSSn$ | $C_{28}H_{47}PSi$ |
| Formula weight | 1236.50 | 673.85 | 442.71 |
| Temperature (K) | 101(2) | 100(2) | 100.00(10) |
| Wavelength | 1.54184 Å | 1.54184 Å | 1.54184 Å |
| Crystal system | Monoclinic | Triclinic | Monoclinic |
| Space group | $P2_1/c$ | $P$-1 | $P2_1/c$ |
| a (Å) | 25.4647(2) | 9.0221(3) | 16.9964(2) |
| b (Å) | 15.01930(10) | 11.9787(4) | 9.51290(10) |
| c (Å) | 17.04440(10) | 15.3582(4) | 18.2550(2) |
| α (°) | 90 | 67.170(3) | 90 |
| β (°) | 107.6870(10) | 84.700(3) | 114.926(2) |
| γ (°) | 90 | 80.845(3) | 90 |
| Volume (Å$^3$) | 6210.69(8) | 1509.44(9) | 2676.63(6) |
| Z | 4 | 2 | 4 |
| Density (calculated) | 1.322 Mg/m$^3$ | 1.483 Mg/m$^3$ | 1.099 Mg/m$^3$ |
| Absorption coefficient | 3.440 mm$^{-1}$ | 8.921 mm$^{-1}$ | 1.404 mm$^{-1}$ |
| F(000) | 2616 | 700 | 976 |
| Crystal dimensions (mm$^3$) | 0.245 x 0.156 x 0.047 | 0.245 × 0.156 × 0.047 | 0.341 × 0.312 × 0.124 |
| Theta range (°) | 3.461 to 77.098 | 3.124 to 67.074 | 2.867 to 76.967 |
| Index ranges | $-32 \le h \le 31$ ,<br>$-16 \le k \le 18$ ,<br>$-21 \le l \le 21$ | $-8 \le h \le 10$ ,<br>$-14 \le k \le 14$ ,<br>$-17 \le l \le 18$ | $-21 \le h \le 20$,<br>$-9 \le k \le 12$,<br>$-21 \le l \le 22$ |
| Reflections collected | 86482 | 14458 | 17306 |
| Independent reflections | 12974<br>[$R$(int) = 0.0596] | 5351<br>[$R$(int) = 0.0495] | 5475<br>[$R$(int)= 0.0320] |
| Data / restraints / parameters | 12974/0/649 | 5351/70/381 | 5475/0/274 |
| Goodness-of-fit on F$^2$ | 1.033 | 1.037 | 1.039 |
| Final R indices [I>2sigma(I)] | $R_1$ = 0.0435,<br>$wR_2$ = 0.1143 | $R_1$ = 0.0691,<br>$wR_2$ = 0.1736 | $R_1$ = 0.0360,<br>$wR_2$ = 0.0961 |
| R indices (all data) | $R_1$ = 0.0449,<br>$wR_2$ = 0.1154 | $R_1$ = 0.0724,<br>$wR_2$ = 0.1787 | $R_1$ = 0.0381,<br>$wR_2$ = 0.09781 |
| Largest diff. peak and hole | 1.256 and -1.300 e.Å$^{-3}$ | 2.653 and -0.694 e.Å$^{-3}$ | 0.455 and -0.398 e.Å$^{-3}$ |

**Table 10**. Crystal data and structure refinement details of compounds **$^{Cy}Y_{Ph}$-SiCl$_3$**, **176** and **179**.

| **Compound** | **$^{Cy}Y_{Ph}$-SiCl$_3$** | **176** | **179** |
|---|---|---|---|
| CCDC No. | | | |
| Empirical formula | $C_{25}$ $H_{38}$ $Cl_3$ P Si | $C_{25}$ $H_{43}$ $Br_2$ P Si | $C_{56}$ $H_{86}$ $Br_2$ $P_2$ $Si_2$ |
| Formula weight | 503.96 | 598.50 | 1037.18 |
| Temperature (K) | 100(2) | 100.00(10) | 100.00(10) |
| Wavelength | 1.54184 Å | 1.54184 Å | 1.54184 Å |
| Crystal system | Monoclinic | Monoclinic | Monoclinic |
| Space group | $P2_1$/c | $P2_1$/m | $P2_1$/n |
| a (Å) | 16.8981(3) | 9.0338(4)(2) | 9.518(2) |
| b (Å) | 9.52090(10) | 14.7460(7) | 14.1905(4) |
| c (Å) | 17.9973(3) | 10.4358(5) | 19.3947(6) |
| α (°) | 90 | 90 | 90 |
| β (°) | 114.909(2) | 92.907(4) | 93.712(3) |
| γ (°) | 90 | 90 | 90 |
| Volume (Å$^3$) | 2626.15(8) | 1388.39(11) | 2614.35(12) |
| Z | 4 | 2 | 2 |
| Density (calculated) | 1.275 Mg/m$^3$ | 1.432 Mg/m$^3$ | 1.318 Mg/m$^3$ |
| Absorption coefficient | 4.241 mm$^{-1}$ | 4.753 mm$^{-1}$ | 3.243 mm$^{-1}$ |
| F(000) | 1072 | 620 | 1100 |
| Crystal dimensions (mm$^3$) | 1.104 x 0.295 x 0.294 | 0.144 x 0.123 x 0.085 | 0.158 x 0.109 x 0.058 |
| Theta range (°) | 2.883 to 77.064 | 4.242 to 79.845° | 3.863 to 77.051°. |
| Index ranges | $-21 \le h \le 20$ ,<br>$-11 \le k \le 11$ ,<br>$-22 \le l \le 20$ | $-11 \le h \le 11$ ,<br>$-18 \le k \le 14$ ,<br>$-13 \le l \le 12$ | $-11 \le h \le 10$,<br>$-15 \le k \le 17$,<br>$-24 \le l \le 23$ |
| Reflections collected | 18308 | 13589 | 18224 |
| Independent reflections | 5347<br>[*R*(int) = 0.0494] | 2976<br>[*R*(int) = 0.0587] | 5285<br>[*R*(int)= 0.0484] |
| Data / restraints / parameters | 5347/0/271 | 2976/0/159 | 5285/0/283 |
| Goodness-of-fit on F$^2$ | 1.026 | 1.128 | 1.044 |
| Final R indices [I>2sigma(I)] | $R_1$ = 0.0425,<br>w$R_2$ = 0.1175 | $R_1$ = 0.0399,<br>w$R_2$ = 0.1005 | $R_1$ = 0.0487,<br>w$R_2$ = 0.01301 |
| R indices (all data) | $R_1$ = 0.0440,<br>w$R_2$ = 0.1190 | $R_1$ = 0.0451,<br>w$R_2$ = 0.1091 | $R_1$ = 0.0561,<br>w$R_2$ = 0.01352 |
| Largest diff. peak and hole | 0.590 and -0.518 e.Å$^{-3}$ | 0.690 and -0.486 e.Å$^{-3}$ | 1.174 and -0.466 e.Å$^{-3}$ |

**Table 11.** Crystal data and structure refinement details of compounds **L1**, **L4** and **P1**.

| Compound | L1 | L4 | P1 |
|---|---|---|---|
| CCDC No. | 2071634 | 2071632 | 2071633 |
| Empirical formula | $C_{44}H_{68}O_2P_2S$ | $C_{32}H_{54}O_2P_2S$ | $C_{38}H_{62}AuClO_2P_2S$ |
| Formula weight | 722.98 | 564.75 | 877.29 |
| Temperature (K) | 100.00(10) | 100.00(10) | 100.00(10) |
| Wavelength | 1.54184 Å | 1.54184 Å | 1.54184 Å |
| Crystal system | Triclinic | Monoclinic | Triclinic |
| Space group | *P*-1 | C2/c | P-1 |
| a (Å) | 10.57894(10) | 38.4015(4) | 10.19965(15) |
| b (Å) | 11.86101(15) | 9.60371(10) | 10.66040(12) |
| c (Å) | 17.34664(17 | 16.96876(19) | 18.20122(17) |
| α (°) | 71.7478(10) | 90 | 91.7698(9) |
| β (°) | 87.4897(8) | 90.9335(10) | 105.8271(11) |
| γ (°) | 78.1942(9) | 90 | 97.7483(11) |
| Volume (Å$^3$) | 2022.89(4) | 6257.19(12) | 1881.89(4) |
| Z | 2 | 8 | 2 |
| Density (calculated) | 1.187 Mg/m$^3$ | 1.199 Mg/m$^3$ | 1.548 Mg/m3 |
| Absorption coefficient | 1.714 mm$^{-1}$ | 2.078 mm$^{-1}$ | 9.558 mm$^{-1}$ |
| F(000) | 788 | 2464 | 896 |
| Crystal dimensions (mm$^3$) | 0.219 × 0.129 × 0.045 | 0.28 × 0.210 × 0.016 | 0.131 x 0.053 x 0.029 |
| Theta range (°) | 2.683 to 77.428 | 4.606 to 77.304 | 2.530 to 77.813 |
| Index ranges | -13 ≤ h ≤ 12 ,<br>-15 ≤ k ≤14 ,<br>-21 ≤ l ≤ 19 | -48 ≤ h ≤ 42,<br>-12 ≤ k ≤ 6,<br>-20 ≤ l ≤ 21 | -12<=h<=12,<br>-11<=k<=13,<br>-19<=l<=22 |
| Reflections collected | 27462 | 19356 | 28727 |
| Independent reflections | 8299<br>[*R*(int) = 0.0215] | 6307<br>[*R*(int)= 0.0248] | 7858<br>[*R*(int)= 0.0305] |
| Data / restraints / parameters | 8299/0/443 | 6307/0/339 | 7858 / 0 / 411 |
| Goodness-of-fit on F$^2$ | 1.055 | 1.057 | 1.145 |
| Final R indices [I>2sigma(I)] | $R_1$ = 0.0411,<br>w$R_2$ = 0.1176 | $R_1$ = 0.0348,<br>w$R_2$ = 0.0910 | $R_1$ = 0.0284,<br>w$R_2$ = 0.0785 |
| R indices (all data) | $R_1$ = 0.0424,<br>w$R_2$ = 0.1187 | $R_1$ = 0.0371,<br>w$R_2$ = 0.0923 | $R_1$ = 0.0290,<br>w$R_2$ = 0.0788 |
| Largest diff. peak and hole | 0.626 and<br>-0.521 e.Å$^{-3}$ | 0.629 and<br>-0.461 e.Å$^{-3}$ | 1.066 and<br>-1.792 e.Å-3 |

**Table 12**. Crystal data and structure refinement details of compounds **P4**, **$^{Cy}Y_{SF}$-H** and **L5**.

| **Compound** | **P4** | **$^{Cy}Y_{SF}$-H** | **L5** |
|---|---|---|---|
| CCDC No. | 2071636 | 2071638 | 2071637 |
| Empirical formula | $C_{39}H_{62}AuClO_2P_2S$ | $C_{23}H_{34}F_9O_2PS$ | $C_{35}H_{55}F_9O_2P_2S$ |
| Formula weight | 889.30 | 576.53 | 772.79 |
| Temperature (K) | 100.00(10) K | 100.00(10) | 100.00(10) |
| Wavelength | 1.54184 Å | 1.54184 Å | 1.54184 Å |
| Crystal system | Triclinic | Orthorhombic | Triclinic |
| Space group | P-1 | Pbca | P-1 |
| a (Å) | 9.28850(14) | 19.6559(2) | 10.75436(10) |
| b (Å) | 14.2022(3) | 11.9311(2) | 13.56365(11) |
| c (Å) | 16.1477(2) | 22.0689(3) | 14.30270(9) |
| α (°) | 70.1408(15) | 90 | 110.3617 |
| β (°) | 89.6651(11) | 90 | 100.4968 |
| γ (°) | 80.1610(14) | 90 | 97.9783 |
| Volume ($Å^3$) | 1970.88(6) | 5176.57(12) | 1876.38(3) |
| Z | 2 | 8 | 2 |
| Density (calculated) | 1.499 | 1.480 | 1.368 $Mg/m^3$ |
| Absorption coefficient | 9.135 | 2.477 | 2.239 $mm^{-1}$ |
| F(000) | 908 | 2400 | 816 |
| Crystal dimensions ($mm^3$) | 0.124 x 0.027 x 0.017 | 0.242 x 0.200 x 0.024 | 0.171 x 0.117 x 0.095 |
| Theta range (°) | 2.914 to 77.653°. | 4.006 to 67.078 | 3.403 to 77.551 |
| Index ranges | -11<=h<=11,<br>-17<=k<=17,<br>-20<=l<=20 | -23 ≤ h ≤ 22,<br>-14 ≤ k ≤ 14,<br>-25 ≤ l ≤ 26 | -13<=h<=13,<br>-15<=k<=17,<br>-18<=l<=16 |
| Reflections collected | 27759 | 64699 | 28860 |
| Independent reflections | 27759<br>[*R*(int)=?] | 4624<br>[*R*(int)= 0.0487] | 7812<br>[*R*(int) = 0.0228] |
| Data / restraints / parameters | 27759 / 405 / 962 | 4624 / 72 / 374 | 7812 / 0 / 442 |
| Goodness-of-fit on $F^2$ | 1.144 | 1.059 | 1.053 |
| Final R indices [I>2sigma(I)] | $R_1$ = 0.0610,<br>w$R_2$ = 0.1750 | $R_1$ = 0.0450,<br>w$R_2$ = 0.1263 | $R_1$ = 0.0281,<br>w$R_2$ = 0.0736 |
| R indices (all data) | $R_1$ = 0.0620,<br>w$R_2$ = 0.1774 | $R_1$ = 0.0469,<br>w$R_2$ = 0.1283 | $R_1$ = 0.0290,<br>w$R_2$ = 0.0742 |
| Largest diff. peak and hole | 2.533 and<br>-0.938 e.Å-3 | 0.531 and<br>-0.425 e.Å-3 | 0.368 and -0.404 e.$Å^{-3}$ |

**Table 13.** Crystal data and structure refinement details of compounds **P5** and **P6**.

| Compound | P5 | P6 |
|---|---|---|
| CCDC No. | 2071635 | 2078561 |
| Empirical formula | $C_{35}H_{55}AuClF_9O_2P_2S$ | $C_{24}H_{37}AuClP$ |
| Formula weight | 1005.20 | 588.92 |
| Temperature (K) | 100(2) | 100(2) |
| Wavelength | 1.54184 Å | 1.54184 Å |
| Crystal system | Monoclinic | Triclinic |
| Space group | P 21/n | P-1 |
| a (Å) | 11.98170(10) | 9.63402(18) |
| b (Å) | 13.78420(10) | 9.91609(15) |
| c (Å) | 24.2263(3) | 13.07001(14) |
| α (°) | 90 | 105.1916(12) |
| β (°) | 90.0340(10) | 104.0487(13)(10) |
| γ (°) | 90 | 99.8202(14) |
| Volume (Å$^3$) | 4001.17(7) | 1131.77(3) |
| Z | 4 | 2 |
| Density (calculated) | 1.669 Mg/m3 | 1.728 Mg/m3 |
| Absorption coefficient | 9.411 mm$^{-1}$ | 13.996 mm$^{-1}$ |
| F(000) | 2016 | 584 |
| Crystal dimensions (mm$^3$) | 0.556 x 0.097 x 0.063 | 0.201 x 0.163 x 0.093 |
| Theta range (°) | 4.115 to 72.244 | 3.676 to 76.973 |
| Index ranges | -14<=h<=14,<br>-16<=k<=12,<br>-29<=l<=29 | -11<=h<=12,<br>-12<=k<=12,<br>-13<=l<=16 |
| Reflections collected | 55890 | 12713 |
| Independent reflections | 7867<br>[*R*(int) = 0.0668] | 4570<br>[*R*(int) = 0.0302] |
| Data / restraints / parameters | 7867 / 0 / 464 | 4570 / 0 / 248 |
| Goodness-of-fit on F$^2$ | 1.040 | 1.040 |
| Final R indices [I>2sigma(I)] | $R_1$ = 0.0308, w$R_2$ = 0.0803 | $R_1$ = 0.0239, w$R_2$ = 0.0622 |
| R indices (all data) | $R_1$ = 0.0333, w$R_2$ = 0.0819 | $R_1$ = 0.0287, w$R_2$ = 0.0639 |
| Largest diff. peak and hole | 1.262 and --2.261 e.Å$^{-3}$ | 1.164 and -1.474 e.Å$^{-3}$ |

# 6. References

[1] B. Cornils, W. A. Herrmann, M. Beller, R. Paciello (Eds.) *Applied homogeneous catalysis with organometallic compounds*, Wiley-VCH Verlag GmbH & Co. KGaA, Weinheim, **2018**.

[2] O. Roelen, German Patent DE849548C, **1938**.

[3] R. Franke, D. Selent, A. Börner, *Chem. Rev.* **2012**, *112*, 5675.

[4] L. H. Pignolet, *Homogeneous Catalysis with Metal Phosphine Complexes*, Springer US, Boston, MA, **1983**.

[5] a) T. P. Clark, C. R. Landis, S. L. Freed, J. Klosin, K. A. Abboud, *J. Am. Chem. Soc.* **2005**, *127*, 5040; b) K. Nozaki, N. Sakai, T. Nanno, T. Higashijima, S. Mano, T. Horiuchi, H. Takaya, *J. Am. Chem. Soc.* **1997**, *119*, 4413.

[6] a) J. A. Osborn, G. Wilkinson, J. J. Mrowca, *Inorg. Synth.* **1967**, 67; b) J. A. Osborn, F. H. Jardine, J. F. Young, G. Wilkinson, *J. Am. Chem. Soc.* **1966**, 1711.

[7] a) R. R. Schrock, *Acc. Chem. Res.* **1990**, *23*, 158; b) R. R. Schrock, A. H. Hoveyda, *Angew. Chem. Int. Ed.* **2003**, *42*, 4592.

[8] a) B. M. Novak, R. H. Grubbs, *J. Am. Chem. Soc.* **1988**, *110*, 960; b) T. M. Trnka, R. H. Grubbs, *Acc. Chem. Res.* **2001**, *34*, 18.

[9] G. C. Vougioukalakis, R. H. Grubbs, *Chem. Rev.* **2010**, *110*, 1746.

[10] Eric L. Dias, SonBinh T. Nguyen, and Robert H. Grubbs, *J. Am. Chem. Soc.* **1997**, *119*, 3887.

[11] a) F. F. Farley, US Patent 3,647,906, **1972**; b) J. C. Mol, *J. Mol. Cat.* **2004**, *213*, 39.

[12] K. Ziegler, E. Holzkamp, H. Breil, H. Martin, *Angew. Chem. Int. Ed.* **1955**, *67*, 426.

[13] G. Natta, P. Pino, P. Corradini, F. Danusso, E. Mantica, G. Mazzanti, G. Moraglio, *J. Am. Chem. Soc.* **1955**, *77*, 1708.

[14] W. Kaminsky, *Angew. Makromolek. Chem.* **1986**, *145*, 149.

[15] K. Tamao, Y. Kiso, K. Sumitani, M. Kumada, *J. Am. Chem. Soc.* **1972**, *94*, 9268.

[16] K. Tamao, K. Sumitani, M. Kumada, *J. Am. Chem. Soc.* **1972**, *94*, 4374.

[17] a) R. F. Heck, *J. Am. Chem. Soc.* **1968**, *90*, 5546; b) R. F. Heck, *J. Am. Chem. Soc.* **1968**, *90*, 5518; c) R. F. Heck, *J. Am. Chem. Soc.* **1968**, *90*, 5538; d) R. F. Heck, *J. Am. Chem. Soc.* **1968**, *90*, 5542; e) R. F. Heck, *J. Am. Chem. Soc.* **1968**, *90*, 5535.

[18] K. Sonogashira, Y. Tohda, N. Hagihara, *Tetrahedron Lett.* **1975**, *16*, 4467.

[19] S. Baba, E. Negishi, *J. Am. Chem. Soc.* **1976**, *98*, 6729.

[20] D. Milstein, J. K. Stille, *J. Am. Chem. Soc.* **1978**, *100*, 3636.

[21] N. Miyaura, A. Suzuki, *Chem. Comm.* **1979**, 866.

[22] F. A. Cotton, *Progress in Inorganic Chemistry*, Wiley, **2009**.

[23] a) W. A. Henderson Jr, S. A. Buckler, *J. Am. Chem. Soc.* **1960**, *82*, 5794; b) W. A. Henderson Jr, C. A. Streuli, *J. Am. Chem. Soc.* **1960**, *82*, 5791.

[24] C. A. Tolman, *Chem. Rev.* **1977**, *77*, 313.

[25] L. Chen, P. Ren, B. P. Carrow, *J. Am. Chem. Soc.* **2016**, *138*, 6392.

[26] O. Diebolt, G. C. Fortman, H. Clavier, A. M. Z. Slawin, E. C. Escudero-Adán, J. Benet-Buchholz, S. P. Nolan, *Organometallics* **2011**, *30*, 1668.

[27] T. Scherpf, C. Schwarz, L. T. Scharf, J.-A. Zur, A. Helbig, V. H. Gessner, *Angew. Chem. Int. Ed.* **2018**, *130*, 13041.

[28] P. Weber, T. Scherpf, I. Rodstein, D. Lichte, L. T. Scharf, L. J. Gooßen, V. H. Gessner, *Angew. Chem. Int. Ed.* **2019**, *58*, 3203.

[29] I. Rodstein, D. S. Prendes, L. Wickert, M. Paaßen, V. H. Gessner, *J. Org. Chem.* **2020**, *85*, 14674.

[30] J. Handelmann, C. N. Babu, H. Steinert, C. Schwarz, T. Scherpf, A. Kroll, V. H. Gessner, *Chem. Sci.* **2021**, doi.org/10.1039/D1SC00105A.

[31] X.-Q. Hu, D. Lichte, I. Rodstein, P. Weber, A.-K. Seitz, T. Scherpf, V. H. Gessner, L. J. Gooßen, *Org. Lett.* **2019**, *21*, 7558.

[32] C. Schwarz, J. Handelmann, D. M. Baier, A. Ouissa, V. H. Gessner, *Catal. Sci. Technol.* **2019**, *9*, 6808.

[33] J. Tappen, I. Rodstein, K. McGuire, A. Großjohann, J. Löffler, T. Scherpf, V. H. Gessner, *Chem. Eur. J.* **2020**, 4281.

[34] a) M. A. Wünsche, P. Mehlmann, T. Witteler, F. Buß, P. Rathmann, F. Dielmann, *Angew. Chem. Int. Ed.* **2015**, *54*, 11857; b) P. Mehlmann, C. Mück‐Lichtenfeld, T. T. Y. Tan, F. Dielmann, *Chem. Eur. J.* **2017**, *23*, 5929.

[35] T. Witteler, H. Darmandeh, P. Mehlmann, F. Dielmann, *Organometallics* **2018**, *37*, 3064.

[36] a) S. Ullrich, B. Kovačević, X. Xie, J. Sundermeyer, *Angew. Chem. Int. Ed.* **2019**, *131*, 10443; b) J. F. Kögel, S. Ullrich, B. Kovačević, S. Wagner, J. Sundermeyer, *Z. Anorg. Allg. Chem.* **2020**, *646*, 923.

[37] a) A. H. Christian, Z. L. Niemeyer, M. S. Sigman, F. D. Toste, *ACS Catal.* **2017**, *7*, 3973; b) D. J. Gorin, F. D. Toste, *Nature* **2007**, *446*, 395; c) Y.-M. Wang, A. D. Lackner, F. D. Toste, *Acc. Chem. Res.* **2014**, *47*, 889; d) G. Zuccarello, M. Zanini, A. M. Echavarren, *Isr. J. Chem.* **2020**, *60*, 360.

[38] A. Aranyos, D. W. Old, A. Kiyomori, J. P. Wolfe, J. P. Sadighi, S. L. Buchwald, *J. Am. Chem. Soc.* **1999**, *121*, 4369.

[39] a) U. Christmann, R. Vilar, *Angew. Chem. Int. Ed.* **2005**, *44*, 366; b) J.-J. Feng, X.-F. Chen, M. Shi, W.-L. Duan, *J. Am. Chem. Soc.* **2010**, *132*, 5562.

[40] R. Martin, S. L. Buchwald, *Acc. Chem. Res.* **2008**, *41*, 1461.

[41] J. P. Stambuli, M. Bühl, J. F. Hartwig, *J. Am. Chem. Soc.* **2002**, *124*, 9346.

[42] S. Z. Tasker, E. A. Standley, T. F. Jamison, *Nature* **2014**, *509*, 299.

[43] J. P. Stambuli, C. D. Incarvito, M. Bühl, J. F. Hartwig, *J. Am. Chem. Soc.* **2004**, *126*, 1184.

[44] a) M. Murata, S. L. Buchwald, *Tetrahedron Lett.* **2004**, *60*, 7397; b) J. Yin, M. P. Rainka, X.-X. Zhang, S. L. Buchwald, *J. Am. Chem. Soc.* **2002**, *124*, 1162.

[45] Z. Hu, X.-J. Wei, J. Handelmann, A.-K. Seitz, I. Rodstein, V. H. Gessner, L. J. Goossen, *Angew. Chem. Int. Ed.* **2021**, 6778.

[46] T. Scherpf, H. Steinert, A. Großjohann, K. Dilchert, J. Tappen, I. Rodstein, V. H. Gessner, *Angew. Chem. Int. Ed.* **2020**, *132*, 20777.

[47] T. E. Barder, M. R. Biscoe, S. L. Buchwald, *Organometallics* **2007**, *26*, 2183.

[48] P. Pérez-Galán, N. Delpont, E. Herrero-Gómez, F. Maseras, A. M. Echavarren, *Chem. Eur. J.* **2010**, *16*, 5324.

[49] P. Kočovský, Š. Vyskočil, I. Císařová, J. Sejbal, I. Tišlerová, M. Smrcina, G. C. Lloyd-Jones, S. C. Stephen, C. P. Butts, M. Murray, *J. Am. Chem. Soc.* **1999**, *121*, 7714.

[50] A. J. Arduengo III, R. L. Harlow, M. Kline, *J. Am. Chem. Soc.* **1991**, *113*, 361.

[51] K. Öfele, *J. Org. Chem.* **1968**, *12*, 42-43.

[52] H. ‐ W. Wanzlick, H. ‐ J. Schönherr, *Angew. Chem. Int. Ed.* **1968**, *7*, 141.

[53] M. N. Hopkinson, C. Richter, M. Schedler, F. Glorius, *Nature* **2014**, *510*, 485.

[54] R. Breslow, *N-Heterocyclic carbenes in organocatalysis*, John Wiley & Sons, **2019**.

[55] T. Schaub, U. D. O. Radius, A. Brucks, M. P. Choules, M. T. Olsen, T. B. Rauchfuss, *Inorg. Synth.* **2010**, 78.

[56] F. Glorius, *N-heterocyclic carbenes in transition metal catalysis*, Springer, **2007**.

[57] C. A. Smith, M. R. Narouz, P. A. Lummis, I. Singh, A. Nazemi, C.-H. Li, C. M. Crudden, *Chem. Rev.* **2019**, *119*, 4986.

[58] L. Oehninger, R. Rubbiani, I. Ott, *Dalton Transactions* **2013**, *42*, 3269.

[59] a) A. Doddi, M. Peters, M. Tamm, *Chem. Rev.* **2019**, *119*, 6994; b) V. Nesterov, D. Reiter, P. Bag, P. Frisch, R. Holzner, A. Porzelt, S. Inoue, *Chem. Rev.* **2018**, *118*, 9678.

[60] J. Li, W.-x. Shen, X.-r. Li, *Curr. Org. Chem.* **2012**, *16*, 2879.

[61] Z. Kelemen, O. Hollóczki, J. Oláh, L. Nyulászi, *RSC advances* **2013**, *3*, 7970.

[62] A. J. Arduengo III, J. R. Goerlich, W. J. Marshall, *Liebigs Ann. Chem.* **1997**, *1997*, 365.

[63] D. Enders, K. Breuer, J. Runsink, J. Henrique Teles, *Liebigs Ann. Chem.* **1996**, *1996*, 2019.

[64] a) V. Lavallo, Y. Canac, C. Präsang, B. Donnadieu, G. Bertrand, *Angew. Chem. Int. Ed.* **2005**, *44*, 5705; b) M. Melaimi, R. Jazzar, M. Soleilhavoup, G. Bertrand, *Angew. Chem. Int. Ed.* **2017**, *56*, 10046; c) M. Soleilhavoup, G. Bertrand, *Acc. Chem. Res.* **2015**, *48*, 256.

[65] a) R. H. Crabtree, *Coord. Chem. Rev.* **2013**, *257*, 755; b) G. Guisado ‐ Barrios, J. Bouffard, B. Donnadieu, G. Bertrand, *Angew. Chem. Int. Ed.* **2010**, *49*, 4759.

[66] D. G. Gusev, *Organometallics* **2009**, *28*, 6458.

[67] M. N. Hopkinson, F. Glorius, *N-Heterocyclic Carbenes in Organocatalysis* **2019**.

[68] A. C. Hillier, W. J. Sommer, B. S. Yong, J. L. Petersen, L. Cavallo, S. P. Nolan, *Organometallics* **2003**, *22*, 4322.

[69] H. Clavier, S. P. Nolan, *Chem. Commun.* **2010**, *46*, 841.

[70] W. A. Herrmann, M. Elison, J. Fischer, C. Köcher, G. R. J. Artus, *Angew. Chem. Int. Ed.* **1995**, *34*, 2371.

[71] T. Weskamp, F. J. Kohl, W. Hieringer, D. Gleich, W. A. Herrmann, *Angew. Chem. Int. Ed.* **1999**, *38*, 2416.

[72] a) C. W. K. Gstöttmayr, V. P. W. Böhm, E. Herdtweck, M. Grosche, W. A. Herrmann, *Angew. Chem. Int. Ed.* **2002**, *41*, 1363; b) W. A. Herrmann, *Angew. Chem. Int. Ed.* **2002**, *114*, 1342.

[73] a) O. Briel, C. S. J. Cazin in *N-Heterocyclic Carbenes in Transition Metal Catalysis and Organocatalysis* (Ed.: C. S.J. Cazin), Springer Netherlands, Dordrecht, **2011**, pp. 315–324; b) C. S.J. Cazin (Ed.) *N-Heterocyclic Carbenes in Transition Metal Catalysis and Organocatalysis*, Springer Netherlands, Dordrecht, **2011**.

[74] a) K. S. Egorova, V. P. Ananikov, *Organometallics* **2017**, *36*, 4071; b) J. D. Hayler, D. K. Leahy, E. M. Simmons, *Organometallics* **2019**, *38*, 36.

[75] P. Anastas, N. Eghbali, *Chem. Soc. Rev.* **2010**, *39*, 301.

[76] P. P. Power, *Nature* **2010**, *463*, 171.

[77] B. E. Hoogenboom, *J. Chem. Ed.* **1998**, *75*, 596.

[78] D. H. Harris, M. F. Lappert, *Chem. Comm.* **1974**, 895.

[79] D. E. Goldberg, D. H. Harris, M. F. Lappert, K. M. Thomas, *Chem. Comm.* **1976**, 261.

[80] T. Fjeldberg, H. Hope, M. F. Lappert, P. P. Power, A. J. Thorne, *Chem. Comm.* **1983**, 639.

[81] D. E. Goldberg, P. B. Hitchcock, M. F. Lappert, K. M. Thomas, A. J. Thorne, T. Fjeldberg, A. Haaland, B. E. R. Schilling, *Dalt. Trans.* **1986**, 2387.

[82] a) E. A. Carter, W. A. Goddard III, *J. Phys. Chem.* **1986**, *90*, 998; b) J. P. Malrieu, G. Trinquier, *J. Am. Chem. Soc.* **1989**, *111*, 5916; c) G. Trinquier, J. P. Malrieu, *J. Am. Chem. Soc.* **1987**, *109*, 5303.

[83] Y. Mizuhata, T. Sasamori, N. Tokitoh, *Chem. Rev.* **2009**, *109*, 3479.

[84] a) P. P. Power, *Chem. Rev.* **1999**, *99*, 3463; b) C. Weetman, *Chem. Eur. J.* **2021**, *27*, 1941.

[85] J.-D. Guo, D. J. Liptrot, S. Nagase, P. P. Power, *Chem. Sci.* **2015**, *6*, 6235.

[86] R. West, M. J. Fink, J. Michl, *Science* **1981**, *214*, 1343.

[87] M. Yoshifuji, I. Shima, N. Inamoto, K. Hirotsu, a. T. Higuchi, *J. Am. Chem. Soc.* **1981**, *103*, 4587.

[88] A. G. Brook, F. Abdesaken, B. Gutekunst, G. Gutekunst, R. K. Kallury, *Chem. Comm.* **1981**, 191.

[89] F. Dahcheh, D. Martin, D. W. Stephan, G. Bertrand, *Angew. Chem. Int. Ed.* **2014**, *53*, 13159.

[90] P. Bissinger, H. Braunschweig, A. Damme, T. Kupfer, A. Vargas, *Angew. Chem. Int. Ed.* **2012**, *51*, 9931.

[91] J. D. Queen, A. Lehmann, J. C. Fettinger, H. M. Tuononen, P. P. Power, *J. Am. Chem. Soc.* **2020**, *142*, 20554.

[92] R. C. Fischer, P. P. Power, *Chem. Rev.* **2010**, *110*, 3877.

[93] C. Cui, M. M. Olmstead, J. C. Fettinger, G. H. Spikes, P. P. Power, *J. Am. Chem. Soc.* **2005**, *127*, 17530.

[94] F. Dielmann, O. Back, M. Henry-Ellinger, P. Jerabek, G. Frenking, G. Bertrand, *Science* **2012**, *337*, 1526.

[95] C. Hering-Junghans, P. Andreiuk, M. J. Ferguson, R. McDonald, E. Rivard, *Angew. Chem. Int. Ed.* **2017**, *56*, 6272.

[96] T. J. Hadlington, M. Hermann, G. Frenking, C. Jones, *J. Am. Chem. Soc.* **2014**, *136*, 3028.

[97] G. D. Frey, V. Lavallo, B. Donnadieu, W. W. Schoeller, G. Bertrand, *Science* **2007**, *316*, 439.

[98] a) G. C. Welch, R. R. San Juan, J. D. Masuda, D. W. Stephan, *Science* **2006**, *314*, 1124; b) G. C. Welch, D. W. Stephan, *J. Am. Chem. Soc.* **2007**, *129*, 1880; c) D. W. Stephan, G. Erker, *Angew. Chem. Int. Ed.* **2010**, *49*, 46; d) D. W. Stephan, *Science* **2016**, *354*.

[99] a) M. K. Sharma, F. Ebeler, T. Glodde, B. Neumann, H.-G. Stammler, R. S. Ghadwal, *J. Am. Chem. Soc.* **2021**, *143*, 121; b) M. K. Sharma, D. Rottschäfer, T. Glodde, B. Neumann, H.-G. Stammler, R. S. Ghadwal, *Angew. Chem. Int. Ed.* **2021**, *60*, 6414.

[100] B. D. Rekken, T. M. Brown, J. C. Fettinger, H. M. Tuononen, P. P. Power, *J. Am. Chem. Soc.* **2012**, *134*, 6504.

[101] S. P. Green, C. Jones, A. Stasch, *Science* **2007**, *318*, 1754.

[102] F. Lips, J. C. Fettinger, A. Mansikkamäki, H. M. Tuononen, P. P. Power, *J. Am. Chem. Soc.* **2014**, *136*, 634.

[103] A. V. Protchenko, K. H. Birjkumar, D. Dange, A. D. Schwarz, D. Vidovic, C. Jones, N. Kaltsoyannis, P. Mountford, S. Aldridge, *J. Am. Chem. Soc.* **2012**, *134*, 6500.

[104] A. V. Protchenko, P. Vasko, D. C. H. Do, J. Hicks, M. Á. Fuentes, C. Jones, S. Aldridge, *Angew. Chem. Int. Ed.* **2019**, *58*, 1808.

[105] a) P. A. Bianconi, I. D. Williams, M. P. Engeler, S. J. Lippard, *J. Am. Chem. Soc.* **1986**, *108*, 311; b) R. N. Vrtis, C. P. Rao, S. G. Bott, S. J. Lippard, *J. Am. Chem. Soc.* **1988**, *110*, 7564; c) A. J. M. Miller, J. A. Labinger, J. E. Bercaw, *J. Am. Chem. Soc.* **2008**, *130*, 11874; d) T. Watanabe, Y. Ishida, T. Matsuo, H. Kawaguchi, *J. Am. Chem. Soc.* **2009**, *131*, 3474.

[106] A. V. Protchenko, A. D. Schwarz, M. P. Blake, C. Jones, N. Kaltsoyannis, P. Mountford, S. Aldridge, *Angew. Chem. Int. Ed.* **2013**, *125*, 596.

[107] D. Wendel, W. Eisenreich, C. Jandl, A. Pöthig, B. Rieger, *Organometallics* **2016**, *35*, 1.

[108] D. Wendel, A. Porzelt, F. A. D. Herz, D. Sarkar, C. Jandl, S. Inoue, B. Rieger, *J. Am. Chem. Soc.* **2017**, *139*, 8134.

[109] M. M. D. Roy, M. J. Ferguson, R. McDonald, Y. Zhou, E. Rivard, *Chem. Sci.* **2019**, *10*, 6476.

[110] D. Wendel, D. Reiter, A. Porzelt, P. J. Altmann, S. Inoue, B. Rieger, *J. Am. Chem. Soc.* **2017**, *139*, 17193.

[111] Y. Peng, J.-D. Guo, B. D. Ellis, Z. Zhu, J. C. Fettinger, S. Nagase, P. P. Power, *J. Am. Chem. Soc.* **2009**, *131*, 16272.

[112] Y. Peng, B. D. Ellis, X. Wang, P. P. Power, *J. Am. Chem. Soc.* **2008**, *130*, 12268.

[113] M. Usher, A. V. Protchenko, A. Rit, J. Campos, E. L. Kolychev, R. Tirfoin, S. Aldridge, *Chem. Eur. J.* **2016**, *22*, 11685.

[114] T. J. Hadlington, C. E. Kefalidis, L. Maron, C. Jones, *ACS Catal.* **2017**, *7*, 1853.

[115] A. Michaelis, H. V. Gimborn, *Chem. Ber.* **1894**, *27*, 272.

[116] a) O. I. Kolodiazhnyi, *Phosphorus Ylides: Chemistry and Applications in Organic Synthesis*, John Wiley & Sons, **2008**; b) A. W. Johnson, R. T. Amel, *J. Org. Chem.* **1969**, *34*, 1240.

[117] S. Pascual, M. Asay, O. Illa, T. Kato, G. Bertrand, N. Saffon-Merceron, V. Branchadell, A. Baceiredo, *Angew. Chem. Int. Ed.* **2007**, *119*, 9236.

[118] C. D. Papageorgiou, Cubillo de Dios, Maria A, S. V. Ley, M. J. Gaunt, *Angew. Chem. Int. Ed.* **2004**, *43*, 4641.

[119] T. Fujii, T. Suzuki, T. Sato, E. Horn, T. Yoshimura, *Tetrahedron Lett.* **2001**, *42*, 6151.

[120] H. S. He, C. W. Y. Chung, T. Y. S. But, P. H. Toy, *Tetrahedron Lett.* **2005**.

[121] R. Sundburg, R. Shepherd, H. Taube, *J. Am. Chem. Soc.* **1972**, *94*, 6558.

[122] a) G. Wittig, U. Schöllkopf, *Chem. Ber.* **1954**, *87*, 1318; b) H. Pommer, *Angew. Chem. Int. Ed.* **1977**, *16*, 423; c) A. Maercker, *Org. React.* **2004**, *14*, 270.

[123] a) H. Lischka, *J. Am. Chem. Soc.* **1977**, *99*, 353; b) D. G. Gilheany, *Chem. Rev.* **1994**, *94*, 1339.

[124] B. J. Walker, J. B. Hobbs, *Organophosphorus Chemistry* **1990**, *21*, 322.

[125] X. M. Zhang, F. G. Bordwell, *J. Am. Chem. Soc.* **1994**, *116*, 968.

[126] M. Schlosser, T. Kadibelban, G. Steinhoff, *Angew. Chem. Int. Ed.* **1966**, *5*, 968.

[127] am van Leusen, B. A. Reith, A. J.W. Iedema, J. Strating, *Rec. Trav. Chim. Pays Bas* **1972**, *91*, 37.

[128] E. J. Corey, J. Kang, *J. Am. Chem. Soc.* **1982**, *104*, 4724.

[129] B. Schaub, T. Jenny, M. Schlosser, *Tetrahedron Lett.* **1984**, *25*, 4097.

[130] B. Schaub, M. Schlosser, *Tetrahedron Lett.* **1985**, *26*, 1623.

[131] K. Korth, J. Sundermeyer, *Tetrahedron Lett.* **2000**, *41*, 5461.

[132] H. J. Bestmann, M. Schmidt, *Angew. Chem. Int. Ed.* **1987**, *26*, 79.

[133] H. J. Bestmann, D. Sandmeter, *Angew. Chem. Int. Ed.* **1975**, *87*, 630.

[134] a) C. Broquet, M. Simalty, *Tetrahedron Lett.* **1972**, *13*, 933; b) C. Broquet, *Tetrahedron Lett.* **1973**, *29*, 3595.

[135] T. Baumgartner, B. Schinkels, D. Gudat, M. Nieger, E. Niecke, *J. Am. Chem. Soc.* **1997**, *119*, 12410.

[136] S. Goumri-Magnet, H. Gornitzka, A. Baceiredo, G. Bertrand, *Angew. Chem. Int. Ed.* **1999**, *38*, 678.

[137] T. Scherpf, R. Wirth, S. Molitor, K.-S. Feichtner, V. H. Gessner, *Angew. Chem. Int. Ed.* **2015**, *54*, 8542.

[138] C. Schwarz, L. T. Scharf, T. Scherpf, J. Weismann, V. H. Gessner, *Chem. Eur. J.* **2019**, *25*, 2793.

[139] A. Garduno-Alva, R. Lenk, Y. Escudié, M. L. González, L. Bousquet, N. Saffon-Merceron, C. A. Toledano, X. Bagan, V. Branchadell, E. Maerten et al., *Eur. J. Inorg. Chem.* **2017**, *2017*, 3494.

[140] R. Tonner, F. Oxler, B. Neumüller, W. Petz, G. Frenking, *Angew. Chem. Int. Ed.* **2006**, *45*, 8038.

[141] L. T. Scharf, D. M. Andrada, G. Frenking, V. H. Gessner, *Chem. Eur. J.* **2017**, *23*, 4422.

[142] L. T. Scharf, V. H. Gessner, *Inorg. Chem.* **2017**, *56*, 8599.

[143] U. Schubert, C. Kappenstein, B. Milewski-Mahrla, H. Schmidbaur, *Chem. Ber.* **1981**, *114*, 3070.

[144] a) R. Tonner, G. Frenking, *Chem. Eur. J.* **2008**, *14*, 3260; b) R. Tonner, G. Frenking, *Chem. Eur. J.* **2008**, *14*, 3273.

[145] H. J. Bestmann, M. Schmidt, *Tetrahedron Lett.* **1987**, *28*, 2111.

[146] a) P. Berno, S. Gambarotta, S. Kotila, G. Erker, *Chem. Commun.* **1996**, 779; b) X. Li, M. Schopf, J. Stephan, K. Harms, J. Sundermeyer, *Organometallics* **2002**, *21*, 2356; c) P. E. Romero, W. E. Piers, R. McDonald, *Angew. Chem. Int. Ed.* **2004**, *116*, 6287; d) R. Zurawinski, C. Lepetit, Y. Canac, M. Mikolajczyk, R. Chauvin, *Inorg. Chem.* **2009**, *48*, 2147; e) A. C. Filippou, D. Wössner, G. Kociok-Köhn, I. Hinz, *J. Org. Chem.* **1997**, *541*, 333.

[147] C. Schwarz, T. Scherpf, I. Rodstein, J. Weismann, K.-S. Feichtner, V. H. Gessner, *ChemistryOpen* **2019**, *8*, 621.

[148] J. Veliks, A. Kazia, *Chem. Eur. J.* **2019**, *25*, 3786.

[149] H. ‐ J. Bestmann, T. Arenz, *Angew. Chem. Int. Ed.* **1986**, *25*, 559.

[150] H. J. Bestmann, T. Röder, M. Bremer, D. Löw, *Chem. Ber.* **1991**, *124*, 199.

[151] a) M. Radius, F. Breher, *Chem. Eur. J.* **2018**, *24*, 15744; b) M. Radius, E. Sattler, H. Berberich, F. Breher, *Chem. Eur. J.* **2019**, *25*, 12206.

[152] T. Scherpf, K.-S. Feichtner, V. H. Gessner, *Angew. Chem. Int. Ed.* **2017**, *56*, 3275.

[153] B. Borthakur, A. K. Phukan in *Structure and Bonding* (Ed.: V. H. Gessner), Springer International Publishing, Cham, **2018**, pp. 1–24.

[154] a) G. Facchin, R. Campostrini, R. A. Michelin, *J. Org. Chem.* **1985**, *294*, c21-c25; b) R. A. Michelin, G. Facchin, D. Braga, P. Sabatino, *Organometallics* **1986**, *5*, 2265; c) R. A. Michelin, M. Mozzon, G. Facchin, D. Braga, P. Sabatino, *Dalt. Trans.* **1988**, 1803.

[155] E. González-Fernández, J. Rust, M. Alcarazo, *Angew. Chem. Int. Ed.* **2013**, *52*, 11392.

[156] a) S.-y. Nakafuji, J. Kobayashi, T. Kawashima, *Angew. Chem. Int. Ed.* **2008**, *120*, 1157; b) J. Kobayashi, S.-y. Nakafuji, A. Yatabe, T. Kawashima, *Chem. Commun.* **2008**, 6233.

[157] a) A. Fürstner, M. Alcarazo, K. Radkowski, C. W. Lehmann, *Angew. Chem. Int. Ed.* **2008**, *120*, 8426; b) A. Fürstner, M. Alcarazo, R. Goddard, C. W. Lehmann, *Angew. Chem. Int. Ed.* **2008**, *120*, 3254.

[158] M. Asay, B. Donnadieu, A. Baceiredo, M. Soleilhavoup, G. Bertrand, *Inorg. Chem.* **2008**, *47*, 3949.

[159] H. Steinert, C. Schwarz, A. Kroll, V. H. Gessner **2020**, 1420.

[160] A. Schmidpeter, H. ‐ P. Schrödel, J. Knizek, *Heteroatom Chemistry* **1998**, *9*, 103.

[161] M. Asay, S. Inoue, M. Driess, *Angew. Chem. Int. Ed.* **2011**, *123*, 9763.

[162] I. Alvarado-Beltran, A. Baceiredo, N. Saffon-Merceron, V. Branchadell, T. Kato, *Angew. Chem. Int. Ed.* **2016**, *55*, 16141.

[163] A. Rosas-Sánchez, I. Alvarado-Beltran, A. Baceiredo, N. Saffon-Merceron, S. Massou, V. Branchadell, T. Kato, *Angew. Chem. Int. Ed.* **2017**, *56*, 10549.

[164] A. Rosas-Sánchez, I. Alvarado-Beltran, A. Baceiredo, N. Saffon-Merceron, S. Massou, D. Hashizume, V. Branchadell, T. Kato, *Angew. Chem. Int. Ed.* **2017**, *56*, 15916.

[165] J. Berthe, J. M. Garcia, E. Ocando, T. Kato, N. Saffon-Merceron, A. de Cózar, F. P. Cossío, A. Baceiredo, *J. Am. Chem. Soc.* **2011**, *133*, 15930.

[166] C. Mohapatra, L. T. Scharf, T. Scherpf, B. Mallick, K.-S. Feichtner, C. Schwarz, V. H. Gessner, *Angew. Chem. Int. Ed.* **2019**, *58*, 7459.

[167] A. Schmidpeter, G. Jochem, *Tetrahedron Lett.* **1992**, *33*, 471.

[168] A. Schmidpeter, H. Nöth, G. Jochem, H. ‐ P. Schrödel, K. Karaghiosoff, *Chem. Ber.* **1995**, *128*, 379.

[169] A. Schmidpeter, G. Jochem, C. Klinger, C. Robl, H. Nöth, *J. Org. Chem.* **1997**, *529*, 87.

[170] a) N. J. Hardman, M. B. Abrams, M. A. Pribisko, T. M. Gilbert, R. L. Martin, G. J. Kubas, R. T. Baker, *Angew. Chem. Int. Ed.* **2004**, *43*, 1955; b) H. Nakazawa, *J. Org. Chem.* **2000**, *611*, 349; c) B. D. Ellis, P. J. Ragogna, C. L. B. Macdonald, *Inorg. Chem.* **2004**, *43*, 7857.

[171] A. Schmidpeter, S. Lochschmidt, A. Willhalm, *Angew. Chem. Int. Ed.* **1983**, *22*, 545.

[172] M. R. Mazieres, C. Roques, M. Sanchez, J. P. Majoral, R. Wolf, *Tetrahedron Lett.* **1987**, *43*, 2109.

[173] A. W. Holderberg, G. Schröder, D. Gudat, H.-P. Schrödel, A. Schmidpeter, *Tetrahedron Lett.* **2000**, *56*, 57.

[174] D. Gudat, *Coord. Chem. Rev.* **1997**, *163*, 71.

[175] A. H. Cowley, R. A. Kemp, *Chem. Rev.* **1985**, *85*, 367.

[176] N. Đorđević, R. Ganguly, M. Petković, D. Vidović, *Inorg. Chem.* **2017**, *56*, 14671.

[177] F. Breitsameter, A. Schmidpeter, H. Nöth, *Chem. Eur. J.* **2000**, *6*, 3531.

[178] R. S. Ghadwal, H. W. Roesky, S. Merkel, J. Henn, D. Stalke, *Angew. Chem. Int. Ed.* **2009**, *48*, 5683.

[179] T. J. Hadlington, J. A. B. Abdalla, R. Tirfoin, S. Aldridge, C. Jones, *Chem. Commun.* **2016**, *52*, 1717.

[180] H. Schmidbaur, W. Malisch, *Angew. Chem. Int. Ed.* **1970**, *9*, 77.

[181] F. Meyer-Wegner, A. Nadj, M. Bolte, N. Auner, M. Wagner, M. C. Holthausen, H.-W. Lerner, *Chem. Eur. J.* **2011**, *17*, 4715.

[182] E. A. Williams, J. D. Cargioli in *Annual Reports on NMR Spectroscopy* (Ed.: G. A. Webb), Academic Press, **1979**, pp. 221–318.

[183] E. A. Williams in *Annual Reports on NMR Spectroscopy* (Ed.: G. A. Webb), Academic Press, **1979**, pp. 235–289.

[184] R. S. Ghadwal, S. S. Sen, H. W. Roesky, G. Tavcar, S. Merkel, D. Stalke, *Organometallics* **2009**, *28*, 6374.

[185] A. C. Filippou, O. Chernov, G. Schnakenburg, *Angew. Chem. Int. Ed.* **2009**, *48*, 5687.

[186] B. Beagley, J. J. Monaghan, T. G. Hewitt, *J. Mol. Struct.* **1971**, *8*, 401.

[187] P. Ghana, M. I. Arz, U. Das, G. Schnakenburg, A. C. Filippou, *Angew. Chem. Int. Ed.* **2015**, *54*, 9980.

[188] C. Jones, *Nat. Rev. Chem.* **2017**, *1*, 59.

[189] J. Wagler, U. Böhme, G. Roewer, *Organometallics* **2004**, *23*, 6066.

[190] a) M. Catellani, C. Mealli, E. Motti, P. Paoli, E. Perez-Carreño, P. S. Pregosin, *J. Am. Chem. Soc.* **2002**, *124*, 4336; b) J. Vignolle, H. Gornitzka, B. Donnadieu, D. Bourissou, G. Bertrand, *Angew. Chem. Int. Ed.* **2008**, *47*, 2271.

[191] L. T. Scharf, I. Rodstein, M. Schmidt, T. Scherpf, V. H. Gessner, *ACS Catal.* **2020**, *10*, 999.

[192] a) C. Burstein, C. W. Lehmann, F. Glorius, *Tetrahedron Lett.* **2005**, *61*, 6207; b) J. Francos, F. Grande-Carmona, H. Faustino, J. Iglesias-Sigüenza, E. Díez, I. Alonso, R. Fernández, J. M. Lassaletta, F. López, J. L. Mascareñas, *J. Am. Chem. Soc.* **2012**, *134*, 14322; c) F. Grande-Carmona, J. Iglesias-Sigüenza, E. Álvarez, E. Díez, R. Fernández, J. M. Lassaletta, *Organometallics* **2015**, *34*, 5073; d) J. Iglesias-Sigüenza, C. Izquierdo, E. Díez, R. Fernández, J. M. Lassaletta, *Dalton Transactions* **2016**, *45*, 10113.

[193] L. Falivene, Z. Cao, A. Petta, L. Serra, A. Poater, R. Oliva, V. Scarano, L. Cavallo, *Nat. Chem.* **2019**, *11*, 872.

[194] C. B. Hubschle, G. M. Sheldrick, B. Dittrich, *J. Appl. Crystallogr.* **2011**, *44*, 1281.

[195] *Dennington, R.; Keith, T. A.; Millam, J. M. GaussView, Version 6.0; Semichem Inc.: Shawnee Mission, 2016.*

[196] *M. J. Frisch, G. W. Trucks, H. B. Schlegel, G. E. Scuseria, M. A. Robb, J. R. Cheeseman, G. Scalmani, V. Barone, G. A. Petersson, H. Nakatsuji et al., Gaussian 16, Revision B.01, Gaussian, Inc., Wallingford CT, 2016.*

[197] *M. J. Frisch, G. W. Trucks, H. B. Schlegel, G. E. Scuseria, M. A. Robb, J. R. Cheeseman, G. Scalmani, V. Barone, G. A. Petersson, H. Nakatsuji et al., Gaussian 16, Revision C.01, Gaussian, Inc., Wallingford CT, 2016.*

[198] a) P. Hohenberg, W. Kohn, *Phys. Rev.* **1964**, *136*, B864-B871; b) W. Kohn, L. J. Sham, *Phys. Rev.* **1965**, *140*, A1133-A1138.

[199] Y. Zhao, D. G. Truhlar, *J. Phys. Chem. A* **2005**, *109*, 5656.

[200] F. Weigend, R. Ahlrichs, *Phys. Chem. Chem. Phys.* **2005**, *7*, 3297.

[201] A. Bergner, M. Dolg, W. Küchle, H. Stoll, H. Preuß, *Mol. Phys.* **1993**, *80*, 1431.

[202] a) S. Grimme, J. Antony, S. Ehrlich, H. Krieg, *J. Chem. Phys.* **2010**, *132*, 154104; b) S. Grimme, S. Ehrlich, L. Goerigk, *J. Comp. Chem.* **2011**, *32*, 1456; c) D. G. A. Smith, L. A. Burns, K. Patkowski, C. D. Sherrill, *J. Phys. Chem. Lett.* **2016**, *7*, 2197.

[203] *NBO 7.0. E. D. Glendening, J. K. Badenhoop, A. E. Reed, J. E. Carpenter, J. A. Bohmann, C. M. Morales, P. Karafiloglou, C. R. Landis, and F. Weinhold, Theoretical Chemistry Institute, University of Wisconsin, Madison, WI (2018)*.

[204] a) R. F. W. Bader, *Chem. Rev.* **1991**, *91*, 893; b) P. S. V. Kumar, V. Raghavendra, V. Subramanian, *J. Chem. Sci.* **2016**, *128*, 1527.

[205] E. R. Johnson, S. Keinan, P. Mori-Sánchez, J. Contreras-García, A. J. Cohen, W. Yang, *J. Am. Chem. Soc.* **2010**, *132*, 6498.

[206] T. Lu, F. Chen, *J. Comp. Chem.* **2012**, *33*, 580.

[207] W. Humphrey, A. Dalke, K. Schulten, *J. Mol. Graph.* **1996**, *14*, 33.

[208] Chemcraft - graphical software for visualization of quantum chemistry computations.

[209] *The GIMP team. GIMP 2.10, 1995-2019.*

[210] M. Schlosser, J. Hartmann, *Angew. Chem.* **1973**, *85*, 544.

[211] a) O. Exner, *Collect. Czech. Chem. Commun.* **1959**, 3562; b) A. Jonczyk, T. Pytlewski, *Synthesis* **1978**, *1978*, 883.

[212] R. Khourzom, F. Rose-Munch, E. Rose, *Tetrahedron Lett.* **1990**, *31*, 2011.

[213] C. Marschner, *Eur. J. Inorg. Chem.* **1998**, *1998*, 221.

[214] B. Schiemenz, P. P. Power, *Angew. Chem. Int. Ed.* **1996**, *35*, 2150.

[215] A. Michaelis, L. Gleichmann, *Ann. Chem* **1885**, *229*, 295.

[216] S. J. Bonyhady, C. Jones, S. Nembenna, A. Stasch, A. J. Edwards, G. J. McIntyre, *Chem. Eur. J.* **2010**, *16*, 938.

[217] a) A. B. Chaplin, A. S. Weller, *Eur. J. Inorg. Chem.* **2010**, 5124; b) R. Anulewicz-Ostrowska, T. Kliś, D. Krajewski, B. Lewandowski, J. Serwatowski, *Tetrahedron Lett.* **2003**, *44*, 7329.

[218] R. Cramer, J. A. McCleverty, J. Bray, *Inorg. Synth.* **1974**, 14.

[219] H. Riihimäki, T. Kangas, P. Suomalainen, H. K. Reinius, S. Jääskeläinen, M. Haukka, A.O.I. Krause, T. A. Pakkanen, J. T. Pursiainen, *J. Mol. Cat.* **2003**, *200*, 81.

# Statutory Declaration

I declare

- that the submitted dissertation with the title:

**"Isolation of metalated ylides and their application in the synthesis of strong donor ligands for homogeneous catalysis and the stabilization of reactive main group compounds"**

is entirely my own work and has been composed without having received unpermitted assistance, and that I have not used other than the declared sources/resources, including entirely or partially included text excerpts as well as graphs, tables and the use of analysis software. I have explicitly marked all material which has been quoted either literally or by content from the used sources.

- that the submitted electronic version corresponds to the printed version of the dissertation and that it, in this or similar form, has not yet been submitted and assessed as a component of another doctoral performance

- that the digital images only contain the original data

- that no commercial brokerage or consultancy services were used

- that I have read, understood and have complied with the DFG-Memorandum ''Safeguarding Good Scientific Practice''

Bochum, 03.05.2021

Heidar Darmandeh

# Declaration (Copyright)

I declare that in the submitted dissertation with the title:

**"Isolation of metalated ylides and their application in the synthesis of strong donor ligands for homogeneous catalysis and the stabilization of reactive main group compounds**"

schemes, figures or other graphical illustrations which were adapted or taken from copyrighted literature (e.g. articles or books), were used with permission from the respective publisher or author.

Bochum, 03.05.2021

Heidar Darmandeh

# Curriculum Vitae

| | |
|---|---|
| Name: | Heidar Darmandeh |
| Place of birth/nationality: | Germany / german |
| Email: | heidar.darmandeh@gmail.com |

## Work Experience

| | |
|---|---|
| since 10/2018 | **Scientific Employee / PhD Candidate**<br>Ruhr Universität Bochum, (Bochum, Germany)<br>Organometallic Chemistry and Homogeneous Catalysis with Prof. Dr. Viktoria H. Gessner |
| Topic: | **"Isolation of metalated ylides and their application in the synthesis of strong donor ligands for homogeneous catalysis and the stabilization of reactive main group compounds. "** |
| 05/2018 – 09/2018 | **Master thesis student**<br>Covestro Deutschland AG (Leverkusen, Germany), |
| 02/2018 – 04/2018 | **Visiting Researcher Supramolecular Chemistry**<br>Institute of Advanced Materials, Universitat Jaume I (Castellón de la Plana, Spain), Supervision by Prof. Eduardo Peris |
| 08/2017 – 01/2018 | **R&D Intern**<br>Covestro Deutschland AG (Leverkusen, Germany), |
| 12/2013 – 06/2017 | **Student Assistant**<br>Institute for Inorganic and Analytical Chemistry<br>Westfälische Wilhelms-Universität Münster |

## Education

| | |
|---|---|
| since 10/2018 | **Dr. rer. nat / PhD – Chemistry**<br>Ruhr-Universität Bochum within the Graduate School of Chemistry and Biochemistry |
| 10/2016 – 09/2018 | **Master of Science – Chemistry**<br>Westfälische Wilhelms-Universität Münster |
| 10/2012 – 08/2016 | **Bachelor of Science - Chemistry**<br>Westfälische Wilhelms-Universität Münster |
| 09/2003 – 06/2012 | **Higher Education entrance qualification**<br>Gymnasium Nepomucenum Coesfeld |

## Accomplishments

| | |
|---|---|
| 01/2020 – 01/2021 | **GDCh Chemento Mentoring Program**<br>▪ Selected Mentee in the official mentoring program of the GDCh (German Chemical Society)<br>▪ 1 year one to one mentoring with an experienced mentor from the chemical industry (Dr. Frank Richter, Covestro AG) |
| 02/2018 – 04/2018 | **DAAD ERASMUS+ Scholarship** |

## Additional Skills

Languages:

- German – native
- Arabic – native
- English – Full professional proficiency
- Spanish – Elementary proficiency

Computer literacy and software:

- Microsoft Office, Microsoft Teams
- MestreNova, SciFinder, ChemDraw

## Poster Presentations

1) _"Isolation, Reactivity and Electronic Structure of a Metalated Ylide"
GDCh Wissenschaftsforum Chemie, Aachen 2019.
2) "Synthesis, Reactivity and Crystal Structures of the Metalated Ylides
[$Cy_3P–C–SO_2Tol$]M (M = Li, K)", Online Workshop on Phosphorus Chemistry, 2021.

## Publications

6) H. Darmandeh, J. Löffler, N. V. Tzouras, T. Scherpf, K.-S. Feichtner, S. V. Broeck, K. V. Hecke, M. Saab, C. S. J. Cazin, S. P. Nolan and V. H. Gessner
"Au···H-C Hydrogen Bonds as Design Principle in Gold(I) Catalysis." *submitted*
5) C. Mohapatra*, H. Darmandeh*, H. Steinert, B. Mallick, K.-S. Feichtner, V.H. Gessner
*equal contribution: "Synthesis of Low-Valent Dinuclear Group 14 Compounds with Element–Element Bonds by Transylidation" *Chem. Eur. J.* , **2020** *26*, 15145–15149.
4) H. Darmandeh, V.H. Gessner
"Selective B (C6F5) 3-Catalyzed Reactions of α-Diazoesters with Heterocycles and Alkenes" *Chem*, **2020**, *9*, 2129-2131.
3) H. Darmandeh, T. Scherpf, K.-S. Feichtner, C. Schwarz, V. H. Gessner
"Synthesis, Isolation and Crystal Structures of the Metalated Ylides [Cy3P-C-SO2Tol]M (M = Li, Na, K)." *Z. Anorg. Allg. Chem.* **2020**, *646*, 1–8.
2) V. Martinez-Agramunt, T. Eder, H. Darmandeh, G. Guisado-Barrios, E. Peris"A Size-Flexible Organometallic Box for the Encapsulation of Fullerenes."
*Angew. Chem. Int. Ed.*, **2019**, *131(17),* 5738–5742.
1) T. Witteler, H. Darmandeh, P. Mehlmann, F. Dielmann
"Dialkyl(1,3-diarylimidazolin-2-ylidenamino)phosphines: Strongly electron-donating, Buchwald-type phosphines" *Organometallics* , **2018**, *37 (18)*, 3064–3072.

# 7. Appendix

## Crystal structure determination of $^{Cy}$Y-H$_2$

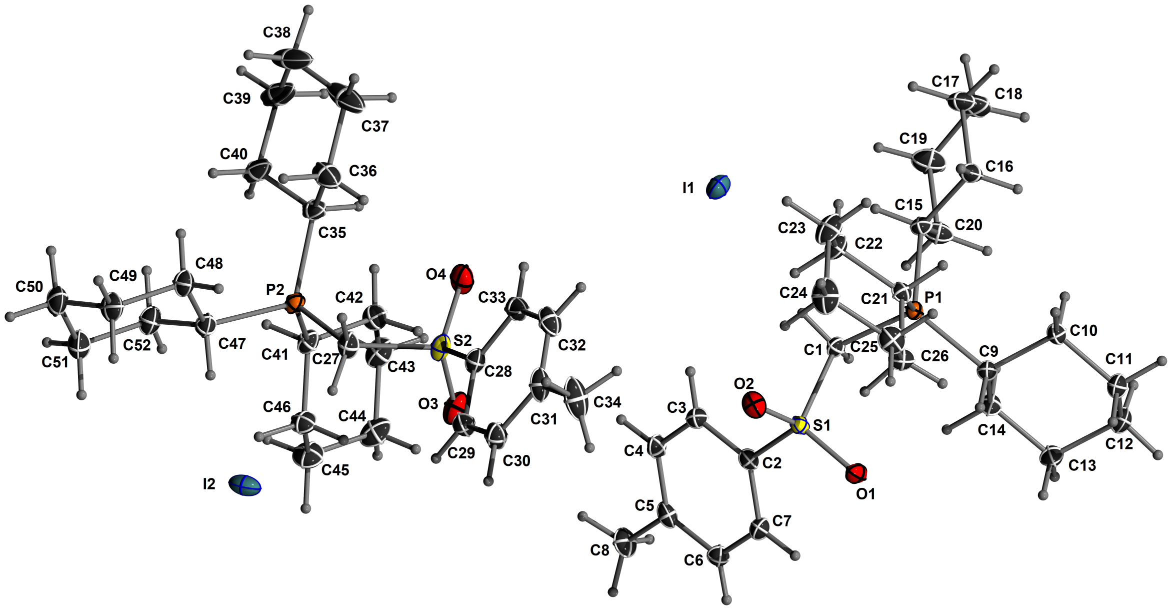
C38
C39
C37
C40
C36
C35
C50
C49
C48
P2
C42
O4
C33
C51
C52
C47
C41
C27
C43
S2
C28
C32
C46
C44
O3
C31
C34
C29
C30
C45
I2
I1
C17
C18
C19
C16
C15
C20
C23
C22
C24
C21
P1
C10
C1
C25
C26
C9
C11
O2
C3
S1
C4
C14
C12
C2
C13
O1
C5
C7
C8
C6

**Figure 52.** ORTEP plot of the iodide of phosphonium salt **$^{Cy}$Y-H$_2$**. Ellipsoids are drawn at 50% probability level.

**Table 14.** Atomic coordinates ( x $10^4$) and equivalent isotropic displacement parameters (Å$^2$x $10^3$)for compound **$^{Cy}$Y-H$_2$**. U(eq) is defined as one third of the trace of the orthogonalized $U^{ij}$ tensor.

| | x | y | z | U(eq) |
|---|---|---|---|---|
| I(1) | 5928(1) | 3049(1) | 5950(1) | 25(1) |
| I(2) | 6708(1) | 4798(1) | 2126(1) | 26(1) |
| S(1) | 5592(1) | 1248(1) | 4874(1) | 14(1) |
| S(2) | 9033(1) | 4374(1) | 3934(1) | 20(1) |
| P(1) | 5416(1) | 1043(1) | 6054(1) | 12(1) |
| P(2) | 9535(1) | 5633(1) | 3580(1) | 15(1) |
| O(1) | 5625(1) | 621(1) | 4837(1) | 18(1) |
| O(2) | 4267(1) | 1550(1) | 4724(1) | 20(1) |
| O(3) | 10132(2) | 4055(1) | 3697(1) | 26(1) |
| O(4) | 9344(2) | 4605(1) | 4452(1) | 26(1) |
| C(1) | 6156(2) | 1451(1) | 5529(1) | 14(1) |
| C(2) | 6966(2) | 1532(1) | 4519(1) | 15(1) |
| C(3) | 7286(2) | 2123(1) | 4554(1) | 18(1) |
| C(4) | 8345(2) | 2343(1) | 4263(1) | 18(1) |
| C(5) | 9086(2) | 1982(1) | 3940(1) | 17(1) |
| C(6) | 8714(2) | 1394(1) | 3904(1) | 18(1) |
| C(7) | 7667(2) | 1162(1) | 4193(1) | 18(1) |
| C(8) | 10289(2) | 2228(1) | 3653(1) | 23(1) |
| C(9) | 6073(2) | 296(1) | 6053(1) | 14(1) |
| C(10) | 5769(2) | -14(1) | 6563(1) | 17(1) |
| C(11) | 6209(2) | -655(1) | 6544(1) | 20(1) |
| C(12) | 7783(2) | -722(1) | 6439(1) | 22(1) |

| | | | | |
|---|---|---|---|---|
| C(13) | 8080(2) | -410(1) | 5934(1) | 19(1) |
| C(14) | 7665(2) | 234(1) | 5946(1) | 17(1) |
| C(15) | 6058(2) | 1481(1) | 6620(1) | 15(1) |
| C(16) | 5293(2) | 1356(1) | 7113(1) | 20(1) |
| C(17) | 5733(2) | 1820(1) | 7523(1) | 25(1) |
| C(18) | 7364(3) | 1846(1) | 7644(1) | 31(1) |
| C(19) | 8134(2) | 1941(1) | 7151(1) | 28(1) |
| C(20) | 7706(2) | 1473(1) | 6742(1) | 22(1) |
| C(21) | 3458(2) | 1055(1) | 6001(1) | 14(1) |
| C(22) | 2888(2) | 1686(1) | 5950(1) | 20(1) |
| C(23) | 1242(2) | 1684(1) | 5940(1) | 27(1) |
| C(24) | 580(2) | 1308(1) | 5493(1) | 29(1) |
| C(25) | 1119(2) | 683(1) | 5553(1) | 22(1) |
| C(26) | 2764(2) | 656(1) | 5568(1) | 18(1) |
| C(27) | 8470(2) | 4965(1) | 3513(1) | 19(1) |
| C(28) | 7488(2) | 3937(1) | 3927(1) | 18(1) |
| C(29) | 6991(2) | 3646(1) | 3470(1) | 20(1) |
| C(30) | 5827(2) | 3273(1) | 3483(1) | 22(1) |
| C(31) | 5173(2) | 3181(1) | 3945(1) | 24(1) |
| C(32) | 5689(2) | 3481(1) | 4393(1) | 25(1) |
| C(33) | 6831(2) | 3867(1) | 4386(1) | 22(1) |
| C(34) | 3935(3) | 2763(1) | 3957(1) | 37(1) |
| C(35) | 9305(2) | 5960(1) | 4211(1) | 21(1) |
| C(36) | 7777(2) | 5919(1) | 4391(1) | 30(1) |
| C(37) | 7792(3) | 6186(2) | 4939(1) | 49(1) |
| C(38) | 8361(4) | 6802(2) | 4962(1) | 57(1) |
| C(39) | 9852(3) | 6839(1) | 4770(1) | 45(1) |
| C(40) | 9867(3) | 6592(1) | 4223(1) | 29(1) |
| C(41) | 11442(2) | 5505(1) | 3512(1) | 17(1) |
| C(43) | 13890(2) | 5174(1) | 3893(1) | 25(1) |
| C(42) | 12308(2) | 5250(1) | 3998(1) | 21(1) |
| C(44) | 14044(2) | 4804(1) | 3408(1) | 29(1) |
| C(45) | 13209(2) | 5073(1) | 2932(1) | 28(1) |
| C(46) | 11615(2) | 5136(1) | 3020(1) | 22(1) |
| C(47) | 8782(2) | 6060(1) | 3017(1) | 18(1) |
| C(48) | 7264(2) | 6295(1) | 3090(1) | 21(1) |
| C(49) | 6634(2) | 6608(1) | 2596(1) | 25(1) |
| C(50) | 7632(2) | 7094(1) | 2442(1) | 27(1) |
| C(51) | 9115(2) | 6847(1) | 2360(1) | 26(1) |
| C(52) | 9793(2) | 6545(1) | 2852(1) | 22(1) |

**Table 15.** Anisotropic displacement parameters (Å2x 103) for compound $^{Cy}$**Y-H$_2$**. The anisotropic displacement factor exponent takes the form: -2p2[ h2 a*2U11 + ... + 2 h k a* b* U12 ].

| | **U11** | **U22** | **U33** | **U23** | **U13** | **U12** |
|---|---|---|---|---|---|---|
| I(1) | 31(1) | 15(1) | 28(1) | 0(1) | 2(1) | -1(1) |
| I(2) | 22(1) | 37(1) | 19(1) | -9(1) | 3(1) | 4(1) |

| | | | | | | |
|---|---|---|---|---|---|---|
| S(1) | 15(1) | 14(1) | 12(1) | 0(1) | 2(1) | -3(1) |
| S(2) | 18(1) | 16(1) | 24(1) | 3(1) | -4(1) | -1(1) |
| P(1) | 12(1) | 12(1) | 11(1) | 0(1) | 1(1) | -1(1) |
| P(2) | 15(1) | 13(1) | 17(1) | -1(1) | -2(1) | 1(1) |
| O(1) | 23(1) | 15(1) | 16(1) | -2(1) | 4(1) | -5(1) |
| O(2) | 16(1) | 24(1) | 19(1) | 3(1) | 1(1) | 0(1) |
| O(3) | 18(1) | 21(1) | 39(1) | 4(1) | 1(1) | 1(1) |
| O(4) | 30(1) | 22(1) | 25(1) | 2(1) | -11(1) | -3(1) |
| C(1) | 16(1) | 12(1) | 15(1) | -1(1) | 2(1) | -1(1) |
| C(2) | 15(1) | 17(1) | 12(1) | 1(1) | 1(1) | -1(1) |
| C(3) | 22(1) | 16(1) | 16(1) | -1(1) | 2(1) | -1(1) |
| C(4) | 22(1) | 14(1) | 17(1) | 2(1) | 1(1) | -5(1) |
| C(5) | 15(1) | 22(1) | 14(1) | 5(1) | 0(1) | -2(1) |
| C(6) | 19(1) | 19(1) | 17(1) | 1(1) | 4(1) | 2(1) |
| C(7) | 21(1) | 14(1) | 18(1) | 0(1) | 2(1) | 0(1) |
| C(8) | 18(1) | 25(1) | 25(1) | 6(1) | 6(1) | -3(1) |
| C(9) | 16(1) | 13(1) | 13(1) | 0(1) | 1(1) | 0(1) |
| C(10) | 20(1) | 15(1) | 16(1) | 2(1) | 4(1) | 1(1) |
| C(11) | 25(1) | 15(1) | 20(1) | 2(1) | 3(1) | 0(1) |
| C(12) | 25(1) | 17(1) | 23(1) | 2(1) | 1(1) | 5(1) |
| C(13) | 19(1) | 20(1) | 20(1) | 0(1) | 4(1) | 4(1) |
| C(14) | 15(1) | 17(1) | 18(1) | 1(1) | 3(1) | 0(1) |
| C(15) | 19(1) | 14(1) | 13(1) | -2(1) | 1(1) | -2(1) |
| C(16) | 26(1) | 21(1) | 14(1) | -4(1) | 4(1) | -2(1) |
| C(17) | 33(1) | 26(1) | 17(1) | -8(1) | 4(1) | -1(1) |
| C(18) | 36(1) | 34(1) | 20(1) | -11(1) | -4(1) | -2(1) |
| C(19) | 25(1) | 34(1) | 26(1) | -10(1) | -4(1) | -9(1) |
| C(20) | 19(1) | 28(1) | 19(1) | -6(1) | 0(1) | -4(1) |
| C(21) | 13(1) | 16(1) | 14(1) | 1(1) | 3(1) | 0(1) |
| C(22) | 17(1) | 17(1) | 26(1) | 0(1) | 1(1) | 2(1) |
| C(23) | 19(1) | 22(1) | 41(1) | 2(1) | 6(1) | 5(1) |
| C(24) | 14(1) | 34(1) | 38(1) | 8(1) | -4(1) | 1(1) |
| C(25) | 15(1) | 27(1) | 24(1) | 1(1) | 1(1) | -5(1) |
| C(26) | 15(1) | 20(1) | 19(1) | -3(1) | 2(1) | -3(1) |
| C(27) | 18(1) | 17(1) | 22(1) | 2(1) | -6(1) | -2(1) |
| C(28) | 18(1) | 16(1) | 20(1) | 2(1) | 0(1) | 1(1) |
| C(29) | 21(1) | 20(1) | 18(1) | 2(1) | 2(1) | -2(1) |
| C(30) | 22(1) | 21(1) | 21(1) | 2(1) | -3(1) | -2(1) |
| C(31) | 18(1) | 25(1) | 29(1) | 11(1) | -1(1) | -1(1) |
| C(32) | 20(1) | 32(1) | 22(1) | 8(1) | 5(1) | 5(1) |
| C(33) | 23(1) | 24(1) | 18(1) | 0(1) | 0(1) | 6(1) |
| C(34) | 25(1) | 45(1) | 39(1) | 21(1) | -3(1) | -12(1) |
| C(35) | 23(1) | 22(1) | 17(1) | -3(1) | -2(1) | 8(1) |
| C(36) | 27(1) | 42(1) | 21(1) | 4(1) | 5(1) | 13(1) |
| C(37) | 46(2) | 82(2) | 20(1) | 2(1) | 7(1) | 39(2) |
| C(38) | 74(2) | 68(2) | 26(1) | -22(1) | -12(1) | 48(2) |

| | | | | | | |
|---|---|---|---|---|---|---|
| C(39) | 64(2) | 36(1) | 31(1) | -17(1) | -24(1) | 24(1) |
| C(40) | 36(1) | 21(1) | 26(1) | -8(1) | -12(1) | 7(1) |
| C(41) | 15(1) | 16(1) | 21(1) | 0(1) | -1(1) | 2(1) |
| C(43) | 17(1) | 23(1) | 34(1) | -2(1) | -5(1) | 2(1) |
| C(42) | 18(1) | 23(1) | 22(1) | -2(1) | -5(1) | 3(1) |
| C(44) | 18(1) | 28(1) | 40(1) | -4(1) | 1(1) | 7(1) |
| C(45) | 22(1) | 33(1) | 31(1) | -2(1) | 6(1) | 4(1) |
| C(46) | 19(1) | 24(1) | 21(1) | -2(1) | 1(1) | 4(1) |
| C(47) | 20(1) | 15(1) | 19(1) | 2(1) | -1(1) | 2(1) |
| C(48) | 21(1) | 21(1) | 21(1) | 3(1) | -1(1) | 5(1) |
| C(49) | 24(1) | 27(1) | 24(1) | 4(1) | -5(1) | 8(1) |
| C(50) | 32(1) | 22(1) | 26(1) | 5(1) | -4(1) | 6(1) |
| C(51) | 31(1) | 22(1) | 27(1) | 6(1) | 1(1) | 0(1) |
| C(52) | 22(1) | 19(1) | 26(1) | 3(1) | 0(1) | 2(1) |

## Crystal structure determination of $^{Cy}$Y-H

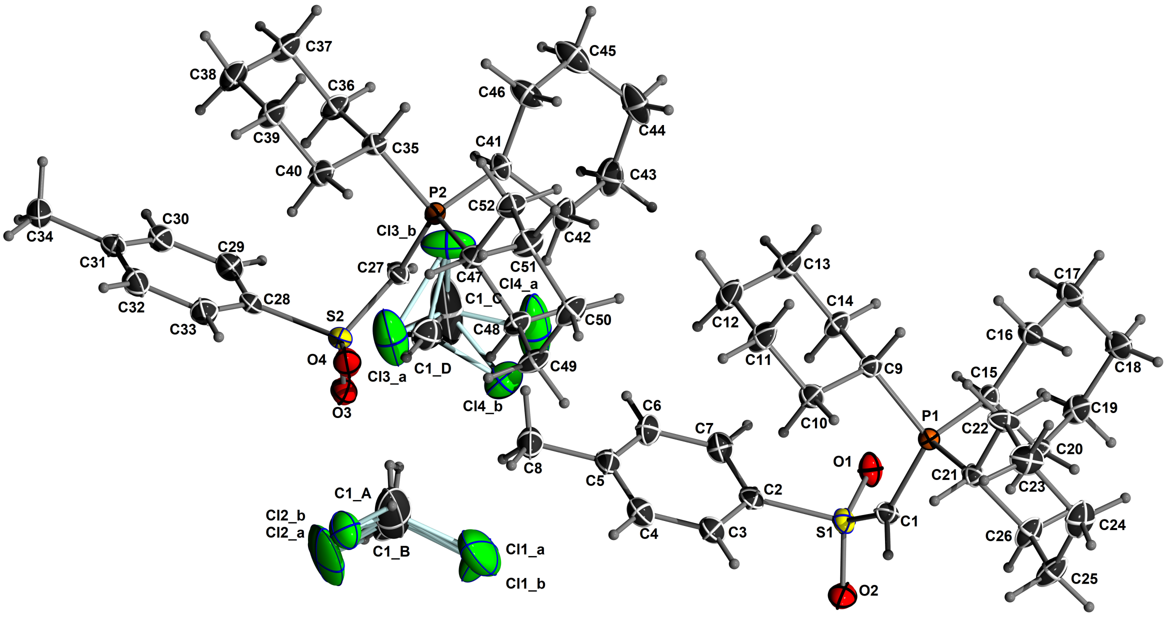
C37
C38
C36
C45
C46
C44
C39
C35
C41
C43
C40
P2
C52
C34
C30
Cl3_b
C42
C31
C29
C27
C47
C51
C13
C28
Cl4_a
C1_C
C17
C32
C33
S2
C14
C12
C48
C50
C16
O4
C11
C9
C18
Cl3_a
C1_D
C49
C15
Cl4_b
C6
C19
O3
C10
P1
C22
C7
O1
C20
C8
C21
C23
C1_A
C5
C2
Cl2_b
Cl2_a
S1
C1
C24
C4
C3
C26
C1_B
Cl1_a
O2
C25
Cl1_b

**Figure 53.** ORTEP plot of compound $^{Cy}$**Y-H**. Ellipsoids are drawn at 50% probability level.

**Table 16.** Atomic coordinates ( x 10$^4$) and equivalent isotropic displacement parameters (Å$^2$x 10$^3$)for compound $^{Cy}$**Y-H**. U(eq) is defined as one third of the trace of the orthogonalized U$^{ij}$ tensor.

| | x | y | z | U(eq) |
|---|---|---|---|---|
| S(1) | 4500(1) | 4252(1) | 7475(1) | 20(1) |
| S(2) | 5231(1) | 4359(1) | 2493(1) | 25(1) |
| P(1) | 5035(1) | 2588(1) | 7787(1) | 14(1) |
| P(2) | 4820(1) | 2658(1) | 2783(1) | 16(1) |
| O(1) | 3658(2) | 3970(2) | 7544(1) | 27(1) |
| O(2) | 4708(2) | 5007(1) | 7761(1) | 30(1) |
| O(3) | 4941(2) | 5103(2) | 2771(1) | 40(1) |
| O(4) | 6093(2) | 4145(2) | 2584(1) | 38(1) |
| C(1) | 5172(2) | 3586(2) | 7741(2) | 19(1) |
| C(2) | 4639(2) | 4389(2) | 6607(2) | 21(1) |
| C(3) | 5421(2) | 4545(2) | 6353(2) | 25(1) |
| C(4) | 5519(2) | 4657(2) | 5681(2) | 27(1) |
| C(5) | 4844(2) | 4605(2) | 5252(2) | 25(1) |
| C(6) | 4068(2) | 4445(2) | 5514(2) | 28(1) |
| C(7) | 3961(2) | 4332(2) | 6188(2) | 26(1) |
| C(8) | 4946(3) | 4731(2) | 4521(2) | 33(1) |
| C(9) | 5032(2) | 2057(2) | 6999(2) | 17(1) |
| C(10) | 5776(2) | 2307(2) | 6579(2) | 23(1) |
| C(11) | 5785(2) | 1881(3) | 5919(2) | 30(1) |
| C(12) | 4983(2) | 1990(3) | 5540(2) | 31(1) |
| C(13) | 4240(2) | 1743(2) | 5954(2) | 26(1) |
| C(14) | 4219(2) | 2182(2) | 6613(2) | 21(1) |
| C(15) | 4058(2) | 2315(2) | 8183(2) | 17(1) |

| | | | | |
|---|---|---|---|---|
| C(16) | 3950(2) | 1428(2) | 8275(2) | 23(1) |
| C(17) | 3068(2) | 1246(2) | 8498(2) | 26(1) |
| C(18) | 2855(2) | 1693(2) | 9130(2) | 29(1) |
| C(19) | 2991(2) | 2569(2) | 9050(2) | 25(1) |
| C(20) | 3874(2) | 2756(2) | 8829(2) | 19(1) |
| C(21) | 5976(2) | 2280(2) | 8227(2) | 17(1) |
| C(22) | 6162(2) | 1395(2) | 8237(2) | 24(1) |
| C(23) | 7032(2) | 1263(2) | 8519(2) | 29(1) |
| C(24) | 7125(2) | 1618(3) | 9201(2) | 34(1) |
| C(25) | 6903(2) | 2483(3) | 9203(2) | 31(1) |
| C(26) | 6034(2) | 2617(2) | 8924(2) | 25(1) |
| C(27) | 4608(2) | 3645(2) | 2748(2) | 20(1) |
| C(28) | 5114(2) | 4478(2) | 1623(2) | 21(1) |
| C(29) | 4337(2) | 4582(2) | 1352(2) | 26(1) |
| C(30) | 4246(2) | 4662(2) | 676(2) | 27(1) |
| C(31) | 4930(2) | 4624(2) | 258(2) | 25(1) |
| C(32) | 5704(2) | 4521(2) | 534(2) | 29(1) |
| C(33) | 5808(2) | 4449(2) | 1214(2) | 26(1) |
| C(34) | 4831(3) | 4683(2) | -482(2) | 36(1) |
| C(35) | 4878(2) | 2142(2) | 1990(2) | 18(1) |
| C(36) | 4111(2) | 2332(2) | 1569(2) | 23(1) |
| C(37) | 4140(2) | 1882(2) | 916(2) | 27(1) |
| C(38) | 4926(2) | 2062(2) | 535(2) | 29(1) |
| C(39) | 5690(2) | 1893(2) | 950(2) | 26(1) |
| C(40) | 5677(2) | 2328(2) | 1606(2) | 22(1) |
| C(41) | 3899(2) | 2274(2) | 3201(2) | 19(1) |
| C(42) | 3855(2) | 2514(2) | 3928(2) | 26(1) |
| C(43) | 3006(2) | 2303(3) | 4216(2) | 34(1) |
| C(44) | 2819(3) | 1430(3) | 4132(2) | 42(1) |
| C(45) | 2884(2) | 1184(2) | 3414(2) | 37(1) |
| C(46) | 3738(2) | 1388(2) | 3128(2) | 30(1) |
| C(47) | 5806(2) | 2441(2) | 3191(2) | 19(1) |
| C(48) | 5960(2) | 2894(2) | 3832(2) | 22(1) |
| C(49) | 6858(2) | 2761(2) | 4051(2) | 28(1) |
| C(50) | 7048(2) | 1895(2) | 4135(2) | 30(1) |
| C(51) | 6862(2) | 1434(2) | 3507(2) | 28(1) |
| C(52) | 5967(2) | 1562(2) | 3285(2) | 24(1) |
| Cl11 | 7392(1) | 5057(2) | 4374(1) | 55(1) |
| Cl21 | 8209(1) | 4958(1) | 3102(1) | 45(1) |

**Table 17.** Anisotropic displacement parameters (Å2x 103) for compound **$^{Cy}$Y-H**. The anisotropic displacement factor exponent takes the form: -2p2[ h2 a*2U11 + ... + 2 h k a* b* U12 ].

| | U11 | U22 | U33 | U23 | U13 | U12 |
|---|---|---|---|---|---|---|
| S(1) | 25(1) | 16(1) | 20(1) | 2(1) | 2(1) | 4(1) |

| | | | | | | |
|---|---|---|---|---|---|---|
| S(2) | 35(1) | 20(1) | 21(1) | 1(1) | -3(1) | -10(1) |
| P(1) | 15(1) | 14(1) | 14(1) | 0(1) | 0(1) | -1(1) |
| P(2) | 16(1) | 16(1) | 15(1) | 0(1) | 1(1) | -1(1) |
| O(1) | 24(1) | 30(1) | 26(1) | 7(1) | 3(1) | 6(1) |
| O(2) | 47(2) | 16(1) | 26(1) | -2(1) | -2(1) | 4(1) |
| O(3) | 75(2) | 20(1) | 24(1) | 0(1) | 2(1) | -6(1) |
| O(4) | 35(1) | 50(2) | 30(1) | 12(1) | -10(1) | -20(1) |
| C(1) | 18(1) | 18(1) | 22(1) | 0(1) | -2(1) | -3(1) |
| C(2) | 26(2) | 14(1) | 23(2) | 1(1) | 1(1) | 0(1) |
| C(3) | 28(2) | 21(2) | 26(2) | 2(1) | 0(1) | -1(1) |
| C(4) | 28(2) | 22(2) | 31(2) | 3(1) | 3(1) | -1(1) |
| C(5) | 37(2) | 16(1) | 22(2) | 0(1) | 2(1) | 1(1) |
| C(6) | 32(2) | 28(2) | 24(2) | 6(1) | -3(1) | 0(1) |
| C(7) | 26(2) | 26(2) | 25(2) | 4(1) | 2(1) | 1(1) |
| C(8) | 47(2) | 27(2) | 24(2) | 3(1) | 5(2) | 3(2) |
| C(9) | 16(1) | 19(1) | 17(1) | -1(1) | -2(1) | -2(1) |
| C(10) | 18(1) | 30(2) | 21(2) | -2(1) | 2(1) | -5(1) |
| C(11) | 22(2) | 48(2) | 22(2) | -10(2) | 6(1) | -5(2) |
| C(12) | 31(2) | 46(2) | 17(2) | -4(1) | 2(1) | -2(2) |
| C(13) | 22(2) | 38(2) | 19(2) | -8(1) | -2(1) | 2(1) |
| C(14) | 17(1) | 26(2) | 18(2) | -4(1) | 0(1) | 2(1) |
| C(15) | 15(1) | 20(1) | 16(1) | 0(1) | 1(1) | 0(1) |
| C(16) | 23(2) | 18(2) | 27(2) | -1(1) | 5(1) | -4(1) |
| C(17) | 23(2) | 27(2) | 29(2) | -1(1) | 8(1) | -8(1) |
| C(18) | 24(2) | 35(2) | 28(2) | -2(2) | 9(1) | -9(2) |
| C(19) | 19(2) | 33(2) | 24(2) | -6(1) | 6(1) | 0(1) |
| C(20) | 19(1) | 21(1) | 19(1) | -4(1) | 2(1) | -1(1) |
| C(21) | 16(1) | 18(1) | 19(2) | 1(1) | -1(1) | -2(1) |
| C(22) | 21(2) | 16(1) | 36(2) | 0(1) | -8(1) | 0(1) |
| C(23) | 22(2) | 26(2) | 39(2) | 1(2) | -7(1) | 6(1) |
| C(24) | 22(2) | 50(2) | 30(2) | 7(2) | -9(1) | 5(2) |
| C(25) | 22(2) | 46(2) | 24(2) | -9(2) | -7(1) | 3(2) |
| C(26) | 19(1) | 36(2) | 20(2) | -2(1) | -4(1) | 7(1) |
| C(27) | 25(2) | 14(1) | 22(2) | 2(1) | 4(1) | -2(1) |
| C(28) | 29(2) | 14(1) | 21(1) | 2(1) | 0(1) | -6(1) |
| C(29) | 28(2) | 25(2) | 27(2) | 2(1) | 2(1) | -3(1) |
| C(30) | 31(2) | 23(2) | 27(2) | 2(1) | -3(1) | -4(1) |
| C(31) | 38(2) | 16(1) | 21(2) | 0(1) | -1(1) | -2(1) |
| C(32) | 32(2) | 27(2) | 28(2) | 3(1) | 7(2) | -3(1) |
| C(33) | 26(2) | 27(2) | 26(2) | 2(1) | -1(1) | -1(1) |
| C(34) | 55(2) | 29(2) | 22(2) | 3(1) | 0(2) | -7(2) |
| C(35) | 16(1) | 19(1) | 18(1) | -3(1) | -1(1) | 0(1) |
| C(36) | 20(1) | 29(2) | 21(2) | -5(1) | -1(1) | 3(1) |
| C(37) | 21(2) | 38(2) | 22(2) | -8(2) | -3(1) | 2(1) |
| C(38) | 29(2) | 39(2) | 18(2) | -4(1) | 0(1) | 2(2) |
| C(39) | 18(2) | 37(2) | 22(2) | -8(1) | 3(1) | -1(1) |

| | | | | | | |
|---|---|---|---|---|---|---|
| C(40) | 19(1) | 29(2) | 19(2) | -5(1) | 5(1) | -3(1) |
| C(41) | 18(1) | 21(2) | 20(2) | 2(1) | 3(1) | 1(1) |
| C(42) | 22(2) | 37(2) | 18(2) | 2(1) | 4(1) | 2(2) |
| C(43) | 27(2) | 46(2) | 28(2) | 2(2) | 9(1) | 5(2) |
| C(44) | 28(2) | 48(3) | 51(3) | 18(2) | 14(2) | -7(2) |
| C(45) | 25(2) | 31(2) | 54(3) | 6(2) | 10(2) | -3(2) |
| C(46) | 23(2) | 21(2) | 44(2) | 3(2) | 8(2) | -2(1) |
| C(47) | 15(1) | 25(2) | 18(1) | -1(1) | 0(1) | -1(1) |
| C(48) | 20(2) | 26(2) | 21(2) | -4(1) | -4(1) | -1(1) |
| C(49) | 21(2) | 34(2) | 27(2) | -8(1) | -8(1) | 0(1) |
| C(50) | 26(2) | 40(2) | 25(2) | -5(2) | -8(1) | 7(2) |
| C(51) | 22(2) | 33(2) | 30(2) | -4(2) | -5(1) | 5(1) |
| C(52) | 21(2) | 25(2) | 26(2) | -2(1) | -5(1) | 3(1) |
| Cl11 | 33(1) | 104(2) | 27(1) | -7(1) | -2(1) | 2(1) |
| Cl21 | 41(1) | 50(1) | 44(1) | 4(1) | 11(1) | -2(1) |

## Crystal structure determination of $^{Cy}$Y-Li·LiI

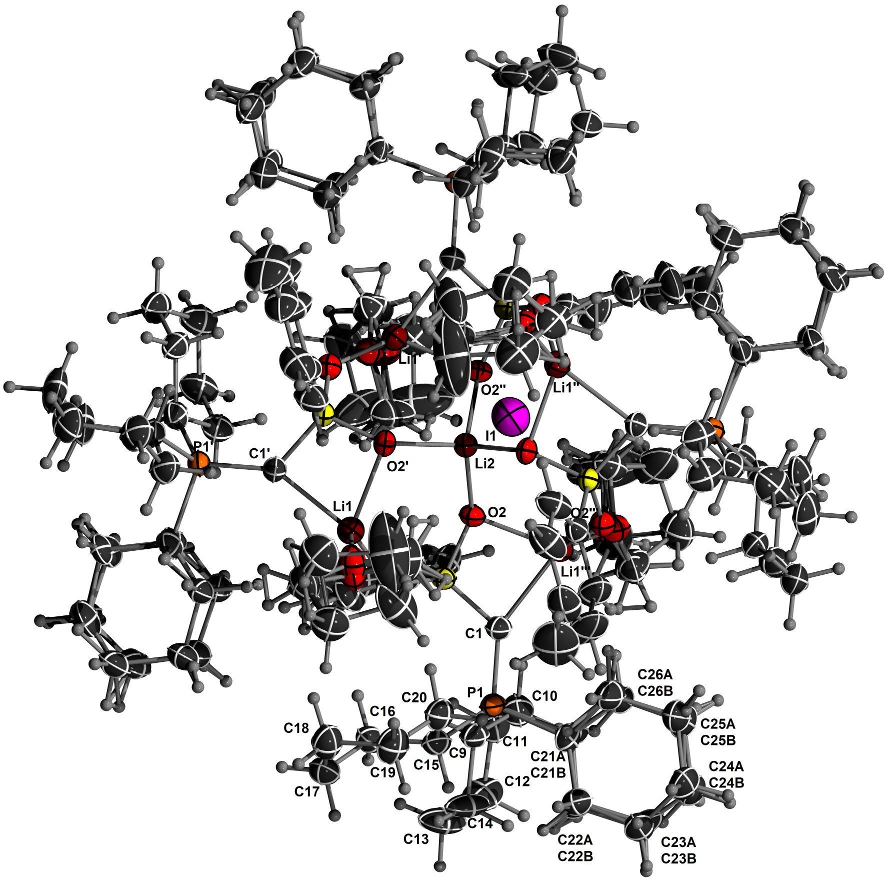
Li1'
O2''
Li1''
I1
P1'
C1'
O2'
Li2
Li1
O2
O2'''
Li1'''
C1
C26A
C26B
P1
C10
C20
C16
C18
C25A
C25B
C11
C9
C15
C21A
C21B
C24A
C24B
C19
C12
C17
C14
C13
C22A
C22B
C23A
C23B

**Figure 54** .ORTEP plot of compound $^{Cy}$**Y-Li·LiI**. Ellipsoids are drawn at 50% probability level.

**Table 18** .Atomic coordinates ( x $10^4$) and equivalent isotropic displacement parameters (Å$^2$x $10^3$)for compound $^{Cy}$**Y-Li·LiI**. U(eq) is defined as one third of the trace of the orthogonalized $U^{ij}$ tensor.

| | x | y | z | U(eq) |
|---|---|---|---|---|
| S(1) | 2032(1) | 4011(1) | 8124(1) | 30(1) |
| Li(1) | 1241(2) | 3372(2) | 6731(3) | 36(1) |
| P(1) | 2504(1) | 5487(1) | 8143(1) | 33(1) |
| O(1) | 1516(1) | 4026(1) | 7484(1) | 37(1) |
| C(1) | 2624(1) | 4612(1) | 8162(2) | 34(1) |
| I(1) | 1135(1) | 2893(1) | 2870(1) | 95(1) |
| O(2) | 2406(1) | 3318(1) | 8159(1) | 31(1) |
| Li(2) | 2500 | 2500 | 7500 | 29(2) |
| C(2) | 1488(1) | 3989(1) | 8967(2) | 37(1) |
| C(4) | 392(2) | 4153(2) | 9625(3) | 81(1) |
| C(3) | 778(2) | 4134(2) | 8934(2) | 60(1) |
| C(5) | 694(2) | 4021(2) | 10317(2) | 66(1) |
| C(6) | 1405(2) | 3875(2) | 10344(2) | 60(1) |
| C(8) | 266(3) | 4023(3) | 11056(3) | 100(2) |
| C(7) | 1803(2) | 3862(2) | 9675(2) | 50(1) |
| C(9) | 2105(1) | 5835(1) | 9039(2) | 37(1) |
| C(10) | 2494(2) | 5599(2) | 9763(2) | 50(1) |
| C(11) | 2068(2) | 5768(2) | 10485(2) | 55(1) |

| | | | | |
|---|---|---|---|---|
| C(12) | 1896(2) | 6551(2) | 10526(2) | 64(1) |
| C(13) | 1533(2) | 6804(2) | 9803(2) | 68(1) |
| C(14) | 1961(2) | 6630(1) | 9076(2) | 58(1) |
| C(15) | 1959(1) | 5857(1) | 7357(2) | 39(1) |
| C(16) | 1163(1) | 5777(1) | 7509(2) | 43(1) |
| C(17) | 731(2) | 6087(2) | 6851(2) | 50(1) |
| C(18) | 918(2) | 5744(2) | 6093(2) | 54(1) |
| C(19) | 1705(2) | 5820(2) | 5923(2) | 55(1) |
| C(20) | 2151(1) | 5520(2) | 6584(2) | 44(1) |
| C(21A) | 3394(6) | 5869(5) | 8144(7) | 39(3) |
| C(22A) | 3449(6) | 6640(7) | 7874(12) | 44(3) |
| C(23A) | 4196(6) | 6929(6) | 7992(12) | 63(4) |
| C(24A) | 4747(3) | 6498(3) | 7601(4) | 59(2) |
| C(25A) | 4677(4) | 5733(4) | 7812(6) | 61(2) |
| C(26A) | 3942(3) | 5445(3) | 7688(5) | 61(2) |
| O(3A) | 1426(8) | 3713(12) | 5667(6) | 43(3) |
| C(27A) | 962(7) | 3903(11) | 5045(8) | 62(4) |
| C(28A) | 1271(4) | 3579(4) | 4350(4) | 76(2) |
| C(29A) | 2059(4) | 3594(11) | 4528(5) | 143(6) |
| C(30A) | 2134(8) | 3689(15) | 5362(7) | 60(5) |
| C(21B) | 3380(7) | 5906(9) | 7918(10) | 34(4) |
| C(22B) | 3419(9) | 6704(9) | 8025(17) | 43(5) |
| C(23B) | 4157(8) | 6971(10) | 7822(18) | 60(6) |
| C(24B) | 4722(4) | 6600(4) | 8245(6) | 51(2) |
| C(25B) | 4689(6) | 5811(6) | 8181(8) | 57(3) |
| C(26B) | 3953(3) | 5522(3) | 8370(5) | 46(2) |
| O(3B) | 1409(12) | 3853(18) | 5765(9) | 43(4) |
| C(27B) | 938(9) | 3908(12) | 5117(10) | 47(4) |
| C(28B) | 1315(5) | 4363(5) | 4557(5) | 66(3) |
| C(29B) | 2068(6) | 4195(9) | 4713(9) | 99(5) |
| C(30B) | 2107(11) | 3780(20) | 5431(11) | 52(4) |

**Table 19.** Anisotropic displacement parameters (Å2x 103) for compound $^{Cy}$**Y-Li·LiI**. The anisotropic displacement factor exponent takes the form: -2p2[ h2 a*2U11 + ... + 2 h k a* b* U12 ].

| | $U_{11}$ | $U_{22}$ | $U_{33}$ | $U_{23}$ | $U_{13}$ | $U_{12}$ |
|---|---|---|---|---|---|---|
| S(1) | 28(1) | 22(1) | 39(1) | -4(1) | 4(1) | 0(1) |
| Li(1) | 33(2) | 32(2) | 42(2) | 1(2) | -3(2) | -1(2) |
| P(1) | 32(1) | 23(1) | 45(1) | -3(1) | 6(1) | -1(1) |
| O(1) | 33(1) | 29(1) | 48(1) | -1(1) | -5(1) | 1(1) |
| C(1) | 31(1) | 24(1) | 45(1) | -4(1) | 6(1) | 0(1) |
| I(1) | 68(1) | 72(1) | 145(1) | -11(1) | 12(1) | 3(1) |
| O(2) | 31(1) | 22(1) | 39(1) | -4(1) | 2(1) | 2(1) |
| Li(2) | 25(2) | 25(2) | 38(4) | 0 | 0 | 0 |
| C(2) | 36(1) | 27(1) | 49(2) | -6(1) | 13(1) | -2(1) |
| C(4) | 52(2) | 90(3) | 100(3) | 29(2) | 41(2) | 25(2) |

| | | | | | | |
|---|---|---|---|---|---|---|
| C(3) | 42(2) | 63(2) | 73(2) | 16(2) | 21(2) | 13(1) |
| C(5) | 71(2) | 51(2) | 75(2) | -1(2) | 42(2) | -1(2) |
| C(6) | 69(2) | 62(2) | 50(2) | -10(2) | 18(2) | -19(2) |
| C(8) | 104(3) | 100(3) | 97(3) | 4(3) | 67(3) | 11(3) |
| C(7) | 43(2) | 58(2) | 48(2) | -11(1) | 9(1) | -11(1) |
| C(9) | 37(1) | 27(1) | 45(1) | -6(1) | 7(1) | -1(1) |
| C(10) | 47(2) | 51(2) | 52(2) | -17(1) | -4(1) | 5(1) |
| C(11) | 57(2) | 59(2) | 50(2) | -13(1) | 1(1) | 5(1) |
| C(12) | 73(2) | 57(2) | 63(2) | -24(2) | 20(2) | -5(2) |
| C(13) | 94(3) | 35(2) | 75(2) | -5(2) | 32(2) | 17(2) |
| C(14) | 81(2) | 27(1) | 67(2) | -7(1) | 29(2) | 2(1) |
| C(15) | 39(1) | 27(1) | 49(2) | 4(1) | 7(1) | -1(1) |
| C(16) | 36(1) | 37(1) | 54(2) | 7(1) | 7(1) | 6(1) |
| C(17) | 45(2) | 40(2) | 64(2) | 11(1) | -1(1) | 5(1) |
| C(18) | 47(2) | 59(2) | 56(2) | 14(2) | -3(1) | -7(1) |
| C(19) | 52(2) | 65(2) | 48(2) | 11(1) | 3(1) | -11(1) |
| C(20) | 38(1) | 45(2) | 49(2) | 3(1) | 10(1) | -5(1) |
| C(21A) | 47(4) | 23(3) | 49(7) | 6(3) | 10(3) | -5(2) |
| C(22A) | 44(5) | 32(5) | 56(6) | 1(4) | 2(3) | -3(3) |
| C(23A) | 66(7) | 31(5) | 91(8) | 2(5) | 6(5) | -18(4) |
| C(24A) | 43(3) | 54(3) | 80(5) | 18(3) | 0(3) | -13(2) |
| C(25A) | 37(3) | 46(3) | 99(7) | 4(4) | 6(4) | -2(2) |
| C(26A) | 40(3) | 40(3) | 103(5) | -6(3) | 18(3) | -3(2) |
| O(3A) | 37(3) | 56(9) | 35(3) | 7(4) | -3(2) | 0(3) |
| C(27A) | 52(6) | 68(10) | 66(6) | 18(6) | -23(4) | 2(6) |
| C(28A) | 87(4) | 86(5) | 55(3) | 14(3) | -18(3) | -8(4) |
| C(29A) | 73(5) | 308(19) | 47(4) | -1(7) | 10(3) | 23(8) |
| C(30A) | 37(4) | 85(13) | 58(5) | 2(6) | 5(4) | -5(5) |
| C(21B) | 29(5) | 38(5) | 36(8) | 9(4) | 10(4) | -4(3) |
| C(22B) | 42(7) | 22(6) | 63(11) | 3(5) | -2(5) | -8(4) |
| C(23B) | 40(8) | 43(8) | 97(14) | 27(7) | 5(6) | -4(5) |
| C(24B) | 38(4) | 47(4) | 68(6) | 6(4) | -5(4) | -13(3) |
| C(25B) | 37(5) | 47(5) | 88(9) | 1(5) | -12(5) | -11(4) |
| C(26B) | 29(3) | 34(3) | 75(6) | 7(3) | -4(3) | -5(3) |
| O(3B) | 33(4) | 48(9) | 50(6) | 5(6) | -3(4) | 0(4) |
| C(27B) | 54(7) | 37(10) | 51(7) | 10(6) | -9(5) | -10(7) |
| C(28B) | 73(5) | 66(5) | 57(5) | 19(4) | -3(4) | -3(4) |
| C(29B) | 68(6) | 120(10) | 108(10) | 51(8) | 43(6) | 25(7) |
| C(30B) | 42(7) | 56(7) | 56(7) | -8(6) | 9(5) | -6(5) |

## Crystal structure determination of $^{Cy}$Y-K

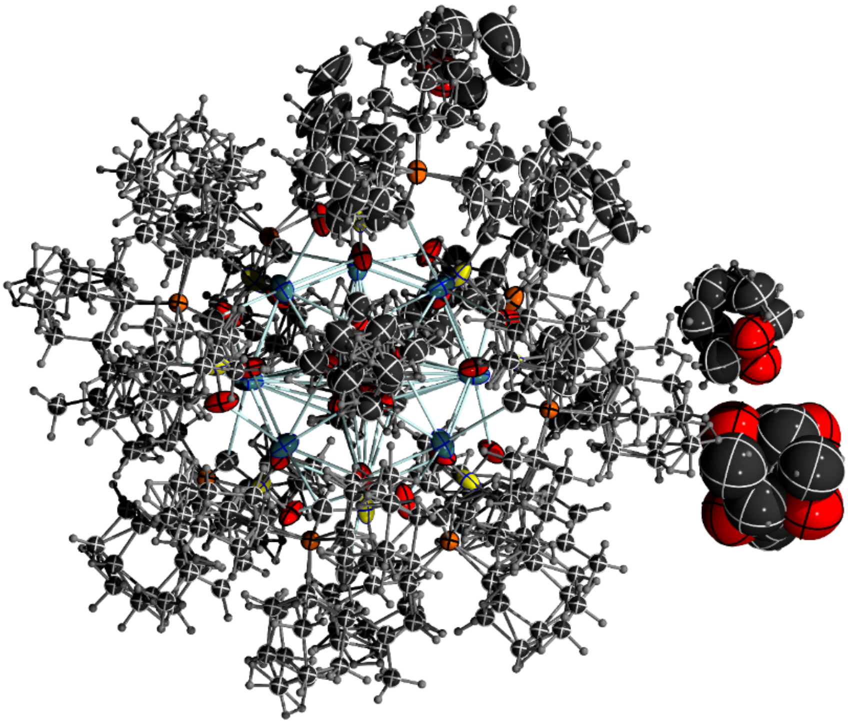

**Figure 55.** ORTEP plot of compound $^{Cy}$**Y-K**. Ellipsoids are drawn at 50% probability level.

**Table 20.** Atomic coordinates ( x $10^4$) and equivalent isotropic displacement parameters ($Å^2$x $10^3$)for compound $^{Cy}$**Y-K**. U(eq) is defined as one third of the trace of the orthogonalized $U^{ij}$ tensor.

| | x | y | z | U(eq) |
|---|---|---|---|---|
| I(1) | 2500 | 2500 | 3569(8) | 52(4) |
| K(3) | 2500 | 2500 | 1920(30) | 52(4) |
| K(1) | 3239(1) | 3608(1) | 4397(1) | 59(1) |
| K(2) | 3816(1) | 2783(1) | 2699(1) | 58(1) |
| S(1) | 2148(1) | 4205(1) | 4768(1) | 50(1) |
| S(2) | 3444(1) | 3971(1) | 2307(1) | 50(1) |
| P(1) | 2720(1) | 4788(1) | 5856(1) | 44(1) |
| P(2) | 4096(1) | 3888(1) | 1009(1) | 51(1) |
| O(1) | 2251(2) | 3804(2) | 4205(2) | 54(1) |
| O(2) | 1704(2) | 4066(2) | 5209(2) | 66(1) |
| O(3) | 3257(2) | 3629(2) | 2903(2) | 54(1) |
| O(4) | 3020(2) | 4190(2) | 1900(2) | 59(1) |
| C(1) | 2652(2) | 4359(2) | 5185(3) | 48(1) |
| C(2) | 1932(2) | 4712(3) | 4199(4) | 59(2) |
| C(3) | 2235(3) | 4897(3) | 3623(4) | 60(2) |
| C(4) | 2085(3) | 5292(3) | 3194(4) | 77(2) |
| C(5) | 1637(4) | 5531(5) | 3326(5) | 108(4) |
| C(6) | 1344(3) | 5366(5) | 3908(6) | 117(4) |
| C(7) | 1487(3) | 4961(4) | 4333(5) | 97(3) |
| C(8) | 1480(5) | 5987(6) | 2867(7) | 172(7) |
| C(9A) | 3359(5) | 4729(7) | 6228(7) | 52(3) |
| C(10A) | 3538(3) | 5103(4) | 6805(6) | 71(3) |

| | | | | |
|---|---|---|---|---|
| C(11A) | 4044(4) | 4989(6) | 7128(6) | 87(4) |
| C(12A) | 4427(4) | 4863(5) | 6569(7) | 83(3) |
| C(13A) | 4258(4) | 4482(5) | 5999(8) | 78(4) |
| C(14A) | 3748(5) | 4603(10) | 5663(8) | 81(5) |
| C(15A) | 2611(5) | 5466(5) | 5554(9) | 49(3) |
| C(16A) | 2941(6) | 5606(5) | 4886(9) | 54(3) |
| C(17A) | 2776(5) | 6109(4) | 4566(6) | 69(3) |
| C(18A) | 2769(5) | 6513(4) | 5156(6) | 80(3) |
| C(19A) | 2463(5) | 6372(4) | 5826(6) | 81(3) |
| C(20A) | 2618(4) | 5865(3) | 6147(5) | 60(2) |
| C(21A) | 2312(6) | 4754(5) | 6706(8) | 58(3) |
| C(22A) | 2317(7) | 4223(6) | 7042(10) | 85(5) |
| C(23A) | 2035(5) | 4234(7) | 7784(7) | 107(5) |
| C(24A) | 1505(5) | 4421(5) | 7683(7) | 103(4) |
| C(25A) | 1489(4) | 4932(5) | 7331(5) | 80(3) |
| C(26A) | 1784(3) | 4928(4) | 6598(4) | 54(2) |
| C(9B) | 3368(10) | 4788(15) | 6157(14) | 47(6) |
| C(10B) | 3485(6) | 4472(11) | 6851(10) | 62(6) |
| C(11B) | 4020(6) | 4538(12) | 7104(10) | 73(6) |
| C(12B) | 4389(7) | 4449(10) | 6489(13) | 69(5) |
| C(13B) | 4269(8) | 4765(11) | 5807(12) | 64(6) |
| C(14B) | 3732(9) | 4680(20) | 5540(13) | 57(6) |
| C(15B) | 2651(12) | 5407(13) | 5620(20) | 58(6) |
| C(16B) | 3026(13) | 5589(11) | 5030(30) | 61(8) |
| C(17B) | 2982(8) | 6143(10) | 4869(19) | 81(6) |
| C(18B) | 2460(9) | 6319(10) | 4737(15) | 83(5) |
| C(19B) | 2103(11) | 6164(8) | 5357(18) | 103(11) |
| C(20B) | 2132(8) | 5597(8) | 5477(16) | 74(7) |
| C(21B) | 2344(16) | 4644(11) | 6644(17) | 62(6) |
| C(22B) | 2359(16) | 4097(11) | 6900(20) | 70(6) |
| C(23B) | 1923(12) | 3973(9) | 7415(15) | 91(7) |
| C(24B) | 1854(13) | 4354(9) | 8025(13) | 94(6) |
| C(25B) | 1814(9) | 4886(9) | 7738(14) | 87(6) |
| C(26B) | 2272(9) | 5018(9) | 7259(13) | 75(6) |
| C(27) | 3889(2) | 3711(2) | 1854(3) | 50(2) |
| C(28) | 3676(2) | 4482(3) | 2863(3) | 53(2) |
| C(29) | 4089(3) | 4396(3) | 3327(4) | 66(2) |
| C(30) | 4288(3) | 4784(4) | 3754(4) | 78(2) |
| C(31) | 4078(3) | 5260(4) | 3717(5) | 79(2) |
| C(32) | 3669(3) | 5340(3) | 3248(5) | 77(2) |
| C(33) | 3468(3) | 4944(3) | 2825(4) | 64(2) |
| C(34) | 4288(4) | 5687(4) | 4183(6) | 107(4) |
| C(35A) | 3589(6) | 3859(6) | 256(7) | 51(3) |
| C(36A) | 3746(5) | 4006(6) | -529(7) | 78(4) |
| C(37A) | 3306(6) | 4035(6) | -1073(8) | 100(4) |
| C(38A) | 3034(5) | 3556(5) | -1096(7) | 88(4) |

| | | | | |
|---|---|---|---|---|
| C(39A) | 2876(6) | 3399(6) | -336(8) | 86(4) |
| C(40A) | 3295(7) | 3380(6) | 239(10) | 97(5) |
| C(41A) | 4360(5) | 4518(5) | 887(10) | 53(3) |
| C(42A) | 4755(4) | 4620(5) | 1486(8) | 75(3) |
| C(43A) | 4984(5) | 5139(5) | 1365(8) | 94(4) |
| C(44A) | 4597(5) | 5527(5) | 1398(6) | 85(3) |
| C(45A) | 4200(5) | 5442(4) | 807(6) | 75(3) |
| C(46A) | 3961(4) | 4927(4) | 899(6) | 57(2) |
| C(47A) | 4533(4) | 3375(4) | 641(6) | 53(3) |
| C(48A) | 4801(5) | 3096(5) | 1261(6) | 82(4) |
| C(49A) | 5126(5) | 2668(5) | 982(7) | 80(5) |
| C(50A) | 5470(4) | 2819(5) | 405(7) | 73(4) |
| C(51A) | 5212(5) | 3103(5) | -238(6) | 81(4) |
| C(52A) | 4880(4) | 3530(4) | 27(5) | 58(3) |
| C(35B) | 3648(12) | 4009(12) | 308(12) | 35(5) |
| C(36B) | 3799(10) | 4265(11) | -419(14) | 63(7) |
| C(37B) | 3351(12) | 4342(11) | -930(17) | 91(7) |
| C(38B) | 3111(14) | 3866(13) | -1090(16) | 92(7) |
| C(39B) | 2950(12) | 3595(13) | -390(18) | 78(6) |
| C(40B) | 3393(14) | 3517(13) | 140(20) | 73(6) |
| C(41B) | 4485(11) | 4467(10) | 970(20) | 52(5) |
| C(42B) | 4948(9) | 4473(9) | 1464(19) | 66(6) |
| C(43B) | 5240(9) | 4958(11) | 1400(20) | 94(7) |
| C(44B) | 4933(11) | 5400(10) | 1528(17) | 86(6) |
| C(45B) | 4471(10) | 5405(9) | 1031(18) | 77(5) |
| C(46B) | 4170(8) | 4924(9) | 1118(16) | 59(5) |
| C(47B) | 4627(10) | 3531(8) | 809(17) | 57(6) |
| C(48B) | 4532(8) | 2981(8) | 914(16) | 65(5) |
| C(49B) | 4939(11) | 2622(9) | 700(20) | 84(9) |
| C(50B) | 5303(11) | 2769(10) | 157(19) | 85(7) |
| C(51B) | 5465(9) | 3310(10) | 240(20) | 102(7) |
| C(52B) | 5025(11) | 3667(10) | 270(20) | 97(9) |
| O11 | 2704(7) | 2818(6) | 2387(8) | 45(4) |
| C11 | 2391(19) | 2404(16) | 2587(11) | 48(6) |
| C21 | 2365(14) | 2057(10) | 1910(15) | 66(6) |
| C31 | 2621(14) | 2350(9) | 1294(12) | 58(6) |
| C41 | 2680(12) | 2878(9) | 1593(10) | 52(5) |
| O12 | 2892(7) | 2617(8) | 5094(11) | 73(5) |
| C12 | 3076(10) | 2673(16) | 5833(14) | 84(8) |
| C22 | 2637(12) | 2813(16) | 6314(16) | 107(10) |
| C32 | 2166(10) | 2723(17) | 5840(20) | 90(8) |
| C42 | 2377(11) | 2460(30) | 5138(17) | 89(9) |
| O13 | 2749(5) | 6312(6) | 2127(10) | 255(7) |
| C13 | 2796(7) | 6796(7) | 2464(12) | 219(8) |
| C23 | 3365(7) | 6835(8) | 2451(11) | 218(8) |
| C33 | 3549(6) | 6570(7) | 1765(11) | 202(7) |

| | | | | |
|---|---|---|---|---|
| C43 | 3127(6) | 6228(6) | 1589(10) | 178(6) |
| O14 | 6986(12) | 3919(12) | 1728(16) | 215(8) |
| C14 | 6681(18) | 3599(11) | 1260(20) | 221(9) |
| C24 | 6525(18) | 3958(15) | 616(18) | 222(9) |
| C34 | 6438(15) | 4428(14) | 1080(20) | 211(9) |
| C44 | 6907(15) | 4442(12) | 1580(20) | 207(9) |
| O15 | 7115(12) | 3677(11) | 1144(19) | 222(8) |
| C15 | 6678(15) | 3648(15) | 680(20) | 225(9) |
| C25 | 6340(10) | 4070(15) | 1020(20) | 212(9) |
| C35 | 6730(15) | 4484(11) | 1060(30) | 209(9) |
| C45 | 7163(14) | 4180(14) | 1440(20) | 202(9) |
| O16 | 7840(50) | 3030(50) | -290(110) | 480(60) |
| C16 | 7430(70) | 2960(50) | -820(60) | 480(60) |
| C26 | 7080(60) | 2600(70) | -400(120) | 480(60) |
| C36 | 7460(80) | 2230(50) | -60(150) | 470(60) |
| C46 | 7920(60) | 2560(70) | 90(110) | 470(60) |

**Table 21.** Anisotropic displacement parameters (Å2x 103) for compound **$^{Cy}$Y-K**. The anisotropic displacement factor exponent takes the form: -2p2[ h2 a*2U11 + ... + 2 h k a* b* U12 ].

| | U11 | U22 | U33 | U23 | U13 | U12 |
|---|---|---|---|---|---|---|
| I(1) | 47(5) | 47(5) | 61(7) | 0 | 0 | 0 |
| K(3) | 47(5) | 47(5) | 61(7) | 0 | 0 | 0 |
| K(1) | 74(1) | 68(1) | 36(1) | -14(1) | -11(1) | 24(1) |
| K(2) | 101(1) | 45(1) | 29(1) | 1(1) | 5(1) | 9(1) |
| S(1) | 37(1) | 81(1) | 33(1) | -17(1) | 8(1) | -14(1) |
| S(2) | 43(1) | 69(1) | 38(1) | 21(1) | 14(1) | 19(1) |
| P(1) | 39(1) | 59(1) | 33(1) | -8(1) | 2(1) | -4(1) |
| P(2) | 48(1) | 68(1) | 37(1) | 18(1) | 16(1) | 12(1) |
| O(1) | 47(2) | 81(3) | 34(2) | -19(2) | 9(2) | -20(2) |
| O(2) | 52(3) | 106(4) | 41(2) | -25(2) | 15(2) | -26(2) |
| O(3) | 45(2) | 78(3) | 38(2) | 25(2) | 18(2) | 16(2) |
| O(4) | 48(2) | 84(3) | 44(2) | 24(2) | 11(2) | 24(2) |
| C(1) | 44(3) | 59(4) | 40(3) | -8(3) | -1(2) | 1(3) |
| C(2) | 34(3) | 92(5) | 51(4) | -18(3) | -1(3) | -2(3) |
| C(3) | 52(4) | 82(5) | 48(4) | -5(3) | 7(3) | 4(3) |
| C(4) | 78(5) | 99(6) | 55(4) | 9(4) | 4(4) | 15(5) |
| C(5) | 88(7) | 166(10) | 69(6) | 16(6) | -8(5) | 45(7) |
| C(6) | 60(5) | 194(12) | 97(7) | 27(8) | -5(5) | 59(7) |
| C(7) | 38(4) | 186(11) | 66(5) | -3(6) | 1(4) | 5(5) |
| C(8) | 166(13) | 220(16) | 129(10) | 55(11) | 3(9) | 120(12) |
| C(9A) | 42(5) | 65(7) | 48(6) | -14(5) | -9(4) | 0(5) |
| C(10A) | 60(5) | 73(7) | 80(7) | -37(5) | -9(5) | 9(5) |
| C(11A) | 62(6) | 121(10) | 77(7) | -46(7) | -25(5) | 9(6) |
| C(12A) | 54(5) | 96(8) | 98(8) | -27(7) | -12(5) | -4(6) |
| C(13A) | 43(5) | 106(10) | 85(8) | -38(7) | 11(5) | -6(6) |

| | | | | | | |
|---|---|---|---|---|---|---|
| C(14A) | 57(6) | 115(12) | 72(7) | -37(8) | -1(5) | -1(6) |
| C(15A) | 48(6) | 60(6) | 40(5) | -6(4) | 3(4) | 0(5) |
| C(16A) | 51(6) | 62(5) | 49(7) | 5(4) | 3(5) | -6(4) |
| C(17A) | 69(7) | 72(6) | 65(6) | 12(5) | 8(5) | 14(6) |
| C(18A) | 82(7) | 66(6) | 91(7) | 4(5) | 5(6) | 3(5) |
| C(19A) | 93(8) | 75(6) | 75(7) | -12(5) | 8(6) | 17(6) |
| C(20A) | 59(6) | 64(5) | 57(5) | -19(4) | -3(4) | 4(4) |
| C(21A) | 50(5) | 88(7) | 34(5) | 0(5) | 12(4) | 11(5) |
| C(22A) | 80(7) | 114(10) | 60(9) | 31(8) | 17(6) | 9(7) |
| C(23A) | 93(9) | 163(12) | 64(8) | 43(8) | 31(7) | 10(8) |
| C(24A) | 81(7) | 165(11) | 62(7) | 33(7) | 28(6) | 4(8) |
| C(25A) | 53(6) | 141(9) | 45(5) | 5(6) | 21(4) | 7(6) |
| C(26A) | 44(4) | 87(7) | 31(4) | -6(4) | 5(3) | 8(4) |
| C(9B) | 39(9) | 72(14) | 32(9) | -15(9) | -4(7) | -4(9) |
| C(10B) | 31(8) | 120(19) | 35(9) | 4(10) | -6(7) | 0(10) |
| C(11B) | 40(8) | 119(16) | 59(9) | -11(11) | -22(7) | 6(10) |
| C(12B) | 34(8) | 85(11) | 86(11) | -2(11) | -5(7) | -2(9) |
| C(13B) | 33(8) | 89(16) | 69(10) | -11(11) | -5(8) | -9(10) |
| C(14B) | 27(8) | 95(15) | 48(10) | 10(10) | 10(7) | -5(9) |
| C(15B) | 59(11) | 65(12) | 51(13) | -12(9) | 11(10) | 1(9) |
| C(16B) | 63(13) | 57(10) | 63(16) | -5(10) | 11(13) | 0(9) |
| C(17B) | 87(11) | 71(9) | 86(14) | 22(11) | 12(10) | 7(10) |
| C(18B) | 87(11) | 72(11) | 91(12) | 15(10) | 18(10) | 12(9) |
| C(19B) | 130(20) | 68(13) | 120(20) | 20(15) | 60(20) | 37(14) |
| C(20B) | 66(11) | 67(12) | 87(18) | 11(12) | 15(11) | 9(10) |
| C(21B) | 49(11) | 93(12) | 45(11) | 1(8) | 6(9) | 6(10) |
| C(22B) | 79(13) | 97(11) | 33(11) | 4(10) | 12(9) | -3(12) |
| C(23B) | 94(15) | 125(14) | 54(13) | 23(10) | 27(12) | 0(14) |
| C(24B) | 84(14) | 148(12) | 51(11) | 22(9) | 32(10) | 12(11) |
| C(25B) | 74(13) | 127(12) | 59(12) | -3(11) | 22(10) | 4(12) |
| C(26B) | 73(12) | 99(12) | 53(10) | -4(9) | 21(9) | 15(11) |
| C(27) | 54(4) | 56(4) | 40(3) | 19(3) | 16(3) | 12(3) |
| C(28) | 50(3) | 71(4) | 38(3) | 13(3) | 23(3) | 15(3) |
| C(29) | 56(4) | 94(6) | 50(4) | 14(4) | 14(3) | 8(4) |
| C(30) | 57(4) | 117(7) | 61(4) | -16(5) | 14(4) | -8(5) |
| C(31) | 69(5) | 101(7) | 66(5) | -16(4) | 40(4) | -23(5) |
| C(32) | 80(6) | 74(5) | 77(5) | -1(4) | 50(5) | 2(4) |
| C(33) | 68(4) | 74(5) | 51(4) | 12(3) | 25(3) | 17(4) |
| C(34) | 85(6) | 127(8) | 110(7) | -39(6) | 56(6) | -34(6) |
| C(35A) | 51(6) | 49(9) | 54(5) | 4(5) | 4(4) | 6(5) |
| C(36A) | 62(6) | 129(13) | 42(6) | 12(8) | -4(4) | 0(7) |
| C(37A) | 96(9) | 138(12) | 66(7) | 25(9) | -31(6) | -14(9) |
| C(38A) | 73(7) | 114(10) | 78(6) | -19(8) | -16(5) | 14(7) |
| C(39A) | 72(7) | 82(10) | 104(7) | -5(7) | -13(6) | -17(7) |
| C(40A) | 115(11) | 71(9) | 104(9) | 13(7) | -35(8) | -24(7) |
| C(41A) | 46(7) | 76(5) | 37(5) | 12(5) | 4(5) | 3(4) |

| | | | | | | |
|---|---|---|---|---|---|---|
| C(42A) | 55(7) | 120(8) | 50(5) | 23(7) | -1(6) | -8(6) |
| C(43A) | 94(8) | 137(10) | 50(6) | -1(8) | -12(7) | -41(7) |
| C(44A) | 110(9) | 108(8) | 37(6) | -1(6) | 10(6) | -45(7) |
| C(45A) | 108(9) | 71(6) | 45(6) | 0(5) | 7(5) | -21(6) |
| C(46A) | 68(7) | 60(5) | 44(6) | 5(4) | 1(5) | 3(5) |
| C(47A) | 43(5) | 76(7) | 41(6) | 12(5) | 14(4) | 16(5) |
| C(48A) | 97(9) | 93(8) | 56(6) | 34(6) | 29(6) | 47(7) |
| C(49A) | 75(9) | 84(7) | 80(9) | 28(6) | 24(7) | 35(7) |
| C(50A) | 61(7) | 76(7) | 82(8) | 11(6) | 11(5) | 23(5) |
| C(51A) | 86(8) | 102(8) | 56(6) | 17(5) | 36(5) | 42(6) |
| C(52A) | 60(6) | 69(6) | 46(5) | 12(5) | 25(5) | 10(5) |
| C(35B) | 35(9) | 49(15) | 22(7) | -5(7) | 22(6) | 9(8) |
| C(36B) | 68(11) | 103(18) | 18(9) | 13(11) | 13(7) | 0(12) |
| C(37B) | 89(13) | 130(17) | 56(12) | 27(14) | -13(10) | -6(14) |
| C(38B) | 74(13) | 133(16) | 69(10) | 10(12) | -22(9) | 2(13) |
| C(39B) | 60(11) | 104(15) | 71(10) | -2(11) | -12(8) | -3(11) |
| C(40B) | 83(12) | 65(14) | 71(10) | 11(10) | -25(9) | -18(10) |
| C(41B) | 44(11) | 78(8) | 34(10) | 16(9) | 15(8) | 1(8) |
| C(42B) | 57(12) | 98(12) | 42(10) | -1(11) | 5(11) | 8(9) |
| C(43B) | 93(14) | 118(13) | 70(14) | -11(12) | 4(13) | -22(9) |
| C(44B) | 103(12) | 103(12) | 51(11) | -16(11) | 10(10) | -32(11) |
| C(45B) | 105(12) | 80(9) | 45(12) | 6(10) | 11(10) | -25(10) |
| C(46B) | 57(11) | 70(8) | 49(12) | 6(9) | 9(9) | -1(8) |
| C(47B) | 55(11) | 74(9) | 42(13) | -5(10) | 6(9) | 8(9) |
| C(48B) | 59(11) | 72(9) | 65(12) | 21(10) | 22(9) | 32(8) |
| C(49B) | 75(16) | 72(10) | 105(18) | 5(13) | 48(14) | 28(11) |
| C(50B) | 79(13) | 99(10) | 76(13) | 7(11) | 37(11) | 27(10) |
| C(51B) | 95(14) | 103(12) | 108(17) | 5(13) | 60(13) | 17(10) |
| C(52B) | 94(15) | 89(13) | 109(18) | 14(14) | 54(13) | 10(11) |
| O11 | 43(9) | 55(9) | 37(7) | 14(6) | -2(7) | 7(7) |
| C11 | 38(12) | 49(11) | 57(8) | 3(8) | -13(9) | 2(9) |
| C21 | 73(12) | 67(9) | 58(11) | -2(8) | 2(10) | -2(9) |
| C31 | 58(13) | 58(11) | 58(8) | 0(7) | -5(9) | 3(8) |
| C41 | 54(11) | 61(9) | 41(8) | -2(8) | 0(8) | 6(8) |
| O12 | 75(11) | 58(11) | 85(9) | 1(9) | -6(8) | -12(10) |
| C12 | 87(12) | 85(17) | 79(11) | -6(13) | 0(9) | 3(13) |
| C22 | 99(15) | 120(20) | 98(13) | -5(14) | 4(11) | 29(14) |
| C32 | 95(12) | 75(16) | 99(15) | 12(13) | 4(10) | 15(13) |
| C42 | 72(14) | 73(18) | 122(13) | -9(16) | 0(10) | -4(14) |
| O13 | 229(11) | 260(12) | 276(14) | -81(11) | 68(10) | -63(10) |
| C13 | 223(12) | 225(14) | 208(15) | -41(12) | 13(12) | -24(12) |
| C23 | 226(12) | 232(15) | 195(13) | -54(11) | 27(12) | -60(12) |
| C33 | 200(12) | 170(13) | 235(14) | -44(11) | 26(11) | -43(10) |
| C43 | 158(11) | 184(12) | 192(13) | -19(10) | 5(9) | -32(9) |
| O14 | 218(13) | 216(12) | 211(13) | -24(11) | -14(11) | 22(10) |
| C14 | 216(15) | 226(12) | 221(14) | -10(11) | -17(12) | 5(11) |

| | | | | | | |
|---|---|---|---|---|---|---|
| C24 | 212(14) | 227(14) | 227(13) | -5(10) | -21(11) | 0(12) |
| C34 | 204(14) | 227(13) | 203(13) | 1(11) | -14(11) | 8(12) |
| C44 | 211(14) | 221(11) | 188(14) | -6(11) | -12(11) | 27(11) |
| O15 | 219(12) | 224(11) | 222(14) | -18(11) | -16(11) | 18(10) |
| C15 | 217(13) | 225(13) | 234(15) | -7(12) | -20(11) | 2(11) |
| C25 | 211(12) | 221(14) | 204(14) | 7(13) | -20(12) | 12(10) |
| C35 | 204(14) | 222(11) | 203(14) | 0(12) | -5(12) | 21(10) |
| C45 | 210(13) | 211(13) | 186(14) | -5(11) | -6(12) | 20(11) |
| O16 | 480(60) | 470(60) | 480(60) | 0(19) | -1(19) | -1(18) |
| C16 | 480(60) | 480(60) | 480(60) | 1(19) | -4(17) | 0(19) |
| C26 | 480(60) | 480(60) | 480(60) | 0(20) | -3(19) | 2(17) |
| C36 | 470(60) | 470(60) | 470(60) | -3(19) | 0(20) | -1(16) |
| C46 | 470(60) | 470(60) | 470(60) | -3(19) | 0(20) | -2(18) |

## Crystal structure determination of $^{\text{Cy}}\text{Y}_2\text{Ge}$

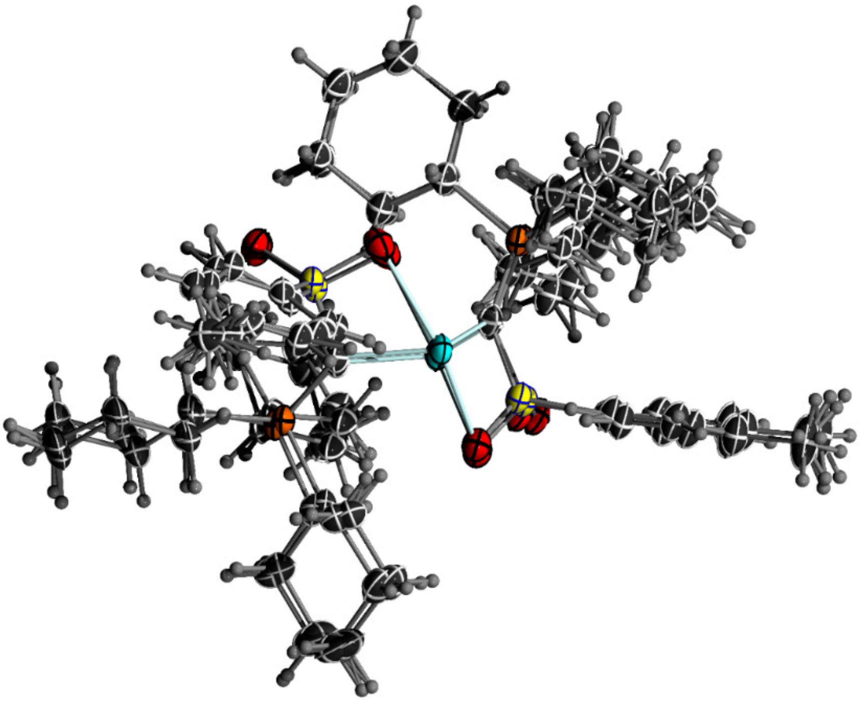

**Figure 56.** ORTEP plot of **$^{\text{Cy}}\text{Y}_2\text{Ge}$**. Ellipsoids drawn at 50% probability level.

**Table 22.** Atomic Coordinates (×$10^4$) and Equivalent Isotropic Displacement Parameters (Å$^2$×$10^3$) for **$^{\text{Cy}}\text{Y}_2\text{Ge}$**. $U_{eq}$ is defined as 1/3 of of the trace of the orthogonalised $U_{ij}$ tensor.

| | *x* | *y* | *z* | U(eq) |
|---|---|---|---|---|
| Ge(1) | 7916.4(5) | 3810.9(4) | 2871.5(2) | 31.43(17) |
| S(1) | 6484.5(13) | 4696.7(13) | 3839.2(4) | 28.6(3) |
| P(2) | 6341.5(12) | 5763.9(10) | 1974.5(4) | 25.5(2) |
| S(2) | 7179.1(10) | 3257.3(9) | 1856.6(4) | 29.7(2) |
| P(1) | 5789.8(15) | 2509.2(15) | 3632.0(7) | 30.9(3) |
| O(1) | 5197(3) | 5216(3) | 4103.4(14) | 37.4(6) |
| O(4) | 6111(3) | 3084(3) | 1541.7(11) | 37.4(6) |
| O(2) | 7134(3) | 5377(2) | 3457.5(11) | 37.0(6) |
| O(3) | 7672(3) | 2405(2) | 2275.6(12) | 38.3(6) |
| C(3) | 7125(4) | 4633(4) | 4913.1(15) | 30.0(9) |
| C(35) | 5490(4) | 5737(3) | 1342.5(14) | 29.4(7) |
| C(2) | 7589(4) | 4409(3) | 4379.5(14) | 28.4(7) |
| C(27) | 6884(3) | 4437(3) | 2209.6(13) | 25.4(7) |
| C(41) | 7692(4) | 6483(3) | 1808.4(16) | 30.0(8) |
| C(9) | 5389(5) | 2443(4) | 4370.9(16) | 37.5(9) |
| C(42) | 8545(4) | 6475(4) | 2297.9(16) | 31.9(9) |
| C(47) | 5255(4) | 6646(3) | 2500.6(15) | 30.6(8) |
| C(5) | 9325(5) | 3801(5) | 5215.7(16) | 34.5(8) |
| C(40) | 4162(4) | 5394(4) | 1435.7(15) | 32.5(8) |
| C(4) | 7991(5) | 4325(5) | 5325.8(14) | 33.3(8) |
| C(6) | 9774(4) | 3594(5) | 4670.5(16) | 36.4(9) |
| C(1) | 6558(4) | 3562(3) | 3467.2(14) | 27.6(7) |
| C(15) | 4184(4) | 2663(3) | 3316.0(16) | 34.1(8) |

| | | | | |
|---|---|---|---|---|
| C(52) | 4194(4) | 6115(4) | 2766.9(15) | 32.2(11) |
| C(14) | 6628(6) | 2006(9) | 4698.8(18) | 40.8(10) |
| C(51) | 3406(4) | 6827(5) | 3236.2(16) | 38.1(12) |
| C(21) | 6854(5) | 1194(4) | 3355(2) | 39.7(9) |
| C(36) | 5287(4) | 6783(3) | 988.2(17) | 35.4(9) |
| C(7) | 8919(4) | 3882(4) | 4255.3(15) | 34.6(8) |
| C(46) | 8600(4) | 5940(4) | 1318.5(18) | 34.9(11) |
| C(28) | 8573(4) | 3097(4) | 1361.9(16) | 34.4(8) |
| C(32) | 10925(4) | 2906(4) | 1167.0(16) | 36.8(9) |
| C(45) | 9678(4) | 6573(4) | 1178.0(19) | 39.1(11) |
| C(48) | 4655(8) | 7837(4) | 2322(3) | 39.6(12) |
| C(50) | 2804(6) | 8015(5) | 3057(2) | 41.4(13) |
| C(30) | 9447(5) | 3137(5) | 446.1(16) | 44.7(12) |
| C(29) | 8374(4) | 3176(6) | 820.6(17) | 39.3(10) |
| C(16) | 3173(4) | 3714(4) | 3540(2) | 37.9(10) |
| C(44) | 10514(4) | 6598(4) | 1660.8(19) | 41.8(11) |
| C(26) | 8309(5) | 1024(5) | 3467(3) | 44.5(14) |
| C(43) | 9654(5) | 7081(5) | 2160.3(18) | 40.3(11) |
| C(39) | 3675(4) | 5132(4) | 891.2(17) | 40.5(10) |
| C(31) | 10749(4) | 3005(4) | 616.0(16) | 40.6(10) |
| C(33) | 9863(4) | 2949(5) | 1542.8(16) | 36.0(9) |
| C(8) | 10244(5) | 3452(5) | 5663.5(18) | 44.5(11) |
| C(22) | 6322(8) | 162(4) | 3506(3) | 47.4(11) |
| C(37) | 4794(4) | 6543(4) | 441.0(16) | 41.3(10) |
| C(49) | 3875(9) | 8546(5) | 2792(3) | 46.1(14) |
| C(10) | 4298(5) | 1822(4) | 4546(2) | 45.6(13) |
| C(38) | 3508(5) | 6104(4) | 513.4(18) | 43.6(11) |
| C(24) | 8629(9) | -1031(5) | 3334(4) | 59.1(16) |
| C(13) | 6249(9) | 2185(8) | 5306.9(19) | 52.4(13) |
| C(25) | 9152(7) | -4(6) | 3168(4) | 52.3(16) |
| C(20) | 4369(4) | 2713(4) | 2697.5(17) | 40.4(10) |
| C(12) | 5141(9) | 1596(4) | 5483.9(19) | 61.4(15) |
| C(23) | 7189(10) | -882(4) | 3224(2) | 58.3(13) |
| C(34) | 11913(5) | 3003(6) | 215(2) | 57.4(14) |
| C(19) | 3031(5) | 2890(5) | 2435(2) | 50.8(12) |
| C(18) | 2020(5) | 3928(5) | 2662(2) | 48.0(12) |
| C(17) | 1831(5) | 3870(5) | 3272(2) | 45.9(11) |
| C(11) | 3934(7) | 1968(5) | 5156(2) | 57.6(16) |
| Ge(1A) | 7279(7) | 3748(4) | 2726(2) | 31.43(17) |
| O(2A) | 6900(30) | 5292(16) | 3329(7) | 37.0(6) |
| O(3A) | 7160(30) | 2354(12) | 2163(6) | 38.3(6) |
| C(27A) | 6280(20) | 4430(11) | 2074(5) | 25.4(7) |
| C(1A) | 6100(20) | 3565(18) | 3389(5) | 27.6(7) |
| S(1A) | 6320(20) | 4650(16) | 3754(6) | 28.6(3) |
| S(2A) | 6873(15) | 3232(11) | 1737(4) | 29.7(2) |
| P(2A) | 6132(18) | 5796(11) | 1876(6) | 25.5(2) |
| P(1A) | 5570(20) | 2449(18) | 3658(8) | 30.9(3) |
| O(1A) | 5090(30) | 5260(30) | 4055(13) | 37.4(6) |

| | | | | |
|---|---|---|---|---|
| C(2A) | 7490(30) | 4310(30) | 4249(9) | 28.4(7) |
| C(7A) | 8840(30) | 3890(50) | 4102(12) | 34.6(8) |
| O(4A) | 5970(30) | 3030(20) | 1333(10) | 37.4(6) |
| C(28A) | 8430(20) | 3130(40) | 1357(9) | 34.4(8) |
| C(35A) | 5320(30) | 5970(20) | 1231(11) | 29.4(7) |
| C(41A) | 7650(30) | 6270(30) | 1800(12) | 30.0(8) |
| C(47A) | 5090(30) | 6690(20) | 2423(14) | 30.6(8) |
| C(9A) | 5230(40) | 2510(40) | 4395(9) | 37.5(9) |
| C(15A) | 3940(30) | 2430(30) | 3363(12) | 34.1(8) |
| C(21A) | 6710(40) | 1160(20) | 3410(20) | 39.7(9) |
| C(3A) | 7160(40) | 4730(60) | 4779(11) | 30.0(9) |
| C(6A) | 9740(30) | 3650(70) | 4504(14) | 36.4(9) |
| C(29A) | 8530(30) | 3050(60) | 801(9) | 39.3(10) |
| C(33A) | 9600(30) | 3080(60) | 1629(12) | 36.0(9) |
| C(40A) | 4100(40) | 5470(40) | 1258(14) | 32.5(8) |
| C(36A) | 5060(50) | 7090(30) | 957(15) | 35.4(9) |
| C(42A) | 8360(40) | 6260(60) | 2330(13) | 31.9(9) |
| C(46A) | 8650(40) | 5710(50) | 1347(18) | 34.9(11) |
| C(52A) | 3980(50) | 6170(40) | 2660(20) | 32.2(11) |
| C(48A) | 4560(90) | 7900(20) | 2260(30) | 39.6(12) |
| C(37A) | 4600(50) | 6980(40) | 383(12) | 41.3(10) |
| C(14A) | 6470(50) | 2010(100) | 4715(14) | 40.8(10) |
| C(10A) | 4050(60) | 2020(70) | 4617(16) | 45.6(13) |
| C(16A) | 2980(40) | 3590(50) | 3490(20) | 37.9(10) |
| C(20A) | 4240(30) | 2320(40) | 2735(12) | 40.4(10) |
| C(26A) | 8140(40) | 1010(50) | 3540(50) | 44.5(14) |
| C(22A) | 6200(70) | 100(20) | 3530(30) | 47.4(11) |
| C(13A) | 6170(80) | 2260(90) | 5322(13) | 52.4(13) |
| C(4A) | 8010(40) | 4340(70) | 5184(11) | 33.3(8) |
| C(5A) | 9340(40) | 3780(70) | 5055(13) | 34.5(8) |
| C(30A) | 9740(30) | 2950(60) | 511(11) | 44.7(12) |
| C(32A) | 10790(30) | 3010(50) | 1333(14) | 36.8(9) |
| C(39A) | 3610(40) | 5390(40) | 698(15) | 40.5(10) |
| C(43A) | 9490(50) | 6870(60) | 2240(20) | 40.3(11) |
| C(45A) | 9770(40) | 6330(60) | 1253(18) | 39.1(11) |
| C(51A) | 3190(60) | 6870(50) | 3140(20) | 38.1(12) |
| C(49A) | 3770(110) | 8590(30) | 2740(40) | 46.1(14) |
| C(38A) | 3340(40) | 6480(40) | 416(16) | 43.6(11) |
| C(11A) | 3780(80) | 2190(70) | 5225(18) | 57.6(16) |
| C(17A) | 1690(40) | 3730(60) | 3200(20) | 45.9(11) |
| C(19A) | 2920(40) | 2440(40) | 2460(16) | 50.8(12) |
| C(25A) | 9040(60) | 10(70) | 3240(60) | 52.3(16) |
| C(23A) | 7120(90) | -910(30) | 3243.81 | 58.3(13) |
| C(12A) | 5010(100) | 1761.2 | 5535(12) | 61.4(15) |
| C(8A) | 10300(50) | 3470(80) | 5488(18) | 44.5(11) |
| C(31A) | 10920(30) | 2900(50) | 777(15) | 40.6(10) |
| C(44A) | 10460(30) | 6360(60) | 1780(20) | 41.8(11) |
| C(50A) | 2650(70) | 8080(60) | 2970(30) | 41.4(13) |

| | | | | |
|---|---|---|---|---|
| C(18A) | 2000(50) | 3610(50) | 2590(20) | 48.0(12) |
| C(24A) | 8540(90) | -1040(50) | 3380(50) | 59.1(16) |
| C(34A) | 12240(30) | 2830(60) | 460(19) | 57.4(14) |

**Table 23.** Anisotropic displacement parameters (Å$^2$×10$^3$) for **$^{Cy}$Y$_2$Ge.** The anisotropic displacement factor exponent takes the form: $-2p^2[ h^2 a^{*2}U^{11} + ... + 2 h k a^* b^* U^{12} ]$

| | $U^{11}$ | $U^{22}$ | $U^{33}$ | $U^{23}$ | $U^{13}$ | $U^{12}$ |
|---|---|---|---|---|---|---|
| Ge(1) | 36.5(3) | 35.8(2) | 20.4(2) | 1.32(16) | 3.58(19) | -6.93(19) |
| S(1) | 30.3(6) | 31.9(4) | 23.1(5) | 0.2(4) | 3.7(4) | -7.8(4) |
| P(2) | 22.7(6) | 32.2(4) | 20.1(6) | 1.0(4) | 2.3(3) | -4.2(4) |
| S(2) | 28.8(6) | 35.5(4) | 23.7(5) | -1.7(4) | 2.5(3) | -6.0(4) |
| P(1) | 31.8(8) | 31.0(5) | 28.3(4) | -0.6(3) | 11.9(4) | -8.0(4) |
| O(1) | 32.7(14) | 42.1(14) | 31.9(13) | -4.6(11) | 4.8(11) | 0.5(11) |
| O(4) | 36.7(15) | 48.5(16) | 28.1(14) | -12.2(12) | 2.7(13) | -13.2(12) |
| O(2) | 45.6(17) | 41.3(14) | 28.6(13) | 5.1(11) | -4.9(12) | -19.0(12) |
| O(3) | 40.2(16) | 38.8(14) | 33.4(14) | -0.7(11) | 7.1(12) | -7.0(12) |
| C(3) | 30.6(17) | 31.2(19) | 26.8(18) | -1.4(18) | 6.4(16) | -6.6(14) |
| C(35) | 28.1(17) | 36(2) | 20.4(16) | 2.2(13) | 2.9(13) | -2.2(15) |
| C(2) | 31.9(17) | 31.6(17) | 22.9(17) | -0.6(14) | 1.7(14) | -11.1(14) |
| C(27) | 22.4(16) | 31.8(16) | 20.1(14) | 1.0(12) | 0.4(12) | -3.4(13) |
| C(41) | 28.9(16) | 29(2) | 30.2(16) | 0.4(14) | 7.1(13) | -5.7(14) |
| C(9) | 44(2) | 32.5(18) | 33.5(17) | -0.2(14) | 17.8(15) | -10.0(17) |
| C(42) | 25.5(19) | 40(3) | 32.0(17) | 0.6(15) | 2.4(14) | -12.1(14) |
| C(47) | 26.7(18) | 37.1(18) | 25.7(17) | -0.2(13) | 5.2(14) | -4.8(14) |
| C(5) | 38.2(19) | 34.7(18) | 31(2) | -1(2) | -0.3(18) | -11.3(15) |
| C(40) | 29.0(17) | 45(2) | 21.6(19) | -2.0(17) | 1.6(15) | -5.9(15) |
| C(4) | 42(2) | 35.5(18) | 22.7(18) | -3(2) | 6.1(17) | -11.4(15) |
| C(6) | 30.6(18) | 44(2) | 32(2) | -1(2) | 5.5(17) | -4.3(15) |
| C(1) | 23.1(17) | 31.3(16) | 27.2(16) | 0.7(13) | 5.3(13) | -5.9(14) |
| C(15) | 31.2(19) | 38(2) | 35.7(18) | -5.3(15) | 10.9(15) | -16.6(15) |
| C(52) | 30(2) | 38.5(19) | 26(2) | -1.7(16) | 3.6(16) | -4.8(16) |
| C(14) | 62(3) | 32.9(18) | 28.4(17) | -0.3(14) | 13.3(17) | -17(2) |
| C(51) | 32(2) | 46(2) | 30(2) | 0.3(18) | 8.1(18) | 0.7(18) |
| C(21) | 46(2) | 37.7(19) | 30.9(19) | 0.8(14) | 11.8(16) | -4.9(16) |
| C(36) | 34(2) | 38(2) | 30.0(17) | 4.7(16) | 0.1(15) | -1.7(18) |
| C(7) | 32.5(18) | 44(2) | 25.8(19) | -5(2) | 8.3(15) | -8.9(15) |
| C(46) | 33.4(18) | 39(3) | 29.1(17) | 0.6(17) | 6.7(14) | -5.6(17) |
| C(28) | 32.9(18) | 37.1(18) | 28.5(16) | -2.5(13) | 4.7(14) | -0.5(15) |
| C(32) | 30.0(18) | 52(2) | 26(2) | -6.3(19) | 1.9(15) | -5.8(17) |
| C(45) | 31.9(19) | 47(3) | 35(2) | 6.3(18) | 9.7(15) | -6.5(18) |
| C(48) | 39(2) | 35.8(19) | 39(3) | -1.0(15) | 9(2) | -2.8(16) |
| C(50) | 36(2) | 45(2) | 35(3) | -2.6(19) | 3(2) | 6.9(17) |
| C(30) | 38(2) | 70(3) | 22.3(17) | -0.5(18) | 1.0(16) | -6(2) |
| C(29) | 32(2) | 52(3) | 32.5(18) | -4.8(16) | 1.8(14) | -8.0(19) |
| C(16) | 34(2) | 40(2) | 38(2) | -2.3(16) | 8.6(16) | -10.2(17) |
| C(44) | 29.2(18) | 52(3) | 44(3) | 4.3(19) | 8.1(17) | -11.7(18) |
| C(26) | 49(3) | 31.9(19) | 46(4) | -0.8(18) | 12(2) | -2.0(18) |
| C(43) | 33(2) | 53(3) | 39(2) | -1.5(19) | 3.5(17) | -19.0(18) |

| | | | | | | |
|---|---|---|---|---|---|---|
| C(39) | 35(2) | 59(3) | 27(2) | -4.4(18) | -1.4(17) | -8.8(19) |
| C(31) | 39(2) | 57(3) | 24.5(19) | -0.8(19) | 5.7(16) | -10.2(19) |
| C(33) | 35(2) | 46(2) | 23.6(17) | -3.7(16) | 6.9(14) | -5(2) |
| C(8) | 49(2) | 46(2) | 38(2) | 0(3) | -9(2) | -10.4(19) |
| C(22) | 62(3) | 34(2) | 45(2) | -6.4(17) | 10(2) | -11.9(19) |
| C(37) | 39(2) | 53(3) | 26.6(17) | 8.7(18) | 0.4(15) | 0(2) |
| C(49) | 46(3) | 42(2) | 45(3) | -9.4(18) | 8(2) | -2.1(18) |
| C(10) | 52(3) | 39(3) | 44(2) | 4.1(18) | 19.5(19) | -13(2) |
| C(38) | 40(2) | 61(3) | 26.6(19) | 0.8(19) | -8.4(16) | -3(2) |
| C(24) | 85(4) | 39(2) | 42(3) | -8.2(18) | -2(3) | 8(2) |
| C(13) | 88(4) | 40(3) | 29.9(18) | -1.1(16) | 17(2) | -23(2) |
| C(25) | 52(3) | 50(2) | 42(4) | -1(2) | 8(2) | 10(2) |
| C(20) | 34(2) | 48(3) | 39(2) | -6.8(18) | 8.1(16) | -13.2(18) |
| C(12) | 109(5) | 46(2) | 34(2) | -3.2(18) | 28(3) | -36(3) |
| C(23) | 79(4) | 38(2) | 53(2) | -10.7(19) | 7(2) | -7(2) |
| C(34) | 40(2) | 105(4) | 29(2) | -6(2) | 7.8(18) | -23(3) |
| C(19) | 42(2) | 65(3) | 49(2) | -12(2) | 0.5(19) | -21(2) |
| C(18) | 36(2) | 61(3) | 51(3) | -5(2) | -3.0(18) | -18(2) |
| C(17) | 35(2) | 51(3) | 54(3) | -5(2) | 5.4(18) | -15.6(19) |
| C(11) | 79(4) | 42(3) | 50(3) | -2(2) | 37(3) | -21(3) |
| Ge(1A) | 36.5(3) | 35.8(2) | 20.4(2) | 1.32(16) | 3.58(19) | -6.93(19) |
| O(2A) | 45.6(17) | 41.3(14) | 28.6(13) | 5.1(11) | -4.9(12) | -19.0(12) |
| O(3A) | 40.2(16) | 38.8(14) | 33.4(14) | -0.7(11) | 7.1(12) | -7.0(12) |
| C(27A) | 22.4(16) | 31.8(16) | 20.1(14) | 1.0(12) | 0.4(12) | -3.4(13) |
| C(1A) | 23.1(17) | 31.3(16) | 27.2(16) | 0.7(13) | 5.3(13) | -5.9(14) |
| S(1A) | 30.3(6) | 31.9(4) | 23.1(5) | 0.2(4) | 3.7(4) | -7.8(4) |
| S(2A) | 28.8(6) | 35.5(4) | 23.7(5) | -1.7(4) | 2.5(3) | -6.0(4) |
| P(2A) | 22.7(6) | 32.2(4) | 20.1(6) | 1.0(4) | 2.3(3) | -4.2(4) |
| P(1A) | 31.8(8) | 31.0(5) | 28.3(4) | -0.6(3) | 11.9(4) | -8.0(4) |
| O(1A) | 32.7(14) | 42.1(14) | 31.9(13) | -4.6(11) | 4.8(11) | 0.5(11) |
| C(2A) | 31.9(17) | 31.6(17) | 22.9(17) | -0.6(14) | 1.7(14) | -11.1(14) |
| C(7A) | 32.5(18) | 44(2) | 25.8(19) | -5(2) | 8.3(15) | -8.9(15) |
| O(4A) | 36.7(15) | 48.5(16) | 28.1(14) | -12.2(12) | 2.7(13) | -13.2(12) |
| C(28A) | 32.9(18) | 37.1(18) | 28.5(16) | -2.5(13) | 4.7(14) | -0.5(15) |
| C(35A) | 28.1(17) | 36(2) | 20.4(16) | 2.2(13) | 2.9(13) | -2.2(15) |
| C(41A) | 28.9(16) | 29(2) | 30.2(16) | 0.4(14) | 7.1(13) | -5.7(14) |
| C(47A) | 26.7(18) | 37.1(18) | 25.7(17) | -0.2(13) | 5.2(14) | -4.8(14) |
| C(9A) | 44(2) | 32.5(18) | 33.5(17) | -0.2(14) | 17.8(15) | -10.0(17) |
| C(15A) | 31.2(19) | 38(2) | 35.7(18) | -5.3(15) | 10.9(15) | -16.6(15) |
| C(21A) | 46(2) | 37.7(19) | 30.9(19) | 0.8(14) | 11.8(16) | -4.9(16) |
| C(3A) | 30.6(17) | 31.2(19) | 26.8(18) | -1.4(18) | 6.4(16) | -6.6(14) |
| C(6A) | 30.6(18) | 44(2) | 32(2) | -1(2) | 5.5(17) | -4.3(15) |
| C(29A) | 32(2) | 52(3) | 32.5(18) | -4.8(16) | 1.8(14) | -8.0(19) |
| C(33A) | 35(2) | 46(2) | 23.6(17) | -3.7(16) | 6.9(14) | -5(2) |
| C(40A) | 29.0(17) | 45(2) | 21.6(19) | -2.0(17) | 1.6(15) | -5.9(15) |
| C(36A) | 34(2) | 38(2) | 30.0(17) | 4.7(16) | 0.1(15) | -1.7(18) |
| C(42A) | 25.5(19) | 40(3) | 32.0(17) | 0.6(15) | 2.4(14) | -12.1(14) |
| C(46A) | 33.4(18) | 39(3) | 29.1(17) | 0.6(17) | 6.7(14) | -5.6(17) |

| | | | | | | |
|---|---|---|---|---|---|---|
| C(52A) | 30(2) | 38.5(19) | 26(2) | -1.7(16) | 3.6(16) | -4.8(16) |
| C(48A) | 39(2) | 35.8(19) | 39(3) | -1.0(15) | 9(2) | -2.8(16) |
| C(37A) | 39(2) | 53(3) | 26.6(17) | 8.7(18) | 0.4(15) | 0(2) |
| C(14A) | 62(3) | 32.9(18) | 28.4(17) | -0.3(14) | 13.3(17) | -17(2) |
| C(10A) | 52(3) | 39(3) | 44(2) | 4.1(18) | 19.5(19) | -13(2) |
| C(16A) | 34(2) | 40(2) | 38(2) | -2.3(16) | 8.6(16) | -10.2(17) |
| C(20A) | 34(2) | 48(3) | 39(2) | -6.8(18) | 8.1(16) | -13.2(18) |
| C(26A) | 49(3) | 31.9(19) | 46(4) | -0.8(18) | 12(2) | -2.0(18) |
| C(22A) | 62(3) | 34(2) | 45(2) | -6.4(17) | 10(2) | -11.9(19) |
| C(13A) | 88(4) | 40(3) | 29.9(18) | -1.1(16) | 17(2) | -23(2) |
| C(4A) | 42(2) | 35.5(18) | 22.7(18) | -3(2) | 6.1(17) | -11.4(15) |
| C(5A) | 38.2(19) | 34.7(18) | 31(2) | -1(2) | -0.3(18) | -11.3(15) |
| C(30A) | 38(2) | 70(3) | 22.3(17) | -0.5(18) | 1.0(16) | -6(2) |
| C(32A) | 30.0(18) | 52(2) | 26(2) | -6.3(19) | 1.9(15) | -5.8(17) |
| C(39A) | 35(2) | 59(3) | 27(2) | -4.4(18) | -1.4(17) | -8.8(19) |
| C(43A) | 33(2) | 53(3) | 39(2) | -1.5(19) | 3.5(17) | -19.0(18) |
| C(45A) | 31.9(19) | 47(3) | 35(2) | 6.3(18) | 9.7(15) | -6.5(18) |
| C(51A) | 32(2) | 46(2) | 30(2) | 0.3(18) | 8.1(18) | 0.7(18) |
| C(49A) | 46(3) | 42(2) | 45(3) | -9.4(18) | 8(2) | -2.1(18) |
| C(38A) | 40(2) | 61(3) | 26.6(19) | 0.8(19) | -8.4(16) | -3(2) |
| C(11A) | 79(4) | 42(3) | 50(3) | -2(2) | 37(3) | -21(3) |
| C(17A) | 35(2) | 51(3) | 54(3) | -5(2) | 5.4(18) | -15.6(19) |
| C(19A) | 42(2) | 65(3) | 49(2) | -12(2) | 0.5(19) | -21(2) |
| C(25A) | 52(3) | 50(2) | 42(4) | -1(2) | 8(2) | 10(2) |
| C(23A) | 79(4) | 38(2) | 53(2) | -10.7(19) | 7(2) | -7(2) |
| C(12A) | 109(5) | 46(2) | 34(2) | -3.2(18) | 28(3) | -36(3) |
| C(8A) | 49(2) | 46(2) | 38(2) | 0(3) | -9(2) | -10.4(19) |
| C(31A) | 39(2) | 57(3) | 24.5(19) | -0.8(19) | 5.7(16) | -10.2(19) |
| C(44A) | 29.2(18) | 52(3) | 44(3) | 4.3(19) | 8.1(17) | -11.7(18) |
| C(50A) | 36(2) | 45(2) | 35(3) | -2.6(19) | 3(2) | 6.9(17) |
| C(18A) | 36(2) | 61(3) | 51(3) | -5(2) | -3.0(18) | -18(2) |
| C(24A) | 85(4) | 39(2) | 42(3) | -8.2(18) | -2(3) | 8(2) |
| C(34A) | 40(2) | 105(4) | 29(2) | -6(2) | 7.8(18) | -23(3) |

## Crystal structure determination of $^{\mathrm{Cy}}\mathrm{Y}_2\mathrm{Sn}$

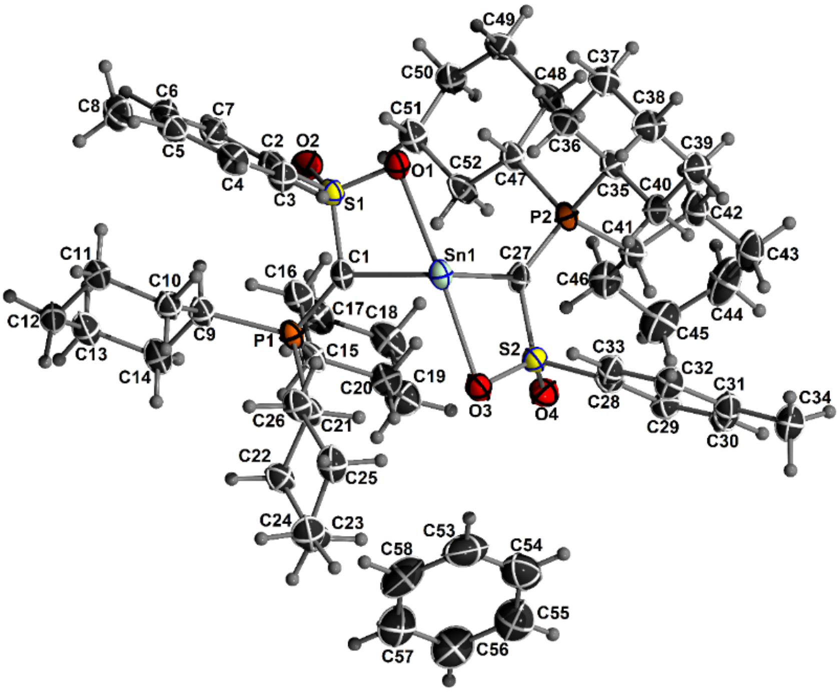
C49
C50
C48
C37
C38
C8
C6
C7
C51
C36
C39
C2
O2
C5
C4
C3
O1
C52
C47
C35
C40
C42
S1
P2
C41
C43
C11
C1
Sn1
C27
C16
C10
C46
C12
C17
C18
C9
C44
C45
P1
C15
S2
C33
C13
C14
C32
C31
C19
C20
O3
O4
C28
C34
C26
C21
C29
C30
C22
C25
C24
C23
C53
C58
C54
C55
C57
C56

**Figure 57.** ORTEP plot of **$^{\mathrm{Cy}}\mathrm{Y}_2\mathrm{Sn}$** containing one benzene molecule. Ellipsoids drawn at 50% probability level.

**Table 24.** Atomic Coordinates (×$10^4$) and Equivalent Isotropic Displacement Parameters (Å$^2$×$10^3$) for **$^{\mathrm{Cy}}\mathrm{Y}_2\mathrm{Sn}$**. $U_{eq}$ is defined as 1/3 of of the trace of the orthogonalised $U_{ij}$ tensor.

| | *x* | *y* | *z* | U(eq) |
|---|---|---|---|---|
| Sn(1) | 2834(1) | 6615(1) | 7989(1) | 28(1) |
| O(1) | 4885(2) | 6241(1) | 8072(1) | 32(1) |
| S(1) | 5234(1) | 6474(1) | 7396(1) | 27(1) |
| P(1) | 3658(1) | 6950(1) | 6202(1) | 25(1) |
| C(1) | 3937(2) | 6723(1) | 7050(1) | 27(1) |
| C(13) | 6066(3) | 7495(1) | 4755(2) | 39(1) |
| C(12) | 6586(3) | 7955(1) | 5150(2) | 37(1) |
| C(11) | 6696(3) | 7872(1) | 5961(2) | 35(1) |
| C(10) | 5466(3) | 7715(1) | 6221(2) | 30(1) |
| C(9) | 5005(3) | 7232(1) | 5835(2) | 30(1) |
| C(8) | 8764(3) | 8168(1) | 8242(2) | 41(1) |
| C(7) | 7437(3) | 6972(1) | 7408(2) | 31(1) |
| C(6) | 8231(3) | 7365(1) | 7600(2) | 33(1) |
| C(5) | 7926(3) | 7733(1) | 8077(2) | 33(1) |
| C(3) | 6005(3) | 7301(1) | 8197(2) | 32(1) |
| O(3) | 800(2) | 6624(1) | 7294(1) | 33(1) |
| C(46) | 902(3) | 4688(1) | 7012(2) | 39(1) |
| C(19) | 1500(3) | 5822(1) | 5189(2) | 42(1) |
| C(30) | -2405(3) | 5744(1) | 8466(2) | 32(1) |
| C(48) | 4102(3) | 4548(1) | 8021(2) | 30(1) |
| C(25) | 1352(3) | 8045(1) | 6930(2) | 38(1) |
| C(47) | 3716(2) | 5075(1) | 7768(1) | 26(1) |
| C(24) | 659(3) | 8231(1) | 6239(2) | 42(1) |
| C(14) | 4860(3) | 7321(1) | 5024(2) | 35(1) |

| | | | | |
|---|---|---|---|---|
| C(52) | 3813(3) | 5131(1) | 6963(1) | 31(1) |
| C(29) | -1564(3) | 5752(1) | 7957(2) | 31(1) |
| P(2) | 2241(1) | 5281(1) | 8064(1) | 24(1) |
| O(2) | 5899(2) | 6156(1) | 6936(1) | 34(1) |
| S(2) | 565(1) | 6080(1) | 7414(1) | 27(1) |
| C(2) | 6316(2) | 6947(1) | 7699(2) | 28(1) |
| C(49) | 5397(3) | 4433(1) | 7823(2) | 33(1) |
| C(26) | 2582(3) | 7809(1) | 6790(2) | 32(1) |
| C(45) | -309(4) | 4419(2) | 6810(2) | 54(1) |
| C(20) | 1959(3) | 6211(1) | 5747(2) | 33(1) |
| C(41) | 985(3) | 4838(1) | 7805(2) | 30(1) |
| C(18) | 2490(3) | 5439(1) | 5059(2) | 41(1) |
| C(4) | 6805(3) | 7689(1) | 8382(2) | 34(1) |
| O(4) | -7(2) | 5811(1) | 6802(1) | 35(1) |
| C(50) | 5512(3) | 4489(1) | 7026(2) | 33(1) |
| C(27) | 1911(2) | 5876(1) | 7771(1) | 25(1) |
| C(40) | 1312(3) | 5445(1) | 9373(2) | 32(1) |
| C(35) | 2459(2) | 5249(1) | 9050(1) | 27(1) |
| C(39) | 1448(3) | 5412(1) | 10184(2) | 38(1) |
| C(34) | -3228(3) | 6059(1) | 9594(2) | 40(1) |
| C(38) | 2578(3) | 5696(1) | 10493(2) | 39(1) |
| C(33) | -447(3) | 6400(1) | 8626(2) | 32(1) |
| C(37) | 3730(3) | 5512(1) | 10178(2) | 35(1) |
| C(32) | -1301(3) | 6386(1) | 9126(2) | 33(1) |
| C(15) | 3112(3) | 6476(1) | 5532(1) | 28(1) |
| C(42) | 903(3) | 4367(1) | 8272(2) | 37(1) |
| C(23) | 522(3) | 7827(1) | 5667(2) | 40(1) |
| C(36) | 3597(3) | 5538(1) | 9359(1) | 30(1) |
| C(31) | -2295(3) | 6056(1) | 9055(2) | 32(1) |
| C(51) | 5115(3) | 5010(1) | 6773(2) | 35(1) |
| C(28) | -569(2) | 6078(1) | 8042(2) | 29(1) |
| C(44) | -462(4) | 3963(2) | 7280(2) | 58(1) |
| C(21) | 2361(3) | 7379(1) | 6251(1) | 28(1) |
| C(17) | 3660(3) | 5694(1) | 4868(2) | 39(1) |
| C(16) | 4117(3) | 6087(1) | 5421(2) | 34(1) |
| C(43) | -317(3) | 4103(1) | 8070(2) | 46(1) |
| C(22) | 1750(3) | 7583(1) | 5541(2) | 33(1) |
| C(53) | -1366(4) | 6476(2) | 5288(3) | 70(1) |
| C(54) | -2304(4) | 6134(2) | 5205(3) | 67(1) |
| C(55) | -2913(4) | 6060(2) | 4544(2) | 59(1) |
| C(56) | -2601(4) | 6328(2) | 3963(2) | 55(1) |
| C(57) | -1663(4) | 6666(2) | 4039(2) | 55(1) |
| C(58) | -1042(4) | 6738(2) | 4701(2) | 62(1) |

**Table 25.** Anisotropic displacement parameters (Å$^2$×10$^3$) for **$^{Cy}$Y$_2$Sn.** The anisotropic displacement factor exponent takes the form: $-2p^2[\ h^2\ a^{*2}U^{11} + ... + 2\ h\ k\ a^*\ b^*\ U^{12}\ ]$

| | $U^{11}$ | $U^{22}$ | $U^{33}$ | $U^{23}$ | $U^{13}$ | $U^{12}$ |
|---|---|---|---|---|---|---|
| Sn(1) | 33(1) | 22(1) | 28(1) | 0(1) | 6(1) | -2(1) |
| O(1) | 34(1) | 27(1) | 34(1) | 6(1) | 3(1) | -5(1) |
| S(1) | 29(1) | 22(1) | 30(1) | 1(1) | 3(1) | -1(1) |
| P(1) | 31(1) | 20(1) | 26(1) | 1(1) | 6(1) | 1(1) |
| C(1) | 29(1) | 26(1) | 26(1) | 3(1) | 8(1) | -3(1) |
| C(13) | 48(2) | 33(2) | 38(2) | 7(1) | 15(1) | 3(1) |
| C(12) | 34(2) | 35(2) | 44(2) | 10(1) | 12(1) | -1(1) |
| C(11) | 33(2) | 32(2) | 41(2) | 8(1) | 5(1) | -1(1) |
| C(10) | 33(1) | 26(1) | 33(1) | 4(1) | 6(1) | 0(1) |
| C(9) | 33(1) | 24(1) | 33(1) | 3(1) | 9(1) | 2(1) |
| C(8) | 45(2) | 34(2) | 44(2) | -1(1) | 2(1) | -8(1) |
| C(7) | 32(1) | 25(1) | 37(2) | 0(1) | 4(1) | 1(1) |
| C(6) | 29(1) | 31(2) | 40(2) | 3(1) | 4(1) | -1(1) |
| C(5) | 37(2) | 26(1) | 33(1) | 3(1) | -2(1) | -2(1) |
| C(3) | 32(1) | 30(1) | 34(1) | 0(1) | 6(1) | -1(1) |
| O(3) | 37(1) | 27(1) | 34(1) | 7(1) | 8(1) | 4(1) |
| C(46) | 45(2) | 38(2) | 32(2) | -10(1) | 4(1) | -8(1) |
| C(19) | 49(2) | 35(2) | 39(2) | -7(1) | -4(1) | -4(1) |
| C(30) | 27(1) | 29(1) | 41(2) | -1(1) | 2(1) | -3(1) |
| C(48) | 37(2) | 23(1) | 30(1) | 1(1) | 4(1) | 1(1) |
| C(25) | 47(2) | 25(1) | 44(2) | -5(1) | 17(1) | 0(1) |
| C(47) | 30(1) | 22(1) | 27(1) | 0(1) | 6(1) | 0(1) |
| C(24) | 42(2) | 35(2) | 52(2) | 0(1) | 16(1) | 11(1) |
| C(14) | 47(2) | 27(1) | 31(1) | 2(1) | 11(1) | -1(1) |
| C(52) | 41(2) | 29(1) | 26(1) | 2(1) | 7(1) | 8(1) |
| C(29) | 30(1) | 30(1) | 33(1) | -1(1) | 1(1) | 1(1) |
| P(2) | 29(1) | 21(1) | 24(1) | 0(1) | 4(1) | -1(1) |
| O(2) | 34(1) | 27(1) | 40(1) | -4(1) | 6(1) | 2(1) |
| S(2) | 29(1) | 26(1) | 28(1) | 2(1) | 4(1) | 1(1) |
| C(2) | 31(1) | 22(1) | 32(1) | 3(1) | 0(1) | 0(1) |
| C(49) | 38(2) | 25(1) | 35(2) | -1(1) | 3(1) | 6(1) |
| C(26) | 41(2) | 23(1) | 35(1) | -2(1) | 8(1) | 1(1) |
| C(45) | 54(2) | 62(2) | 46(2) | -24(2) | 0(2) | -15(2) |
| C(20) | 39(2) | 30(1) | 30(1) | -4(1) | 4(1) | -2(1) |
| C(41) | 31(1) | 27(1) | 31(1) | -2(1) | 4(1) | -2(1) |
| C(18) | 65(2) | 26(2) | 31(2) | -7(1) | -2(1) | -2(1) |
| C(4) | 42(2) | 30(2) | 30(1) | -1(1) | 2(1) | 0(1) |
| O(4) | 33(1) | 42(1) | 31(1) | 1(1) | 2(1) | 0(1) |
| C(50) | 37(2) | 27(1) | 36(2) | -1(1) | 8(1) | 4(1) |
| C(27) | 26(1) | 20(1) | 30(1) | -1(1) | 7(1) | -3(1) |
| C(40) | 32(1) | 36(2) | 29(1) | 2(1) | 6(1) | 1(1) |
| C(35) | 31(1) | 26(1) | 25(1) | 0(1) | 5(1) | 0(1) |
| C(39) | 36(2) | 50(2) | 28(1) | 3(1) | 8(1) | 5(1) |
| C(34) | 39(2) | 40(2) | 42(2) | -3(1) | 11(1) | -6(1) |
| C(38) | 41(2) | 50(2) | 27(1) | -5(1) | 5(1) | 7(1) |

| | | | | | | |
|---|---|---|---|---|---|---|
| C(33) | 30(1) | 29(1) | 37(2) | -1(1) | 6(1) | 0(1) |
| C(37) | 38(2) | 38(2) | 28(1) | -2(1) | 1(1) | 0(1) |
| C(32) | 32(1) | 32(2) | 34(1) | -5(1) | 5(1) | -2(1) |
| C(15) | 40(2) | 24(1) | 21(1) | 0(1) | 5(1) | 1(1) |
| C(42) | 41(2) | 25(1) | 45(2) | 1(1) | 10(1) | -5(1) |
| C(23) | 37(2) | 39(2) | 45(2) | 0(1) | 4(1) | 10(1) |
| C(36) | 33(1) | 33(1) | 24(1) | -1(1) | 2(1) | 0(1) |
| C(31) | 31(1) | 28(1) | 38(2) | 2(1) | 7(1) | -1(1) |
| C(51) | 45(2) | 25(1) | 36(2) | -1(1) | 15(1) | 4(1) |
| C(28) | 28(1) | 28(1) | 32(1) | 2(1) | 1(1) | 4(1) |
| C(44) | 52(2) | 47(2) | 75(3) | -26(2) | 13(2) | -23(2) |
| C(21) | 32(1) | 21(1) | 31(1) | 1(1) | 7(1) | 0(1) |
| C(17) | 60(2) | 28(2) | 31(1) | -2(1) | 10(1) | 5(1) |
| C(16) | 44(2) | 24(1) | 34(2) | -2(1) | 11(1) | 2(1) |
| C(43) | 48(2) | 31(2) | 62(2) | -3(1) | 15(2) | -11(1) |
| C(22) | 37(2) | 30(1) | 32(1) | 2(1) | 4(1) | 5(1) |
| C(53) | 48(2) | 97(4) | 63(3) | 5(2) | -6(2) | 18(2) |
| C(54) | 65(3) | 61(3) | 75(3) | 16(2) | 15(2) | 20(2) |
| C(55) | 60(2) | 47(2) | 73(3) | -11(2) | 14(2) | 0(2) |
| C(56) | 56(2) | 56(2) | 53(2) | -22(2) | 8(2) | 2(2) |
| C(57) | 57(2) | 53(2) | 57(2) | -10(2) | 18(2) | 5(2) |
| C(58) | 39(2) | 76(3) | 71(3) | -20(2) | 4(2) | -4(2) |

## Crystal structure determination of ($^{Cy}$YSnCl)$_2$ (170)

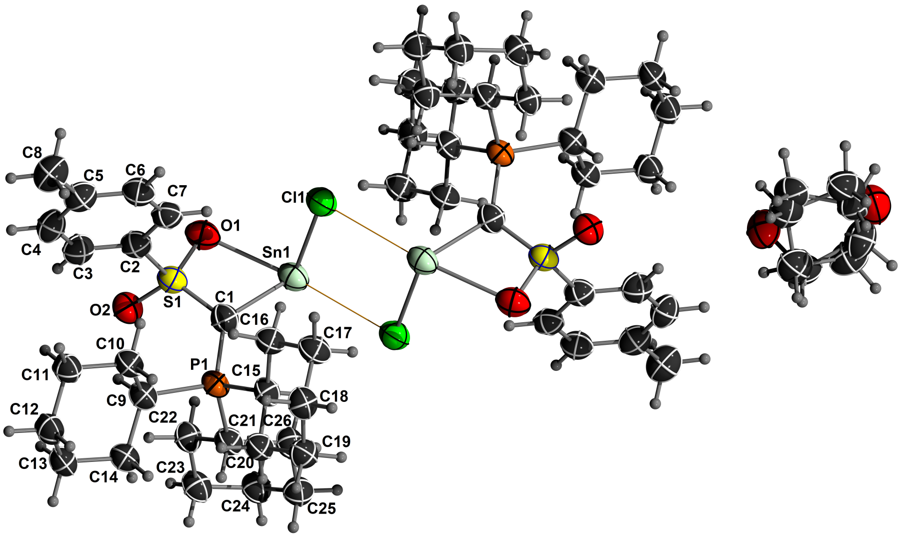

**Figure 58.** ORTEP plot of **170** containing one THF molecule (disordered). Ellipsoids drawn at 50% probability level.

**Table 26.** Atomic Coordinates (×10$^4$) and Equivalent Isotropic Displacement Parameters (Å$^2$×10$^3$) for **170**. U$_{eq}$ is defined as 1/3 of of the trace of the orthogonalised U$_{ij}$ tensor.

| | *x* | *y* | *z* | **U(eq)** |
|---|---|---|---|---|
| Sn(1) | 5562(1) | 8057(1) | 768(1) | 52(1) |
| P(1) | 2455(1) | 7821(1) | 2484(1) | 43(1) |
| O(1) | 6999(4) | 6879(3) | 2139(3) | 59(1) |
| Cl(1) | 6712(1) | 9977(1) | 560(1) | 58(1) |
| S(1) | 5696(1) | 6813(1) | 2826(1) | 48(1) |
| C(1) | 4336(5) | 7721(4) | 2126(3) | 48(1) |
| C(2) | 6199(5) | 7445(4) | 3624(4) | 47(1) |
| O(2) | 5405(4) | 5584(3) | 3436(3) | 54(1) |
| C(3) | 6220(6) | 6748(5) | 4584(4) | 54(1) |
| C(4) | 6486(6) | 7274(5) | 5211(4) | 54(1) |
| C(5) | 6759(6) | 8479(5) | 4886(4) | 55(1) |
| C(6) | 6751(6) | 9156(5) | 3914(4) | 54(1) |
| C(7) | 6475(5) | 8653(5) | 3275(4) | 49(1) |
| C(8) | 6992(7) | 9054(6) | 5562(5) | 66(1) |
| C(9) | 2174(5) | 7255(4) | 3781(3) | 45(1) |
| C(10) | 2534(5) | 8147(4) | 4216(3) | 46(1) |
| C(11) | 2495(6) | 7544(5) | 5294(3) | 51(1) |
| C(12) | 970(6) | 7138(5) | 5669(4) | 56(1) |
| C(13) | 591(5) | 6267(4) | 5240(3) | 50(1) |
| C(14) | 621(5) | 6836(4) | 4167(3) | 47(1) |
| C(15) | 1586(5) | 9415(4) | 1917(3) | 44(1) |
| C(16) | 2517(5) | 10346(4) | 1982(4) | 48(1) |
| C(17) | 1741(6) | 11658(4) | 1487(4) | 53(1) |
| C(18) | 147(6) | 11815(4) | 1882(4) | 53(1) |
| C(19) | -772(5) | 10936(4) | 1747(4) | 52(1) |
| C(20) | -51(5) | 9605(4) | 2248(4) | 48(1) |
| C(21) | 1417(5) | 6902(4) | 2102(3) | 46(1) |
| C(22) | 2097(5) | 5536(4) | 2529(3) | 48(1) |

| | | | | |
|---|---|---|---|---|
| C(23) | 1190(6) | 4757(4) | 2254(4) | 52(1) |
| C(24) | 1159(6) | 5161(4) | 1191(4) | 53(1) |
| C(25) | 502(6) | 6519(4) | 745(4) | 53(1) |
| C(26) | 1366(6) | 7328(4) | 1019(3) | 50(1) |
| O1A1 | 3751(11) | 7497(8) | 7414(6) | 73(3) |
| C1A1 | 3300(20) | 6291(19) | 7717(12) | 61(4) |
| C2A1 | 3760(20) | 5575(18) | 8715(12) | 61(4) |
| C3A1 | 4170(30) | 6542(17) | 9035(13) | 74(5) |
| C4A1 | 4747(19) | 7458(16) | 8071(14) | 68(4) |
| O1B1 | 3418(16) | 6089(14) | 9251(8) | 93(4) |
| C1B1 | 4520(30) | 6920(20) | 8880(17) | 77(5) |
| C2B1 | 4820(20) | 7156(18) | 7851(14) | 70(5) |
| C3B1 | 3710(30) | 6500(20) | 7626(15) | 67(5) |
| C4B1 | 3330(30) | 5550(20) | 8610(17) | 79(6) |

**Table 27.** Anisotropic displacement parameters ($Å^2 \times 10^3$) for **170**. The anisotropic displacement factor exponent takes the form: $-2p^2[\, h^2 a^{*2} U^{11} + \ldots + 2 h k a^* b^* U^{12}\,]$

| | $U^{11}$ | $U^{22}$ | $U^{33}$ | $U^{23}$ | $U^{13}$ | $U^{12}$ |
|---|---|---|---|---|---|---|
| Sn(1) | 53(1) | 56(1) | 50(1) | -25(1) | 10(1) | -12(1) |
| P(1) | 44(1) | 42(1) | 43(1) | -17(1) | 5(1) | -8(1) |
| O(1) | 50(2) | 65(2) | 64(2) | -31(2) | 10(2) | -6(2) |
| Cl(1) | 59(1) | 62(1) | 55(1) | -22(1) | 5(1) | -21(1) |
| S(1) | 45(1) | 48(1) | 52(1) | -22(1) | 4(1) | -5(1) |
| C(1) | 50(2) | 48(2) | 46(2) | -19(2) | 2(2) | -6(2) |
| C(2) | 42(2) | 52(2) | 50(2) | -24(2) | 2(2) | -3(2) |
| O(2) | 58(2) | 48(2) | 56(2) | -20(2) | -1(2) | -7(1) |
| C(3) | 51(2) | 50(2) | 60(3) | -21(2) | -4(2) | -1(2) |
| C(4) | 56(3) | 54(2) | 52(3) | -22(2) | -8(2) | 3(2) |
| C(5) | 50(2) | 57(3) | 62(3) | -28(2) | -5(2) | 1(2) |
| C(6) | 49(2) | 55(2) | 58(3) | -25(2) | 3(2) | -7(2) |
| C(7) | 40(2) | 56(2) | 53(3) | -23(2) | 3(2) | -6(2) |
| C(8) | 69(3) | 68(3) | 69(3) | -38(3) | -9(3) | 4(2) |
| C(9) | 46(2) | 43(2) | 45(2) | -17(2) | 4(2) | -8(2) |
| C(10) | 47(2) | 43(2) | 47(2) | -16(2) | 3(2) | -8(2) |
| C(11) | 53(3) | 56(2) | 46(2) | -21(2) | 4(2) | -12(2) |
| C(12) | 61(3) | 61(3) | 45(2) | -20(2) | 7(2) | -14(2) |
| C(13) | 53(2) | 47(2) | 46(2) | -12(2) | 7(2) | -11(2) |
| C(14) | 46(2) | 45(2) | 49(2) | -19(2) | 5(2) | -9(2) |
| C(15) | 49(2) | 39(2) | 43(2) | -14(2) | 2(2) | -9(2) |
| C(16) | 47(2) | 46(2) | 51(2) | -19(2) | 1(2) | -9(2) |
| C(17) | 53(3) | 45(2) | 61(3) | -20(2) | 6(2) | -11(2) |
| C(18) | 58(3) | 46(2) | 52(3) | -19(2) | 1(2) | -4(2) |
| C(19) | 49(2) | 45(2) | 55(3) | -14(2) | 0(2) | -3(2) |
| C(20) | 47(2) | 44(2) | 50(2) | -16(2) | 3(2) | -7(2) |
| C(21) | 47(2) | 42(2) | 47(2) | -15(2) | 3(2) | -6(2) |
| C(22) | 55(2) | 42(2) | 46(2) | -16(2) | 1(2) | -7(2) |
| C(23) | 66(3) | 42(2) | 52(3) | -20(2) | 5(2) | -16(2) |

| | | | | | | |
|---|---|---|---|---|---|---|
| C(24) | 64(3) | 46(2) | 51(3) | -19(2) | 0(2) | -13(2) |
| C(25) | 57(3) | 53(2) | 52(3) | -20(2) | -2(2) | -13(2) |
| C(26) | 60(3) | 45(2) | 45(2) | -17(2) | -1(2) | -11(2) |
| O1A1 | 91(6) | 74(6) | 63(5) | -33(4) | -3(4) | -14(4) |
| C1A1 | 56(11) | 74(8) | 62(7) | -39(6) | 6(6) | -5(6) |
| C2A1 | 60(11) | 69(7) | 60(6) | -28(5) | 0(6) | -14(6) |
| C3A1 | 98(17) | 68(11) | 62(7) | -33(7) | -18(7) | 1(7) |
| C4A1 | 56(7) | 68(8) | 87(9) | -38(7) | -4(6) | -5(6) |
| O1B1 | 91(9) | 100(9) | 69(6) | -15(6) | 4(6) | -12(6) |
| C1B1 | 70(10) | 89(15) | 86(11) | -50(11) | -9(8) | -2(8) |
| C2B1 | 61(8) | 65(9) | 80(10) | -26(7) | -2(7) | 2(6) |
| C3B1 | 52(12) | 78(13) | 68(8) | -30(7) | -1(7) | 5(7) |
| C4B1 | 61(14) | 62(8) | 101(12) | -20(7) | 3(9) | -6(7) |

## Crystal structure determination of $^{Cy}$Y(Cl)Ge-Ge(Cl)$^{Cy}$Y (169)

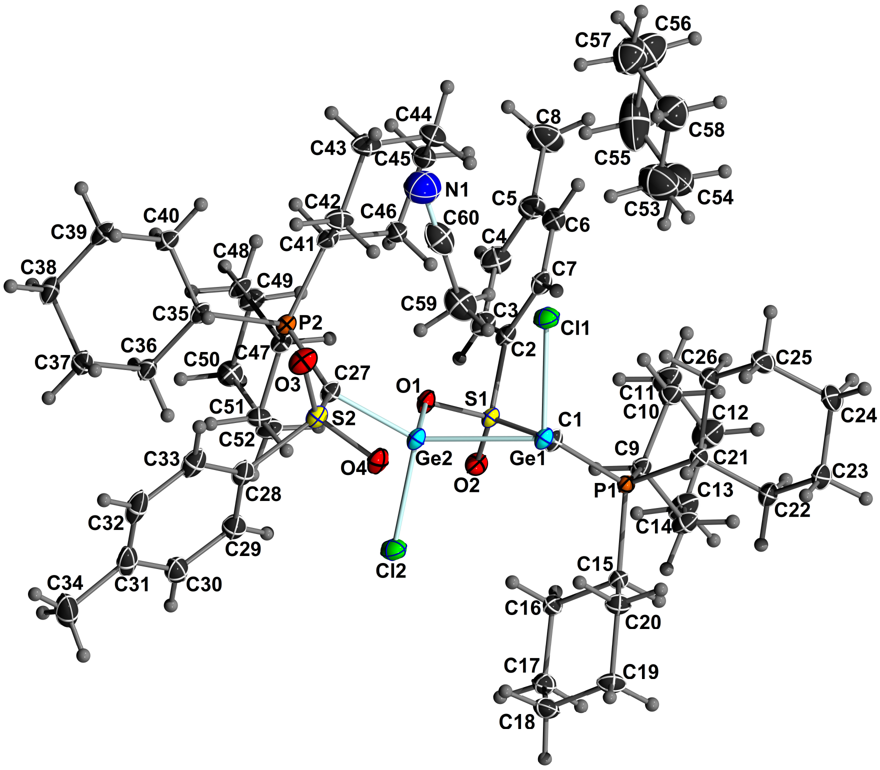
C57
C56
C44
C8
C58
C43
C45
C55
N1
C42
C46
C60
C5
C53
C54
C39
C40
C41
C4
C6
C48
C49
C7
C38
C59
C3
Cl1
C35
P2
C2
C26
C25
C37
C36
C47
C27
C11
C50
O3
O1
S1
C1
C10
C12
C24
C51
S2
C52
C9
C21
C33
O4
Ge2
Ge1
C23
O2
P1
C13
C28
C22
C32
C14
C29
Cl2
C15
C34
C31
C30
C16
C20
C17
C19
C18

**Figure 59.** ORTEP plot of **169** containing non-coordinating solvent molecules (acetonitrile and cyclohexane). Ellipsoids drawn at 50% probability level.

**Table 28.** Atomic Coordinates (×10$^4$) and Equivalent Isotropic Displacement Parameters (Å$^2$×10$^3$) for **169**. U$_{eq}$ is defined as 1/3 of of the trace of the orthogonalised U$_{ij}$ tensor.

| | *x* | *y* | *z* | U(eq) |
|---|---|---|---|---|
| Ge(1) | 3181(1) | 4050(1) | 6613(1) | 15(1) |
| C(1) | 3648(1) | 3232(2) | 6267(1) | 15(1) |
| Cl(1) | 3694(1) | 5138(1) | 7372(1) | 24(1) |
| S(1) | 3882(1) | 2571(1) | 7099(1) | 16(1) |
| P(1) | 3715(1) | 2994(1) | 5301(1) | 13(1) |
| O(1) | 3602(1) | 2937(1) | 7669(1) | 20(1) |
| N(1) | 2454(1) | -505(2) | 6321(2) | 50(1) |
| Ge(2) | 2280(1) | 4187(1) | 6895(1) | 15(1) |
| P(2) | 1762(1) | 6118(1) | 6367(1) | 13(1) |
| O(2) | 3823(1) | 1622(1) | 6944(1) | 23(1) |
| S(2) | 2494(1) | 5446(1) | 5464(1) | 13(1) |
| Cl(2) | 1869(1) | 3054(1) | 5959(1) | 24(1) |
| C(2) | 4604(1) | 2741(2) | 7583(1) | 20(1) |
| C(3) | 4815(1) | 3598(2) | 7707(2) | 23(1) |
| O(3) | 2927(1) | 4728(1) | 5572(1) | 16(1) |
| C(4) | 5374(1) | 3725(2) | 8082(2) | 27(1) |
| O(4) | 2716(1) | 6329(1) | 5447(1) | 18(1) |
| C(5) | 5730(1) | 2997(2) | 8346(2) | 29(1) |
| C(6) | 5510(1) | 2149(2) | 8213(2) | 30(1) |
| C(7) | 4951(1) | 2009(2) | 7835(2) | 25(1) |
| C(8) | 6334(1) | 3156(3) | 8783(2) | 41(1) |

| | | | | |
|---|---|---|---|---|
| C(9) | 4314(1) | 2264(2) | 5421(1) | 16(1) |
| C(10) | 4874(1) | 2747(2) | 5736(2) | 18(1) |
| C(11) | 5342(1) | 2063(2) | 5952(2) | 21(1) |
| C(12) | 5329(1) | 1491(2) | 5204(2) | 23(1) |
| C(13) | 4769(1) | 1047(2) | 4850(2) | 20(1) |
| C(14) | 4298(1) | 1722(2) | 4643(1) | 19(1) |
| C(15) | 3751(1) | 4037(1) | 4767(1) | 14(1) |
| C(16) | 4151(1) | 4736(2) | 5281(1) | 18(1) |
| C(18) | 4136(1) | 5514(2) | 3952(2) | 20(1) |
| C(17) | 4069(1) | 5624(2) | 4812(2) | 20(1) |
| C(19) | 3748(1) | 4803(2) | 3455(1) | 19(1) |
| C(20) | 3836(1) | 3911(2) | 3916(1) | 17(1) |
| C(21) | 3134(1) | 2377(2) | 4616(1) | 16(1) |
| C(22) | 2595(1) | 2911(2) | 4318(2) | 21(1) |
| C(23) | 2152(1) | 2346(2) | 3707(2) | 26(1) |
| C(24) | 2058(1) | 1462(2) | 4083(2) | 30(1) |
| C(25) | 2593(1) | 943(2) | 4416(2) | 25(1) |
| C(26) | 3032(1) | 1506(2) | 5028(2) | 22(1) |
| C(53) | 643(2) | 1793(3) | 5233(3) | 61(1) |
| C(52) | 1386(1) | 7878(2) | 5791(2) | 21(1) |
| C(51) | 1295(1) | 8524(2) | 5064(2) | 28(1) |
| C(50) | 863(1) | 8192(2) | 4291(2) | 31(1) |
| C(49) | 998(1) | 7258(2) | 4057(2) | 27(1) |
| C(48) | 1074(1) | 6619(2) | 4781(1) | 20(1) |
| C(47) | 1540(1) | 6951(2) | 5534(1) | 16(1) |
| C(46) | 845(1) | 4937(2) | 5940(2) | 21(1) |
| C(45) | 442(1) | 4405(2) | 6256(2) | 26(1) |
| C(44) | 60(1) | 5022(2) | 6544(2) | 30(1) |
| C(43) | 395(1) | 5666(2) | 7200(2) | 27(1) |
| C(42) | 802(1) | 6211(2) | 6891(2) | 22(1) |
| C(41) | 1182(1) | 5578(2) | 6604(1) | 17(1) |
| C(40) | 2673(1) | 7123(2) | 7186(1) | 16(1) |
| C(39) | 3004(1) | 7651(2) | 7942(2) | 21(1) |
| C(38) | 3119(1) | 7106(2) | 8734(2) | 24(1) |
| C(37) | 2589(1) | 6727(2) | 8842(1) | 21(1) |
| C(36) | 2272(1) | 6176(2) | 8092(1) | 19(1) |
| C(35) | 2140(1) | 6738(2) | 7301(1) | 14(1) |
| C(34) | 1079(1) | 4807(3) | 1938(2) | 41(1) |
| C(33) | 1675(1) | 4578(2) | 4265(1) | 18(1) |
| C(32) | 1352(1) | 4448(2) | 3454(2) | 22(1) |
| C(31) | 1428(1) | 4958(2) | 2814(2) | 26(1) |
| C(30) | 1839(1) | 5606(2) | 3003(2) | 27(1) |
| C(29) | 2165(1) | 5748(2) | 3807(2) | 21(1) |
| C(28) | 2079(1) | 5235(2) | 4434(1) | 16(1) |
| C(27) | 2152(1) | 5261(2) | 6137(1) | 14(1) |
| C(54) | 469(2) | 2563(3) | 4655(3) | 59(1) |
| C(55) | 545(2) | 2359(3) | 3822(3) | 68(1) |
| C(56) | 246(2) | 1518(3) | 3453(3) | 58(1) |

| | | | | |
|---|---|---|---|---|
| C(57) | 425(2) | 739(2) | 4049(3) | 50(1) |
| C(58) | 346(2) | 953(3) | 4869(2) | 48(1) |
| C(59) | 2536(1) | 1055(2) | 6999(2) | 35(1) |
| C(60) | 2490(1) | 184(2) | 6612(2) | 35(1) |

**Table 29.** Anisotropic displacement parameters ($Å^2 \times 10^3$) for **169**. The anisotropic displacement factor exponent takes the form: $-2p^2[\ h^2\ a^{*2}U^{11} + ... + 2\ h\ k\ a^*\ b^*\ U^{12}\ ]$

| | $U^{11}$ | $U^{22}$ | $U^{33}$ | $U^{23}$ | $U^{13}$ | $U^{12}$ |
|---|---|---|---|---|---|---|
| Ge(1) | 18(1) | 15(1) | 14(1) | 1(1) | 8(1) | 2(1) |
| C(1) | 18(1) | 14(1) | 14(1) | 1(1) | 7(1) | 4(1) |
| Cl(1) | 27(1) | 18(1) | 24(1) | -4(1) | 5(1) | 1(1) |
| S(1) | 20(1) | 16(1) | 14(1) | 3(1) | 7(1) | 3(1) |
| P(1) | 16(1) | 12(1) | 13(1) | 0(1) | 6(1) | 1(1) |
| O(1) | 22(1) | 24(1) | 15(1) | 2(1) | 10(1) | 4(1) |
| N(1) | 54(2) | 44(2) | 53(2) | -7(1) | 18(2) | -8(1) |
| Ge(2) | 18(1) | 15(1) | 14(1) | 1(1) | 8(1) | 2(1) |
| P(2) | 14(1) | 14(1) | 12(1) | -1(1) | 5(1) | 1(1) |
| O(2) | 32(1) | 15(1) | 22(1) | 4(1) | 11(1) | 3(1) |
| S(2) | 16(1) | 13(1) | 13(1) | 1(1) | 7(1) | 1(1) |
| Cl(2) | 27(1) | 18(1) | 24(1) | -4(1) | 5(1) | 1(1) |
| C(2) | 20(1) | 26(1) | 14(1) | 3(1) | 6(1) | 6(1) |
| C(3) | 22(1) | 27(1) | 19(1) | 2(1) | 7(1) | 4(1) |
| O(3) | 18(1) | 18(1) | 14(1) | 2(1) | 7(1) | 5(1) |
| C(4) | 22(1) | 38(2) | 21(1) | -2(1) | 8(1) | 2(1) |
| O(4) | 22(1) | 14(1) | 20(1) | 0(1) | 10(1) | -2(1) |
| C(5) | 21(1) | 51(2) | 16(1) | 2(1) | 8(1) | 9(1) |
| C(6) | 29(1) | 44(2) | 19(1) | 7(1) | 10(1) | 20(1) |
| C(7) | 30(1) | 28(1) | 18(1) | 6(1) | 11(1) | 11(1) |
| C(8) | 21(1) | 72(2) | 27(1) | -1(1) | 5(1) | 9(1) |
| C(9) | 19(1) | 12(1) | 17(1) | 0(1) | 7(1) | 3(1) |
| C(10) | 18(1) | 16(1) | 21(1) | -2(1) | 9(1) | 1(1) |
| C(11) | 19(1) | 20(1) | 25(1) | -1(1) | 8(1) | 3(1) |
| C(12) | 23(1) | 21(1) | 29(1) | -1(1) | 14(1) | 6(1) |
| C(13) | 27(1) | 16(1) | 22(1) | -2(1) | 11(1) | 6(1) |
| C(14) | 24(1) | 16(1) | 17(1) | -2(1) | 7(1) | 4(1) |
| C(15) | 17(1) | 12(1) | 13(1) | 1(1) | 6(1) | 1(1) |
| C(16) | 21(1) | 15(1) | 17(1) | -2(1) | 5(1) | -2(1) |
| C(18) | 25(1) | 15(1) | 22(1) | 4(1) | 9(1) | -1(1) |
| C(17) | 26(1) | 13(1) | 22(1) | -2(1) | 7(1) | -1(1) |
| C(19) | 26(1) | 17(1) | 15(1) | 3(1) | 8(1) | 1(1) |
| C(20) | 23(1) | 14(1) | 15(1) | 1(1) | 9(1) | 1(1) |
| C(21) | 20(1) | 15(1) | 15(1) | -3(1) | 7(1) | -1(1) |
| C(22) | 17(1) | 20(1) | 24(1) | -6(1) | 5(1) | 0(1) |
| C(23) | 20(1) | 25(1) | 30(1) | -9(1) | 2(1) | 2(1) |
| C(24) | 24(1) | 28(1) | 36(2) | -10(1) | 9(1) | -8(1) |
| C(25) | 30(1) | 20(1) | 24(1) | -4(1) | 7(1) | -7(1) |
| C(26) | 28(1) | 19(1) | 20(1) | -1(1) | 7(1) | -6(1) |

| | | | | | | |
|---|---|---|---|---|---|---|
| C(53) | 53(2) | 61(3) | 57(2) | -2(2) | 0(2) | 3(2) |
| C(52) | 29(1) | 18(1) | 16(1) | 0(1) | 6(1) | 6(1) |
| C(51) | 40(2) | 20(1) | 23(1) | 4(1) | 9(1) | 8(1) |
| C(50) | 42(2) | 29(1) | 20(1) | 7(1) | 6(1) | 13(1) |
| C(49) | 34(1) | 32(1) | 14(1) | 1(1) | 4(1) | 9(1) |
| C(48) | 21(1) | 22(1) | 16(1) | -1(1) | 3(1) | 4(1) |
| C(47) | 18(1) | 17(1) | 14(1) | 1(1) | 5(1) | 4(1) |
| C(46) | 19(1) | 24(1) | 21(1) | -6(1) | 9(1) | -3(1) |
| C(45) | 22(1) | 31(1) | 27(1) | -8(1) | 10(1) | -10(1) |
| C(44) | 19(1) | 41(2) | 32(1) | -10(1) | 12(1) | -9(1) |
| C(43) | 21(1) | 36(1) | 28(1) | -10(1) | 15(1) | -5(1) |
| C(42) | 19(1) | 26(1) | 23(1) | -6(1) | 10(1) | 0(1) |
| C(41) | 15(1) | 21(1) | 16(1) | -4(1) | 6(1) | -2(1) |
| C(40) | 16(1) | 18(1) | 15(1) | -2(1) | 6(1) | -2(1) |
| C(39) | 21(1) | 22(1) | 21(1) | -4(1) | 7(1) | -5(1) |
| C(38) | 21(1) | 28(1) | 19(1) | -4(1) | 1(1) | -5(1) |
| C(37) | 27(1) | 22(1) | 13(1) | 0(1) | 3(1) | -4(1) |
| C(36) | 22(1) | 18(1) | 16(1) | 1(1) | 5(1) | -2(1) |
| C(35) | 14(1) | 15(1) | 13(1) | -2(1) | 4(1) | 0(1) |
| C(34) | 42(2) | 58(2) | 19(1) | 1(1) | 1(1) | -5(2) |
| C(33) | 21(1) | 19(1) | 17(1) | 1(1) | 9(1) | 2(1) |
| C(32) | 20(1) | 24(1) | 22(1) | -4(1) | 6(1) | 0(1) |
| C(31) | 27(1) | 32(1) | 17(1) | -1(1) | 4(1) | 5(1) |
| C(30) | 35(1) | 31(1) | 16(1) | 6(1) | 9(1) | 1(1) |
| C(29) | 26(1) | 21(1) | 18(1) | 2(1) | 9(1) | 0(1) |
| C(28) | 20(1) | 15(1) | 15(1) | 0(1) | 7(1) | 4(1) |
| C(27) | 17(1) | 14(1) | 14(1) | 2(1) | 8(1) | 2(1) |
| C(54) | 44(2) | 51(2) | 70(3) | -16(2) | -1(2) | 5(2) |
| C(55) | 52(2) | 50(2) | 116(4) | 34(2) | 47(3) | 15(2) |
| C(56) | 73(3) | 61(2) | 48(2) | 0(2) | 30(2) | 1(2) |
| C(57) | 51(2) | 42(2) | 61(2) | -3(2) | 24(2) | 0(2) |
| C(58) | 50(2) | 49(2) | 45(2) | 4(2) | 12(2) | 7(2) |
| C(59) | 33(2) | 28(1) | 41(2) | 10(1) | 6(1) | -1(1) |
| C(60) | 30(1) | 38(2) | 35(2) | 8(1) | 8(1) | -5(1) |

## Crystal structure determination of $^{Cy}Y_{Ph}$-TMS

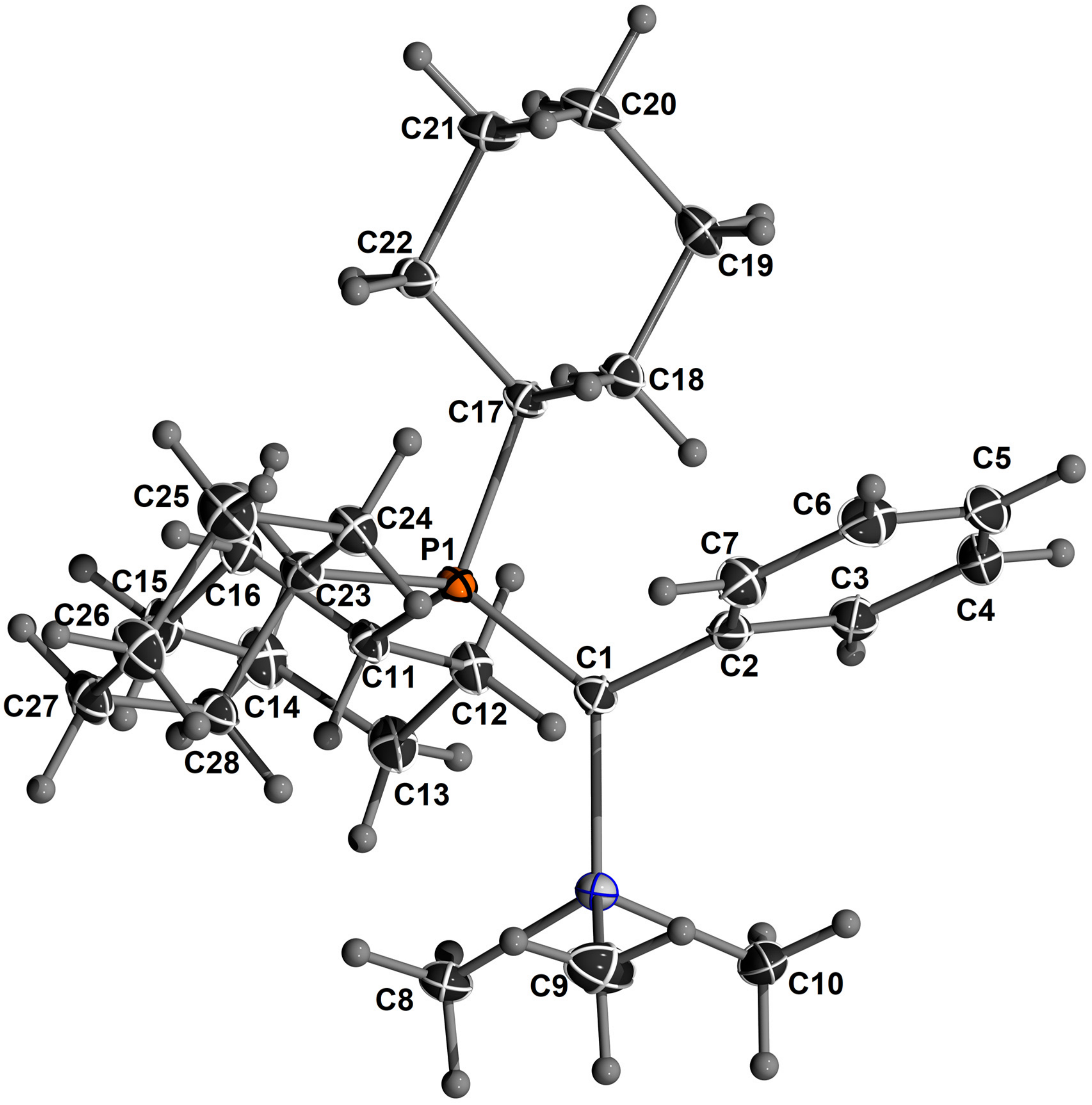
C21
C20
C22
C19
C18
C17
C25
C24
P1
C6
C5
C7
C3
C15
C16
C23
C26
C4
C1
C2
C11
C12
C27
C14
C28
C13
C8
C9
C10

**Figure 60.** ORTEP plot of **$^{Cy}Y_{Ph}$-TMS**. Ellipsoids drawn at 50% probability level.

**Table 30.** Atomic Coordinates (×$10^4$) and Equivalent Isotropic Displacement Parameters (Å$^2$×$10^3$) for **$^{Cy}Y_{Ph}$-TMS**. $U_{eq}$ is defined as 1/3 of of the trace of the orthogonalised $U_{ij}$ tensor.

| | *x* | *y* | *z* | U(eq) |
|---|---|---|---|---|
| P(1) | 7507(1) | 3078(1) | 3040(1) | 11(1) |
| Si(1) | 8250(1) | 4197(1) | 4840(1) | 16(1) |
| C(1) | 7533(1) | 3133(1) | 3982(1) | 14(1) |
| C(2) | 6979(1) | 2119(1) | 4188(1) | 16(1) |
| C(5) | 5892(1) | 273(2) | 4565(1) | 28(1) |
| C(4) | 5686(1) | 1689(2) | 4425(1) | 27(1) |
| C(3) | 6223(1) | 2587(1) | 4242(1) | 21(1) |
| C(6) | 6639(1) | -223(2) | 4527(1) | 27(1) |
| C(7) | 7179(1) | 685(1) | 4350(1) | 21(1) |
| C(13) | 7104(1) | 7399(1) | 2571(1) | 20(1) |
| C(15) | 7752(1) | 6453(1) | 1659(1) | 20(1) |

| | | | | |
|---|---|---|---|---|
| C(14) | 7121(1) | 7512(1) | 1742(1) | 22(1) |
| C(8) | 8852(1) | 5674(1) | 4615(1) | 20(1) |
| C(9) | 9081(1) | 3068(2) | 5640(1) | 32(1) |
| C(20) | 4872(1) | 1407(1) | 989(1) | 21(1) |
| C(21) | 5710(1) | 619(1) | 1138(1) | 21(1) |
| C(22) | 6513(1) | 1542(1) | 1576(1) | 17(1) |
| C(23) | 8411(1) | 2176(1) | 2904(1) | 14(1) |
| C(24) | 8515(1) | 659(1) | 3220(1) | 18(1) |
| C(25) | 9226(1) | -116(1) | 3072(1) | 24(1) |
| C(26) | 10093(1) | 652(1) | 3476(1) | 25(1) |
| C(27) | 10007(1) | 2180(1) | 3196(1) | 21(1) |
| C(28) | 9279(1) | 2949(1) | 3322(1) | 17(1) |
| C(10) | 7635(1) | 5098(2) | 5355(1) | 32(1) |
| C(12) | 6891(1) | 5899(1) | 2733(1) | 17(1) |
| C(11) | 7548(1) | 4861(1) | 2661(1) | 14(1) |
| C(17) | 6528(1) | 2112(1) | 2368(1) | 14(1) |
| C(16) | 7535(1) | 4948(1) | 1814(1) | 17(1) |
| C(19) | 4896(1) | 1992(1) | 1776(1) | 20(1) |
| C(18) | 5689(1) | 2941(1) | 2190(1) | 17(1) |

**Table 31.** Anisotropic displacement parameters (Å$^2$×10$^3$) for **$^{Cy}$Y$_{Ph}$-TMS**. The anisotropic displacement factor exponent takes the form: -2p$^2$[ h$^2$ a*$^2$U$^{11}$ + ... + 2 h k a* b* U$^{12}$ ]

| | $U^{11}$ | $U^{22}$ | $U^{33}$ | $U^{23}$ | $U^{13}$ | $U^{12}$ |
|---|---|---|---|---|---|---|
| Si(1) | 16(1) | 16(1) | 15(1) | -2(1) | 6(1) | -3(1) |
| C(1) | 16(1) | 12(1) | 16(1) | -1(1) | 8(1) | -2(1) |
| C(2) | 19(1) | 16(1) | 14(1) | -2(1) | 6(1) | -5(1) |
| C(5) | 34(1) | 29(1) | 23(1) | -4(1) | 16(1) | -18(1) |
| C(4) | 24(1) | 33(1) | 27(1) | -7(1) | 15(1) | -10(1) |
| C(3) | 23(1) | 19(1) | 22(1) | -3(1) | 11(1) | -4(1) |
| C(6) | 40(1) | 18(1) | 24(1) | 1(1) | 13(1) | -9(1) |
| C(7) | 26(1) | 17(1) | 22(1) | 2(1) | 11(1) | -1(1) |
| C(13) | 23(1) | 11(1) | 30(1) | 1(1) | 15(1) | 1(1) |
| C(15) | 25(1) | 16(1) | 24(1) | 3(1) | 15(1) | -1(1) |
| C(14) | 26(1) | 14(1) | 30(1) | 6(1) | 14(1) | 1(1) |
| C(8) | 19(1) | 18(1) | 20(1) | -4(1) | 6(1) | -5(1) |
| C(9) | 31(1) | 31(1) | 23(1) | 5(1) | 1(1) | -5(1) |
| C(20) | 16(1) | 17(1) | 24(1) | -2(1) | 2(1) | -4(1) |
| C(21) | 19(1) | 16(1) | 23(1) | -5(1) | 4(1) | -2(1) |
| C(22) | 15(1) | 16(1) | 18(1) | -4(1) | 6(1) | -1(1) |
| C(23) | 13(1) | 12(1) | 17(1) | -1(1) | 6(1) | 1(1) |
| C(24) | 17(1) | 12(1) | 26(1) | 1(1) | 9(1) | 2(1) |
| C(25) | 22(1) | 15(1) | 37(1) | -1(1) | 13(1) | 4(1) |
| C(26) | 18(1) | 22(1) | 36(1) | 1(1) | 11(1) | 6(1) |
| C(27) | 16(1) | 20(1) | 29(1) | -2(1) | 11(1) | 1(1) |
| C(28) | 14(1) | 15(1) | 22(1) | -3(1) | 8(1) | 0(1) |
| C(10) | 28(1) | 42(1) | 30(1) | -20(1) | 17(1) | -14(1) |

| | | | | | | |
|---|---|---|---|---|---|---|
| C(12) | 18(1) | 11(1) | 24(1) | 2(1) | 12(1) | 1(1) |
| C(11) | 14(1) | 11(1) | 18(1) | 0(1) | 7(1) | -1(1) |
| C(17) | 14(1) | 11(1) | 16(1) | -1(1) | 6(1) | -1(1) |
| C(16) | 21(1) | 13(1) | 19(1) | 2(1) | 11(1) | 0(1) |
| C(19) | 14(1) | 21(1) | 26(1) | 1(1) | 7(1) | -2(1) |
| C(18) | 15(1) | 16(1) | 20(1) | -2(1) | 7(1) | 0(1) |

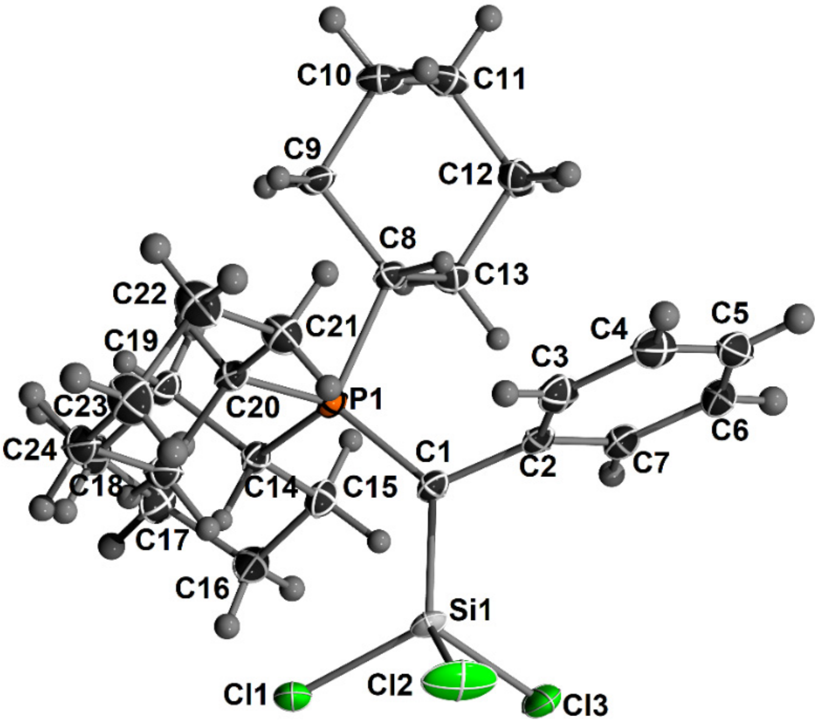
C10
C11
C9
C12
C8
C13
C22
C21
C4
C5
C19
C3
P1
C23
C20
C6
C24
C1
C2
C7
C18
C14
C15
C17
C16
Si1
Cl1
Cl2
Cl3

**Figure 61.** ORTEP plot of **$^{Cy}Y_{Ph}$-$SiCl_3$**. Ellipsoids drawn at 50% theory level.

**Table 32.** Atomic Coordinates ($\times 10^4$) and Equivalent Isotropic Displacement Parameters ($Å^2 \times 10^3$) for **$^{Cy}Y_{Ph}$-$SiCl_3$**. $U_{eq}$ is defined as 1/3 of of the trace of the orthogonalised $U_{ij}$ tensor.

| | *x* | *y* | *z* | U(eq) |
|---|---|---|---|---|
| P(1) | 7445(1) | 3059(1) | 6901(1) | 14(1) |
| Cl(1) | 6069(1) | 5690(1) | 5318(1) | 27(1) |
| Si(1) | 6816(1) | 4182(1) | 5110(1) | 18(1) |
| C(1) | 7441(1) | 3085(2) | 5941(1) | 17(1) |
| C(2) | 8009(1) | 2055(2) | 5746(1) | 19(1) |
| Cl(2) | 5974(1) | 3107(1) | 4089(1) | 49(1) |
| Cl(3) | 7542(1) | 5334(1) | 4643(1) | 33(1) |
| C(3) | 7789(1) | 644(2) | 5563(1) | 25(1) |
| C(4) | 8342(1) | -287(2) | 5419(1) | 31(1) |
| C(5) | 9126(1) | 177(2) | 5433(1) | 32(1) |
| C(6) | 9351(1) | 1584(2) | 5588(1) | 29(1) |
| C(7) | 8799(1) | 2504(2) | 5744(1) | 23(1) |
| C(9) | 8422(1) | 1515(2) | 8381(1) | 20(1) |
| C(8) | 8423(1) | 2093(2) | 7581(1) | 16(1) |
| C(10) | 9223(1) | 580(2) | 8817(1) | 24(1) |
| C(11) | 10073(1) | 1359(2) | 8987(1) | 24(1) |
| C(12) | 10062(1) | 1985(2) | 8198(1) | 23(1) |
| C(13) | 9267(1) | 2933(2) | 7781(1) | 19(1) |
| C(14) | 7409(1) | 4844(2) | 7273(1) | 16(1) |
| C(15) | 8058(1) | 5886(2) | 7183(1) | 19(1) |
| C(16) | 7811(1) | 7384(2) | 7316(1) | 23(1) |
| C(17) | 7785(1) | 7523(2) | 8151(1) | 25(1) |

| | | | | |
|---|---|---|---|---|
| C(18) | 7182(1) | 6436(2) | 8262(1) | 23(1) |
| C(19) | 7432(1) | 4938(2) | 8135(1) | 20(1) |
| C(20) | 6517(1) | 2163(2) | 6986(1) | 17(1) |
| C(21) | 6420(1) | 656(2) | 6661(1) | 24(1) |
| C(22) | 5691(1) | -116(2) | 6791(1) | 33(1) |
| C(23) | 4824(1) | 658(2) | 6360(1) | 33(1) |
| C(24) | 4904(1) | 2178(2) | 6648(1) | 25(1) |
| C(25) | 5646(1) | 2952(2) | 6547(1) | 21(1) |

**Table 33.** Anisotropic displacement parameters (Å$^2$×10$^3$) for **$^{Cy}$Y$_{Ph}$-SiCl$_3$**. The anisotropic displacement factor exponent takes the form: $-2p^2[h^2 a^{*2}U^{11} + ... + 2 h k a^* b^* U^{12}]$

| | $U^{11}$ | $U^{22}$ | $U^{33}$ | $U^{23}$ | $U^{13}$ | $U^{12}$ |
|---|---|---|---|---|---|---|
| Si(1) | 16(1) | 16(1) | 15(1) | -2(1) | 6(1) | -3(1) |
| C(1) | 16(1) | 12(1) | 16(1) | -1(1) | 8(1) | -2(1) |
| C(2) | 19(1) | 16(1) | 14(1) | -2(1) | 6(1) | -5(1) |
| C(5) | 34(1) | 29(1) | 23(1) | -4(1) | 16(1) | -18(1) |
| C(4) | 24(1) | 33(1) | 27(1) | -7(1) | 15(1) | -10(1) |
| C(3) | 23(1) | 19(1) | 22(1) | -3(1) | 11(1) | -4(1) |
| C(6) | 40(1) | 18(1) | 24(1) | 1(1) | 13(1) | -9(1) |
| C(7) | 26(1) | 17(1) | 22(1) | 2(1) | 11(1) | -1(1) |
| C(13) | 23(1) | 11(1) | 30(1) | 1(1) | 15(1) | 1(1) |
| C(15) | 25(1) | 16(1) | 24(1) | 3(1) | 15(1) | -1(1) |
| C(14) | 26(1) | 14(1) | 30(1) | 6(1) | 14(1) | 1(1) |
| C(8) | 19(1) | 18(1) | 20(1) | -4(1) | 6(1) | -5(1) |
| C(9) | 31(1) | 31(1) | 23(1) | 5(1) | 1(1) | -5(1) |
| C(20) | 16(1) | 17(1) | 24(1) | -2(1) | 2(1) | -4(1) |
| C(21) | 19(1) | 16(1) | 23(1) | -5(1) | 4(1) | -2(1) |
| C(22) | 15(1) | 16(1) | 18(1) | -4(1) | 6(1) | -1(1) |
| C(23) | 13(1) | 12(1) | 17(1) | -1(1) | 6(1) | 1(1) |
| C(24) | 17(1) | 12(1) | 26(1) | 1(1) | 9(1) | 2(1) |
| C(25) | 22(1) | 15(1) | 37(1) | -1(1) | 13(1) | 4(1) |
| C(26) | 18(1) | 22(1) | 36(1) | 1(1) | 11(1) | 6(1) |
| C(27) | 16(1) | 20(1) | 29(1) | -2(1) | 11(1) | 1(1) |
| C(28) | 14(1) | 15(1) | 22(1) | -3(1) | 8(1) | 0(1) |
| C(10) | 28(1) | 42(1) | 30(1) | -20(1) | 17(1) | -14(1) |
| C(12) | 18(1) | 11(1) | 24(1) | 2(1) | 12(1) | 1(1) |
| C(11) | 14(1) | 11(1) | 18(1) | 0(1) | 7(1) | -1(1) |
| C(17) | 14(1) | 11(1) | 16(1) | -1(1) | 6(1) | -1(1) |
| C(16) | 21(1) | 13(1) | 19(1) | 2(1) | 11(1) | 0(1) |
| C(19) | 14(1) | 21(1) | 26(1) | 1(1) | 7(1) | -2(1) |
| C(18) | 15(1) | 16(1) | 20(1) | -2(1) | 7(1) | 0(1) |

## Crystal structure determination of 176

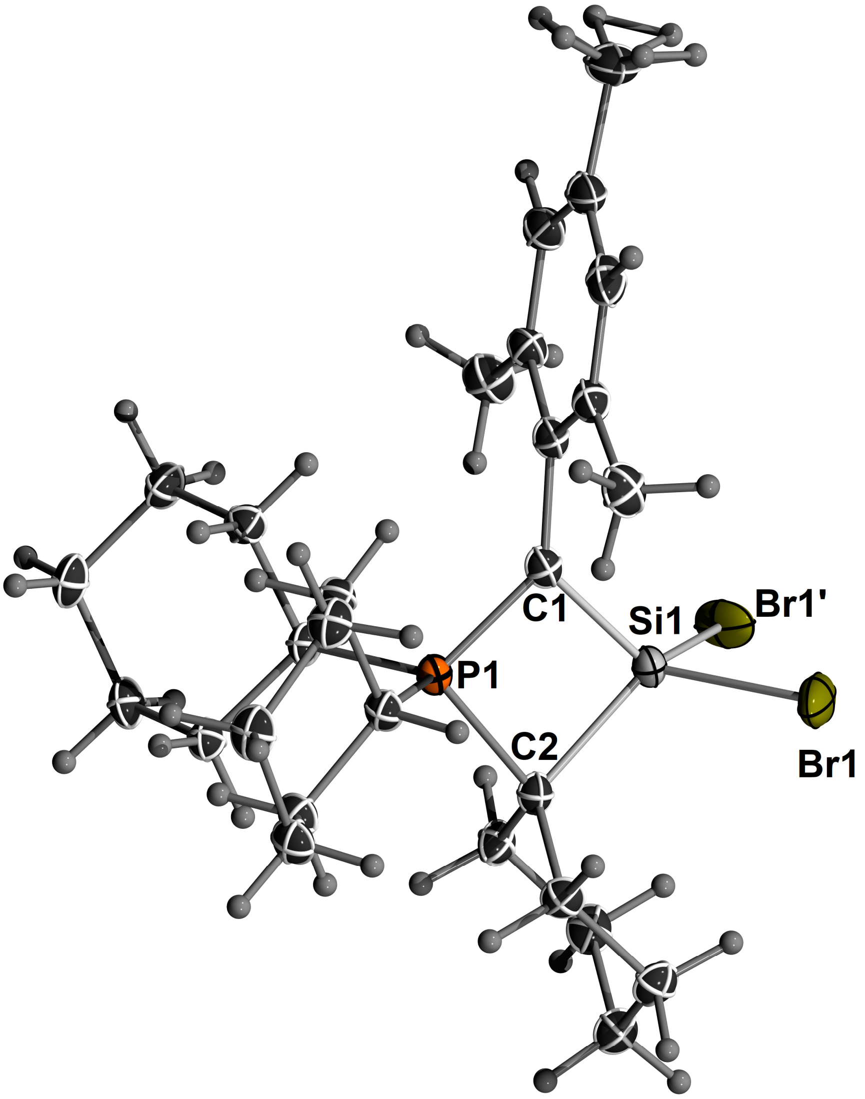

**Figure 62:** ORTEP plot of **176**. Ellipsoids drawn at the 50% probability level.

**Table 34.** Atomic Coordinates ($\times 10^4$) and Equivalent Isotropic Displacement Parameters ($Å^2 \times 10^3$) for **176**. $U_{eq}$ is defined as 1/3 of of the trace of the orthogonalised $U_{ij}$ tensor.

| | *x* | *y* | *z* | U(eq) |
|---|---|---|---|---|
| Br(1) | 6719(1) | 6311(1) | 5704(1) | 40(1) |
| C(1) | 4667(3) | 7500 | 3401(3) | 18(1) |
| Si(1) | 5318(1) | 7500 | 5014(1) | 20(1) |
| P(1) | 2839(1) | 7500 | 3799(1) | 16(1) |
| C(3) | 5450(3) | 7500 | 2175(3) | 19(1) |
| C(2) | 3339(3) | 7500 | 5573(3) | 18(1) |
| C(4) | 5885(3) | 6677(2) | 1604(2) | 22(1) |
| C(8) | 8179(5) | 7500 | -1137(4) | 41(1) |
| C(7) | 5530(3) | 5763(2) | 2169(3) | 29(1) |
| C(6) | 7176(4) | 7500 | -24(4) | 29(1) |
| C(5) | 6719(3) | 6696(2) | 518(3) | 27(1) |

| | | | | |
|---|---|---|---|---|
| C(9) | 2857(3) | 8357(2) | 6297(2) | 20(1) |
| C(10) | 3442(3) | 8349(2) | 7704(2) | 23(1) |
| C(11) | 2963(4) | 7500 | 8401(3) | 23(1) |
| C(12) | 1807(3) | 6474(2) | 3284(2) | 18(1) |
| C(13) | 219(3) | 6325(2) | 3709(2) | 21(1) |
| C(14) | -233(3) | 5344(2) | 3405(3) | 24(1) |
| C(15) | -152(3) | 5138(2) | 1978(2) | 26(1) |
| C(16) | 1379(3) | 5357(2) | 1492(2) | 25(1) |
| C(17) | 1823(3) | 6334(2) | 1818(2) | 22(1) |

**Table 35.** Anisotropic displacement parameters ($Å^2 \times 10^3$) for **176**. The anisotropic displacement factor exponent takes the form: $-2p^2[ h^2 a^{*2}U^{11} + ... + 2 h k a^* b^* U^{12} ]$

| | $U^{11}$ | $U^{22}$ | $U^{33}$ | $U^{23}$ | $U^{13}$ | $U^{12}$ |
|---|---|---|---|---|---|---|
| Br(1) | 33(1) | 57(1) | 30(1) | 5(1) | 0(1) | 26(1) |
| C(1) | 16(1) | 16(2) | 22(2) | 0 | 1(1) | 0 |
| Si(1) | 14(1) | 25(1) | 21(1) | 0 | -1(1) | 0 |
| P(1) | 14(1) | 14(1) | 19(1) | 0 | 0(1) | 0 |
| C(3) | 15(1) | 21(2) | 21(2) | 0 | 0(1) | 0 |
| C(2) | 16(1) | 20(2) | 19(2) | 0 | -1(1) | 0 |
| C(4) | 17(1) | 25(1) | 24(1) | -2(1) | 0(1) | 3(1) |
| C(8) | 32(2) | 67(3) | 25(2) | 0 | 8(2) | 0 |
| C(7) | 28(1) | 22(1) | 37(1) | -1(1) | 2(1) | 6(1) |
| C(6) | 19(2) | 46(2) | 21(2) | 0 | 0(1) | 0 |
| C(5) | 22(1) | 32(2) | 28(1) | -5(1) | -2(1) | 7(1) |
| C(9) | 22(1) | 18(1) | 21(1) | -1(1) | 0(1) | 4(1) |
| C(10) | 27(1) | 18(1) | 24(1) | -4(1) | 0(1) | 2(1) |
| C(11) | 26(2) | 21(2) | 23(2) | 0 | 0(1) | 0 |
| C(12) | 18(1) | 17(1) | 20(1) | 0(1) | 0(1) | -2(1) |
| C(13) | 19(1) | 21(1) | 23(1) | -2(1) | 1(1) | -3(1) |
| C(14) | 20(1) | 23(1) | 29(1) | 1(1) | -1(1) | -6(1) |
| C(15) | 26(1) | 22(1) | 28(1) | -5(1) | -6(1) | -5(1) |
| C(16) | 28(1) | 23(1) | 23(1) | -6(1) | -2(1) | 0(1) |
| C(17) | 22(1) | 23(1) | 20(1) | 0(1) | 0(1) | -1(1) |

## Crystal structure determination of 179

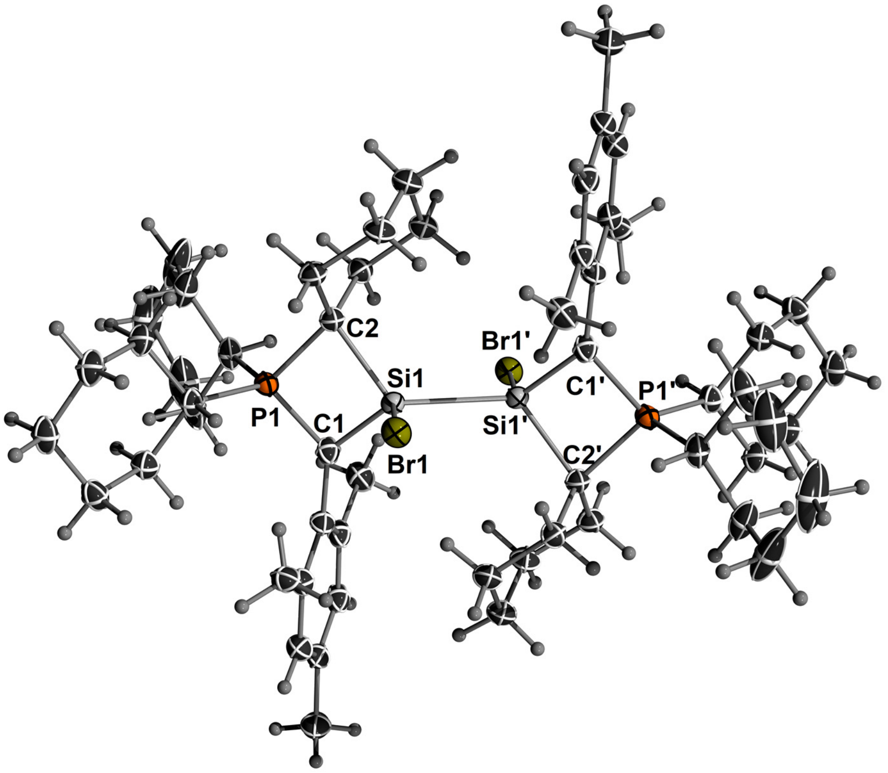

**Figure 63:** ORTEP plot of **179**. Ellipsoids drawn at the 50% probability level.

**Table 36.** Atomic Coordinates ($\times 10^4$) and Equivalent Isotropic Displacement Parameters ($\text{Å}^2 \times 10^3$) for **179**. $U_{eq}$ is defined as 1/3 of of the trace of the orthogonalised $U_{ij}$ tensor.

| | *x* | *y* | *z* | **U(eq)** |
|---|---|---|---|---|
| Br(1) | 2121(1) | 5362(1) | 4730(1) | 26(1) |
| C(1) | 3895(3) | 3986(2) | 5996(1) | 22(1) |
| P(1) | 3560(1) | 4736(1) | 6668(1) | 20(1) |
| Si(1) | 4120(1) | 4956(1) | 5413(1) | 20(1) |
| C(4) | 4877(3) | 1389(2) | 5991(2) | 28(1) |
| C(3) | 4967(3) | 2359(2) | 6093(2) | 24(1) |
| C(2) | 4164(3) | 5792(2) | 6208(1) | 21(1) |
| C(6) | 2467(3) | 1524(2) | 5601(2) | 27(1) |
| C(5) | 3629(4) | 954(2) | 5751(2) | 29(1) |
| C(9) | 6359(3) | 2760(2) | 6363(2) | 28(1) |
| C(8) | 1210(3) | 3048(2) | 5437(2) | 28(1) |
| C(7) | 2520(3) | 2503(2) | 5672(2) | 24(1) |
| C(10) | 3542(4) | -99(2) | 5649(2) | 36(1) |
| C(12) | 5689(3) | 6079(2) | 6441(2) | 25(1) |
| C(11) | 3785(3) | 2943(2) | 5928(2) | 22(1) |
| C(13) | 6249(3) | 6830(2) | 5970(2) | 28(1) |
| C(14) | 5289(4) | 7692(2) | 5915(2) | 32(1) |
| C(15) | 3792(3) | 7402(2) | 5682(2) | 30(1) |
| C(16) | 3221(3) | 6669(2) | 6172(2) | 26(1) |
| C(17) | 4610(3) | 4547(2) | 7484(2) | 26(1) |

| | | | | |
|---|---|---|---|---|
| C(18) | 4496(4) | 5298(3) | 8043(2) | 38(1) |
| C(19) | 5697(4) | 5165(4) | 8603(2) | 58(1) |
| C(20) | 5681(4) | 4173(5) | 8905(2) | 72(2) |
| C(21) | 5645(4) | 3409(4) | 8364(2) | 55(1) |
| C(22) | 4465(3) | 3565(3) | 7805(2) | 38(1) |
| C(23) | 1678(3) | 4819(2) | 6845(2) | 22(1) |
| C(24) | 1138(3) | 3870(2) | 7117(2) | 26(1) |
| C(25) | -458(3) | 3852(2) | 7070(2) | 29(1) |
| C(26) | -1059(3) | 4681(2) | 7456(2) | 31(1) |
| C(27) | -474(3) | 5621(2) | 7224(2) | 30(1) |
| C(28) | 1134(3) | 5622(2) | 7288(2) | 26(1) |

**Table 37.** Anisotropic displacement parameters ($Å^2 \times 10^3$) for **179**. The anisotropic displacement factor exponent takes the form: $-2p^2[ h^2 a^{*2}U^{11} + ... + 2 h k a^* b^* U^{12} ]$

| | $U^{11}$ | $U^{22}$ | $U^{33}$ | $U^{23}$ | $U^{13}$ | $U^{12}$ |
|---|---|---|---|---|---|---|
| Br(1) | 23(1) | 28(1) | 28(1) | 3(1) | 0(1) | 1(1) |
| C(1) | 22(1) | 22(1) | 23(1) | 1(1) | 3(1) | 2(1) |
| P(1) | 19(1) | 20(1) | 20(1) | 1(1) | 3(1) | 0(1) |
| Si(1) | 21(1) | 19(1) | 21(1) | 0(1) | 3(1) | -1(1) |
| C(4) | 31(2) | 24(2) | 30(2) | 2(1) | 10(1) | 4(1) |
| C(3) | 26(1) | 22(1) | 26(1) | 5(1) | 7(1) | 2(1) |
| C(2) | 22(1) | 19(1) | 23(1) | -2(1) | 4(1) | -2(1) |
| C(6) | 32(2) | 24(2) | 25(1) | 0(1) | 5(1) | -5(1) |
| C(5) | 42(2) | 19(1) | 27(2) | 1(1) | 13(1) | -3(1) |
| C(9) | 23(1) | 25(2) | 37(2) | 5(1) | 4(1) | 4(1) |
| C(8) | 24(1) | 26(2) | 32(2) | -2(1) | 1(1) | -5(1) |
| C(7) | 27(1) | 23(1) | 22(1) | 1(1) | 6(1) | -2(1) |
| C(10) | 49(2) | 23(2) | 38(2) | -1(1) | 12(2) | -1(1) |
| C(12) | 24(1) | 25(1) | 25(1) | -3(1) | 3(1) | -1(1) |
| C(11) | 25(1) | 18(1) | 24(1) | 2(1) | 6(1) | 1(1) |
| C(13) | 29(2) | 26(2) | 30(2) | -4(1) | 4(1) | -7(1) |
| C(14) | 39(2) | 23(2) | 34(2) | -2(1) | 9(1) | -7(1) |
| C(15) | 36(2) | 19(1) | 34(2) | 2(1) | 4(1) | 1(1) |
| C(16) | 28(1) | 20(1) | 31(2) | -3(1) | 6(1) | 0(1) |
| C(17) | 20(1) | 36(2) | 21(1) | 4(1) | 3(1) | 0(1) |
| C(18) | 25(2) | 63(3) | 24(2) | -9(2) | 3(1) | 2(2) |
| C(19) | 27(2) | 119(4) | 29(2) | -26(2) | 0(2) | 6(2) |
| C(20) | 36(2) | 155(6) | 25(2) | 19(3) | -4(2) | 24(3) |
| C(21) | 31(2) | 91(3) | 42(2) | 32(2) | 3(2) | 18(2) |
| C(22) | 26(2) | 51(2) | 38(2) | 21(2) | 6(1) | 7(1) |
| C(23) | 21(1) | 26(1) | 20(1) | 1(1) | 1(1) | 0(1) |
| C(24) | 24(1) | 28(2) | 25(1) | 0(1) | 1(1) | 0(1) |
| C(25) | 22(1) | 34(2) | 29(2) | 2(1) | 0(1) | -7(1) |
| C(26) | 20(1) | 43(2) | 31(2) | 2(1) | 5(1) | 2(1) |
| C(27) | 24(2) | 34(2) | 32(2) | 2(1) | 5(1) | 7(1) |
| C(28) | 23(1) | 30(2) | 27(1) | -2(1) | 7(1) | 2(1) |

## Crystal structure determination of $^{Cy}Y_s$-PCy$_2$ (L1)

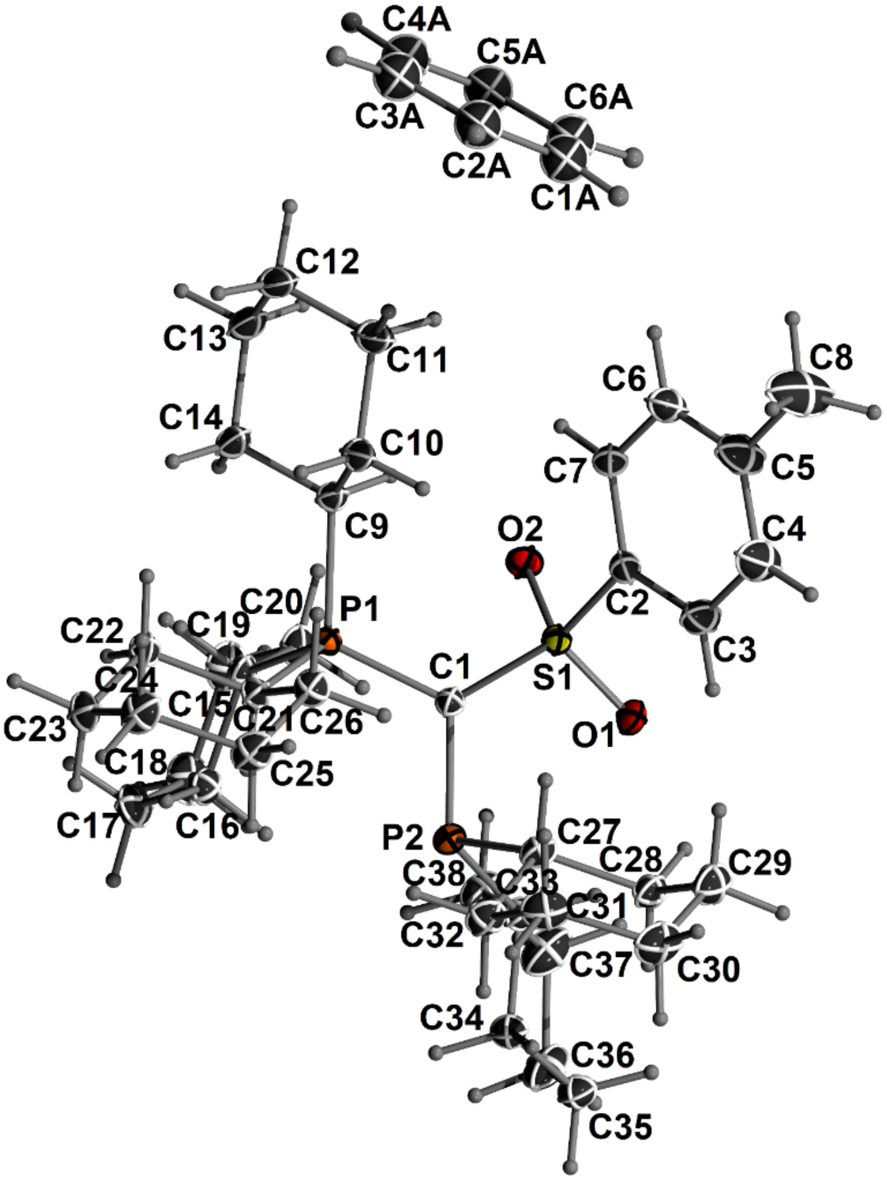
C4A
C5A
C6A
C3A
C2A
C1A
C12
C13
C11
C14
C10
C9
C6
C8
C7
C5
O2
C4
C2
C3
C22
C19
C20
P1
C1
S1
C24
C15
C21
C26
C23
O1
C18
C25
C17
C16
P2
C27
C28
C29
C38
C33
C31
C32
C37
C30
C34
C36
C35

**Figure 64.** ORTEP plot of **L1** with one molecule of benzene. Ellipsoids drawn at 50% probability level.

**Table 38.** Atomic Coordinates (×10$^4$) and Equivalent Isotropic Displacement Parameters (Å$^2$×10$^3$) for **L1**. $U_{eq}$ is defined as 1/3 of of the trace of the orthogonalised $U_{ij}$ tensor.

| | *x* | *y* | *z* | **U(eq)** |
|---|---|---|---|---|
| S(1) | 6801(1) | 5451(1) | 3433(1) | 15(1) |
| P(1) | 4626(1) | 5511(1) | 2336(1) | 13(1) |
| P(2) | 7311(1) | 5372(1) | 1673(1) | 15(1) |
| O(1) | 8044(1) | 5808(1) | 3308(1) | 22(1) |
| O(2) | 5789(1) | 6164(1) | 3779(1) | 18(1) |
| C(1) | 6274(1) | 5372(1) | 2537(1) | 14(1) |
| C(2) | 7145(2) | 3997(2) | 4188(1) | 19(1) |
| C(3) | 8360(2) | 3263(2) | 4224(1) | 30(1) |
| C(4) | 8660(2) | 2166(2) | 4833(1) | 38(1) |
| C(5) | 7749(2) | 1764(2) | 5409(1) | 36(1) |
| C(6) | 6548(2) | 2524(2) | 5377(1) | 26(1) |
| C(7) | 6252(2) | 3638(2) | 4780(1) | 20(1) |

| | | | | |
|---|---|---|---|---|
| C(8) | 8054(3) | 542(2) | 6054(2) | 59(1) |
| C(9) | 3643(2) | 5073(2) | 3256(1) | 18(1) |
| C(10) | 3802(2) | 3685(2) | 3622(1) | 21(1) |
| C(11) | 3106(2) | 3341(2) | 4430(1) | 29(1) |
| C(12) | 1673(2) | 3929(2) | 4320(1) | 33(1) |
| C(13) | 1481(2) | 5300(2) | 3942(1) | 31(1) |
| C(14) | 2189(2) | 5666(2) | 3138(1) | 24(1) |
| C(15) | 3807(2) | 7064(1) | 1763(1) | 17(1) |
| C(16) | 4229(2) | 7494(2) | 878(1) | 20(1) |
| C(17) | 3496(2) | 8776(2) | 440(1) | 25(1) |
| C(18) | 3659(2) | 9667(2) | 883(1) | 29(1) |
| C(19) | 3238(2) | 9243(2) | 1758(1) | 26(1) |
| C(20) | 3967(2) | 7963(2) | 2210(1) | 20(1) |
| C(21) | 4484(2) | 4623(1) | 1654(1) | 16(1) |
| C(22) | 3085(2) | 4708(2) | 1393(1) | 19(1) |
| C(23) | 3079(2) | 4136(2) | 716(1) | 23(1) |
| C(24) | 3832(2) | 2832(2) | 962(1) | 26(1) |
| C(25) | 5208(2) | 2746(2) | 1243(1) | 24(1) |
| C(26) | 5200(2) | 3293(1) | 1936(1) | 18(1) |
| C(27) | 8503(2) | 3880(1) | 1991(1) | 18(1) |
| C(28) | 9870(2) | 3845(2) | 2273(1) | 20(1) |
| C(29) | 10620(2) | 2530(2) | 2589(1) | 25(1) |
| C(30) | 10671(2) | 1879(2) | 1955(1) | 30(1) |
| C(31) | 9326(2) | 1950(2) | 1638(1) | 28(1) |
| C(32) | 8603(2) | 3268(2) | 1320(1) | 22(1) |
| C(33) | 8360(2) | 6505(1) | 1556(1) | 18(1) |
| C(34) | 9136(2) | 6623(2) | 773(1) | 22(1) |
| C(35) | 10104(2) | 7441(2) | 732(1) | 25(1) |
| C(36) | 9416(2) | 8694(2) | 753(1) | 32(1) |
| C(37) | 8553(2) | 8614(2) | 1486(1) | 31(1) |
| C(38) | 7616(2) | 7766(2) | 1536(1) | 24(1) |
| C1A1 | 4180(4) | -339(3) | 6393(2) | 83(1) |
| C2A1 | 3177(3) | -799(3) | 6191(2) | 74(1) |
| C3A1 | 1932(3) | -129(3) | 6118(2) | 71(1) |
| C4A1 | 1695(4) | 953(3) | 6289(2) | 69(1) |
| C5A1 | 2647(4) | 1388(3) | 6490(2) | 73(1) |
| C6A1 | 3923(4) | 712(3) | 6569(2) | 76(1) |

**Table 39.** Anisotropic displacement parameters (Å$^2$×10$^3$) for **L1.** The anisotropic displacement factor exponent takes the form: $-2\pi^2[ h^2 a^{*2}U^{11} + ... + 2 h k a^* b^* U^{12} ]$

| | $U^{11}$ | $U^{22}$ | $U^{33}$ | $U^{23}$ | $U^{13}$ | $U^{12}$ |
|---|---|---|---|---|---|---|
| S(1) | 12(1) | 20(1) | 14(1) | -7(1) | 0(1) | -3(1) |
| P(1) | 11(1) | 16(1) | 13(1) | -6(1) | 0(1) | -2(1) |
| P(2) | 12(1) | 17(1) | 15(1) | -5(1) | 1(1) | -3(1) |
| O(1) | 15(1) | 33(1) | 20(1) | -10(1) | 1(1) | -10(1) |
| O(2) | 18(1) | 21(1) | 19(1) | -11(1) | 2(1) | -3(1) |
| C(1) | 11(1) | 18(1) | 13(1) | -6(1) | 0(1) | -2(1) |
| C(2) | 16(1) | 25(1) | 15(1) | -6(1) | -2(1) | 0(1) |
| C(3) | 21(1) | 38(1) | 22(1) | -3(1) | 4(1) | 4(1) |
| C(4) | 29(1) | 39(1) | 29(1) | -1(1) | 4(1) | 12(1) |

| | | | | | | |
|---|---|---|---|---|---|---|
| C(5) | 36(1) | 33(1) | 25(1) | 1(1) | 4(1) | 8(1) |
| C(6) | 26(1) | 28(1) | 18(1) | -4(1) | 4(1) | -1(1) |
| C(7) | 17(1) | 25(1) | 17(1) | -8(1) | 1(1) | -2(1) |
| C(8) | 56(2) | 43(1) | 44(1) | 14(1) | 14(1) | 19(1) |
| C(9) | 14(1) | 27(1) | 16(1) | -10(1) | 3(1) | -7(1) |
| C(10) | 22(1) | 28(1) | 17(1) | -8(1) | 3(1) | -12(1) |
| C(11) | 31(1) | 42(1) | 18(1) | -9(1) | 6(1) | -20(1) |
| C(12) | 27(1) | 58(1) | 22(1) | -16(1) | 10(1) | -24(1) |
| C(13) | 18(1) | 56(1) | 27(1) | -22(1) | 8(1) | -12(1) |
| C(14) | 14(1) | 37(1) | 24(1) | -15(1) | 5(1) | -6(1) |
| C(15) | 13(1) | 18(1) | 19(1) | -8(1) | -1(1) | 0(1) |
| C(16) | 19(1) | 20(1) | 20(1) | -6(1) | -1(1) | -2(1) |
| C(17) | 27(1) | 21(1) | 23(1) | -2(1) | -4(1) | -3(1) |
| C(18) | 34(1) | 17(1) | 34(1) | -4(1) | -6(1) | -3(1) |
| C(19) | 25(1) | 20(1) | 36(1) | -13(1) | -4(1) | 2(1) |
| C(20) | 18(1) | 20(1) | 24(1) | -10(1) | -2(1) | 0(1) |
| C(21) | 15(1) | 19(1) | 15(1) | -8(1) | 1(1) | -4(1) |
| C(22) | 15(1) | 23(1) | 20(1) | -10(1) | -1(1) | -5(1) |
| C(23) | 22(1) | 32(1) | 22(1) | -14(1) | -1(1) | -10(1) |
| C(24) | 25(1) | 31(1) | 31(1) | -20(1) | 3(1) | -10(1) |
| C(25) | 22(1) | 26(1) | 30(1) | -18(1) | 4(1) | -6(1) |
| C(26) | 18(1) | 18(1) | 21(1) | -9(1) | 1(1) | -4(1) |
| C(27) | 15(1) | 17(1) | 20(1) | -6(1) | 3(1) | -3(1) |
| C(28) | 15(1) | 20(1) | 22(1) | -5(1) | 1(1) | -2(1) |
| C(29) | 19(1) | 23(1) | 29(1) | -5(1) | 0(1) | 1(1) |
| C(30) | 26(1) | 23(1) | 35(1) | -8(1) | 5(1) | 4(1) |
| C(31) | 31(1) | 23(1) | 32(1) | -13(1) | 6(1) | -4(1) |
| C(32) | 20(1) | 24(1) | 26(1) | -12(1) | 2(1) | -4(1) |
| C(33) | 15(1) | 18(1) | 20(1) | -5(1) | 1(1) | -4(1) |
| C(34) | 20(1) | 25(1) | 20(1) | -4(1) | 2(1) | -6(1) |
| C(35) | 19(1) | 29(1) | 25(1) | -2(1) | 3(1) | -8(1) |
| C(36) | 24(1) | 24(1) | 43(1) | 1(1) | 1(1) | -10(1) |
| C(37) | 26(1) | 20(1) | 50(1) | -11(1) | 4(1) | -6(1) |
| C(38) | 18(1) | 18(1) | 33(1) | -5(1) | 3(1) | -4(1) |
| C1A1 | 100(3) | 54(2) | 89(3) | -8(2) | -34(2) | -15(2) |
| C2A1 | 79(2) | 47(2) | 100(3) | -32(2) | -31(2) | -1(2) |
| C3A1 | 71(2) | 61(2) | 92(2) | -40(2) | -12(2) | -6(2) |
| C4A1 | 100(3) | 49(2) | 61(2) | -20(1) | 14(2) | -18(2) |
| C5A1 | 122(3) | 60(2) | 49(2) | -26(1) | 24(2) | -38(2) |
| C6A1 | 108(3) | 80(2) | 56(2) | -21(2) | -4(2) | -54(2) |

## Crystal structure determination of $^{Cy}Y_S$-P*i*Pr$_2$ (L4)

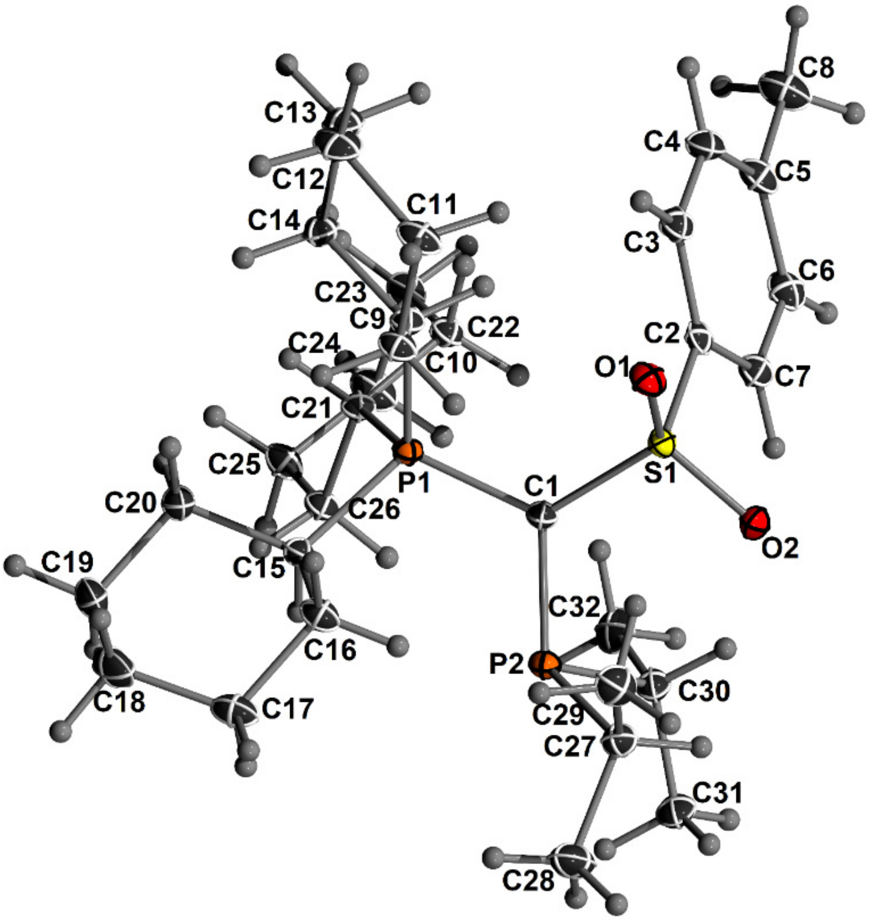
C8
C13
C4
C5
C12
C11
C14
C3
C6
C23
C9
C22
C2
C24
C10
O1
C7
C21
S1
C25
P1
C1
C20
C26
O2
C19
C15
C32
C16
P2
C30
C29
C18
C17
C27
C31
C28

**Figure 65.** ORTEP plot of **L4**. Ellipsoids drawn at 50% probability level.

**Table 40.** Atomic Coordinates (×10$^4$) and Equivalent Isotropic Displacement Parameters (Å$^2$×10$^3$) for **L4**. U$_{eq}$ is defined as 1/3 of of the trace of the orthogonalised U$_{ij}$ tensor.

| | *x* | *y* | *z* | U(eq) |
|---|---|---|---|---|
| S(1) | 3677(1) | 5130(1) | 3234(1) | 13(1) |
| P(1) | 3839(1) | 4495(1) | 4964(1) | 11(1) |
| P(2) | 3922(1) | 2210(1) | 3756(1) | 14(1) |
| O(1) | 3870(1) | 6429(1) | 3267(1) | 17(1) |
| O(2) | 3685(1) | 4362(1) | 2497(1) | 17(1) |
| C(1) | 3797(1) | 3983(1) | 3970(1) | 13(1) |
| C(2) | 3231(1) | 5651(2) | 3323(1) | 14(1) |
| C(3) | 3146(1) | 6950(2) | 3628(1) | 17(1) |
| C(4) | 2798(1) | 7326(2) | 3695(1) | 19(1) |
| C(5) | 2532(1) | 6439(2) | 3448(1) | 19(1) |
| C(6) | 2623(1) | 5166(2) | 3105(1) | 19(1) |
| C(7) | 2969(1) | 4770(2) | 3049(1) | 17(1) |
| C(8) | 2154(1) | 6822(2) | 3558(1) | 26(1) |
| C(9) | 3880(1) | 6399(1) | 5044(1) | 13(1) |
| C(10) | 4250(1) | 6913(2) | 4863(1) | 16(1) |
| C(11) | 4252(1) | 8501(2) | 4791(1) | 20(1) |
| C(12) | 4117(1) | 9195(2) | 5537(1) | 23(1) |
| C(13) | 3756(1) | 8646(2) | 5736(1) | 20(1) |

| | | | | |
|---|---|---|---|---|
| C(14) | 3754(1) | 7059(2) | 5816(1) | 16(1) |
| C(15) | 4202(1) | 3574(2) | 5451(1) | 14(1) |
| C(16) | 4552(1) | 3610(2) | 5030(1) | 18(1) |
| C(17) | 4803(1) | 2572(2) | 5416(1) | 22(1) |
| C(18) | 4858(1) | 2883(2) | 6292(1) | 28(1) |
| C(19) | 4510(1) | 2929(2) | 6718(1) | 25(1) |
| C(20) | 4254(1) | 3952(2) | 6326(1) | 19(1) |
| C(21) | 3465(1) | 4041(1) | 5587(1) | 13(1) |
| C(22) | 3122(1) | 4579(2) | 5216(1) | 15(1) |
| C(23) | 2810(1) | 4256(2) | 5734(1) | 18(1) |
| C(24) | 2786(1) | 2702(2) | 5903(1) | 22(1) |
| C(25) | 3122(1) | 2184(2) | 6292(1) | 18(1) |
| C(26) | 3440(1) | 2478(2) | 5784(1) | 15(1) |
| C(27) | 4258(1) | 2226(2) | 2951(1) | 19(1) |
| C(28) | 4495(1) | 941(2) | 3055(1) | 27(1) |
| C(29) | 4487(1) | 3522(2) | 2881(1) | 23(1) |
| C(30) | 3549(1) | 1411(2) | 3188(1) | 17(1) |
| C(31) | 3648(1) | -26(2) | 2865(1) | 23(1) |
| C(32) | 3228(1) | 1263(2) | 3704(1) | 23(1) |

**Table 41.** Anisotropic displacement parameters (Å$^2$×10$^3$) for **L4.** The anisotropic displacement factor exponent takes the form: $-2\pi^2[\ h^2\ a^{*2}U^{11} + \ldots\ + 2\ h\ k\ a^*\ b^*\ U^{12}\ ]$

| | $U^{11}$ | $U^{22}$ | $U^{33}$ | $U^{23}$ | $U^{13}$ | $U^{12}$ |
|---|---|---|---|---|---|---|
| S(1) | 15(1) | 12(1) | 12(1) | 1(1) | 1(1) | 1(1) |
| P(1) | 12(1) | 10(1) | 12(1) | 0(1) | 0(1) | 0(1) |
| P(2) | 17(1) | 11(1) | 13(1) | 0(1) | 0(1) | 1(1) |
| O(1) | 20(1) | 13(1) | 18(1) | 3(1) | 1(1) | -1(1) |
| O(2) | 22(1) | 16(1) | 12(1) | 0(1) | 2(1) | 3(1) |
| C(1) | 16(1) | 10(1) | 12(1) | 0(1) | -1(1) | 1(1) |
| C(2) | 16(1) | 14(1) | 11(1) | 4(1) | 0(1) | 2(1) |
| C(3) | 21(1) | 13(1) | 18(1) | 2(1) | -3(1) | 0(1) |
| C(4) | 22(1) | 13(1) | 22(1) | 1(1) | -1(1) | 4(1) |
| C(5) | 19(1) | 16(1) | 21(1) | 6(1) | 0(1) | 1(1) |
| C(6) | 20(1) | 15(1) | 21(1) | 4(1) | -2(1) | -3(1) |
| C(7) | 21(1) | 14(1) | 16(1) | 2(1) | -1(1) | 0(1) |
| C(8) | 19(1) | 21(1) | 38(1) | 4(1) | 1(1) | 2(1) |
| C(9) | 15(1) | 10(1) | 15(1) | 0(1) | 0(1) | 0(1) |
| C(10) | 15(1) | 12(1) | 20(1) | 2(1) | 0(1) | -1(1) |
| C(11) | 18(1) | 14(1) | 28(1) | 5(1) | 0(1) | -1(1) |
| C(12) | 26(1) | 10(1) | 33(1) | -1(1) | -2(1) | -2(1) |
| C(13) | 26(1) | 13(1) | 22(1) | -2(1) | 2(1) | 1(1) |
| C(14) | 21(1) | 12(1) | 16(1) | -2(1) | 2(1) | 0(1) |
| C(15) | 15(1) | 11(1) | 16(1) | 0(1) | -2(1) | 2(1) |
| C(16) | 14(1) | 18(1) | 23(1) | 2(1) | 0(1) | 1(1) |
| C(17) | 16(1) | 19(1) | 32(1) | 1(1) | -1(1) | 4(1) |
| C(18) | 23(1) | 27(1) | 35(1) | -1(1) | -12(1) | 7(1) |
| C(19) | 31(1) | 24(1) | 21(1) | 1(1) | -9(1) | 8(1) |
| C(20) | 23(1) | 17(1) | 17(1) | -2(1) | -5(1) | 4(1) |

| | | | | | | |
|---|---|---|---|---|---|---|
| C(21) | 14(1) | 12(1) | 14(1) | 0(1) | 1(1) | 0(1) |
| C(22) | 16(1) | 13(1) | 15(1) | 2(1) | 0(1) | 1(1) |
| C(23) | 16(1) | 17(1) | 20(1) | 3(1) | 2(1) | 1(1) |
| C(24) | 16(1) | 19(1) | 31(1) | 7(1) | 1(1) | -2(1) |
| C(25) | 19(1) | 15(1) | 20(1) | 5(1) | 1(1) | -1(1) |
| C(26) | 16(1) | 12(1) | 16(1) | 2(1) | 0(1) | 0(1) |
| C(27) | 21(1) | 19(1) | 17(1) | 0(1) | 2(1) | 5(1) |
| C(28) | 29(1) | 24(1) | 29(1) | 2(1) | 6(1) | 11(1) |
| C(29) | 21(1) | 24(1) | 23(1) | 4(1) | 6(1) | 2(1) |
| C(30) | 23(1) | 13(1) | 16(1) | 0(1) | -3(1) | -1(1) |
| C(31) | 33(1) | 13(1) | 21(1) | -4(1) | -5(1) | -1(1) |
| C(32) | 24(1) | 22(1) | 22(1) | -1(1) | -2(1) | -6(1) |

## Crystal structure determination of $[Au({}^{Cy}Y_{S}\text{-}PCy_2)Cl]$ (P1)

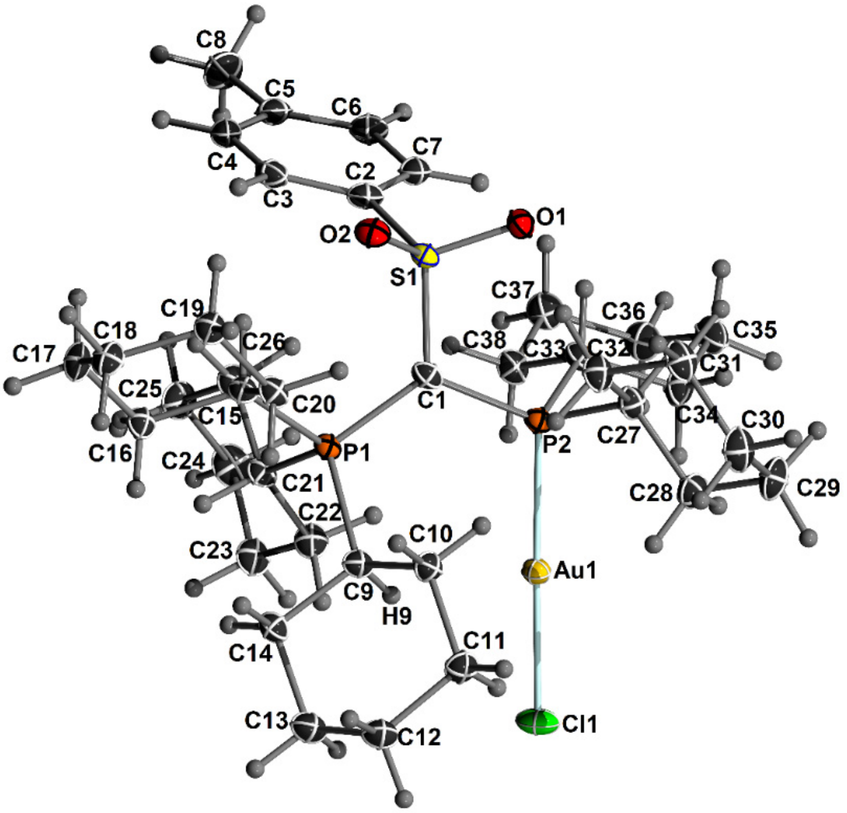
C8
C5
C6
C7
C4
C2
C3
O2
O1
S1
C37
C36
C35
C19
C18
C17
C26
C38
C33
C32
C31
C25
C20
C1
C15
C34
C30
C16
C24
P1
P2
C27
C21
C22
C28
C29
C10
C23
Au1
C9
H9
C11
C14
Cl1
C13
C12

**Figure 66.** ORTEP plot of **P1**. Ellipsoids drawn at 50% probability level.

**Table 42.** Atomic Coordinates ($\times10^4$) and Equivalent Isotropic Displacement Parameters ($Å^2\times10^3$) for **P1**. $U_{eq}$ is defined as 1/3 of of the trace of the orthogonalised $U_{ij}$ tensor.

| | *x* | *y* | *z* | U(eq) |
|---|---|---|---|---|
| Au(1) | 4950(1) | 1185(1) | 7347(1) | 16(1) |
| Cl(1) | 5909(1) | -180(1) | 6723(1) | 27(1) |
| S(1) | 3433(1) | 5141(1) | 8199(1) | 15(1) |
| P(1) | 4075(1) | 4355(1) | 6707(1) | 13(1) |
| P(2) | 4080(1) | 2519(1) | 8018(1) | 15(1) |
| O(1) | 3169(2) | 4477(2) | 8839(1) | 19(1) |
| O(2) | 2374(2) | 5818(2) | 7766(1) | 19(1) |
| C(1) | 3874(3) | 4026(3) | 7622(2) | 16(1) |
| C(2) | 4870(3) | 6342(3) | 8608(2) | 17(1) |
| C(3) | 5035(4) | 7476(3) | 8270(2) | 20(1) |
| C(4) | 6204(4) | 8353(3) | 8573(2) | 21(1) |
| C(5) | 7212(4) | 8126(3) | 9228(2) | 23(1) |
| C(6) | 6991(4) | 7014(3) | 9587(2) | 22(1) |
| C(7) | 5833(4) | 6126(3) | 9282(2) | 19(1) |
| C(8) | 8504(4) | 9057(4) | 9540(2) | 31(1) |
| C(9) | 3472(3) | 2945(3) | 6024(2) | 15(1) |
| C(10) | 2085(3) | 2174(3) | 6017(2) | 19(1) |
| C(11) | 1880(4) | 906(3) | 5554(2) | 21(1) |
| C(12) | 1979(4) | 1088(3) | 4738(2) | 22(1) |
| C(13) | 3327(4) | 1911(3) | 4747(2) | 22(1) |
| C(14) | 3513(3) | 3192(3) | 5199(2) | 18(1) |

| | | | | |
|---|---|---|---|---|
| C(15) | 3158(3) | 5675(3) | 6337(2) | 15(1) |
| C(16) | 3647(3) | 6399(3) | 5715(2) | 18(1) |
| C(17) | 2921(4) | 7559(3) | 5537(2) | 21(1) |
| C(18) | 1355(3) | 7213(3) | 5304(2) | 21(1) |
| C(19) | 877(3) | 6469(3) | 5916(2) | 19(1) |
| C(20) | 1580(3) | 5288(3) | 6073(2) | 17(1) |
| C(21) | 5876(3) | 4838(3) | 6677(2) | 16(1) |
| C(22) | 6761(3) | 3759(3) | 6779(2) | 20(1) |
| C(23) | 8227(3) | 4249(3) | 6757(2) | 22(1) |
| C(24) | 8900(4) | 5328(4) | 7359(2) | 26(1) |
| C(25) | 8061(4) | 6421(4) | 7235(2) | 24(1) |
| C(26) | 6572(3) | 5981(3) | 7247(2) | 20(1) |
| C(27) | 2453(3) | 1702(3) | 8198(2) | 18(1) |
| C(28) | 2270(4) | 270(3) | 7961(2) | 22(1) |
| C(29) | 1007(4) | -469(4) | 8140(2) | 27(1) |
| C(30) | -301(4) | 87(4) | 7774(2) | 27(1) |
| C(31) | -125(4) | 1487(4) | 8028(2) | 24(1) |
| C(32) | 1115(3) | 2244(3) | 7832(2) | 22(1) |
| C(33) | 5366(3) | 2751(3) | 8971(2) | 18(1) |
| C(34) | 5524(4) | 1498(3) | 9361(2) | 21(1) |
| C(35) | 6602(4) | 1710(4) | 10140(2) | 25(1) |
| C(36) | 7989(4) | 2395(4) | 10097(2) | 26(1) |
| C(37) | 7827(4) | 3627(4) | 9700(2) | 24(1) |
| C(38) | 6772(3) | 3379(3) | 8912(2) | 20(1) |

**Table 43.** Anisotropic displacement parameters (Å$^2$×10$^3$) for **P1**. The anisotropic displacement factor exponent takes the form: -2π$^2$[ h$^2$ a*$^2$U$^{11}$ + ... + 2 h k a* b* U$^{12}$ ]

| | $U^{11}$ | $U^{22}$ | $U^{33}$ | $U^{23}$ | $U^{13}$ | $U^{12}$ |
|---|---|---|---|---|---|---|
| Au(1) | 16(1) | 17(1) | 16(1) | 1(1) | 5(1) | 4(1) |
| Cl(1) | 28(1) | 31(1) | 26(1) | -6(1) | 8(1) | 11(1) |
| S(1) | 14(1) | 18(1) | 14(1) | 0(1) | 5(1) | 3(1) |
| P(1) | 11(1) | 14(1) | 14(1) | 1(1) | 4(1) | 2(1) |
| P(2) | 14(1) | 15(1) | 16(1) | 2(1) | 6(1) | 3(1) |
| O(1) | 20(1) | 20(1) | 17(1) | 2(1) | 8(1) | 2(1) |
| O(2) | 16(1) | 23(1) | 20(1) | 0(1) | 5(1) | 6(1) |
| C(1) | 15(1) | 20(2) | 15(1) | 1(1) | 5(1) | 1(1) |
| C(2) | 14(1) | 19(2) | 17(1) | -5(1) | 4(1) | 2(1) |
| C(3) | 24(2) | 23(2) | 14(1) | 1(1) | 4(1) | 7(1) |
| C(4) | 31(2) | 16(2) | 19(2) | 1(1) | 11(1) | 5(1) |
| C(5) | 27(2) | 19(2) | 24(2) | -6(1) | 11(1) | 1(1) |
| C(6) | 20(2) | 24(2) | 19(2) | -3(1) | 2(1) | 3(1) |
| C(7) | 23(2) | 18(2) | 18(2) | 0(1) | 7(1) | 5(1) |
| C(8) | 28(2) | 28(2) | 33(2) | -2(2) | 6(2) | -2(2) |
| C(9) | 12(1) | 17(1) | 16(1) | -2(1) | 4(1) | 1(1) |
| C(10) | 18(2) | 19(2) | 18(2) | 0(1) | 6(1) | 0(1) |
| C(11) | 20(2) | 19(2) | 20(2) | -1(1) | 2(1) | -1(1) |
| C(12) | 23(2) | 23(2) | 21(2) | -3(1) | 5(1) | 2(1) |

| | | | | | | |
|---|---|---|---|---|---|---|
| C(13) | 21(2) | 25(2) | 20(2) | -4(1) | 7(1) | 2(1) |
| C(14) | 17(2) | 21(2) | 16(1) | 2(1) | 6(1) | 4(1) |
| C(15) | 14(1) | 16(1) | 15(1) | 1(1) | 4(1) | 3(1) |
| C(16) | 16(2) | 18(2) | 21(2) | 4(1) | 8(1) | 4(1) |
| C(17) | 19(2) | 18(2) | 26(2) | 8(1) | 6(1) | 4(1) |
| C(18) | 18(2) | 20(2) | 25(2) | 4(1) | 5(1) | 5(1) |
| C(19) | 15(2) | 20(2) | 23(2) | 2(1) | 6(1) | 4(1) |
| C(20) | 12(1) | 21(2) | 17(1) | 1(1) | 5(1) | 0(1) |
| C(21) | 12(1) | 19(2) | 20(1) | 2(1) | 8(1) | 3(1) |
| C(22) | 13(2) | 23(2) | 24(2) | 5(1) | 6(1) | 6(1) |
| C(23) | 14(2) | 25(2) | 31(2) | 6(1) | 11(1) | 6(1) |
| C(24) | 10(2) | 39(2) | 29(2) | 5(2) | 4(1) | 2(1) |
| C(25) | 16(2) | 25(2) | 31(2) | 0(1) | 8(1) | -2(1) |
| C(26) | 13(2) | 24(2) | 22(2) | 0(1) | 5(1) | 1(1) |
| C(27) | 16(2) | 19(2) | 18(2) | 3(1) | 5(1) | 0(1) |
| C(28) | 21(2) | 21(2) | 24(2) | 2(1) | 7(1) | -1(1) |
| C(29) | 25(2) | 21(2) | 35(2) | 7(1) | 9(2) | -2(1) |
| C(30) | 18(2) | 30(2) | 30(2) | 7(2) | 4(1) | -4(1) |
| C(31) | 17(2) | 31(2) | 26(2) | 7(1) | 9(1) | 2(1) |
| C(32) | 16(2) | 24(2) | 25(2) | 6(1) | 8(1) | 4(1) |
| C(33) | 16(2) | 22(2) | 16(1) | 1(1) | 4(1) | 2(1) |
| C(34) | 20(2) | 20(2) | 24(2) | 7(1) | 7(1) | 6(1) |
| C(35) | 29(2) | 29(2) | 22(2) | 7(1) | 8(1) | 13(2) |
| C(36) | 25(2) | 30(2) | 22(2) | 5(1) | 2(1) | 10(2) |
| C(37) | 21(2) | 28(2) | 23(2) | 2(1) | 3(1) | 2(1) |
| C(38) | 16(2) | 24(2) | 18(2) | 2(1) | 4(1) | 2(1) |

## Crystal structure determination of [Au($^{Cy}$Y$_S$-P*i*Pr$_2$)Cl] (P4)

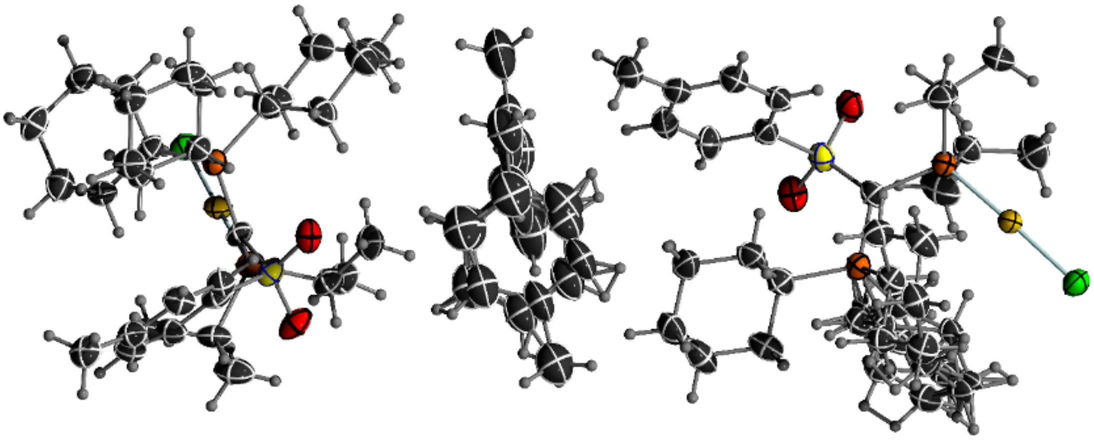

**Figure 67.** ORTEP plot of **P4 $^{Cy}$Y$_S$-P*i*Pr$_2$-AuCl** crystallizes as a twin with two molecules of toluene. Ellipsoids drawn at 50% probability level.

**Table 44.** Atomic Coordinates (×10$^4$) and Equivalent Isotropic Displacement Parameters (Å$^2$×10$^3$) for **P4**. U$_{eq}$ is defined as 1/3 of of the trace of the orthogonalised U$_{ij}$ tensor.

| | *x* | *y* | *z* | U(eq) |
|---|---|---|---|---|
| Au(1) | 5439(1) | 255(1) | 1841(1) | 36(1) |
| Au(2) | -250(1) | 10122(1) | 6871(1) | 38(1) |
| Cl(1) | 7579(4) | -839(3) | 2495(3) | 46(1) |
| Cl(2) | -2397(4) | 11202(3) | 6883(3) | 51(1) |
| S(1) | 2175(4) | 3217(3) | -339(2) | 40(1) |
| S(2) | 2991(4) | 7164(3) | 6450(2) | 41(1) |
| P(1) | 5418(4) | 2392(3) | -298(2) | 35(1) |
| P(2) | 3377(4) | 1362(3) | 1192(2) | 37(1) |
| P(3) | -251(4) | 8017(3) | 6019(2) | 35(1) |
| P(4) | 1811(4) | 9016(3) | 6878(2) | 37(1) |
| O(1) | 2552(13) | 4223(9) | -554(7) | 46(2) |
| O(2) | 976(12) | 2998(10) | 232(7) | 50(3) |
| O(3) | 4184(13) | 7367(10) | 6896(8) | 51(3) |
| O(4) | 2597(14) | 6171(9) | 6823(7) | 47(2) |
| C(1) | 3669(14) | 2251(10) | 143(8) | 32(2) |
| C(2) | 1581(15) | 3153(12) | -1364(9) | 38(3) |
| C(3) | 1185(16) | 2259(13) | -1400(10) | 43(3) |
| C(4) | 731(17) | 2228(12) | -2197(11) | 44(3) |
| C(5) | 655(16) | 3065(12) | -2983(10) | 42(3) |
| C(6) | 1021(17) | 3962(12) | -2915(11) | 44(3) |
| C(7) | 1482(17) | 4008(12) | -2111(10) | 41(3) |
| C(8) | 240(20) | 2997(15) | -3846(12) | 50(4) |
| C(9) | 6456(15) | 1140(12) | -213(9) | 38(3) |
| C(10) | 5670(17) | 482(13) | -573(13) | 48(4) |
| C(11) | 6480(20) | -620(13) | -226(12) | 54(4) |
| C(12) | 8074(19) | -674(14) | -519(11) | 50(4) |
| C(13) | 8841(18) | 18(15) | -225(11) | 51(4) |
| C(14) | 8022(15) | 1120(12) | -538(10) | 39(3) |

| | | | | |
|---|---|---|---|---|
| C(15) | 5299(16) | 3261(11) | -1467(9) | 38(3) |
| C(16) | 4937(16) | 2752(11) | -2114(9) | 38(3) |
| C(17) | 4780(18) | 3507(15) | -3069(10) | 46(4) |
| C(18) | 6167(18) | 3939(13) | -3329(10) | 47(3) |
| C(19) | 6558(18) | 4451(13) | -2684(11) | 48(3) |
| C(20) | 6722(17) | 3707(12) | -1734(10) | 42(3) |
| C(21) | 6590(17) | 2927(13) | 292(10) | 44(3) |
| C(22) | 7150(20) | 2226(15) | 1213(12) | 49(4) |
| C(23) | 8190(20) | 2726(16) | 1612(11) | 55(4) |
| C(24) | 7470(30) | 3775(18) | 1597(13) | 65(5) |
| C(25) | 6950(30) | 4460(17) | 661(13) | 62(5) |
| C(26) | 5860(20) | 3986(13) | 258(12) | 48(4) |
| C(27) | 2576(17) | 2025(13) | 1970(10) | 45(3) |
| C(28) | 3030(20) | 3040(17) | 1817(12) | 58(4) |
| C(29) | 3040(20) | 1349(17) | 2935(10) | 55(4) |
| C(30) | 1937(15) | 632(13) | 1079(10) | 44(3) |
| C(31) | 2524(17) | -134(14) | 640(12) | 52(4) |
| C(32) | 1370(20) | 54(18) | 1968(13) | 62(5) |
| C(33) | 1532(16) | 8125(11) | 6356(9) | 37(3) |
| C(34) | 3617(15) | 7216(12) | 5389(10) | 39(3) |
| C(35) | 3966(16) | 8111(12) | 4803(10) | 40(3) |
| C(36) | 4468(18) | 8124(13) | 3982(12) | 48(3) |
| C(37) | 4634(17) | 7244(13) | 3757(12) | 46(3) |
| C(38) | 4310(20) | 6355(13) | 4372(12) | 51(4) |
| C(39) | 3806(18) | 6338(12) | 5175(10) | 44(3) |
| C(40) | 5110(20) | 7259(18) | 2862(13) | 58(5) |
| C(41) | -157(17) | 7125(12) | 5403(10) | 41(3) |
| C(42) | -1610(20) | 6722(14) | 5386(12) | 50(4) |
| C(43) | -1420(20) | 5931(14) | 4913(14) | 62(5) |
| C(44) | -960(20) | 6356(17) | 3996(14) | 60(5) |
| C(45) | 460(20) | 6760(20) | 4009(17) | 68(6) |
| C(46) | 263(18) | 7566(14) | 4447(11) | 48(3) |
| C(47A) | -1480(20) | 7502(13) | 6909(13) | 35(4) |
| C(48A) | -2020(20) | 8224(16) | 7410(13) | 37(5) |
| C(49A) | -3010(30) | 7770(17) | 8129(15) | 38(6) |
| C(50A) | -2290(30) | 6729(15) | 8752(15) | 49(5) |
| C(51A) | -1770(30) | 6002(17) | 8261(15) | 48(5) |
| C(52A) | -800(40) | 6430(20) | 7520(20) | 40(8) |
| C(47B) | -1060(40) | 7610(30) | 7112(18) | 35(8) |
| C(48B) | -2700(40) | 7980(30) | 7110(20) | 44(11) |
| C(49B) | -3240(60) | 7660(40) | 8040(30) | 41(12) |
| C(50B) | -2790(40) | 6520(30) | 8530(30) | 50(8) |
| C(51B) | -1150(50) | 6160(30) | 8530(30) | 45(8) |
| C(52B) | -590(80) | 6470(40) | 7610(40) | 35(10) |
| C(53) | -1257(16) | 9270(11) | 5333(9) | 39(3) |
| C(54) | -435(19) | 9876(12) | 4580(11) | 46(3) |

| | | | | |
|---|---|---|---|---|
| C(55) | -1220(20) | 10996(14) | 4239(13) | 60(5) |
| C(56) | -2790(20) | 11065(13) | 3907(12) | 51(4) |
| C(57) | -3620(20) | 10392(14) | 4617(11) | 53(4) |
| C(58) | -2803(17) | 9285(13) | 4984(10) | 44(3) |
| C(59) | 3267(17) | 9730(13) | 6335(11) | 45(3) |
| C(60) | 2725(18) | 10510(14) | 5433(11) | 50(4) |
| C(61) | 3830(20) | 10295(16) | 6882(15) | 54(5) |
| C(62) | 2565(18) | 8333(14) | 8057(11) | 48(4) |
| C(63) | 2130(30) | 7331(19) | 8486(12) | 69(6) |
| C(64) | 2110(20) | 9028(19) | 8604(13) | 64(5) |
| C11 | 5830(40) | 3840(20) | 3964(19) | 87(8) |
| C21 | 4830(50) | 4466(18) | 3250(16) | 92(10) |
| C31 | 3320(70) | 4500(30) | 3280(20) | 127(18) |
| C41 | 2860(50) | 3910(30) | 3980(20) | 114(13) |
| C51 | 3740(40) | 3290(20) | 4680(20) | 98(9) |
| C61 | 5260(40) | 3240(20) | 4686(17) | 85(8) |
| C71 | 7400(50) | 3850(30) | 3940(30) | 120(13) |
| C1A2 | -400(60) | 6600(40) | 1270(40) | 68(8) |
| C2A2 | 320(50) | 7260(40) | 1490(40) | 71(9) |
| C3A2 | 1810(50) | 7170(50) | 1390(60) | 80(8) |
| C4A2 | 2590(60) | 6450(50) | 1120(60) | 80(13) |
| C5A2 | 1850(70) | 5860(100) | 850(110) | 81(12) |
| C6A2 | 360(60) | 5930(50) | 900(60) | 69(9) |
| C7A2 | -2020(50) | 6670(40) | 1350(30) | 80(11) |
| C1B2 | 2330(60) | 6610(60) | 980(60) | 77(13) |
| C2B2 | 1870(80) | 5860(100) | 730(110) | 78(11) |
| C3B2 | 480(60) | 5670(50) | 920(60) | 72(10) |
| C4B2 | -510(70) | 6260(40) | 1240(40) | 74(10) |
| C5B2 | -20(60) | 6950(40) | 1510(40) | 74(9) |
| C6B2 | 1400(60) | 7120(60) | 1430(60) | 78(9) |
| C7B2 | 3880(50) | 6760(40) | 870(30) | 79(12) |

**Table 45.** Anisotropic displacement parameters ($Å^2 \times 10^3$) for **P4**. The anisotropic displacement factor exponent takes the form: $-2\pi^2[\, h^2 a^{*2} U^{11} + \ldots + 2 h k a^* b^* U^{12} \,]$

| | $U^{11}$ | $U^{22}$ | $U^{33}$ | $U^{23}$ | $U^{13}$ | $U^{12}$ |
|---|---|---|---|---|---|---|
| Au(1) | 33(1) | 45(1) | 31(1) | -10(1) | 2(1) | -12(1) |
| Au(2) | 32(1) | 50(1) | 42(1) | -25(1) | 6(1) | -14(1) |
| Cl(1) | 38(2) | 55(2) | 42(2) | -13(2) | -3(1) | -5(1) |
| Cl(2) | 36(2) | 67(2) | 57(2) | -34(2) | 4(1) | -3(2) |
| S(1) | 40(2) | 46(2) | 32(2) | -12(1) | 3(1) | -3(1) |
| S(2) | 44(2) | 42(2) | 36(2) | -15(1) | -5(1) | -3(1) |
| P(1) | 35(2) | 42(2) | 28(2) | -12(1) | 3(1) | -10(1) |
| P(2) | 34(2) | 46(2) | 30(2) | -10(1) | 2(1) | -10(1) |
| P(3) | 38(2) | 36(2) | 30(2) | -11(1) | 2(1) | -8(1) |
| P(4) | 33(2) | 47(2) | 38(2) | -22(2) | 6(1) | -10(1) |

| | | | | | | |
|---|---|---|---|---|---|---|
| O(1) | 56(6) | 46(6) | 41(5) | -21(5) | 3(5) | -5(5) |
| O(2) | 43(5) | 66(7) | 32(5) | -11(5) | 6(4) | 3(5) |
| O(3) | 49(6) | 63(7) | 44(6) | -28(5) | -5(5) | -2(5) |
| O(4) | 60(6) | 39(5) | 38(5) | -11(4) | -4(5) | -4(5) |
| C(1) | 30(6) | 38(7) | 26(6) | -9(5) | 3(4) | -5(5) |
| C(2) | 32(6) | 50(8) | 28(6) | -9(5) | 7(5) | -8(5) |
| C(3) | 40(7) | 54(9) | 37(7) | -13(6) | 5(6) | -19(6) |
| C(4) | 40(7) | 41(8) | 48(8) | -10(6) | 3(6) | -13(6) |
| C(5) | 33(6) | 50(8) | 44(8) | -15(6) | 3(6) | -9(6) |
| C(6) | 43(7) | 37(8) | 43(8) | -4(6) | -3(6) | -8(6) |
| C(7) | 40(7) | 40(8) | 40(7) | -13(6) | -2(6) | -4(6) |
| C(8) | 53(9) | 55(10) | 40(8) | -13(7) | 4(7) | -11(7) |
| C(9) | 37(7) | 46(8) | 32(6) | -15(5) | 9(5) | -5(5) |
| C(10) | 35(7) | 54(9) | 64(10) | -29(8) | 13(7) | -15(6) |
| C(11) | 65(10) | 42(9) | 53(9) | -15(7) | 14(8) | -11(7) |
| C(12) | 50(9) | 47(9) | 45(8) | -13(7) | 4(7) | 6(7) |
| C(13) | 42(8) | 71(11) | 41(8) | -25(7) | 4(6) | -2(7) |
| C(14) | 29(6) | 51(8) | 38(7) | -16(6) | 3(5) | -5(5) |
| C(15) | 42(7) | 42(7) | 32(7) | -11(6) | 5(5) | -12(6) |
| C(16) | 40(7) | 44(8) | 30(7) | -12(6) | 5(5) | -8(6) |
| C(17) | 46(8) | 62(10) | 29(7) | -11(7) | 0(6) | -14(7) |
| C(18) | 49(8) | 56(9) | 30(7) | -6(6) | 9(6) | -14(7) |
| C(19) | 43(8) | 50(9) | 44(8) | -6(7) | 9(6) | -15(7) |
| C(20) | 42(7) | 49(8) | 36(7) | -11(6) | 3(6) | -18(6) |
| C(21) | 44(7) | 54(9) | 39(7) | -19(6) | -2(6) | -16(6) |
| C(22) | 44(9) | 56(10) | 45(9) | -12(7) | 3(7) | -17(7) |
| C(23) | 50(9) | 84(13) | 34(7) | -17(8) | 5(6) | -29(9) |
| C(24) | 73(12) | 85(14) | 51(10) | -28(9) | 4(9) | -42(11) |
| C(25) | 87(14) | 64(12) | 46(9) | -20(8) | 2(9) | -39(11) |
| C(26) | 56(9) | 48(9) | 45(8) | -16(7) | 6(7) | -23(7) |
| C(27) | 42(7) | 53(9) | 39(8) | -14(6) | 5(6) | -6(6) |
| C(28) | 64(10) | 80(13) | 43(9) | -35(9) | 8(8) | -16(9) |
| C(29) | 48(8) | 84(13) | 30(7) | -18(7) | 2(6) | -10(8) |
| C(30) | 30(6) | 56(9) | 44(8) | -9(6) | 0(6) | -17(6) |
| C(31) | 36(7) | 66(10) | 56(9) | -17(8) | -5(6) | -24(7) |
| C(32) | 54(12) | 77(14) | 53(11) | -11(9) | 9(8) | -33(10) |
| C(33) | 39(7) | 45(8) | 30(6) | -16(6) | -6(5) | -8(6) |
| C(34) | 36(7) | 46(8) | 38(7) | -20(6) | -1(5) | -5(6) |
| C(35) | 38(7) | 43(8) | 44(7) | -19(6) | -3(6) | -9(6) |
| C(36) | 45(8) | 51(9) | 51(9) | -21(7) | 4(7) | -14(7) |
| C(37) | 36(7) | 58(9) | 53(9) | -28(7) | 4(6) | -13(6) |
| C(38) | 57(9) | 45(9) | 56(9) | -26(7) | 0(7) | -6(7) |
| C(39) | 51(8) | 37(7) | 40(8) | -14(6) | -1(6) | -1(6) |
| C(40) | 61(11) | 72(12) | 52(10) | -33(9) | 7(8) | -21(9) |
| C(41) | 43(7) | 40(8) | 40(7) | -13(6) | -2(6) | -7(6) |
| C(42) | 54(9) | 52(9) | 47(9) | -11(7) | -7(7) | -24(7) |

| | | | | | | |
|---|---|---|---|---|---|---|
| C(43) | 62(11) | 42(9) | 80(13) | -22(9) | -30(9) | -4(8) |
| C(44) | 59(10) | 70(12) | 66(12) | -41(10) | -10(9) | -11(9) |
| C(45) | 46(9) | 102(17) | 82(14) | -66(13) | 4(9) | -12(10) |
| C(46) | 42(7) | 65(10) | 47(8) | -27(7) | 3(6) | -18(7) |
| C(47A) | 40(10) | 40(8) | 30(8) | -15(6) | 7(8) | -16(7) |
| C(48A) | 39(11) | 47(10) | 32(9) | -20(7) | 4(7) | -14(8) |
| C(49A) | 34(9) | 55(9) | 38(9) | -26(7) | 3(7) | -24(7) |
| C(50A) | 50(12) | 60(10) | 41(10) | -17(7) | 9(8) | -23(8) |
| C(51A) | 56(12) | 47(10) | 40(10) | -9(7) | 6(9) | -20(9) |
| C(52A) | 46(13) | 44(8) | 33(10) | -13(7) | 0(10) | -12(8) |
| C(47B) | 41(15) | 42(12) | 25(14) | -11(10) | 8(12) | -17(11) |
| C(48B) | 41(16) | 60(20) | 35(15) | -16(14) | 6(13) | -9(14) |
| C(49B) | 41(17) | 59(14) | 32(13) | -22(12) | 3(13) | -18(13) |
| C(50B) | 50(15) | 61(14) | 43(17) | -14(12) | 3(13) | -24(11) |
| C(51B) | 52(14) | 45(16) | 38(13) | -8(11) | 4(12) | -21(12) |
| C(52B) | 43(18) | 40(11) | 30(13) | -17(10) | -7(13) | -18(11) |
| C(53) | 41(7) | 40(7) | 32(7) | -8(5) | -6(5) | -6(6) |
| C(54) | 48(8) | 40(8) | 44(8) | -7(6) | 6(6) | -12(6) |
| C(55) | 81(13) | 43(9) | 51(9) | -5(7) | -11(9) | -21(8) |
| C(56) | 67(11) | 40(8) | 46(9) | -14(6) | -9(8) | -4(7) |
| C(57) | 50(9) | 58(10) | 42(8) | -14(7) | -12(7) | 3(7) |
| C(58) | 41(8) | 50(9) | 40(8) | -14(6) | -3(6) | -10(6) |
| C(59) | 39(7) | 55(9) | 53(9) | -28(7) | 7(6) | -18(6) |
| C(60) | 45(8) | 64(10) | 48(8) | -22(7) | 13(7) | -26(7) |
| C(61) | 44(10) | 59(11) | 69(12) | -28(9) | 8(8) | -22(8) |
| C(62) | 44(8) | 59(10) | 43(8) | -22(7) | -4(6) | -7(7) |
| C(63) | 80(13) | 96(16) | 34(8) | -15(9) | -7(8) | -36(12) |
| C(64) | 63(11) | 94(15) | 42(9) | -34(10) | -5(8) | -13(10) |
| C11 | 130(20) | 74(15) | 85(18) | -52(14) | 25(16) | -27(15) |
| C21 | 180(40) | 48(12) | 48(11) | -24(9) | 5(16) | -15(16) |
| C31 | 220(50) | 80(20) | 66(18) | -37(16) | -50(30) | 20(30) |
| C41 | 160(30) | 100(20) | 80(20) | -46(18) | -40(20) | 0(20) |
| C51 | 130(30) | 100(20) | 70(15) | -29(14) | -2(16) | -34(19) |
| C61 | 140(30) | 63(14) | 53(12) | -24(10) | 0(14) | -7(15) |
| C71 | 160(40) | 100(20) | 130(30) | -80(20) | 10(30) | -30(20) |
| C1A2 | 97(14) | 60(20) | 56(13) | -29(15) | -7(12) | -21(12) |
| C2A2 | 101(17) | 60(20) | 58(16) | -28(16) | -12(15) | -23(14) |
| C3A2 | 101(17) | 63(15) | 69(16) | -12(13) | -12(17) | -21(15) |
| C4A2 | 108(18) | 60(20) | 50(30) | 0(20) | -15(19) | -7(16) |
| C5A2 | 109(13) | 70(15) | 50(30) | -10(17) | 3(12) | -15(12) |
| C6A2 | 110(13) | 50(30) | 48(14) | -10(20) | 2(12) | -18(13) |
| C7A2 | 98(15) | 70(30) | 70(30) | -20(20) | -1(17) | -18(17) |
| C1B2 | 105(17) | 60(20) | 50(30) | 0(20) | -15(19) | -8(16) |
| C2B2 | 109(14) | 69(15) | 50(30) | -12(17) | 4(13) | -18(12) |
| C3B2 | 109(14) | 50(30) | 48(14) | -10(20) | 0(12) | -15(14) |
| C4B2 | 97(16) | 70(20) | 60(16) | -24(17) | -6(14) | -19(14) |

| | | | | | | |
|---|---|---|---|---|---|---|
| C5B2 | 102(16) | 70(20) | 57(14) | -23(15) | -7(14) | -21(14) |
| C6B2 | 101(18) | 61(16) | 67(15) | -15(13) | -8(16) | -19(15) |
| C7B2 | 105(18) | 80(30) | 50(30) | -20(20) | -18(18) | -11(18) |

## Crystal structure determination of $^{Cy}\mathbf{Y}_{SF}$-H

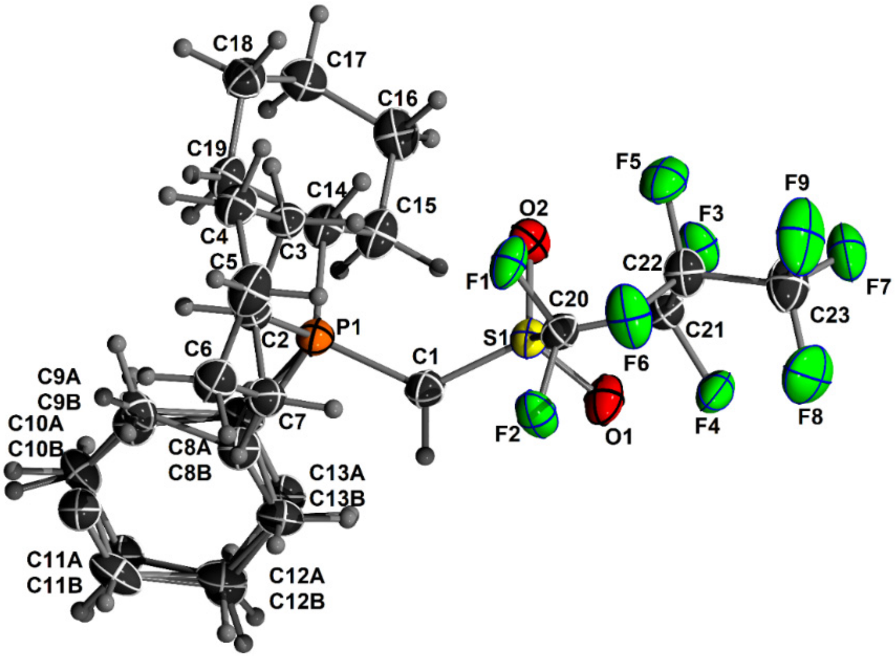
C18
C17
C16
C19
C14
C15
F5
F9
O2
F3
C4
C3
C5
C22
F7
F1
C20
C23
C2
P1
S1
C6
C1
C21
F6
C9A
C9B
C10A
C10B
C8A
C8B
C7
F2
O1
F4
F8
C13A
C13B
C11A
C11B
C12A
C12B

**Figure 68.** ORTEP plot of $^{Cy}\mathbf{Y}_{SF}$**-H**. Ellipsoids drawn at 50% probability level.

**Table 46.** Atomic Coordinates (×$10^4$) and Equivalent Isotropic Displacement Parameters (Å$^2$×$10^3$) for $^{Cy}\mathbf{Y}_{SF}$**-H**. $U_{eq}$ is defined as 1/3 of of the trace of the orthogonalised $U_{ij}$ tensor.

| | *x* | *y* | *z* | U(eq) |
|---|---|---|---|---|
| S(1) | 3693(1) | 3486(1) | 6401(1) | 29(1) |
| F(1) | 4928(1) | 3371(1) | 5924(1) | 39(1) |
| O(1) | 3369(1) | 2670(2) | 6788(1) | 40(1) |
| P(1) | 3771(1) | 6037(1) | 6406(1) | 28(1) |
| C(1) | 3747(1) | 4713(2) | 6730(1) | 31(1) |
| C(2) | 4644(1) | 6522(2) | 6262(1) | 28(1) |
| O(2) | 3499(1) | 3553(2) | 5776(1) | 35(1) |
| F(2) | 4881(1) | 3026(1) | 6893(1) | 42(1) |
| F(3) | 4101(1) | 1333(1) | 5806(1) | 39(1) |
| C(3) | 4940(1) | 6052(2) | 5669(1) | 28(1) |
| C(4) | 5679(1) | 6426(2) | 5581(1) | 33(1) |
| F(4) | 4426(1) | 1018(1) | 6736(1) | 43(1) |
| C(5) | 6119(2) | 6115(3) | 6125(2) | 40(1) |
| F(5) | 5312(1) | 1395(2) | 5389(1) | 48(1) |
| C(6) | 5834(2) | 6610(3) | 6704(1) | 38(1) |
| F(6) | 5777(1) | 1661(2) | 6267(1) | 52(1) |
| C(7) | 5098(2) | 6231(3) | 6806(1) | 33(1) |
| F(7) | 4832(1) | -666(2) | 5837(1) | 53(1) |
| F(8) | 5453(1) | -399(2) | 6625(1) | 68(1) |
| F(9) | 5910(1) | -435(2) | 5747(1) | 75(1) |
| C(14) | 3309(1) | 6081(2) | 5690(1) | 30(1) |
| C(15) | 2571(1) | 5659(3) | 5733(1) | 35(1) |
| C(16) | 2289(1) | 5533(3) | 5092(1) | 39(1) |
| C(17) | 2313(2) | 6642(3) | 4747(1) | 39(1) |
| C(18) | 3027(2) | 7145(3) | 4747(1) | 37(1) |

| | | | | |
|---|---|---|---|---|
| C(19) | 3313(1) | 7248(2) | 5389(1) | 32(1) |
| C(20) | 4559(1) | 2852(2) | 6361(1) | 29(1) |
| C(21) | 4570(1) | 1582(2) | 6226(1) | 29(1) |
| C(22) | 5259(1) | 1151(2) | 5980(1) | 35(1) |
| C(23) | 5361(2) | -120(3) | 6052(2) | 45(1) |
| C(8) | 3340(2) | 7014(3) | 6925(2) | 46(1) |
| C(9) | 3610(2) | 8207(3) | 6902(1) | 37(1) |
| C(10) | 3218(2) | 9007(3) | 7302(2) | 53(1) |
| C(11) | 3126(2) | 8592(3) | 7921(2) | 61(1) |
| C(12) | 2834(2) | 7406(3) | 7953(1) | 39(1) |
| C(13) | 3234(2) | 6594(3) | 7549(2) | 54(1) |

**Table 47.** Anisotropic displacement parameters (Å$^2$×10$^3$) for **$^{Cy}$Y$_{SF}$-H**. The anisotropic displacement factor exponent takes the form: $-2\pi^2[\ h^2\ a^{*2}U^{11} + \ldots\ + 2\ h\ k\ a^*\ b^*\ U^{12}\ ]$

| | $U^{11}$ | $U^{22}$ | $U^{33}$ | $U^{23}$ | $U^{13}$ | $U^{12}$ |
|---|---|---|---|---|---|---|
| S(1) | 25(1) | 27(1) | 33(1) | 1(1) | 4(1) | 1(1) |
| F(1) | 31(1) | 31(1) | 57(1) | 11(1) | 13(1) | 0(1) |
| O(1) | 36(1) | 32(1) | 52(1) | 3(1) | 16(1) | -2(1) |
| P(1) | 28(1) | 27(1) | 29(1) | 0(1) | 7(1) | 1(1) |
| C(1) | 35(2) | 30(1) | 29(1) | 1(1) | 7(1) | 2(1) |
| C(2) | 29(1) | 26(1) | 27(1) | 0(1) | 3(1) | -1(1) |
| O(2) | 33(1) | 34(1) | 38(1) | -3(1) | -4(1) | 6(1) |
| F(2) | 45(1) | 35(1) | 46(1) | -6(1) | -18(1) | 5(1) |
| F(3) | 29(1) | 38(1) | 51(1) | -10(1) | -9(1) | 0(1) |
| C(3) | 28(1) | 28(1) | 28(1) | 0(1) | 5(1) | -1(1) |
| C(4) | 29(1) | 34(2) | 37(2) | 2(1) | 7(1) | 0(1) |
| F(4) | 58(1) | 31(1) | 40(1) | 8(1) | 15(1) | 3(1) |
| C(5) | 26(1) | 40(2) | 53(2) | 9(1) | 0(1) | 0(1) |
| F(5) | 50(1) | 49(1) | 46(1) | 6(1) | 19(1) | 2(1) |
| C(6) | 33(2) | 40(2) | 41(2) | 6(1) | -11(1) | -5(1) |
| F(6) | 28(1) | 43(1) | 84(1) | -9(1) | -14(1) | 2(1) |
| C(7) | 35(2) | 36(2) | 29(1) | 1(1) | -1(1) | -2(1) |
| F(7) | 56(1) | 33(1) | 71(1) | -11(1) | 10(1) | -6(1) |
| F(8) | 86(2) | 46(1) | 72(1) | 12(1) | -10(1) | 24(1) |
| F(9) | 55(1) | 44(1) | 125(2) | -4(1) | 38(1) | 14(1) |
| C(14) | 24(1) | 29(1) | 38(1) | 3(1) | 5(1) | 2(1) |
| C(15) | 23(1) | 35(2) | 48(2) | 7(1) | 4(1) | 2(1) |
| C(16) | 26(1) | 38(2) | 51(2) | -4(1) | 0(1) | 1(1) |
| C(17) | 35(2) | 42(2) | 39(2) | -1(1) | -3(1) | 3(1) |
| C(18) | 39(2) | 35(2) | 36(2) | 3(1) | 1(1) | 2(1) |
| C(19) | 30(1) | 29(1) | 38(2) | 4(1) | 2(1) | 1(1) |
| C(20) | 28(1) | 29(1) | 30(1) | 3(1) | 0(1) | -2(1) |
| C(21) | 28(1) | 30(1) | 28(1) | 4(1) | 1(1) | -1(1) |
| C(22) | 28(1) | 33(2) | 44(2) | -1(1) | 0(1) | 0(1) |
| C(23) | 42(2) | 34(2) | 60(2) | -2(2) | 8(2) | 6(1) |
| C(8) | 51(2) | 36(2) | 51(2) | -7(1) | 23(2) | 1(1) |
| C(9) | 39(2) | 34(2) | 39(2) | -6(1) | 4(1) | -1(1) |
| C(10) | 49(2) | 39(2) | 69(2) | -15(2) | 18(2) | -1(2) |

| | | | | | | |
|---|---|---|---|---|---|---|
| C(11) | 76(3) | 57(2) | 49(2) | -22(2) | 10(2) | 4(2) |
| C(12) | 37(2) | 51(2) | 29(1) | -5(1) | 3(1) | 6(1) |
| C(13) | 77(3) | 45(2) | 39(2) | -5(2) | 20(2) | -1(2) |

## Crystal structure determination of $^{\mathrm{Cy}}\mathrm{Y}_{\mathrm{SF}}$-PCy$_2$ (L5)

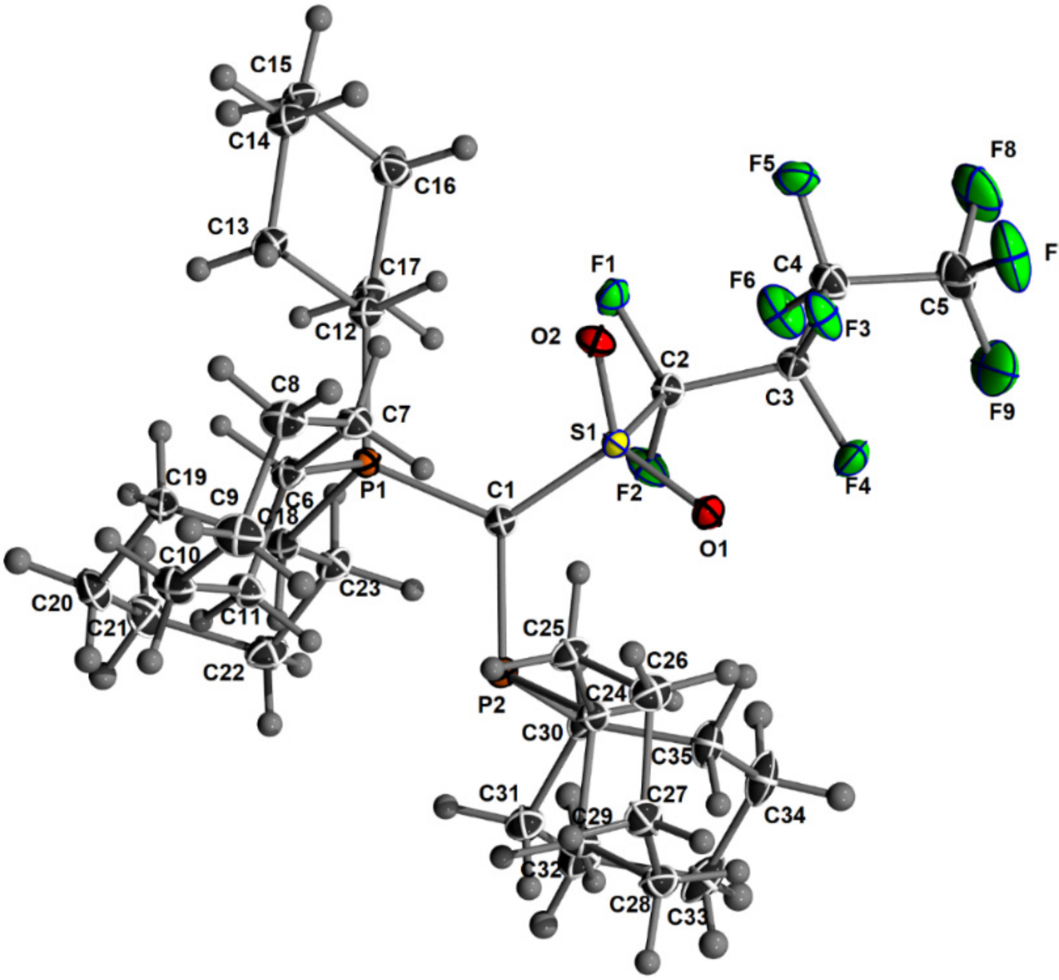
C15
C14
C16
C13
C17
C12
F5
F8
F1
F6
C4
F7
O2
F3
C5
C2
C8
C7
C3
F9
S1
C19
C9
C6
P1
C18
C1
F2
F4
O1
C10
C23
C20
C21
C11
C25
C26
C22
P2
C24
C30
C35
C31
C27
C34
C29
C32
C28
C33

**Figure 69.** ORTEP plot of **L5**. Ellipsoids drawn at 50% probability level.

**Table 48.** Atomic Coordinates (×10$^4$) and Equivalent Isotropic Displacement Parameters (Å$^2$×10$^3$) for **L5**. U$_{eq}$ is defined as 1/3 of of the trace of the orthogonalised U$_{ij}$ tensor.

| | ***x*** | ***y*** | ***z*** | **U(eq)** |
|---|---|---|---|---|
| S(1) | 6664(1) | 8451(1) | 3317(1) | 13(1) |
| P(1) | 4365(1) | 7094(1) | 3573(1) | 11(1) |
| P(2) | 6823(1) | 6272(1) | 3488(1) | 13(1) |
| F(1) | 5041(1) | 8646(1) | 1778(1) | 20(1) |
| F(2) | 6047(1) | 7340(1) | 1286(1) | 23(1) |
| F(3) | 7653(1) | 10047(1) | 2487(1) | 25(1) |
| F(4) | 8167(1) | 8619(1) | 1474(1) | 29(1) |
| F(5) | 5872(1) | 10084(1) | 1014(1) | 28(1) |
| F(6) | 5886(1) | 8467(1) | -30(1) | 30(1) |
| F(7) | 8475(1) | 10708(1) | 1039(1) | 46(1) |
| F(8) | 7046(1) | 10193(1) | -397(1) | 45(1) |
| F(9) | 8290(1) | 9160(1) | -146(1) | 52(1) |

| | | | | |
|---|---|---|---|---|
| O(1) | 8041(1) | 8536(1) | 3459(1) | 19(1) |
| O(2) | 6198(1) | 9383(1) | 3860(1) | 18(1) |
| C(1) | 5946(1) | 7304(1) | 3386(1) | 13(1) |
| C(2) | 6194(1) | 8366(1) | 1950(1) | 15(1) |
| C(3) | 7184(1) | 9104(1) | 1680(1) | 17(1) |
| C(4) | 6618(1) | 9372(1) | 741(1) | 20(1) |
| C(5) | 7640(2) | 9868(1) | 302(1) | 30(1) |
| C(6) | 4334(1) | 7327(1) | 4914(1) | 14(1) |
| C(7) | 5127(1) | 8456(1) | 5648(1) | 16(1) |
| C(8) | 4962(1) | 8693(1) | 6740(1) | 21(1) |
| C(9) | 5327(1) | 7830(1) | 7132(1) | 24(1) |
| C(10) | 4554(1) | 6711(1) | 6390(1) | 21(1) |
| C(11) | 4733(1) | 6461(1) | 5299(1) | 16(1) |
| C(12) | 3374(1) | 7968(1) | 3196(1) | 14(1) |
| C(13) | 2343(1) | 8274(1) | 3807(1) | 18(1) |
| C(14) | 1705(1) | 9099(1) | 3504(1) | 22(1) |
| C(15) | 1111(1) | 8696(1) | 2349(1) | 22(1) |
| C(16) | 2099(1) | 8333(1) | 1733(1) | 20(1) |
| C(17) | 2710(1) | 7498(1) | 2036(1) | 16(1) |
| C(18) | 3589(1) | 5657(1) | 2863(1) | 14(1) |
| C(19) | 2208(1) | 5352(1) | 2984(1) | 17(1) |
| C(20) | 1746(1) | 4124(1) | 2548(1) | 22(1) |
| C(21) | 1829(1) | 3605(1) | 1434(1) | 24(1) |
| C(22) | 3192(1) | 3937(1) | 1320(1) | 19(1) |
| C(23) | 3620(1) | 5168(1) | 1726(1) | 16(1) |
| C(24) | 8448(1) | 6960(1) | 4398(1) | 15(1) |
| C(25) | 8414(1) | 7832(1) | 5412(1) | 17(1) |
| C(26) | 9794(1) | 8366(1) | 6091(1) | 20(1) |
| C(27) | 10508(1) | 7538(1) | 6302(1) | 20(1) |
| C(28) | 10485(1) | 6620(1) | 5306(1) | 20(1) |
| C(29) | 9100(1) | 6105(1) | 4634(1) | 18(1) |
| C(30) | 7240(1) | 5653(1) | 2217(1) | 15(1) |
| C(31) | 7024(1) | 4421(1) | 1888(1) | 19(1) |
| C(32) | 7182(1) | 3882(1) | 795(1) | 24(1) |
| C(33) | 8509(1) | 4352(1) | 710(1) | 26(1) |
| C(34) | 8730(1) | 5571(1) | 1031(1) | 25(1) |
| C(35) | 8573(1) | 6122(1) | 2122(1) | 20(1) |

**Table 49** Anisotropic displacement parameters (Å$^2$×10$^3$) for **L5**. The anisotropic displacement factor exponent takes the form: $-2\pi^2[\, h^2 a^{*2}U^{11} + \dots + 2 h k a^* b^* U^{12} \,]$

| | $U^{11}$ | $U^{22}$ | $U^{33}$ | $U^{23}$ | $U^{13}$ | $U^{12}$ |
|---|---|---|---|---|---|---|
| S(1) | 13(1) | 12(1) | 15(1) | 6(1) | 3(1) | 2(1) |
| P(1) | 12(1) | 11(1) | 12(1) | 4(1) | 3(1) | 3(1) |
| P(2) | 13(1) | 12(1) | 14(1) | 5(1) | 5(1) | 4(1) |
| F(1) | 13(1) | 30(1) | 23(1) | 15(1) | 4(1) | 5(1) |
| F(2) | 35(1) | 15(1) | 17(1) | 5(1) | 6(1) | 3(1) |

| | | | | | | |
|---|---|---|---|---|---|---|
| F(3) | 26(1) | 21(1) | 22(1) | 10(1) | -1(1) | -6(1) |
| F(4) | 20(1) | 42(1) | 42(1) | 28(1) | 17(1) | 17(1) |
| F(5) | 31(1) | 32(1) | 31(1) | 20(1) | 11(1) | 17(1) |
| F(6) | 40(1) | 27(1) | 18(1) | 9(1) | 1(1) | -2(1) |
| F(7) | 47(1) | 46(1) | 42(1) | 22(1) | 11(1) | -14(1) |
| F(8) | 55(1) | 57(1) | 41(1) | 39(1) | 15(1) | 10(1) |
| F(9) | 69(1) | 58(1) | 62(1) | 37(1) | 52(1) | 31(1) |
| O(1) | 13(1) | 21(1) | 25(1) | 13(1) | 2(1) | 2(1) |
| O(2) | 21(1) | 13(1) | 18(1) | 5(1) | 4(1) | 4(1) |
| C(1) | 13(1) | 13(1) | 15(1) | 6(1) | 4(1) | 3(1) |
| C(2) | 14(1) | 15(1) | 17(1) | 7(1) | 4(1) | 3(1) |
| C(3) | 14(1) | 19(1) | 20(1) | 10(1) | 5(1) | 4(1) |
| C(4) | 23(1) | 20(1) | 20(1) | 10(1) | 6(1) | 5(1) |
| C(5) | 36(1) | 32(1) | 29(1) | 19(1) | 14(1) | 7(1) |
| C(6) | 15(1) | 15(1) | 13(1) | 5(1) | 5(1) | 5(1) |
| C(7) | 18(1) | 14(1) | 15(1) | 4(1) | 5(1) | 4(1) |
| C(8) | 28(1) | 19(1) | 15(1) | 3(1) | 5(1) | 7(1) |
| C(9) | 33(1) | 25(1) | 14(1) | 6(1) | 4(1) | 9(1) |
| C(10) | 28(1) | 22(1) | 16(1) | 10(1) | 8(1) | 9(1) |
| C(11) | 20(1) | 16(1) | 14(1) | 6(1) | 5(1) | 6(1) |
| C(12) | 14(1) | 13(1) | 17(1) | 6(1) | 4(1) | 5(1) |
| C(13) | 17(1) | 19(1) | 21(1) | 8(1) | 8(1) | 8(1) |
| C(14) | 20(1) | 20(1) | 31(1) | 10(1) | 9(1) | 10(1) |
| C(15) | 15(1) | 20(1) | 34(1) | 14(1) | 4(1) | 6(1) |
| C(16) | 18(1) | 20(1) | 23(1) | 12(1) | 1(1) | 4(1) |
| C(17) | 15(1) | 16(1) | 17(1) | 7(1) | 3(1) | 4(1) |
| C(18) | 14(1) | 13(1) | 15(1) | 5(1) | 4(1) | 3(1) |
| C(19) | 15(1) | 16(1) | 19(1) | 7(1) | 6(1) | 2(1) |
| C(20) | 22(1) | 18(1) | 27(1) | 9(1) | 6(1) | -1(1) |
| C(21) | 22(1) | 16(1) | 26(1) | 3(1) | 4(1) | -1(1) |
| C(22) | 20(1) | 16(1) | 19(1) | 2(1) | 3(1) | 5(1) |
| C(23) | 15(1) | 16(1) | 14(1) | 4(1) | 4(1) | 3(1) |
| C(24) | 15(1) | 15(1) | 15(1) | 6(1) | 4(1) | 5(1) |
| C(25) | 16(1) | 17(1) | 16(1) | 4(1) | 3(1) | 6(1) |
| C(26) | 18(1) | 18(1) | 20(1) | 3(1) | 2(1) | 4(1) |
| C(27) | 17(1) | 22(1) | 21(1) | 9(1) | 0(1) | 2(1) |
| C(28) | 18(1) | 19(1) | 24(1) | 10(1) | 3(1) | 7(1) |
| C(29) | 19(1) | 16(1) | 18(1) | 6(1) | 3(1) | 6(1) |
| C(30) | 14(1) | 16(1) | 15(1) | 5(1) | 5(1) | 4(1) |
| C(31) | 21(1) | 17(1) | 20(1) | 4(1) | 8(1) | 5(1) |
| C(32) | 24(1) | 22(1) | 21(1) | 1(1) | 8(1) | 5(1) |
| C(33) | 21(1) | 35(1) | 18(1) | 2(1) | 8(1) | 10(1) |
| C(34) | 18(1) | 36(1) | 17(1) | 6(1) | 8(1) | 1(1) |
| C(35) | 16(1) | 24(1) | 17(1) | 6(1) | 7(1) | 1(1) |

## Crystal Structure of [Au($^{Cy}Y_{SF}$-PCy$_2$)Cl] (P5)

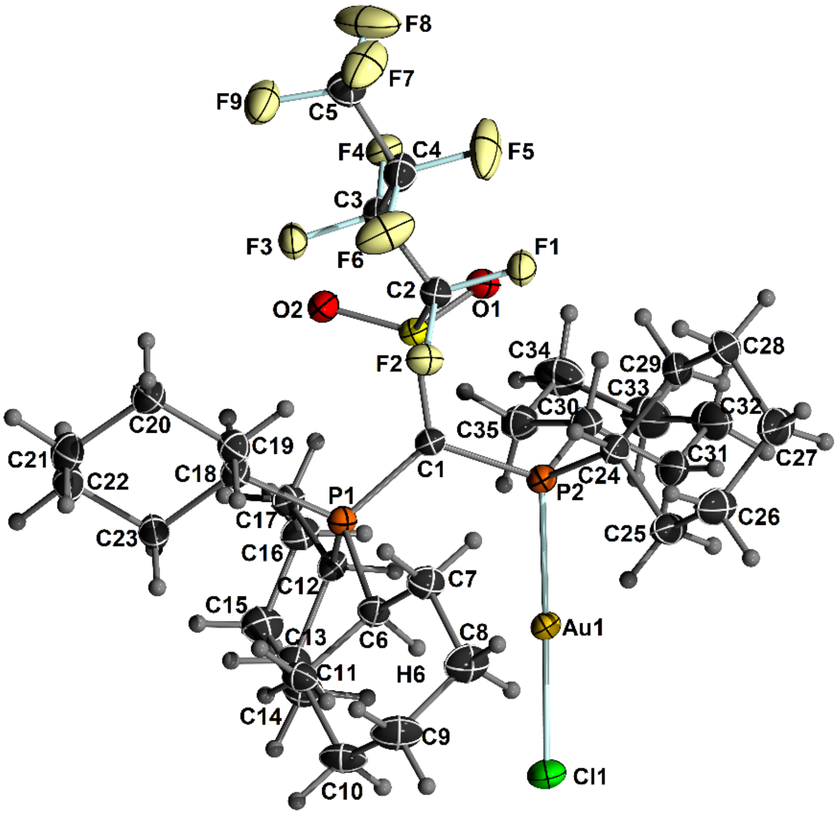
F8
F7
F9
C5
F4
C4
F5
C3
F3
F6
F1
C2
O2
O1
C34
C28
C29
F2
C33
C32
C30
C35
C20
C19
C21
C18
C22
C1
C31
C27
P1
C24
P2
C17
C23
C26
C16
C25
C7
C12
C15
C8
C13
C6
Au1
C11
H6
C14
C9
Cl1
C10

**Figure 70.** ORTEP plot of **P5**. Ellipsoids drawn at 50% probability level.

**Table 50.** Atomic Coordinates (×$10^4$) and Equivalent Isotropic Displacement Parameters (Å$^2$×$10^3$) for **P5**. $U_{eq}$ is defined as 1/3 of of the trace of the orthogonalised $U_{ij}$ tensor.

| | *x* | *y* | *z* | U(eq) |
|---|---|---|---|---|
| Au(1) | 3027(1) | 2046(1) | 7015(1) | 24(1) |
| Cl(1) | 2765(1) | 2390(1) | 7929(1) | 40(1) |
| O(1) | 4015(2) | 3663(2) | 4801(1) | 27(1) |
| S(1) | 3650(1) | 2754(1) | 5030(1) | 22(1) |
| F(1) | 2339(2) | 1462(1) | 4534(1) | 30(1) |
| P(1) | 2961(1) | 3978(1) | 6027(1) | 21(1) |
| C(1) | 3274(3) | 2843(2) | 5699(1) | 22(1) |
| F(2) | 1430(2) | 2724(1) | 4824(1) | 29(1) |
| P(2) | 3312(1) | 1739(1) | 6108(1) | 23(1) |
| O(2) | 4323(2) | 1905(2) | 4940(1) | 28(1) |
| C(2) | 2395(3) | 2433(2) | 4581(1) | 26(1) |
| C(3) | 2444(3) | 2871(2) | 3992(1) | 26(1) |
| F(3) | 2352(2) | 3845(1) | 4030(1) | 31(1) |
| C(4) | 1508(3) | 2539(2) | 3589(1) | 33(1) |
| F(4) | 3433(2) | 2648(1) | 3769(1) | 31(1) |
| F(5) | 524(2) | 2852(2) | 3780(1) | 52(1) |
| C(5) | 1638(3) | 2912(2) | 2990(2) | 33(1) |
| C(6) | 1667(3) | 3857(2) | 6428(1) | 25(1) |
| F(6) | 1484(3) | 1571(2) | 3557(1) | 64(1) |
| C(7) | 753(3) | 3240(2) | 6148(1) | 29(1) |
| F(7) | 1755(2) | 3852(2) | 2979(1) | 46(1) |

| | | | | |
|---|---|---|---|---|
| C(8) | -164(3) | 3001(3) | 6566(2) | 38(1) |
| F(8) | 2528(3) | 2525(2) | 2751(1) | 67(1) |
| F(9) | 744(2) | 2677(2) | 2701(1) | 53(1) |
| C(9) | -656(3) | 3912(3) | 6825(2) | 42(1) |
| C(10) | 256(3) | 4542(3) | 7078(1) | 35(1) |
| C(12) | 4105(2) | 4181(2) | 6514(1) | 22(1) |
| C(11) | 1137(3) | 4803(2) | 6650(1) | 29(1) |
| C(14) | 4868(3) | 4781(3) | 7417(1) | 32(1) |
| C(13) | 3873(3) | 4814(2) | 7027(1) | 27(1) |
| C(15) | 5954(3) | 5059(3) | 7133(1) | 35(1) |
| C(16) | 6165(3) | 4435(2) | 6625(1) | 31(1) |
| C(23) | 2956(3) | 6019(2) | 5826(1) | 29(1) |
| C(22) | 2983(3) | 6814(2) | 5386(2) | 35(1) |
| C(21) | 1975(3) | 6767(3) | 5007(2) | 37(1) |
| C(20) | 1875(3) | 5764(2) | 4743(1) | 33(1) |
| C(19) | 1822(3) | 4971(2) | 5183(1) | 27(1) |
| C(18) | 2872(3) | 5006(2) | 5547(1) | 24(1) |
| C(17) | 5192(3) | 4490(2) | 6221(1) | 26(1) |
| C(30) | 4674(3) | 1124(2) | 6053(1) | 28(1) |
| C(31) | 4741(3) | 309(2) | 6489(1) | 36(1) |
| C(32) | 5852(4) | -234(3) | 6439(2) | 47(1) |
| C(33) | 6832(4) | 449(3) | 6500(2) | 49(1) |
| C(34) | 6760(3) | 1287(3) | 6094(2) | 43(1) |
| C(35) | 5652(3) | 1826(3) | 6134(1) | 32(1) |
| C(24) | 2241(3) | 887(2) | 5825(1) | 28(1) |
| C(25) | 1457(3) | 513(3) | 6279(1) | 34(1) |
| C(26) | 469(3) | -37(3) | 6023(2) | 42(1) |
| C(27) | 876(4) | -877(3) | 5666(2) | 44(1) |
| C(28) | 1693(4) | -519(2) | 5229(2) | 39(1) |
| C(29) | 2682(3) | 30(2) | 5478(1) | 32(1) |

**Table 51.** Anisotropic displacement parameters (Å$^2$×10$^3$) for **P5**. The anisotropic displacement factor exponent takes the form: $-2\pi^2[h^2 a^{*2}U^{11} + ... + 2 h k a^* b^* U^{12}]$

| | $U^{11}$ | $U^{22}$ | $U^{33}$ | $U^{23}$ | $U^{13}$ | $U^{12}$ |
|---|---|---|---|---|---|---|
| Au(1) | 32(1) | 22(1) | 18(1) | 1(1) | 3(1) | -1(1) |
| Cl(1) | 63(1) | 35(1) | 21(1) | -1(1) | 7(1) | 0(1) |
| O(1) | 32(1) | 25(1) | 23(1) | 2(1) | 3(1) | -3(1) |
| S(1) | 26(1) | 22(1) | 18(1) | 0(1) | 2(1) | -1(1) |
| F(1) | 44(1) | 20(1) | 27(1) | 2(1) | -3(1) | -5(1) |
| P(1) | 22(1) | 20(1) | 19(1) | 0(1) | 0(1) | 1(1) |
| C(1) | 27(2) | 23(1) | 17(1) | 1(1) | 2(1) | 0(1) |
| F(2) | 28(1) | 34(1) | 24(1) | -3(1) | 2(1) | -2(1) |
| P(2) | 30(1) | 20(1) | 18(1) | 1(1) | 3(1) | -1(1) |
| O(2) | 33(1) | 29(1) | 22(1) | -2(1) | 4(1) | 4(1) |
| C(2) | 31(2) | 23(1) | 23(1) | -1(1) | 3(1) | -1(1) |
| C(3) | 31(2) | 20(1) | 25(2) | 0(1) | 0(1) | -2(1) |
| F(3) | 44(1) | 20(1) | 30(1) | 1(1) | -4(1) | -2(1) |

| | | | | | | |
|---|---|---|---|---|---|---|
| C(4) | 43(2) | 26(2) | 31(2) | 4(1) | -7(1) | -7(1) |
| F(4) | 38(1) | 32(1) | 24(1) | 2(1) | 5(1) | 0(1) |
| F(5) | 33(1) | 89(2) | 35(1) | 10(1) | -4(1) | -11(1) |
| C(5) | 37(2) | 35(2) | 28(2) | -3(1) | -5(1) | -1(1) |
| C(6) | 24(1) | 26(1) | 25(1) | -1(1) | 1(1) | 0(1) |
| F(6) | 111(2) | 29(1) | 53(1) | 8(1) | -42(2) | -26(1) |
| C(7) | 24(2) | 33(2) | 29(2) | -4(1) | 2(1) | -3(1) |
| F(7) | 68(2) | 36(1) | 35(1) | 9(1) | -9(1) | -11(1) |
| C(8) | 28(2) | 47(2) | 38(2) | -3(1) | 5(2) | -9(1) |
| F(8) | 77(2) | 98(2) | 27(1) | -9(1) | -1(1) | 37(2) |
| F(9) | 66(2) | 59(1) | 35(1) | 10(1) | -22(1) | -25(1) |
| C(9) | 26(2) | 62(2) | 38(2) | -7(2) | 10(1) | -1(2) |
| C(10) | 30(2) | 48(2) | 28(2) | -7(1) | 5(1) | 8(1) |
| C(12) | 23(1) | 24(1) | 20(1) | 2(1) | 1(1) | -2(1) |
| C(11) | 29(2) | 30(2) | 27(2) | -5(1) | 2(1) | 7(1) |
| C(14) | 34(2) | 36(2) | 25(2) | -3(1) | -3(1) | 1(1) |
| C(13) | 32(2) | 26(1) | 24(1) | -3(1) | -1(1) | -1(1) |
| C(15) | 33(2) | 42(2) | 30(2) | -4(1) | -6(1) | -6(1) |
| C(16) | 28(2) | 36(2) | 29(2) | 0(1) | 0(1) | 0(1) |
| C(23) | 38(2) | 21(1) | 28(2) | 0(1) | -3(1) | -1(1) |
| C(22) | 42(2) | 22(1) | 41(2) | 2(1) | -1(2) | 0(1) |
| C(21) | 48(2) | 29(2) | 34(2) | 6(1) | -5(2) | 9(1) |
| C(20) | 43(2) | 31(2) | 26(2) | 1(1) | -2(1) | 7(1) |
| C(19) | 30(2) | 27(2) | 26(1) | -2(1) | -2(1) | 3(1) |
| C(18) | 30(2) | 22(1) | 21(1) | 1(1) | -1(1) | 1(1) |
| C(17) | 27(2) | 27(2) | 24(1) | 0(1) | 1(1) | -6(1) |
| C(30) | 34(2) | 26(2) | 24(1) | 2(1) | 1(1) | 5(1) |
| C(31) | 50(2) | 28(2) | 29(2) | 7(1) | 4(1) | 10(1) |
| C(32) | 64(3) | 40(2) | 35(2) | 3(2) | 3(2) | 24(2) |
| C(33) | 51(2) | 57(2) | 40(2) | 0(2) | -4(2) | 26(2) |
| C(34) | 36(2) | 55(2) | 38(2) | -3(2) | 0(2) | 12(2) |
| C(35) | 33(2) | 35(2) | 28(2) | 0(1) | -1(1) | 3(1) |
| C(24) | 36(2) | 24(1) | 24(1) | 0(1) | 3(1) | -6(1) |
| C(25) | 41(2) | 35(2) | 26(2) | -3(1) | 7(1) | -12(1) |
| C(26) | 48(2) | 44(2) | 34(2) | -8(2) | 8(2) | -20(2) |
| C(27) | 63(3) | 36(2) | 34(2) | -5(1) | 7(2) | -22(2) |
| C(28) | 61(2) | 26(2) | 31(2) | -6(1) | 8(2) | -13(2) |
| C(29) | 47(2) | 22(1) | 28(2) | -1(1) | 5(1) | -4(1) |

## Crystal structure determination of [Au(Cy-$^{Cy}$JohnPhos)Cl] (P6)

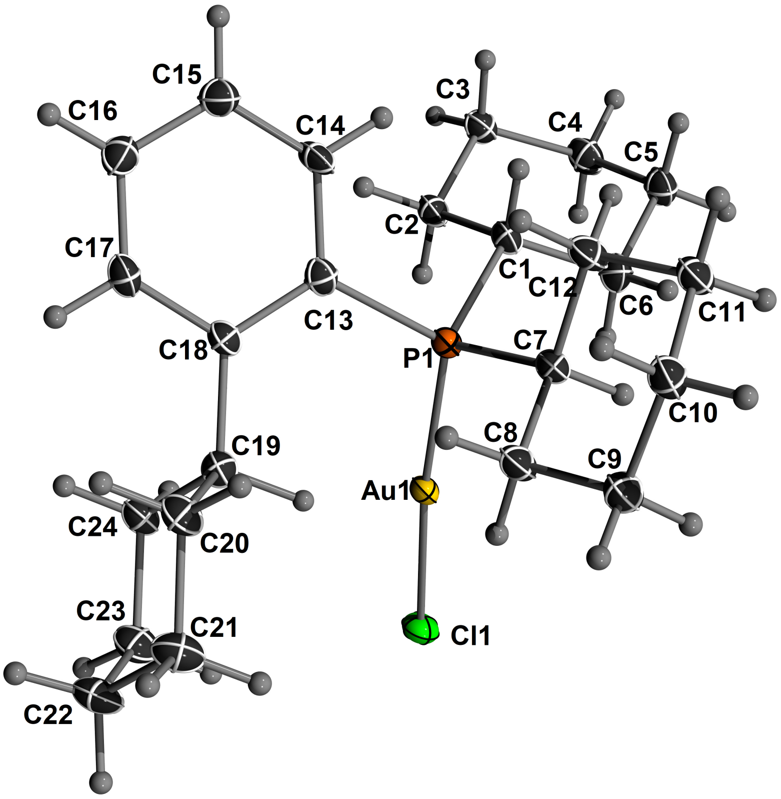

**Figure 71.** ORTEP plot of **P6**. Ellipsoids drawn at 50% probability level.

**Table 52.** Atomic Coordinates (×$10^4$) and Equivalent Isotropic Displacement Parameters (Å$^2$×$10^3$) for **P6**. $U_{eq}$ is defined as 1/3 of of the trace of the orthogonalised $U_{ij}$ tensor.

| | *x* | *y* | *z* | U(eq) |
|---|---|---|---|---|
| Au(1) | 6055(1) | 4981(1) | 2314(1) | 16(1) |
| Cl(1) | 7968(1) | 3886(1) | 2274(1) | 22(1) |
| C(1) | 2512(4) | 4599(3) | 1103(3) | 18(1) |
| P(1) | 4114(1) | 5967(1) | 2159(1) | 15(1) |
| C(2) | 2110(4) | 3263(4) | 1449(3) | 19(1) |
| C(3) | 730(4) | 2187(4) | 589(3) | 20(1) |
| C(5) | 1396(4) | 3096(4) | -905(3) | 23(1) |
| C(4) | 914(4) | 1765(4) | -570(3) | 24(1) |
| C(6) | 2770(4) | 4160(4) | -42(3) | 23(1) |
| C(8) | 5699(4) | 8744(4) | 2357(3) | 21(1) |
| C(7) | 4380(3) | 7487(3) | 1599(3) | 17(1) |
| C(13) | 3496(4) | 6554(3) | 3387(3) | 17(1) |
| C(12) | 2978(4) | 8039(4) | 1311(3) | 21(1) |
| C(11) | 3227(4) | 9181(4) | 735(3) | 22(1) |
| C(10) | 4571(4) | 10429(4) | 1449(3) | 22(1) |
| C(9) | 5953(4) | 9889(4) | 1782(3) | 23(1) |
| C(14) | 1973(4) | 6306(4) | 3225(3) | 20(1) |
| C(15) | 1394(4) | 6579(4) | 4103(3) | 23(1) |
| C(16) | 2334(4) | 7131(4) | 5183(3) | 22(1) |
| C(17) | 3844(4) | 7423(4) | 5352(3) | 21(1) |

| | | | | |
|---|---|---|---|---|
| C(18) | 4468(3) | 7176(3) | 4481(3) | 16(1) |
| C(19) | 6152(4) | 7585(4) | 4777(3) | 19(1) |
| C(20) | 6806(4) | 9186(4) | 5469(3) | 22(1) |
| C(21) | 8490(4) | 9593(4) | 5751(3) | 28(1) |
| C(22) | 9180(4) | 8630(4) | 6356(3) | 29(1) |
| C(23) | 8529(4) | 7038(4) | 5681(3) | 26(1) |
| C(24) | 6851(4) | 6624(4) | 5389(3) | 20(1) |

**Table 53.** Anisotropic displacement parameters ($Å^2 \times 10^3$) for **P6**. The anisotropic displacement factor exponent takes the form: $-2\pi^2[ h^2 a^{*2}U^{11} + ... + 2 h k a^* b^* U^{12} ]$

| | $U^{11}$ | $U^{22}$ | $U^{33}$ | $U^{23}$ | $U^{13}$ | $U^{12}$ |
|---|---|---|---|---|---|---|
| Au(1) | 14(1) | 20(1) | 13(1) | 5(1) | 2(1) | 5(1) |
| Cl(1) | 17(1) | 27(1) | 23(1) | 8(1) | 4(1) | 10(1) |
| C(1) | 16(2) | 21(2) | 13(1) | 5(1) | 2(1) | 3(1) |
| P(1) | 13(1) | 19(1) | 13(1) | 5(1) | 2(1) | 5(1) |
| C(2) | 17(2) | 23(2) | 15(2) | 6(1) | 1(1) | 4(1) |
| C(3) | 17(2) | 21(2) | 19(2) | 7(1) | 2(1) | 3(1) |
| C(5) | 23(2) | 26(2) | 15(2) | 5(1) | 3(1) | 6(1) |
| C(4) | 23(2) | 23(2) | 19(2) | 2(1) | 2(1) | 4(1) |
| C(6) | 23(2) | 28(2) | 16(2) | 6(1) | 6(1) | 5(1) |
| C(8) | 17(2) | 24(2) | 20(2) | 9(1) | 0(1) | 4(1) |
| C(7) | 14(1) | 22(2) | 15(1) | 7(1) | 2(1) | 4(1) |
| C(13) | 19(2) | 16(1) | 16(2) | 5(1) | 4(1) | 3(1) |
| C(12) | 17(2) | 23(2) | 22(2) | 9(1) | 1(1) | 6(1) |
| C(11) | 18(2) | 25(2) | 20(2) | 10(1) | 1(1) | 5(1) |
| C(10) | 23(2) | 23(2) | 19(2) | 8(1) | 3(1) | 5(1) |
| C(9) | 21(2) | 26(2) | 23(2) | 10(1) | 3(1) | 5(1) |
| C(14) | 15(2) | 24(2) | 14(2) | 1(1) | -2(1) | 6(1) |
| C(15) | 19(2) | 27(2) | 21(2) | 4(1) | 6(1) | 6(1) |
| C(16) | 24(2) | 24(2) | 20(2) | 7(1) | 10(1) | 7(1) |
| C(17) | 22(2) | 23(2) | 14(2) | 4(1) | 2(1) | 4(1) |
| C(18) | 16(2) | 16(1) | 15(1) | 6(1) | 3(1) | 5(1) |
| C(19) | 18(2) | 22(2) | 17(2) | 7(1) | 4(1) | 4(1) |
| C(20) | 21(2) | 21(2) | 22(2) | 7(1) | 3(1) | 7(1) |
| C(21) | 20(2) | 25(2) | 33(2) | 7(2) | 3(2) | 2(1) |
| C(22) | 16(2) | 32(2) | 30(2) | 6(2) | -1(1) | 4(1) |
| C(23) | 21(2) | 29(2) | 28(2) | 11(2) | 4(1) | 11(1) |
| C(24) | 18(2) | 21(2) | 19(2) | 6(1) | 1(1) | 3(1) |